UNIVERSITY *of the*
WESTERN CAPE

The Effects of Various Combinations of Different Classes of Anticancer Drugs and Tyrosine Kinase Inhibitors on the Human MCF-7 and Triple-Negative MDA-MB 231 Breast Carcinoma Cell Lines

by

Beynon Abrahams

Student Number: 2317457

Thesis Submitted in Fulfilment of the Requirements for the Degree:

Doctor of Philosophy (PhD)

Department of Medical Biosciences

Faculty of Natural Sciences

University of the Western Cape

Supervisor	**Co-Supervisor**
Prof Donavon Hiss	Dr Tonie Gerber

23 November 2020

DECLARATION AND ATTRIBUTION

I, Beynon Abrahams, declare that "**The Effects of Various Combinations of Different Classes of Anticancer Drugs and Tyrosine Kinase Inhibitors on the Human MCF-7 and Triple-Negative MDA-MB 231 Breast Carcinoma Cell Lines**" is my original work and that all the sources I have used or cited have been indicated and acknowledged by means of complete references in strict accordance with appropriate statutory rules, and the terms and conditions of the Creative Commons Attribution (https://creativecommons.org/licenses/by/4.0/).

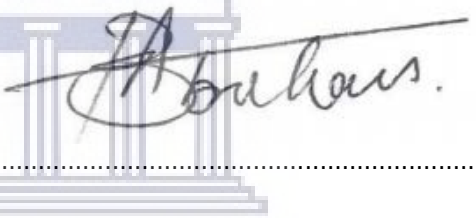

Beynon Abrahams	:	.....
Student Number	:	2317457
Place	:	University of the Western Cape
Date	:	23 November 2020

DEDICATION

"In memory of Margaret Adams (Née Van Wyk) 5 November 1958 – 19 August 2007, forever in our hearts"

To my family

LITERARY QUOTATIONS

There can be life after breast cancer. The prerequisite is early detection.

Ann Jillian (1950-)
American actress.
(http://www.brainyquote.com/quotes/authors/a/ann_jillian.ht ml, accessed October 20, 2013)

Breast cancer changes you, and the change can be beautiful.

Alyssa-Jane Cook
Breast cancer Survivor
(AZQuotes.com. Wind and Fly LTD, 2020. 03 July 2020. https://www.azquotes.com/quote/597770)

A carcinoma does not give rise to the same danger [as a carbuncle] unless it is irritated by imprudent treatment. This disease occurs mostly in the upper parts of the body, in the region of the face, nose, ears, lips, and in the breasts of women, but it may also arise in an ulceration, or in the spleen . . .. At times the part becomes harder or softer than natural . . .. After excision, even when a scar has formed, none the less the disease has returned, and caused death.

Aulus Aurelius Cornelius Celsus
(25 BC – AD 50) [1]

The difference between cancerous swelling and induration. The latter is a slumbering silent mass, which ... is painless, and stationary ... A cancerous swelling progressively increases in size, is destructive, and spreads roots which insinuate themselves amongst the tissue-elements.

Avicenna
(981–1037) [1]

ACKNOWLEDGEMENTS

All honor and glory goes to God Almighty for His grace and mercy that allowed me to see through this project.

- To my parents, for their sacrifices they made that allowed me to pursue this journey in medical sciences, and instilling a culture of hard work and character within me. I am forever grateful to you.

- To my girlfriend, Lize Von Schlicht, for her unwavering love, support and encouragement when I needed it the most. This project is as much yours as it is mine. I love you!

- To my family and friends for their continued support and words of encouragement. I am grateful to you for always standing behind me.

- I would like to extent my gratitude to my colleagues and the executive, particularly my HOD, Dr Sanet Van Zyl, in the Department of Basic Medical Sciences as well as the School of Biomedical Sciences and the Faculty of Health Sciences at UFS for accommodating me and helping me to attain this goal.

- Funding support from the Department of Higher Education and Training (DHET) and the National Research Foundation (NRF), the University of the Western Cape (UWC) and the University of the Free State (UFS) that made this research project possible, is gratefully acknowledged.

- "This work is based on the research supported wholly by the National Research Foundation of South Africa (Grant Numbers: 114600)"

Special thank you to:

- My supervisor, friend and mentor, Prof Donavon Charles Hiss. Thank you for all you

have done for me from Hons to PhD level of studies. This journey has been tremendous! Thank you for rarely saying NO to me and always supporting me in taking this project in the direction where I wanted it to go. You are an inspiration to me and I have so much that I still want to learn from you. Thank you for your expert technical assistance and guidance in my research project, it is highly appreciated. I'm looking forward to continue working with you.

- My co-supervisor, Dr Anthonie Marthinus Gerber. You have been a tremendous support to me at the in the department from day one, when I started this journey and was searching for a space to work. I value your technical input in my studies and also miss the coffee sessions we had that helped me to relax and re-energize my mind.

- Prof Arnold Crous my nGAP mentor, for your willingness to take the academic load of my shoulders when I needed to run my experiments or wanted to attend a conference to gain valuable research insight.

- Profs Gilbert Matsabisa and Andrew Walubo at the department of Pharmacology, for allowing me to use their tissue culture laboratory and execute my laboratory experiments for this study at the University of the Free State.

- Dr Mamello Sekhoacha and Ms Sunelle Rademan for your excellent assistance in the laboratory during cell cultures at the Pharmacology department.

- The HOD of Medical Biosciences, Prof Ralf Henkel, the department and Science Faculty at that allowed me to register and complete my studies at the University of the Western Cape.

- The New Generation of Academics Program (nGAP) which forms part of the Staffing South Africa's University Framework (SSAUF) implemented by the DHET, that allowed me this opportunity to pursue my studies as well as develop as an academic at the University of the Free State.

ABSTRACT

Globally, breast cancer is the most common cancer affecting women and it is predicted that in 2030 about 12 million deaths will occur with approximately 21.7 million new cases [2]. Genetic risk factors as well as race and ethnicity, account for about 5-10% of all breast cancer occurrences. Triple negative breast cancer (TNBC), tumors that tested negative for oestrogen receptor (ER), progesterone receptor (PR) and human epidermal growth factor receptor 2 (HER2), contribute to 10-20% of all breast carcinomas [3,4] and is known to be a more aggressive type of cancer with varying degree of response to chemotherapeutic and radiation therapy [5,6]

The epidermal growth factor receptor (EGFR) is abnormally activated in many cancers and its signal transduction pathways play an important role in regulating cell proliferation and survival. It is often overexpressed in TNBC [7]. P-glycoprotein (P-gp) is a transmembrane glycoprotein responsible for active transport of substances across the cell membrane out of a cell. It functions as an efflux pump and is overexpressed in many cancer cells. The altered expression of both EGFR and P-gp parallels an aggressive clinical course and the development of resistance to anticancer and adjuvant endocrine therapies.

Anti-EGFR compounds that specifically target the intracellular and extracellular domains of the EGFR include tyrosine kinase inhibitors (TKIs), e.g., gefitinib and erlotinib and monoclonal antibodies, e.g., cetuximab and trastuzamab, that are amongst the most effective agents that are currently used together with chemotherapeutic agents in clinical practice. However, the emergence of multidrug resistance (MDR), a mechanism that is not well understood, has, over time, eclipsed

the progress that has been made in drug therapeutics.In this study we examined the effects of doxorubicin (DOX), cisplatin (CDDP) and one investigational TKI (EGFR inhibitor I, hereinafter referred to as EGFRi), individually and in combination, on human MCF-7 breast carcinoma cells and a triple negative breast cancer (TNBC) cell line (MDA-MB-231), with specific focus on P-gp and EGFR inhibition.

Analyses of MCF-7 and MDA-MB-231 TNB carcinoma cells exposure to DOX, CDDP and EGFRi included growth and dose-response curves (cytotoxicity assays), caspase-3/7 assays for apoptosis detection, P-glycoprotein function (intracellular Calcein-AM accumulation) and *EGFR* and P-glycoprotein (*ABCB1* gene) mRNA expression, using quantitative Real-Time PCR.

When used as an individual treatment, EGFRi demonstrated a higher growth inhibition in both MCF-7 and MDA-MB 231 cell lines, compared to DOX and CDDP. Combination treatment of DOX with CDDP at equimolar log dose concentrations, synergistically inhibited cell growth that was significantly different to the compounds used individually. The pairwise combinations of EGFRi with both DOX and CDDP also demonstrated synergistic and antagonistic drug interactions consistent with the Bliss independence and Loewe additivity synergy models.

Apoptosis was confirmed in both MCF-7 and MDA-MB-231 TNBC cells after 24-hour drug treatments. Intracellular calcein accumulation that is indicative of P-glycoprotein inhibition, was determined using the Calcein-AM assay. Drug treatments significantly increased the intracellular accumulation of calcein inside the cells, but only at very high concentrations in MCF-7 cells. No significant levels of calcein accumulation were detected in MDA-MB-231 cells, following individual treatment with EGFRi, DOX and CDDP.

The pairwise combination drug treatments of EGFRi + DOX demonstrated significant accumulation of calcein only in MCF-7 cells. RT-qPCR was utilized to quantify the gene expression levels of *EGFR* and *ABCB1* in both MCF-7 and MDA-MB-231 TNBC cell lines following drug treatment. The expression levels of *EGFR* gene were significantly reduced in both cells following drug treatment, which correlates with the cellular growth inhibition results. The expression levels of *ABCB1* gene could not be quantitated following optimization of expression due to undesirable C_T values that was outside the normal acceptable ranges. This is a due to the undetectably low expression levels of *ABCB1* gene in our samples.

Our scientific findings confirmed our hypothesis of the EGFRi's ability to successfully reduce the efflux function of P-glycoprotein as well as demonstrating its combinatorial potential with DOX and CDDP, as compounds from different classes are more effective in enhancing growth inhibition efficacy in the two human breast carcinoma cell lines.

Keywords: breast cancer, MCF-7 breast carcinoma cells, MDA-MB-231 TNBC cells, tyrosine kinase inhibitor, EGFR inhibitor, doxorubicin, cisplatin, drug combinations, drug interactions, Bliss independence, Loewe additivity, P-gp, EGFR, apoptosis, dose-response, drug efflux, *EGFR* and *ABCB1* gene expression

ABBREVIATIONS AND ACRONYMS

ABC	Advanced Breast Cancer
ABC	Adenosine Triphosphate (ATP)-Binding Cassette
ABCB1/MDR1/P-gp	Multidrug Resistance-Associated Protein-1 or P-Glycoprotein
AIs	Aromatase Inhibitors
AIDS	Acquired Immunodeficiency Syndrome
AJCC	American Joint Committee on Cancer
ANOVA	One-Way Analysis of Variance
ATP	Adenosine-5′-Triphosphate
BC/BRCA	Breast Cancer
BCRP/ABCG2	Breast Cancer Resistance Protein
BCS	Breast-Conserving Surgery
BCS	Breast Cancer Survivors
bCSCs/MaSCs	Breast Cancer Stem Cells/Mammary Stem Cells
BCSS	Breast Cancer-Specific Survival
Calcein-AM	Calcein–Acetoxymethylester
CDDP	Cisplatin (Cis-DiammineDichloroPlatinum)
95%CI	95% Confidence Interval
CI	Combination Index
CNAs	Copy Number Aberrations
COSMIC	Catalogue of Somatic Mutations in Cancer
CR	Cross-Resistance
CS	Collateral Sensitivity
CT	Threshold Cycle
Cq	Quantification Cycle
DDIs	Drug–Drug Interactions
DFS	Disease-Free Survival
DOX	Doxorubicin
DRI	Drug/Dose Reduction Index. Potency is the Concentration of Drug Required to Achieve a Particular Effect. Commonly Quantified by the IC_{50}, the Drug Concentration Required to Achieve a Half-Maximal Effect ($E_{max}/2$). The potency Ratio (PR) is Also Referred to as the Dose-Reduction Index (DRI)
EGFR-2	Epidermal Growth Factor Receptor 2 (HER2, ERBB2)
EGFRi	EGFR Inhibitor I
E_0	The Minimum Effect of a Drug

E_{max}	The Maximum Effect of a Drug (Once this magnitude of effect is achieved, higher doses of the drug will not produce an increase in the magnitude of effect)
$E_{max}/2$	The Half-Maximal Effect of a Drug
EMT	Epithelial to Mesenchymal Transition
ER	Estrogen Receptor
ERS	Endoplasmic Reticulum Stress
ERBB2/ ErbB2	v-erb-b2 Avian Erythroblastic Leukemia Viral Oncogene Homolog 2, Also Known as HER2 and Neu) is a Gene That Encodes for the Receptor Tyrosine-Protein Kinase erbB-2.
ESMO	European Society for Medical Oncology
FDA	Food and Drug Administration, US
FBS	Fetal Bovine Serum
FICs	Sum of Fractional Inhibitory Concentrations
GBD	Global Burden of Disease
GEP	Genomic Expression Profile
GLOBOCAN	Global Cancer Observatory - Part of IARC
GOF	Gain of Function
HBOC	Hereditary Breast/Ovarian Cancer Syndrome
HER1	Human Epidermal Growth Factor Receptor 1
HER2/neu	Human Epidermal Growth Factor Receptor 2
HIF-1α	Hypoxia-Inducible Factor–1α
HIFBS	Heat-Inactivated Fetal Bovine Serum
HIV	Human Immunodeficiency Virus
HTS	High Throughput Screening
IACR	International Association of Cancer Registries
IARC	International Agency for Research on Cancer
IC	Institutional Cohort
IC_{50}	Potency is the Concentration of Drug Required to Achieve a Particular Effect. Commonly Quantified by the IC_{50}, the Drug Concentration Required to Achieve a Half-Maximal Effect ($E_{max}/2$).
ICGC	International Cancer Genome Consortium
IHC	Immunohistochemistry/Immunohistochemical
LOF	Loss of Function
mAB	Monoclonal Antibody
MaSCs/bCSCs	Mammary Stem Cells/Breast Cancer Stem Cells
MBC	Metastatic Breast Cancer
MDR	Multidrug Resistance
METABRIC	Molecular Taxonomy of Breast Cancer International Consortium

MRPs/ABCCs	Multidrug Resistance-Associated Proteins
MRP1	Multidrug Resistance-Associated Protein-1
MuSiCa	Mutational Signatures in Cancer
NAC/NACT	Neoadjuvant Chemotherapy
NAT	Neoadjuvant Therapy
NBDs	Nucleotide-Binding Domains
NCCN	National Comprehensive Cancer Network
NSCLC	Non-Small Cell Lung Cancer
NRT	No Reverse Transcriptase Control
NTC	No Template Control
OET	Oral Endocrine Therapy
OS	Overall Survival
PBCRs	Population-Based Cancer Registries
PCAWG	Pan-Cancer Analysis of Whole Genomes
PCD	Programmed Cell Death
pCR	Pathological Complete Response
PFS	Progression-Free Survival
P-gp	P-Glycoprotein
PR	Potency is the Concentration of Drug Required to Achieve a Particular Effect. Commonly Quantified by the IC_{50}, the Drug Concentration Required to Achieve a Half-Maximal Effect ($E_{max}/2$). PR is Also Referred to as the Dose-Reduction Index (DRI)
PR	Progesterone Receptor
QNBC	Quadruple Negative Breast Cancer
ROS	Reactive Oxygen Species
RSM(s)	Response Surface Model(s)
RTKs/NRTKs	Receptor Tyrosine Kinases/Non-Receptor Tyrosine Kinases
RT-qPCR -	Quantitative Real-Time polymerase Chain Reaction
SEER	Surveillance, Epidemiology and End Results
SEM	Standard Error of the Mean
STKs	Serine–Threonine Kinases
Ta	Annealing Temperature
TAMs	Tumor-Associated Macrophages
TCGA	The Cancer Genome Atlas
TKD	Tyrosine Kinase Domain
TKs	Tyrosine Kinases
TKI	Tyrosine Kinase Inhibitor

TKRs	Tyrosine Kinase Receptors
Tm	Melting Temperature
TMDs	Transmembrane Domains
TME	Tumor Microenvironment
TNBC	Triple-Negative Breast Cancer
TNM	Tumor, Node, Metastasis Staging System
UICC	Union for International Cancer Control
UPR	Unfolded Protein Response
USA	United States of America
VEGF	Vascular Endothelial Growth Factor
WLWHA	Women Living with HIV/AIDS
WHO	World Health Organization

CONTENTS

LIST OF FIGURES

LIST OF TABLES

CHAPTER 1

INTRODUCTION AND LITERATURE REVIEW

SECTION A: CANCER

A.1 The Hallmarks of Cancer

Cancer is a non-communicable heterogeneous disease in etiology and pathology that is brought about by the uncontrolled growth of aberrant cells [2]. The ability of normal cells to develop and progress into a malignant mass of cells, known as a tumor is better described by a concept known as The Hallmarks of Cancer [8,9]. This concept describes six biological capabilities that are acquired during neoplastic disease development and is used to better understand the complexity and heterogeneity of cancer as a disease. The six characteristic traits encompass sustained proliferative signalling, evasion of growth suppression, resistance to cell death, limitless replicative potential, induction of angiogenesis and tissue invasion and metastasis [8-10].

A.1.1 Sustained Proliferative Signaling

In contrast to normal cells that require constant signalling for growth, tumor cells generate and sustain their own proliferative signals and thus demonstrate their independence from their normal tissue environment. Normal growth factor receptors expressed in somatic cells promote growth signalling through growth factors. In cancer cells, these signals are often deregulated by the overexpression of surface tyrosine kinase receptors (TKRs).

In cancer cells, these signals are often deregulated by the overexpression of surface tyrosine kinase receptors (TKRs). Cancer cells may also promote constant proliferative signaling by generating their own growth factor ligands resulting in autocrine activation that can lead to tumor development [8,9,11].

A.1.2 Evasion of Growth Suppressors

Normal cells are constantly regulated by different mechanisms to ensure homeostasis in the tissue and this includes growth inhibitory regulation. This usually takes place during cell cycle progression. In all cells, this process is brought about by extracellular or intracellular tumor suppressor proteins (e.g., TP53) and Retinoblastoma protein (RB), which control cell proliferation. Many cancer cells can either turn off molecules that send antiproliferative signals or dysregulate any signaling that relates to the activation of the tumor suppressor proteins [8,9].

A.1.3 Resistance to Programmed Cell Death or Apoptosis

Apoptosis, also known as programmed cell death, is a process that all cell types undergo. The process involves the recruitment of sensors that monitor the extracellular and intracellular environments for any changes that might occur. Depending on the conditions, favorable or unfavorable, these sensors will either stimulate signals to promote growth of the cell or induce cell death. Cell death involves numerous physiological events, including membrane disruption, cytosol expulsion, degradation and fragmentation of the nuclear material.

Tumor suppressor protein (TP53) is implicated in the induction of apoptosis that is stimulated by DNA damage. Many cancer cells evade cell death by dysregulating TP53 function. Furthermore, tumor cells may also downregulate the pro-apoptotic protein (Bax) and upregulate the pro-survival (anti-apoptotic) protein (Bcl-2) as well as

make use of the autophagy which have overlapping signals with apoptosis and may either promote cell survival or cell death [8,9,12].

A.1.4 Limitless Replicative Potential

Most cell types have automated internal processes that regulate and stop cellular replication after several cycles, independent of the growth signals elicited. This process is referred to as senescence. However, certain cells have the ability to bypass senescence and continue multiplying until they reach a crisis state, in which all the cells die. This process of senescence and crisis is dictated by telomerase activity in cells. The higher the telomerase activity, the longer the telomeric DNA and the longer the cell replication cycle and *vice versa*. Many neoplastic cells have developed the ability to overcome senescence and sustain telomerase activity and develop tumors [8,9].

A.1.5 Induction of Angiogenesis

All cellular and tissue survival mechanisms are dependent on oxygen and nutrient supply. Hence, angiogenesis, the formation of new blood vessels, is not only essential to all cells, but critical to new tissue development. Angiogenesis is upregulated during the process of tumorigenesis and is continuously producing more blood vessels from normal dormant vasculature. Angiogenesis can either be induced or suppressed, this is referred to as the “angiogenic switch”. This is mediated by angiogenesis inhibitors, e.g., vascular endothelial growth factor (VEGF), fibroblast growth factor (FGF) and inhibitor thrombospondin-1 (TSP-1). These compounds bind to either stimulatory or inhibitory transmembrane receptors exposed on vascular cells. Upregulation of VEGF genes that encode ligands together with the overexpression of the receptors and signal transduction of FGF have been implicated in tumor angiogenesis [8,9].

A.1.6 Tissue Invasion and Metastasis

Tumorigenesis is promoted by the ability of cells to migrate from the primary tumor site, invading other tissues and metastasizing to other (secondary) sites. The ability of cancer cells to metastasize and invade other tissues is made possible by all the other aforementioned characteristics and abilities which constitute the *Hallmarks of Cancer*. It is also further facilitated by the loss of the cell adhesion molecule, E-cadherin, a molecule that the once normal epithelial cell contained and is lost in cancer cells [13,14]. This allows cancer cells to invade distant sites and replace adjacent cells. Furthermore, changes in cell-cell adhesion molecules (CAMs) and proteins involved in forming junctions also permit primary neoplastic masses in invasion and metastasis to progress in distant sites [8-10,15].

A.1.7 The Hallmarks of Cancer Are the Sine Qua Non for Cancer Therapy

In a follow-up review by Hanahan and Weinberg, two additional hallmarks were added to cancer tumorigenesis and progression, viz., *Deregulation of Cellular Energetics* where normal cellular metabolism programming is modified to support cancer cell growth and, *Surviving Immune Destruction*, in which cancer cells effectively evade immunological destruction by T and B lymphocytes and natural killer cells [9]. Following their initial publication during a time where the complexity of cancer was not very well understood, Hanahan and Weinberg received a lot of criticism with regards to their attempt to simplify the diverse nature of cancer. Several authors keenly alluded to the shortcomings and provided suggestions that could be incorporated in future reviews [11,12,16-18]. However, *The Hallmarks of Cancer* remain the mainstay in understanding the extraordinary molecular heterogeneity and variability embedded in the tumor microenvironment and provide a system-based rationale for targeting diverse cancers for individualized therapies [19-23].

Figure 1.1 illustrates that the hallmarks of cancer should more precisely include the stress phenotypes of cancer, including DNA damage and DNA replication stress (genomic instability, oncogene addiction and tumor suppressor gene hypersensitivity), metabolic stress, proteotoxic stress, mitotic stress and oxidative stress mechanisms to consolidate the autonomy in tumor growth factor signaling and insensitivity to growth regulation into the unified hallmark of activated growth signaling [11,24,25].

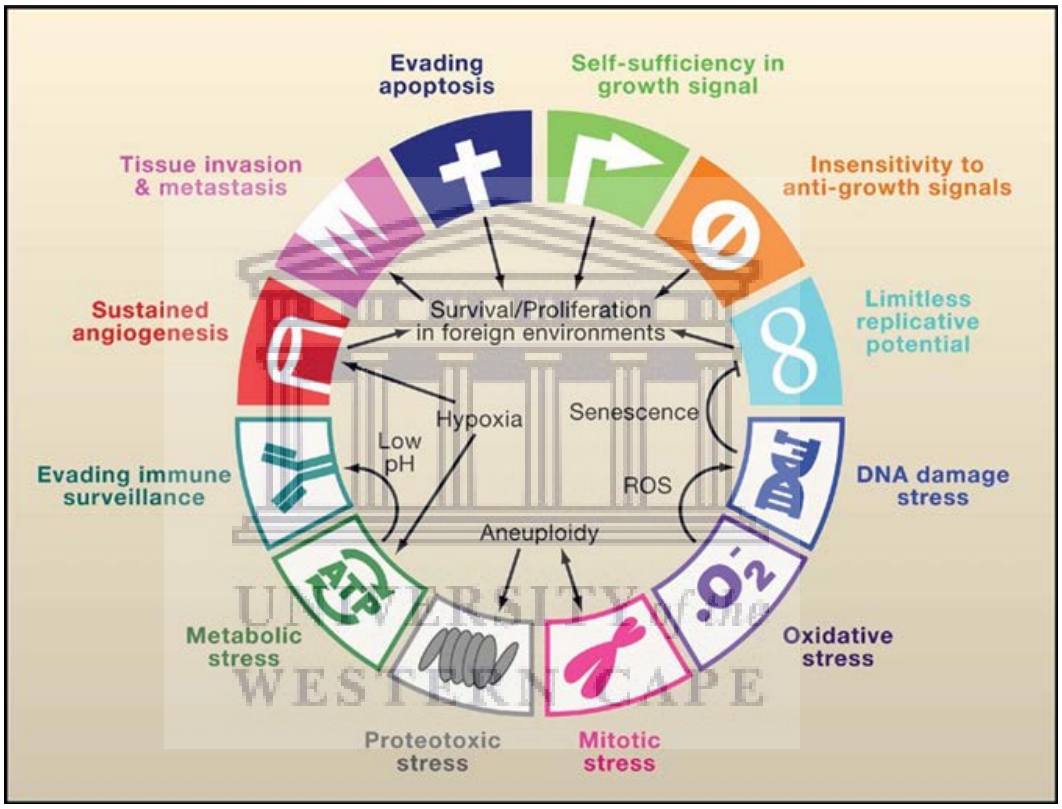

Sources: [24]: In addition to the six hallmarks originally proposed by Hanahan and Weinberg [9] (top half, white symbols) and evasion of immune surveillance proposed by Kroemer and Pouyssegur [26], a new set of additional hallmarks depicts the stress phenotypes of cancer cells (lower half, colored symbols). These include metabolic stress, proteotoxic stress, mitotic stress, oxidative stress, and DNA damage stress. Functional interplays among these hallmarks promote the tumorigenic state and suppress oncogenic stress. For example, the utilization of glycolysis allows tumor cells to adapt to hypoxia and acidify its microenvironment to evade immune surveillance. Increased mitotic stress promotes aneuploidy, which leads to proteotoxic stress that requires compensation from the heat shock response pathway. Elevated levels of reactive oxygen species (ROS) result in increased levels of DNA damage that normally elicits senescence or apoptosis, but is overcome by tumor cells.

Figure 1.1: Proposed revision of the hallmarks of cancer to include genomic instability, and to consolidate the self-sufficiency in growth signals and insensitivity to anti-growth signals into the single hallmark of activated growth signaling.

Since this study focuses on the effects of various combinations of different classes of anticancer drugs and tyrosine kinase inhibitors (TKIs) on the human MCF-7 and triple-negative MDA-MB 231 breast carcinoma cell lines, a degree of objectivity in this thesis will be maintained insofar as the importance and relevance of specific breast cancer hallmarks and oncogenic determinants are concerned [21,27-35].

A.2 Epidemiology, Etiology and Prevention of Breast Cancer

Epidemiological studies have been invaluable in enhancing our understanding of the pathogenesis of cancer, i.e., surveying global trends and identifying cancer prevention strategies [36-39]. In 1981, an epidemiological study by Richard Doll and Richard Peto [40], described cancer as a disease that can be avoided, in an attempt to prevent its onset (initiation), progression (proliferation) and hematogenous spread (metastasis). This notion followed the understanding of a World Health Organization (WHO) expert committee in 1964 who were of the opinion that environmental factors are responsible for the majority of cancer cases and, as such, can be avoided in an attempt to prevent the onset of cancer [41].

The epidemiological study of 1981 broadly categorized and associated specific types of cancers with their causes based on the literature available at the time, such as the association of tobacco smoking with the incidence of lung cancer. The study also looked at migration patterns of specific ethnic groups in which a certain type of cancer would be more prevalent in a particular region of the world, such as the incidence rates of oral cancer in Indians and how migration to Fiji and South Africa significantly reduced their high risk of developing oral cancer. The major factors that were listed as avoidable factors were environmental (extrinsic) factors that included tobacco smoking, alcohol usage, dietary intake, reproductive factors (hormonal imbalance) as modifiable factors and, to a lesser extent, occupational hazards (exposure to

chemicals) and pollution [40]. One limitation of this classic epidemiological study was that it did not focus on intrinsic factors such as the tumor microenvironment (TME) and genetic mutations or aberrations that are typically associated with cancer [42-46]. However, epidemiological studies have contributed significantly to identifying links between lifestyle factors and the risks of developing cancer which could be confirmed by laboratory investigations [47-51]. This includes the association of the tobacco smoking with the development of lung cancer which were directly involved in the establishment of prevention strategies of tobacco use in the United States of America (USA), as well as the link between obesity and physical inactivity with development of postmenopausal breast cancer, and prostate and pancreatic cancer [47].

Despite all this knowledge and the major advances in cancer prevention over the last 30 years, the global cancer burden persists and cancer remains the leading cause of mortality in women in both developed and developing countries [52]. In recent years, there has been a dramatic shift in the prevalence of certain cancers. Cancers with a high incidence in predominantly developed countries have become more prevalent in developing countries. This trend is due to the increase in risk factors such as smoking, obesity and physical inactivity and reproductive factors that are directly linked to the increase in population size over the years as well delay in early diagnosis and access to treatment [52].

Approximately 19% of all cancers are caused by tobacco smoking, which can be prevented [53-58]. Likewise, cancers (e.g., lung, breast, cervical, oropharyngeal, liver and colorectal) that are caused by viruses such as human papilloma virus (HPV) [53,59,60] and hepatitis B (HBV) [61-63] or hepatitis C (HBC) [64] may be prevented by vaccination [2,65,66]. However, innovative multimodal approaches to epidemiological studies are still needed, specifically at the spectrum of early diagnosis

and treatment where biomarkers and environmental, lifestyle and nutritional indicators that are associated with tumorigenesis and cancer progression, and responses to paradigmatic cancer therapeutics and customized interventions may be validated in specific population groups [36,48,51,65,67-76].

Globally, cancer is the second major cause of death after cardiovascular disease, and breast cancer is the leading cancer among women [39,77,78]. A recent Global Burden of Disease (GBD) Cancer Collaboration systematic analysis showed that the principal cause of cancer deaths and disability-adjusted life-years (DALYs) was tracheal, bronchus, and lung cancer (1.2 million deaths and 25.4 million DALYs). By comparison, in women, the predominant cancer and the leading cause of cancer deaths and DALYs was breast cancer (1.7 million incident cases, 535 000 deaths, and 14.9 million DALYs) [77].

Worldwide, 1 in 20 women will develop breast cancer over a lifetime and the odds of developing breast cancer is highest in high socioeconomic status or sociodemographic index (SDI)[1] countries (1 in 10), and the lowest in low SDI countries (1 in 50). It is not surprising that for women, breast cancer was found to be the most common cancer in 131 countries and the most common cause of cancer deaths in 112 countries [79].

Currently, GLOBOCAN (Global Cancer Observatory 2018) and the WHO International Agency for Research on Cancer (IARC) estimated that by 2018, 18.1 million new cancer cases and 9.6 million cancer deaths will be registered [80]. In both sexes combined, the incidences of lung and breast cancer are similar, i.e., 11.6% of the total

[1] The SDI (socioeconomic status) is a composite indicator, including fertility, education, and income, and it has been shown to correlate well with health outcomes.

cases most commonly diagnosed, whereas, of the 10 most common newly-diagnosed cancers, the mortality rate for breast cancer (6.6% of 9.6 million cancer deaths) is only eclipsed by that of lung cancer (18.4% of 9.6 million cancer deaths, Figure 1.2). Global research trends have confirmed that breast cancer (BRCA) remains the most frequent type of cancer (Figure 1.3) diagnosed in females, in addition to being the leading cause of death amongst females in underdeveloped countries [81,82].

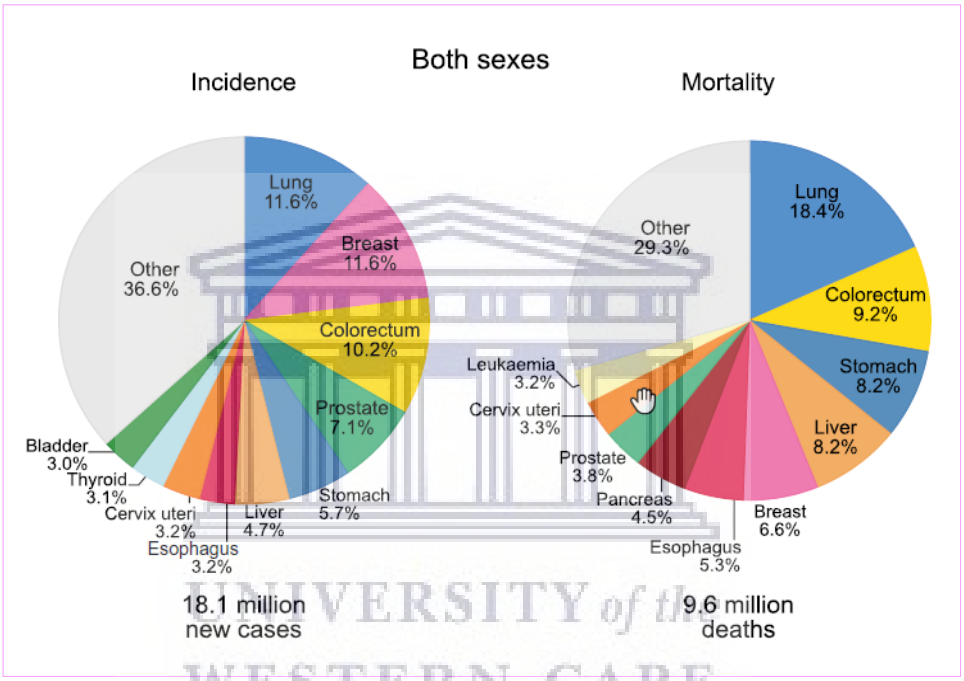

Source: IARC Globocan [80]

Figure 1.2: Globocan incidence and mortality rates for the most common cancers in 2018 for both sexes

Recent incidence data compiled by population-based cancer registries (PBCRs) and published in *Volume XI of the International Association of Cancer Registries' (IACR's) Cancer Incidence in Five Continents* indicate that cancer is a growing health problem in Africa because of ageing and population upsurge, as well as heightened risk due to changing prevalence of risk factors associated with social and economic transition (including smoking, alcohol, obesity, physical inactivity, and reproductive behaviors).

The number of new cancer cases will more than double between 2018 and 2040, faster than any other region of the world—simply because of demographic changes such as urbanization and associated changes in lifestyles [78,80,83].

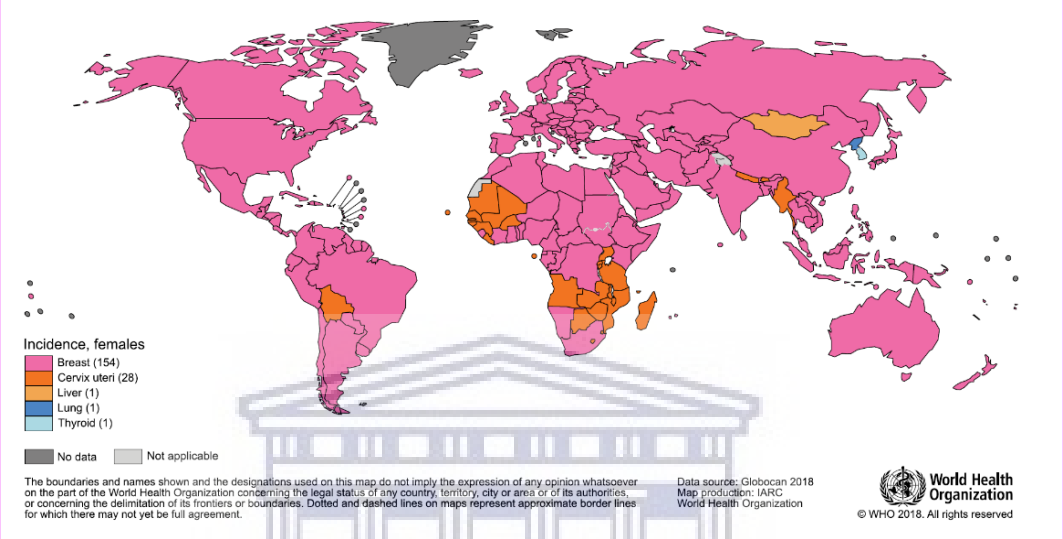

Source: IARC Globocan [78]

Figure 1.3:Rank of female cancers surveyed by country, 2018

Moreover, the last two decades, breast cancer incidence rates have increased steadily in developed and transitioning countries such as South America, Africa and Asia [78,84], most likely due to a plethora of global demographic factors linked to social and economic development, including the postponement of childbearing and having fewer children, greater levels of obesity (high body mass index and physical inactivity) [85], increases in breast cancer screening and awareness, and a waning in the use of postmenopausal hormonal treatment often linked to increased breast cancer risk [85-89]. Well-established risk factors for breast cancer as evidenced by epidemiologic/demographic studies include race/ethnicity [90-95], gender [96,97], family history of cancer and genetic traits [97-102], as well as modifiable exposures

[103] such as increased alcohol consumption [104,105], physical inactivity, exogenous hormones/contraceptives [106], marital status [107], certain female reproductive factors and women living with HIV/AIDS (WLWHA) [108]. Interestingly, younger age at menarche, parity and older age at first full-term pregnancy may also influence breast cancer risk through long-term effects on sex hormone levels or by other pathophysiological mechanisms [109].

Recent studies have suggested that triple negative breast cancer (TNBC) may have a distinct etiology [110-113]. Genetic variants and mutations in genes that code for proteins regulating DNA repair pathways and the homologous recombination of DNA double stranded breaks (APEX1, BRCA1, BRCA2, XRCC2, XRCC3, ATM, CHEK2, PALB2, RAD51, XPD) have been implicated in some cases of breast cancer [109].

Based on the latest global breast cancer incidence and mortality rates, it seems likely that primary risk factors for breast cancer are not easily modifiable because they stem from prolonged endogenous hormonal exposures (e.g., oral contraceptives and extended, current or recent use of hormone replacement therapy), even though risk factor awareness and the promotion of breastfeeding may prove beneficial [114-118]. South African breast cancer incidence trends are consistent with global trends, demonstrating a steady increase from 39 per 100 000 in 2012 to 46 per 100 000 in 2018 [80,119].

A.3 Pathology of Breast Cancer

A.3.1 Molecular Pathogenesis of Breast Cancer

In Section A.2, it was noted that several non-hereditary factors have been implicated in the etiology of human breast cancer and the prospects for their prevention remain challenging [120].

Recent evidence support the notion that the development of breast cancer may be influenced by the intrauterine environment, exposures during adolescence, and pregnancy that has a bi-directional impact on breast cancer risk, viz., an early increase followed by long-term protection [121].

Several plausible models have been proposed that breast cancer stem cells (BCSCs) most likely give rise to tumor progression, spreading and resistance to conventional therapies [46,122-128].

Figure 1.4 illustrates the breast structure, risk factors and stages of cancer development, whereas models of BCSC formation are depicted in Figure 1.5.

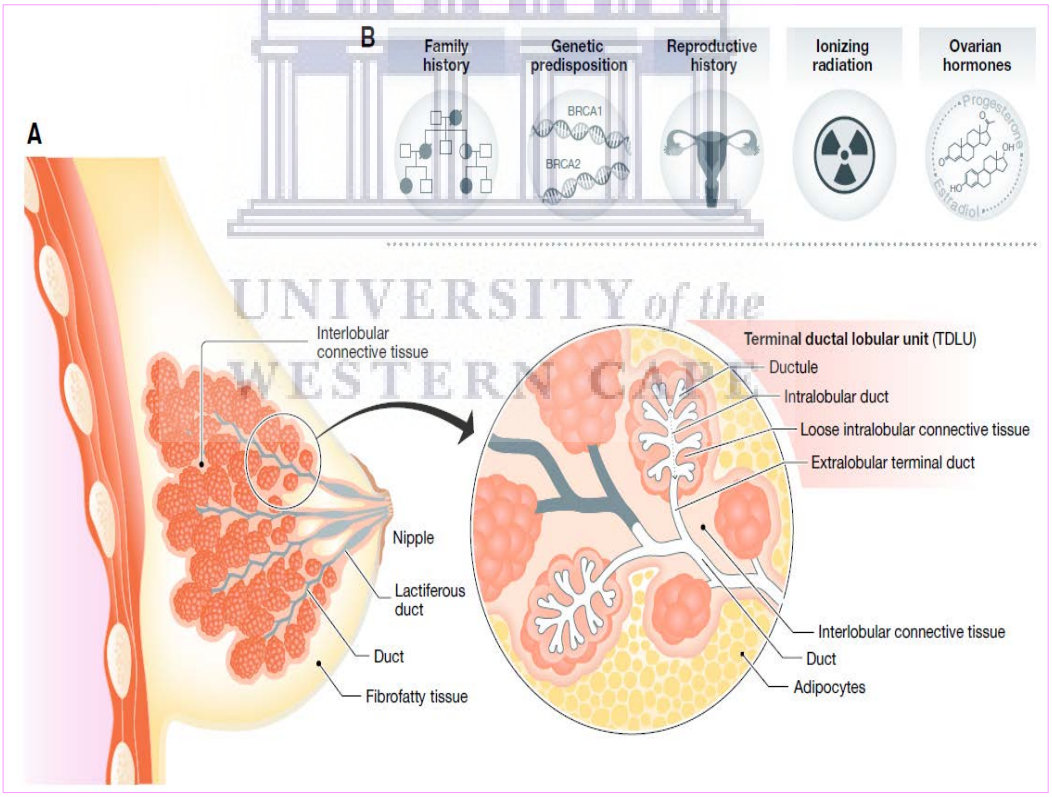

Source: [122]. **(A)** Schematic of the human breast highlighting terminal ductal lobular units (TDLUs), the site of origin in a number of breast cancers. **(B)** Some of the major risk factors underlying high-risk status for breast cancer.

Figure 1.4: The breast: structure, risk factors and stages of cancer development

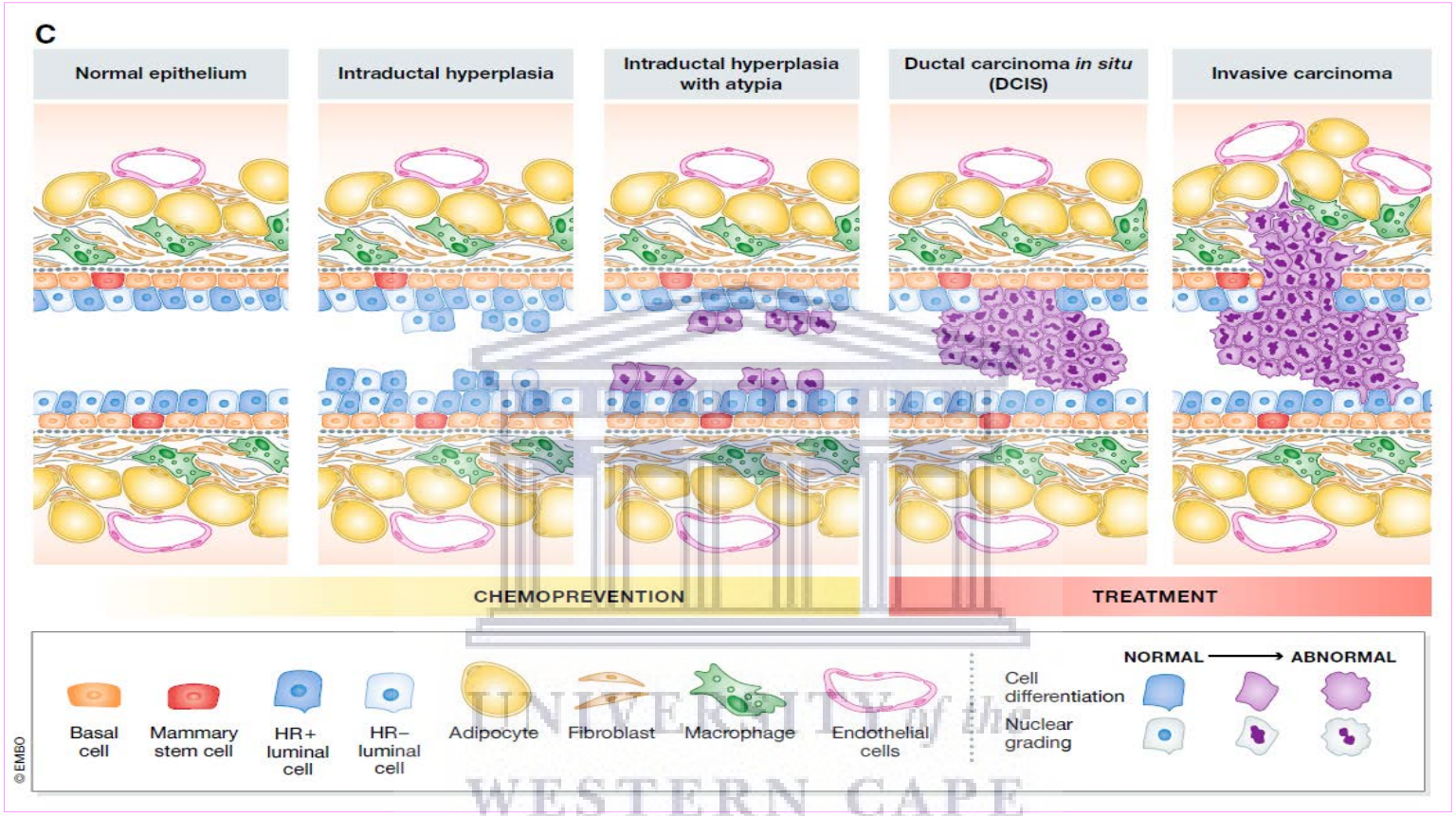

(C) Schematic of a ductal cross-section, depicting the progression of breast cancer from normal bi-layered epithelium to hyperplasia, to hyperplasia with atypia, to ductal carcinoma in situ, and finally to invasive disease.

Figure 1.4: The breast: structure, risk factors and stages of cancer development (*continued)*

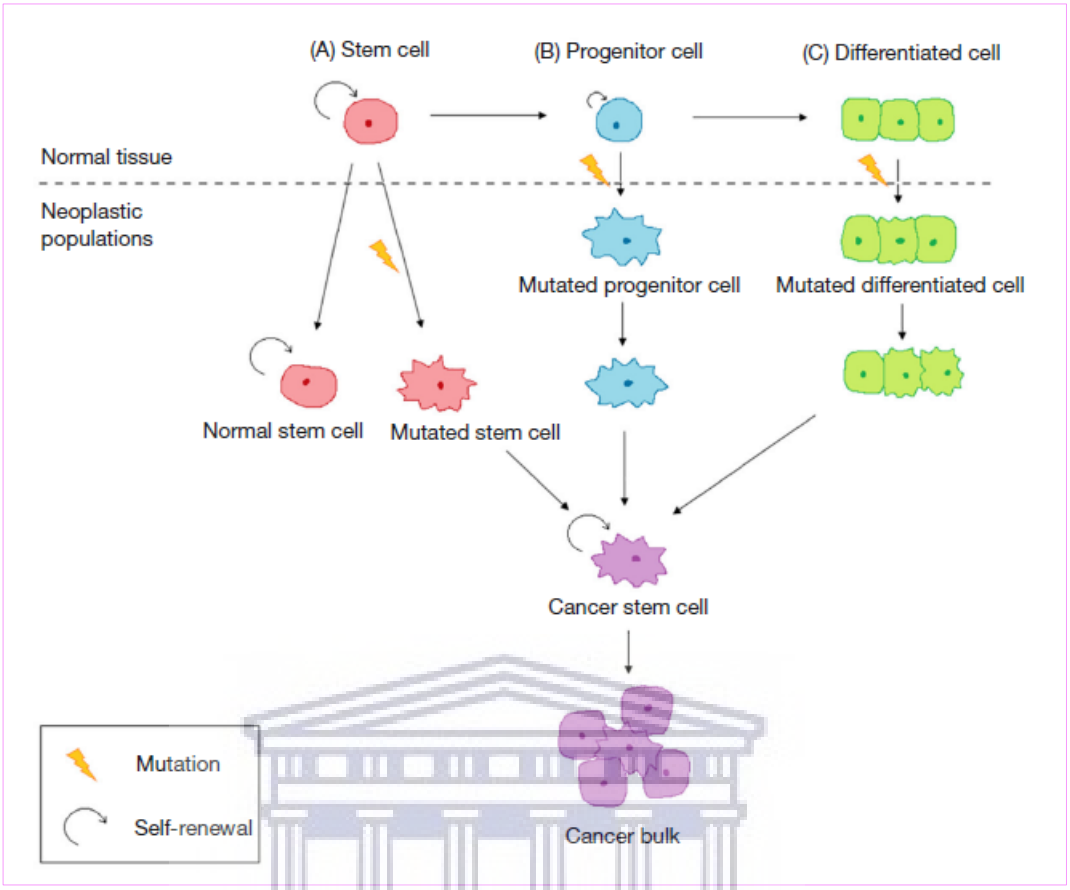

Source: [129]. **(A)** Model 1: Breast cancer stem cells (BCSCs) originate from mammary stem cells. Several effective mutations that occurred during the quiescent state of stem cells initiate oncogenic transformation; **(B)** Model 2: BCSCs originate from mammary progenitor cells. Accumulation of multiple mutations at the level of transient amplifying progenitor cell leads to transformation and initiate malignancy; **(C)** Model 3: BCSCs originate from differentiated mammary cells. Differentiated cells are de-differentiated to re-acquire stem-cell properties.

Figure 1.5: Models of breast cancer stem cell (BCSC) formation

Great variation exists in the anatomical and physiological development of the breast ductal system already in the newborn and, by inference, in utero, while pregnancy induces permanent structural changes in the mammary gland. It has been suggested that these developmental alterations be fitted into an etiological model with the following key components:

- **Breast cancer risk** correlates with the number of cells at risk, the susceptibility of individual cells to oncogenic/tumorigenic transformation, and on the rate of cellular proliferation, especially cells which act as founders of breast cancer;

- **The number of target cells** is controlled by the hormonal system principally early in life, conceivably in utero;

- **In adult life**, non-genotoxic hormones increase breast cancer risk by promoting selective cell proliferation and thus the population of target cells and the risk of retention of canonical somatic mutations;

- **Pregnancy** promotes the expansion of resident malignant cells or cells close to malignant transformation in the breast tissue milieu (and potentially engenders some short-term risk increase)—the dominating long-term protection occurs due to irreversible architectural breast tissue changes, terminal differentiation and presumably arrest of cellular proliferation [121].

These components have recently been conceptualized as the developmental windows of breast cancer risk that provide vistas for targeted chemoprevention [120] as depicted in Figure 1.6.

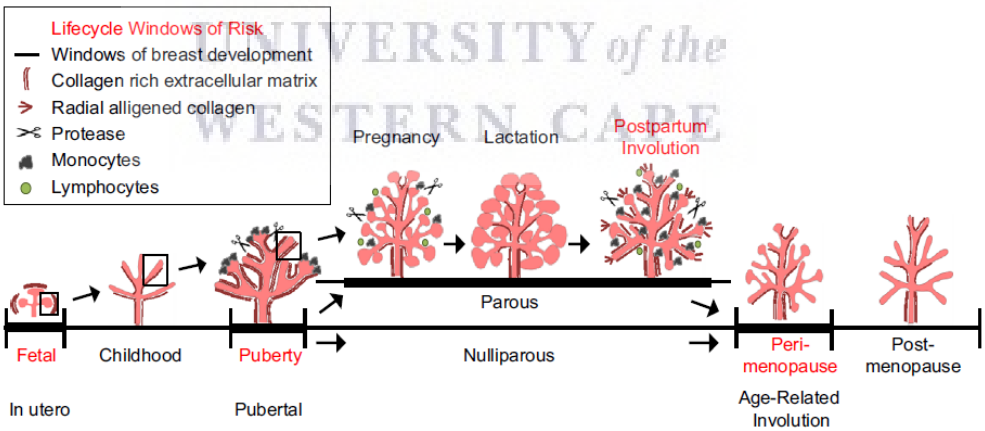

Source: [120]. Schematic presentation of the life cycle of breast development in women. The pregnancy, lactation, and involution cycle of the breast is offset to distinguish parous from women who have never been pregnant (nulliparous). The four windows of cancer vulnerability are defined by red text: fetal, puberty, postpartum involution, and age-related involution.

Figure 1.6:Life cycle windows of risk for breast cancer

According to the developmental windows of breast cancer risk concept, the 'lifecycle' of the breast can be divided into five windows of cancer vulnerability: in utero, pubertal, pregnancy, postpartum involution and age-related involution [120]. Hence, weighing these 'lifecycle windows' of risk together with known risk factor assessments, possibly in conjunction with genetic analysis of breast cancer susceptibility loci, may assist in overcoming several barriers that limit breast cancer prevention and successful treatment outcome in high risk cohorts.

It is widely recognized that specific genes are associated with an elevated lifetime incidence risk of breast cancer, and the molecular mechanisms that drive breast tumor formation are rapidly being delineated [130-136]. Cancer is driven by numerous genetic (chromosomal) and epigenetic alterations that trigger pathological changes that define the tumor phenotype [20,137]. These hallmark adaptations display disease heterogeneity and prospective anticancer therapeutic targets [20,21,138]. Recent advances in genomics and proteomics, together with the advent of genome-wide sequencing, including COSMIC, the Catalogue of Somatic Mutations in Cancer (https://cancer.sanger.ac.uk) [139], Mutational Signatures in Cancer (MuSiCa) [140], Pan-Cancer Analysis of Whole Genomes (PCAWG) Consortium of the International Cancer Genome Consortium (ICGC) and The Cancer Genome Atlas (TCGA), have enhanced systematic online documentation of genetic variation of cancers on a global scale [140-144]. Figure 1.7 represents a panoramic glimpse of driver mutations in more than 2,500 tumors, including breast adenocarcinoma, of PCAWG accessed and analysed from the ICGC/TCGA PCAWG Consortium (http://docs.icgc.org/pcawg) [141]. Likewise, CancerGeneNet (https://signor.uniroma2.it/CancerGeneNet/) is a resource that links genes that are frequently mutated in cancers to cancer phenotypes [20]. CancerGeneNet links proteins whose activities are triggered by cancer drivers to proteins that impact on the hallmarks of cancer.

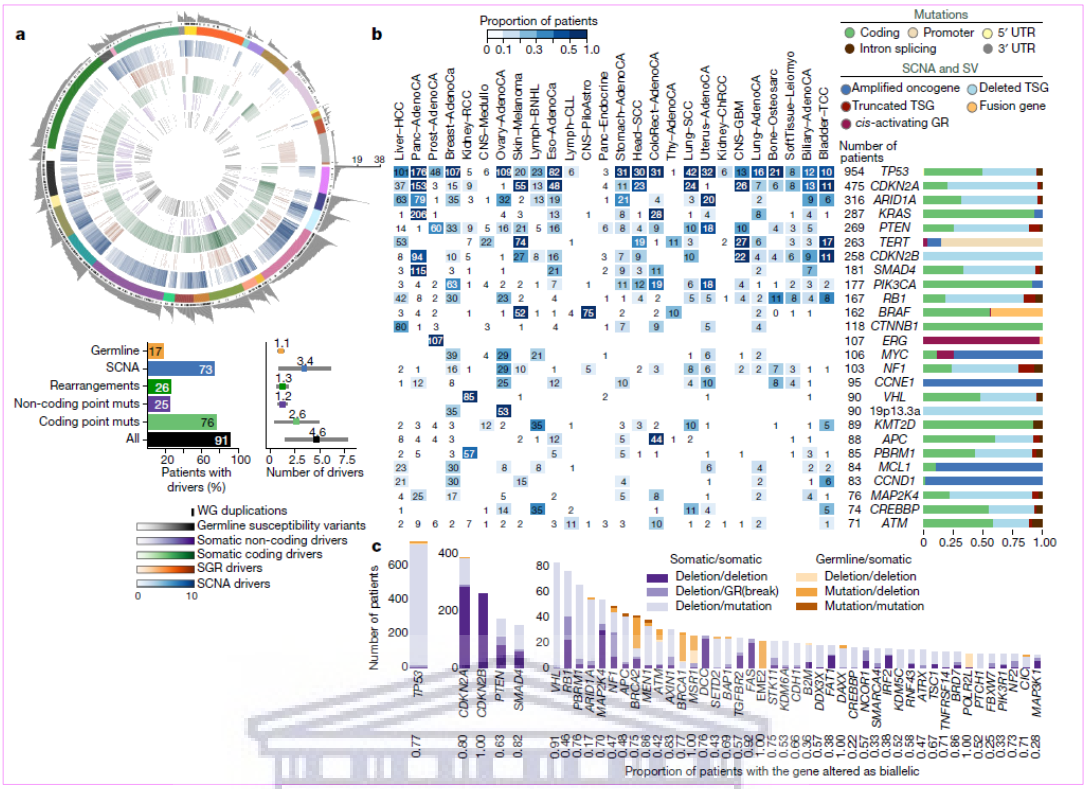

Source: [141]; **Panorama of driver mutations in PCAWG**. **a,** Top, putative driver mutations in PCAWG, represented as a circos plot. Each sector represents a tumor in the cohort. From the periphery to the centre of the plot the concentric rings represent: (1) the total number of driver alterations; (2) the presence of whole-genome (WG) duplication; (3) the tumor type; (4) the number of driver CNAs; (5) the number of driver genomic rearrangements; (6) driver coding point mutations; (7) driver non-coding point mutations; and (8) pathogenic germline variants. Bottom, snapshots of the panorama of driver mutations. The horizontal bar plot (left) represents the proportion of patients with different types of drivers. The dot plot (right) represents the mean number of each type of driver mutation across tumors with at least one event (the square dot) and the standard deviation (grey whiskers), based on n = 2,583 patients. **b,** Genomic elements targeted by different types of mutations in the cohort altered in more than 65 tumors. Both germline and somatic variants are included. Left, the heat map shows the recurrence of alterations across cancer types. The colour indicates the proportion of mutated tumors and the number indicates the absolute count of mutated tumors. Right, the proportion of each type of alteration that affects each genomic element. **c,** Tumor-suppressor genes with biallelic inactivation in 10 or more patients. The values included under the gene labels represent the proportions of patients who have biallelic mutations in the gene out of all patients with a somatic mutation in that gene. GR, genomic rearrangement; SCNA, somatic copy-number alteration; SGR, somatic genome rearrangement; TSG, tumor suppressor gene; UTR, untranslated region. Pan-Cancer Analysis of Whole Genomes (PCAWG); Consortium of the International Cancer Genome Consortium (ICGC); The Cancer Genome Atlas (TCGA)

Figure 1.7:Integrative analysis of 2,658 whole-cancer genomes and their matching normal tissues across 38 tumor types from the PCAWG Consortium of the ICGC and TCGA

Breast cancer is a complex disease encompassing multiple oncogenic signatures, distinct morphologies, behaviors and clinical correlations [30]. In addition to the estrogen receptor (ER), progesterone receptor (PR) and the human epidermal growth factor receptor 2 (EGFR-2, HER2, ERBB2), novel predictive and prognostic

biomarkers have further mystified our insight into the variability of such cancers. Nonetheless, the dominant hallmarks (biomarkers) that drive inter- and intra-breast cancer heterogeneity present new perspectives in the breast cancer landscape encompassing differential diagnosis, treatment, prognosis and management [136,145]. Table 1.1 summarizes key hallmarks that drive breast cancer heterogeneity with a focus on commonly identified biomarkers and the associated molecular subtypes.

A.3.2 Breast Cancer Classification, Staging and Molecular Subtypes

Breast cancer is generally regarded as a highly heterogeneous disease presenting with distinct phenotypic and morphologic traits, and an expanding number of diagnosable molecular or biological subtypes that correlate with clinical prognosis [128,134,146-151]. Breast cancer is categorized into three basic therapeutic groups, in line with their immunohistochemical (IHC) properties or hormone receptor (HR) status, viz., they are (1) HR-positive, (2) human epidermal growth factor receptor 2 positive (EGFR-2/ERBB2HER2/neu) and (3) triple-negative breast cancers (TNBC), i.e., tumors that tested negative for estrogen receptor (ER), progesterone receptor (PR) and HER2/neu. HR-positive cancers are those that are ER^+ and PR^+. The majority of breast cancers are HR^+ (85%) and are candidates for endocrine therapies such as tamoxifen and the aromatase inhibitors (AIs) anastrozole (Arimidex), letrozole (Femara), or exemestane (Aromasin) [146,147]. Breast tumors are further classified by molecular subtyping using cDNA microarrays based into four intrinsic groups, viz., ER/luminal-like (gene expression profile of luminal cells and ER), basal-like (gene expression profiles of basal epithelial cells), $ERBB2^+$ (over expression gene profile at ERBB2 locus on chromosome 17) and normal breast (high gene expression of basal epithelia and adipocyte genes and low expression of luminal epithelia genes) [134,149,152].

Table 1.1: Hallmarks that drive breast cancer heterogeneity based on diagnostic biomarkers and the associated subtypes

Cancer Hallmark	Breast Cancer Biomarkers	Clinical Characteristics and Associated Subtypes	References
Self-sufficiency in growth and survival signaling*	ER, PR, HER2/neu, AR, Ki67, Topo-IIα	These hormonal and growth receptors define basic breast tumor molecular subtypes and mediate cell growth signaling. ER-, PR- and HER2-negative tumors have relatively poorer prognosis than any of the HR-positive tumors. ER plays a pivotal role in breast carcinogenesis, and its inhibition forms the basis of breast cancer endocrine therapy. Absence of PR expression in ER+ tumors may suggest aberrant growth factor signaling that, in turn, contributes to tamoxifen resistance of such tumors. HER2-positivity is associated with relative, but not absolute resistance to endocrine therapies. Besides ER, PR and HER2, androgen receptor (AR) is used in breast cancer subtyping since it is the prevalent sex steroid hormone receptor expressed in 90% ER+ and 55% ER- tumors. AR expression inversely correlates with immune cell infiltration in HER2-positive breast cancer. KI67 is the most widely used proliferation marker in breast cancer since it is present in actively cycling cells. Positive Ki67 expression is also associated with a poor 5-year survival outcome. Aberration of Topo-IIα (TOP2A) which catalyzes the breakage and reunion of double-stranded DNA is found in 30–90% of HER2-amplified breast cancer and correlates with Ki67 as well as increased responsiveness to anthracycline-based chemotherapy.	[30,136,153-161]
Tissue invasion and metastasis*	ER, PR, HER2/neu, CK5/6, 14, 17, 8/18, EGFR, AR, Ki67, EMT genes primarily include VIM, SNAI1, SNAI2, TWIST1, TWIST2, ZEB1, ZEB2, CDH1, CLDN3 (claudin 3), CLDN4 (claudin 4), CLDN7 (claudin 7), CD44, CD24, EpCAM, CD10, CD49, CD29, MUC1, THY1 and ALDH1A1	ER-PR-HER2-tumors are clinically the most aggressive subtype of breast cancer due to lack of targeted therapies. The most rational and widely accepted definition of the basal subtype is ER-PR-HER2-, i.e., TNBC tumors with positive expression of CK5/6 and EGFR. QNBC lacking the expression of ER, PR, HER2 and AR is regarded as one breast cancer subtype with the worst prognosis because QNBC is insensitive to conventional chemotherapeutic agents and has no efficient treatment targets. The poor prognosis of TNBC is associated with the 'activating invasion and metastasis' hallmark. Stem cell markers (e.g., EMT genes) such as CD44, CD24, EpCAM, CD10, CD49, CD29, MUC1, THY1 and ALDH1A1 which confer an aggressive malignant phenotype are enriched in TNBC.	[32,162-164]
Evading immune surveillance & destruction*	ER, PR, HER2/neu, STAT1, SP110	ER-PR-HER2- tumors that overexpress interferon-regulated genes (e.g., STAT1 and SP110) constitute 10% of breast tumor cases. SP110 reportedly has prognostic value associated with activation of complement and immune response pathways.	[32,165,166]

/Continued

Table 1.1: Hallmarks that drive breast cancer heterogeneity based on diagnostic biomarkers and the associated subtypes (*continued*)

Cancer Hallmark	Breast Cancer Biomarkers	Clinical Characteristics and Associated Subtypes	References
Bypassing apoptosis (programmed cell death)	BCL2, BCSC biomarkers ($CD44^+$, CD24, ALDH1, CD49f, CD61, $CD133/2^+$)	The proto-oncogene BCL2 is a suppressor of apoptosis, i.e., an antiapoptotic protein. BLC2 is associated with several favourable prognostic features, such as low mitotic count, low S-phase fraction size, low cathepsin D expression, downregulated p53 and TNF, and a high histological grade of differentiation. Patients with $BCL2^+$ tumors have a more favourable short-term, but similar long-term breast cancer specific death as compared with those carrying BCL2- tumors. BCL2 is a clinically valid and robust prognostic marker for all types of early-stage breast cancer, independent of ER, HER2 and adjuvant therapy received and its strong correlation with hormonal receptor might contribute to the superior survival observed for $BCL2^+$ breast patients. Tumor-initiating cells drive breast cancer tumorigenesis and resistance to radiation and chemotherapy, and a reduced propensity to undergo apoptosis or senescence.	[129,167-172]
Genomic instability and mutation	TP53 (p53), Ki67, BRCA1	The tumor suppressor TP53 or p53 plays a critical role in the cellular signaling axis, controlling cell proliferation, survival, apoptosis and, most importantly, genomic integrity (it is hailed as the guardian of the genome). The expression of p53, KI67 and BRCA1 in different molecular subtypes of breast cancer (BC) are related to pathological features and are thus helpful in predicting the prognosis, diagnosis, and treatment of BC. TP53-PR tumors are associated with the worst prognosis among all breast cancers. Genome instability and mutation contributes to tumor drug resistance regardless of which BC subtype it belongs.	[30,156,173,174]
Deregulating cellular energetics	VDR, AR, ER	High levels of circulating vitamin D metabolites correlate with decreased breast cancer risk. The receptor status of VDR, AR and ER correlates with tumor differentiation state and predicts clinical outcome. BC could be quantitatively classified into 4 categories, i.e., HR3 (ER+AR+VDR+), HR2 (ER+AR+, AR+VDR+, ER+VDR+), HR1 (ER+, VDR+, AR+), and HR0 (ER-AR-VDR-), with HR3 tumors being associated with the best survival and HR1 and HR0 tumors the most aggressive.	[175-179]

Adapted from [30]. *Markers representing these three cancer hallmarks contribute to the current breast tumor classification [30]. IHC, Immunohistochemistry; HR, hormone receptor; ER, estrogen receptor; PR, progesterone receptor; HER2, human epidermal growth factor receptor 2 (HER2); AR, androgen receptor; CK, cytokeratins; EGFR, epidermal growth factor receptor; VDR, vitamin D receptor; TNBC, triple-negative breast cancer; QNBC, quadruple negative breast cancer; Topo-IIα (TOP2A), topoisomerase II alpha; EMT, epithelial to mesenchymal transition; BCSC, breast cancer stem cell.

Expansion of the luminal-like group into two luminal subgroups, Luminal A and Luminal B is based on the expression of luminal genes [146,180]. Luminal A tumors tend to be ER^+ and/or PR^+ and $HER2^-$ with low Ki67 proliferative genes, whereas Luminal B tend to be ER^+ and/or PR^+ and $HER2^+$ with high Ki67 proliferative genes. Luminal A is considered the subtype with best prognosis, whereas Luminal B is the more aggressive subtype [181]. Basal-like tumors lack ER, PR and HER2 expression, but express cytokeratins 5, 6 and 17, and are also referred to as TNBC. ERBB2 tumors overexpress HER2, but can be ER^- and PR^- or ER^+ or PR^+, or both [90,146,152,180,182]. Normal breast-like tumors, expressed one fibroadenoma containing three normal breast specimens in the study of *Molecular Portraits of Human Breast Tumors* [149]. The heterogeneity of these subtypes is not limited to its classification, but also in their prognosis and chemotherapeutic responses.

Breast cancer thus represents a diverse group of diseases encompassing several biological subtypes that have distinct behaviors and responses to therapy [123]. Genomic profiling studies have identified several intrinsic genes that differentiate these subtypes according to clusters of genes relating to estrogen receptor (ER) expression (the luminal cluster), human epidermal growth factor 2 (HER2) expression, proliferation, and a distinctive cluster of genes called the basal cluster [183-185].

Breast cancers are typically divided into five intrinsic or molecular subtypes that are based on the expression pattern of certain genes that have both biologic and clinical relevance (Table 1.2)[123]. Furthermore, histological classification entails grading based on tumor appearance and then staging based on tumor size and invasion of the chest wall, the number of lymph nodes involved and finally the presence or absence of metastasis.

Table 1.2: Molecular/intrinsic subtypes of breast cancers

Subtypes	Molecular Signatures	Characteristics	Treatment options[a]
Luminal A	ER+, PR±, HER2-, Low Ki67	~70%, Most common Best prognosis	Hormonal Therapy Targeted Therapy
Luminal B	ER+, PR±, HER2±, High Ki67	10%–20% Lower survival than Luminal A	Hormonal Therapy Targeted Therapy
HER2	ER-, PR-, HER2+	5%–15%	Targeted Therapy
Triple Negative	ER-, PR-, HER2-	15%–20% More common in black women Diagnosed at younger age Worst prognosis	Limited Targeted Therapy
Normal-like	ER+, PR±, HER2-, Low Ki67	Rare Low proliferation gene cluster expression	Hormonal Therapy Targeted Therapy

[a] Besides conventional surgical and non-surgical treatment.

Adapted from [123]

This is followed by a stage assignment according to the conventional tumor, node, metastasis (TNM) staging system as depicted in Table 1.3 [151,181,186], even though diagnosis hinges on more complex hierarchical histological or cytological assessment since a breast cancer specimen inevitably represents a combination of different cell types in a single breast tumor [95,123,187-189]. The first two stages classify early stage and the latter two the late stage of diagnosis. The type of anticancer treatment plan is determined by this TNM staging system [147,190,191]. The clinical staging of breast cancer is undifferentiated across breast cancer subtypes according to the American Joint Committee on Cancer (AJCC) and the International Union for Cancer Control (UICC) Tumor, Node, and Metastasis (TNM) Breast Cancer Staging System, viz., Stage 0, Stage I, Stage II, Stage III and Stage IV, as itemized in Table 1.4 [123].

Table 1.3: TNM staging system for breast cancer

Stage	Tumor description
T1	Tumor less than 2 cm in diameter
T2	Tumor 2–5 cm in diameter
T3	Tumor more than 5 cm
T4	Tumor of any size with direct extension to chest wall or skin
N0	No palpable node involvement
N1	Mobile ipsilateral node(s)
N2	Fixed ipsilateral nodes
N3	Supraclavicular or infraclavicular nodes or edema of arm
M0	No distant metastases
M1	Distant metastases

Adapted from [1]

Table 1.4: Anatomic stage groups of breast cancer

Stages		Definition
Stage 0		Ductal Carcinoma In Situ
Stage I	IA	Primary invasive tumor with a size of ≤20 mm No nodal involvement
	IB	Nodal micrometastases (>0.2 mm, <2.0 mm) with or without ≤ 20 mm primary tumor
Stage II	IIA	Movable ipsilateral Level I, II lymph node metastases with ≤20 mm primary tumor; Or > 20 mm, ≤ 50 mm tumor with no nodal involvement
	IIB	Movable ipsilateral Level I, II lymph node metastases with >20 mm, ≤ 50 mm tumor; Or > 50 mm tumor with no nodal involvement
Stage III	IIIA	Movable ipsilateral Level I, II lymph node metastases with >50 mm tumor; Or any size primary tumor with fixed ipsilateral Level I, II or internal lymph node metastases
	IIIB	Primary tumor with chest wall and/or skin invasion
	IIIC	Any size primary tumor with supraclavicular or ipsilateral Level III lymph node metastases; Or with ipsilateral Level I, II and internal lymph node metastases
Stage IV		Any case with distant organ metastasis

Notes: 1). Lobular carcinoma in situ is now considered benign thus removed from the breast cancer staging system.
2). The Anatomic Stage Group is to be used when biomarker tests are not available.
Source: AJCC Cancer Staging Manual, Eighth Edition, The American College of Surgeons (ACS), Chicago, IL, USA. With reprint permission of ACS.

Adapted from [123]

The TNM classification of the AJCC for breast cancer has recently been revised as adjudicated by a multidisciplinary team of breast cancer experts. The panel incorporated biologic factors such as tumor grade, proliferation rate, estrogen and progesterone receptor expression, human epidermal growth factor 2 (HER2) expression, and gene expression prognostic panels into the staging system. AJCC levels of evidence and guidelines for all tumor types were followed as much as possible. The panel felt that, to sustain universal merit, the tumor staging system should remain based on TNM anatomic factors. However, the recognition of the prognostic influence of grade, hormone receptor expression, and HER2 amplification mandated their inclusion into the staging system [187,192]. In spite of this, to date, the prognostic staging system did not provide better discriminatory power in predicting TNBCs prognosis than the AJCC anatomic staging system [193].

A.3.3 Triple Negative Breast Cancer (TNBC)

Triple-negative breast cancer (TNBC) makes up 15% of the total number of breast cancer cases diagnosed worldwide. TNBC is a complex disease, because this type of breast cancer does not overexpress receptors, which makes targeted therapies exceedingly difficult. In the clinical setting, TNBC is treated with a combination of surgery, radiotherapy, and chemotherapy. TNBCs have by far the worst prognosis because of the lack of targeted treatments and a higher chance of recurrence [146]. The diverse molecular heterogeneity of TNBC is one of the most important determinants of the success of any treatment strategy and as such also the development of resistance. Recently, six subtypes of TNBC, viz., luminal androgen receptor (LAR), mesenchymal (M) and mesenchymal stem-like (MSL), immunomodulatory (IM) and two basal like subtypes (BL1 and BL2) have been identified [194]. In a follow-up study, the two subtypes, namely, IM and MSL were removed as they were not representative of the TNBC biology, based on

histopathological quantification and laser-capture microdissection. Therefore, the TNBC subtypes have been refined to four groups, viz., BL1, BL2, LAR and M [195,196]. This further highlights the heterogeneity of TNBC, each subtype with a distinct presentation, behaviour, pathology and response to treatment [197]. Various research groups [194,195,198,199] have applied genomic expression profile (GEP) assays for molecular characterization of TNBC subgroups to categorize their observed "molecular fingerprints". Figure 1.8 summarizes the intersections between the proposed subclassification groups.

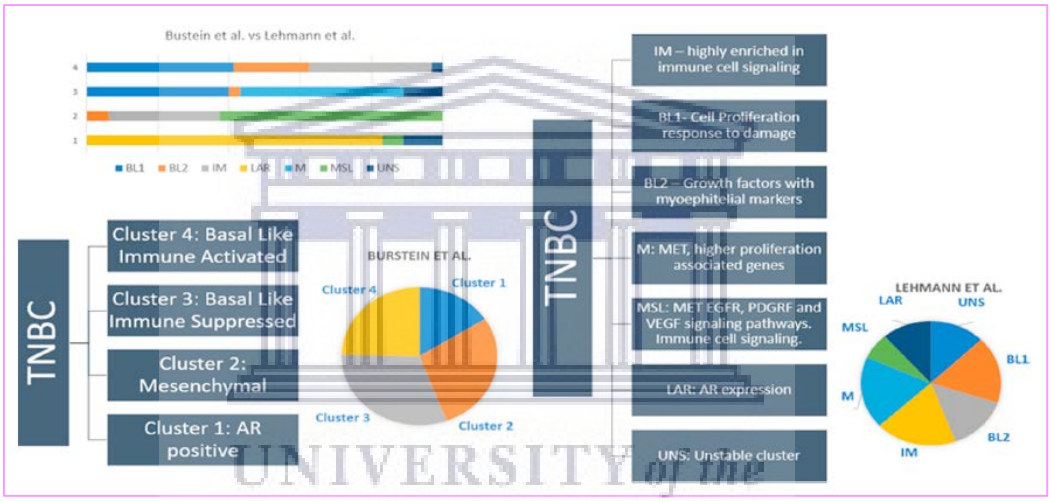

Source: [200]. Intersections of the subclassifications of Burstein et al. and Lehmann et al. Lehmann et al. in 2011 proposed a division of TNBCs into 7 molecular subtypes: immunomodulatory (IM), mesenchymal (NI), mesenchymal stem-like (MSL): luminal androgen receptor (LAIR.). unstable (UNS) subtype and two basal-like subtypes (BL1 and BL2). in 2015: Burstein et al. used DNA profiling to identify TNBC subtypes: Cluster 1: luminal AR (AI), cluster 2: mesenchymal (MES), cluster 3: basal-like immunosuppressed (BLIS), and cluster 4: basal-like immune-activated (B LIA).Comparing the two classifications, cluster 1 contains all of Lehmann's LAR tumors and cluster 2 contains most of Lehmann's mesenchymal stem—like. Lehmann's basal-like 1 and basal-like 2 tumors are split between clusters 3 and 4, mesenchymal tumors reside in cluster 3, whereas the immunomodulatory tumors are distributed across clusters 2 and 4: which express common signaling pathways.

Figure 1.8: Intersections of the subclassifications of TNBCs

It is also widely recognized that microRNAs (miRNAs/miRs) play pivotal roles in the pathogenesis, progression and prognosis of triple-negative breast cancer (TNBC) [201-203] and luminal breast cancer [204].

TNBCs are clinically heterogeneous, but predominantly aggressive malignancies lacking expression of the estrogen, progesterone and HER2 (ERBB2/NEU) receptors. Recent studies demonstrated that basal endoplasmic reticulum stress (ERS) is constitutively activated in TNBC and converges with hypoxia-inducible factor–1α (HIF-1α) signaling to promote tumor progression and relapse—ERS and hypoxia signalling responses may thus represent novel hallmarks of TNBC and a paradigm for targeting HIF-1α and the unfolded protein response (UPR) in TNBC [32]. Similarly, observations that the TP53 mutation occurs frequently in TNBC and is correlated with a predominantly poor survival outcome [205-207] and BRCA1 promoter methylation in peripheral blood is associated with the risk of TNBC [208], may connote proof-of-concept for targeted therapy. Several reliable predictive and prognostic biomarkers in TNBC have recently been reviewed [200] and are summarized in Table 1.5.

A.3.4 Quadruple Negative Breast Cancer (QNBC)

Breast cancers which lack the expression of ER, PR, HER2 and AR are classified as quadruple negative breast cancers (QNBC) [162,209,210]. Compared to AR+ TNBC, QNBC predominantly exhibits a basal-like molecular subtype, and is regarded as one breast cancer subtype with the worst prognosis [210]. Figure 1.9 is a schematic of the current TNBC and QNBC subtyping systems based on applied probabilistic graphical models to a previously published TNBC cohort [210,211]. Since QNBC is a highly retractable to conventional chemotherapeutic agents, it lacks efficient treatment strategies and a dire need exists to elucidate targetable signal transduction pathways for this type of breast cancer. In recent years, QNBC has been shown to express unique proteins, including ACSL4, SKP2, immune checkpoint inhibitors, EGFR, microRNA signatures and Engrailed 1 that may be exploited for the potential development of targeted therapies [162].

Table 1.5: Predictive and prognostic biomarkers in TNBC

Molecular Biomarker	% of TNBC with expression/mutations	Main Function	Prognostic significance	Targeted therapies	References
TP53 gene	75–80% (somatic mutations)	Apoptosis	Low gene expression in TP53 missense mutations correlate with poor prognosis (worst DFS, but conflicting data).	NA	Kim et al., 2016; Synnott et al., 2017
Ki-67	45–53% (high expression, >20%)	Cell proliferation	High index and high expression correlate with shorter DFS and OS.	NA	Wang et al., 2016a, 2016b; Ilie et al., 2018
EGFR	13–78%	Cellular growth	Increased expression associates with worst DFS.	Erlotinib, gefitinib, afatinib	Gumuskaya et al., 2016; Gluz et al., 2009; Porta et al., 2014
c-KIT	50%	Cell transformation and differentiation	Predictor of poor cancer-specific survival in patients with TNBC	Imatinib	Kashiwagi et al., 2013; Sørlie et al., 2001); Jansson et al., 2014
VEGF	32–62%	Angiogenesis	High levels associate with disease progression and metastasis rates.	Bevacizumab	Linderholm et al., 2009; Ali et al., 2011; El-Arab et al., 2012
Androgen receptor	10–55%	Cell proliferation and dedifferentiation	Positive expression correlates with higher DFS. May be associated with chemoresistance.	Bicalutamide, enzalutamide, abiraterone	Niemeier et al., 2010; He et al., 2012; Galal et al., 2013; Gucalp and Traina, 2016; Wang et al., 2016b
BRCA1 and BRCA2 genes	14–20 % (germline mutations)	DNA-double strand break repair	Mutated status correlates with increased DFS.	PARP inhibitors - Olaparib	Gonzalez-Ângulo et al., 2012; Loibl et al., 2018; Robson et al., 2019; Abkevich et al., 2012
PD-L1 protein	15–30%	Tumor immune evasion process	High expression correlates with a higher survival rates in trials with checkpoint inhibitors	Immune Checkpoint inhibitor —atezolizumab	Castaneda et al., 2016a,2016b; Ghebeh et al., 2006; Castaneda et al., 2016b; Beckers et al., 2016; Schalper et al., 2014
Notch pathway	~10%	Cell proliferation and differentiation	Potential target under development	AL101	Broner et al., 2019; Pineda et al., 2018
PI3-kinase pathway	~25%	Cell Proliferation	Multiple genomic alterations lead to activated PI3-Kinase pathway, including activation in PIK3CA, AKT and mTOR or inactivation in tumor suppressor genes such as PTEN.	PI3K inhibitor – alpelisib AKT Inhibitors – ipatasertib, capivasertib	Baselga, 2011; Speiser et al., 2013; Pascual and Turner, 2019; Baselga, 2011; Kim et al., 2017; Porta et al., 2014

Adapted from [200]. NA: not applicable; DFS: disease free survival; OS: overall survival. Cross-references are cited in [200].

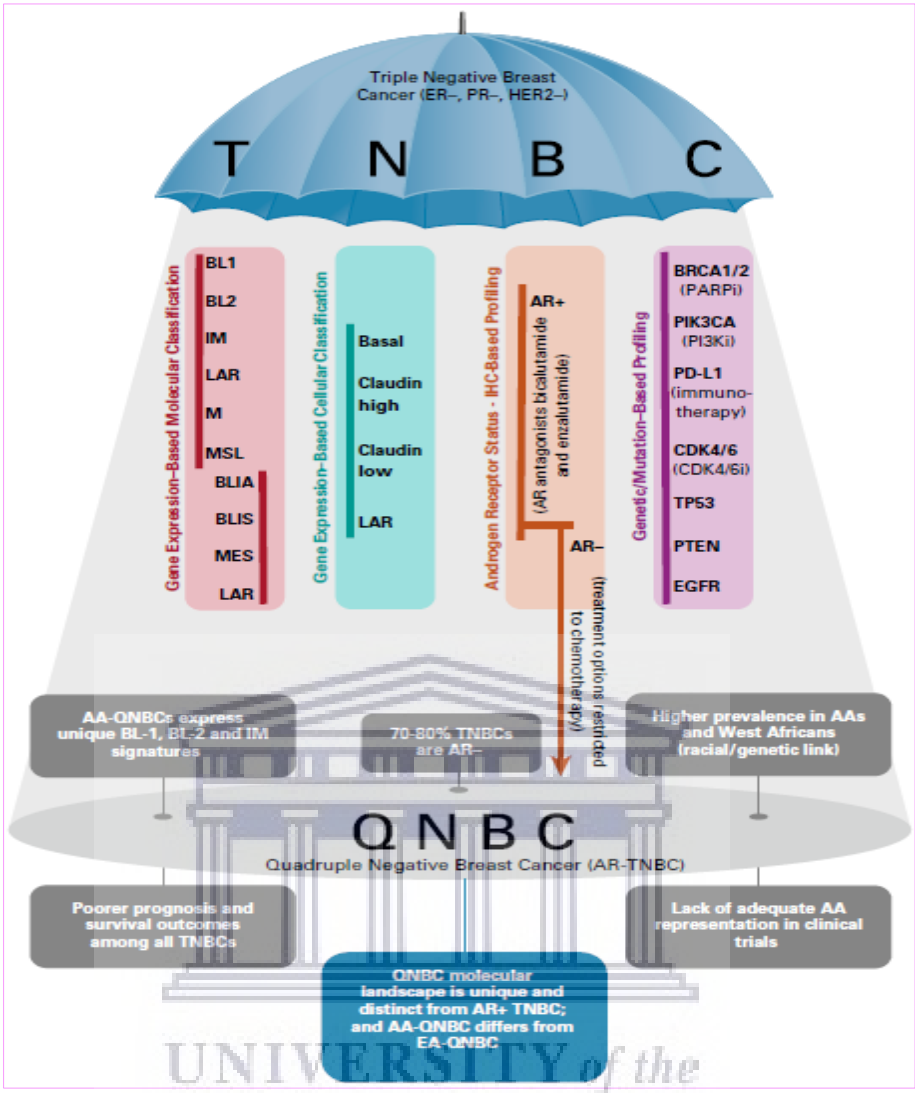

Source: [210]. Triple-negative breast cancers (TNBCs) make up a highly heterogeneous group that can be classified variously, as outlined in the long columns. Quadruple-negative breast cancer (QNBC) is clinically defined as an androgen receptor (AR)–negative TNBC and is briefly characterized in the lower half of the schematic. There is a pressing need to extricate QNBC from the shadows of TNBC and classify it as a unique, clinically relevant BC subtype. AA, African American; BL, basal-like; BLIA, basal-like immune associated; BLIS, basal-like immune suppressed; CDK4/6i, CDK4/6 inhibitors; IHC, immunohistochemistry; IM, immunomodulatory; LAR, luminal androgen receptor; M, mesenchymal; ML, mesenchymal stem-like; PARPi, PARP inhibitor; PI3Ki, PI3K inhibitor.

Figure 1.9: Comparison of TNBC and QNBC subtypes

A.3.5 Breast Cancer Molecular Evolutionary Pathways

Recent genomic and transcriptomic analyses imply that breast cancer develops and evolves along two distinct molecular evolutionary pathways, i.e., the ‘low-grade-like’ molecular pathway and a ‘high-grade-like’ molecular pathway as illustrated in Figure 1.10 [128]. At the genetic level, these two pathways are distinguished by either the

presence or absence of chromosome 1q, 16q, 13q, gain of chromosomal region 11q13 and amplification of the 17q12. In addition, these pathways positively correlate with the transcriptomic equivalent of tumor grade/proliferation.

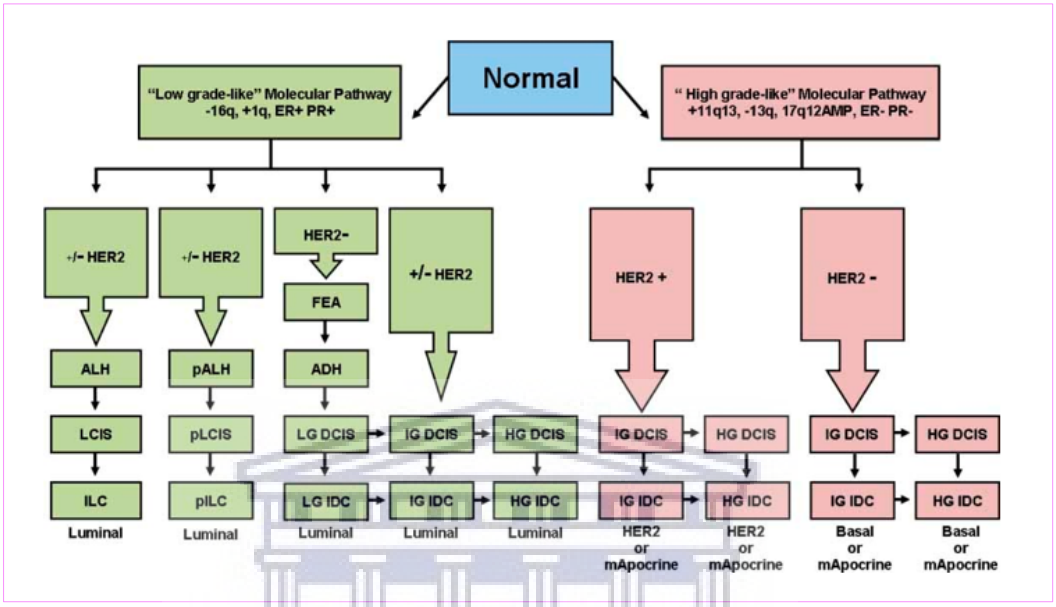

Source: [128]. Genomic and transcriptomic data in combination with morphological and immunohistochemical data stratify the majority of breast cancers into a 'low-grade-like' molecular pathway and a 'high-grade-like' molecular pathway. The low-grade-like pathway (left-hand side) is characterized by recurrent chromosomal loss of 16q, gains of 1q, a low-grade-like gene expression signature and the expression of oestrogen and progesterone receptors (ER+ and PR+). The progression (vertical arrows) along this pathway (green rectangles) culminates with the formation of low- and intermediate-grade invasive ductal (LG IDC and IG IDC) and invasive lobular carcinomas, including both the classic (ILC) and the pleomorphic (pILC) variants. The tumors arising from the low-grade pathway are classified as luminal, consisting of a continuum of gene expression frequently associated with the absence (luminal A) or presence (luminal B) of HER2 expression. The vast majority of ILCs and pILCs and their precursors cluster together within the luminal subtype. The high-grade-like gene expression molecular pathway (right-hand side) is characterized by recurrent gain of 11q13 (+11q13), loss of 13q (13q−), expression of a high-grade-like gene expression signature, amplification of 17q12 (17q12AMP), and lack of oestrogen and progesterone receptors expression (ER− and PR−). The progression along this pathway (red rectangles) includes intermediate- and high-grade ductal carcinomas that are stratified as HER2 or basal-like, depending on the expression/amplification of HER2. The molecular apocrine subtype, characterized by the lack of ER expression and presence of AR expression, arises from the high-grade pathway. The model also depicts intra-pathway tumor grade progression (horizontal arrows). ALH, atypical lobular hyperplasia; DCIS, ductal carcinoma in situ; LCIS, lobular carcinoma in situ; pALH, pleomorphic atypical lobular hyperplasia; pLCIS, pleomorphic lobular carcinoma in situ; FEA, flat epithelial atypia; ADH, atypical ductal hyperplasia; Basal, basal-like; mApocrine, molecular apocrine. ±HER2 in which the '−' sign is bold indicates that the majority of tumors in the pathway lack HER2 over-expression.

Figure 1.10: Divergent evolutionary pathways of breast cancer progression

A.3.6 Genetic Alterations and Oncogenes in Breast Cancer

It is widely accepted that hereditary predisposition to breast cancer significantly influences screening and management of high-risk women [109]. In patients with a family history of breast cancer (for a definition of 'familial' breast cancer, and generally accepted criteria, cf. National Comprehensive Cancer Network (NCCN) guidelines; https://www.nccn.org/professionals/physician_gls/pdf/genetics_bop.pdf), a specific predisposing gene is identified in <30% of cases and up to 25% of hereditary cases are due to a mutation in one of the few identified rare, but high-penetrance genes (*BRCA1, BRCA2, PTEN, TP53, CDH1*, and *STK11*), which present up to an 80% lifetime risk of breast cancer. Moderate-penetrance genes (e.g., *CHEK2, BRIP1, ATM*, and *PALB2*) account for ~2%–3% of cases due to mutations and are each associated with a twofold increase in risk [212]. Earlier prediction models suggested that additional yet-to-be-identified high-penetrance genes were unlikely to emerge [102], but intriguing candidates in the predisposition to breast and/or ovarian cancer could be incorporated in current diagnostic panels for the assessment of cancer risk [213].

BRCA1, located on chromosome 17 by linkage analysis in families with suggestive pedigrees, was the first major gene associated with hereditary breast cancer [214,215]. Thereafter, *BRCA2* was mapped to chromosome 13 [216]. Predictably, a mutation in either *BRCA1* or *BRCA2* (collectively termed as *BRCA* or *BRCA1*/2) confers an increased risk of breast and other cancers [98,217,218]. The clinical behavior seen in in *BRCA* mutation carriers is referred to as the *Hereditary Breast/Ovarian Cancer (HBOC)* syndrome, though there are patients matching clinical pictures who tested negative for mutations in both *BRCA1* and *BRCA2* [219,220]. Tumors that overexpress *BRCA1* tend to have a basal-like phenotype and a high histologic grade, and do not commonly express ER, PR, or Her2/neu, the so-called TNBC [208].

By contrast, *BRCA2*-related tumors more closely resemble sporadic tumors [217,221]. *BRCA1/2* mutations are inherited in an autosomal dominant fashion, but act recessively on the cellular level as tumor suppressor genes involved in double-stranded DNA (dsDNA) break repair [222]. Female carriers of *BRCA1/2* mutations have a lifetime risk of breast cancer of 50%–85% [218,223]. Male carries of *BRCA1* have an increased risk of breast cancer, though to a lesser degree than carriers of *BRCA2* who have an estimated 5%–10% lifetime risk [224].

In a contemporary prospective cohort of 9856 mutation carriers, chiefly verified through cancer genetic clinics, the cumulative breast cancer risk to age 80 years was 72% for *BRCA1* and 69% for *BRCA2* carriers. The cumulative ovarian cancer risk to age 80 years was 44% for *BRCA1* and 17%for *BRCA2* carriers. Cancer risks varied by family history and mutation position [225]. Current rates of genetic testing and screening young women with breast cancer for *BRCA1/2* mutations consistent with the NCCN guidelines are intensifying since genetic risk not only provides better leverage to surgical decisions and systemic therapeutic trial eligibility, but also improves cancer management, genetic counselling and prevention of BRCA-related cancers [226-230].

Additional rare, yet highly penetrant genes include *PTEN* [213,231], *TP53* [100,174,205,213], *CDH1* [213,232] and *STK11* [141,213,229], each conferring a distinct clinical syndrome (Table 1.6 and Table 1.7). The most frequently mutated and/or amplified genes in the tumor cells are *TP53* (41% of tumors), *PIK3CA* (30%), *MYC* (20%), *PTEN* (16%), *CCND1* (16%), *ERBB2* (13%), *FGFR1* (11%) and *GATA3* (10%), as portrayed in Figure 1.10. These genes encode cell-cycle modulators that are either supressed, e.g., *p53*, or activated, e.g., *cyclin D1*), sustaining proliferation and/or inhibiting apoptosis, inhibiting oncogenic pathways that are activated (*MYC*,

HER2 and *FGFR1*) or inhibiting elements that are no longer repressed (*PTEN*). The mutations affecting 100 putative breast cancer drivers are predominantly sporadic [233], implying that most breast cancers are caused by multiple, low-penetrant mutations that act cumulatively.

Table 1.6: Main genes associated with breast cancer (BC)/ovarian cancer (OC) with associated syndromes and BC/OC risk estimate

Syndrome Associated	Gene	Locus	BC Risk *	OC Risk *	References
Hereditary Breast and Ovarian Cancer (AD)	*BRCA1* *BRCA2*	17q21.31 13q13.1	57–65% (by age 70) 45–55% (by age 70)	39–44% (by age 70) 11–18% (by age 70)	[20–22]
Peutz-Jeghers syndrome (AD)	*STK11*	19p13.3	32–54%	18–21%	[23]
Cowden syndrome (AD)	*PTEN*	10q23.31	25–85%	NA	[24]
Li-Fraumeni syndrome (AD)	*TP53*	17p13.1	25–79%	NA	[25]
Hereditary Diffuse Gastric Cancer (AD)	*CDH1*	16q22.1	39–52% (by age 80)	NA	[26,27]
Ataxia–telangiectasia (AR)	*ATM*	11q22.3	17–52%	NA	[28]
-	*CHEK2*	22q12.1	25–39%	NA	[29]
-	*BARD1*	2q35	NA	NA	[30]
Neurofibromatosis type I (AD)	*NF1*	17q11.2	~8% (by age 50)	NA	[31]
Nijmegen breakage syndrome (AR)	*NBN*	8q21.3	12–30%	NA	[32]
Fanconi anemia (AR)	*PALB2* *BRIP1*	16p12.2 17q23.2	44–63% (by age 80) NA	2–10% (by age 80) ~6%	[33] [34]
-	*RAD51C*	17q22	NA	~7%	[35,36]
-	*RAD51D*	17q12	NA	~15%	[35,37]
Lynch syndrome (AD)	*MLH1* *MSH2* *MSH6* *PMS2* *EPCAM*	3p22.2 2p21-p16 2p16.3 7p22.1 2p21	NA	4–12%	[38]

AD: autosomal dominant; AR: autosomal recessive; NA: not assessed. * The percentages represent lifetime risks unless otherwise specified.

Source and cross-references: [213].

It has been shown that TNBCs are significantly correlated with *BRCA1* germline mutations and high levels of genomic instability, *TP53* (82%) and *PIK3CA* (10%) being the two most frequently mutated somatic genes [234]. TNBC subtypes display considerable genomic heterogeneity that can be exploited to improve existing knowledge of disease biology and allow identification of candidate targets for novel therapeutic intervention of TNBC [232].

Table 1.7: The most frequently inherited breast cancer syndromes

Syndrome or key gene*	Mutation characteristics	Penetrance	Prevalence	Breast cancer types
BRCA1 hereditary breast cancer syndrome, and *BRCA1* breast and ovarian breast cancer syndrome	*BRCA1*; mutations: no hot spots; tumour suppressor; DNA repair of double-stranded DNA breaks	Cumulative risk of breast cancer at age 70 years of 65%; very high penetrance	• Autosomal dominant, 3 in 1,000 • Rare • Average relative risk 11.4	• Adenocarcinoma NST • Medullary-like • Metaplasic • Triple-negative • 80% basal-like • Female and male
BRCA2 hereditary breast cancer syndrome, and *BRCA2* breast and ovarian breast cancer syndrome	*BRCA2*; mutations: no hot spots; tumour suppressor; DNA repair of double-stranded DNA breaks	Cumulative risk of breast cancer at age 70 years of 45%; high penetrance	• Autosomal dominant, 7 in 1,000 • Rare • Average relative risk 11.7	• Adenocarcinoma • No distinct phenotype • Female and male
Li Fraumeni syndrome and Li Fraumeni-like syndrome	*TP53*; mutations: no hot spots; *BRCA2*, Fanconi genes, *MMR* also mutated; tumour suppressor, cell cycle control, DNA repair, apoptosis and DNA replication	Cumulative risk of breast cancer at age 60 years of 50%; very high penetrance	• Autosomal dominant, 1 in 20,000–1 in 5,000 • Very rare • Average relative risk 10.5	• Phyllodes tumours • Adenocarcinoma NST • 80% HER2+ female
PALB2	*PALB2* monoallelic germline mutations; if biallelic: Fanconi anaemia; DNA repair of double-stranded DNA breaks	Cumulative risk of breast cancer in one's lifetime of 33–58%; moderate to high penetrance	• Autosomal dominant • Average relative risk 5.3	• Adenocarcinoma NST • No distinct class • Pancreas, ovary
CHEK2	*CHECK2* mutations (*CHEK2*1100delC* more frequent than 470C>T or I157Thr missense variants); cell cycle checkpoint kinase, DNA repair, activated BRCA1 and p53	Cumulative risk of breast cancer in one's lifetime of 20–30%; moderate to low penetrance	• Autosomal dominant • Average relative risk 2.26 for women and 3.13 for men • Higher in cases of family history • Missense variants confer lower risk[329]	• Adenocarcinoma NST • ER positivity varies according to the type of mutations • Female and male • Colorectal cancer risk in *CHEK2*1100delC* mutation carriers
Ataxia telangiectasia	*ATM*; mutations: no hot spots; homozygotes more affected than heterozygotes; protein kinase DNA damage response through p53, BRCA1 and CHECK2 pathways	Cumulative risk of breast cancer in one's lifetime of 20%; low to moderate penetrance	• Autosomal recessive, 1–2.5 in 100,000 • Common • Average relative risk 2.8	• Adenocarcinoma NST • No distinct class
Cowden syndrome	*PTEN*; germline mutations, variants and epimutations; tumour suppressor, PIK3CA pathway	Cumulative risk of breast cancer in one's lifetime of 85%; very high penetrance	• Autosomal dominant, 1 in 250,000 • Average relative risk of 25% • Very rare	• Adenocarcinoma NST • No distinct class • Female and male • Benign breast lesions
Hereditary diffuse gastric cancer syndrome	Germline *CDH1*; mutations: no hot spots; cell invasion suppressor and cell–cell adhesion	Cumulative risk of breast cancer in one's lifetime of 42–60%; high penetrance	• Autosomal dominant, <0.1 in 100,000 • Average relative risk of 6.6	• Invasive lobular carcinoma • Female
Peutz–Jegher syndrome	*STK11*; mutations: no hot spots; tumour suppressor gene, cell-cycle regulation and apoptosis	Cumulative risk of breast cancer at age 60 years of 32–54%; high penetrance	• Autosomal dominant • Insufficient data to determine average relative risk	• Adenocarcinoma NST • No distinct class
Neurofibromatosis	*NF1* germline mutations; tumour suppressor and negative regulation of the RAS signalling pathway	Cumulative risk of breast cancer in one's lifetime of 17%; low to moderate penetrance[330]	• Autosomal dominant, 1–5 in 10,000 • Average relative risk of 2.6	• Adenocarcinoma NST • Higher prevalence of metaplastic carcinoma[331] • Female and male

+, positive; ER, oestrogen receptor; HER2, human epidermal growth factor receptor 2; NST, no special type (also known as invasive ductal carcinoma). Data from REFS[14–16,312,313]. *Lynch syndrome may also be associated with an increased frequency of breast cancer, but the link is not clear.

Source and cross-references: [147].

A recent study that evaluated the genomic aberrations that drive each of the TNBC molecular subtypes by integrative analysis conflating somatic mutation, copy number aberrations (CNAs) and gene expression profiles of 550 TNBC [235] derived from the Molecular Taxonomy of Breast Cancer International Consortium (METABRIC) [236]

and The Cancer Genome Atlas (TCGA) [237] consortia, summarized genes most frequently gained/amplified (GAIN/AMP)—*MYC* (64%), *PIK3CA* (51%) and *CDK6* (39%); most frequently subject to hemizygous (HETD) or homozygous deletion (HOMD)—*MAP2K4* (55%), *TP53* (55%) and *NCOR1* (54%) Figure 1.11.

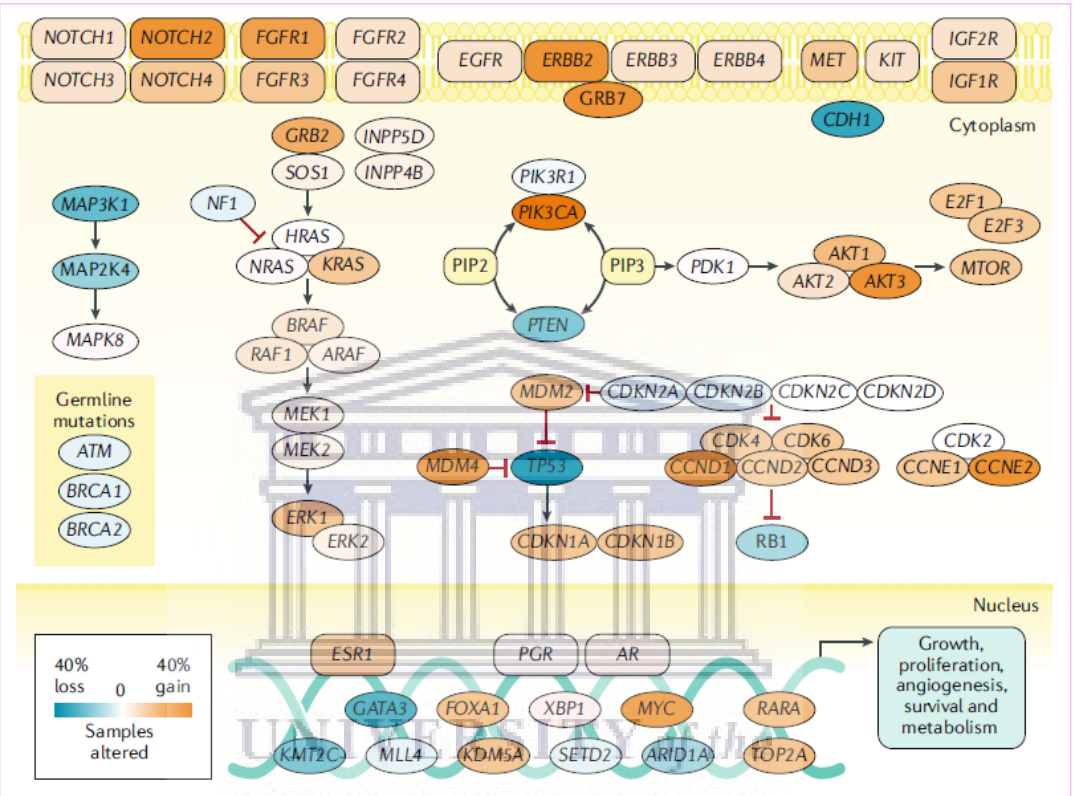

Source: [147]. The Cancer Genome Atlas data on breast tumor DNA copy number and somatic mutations were used to identify the frequency of each genetic alteration across 792 patients with breast cancer (all subtypes)322. Each gene is shaded according to the overall frequency of alteration. Orange indicates a high level of amplification and/or likely gain- of-function mutations; blue represents homozygous deletions and/or likely loss-of-function mutations.

Figure 1.10: Most frequent molecular mutations in breast cancer

This study underscores the significant genetic heterogeneity that embodies the fundamental TNBC molecular subtypes at the somatic mutation, copy number and gene expression levels, which may further pinpoint several candidate genes for targeted therapy of TNBC [152,196,232].

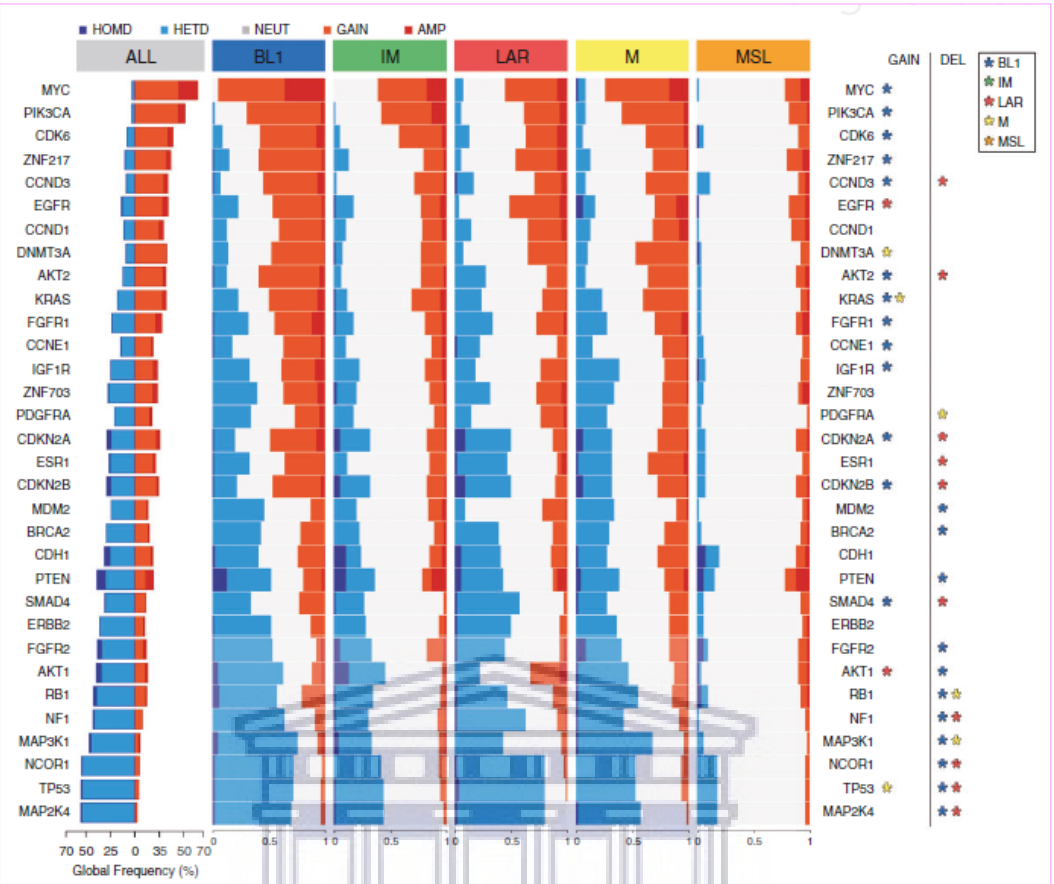

Source: [232]. CNA frequencies for the 32 breast cancer copy number driver genes across each TNBC molecular subtype. Significant differences (FDR<5%, one-sided Fisher test) are shown with an asterisk. CNAs: copy number aberrations; FDR: Benjamini–Hochberg false discovery rate; HOMD: homozygous deletion; HETD: heterozygous deletion; NEUT: neutral; GAIN: genes most frequently gained; AMP: genes most frequently amplified; BL1: basal-like subtypes 1; IM: immunomodulatory; LAR: luminal androgen receptor; M: mesenchymal; MSL: mesenchymal stem-like.

Figure 1.11: Genomic instability within each TNBC molecular subtype

A.4 The Evolving Landscape of Breast Cancer Management

A.4.1 Current Evidence-Based Breast Cancer Therapeutics

At the molecular level, breast cancer is a heterogeneous disease categorized into various subtypes [238], depending on the presence or absence of molecular markers for estrogen (ER) or progesterone (PR) receptors and human epidermal growth factor-2 (ERBB2/neu): $ER^+/PR^+/ERBB2^-$ (70% of patients), $ERBB2^+$ (15%-20%), and triple-negative (tumors lacking all three standard molecular markers; 15%) and/or *BRCA* mutations [147,182,239].

Over the past two decades, breast cancer heterogeneity has become an important consideration for the multidisciplinary management of the disease, accentuating biological-directed and personalized therapies and treatment de-escalation to moderate adverse events in ~70–80% of patients with early-stage, non-metastatic disease [147]. Advanced stage breast cancer with distant organ metastases is recalcitrant to current therapeutic modalities [146,240,241]. In most cases (>90%), breast cancers are not initially diagnosed as metastatic and the therapeutic goals for patients presenting without metastatic disease include tumor eradication and preventing recurrence.

However, TNBC has a higher recurrence than the other 2 subtypes, with 85% 5-year breast cancer–specific survival for stage I TNBC vs 94–99% for hormone receptor positive and ERBB2 positive breast cancers [239]. Multidisciplinary therapeutic rationales for breast cancer encompass locoregional (surgery and radiation therapy) and systemic therapy [147,182,239,242]. Systemic therapies incorporate endocrine therapy for hormone receptor-positive disease [243,244], chemotherapy [245-247], anti-HER2 therapy for $HER2^{+}$ disease [248-250], bone stabilizing agents [251], poly(ADP-ribose) polymerase (PARP) inhibitors [252,253] for *BRCA* mutation carriers and, currently, immunotherapy [254,255].

Other current BC treatment strategies include breast-conserving surgery (BCS, surgical elimination of the tumor and adjacent tissue) [256-259] or mastectomy (surgical ablation of the breast) [260-262]. Neoadjuvant therapy (NAT)/neoadjuvant chemotherapy (NAC) for operable breast cancer may facilitate more breast-conserving surgery (BCS) [242,257,263]. Generally, the standard treatment options for HR-positive tumors are endocrine therapies such as tamoxifen and aromatase inhibitors [264-266].

In some instances, Luminal B is treated with endocrine therapy as well as chemotherapy because of the high Ki-67 association. HER2-positive tumors are normally treated with anti-HER2 drugs such as trastuzumab and anthracycline-based chemotherapy. TNBC tumors, lack the hormonal biomarkers for targeted treatment and is usually treated with a combination of surgery, radiation and chemotherapy (anthracycline and taxanes) [146,147,182]. Various chemotherapeutic options that are currently available for metastatic breast cancer (MBC) are summarized in Figure 1.12 [147].

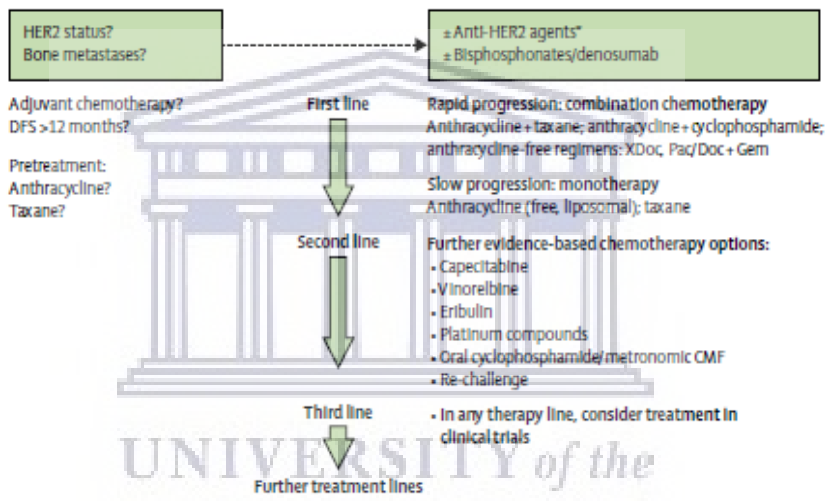

Source: [147]. DFS=disease-free survival. XDoc= capecitabine and docetaxel. Pac=paclitaxel. Doc=docetaxel. Gem=gemcitabine. CMF=cyclophosphamide, methotrexate, and 5-fluorouracil. *Approved targeted drugs for addition to chemotherapy: trastuzumab, pertuzumab, or lapatinib for HER2-positive tumors; bevacizumab (first-line therapy) for HER2-negative tumors.

Figure 1.12: Evidence-based chemotherapeutic modalities for metastatic breast cancer

A.4.2 Breast Cancer Treatment Algorithms

A treatment algorithm for advanced breast cancer is depicted in Figure 1.13 [147]. According to this algorithm, treatment options are focused on approved therapies, systemic therapy is guided by biology and the relative distribution of subtypes. Several lines of endocrine-based therapy should be used for all luminal-like metastatic breast

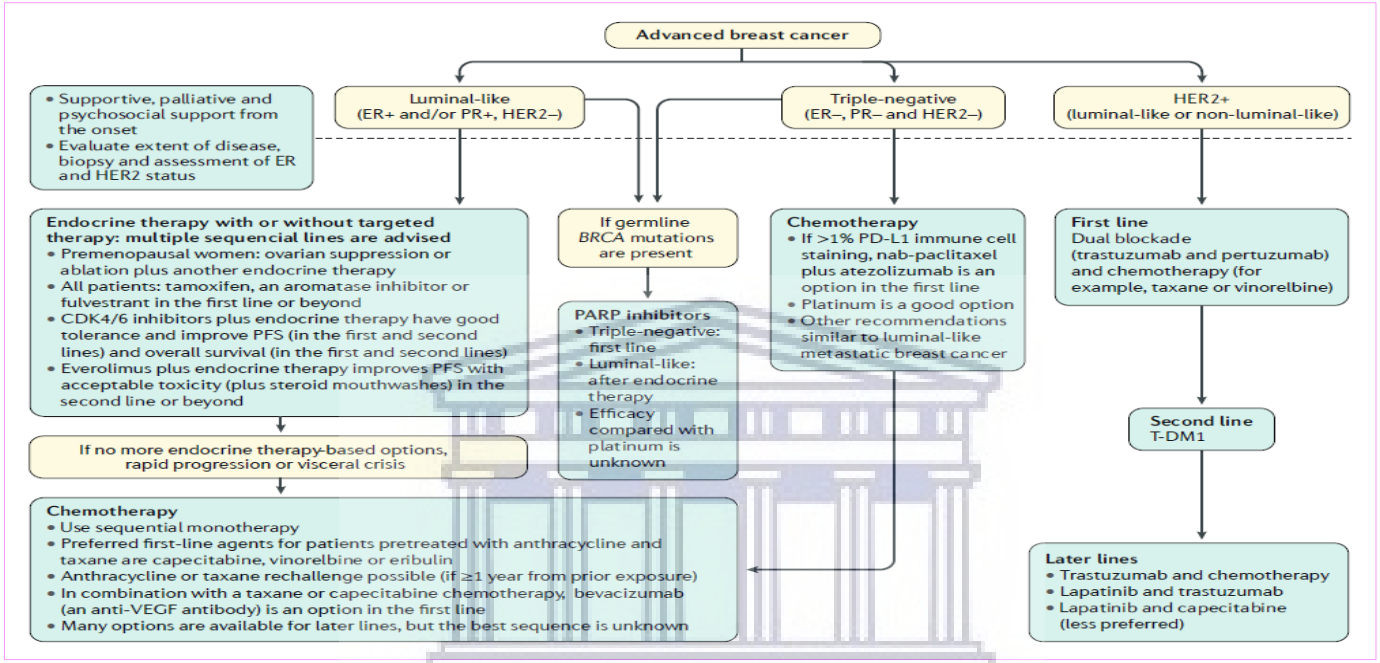

Source: [147]. Management of advanced breast cancer with distant metastases should be according to subtype as well as disease characteristics and patient preferences. Supportive, palliative and psychosocial support are crucial from the time of diagnosis. Biopsy of a metastatic site and assessment of oestrogen receptor (ER), progesterone receptor (PR) and human epidermal growth factor receptor 2 (HER2) status, at least once in the metastatic setting, are also necessary. Endocrine therapy , with or without targeted therapy , is the mainstay for luminal- like disease, and — unless life- threatening — several lines are to be used before commencing chemotherapy. When chemotherapy is used, sequential monotherapy is advised. For triple- negative disease, chemotherapy is the main treatment, with no specific recommendations except that platinum is one of the preferred options. Triple- negative tumors with immune cells expressing programmed death- ligand 1 (PD- L1) may be candidates for first- line immunotherapy. For HER2-positive disease, it is crucial to continue blocking the HER2 pathway , with a sequence of anti- HER2 agents and chemotherapy; combinations of endocrine therapy with anti- HER2 therapy can also be used in ER- positive, HER2-positive disease, preferentially as maintenance therapy. For women harbouring germline BRCA mutations, poly(ADP- ribose) polymerase (PARP) inhibitors are an additional therapy option. The management algorithm takes evidence- based registered therapy options into account. Availability and reimbursement of individual diagnostic or therapeutic options may differ regionally and require adjustments of the treatment concepts outlined here. −, negative; +, positive; PFS, progression- free survival; T- DM1, ado- trastuzumab emtansine; VEGF, vascular endothelial growth factor.

Figure 1.13: Treatment algorithm for advanced breast cancer focusing on approved therapies

cancers (MBCs) until endocrine resistance is observed. To overcome endocrine resistance, CDK4/6 inhibitors (palbociclib, ribociclib and abemaciclib) and mammalian target of rapamycin (mTOR) inhibitors (e.g., everolimus) can be used. For HER2-positive advanced breast cancer (including ER+ and ER-, HER2+ disease), anti-HER2 agents should be started early and continued beyond progression [147]. The algorithm does not provide different or specific chemotherapy recommendations for TNBC patients without *BRCA* mutations, but for BRCA-associated advanced TNBC, a platinum agent is the preferred selection [147].

A.4.3 Breast Cancer Metronomic Therapy

Interestingly also, several studies have strongly recommended low-dose metronomic (continuous) treatment (e.g., capecitabine, cyclophosphamide, methotrexate, bevacizumab, erlotinib) to lower VEGF (considered as predictive biomarker of the angiogenic suppression response in MBC) as an alternative strategy for metastatic breast (MBC) or HER2$^-$, ER- and PR-poor advanced breast cancer patients since it has fewer side effects and its efficacy (overall survival benefit) in most patients may have potentially significant cost-effective advantages for public health [200,267-272].

A.4.5 Immunotherapeutic Implications of the Tumor Microenvironment

In recent years, participation of the tumor microenvironment (TME)—also referred to as the mammary stem cell (MaSC) niche—in driving metastatic spread and breast cancer chemoresistance, all of which impact the cancer's response to therapy, is increasingly being documented [46,122,123,273-277]. Components of the TME include mammary stem cells (MaSCs), immune cells (such as pericytes, endothelial cells, macrophages, eosinophils, neutrophils, and mast cells), extracellular matrix (ECM) components (such as collagen, fibronectin, hyaluronan, laminin, and matrix remodeling enzymes/matrix metalloproteases–MMPs), epithelial-stromal cells (such

as pre-adipocytes, adipocytes, mesenchymal stem cells (MSCs), cancer-associated fibroblasts (CAFs), tumor-associated leukocytes (TILs), dendritic cells, $CD8^+$ T cells, CD4+ T cells and tumor-associated macrophages (TAMs). Dynamic interactions of these TME elements are collectively responsible for releasing cytokines, chemokines, growth factors and inflammatory mediators (such as interleukin-6/8, TGF-ß, IF-γ, TNF-α, oncostatin) that regulate breast cancer stem cell (bCSC/MaSC) plasticity [278], expansion, promotion of chemoresistance and relapse [46,273,275,279].

Remarkably, TAMs can undergo differential polarization by altering their phenotype in response to dynamic TME signals, i.e., they can either be antitumoral (by direct tumor cell killing/inhibition of angiogenesis or by the activation of T cells) or protumoral (by stimulating cancer cell growth and metastasis) [279,280]. Hence, targeting the various interactions of TAMs in the TME may yield as yet untapped potential therapeutic targets in breast cancer [46,275,279,281]. An elevated density of cells expressing macrophage-associated markers in primary breast cancer (typically 50% of the number of cells within the tumor) correlates with worse patient prognosis. TAMs mediate tumor growth and progression by secretion of cytokines such as matrix metalloproteases (MMPs), vascular endothelial growth factor A (VEGF-A), CCL18 and IL-10, and thus promote therapy resistance (Figure 1.14) [273,282].

Several drugs have been designed to target TAMs in the TME (Figure 1.15) and some that have entered Phase I trials clinical trials produced efficacious outcomes [283]. Other strategies currently being employed in TAM targeting include *inhibition of*: colony stimulating factor-1 (CSF1)-CSF1 receptor (CSF1R) axis, CD47-SIRPα, CCL2-CCR2, Ang2-TIE2, COX-2 (with celecoxib), and *stimulation of*: CD40, CR3, toll-like receptor 7 (TLR7). Promising oncolytic agents that may perturb macrophages include bisphosphonates such as zoledronic acid (induce apoptosis in macrophages

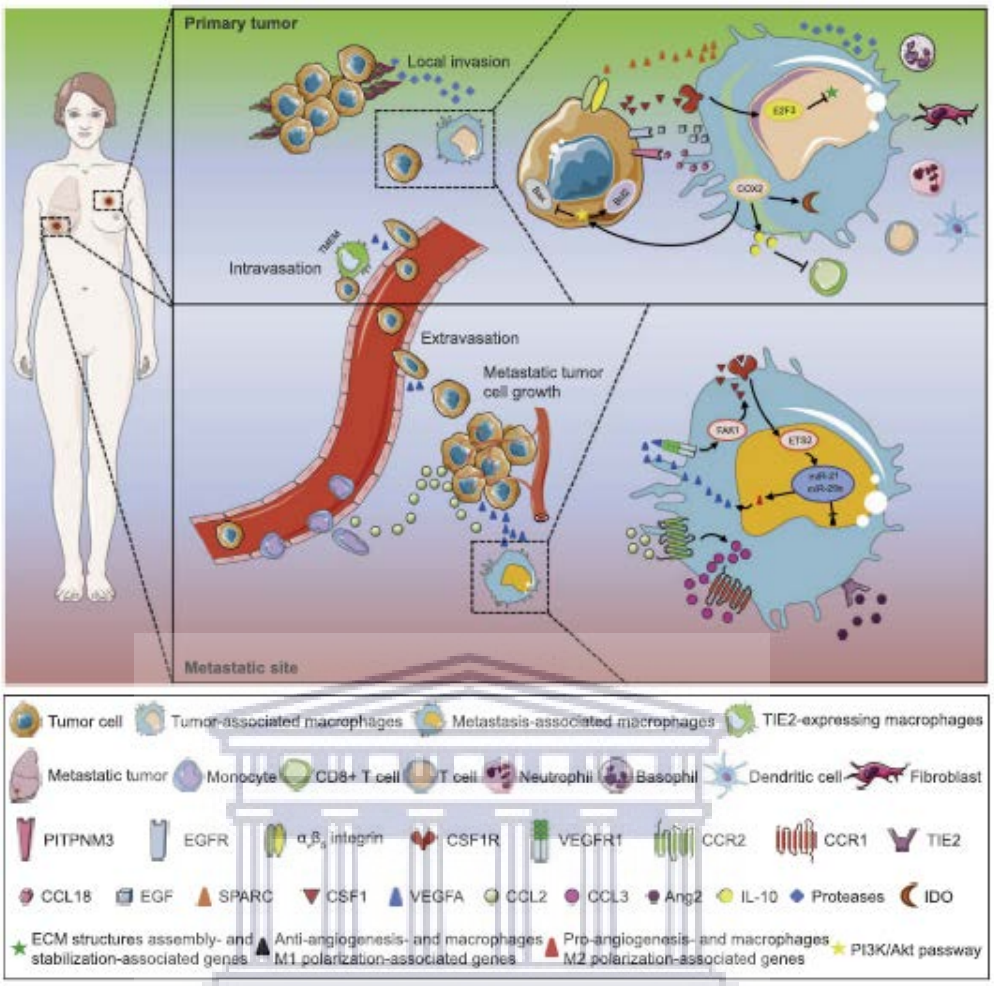

Source: [273]. **Tumor growth:** Over-expression of cyclooxygenase-2 (COX-2) in TAMs increases the expression of interleukin 10 (IL-10) and indoleamine 2,3-dioxygenase (IDO) and further suppresses CD8+ T cell proliferation and interferon-γ(IFN-γ) production. Thereby, this reduces tumor cell killing by CD8+ T cells. In addition, COX-2+ TAMs activate the PI3K-Akt pathway in cancer cells and increase the anti-apoptotic factor Bcl-2 and decrease the pro-apoptotic factor Bax expression. Together, these promote tumor cell growth. **Local invasion:** TAMs secret proteases that degrade extracellular matrix (ECM). Furthermore, TAMs facilitate tumor cell migration and invasion through interacting with each other. These interactions include secreted protein acidic and rich in cysteine (SPARC) and αvβ5 integrins, Chemokine (CC motif) ligand 18 (CCL18) and phosphatidylinositol transfer protein 3 (PITPNM3), epidermal growth factor (EGF) and EGF receptor (EGFR), colony stimulating factor-1 (CSF1) and CSF1 receptor (CSF1R). **Intravasation:** Vascular endothelial growth factor A (VEGF-A) is secreted from macrophages in the tumor microenvironment of metastasis (TMEM) structure, which consists of the direct contact of a TIE2-expressing TAM, a mammalian enabled overexpressing tumor cell and an endothelial cell. TMEM-derived VEGF-A promotes tumor cell intravasation. **Extravasation:** In the metastatic sites, macrophages contribute to premetastatic niche establishment. The metastasis-associated macrophages (MAMs) derived VEGF-A promotes tumor cell extravasation. **Metastatic tumor cell growth:** VEGF-A promotes breast tumor cell seeding and persistent growth after seeding through activation of the VEGFR1-Focal adhesion kinase (FAK1)-CSF1-C-ets-2 (ETS2)-microRNAs signaling in MAMs. In return, tumor cells secrete CCL2 to recruit monocytes which further develop into MAMs. Moreover, the CCL2-CCR2 signaling in MAMs can activate the CCL3-CCR1 signaling, which prolongs the retention of MAMs in the metastatic site and eventually promotes tumor cell extravasation and seeding. In addition, the angiopoietin-2 (Ang2)-TIE2 signaling promote the postseeding tumor cell growth. Macrophages also interact with other immune cells in the tumor microenvironment.

Figure 1.14: Mechanisms of tumor-associated macrophages (TAMs) in promoting breast tumor growth and metastasis

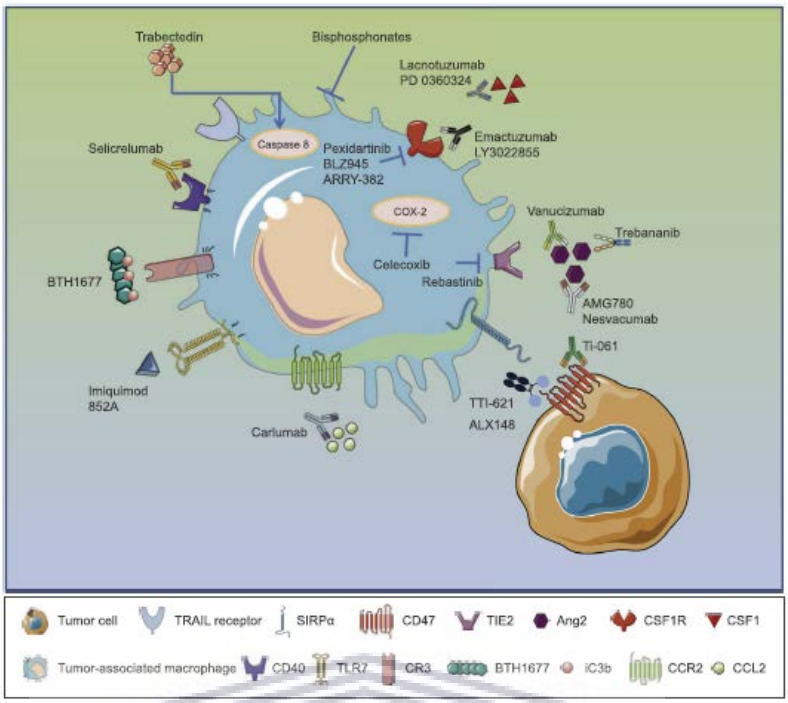

Source: [273]. Macrophage-targeted therapies are aimed at activating macrophages' tumor killing activity, or inhibiting their recruitment and tumor-promoting functions. Activation of macrophages' antitumor activity can be achieved by stimulating the co-stimulatory receptor CD40, complement receptor 3 (CR3) and Toll-like receptor 7 (TLR7). These treatment strategies have been demonstrated to repolarize the tumor-promoting M2-like tumor-associated macrophages (TAMs) to an antitumor M1-like phenotype. In addition, blocking the interaction between CD47 and signal-regulatory protein alpha (SIRPα), a 'don't eat me' signal, can enhance macrophages' phagocytic function and thereby improve their antitumor activity. Inhibition of macrophage accumulation within the breast tumor microenvironment has been demonstrated to reduce tumor growth and metastasis in preclinical studies. This treatment strategy includes inhibition of colony stimulating factor 1 (CSF1)-CSF1 receptor (CSF1R) axis or chemokine (C-C motif) ligand 2 (CCL2)-CCL2 receptor (CCR2) axis. Besides, caspase-8 dependent TRAIL receptor-mediated monocyte apoptosis induced by a DNA-binding marine alkaloid trabectedin has also shown to cause TAMs depletion in tumor microenvironment. Other macrophage-targeted therapies in breast cancer include angiopoietin 2 (Ang2)-TIE2 axis inhibition, cyclooxygenase-2 (COX-2) inhibition and bisphosphonates. The Ang2-TIE2 signaling mediates angiogenesis and metastasis. Expression of COX-2 in TAMs is essential to maintain their immunosuppressive function and promote tumor cell proliferation. Bisphosphonates have been widely used in breast cancer. Only preclinical evidencesuggests that bisphosphonates cause TAM apoptosis.

Figure 1.15: Macrophage-targeted therapies in breast cancer

in vitro) [284], celecoxib (disappointing in breast cancer patients) [285], trabectedin, a DNA intercalator (reduces TAM viability and inflammatory mediators CCL2 and IL-6 production by TAMs and tumor cells) in combination with paclitaxel and trastuzumab (but limited clinical efficacy in patients with metastatic breast cancer) [286,287].

A.4.6 Drug Combinations in Breast Cancer Therapy

A.4.6.1 Clarification of the Concepts of Combination Therapy

Combination therapy is a central concept in modern medicine [288-295]. Multi-agent therapies and repurposing of drugs are fundamental to the advancement and efficacy of treatment modalities in a wide assortment of diseases, including cancer [289,296-300] and infectious diseases (such as HIV/AIDS and other viruses, parasitic, bacterial and fungal infections, tuberculosis and malaria) [301,302]. The rationale for using synergistic drug combination therapy are summarized in Table 1.8 [288].

Diseases such as cancer, diabetes, infectious diseases, and cardiovascular diseases are characterized by complex and multiple alterations in molecular pathways and interactions at the cellular and organ levels [277,303-306]. The Cancer Genome Atlas (TCGA), a cancer genomics program, is a repository of the molecular (genomic, epigenomic, transcriptomic, and proteomic) signatures of about 20,000 primary cancers derived from patients and matched normal samples covering more than 33 cancer types (https://www.cancer.gov/about-nci/organization/ccg/research/structural-genomics/tcga). The TCGA makes specific reference that cancer phenotypes have multiple underlying molecular networks which embrace the notion of personalized, targeted and precision medicine as guided by these molecular disease classifications in individual patients [307-309].

Accordingly, current drug treatment strategies in complex diseases have shifted emphasis away from the narrow sense of single-target monotherapy (or single-agent therapy)—since disease phenotypes are rarely driven by single molecular entities and this, as such, imposes serious limitations on optimal treatment effects—towards more inclusive and efficacious combinatorial drug therapies [289,290,310-312].

Table 1.8: Advantages of therapeutic drug combinations

❄ By targeting multiple mechanisms of a disease, the potency and efficacy of treatment can be increased while maintaining or even reducing negative side effects.
❄ Use of combination therapy leverages the development of otherwise ineffective drugs, and allows for repurposing of existing, clinically-approved agents, greatly accelerating the discovery and development of new therapies.
❄ Combination therapy to prevent or treat cancer, whether the agents used are natural or pharmacologic, has the potential to be more effective than single agent therapy.
❄ When using combination therapy, interactions may be beneficial (additive or synergistic), neutral or harmful (by increasing toxicity and/or decreasing efficacy).
❄ Both plant- and animal-derived natural compounds have demonstrated efficacy in cancer.
❄ A limitation to progress in the use of natural compounds has been our lack of understanding of their mechanism(s) of action.
❄ There are extensive ongoing global and commercial efforts to translate natural products into effective chemopreventive and chemotherapeutic agents.
❄ Toxicity assessment is critical to the development of natural products, whether evaluating single agents or agents used in combination.
❄ The use of combination therapy leverages the enhancement of otherwise ineffective drugs, and expedites for repurposing of existing, clinically-approved agents, significantly fast-tracking the discovery and development of novel therapies.
❄ Development of therapeutic drug combinations has exploded over the past three decades and this explosion of the number of agents that can be used in a combination introduced some challenges since it has become intrinsically insuperable to evaluate all possible combination therapies in a clinical setting, or even in in vivo preclinical studies.
❄ Successful drug combinations currently in use and those emerging in clinical trials suggest that greater emphasis should be directed towards the greater tumor microenvironment (TME).
Sources: [288,290,300,313]

Figure 1.16 is a schematic of the possible rationales for the effects of combination therapies [290]. In the broader context of models of drug-drug interactions (DDIs) and combination analyses [291,314-327], two forms of combination efficacy demonstrate the power of a robust combination evaluation method, viz., synergy-driven efficacy and potency-driven efficacy as illustrated in Figure 1.17 [288]. DDIs are critical to the success of combination therapy, and can be either beneficial or detrimental.

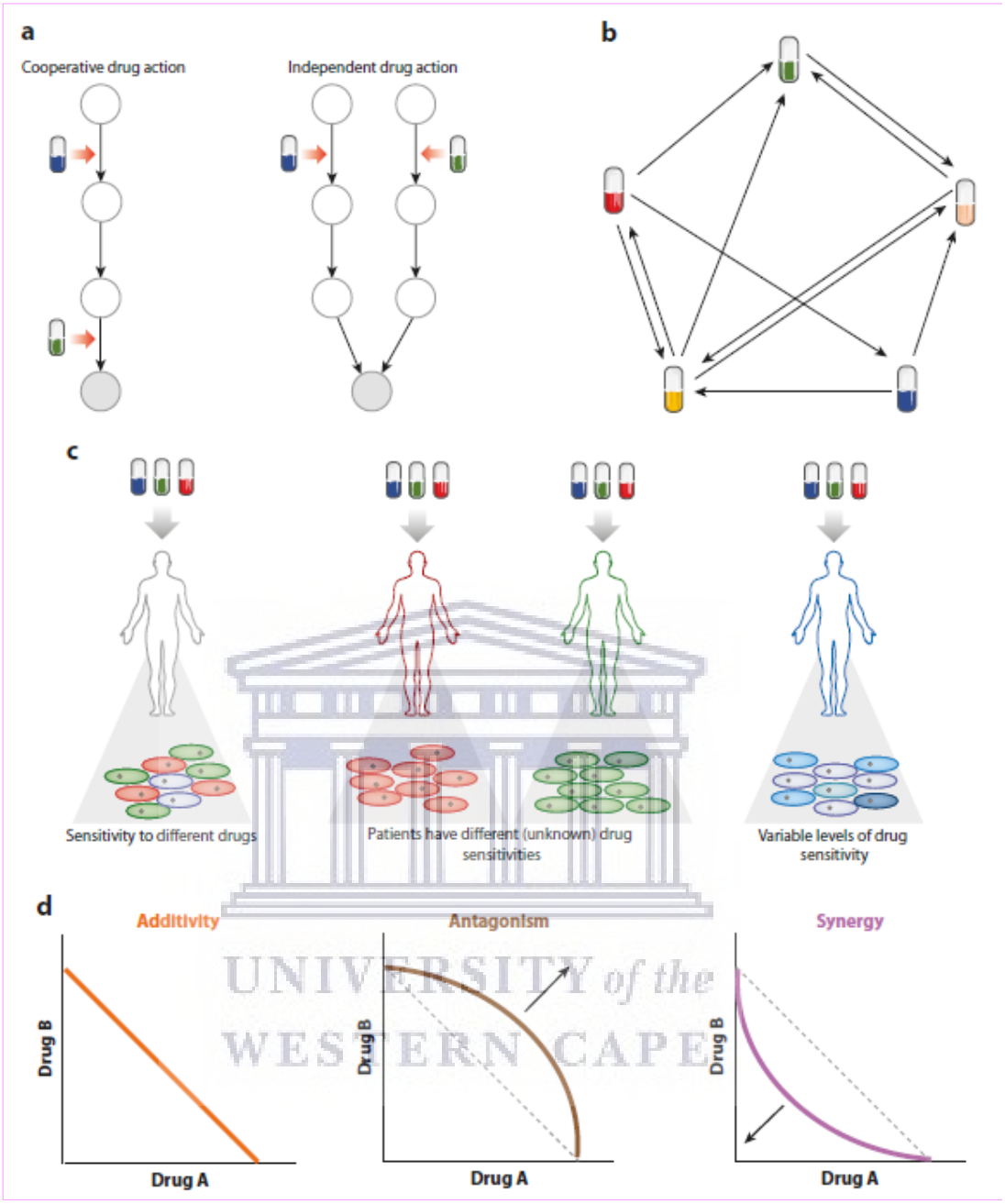

Source: [290]. Several rationales exist for the effects of combination therapies. **(a)** Drugs may act in combination either in a serial fashion (left) or in a parallel fashion (right) on a signaling pathway component (white circles) that is associated with a downstream effect (gray circle). **(b)** The occurrence of collateral sensitivity, here depicted as a network of relationships between drug resistance (arrow origin) and associated drug sensitivity, can be exploited to design combinatorial therapies to restore drug sensitivity. **(c)** Heterogeneity in cellular drug sensitivity within patients (left) and between patients (middle) forms an important rationale for combinatorial regimens. Relative variability in drug sensitivity across cell types (right) can be addressed using resensitizing combination regimens. **(d)** Additive, synergistic, and antagonistic combinatory drug effects may be quantified by isobologram analysis. Collateral sensitivity network depicting relationships between drug resistance (arrow origin) and associated drug sensitivity.

Figure 1.16: Rationales for drug combination effects

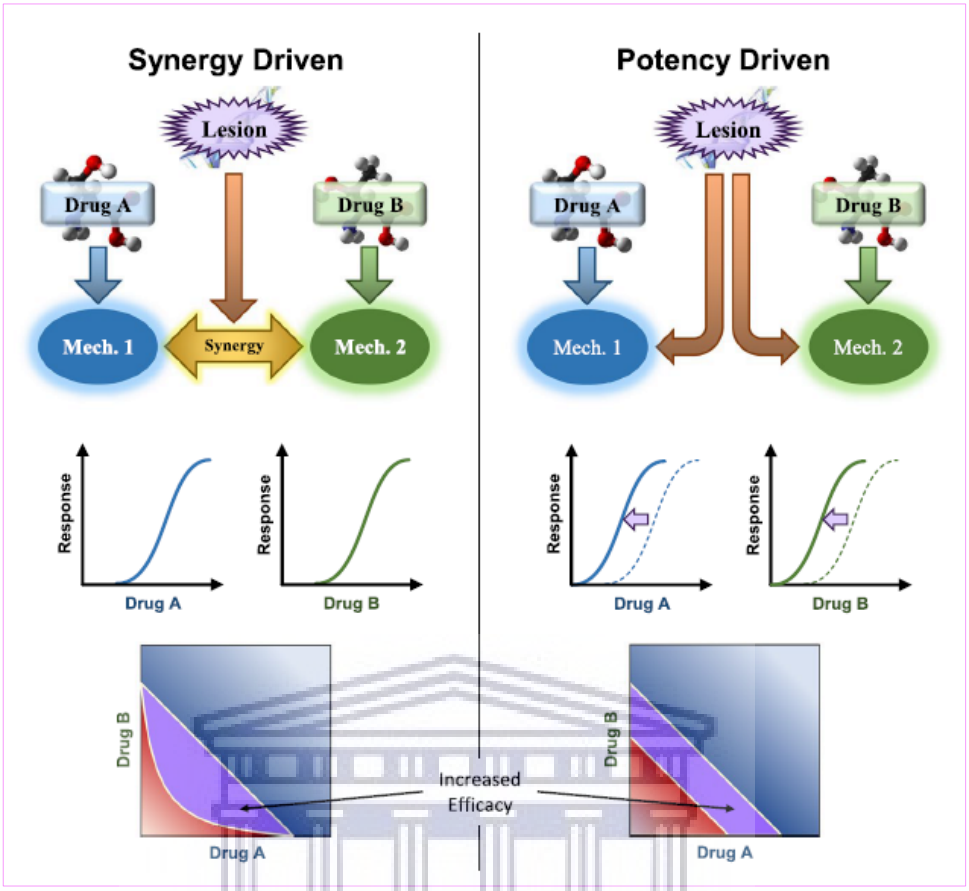

Source: [288]. In synergy driven efficacy, a sample condition such as a genetic lesion drives a distinct mechanism that increases the synergy between mechanism 1 and mechanism 2. The effects of drug A and drug B are unaffected by the lesion, but their combined effect is increased, and a set of combination dose pairs that would not have produced a sufficient efficacy now do; the combination is more effective. In potency-driven efficacy, the lesion simply increases the sensitivity to mechanisms 1 and 2 simultaneously, causing both drugs to be more potent. The degree of synergy is unchanged, but again the combination shows greater efficacy.

Figure 1.17: Synergy-driven vs potency-driven combination efficacy

The observed interactions can provide illuminating insights into the agents' mechanisms of action, viz., synergistic interactions indicate distinct sites of action whereas additive interactions suggest a shared (mutual) site of action. There are four plausible effects of drug combinations as summarized in Table 1.9. Besides DDIs (synergy and antagonism) [323], collateral sensitivity (CS) among the drugs in the combination regimen plays a pivotal role in driving the development of resistance against drug combinations [300,313,328-332].

Table 1.9: Potential effects of drug combinations

Synergism	This is defined as the combined activity of two or more drugs that produce a greater than simply additive effect, i.e., supra-additive. An advantage of drug synergy is that it permits therapeutic efficacy to be accomplished with lower doses of individual component interventions, which also reduces probable adverse events. Two compounds may exhibit synergy if they target parallel pathways or if one increases the bioavailability of the other.
Additivity	If two interventions act additively, then the effect of the combination of half the dose of each agent produces the same effect as a full dose of one parent agent.
Antagonism	An antagonistic or counteracting interaction is observed when the combined activity of two or more compounds is less than their expected individual activities, i.e., infra-additive.
Potentiation	Potentiation occurs when one drug increases the effects of a second, often by increasing the bioavailability of the second drug. Like synergy, potentiation can increase the beneficial effects of the second drug, but may also increase its toxic effects.
Sources: [290,296,300].	

CS and resistance, also known as cross-resistance (CR), are observed when mutations conferring resistance to one drug increase or decrease sensitivity to another drug (Figure 1.18). Collateral susceptibility alterations were conceptualized in the early 1950s [333] and has since been reported for many different drugs and bacterial species, as well as for viruses, cancer cell lines, and plants [306,330,332,334].

CS is a highly selective phenomenon that renders drugs particularly effective against drug-resistant cells and can thus can be regarded as a type of *synthetic lethality* [292,335-337] in which the genetic alteration that confers resistance to a drug sensitizes it to other drugs, i.e., CR. Therefore, CS can be used to rationally design drug cycling regimens that limit the evolution of resistance, a sustainable treatment paradigm that may be generally applicable to infectious diseases and cancer [332,334,338,339].

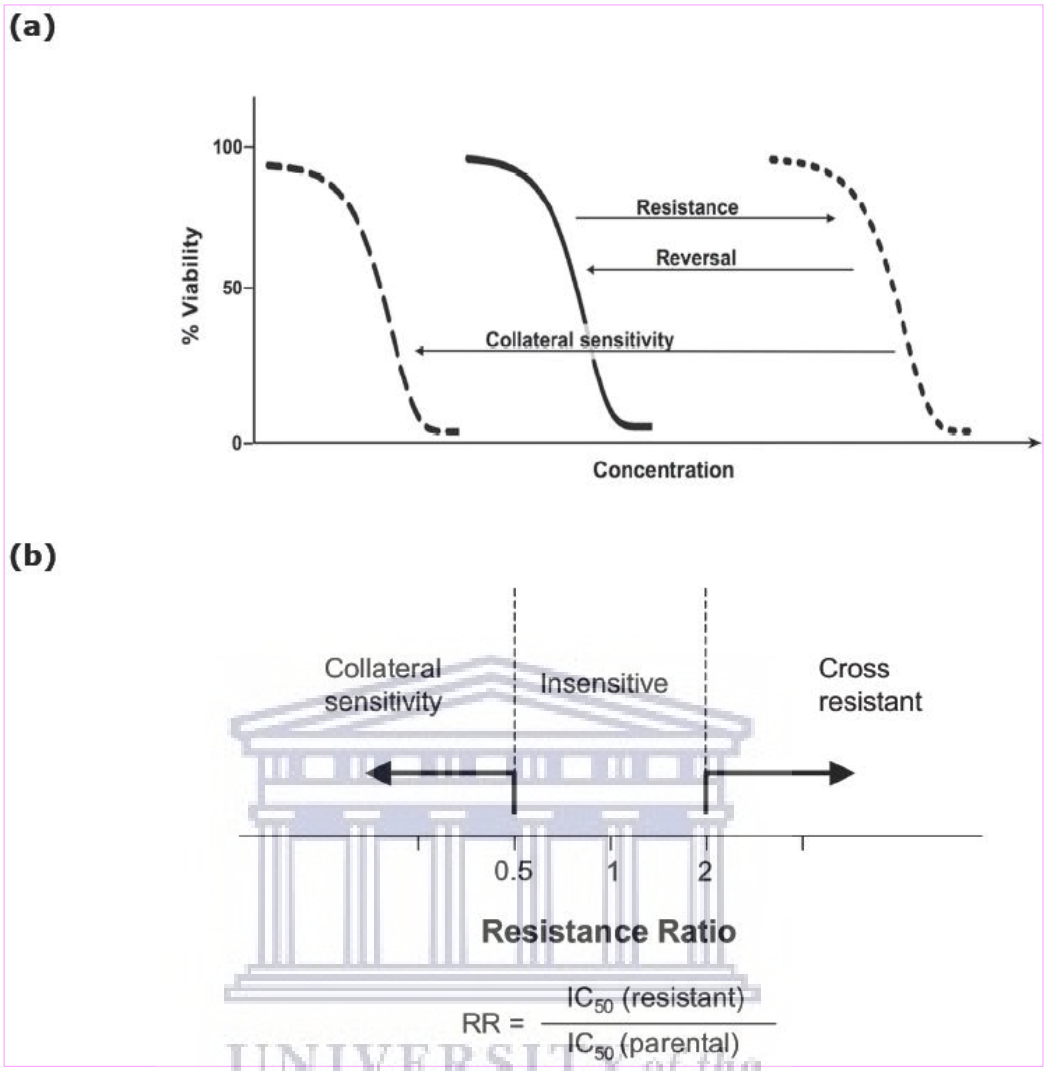

Collateral sensitivity: the phenomenon in which an organism that has developed resistance to one drug displays increased sensitivity to a second drug.

Cross-resistance: the phenomenon in which an organism that has developed resistance to one drug displays decreased sensitivity to a second drug.

Source: [339] Collateral sensitivity defined schematically. **(a)** Representative dose-response curve of a parental cell line (solid line, center). Development of resistance to a drug, and concomitant cross-resistance to a variety of cytotoxic agents conferred by ABC transporters such as P-gp, results in a loss of sensitivity of possibly several orders of magnitude (dotted line, right). Inhibitors of P-gp (so-called reversal agents) inhibit the efflux function of P-gp, restoring cellular accumulation and re-sensitizing cross-resistant cells to levels approaching that of the original parental cells. A small number of agents have been demonstrated to sensitize multidrug-resistant cells to a greater degree than the original parental cells (dashed line, left). This property is termed collateral sensitivity (CS). **(b)** The determination of collateral sensitivity (≤0.5) and multidrug resistance (≥2) as defined in this review. It is important to emphasize that a lack of cross-resistance to an agent—the same drug response for a parental and resistant line—is not collateral sensitivity, but merely a lack of resistance. This occurs, for example, with the P-gp substrate vinblastine against cisplatin-resistant 7407-CP human liver carcinoma cells which do not express P-gp as part of their resistance phenotype [340].

Figure 1.18: Collateral sensitivity and cross-resistance explained

CS can be assessed *in* vitro straightforwardly by calculating the half-maximal cytotoxicity (IC_{50}) of a drug against a parental cell line and its matched MDR derivative (Figure 1.17). A drug that exhibits CR will display lower efficacy against the MDR cell line compared to the parental cell line, and hence yield a resistance ratio >1 (RR, determined by dividing the IC_{50} against a drug-resistant cell line by the IC_{50} against a parental cell line).

Conversely, a CS agent will show greater toxicity against the MDR cell line than the parental cell line, and therefore the RR will be <1. In the case of both CS and CR, at least a two-fold effect is most likely required to be considered significant [339,341]. Research estimating the combined action of drugs places substantial emphasis on the identification of synergy, in which the combined effects of drugs yields greater potency than any of the individual drugs in the combination, while antagonism is observed in which the combination is less potent than expected. The type of interaction of drugs in the combination is based on the hypothesis that synergistic combinations hold greater promise than antagonistic ("counteracting") or non-interacting combinations.

The most popular combination evaluation models [318,319]—are the *Combination Index* (CI) [327], *Loewe Additivity* [342-344] and *Bliss Independence* [317]. CI also appears under other names, including the drug interaction index (I) or sum of fractional inhibitory concentrations (FICs) [345]. Median effect analysis of the quantitative metrics of drug combinations: isoboles, combination index (CI) and dose-reduction index (DRI) is covered in detail in the cited references in this section [299,315,316,324,327,346-348]. Synergy Finder (https://synergyfinder.fimm.fi) is a stand-alone web-application for interactive analysis and visualization of drug combination screening data. Other commercially as well as freely available software to analyze combination datasets have adequately been reviewed [349,350].

A.4.6.2 Current Drug Combination Rationales Used in Breast Cancer

Intratumor heterogeneity, encompassing different molecular subtypes and the TME, is a major impediment to effective breast cancer treatment and personalized medicine [46,351]. Therefore, breast cancer therapy necessitates a multidisciplinary approach consisting of surgery, radiotherapy, neoadjuvant and adjuvant therapy (Figure 1.19) [147,182,239]. Neoadjuvant therapy is the administration of therapeutic agents before the main treatment, e.g., hormone therapy or chemotherapy prior to radical radiotherapy for breast adenocarcinoma. On the other hand, adjuvant therapy, also known as adjunct therapy, add-on therapy, and adjuvant care, is therapy that is given in addition to the primary or initial therapy to maximize its efficacy.

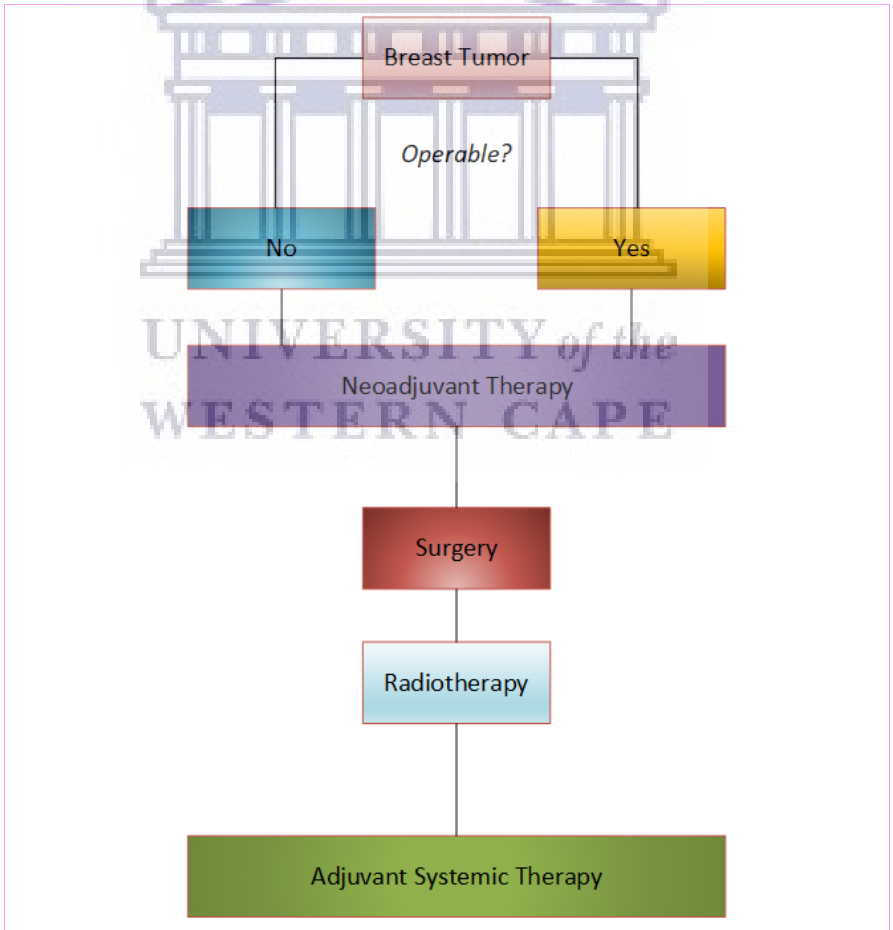

Source: [352]

Figure 1.19: Treatment strategies for breast cancer

Systemic therapy prior to surgery (neoadjuvant) in women with bulky tumors for whom reducing the tumor burden is preferred may have pre-surgical prognostic value (e.g., in $HER2^+$ disease or TNBC [147,353,354]. Neoadjuvant chemotherapy together with anti-HER2 therapy has become the standard of care in $HER2^+$ early breast cancer since pathological complete response (pCR) is correlated with improved outcome, i.e., disease-free (DFS) and overall survival (OS) and adjuvant therapy selection may thus also be influenced by pCR status [354]. The extensive application of neoadjuvant systemic therapy to reduce tumor size has not only made breast-conserving surgery (BCS) more practical, but also led to the improvement of advanced oncoplastic techniques [147,355]. Chemotherapy can be administered before (neoadjuvant) or after (adjuvant) surgery with similar effects outcomes [147,356].

In the adjuvant setting, tamoxifen (which binds to and inhibits the ER) is the standard of care and aromatase inhibitors should therefore not be used as monotherapy (as they are associated with worse survival) [147]. Globally, recommendations for adjuvant chemotherapy and radiation therapy are analogous for patients with luminal early breast cancer, as are the updated European Society for Medical Oncology (ESMO) Clinical Practice Guidelines for management of advanced breast cancer [357].

Clearly, effective therapy of breast cancer is based on the maxim of the highest therapeutic efficacy, with insignificant side effects, to predict a good quality of life for patients [352]. Therefore, prudent selection of combinatorial therapeutic interventions affords patients with the prospect of receiving maximum benefit from therapy while minimizing or eliminating recurrence, resistance and toxic side effects, as well as ensuring that patients have a good quality of life. Figure 1.20 illustrates the most important therapeutic combinations that can be exploited in breast cancer treatment.

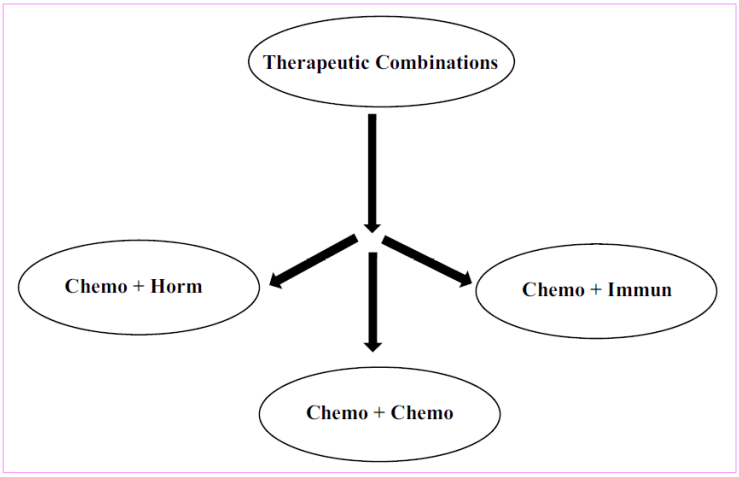

Source: [352]. Key: Chemo = chemotherapy; Horm = hormononal therapy; Immun = immunotherapy

Figure 1.20: Outline of options for treatment combinations in breast cancer

Anthracyclines and taxanes in a combination or in sequence over a period of 18–24 weeks is the current chemotherapy standard in early breast cancer and, as a rule, recommended regimens do not vary between neoadjuvant and adjuvant settings [182]. The Early Breast Cancer Trialists' Collaborative Group (EBCTCG) meta-analysis study reported that anthracycline-containing and taxane-containing chemotherapy reduced 10-year breast cancer mortality by about a third [358]. Combination therapy has thus become a cornerstone in breast cancer treatment to potentiate therapeutic effectiveness and overcome drug resistance and metastasis [359], and a vast literature on clinical trials with a multitude of different therapeutic combinations for various types of breast cancer attests to this [113,297,352,359-367], but further consideration of such combinations is beyond the scope of this thesis. However, as mentioned in Section A.1.7, cancer is a complex assembly of distinct and heterogeneous genetic diseases united by common hallmarks that can be exploited for combinatorial orthogonal cancer therapies in order to robustly reduce the probability of emergence of a resistant cancer cell population and to improve patient survival benefit (i.e., progression-free survival or PFS) [5,19,25,152,196,278,298,368-

371]. Two therapies are regarded as orthogonal, and therefore act synergistically, when they attack a cancer via two different mechanisms such that a suppressor mutation for the first therapy cannot suppress the second therapy and vice versa [25].

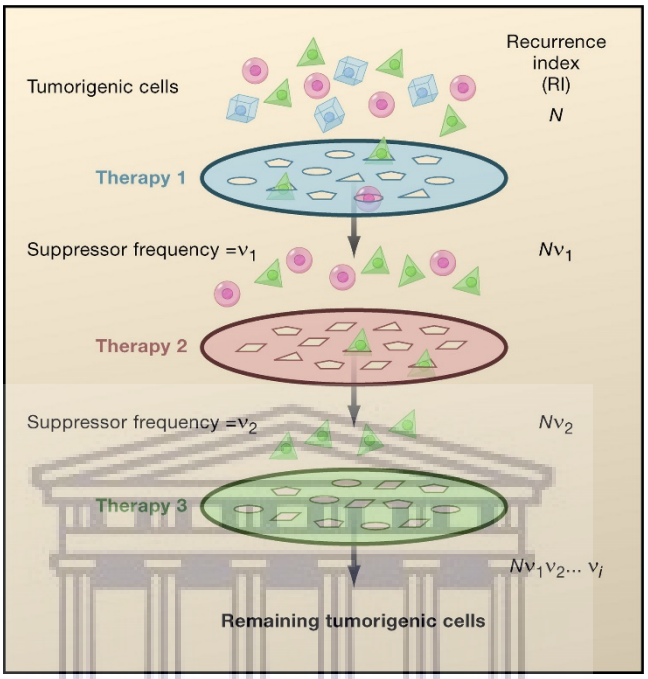

Source: [25]. A tumor consists of genetically distinct subpopulations of cancer cells (represented by the different cell shapes), each with its own characteristic sensitivity profile to a given therapeutic agent. Each cancer therapy can be viewed as a filter that removes a subpopulation of cancer cells that are sensitive to this treatment while allowing other insensitive subpopulations to escape. This escape occurs as a result of suppressor mutations that occur at a given frequency (v) unique to each therapy and tumor type. By combining therapies with orthogonal modes of action, a combinatorial filter can be set up to minimize the recurrence index (RI) of the cancer. N represents the total number of cancer cells in the tumor. A combination of orthogonal therapies that result in RI < 1 would greatly enhance the likelihood of preventing tumor recurrence.

Figure 1.21: The combinatorial strategy of orthogonal cancer therapies

A.4.7 Breast Cancer Survival, Clinical Drug Resistance and Recurrence

According to GLOBOCAN estimates of the worldwide incidence and mortality from 36 cancers and for all cancers combined for the year 2018, breast cancer was the most frequently diagnosed cancer in women in all regions of the world, except in Eastern Africa where cervical cancer eclipsed all other cancers. Also, breast cancer was the most frequent cause of death from cancer in 11 regions of the world, lung cancer in

five regions and cervical cancer in the four regions of sub-Saharan Africa [80]. An estimated 6.8 million women worldwide survived breast cancer after being diagnosed within the 5 years preceding 2018, however, it is not known how many of the survivors are living with metastatic disease and how many are cancer-free [78]. Breast cancer is curable in ~70–80% of patients with early-stage, non-metastatic disease. Nonetheless, advanced breast cancer with distant organ metastases is considered incurable with currently approved treatment regimens [147].

It has been reported that after 5 years of endocrine therapy, recurrences still occur in early breast cancer patients over at least 20 years, at rates that strongly correlate with the initial tumor burden [372]. The CREATEx trial, e.g., found that additional adjuvant capecitabine improved DFS and OS, with the survival benefit being most pronounced in TNBC [373]. Currently, advanced breast cancer is treatable, but virtually incurable, with metastases (Figure 1.22) being the cause of death in most patients, and a median OS of 2–3 years [374].

The breast cancer mortality rate is generally higher in many low- and middle-income countries, such as those in sub-Saharan Africa [375] and developing Asian countries [376]. Real-world evidence for 37.5 million patients diagnosed with one of 18 cancers between 2000 and 2014 across 71 countries in the CONCORD cancer survival program, indicated that the differences in 5-year survival between countries were wide-ranging [377]. Good exemplars are: the 5-year survival for lung cancer was approximately 33% in Japan, but 4% in India; 5-year survival for breast cancer was 90% in the United States, but 40% in South Africa [377,378]. It is important to note that the extent of breast cancer outcome disparity can be measured by comparing Surveillance, Epidemiology, and End Results (SEER) breast cancer-specific survival (BCSS) by region and with institutional cohort (IC) rates.

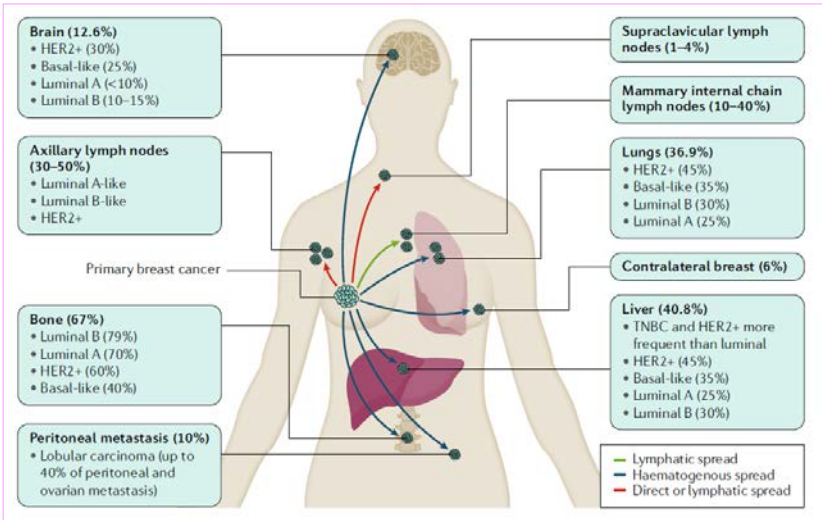

Sources: [147,379]. The most frequent nodal site is the axillary lymph nodes and the frequency of involvement depends on the size of the tumor. 10–40% of breast cancers have metastasis in the internal mammary chain, influenced by the topography of the tumor in the breast (inner quadrant versus outer quadrant and the size). Controversy abounds with regard to the value of staging and treatment of these nodes, for example, whether or not they need to be dealt with surgically or by radiation therapy. Breast cancer hones to distant metastatic sites differentially according to the molecular subtype according to data from the US Surveillance, Epidemiology , and End Results Program (SEER) database (data from 2010 to 2014, 295,213 patients with invasive breast cancer). Locoregional lymphatic spread is less frequent in triple- negative breast cancer (TNBC) than in other subtypes. The opposite is true for brain metastases, which are more frequent in TNBC than luminal tumors. Additionally , metastatic disease occurs at different time points in the natural history ; for example, luminal A cancers typically show late metastatic occurrence (5–10 years after diagnosis) and long survival is possible. By contrast, basal- like subtypes usually metastasize within 2 years, and long survival durations are uncommon. The percentage of metastases found at that site are shown in parentheses. +, positive; HER2, human epidermal growth factor receptor 2.

Figure 1.22: Common metastatic sites in breast cancer

In the USA, over 2 decades, the survival of patients with metastatic breast cancer improved nationally, but with regional survival disparity and differential improvement. To espouse equitable outcomes, access and treatment practices will need to be identified and implemented [91]. Therefore, further treatment advances as well as equal worldwide access to such remain a global challenge in multidisciplinary breast

cancer care for the future, with the hope to prolong DFS and minimize treatment-associated adverse events to maintain or improve quality of life (i.e., improved quality-adjusted life expectancy) [147]. Recently, the Advanced Breast Cancer (ABC) Global Alliance (https://www.abcglobalalliance.org/abc-global-charter/) was created to lobby for scientific advances, a deeper understanding of the needs of breast cancer patients and their rights, better survival and quality of life, accurate information, access to multidisciplinary and high-quality care, early access to supportive and palliative interventions [147].

Various hypotheses that are currently under investigation for the prevention of breast cancer recurrence [380]. It has long been known that factors that influence the success of treatment strategies, recurrence of disease and survival of breast cancer patients include hormone receptor status, tumor grade, multidrug resistance (P-glycoprotein) and human epidermal growth factor receptor (EGFR 1/HER2) status [249,381-385]. P-gp will be reviewed in Section B and EGFR/HER2 in Section C.

A.4.8 Adverse Effects Associated with Breast Cancer Therapies

In 75% of ER^+ breast cancer survivors (BCS), recurrence and mortality are reduced by oral endocrine therapy (OET) such as tamoxifen or aromatase inhibitors (AIs) [386]. However, many BCS do not adhere to OET due to therapy-associated side effects. Typical tamoxifen side effects are hot flashes, weight gain, and loss of libido and, less frequently, thromboembolic disease or endometrial pathologies [387].

AI side effects include hot flashes, arthralgia, increased fractures, rash, and gastrointestinal upset [386,387]. Therefore, a dire need exists to provide decisional support to non-adherent BCS experiencing OET side effects [387-389]. Current consensus opinion in the management of early stage breast cancer emphasizes that

an individualized approach is required for every patient and that the adverse effects of OET should be weighed against the potential benefits of extended therapy to better inform decision-making [390,391].

SECTION B: MULTIDRUG RESISTANCE (MDR) TRANSPORTERS

B.1 Overview of the ABC Transporter Superfamily

The mammalian adenosine triphosphate (ATP)-binding cassette (ABC) superfamily of transporters comprise a large number of functionally diverse transmembrane proteins which have been subdivided into 7 families designated ABCA to ABCG, and 49 ABC transporter subtypes, based on structure, domains and amino acid sequence homology [392-394]. In humans, ABC transporters export a variety of diverse drugs, drug conjugates, xenobiotics, lipids and hormones, and metabolites out of cells to maintain intracellular homeostasis.

The ABC transporters play a protective role in sanctuary sites such as the blood-brain barrier by excreting exogenous compounds and preventing the accumulation of toxins in normal tissue [395,396]. ABC transporters exist as either full transporters (TMD1-NBD1-TMD2-NBD2) or half transporters (TMD-NBD), i.e., full functional transporters typically contain two nucleotide-binding domains (NBDs) and two transmembrane domains (TMDs), whereas half transporters only contain half the complement of each. Humans possess 48 ABC transporter genes, with 3 pseudogenes. Functionally, the ABC proteins are categorized in two groups, those that utilize ATP hydrolysis to transport molecules across the plasma membrane and those that recruit transporter facilitators that undergo a conformational change when ATP binds [397]. No fewer

than 11 ABC superfamily transporters, including P-glycoprotein (P-gp/MDR1/ABCB1), multidrug resistance-associated proteins (MRPs/ABCCs) [398,399], and breast cancer resistance protein (BCRP/ABCG2) are involved in multidrug resistance (MDR) development [392,397]. The TMDs consist of six transmembrane-spanning α-helices and confer substrate specificity. The NBDs are highly conserved throughout the different ABC transporters and face the cytoplasmic side of the membrane to transfer the energy to transport the substrate across the membrane [398,400]. While roles in cancer MDR have been unequivocally confirmed for P-glycoprotein (P-gp), breast cancer resistance protein (BCRP) and multidrug resistance protein 1 (MRP1) [397,399]. Analysis of RNA sequencing data from The Cancer Genome Atlas (TCGA) database corroborated that expression levels of both P-gp/*ABCB1* and *BCRP*/*ABCG2* in a variety of patient tumor samples range over several 1,000-fold (log_{10} increments) (Figure 1.23), a significant wider range of expression than previously arrived at with standard protocols [396].

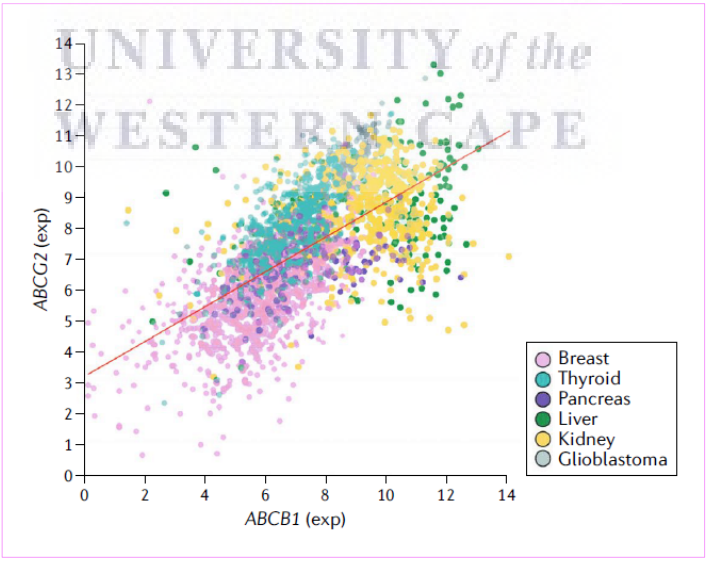

Source: [396] Data from TCGA database https://www.cancer.gov/about-nci/organization/ccg/research/structural-genomics/tcga) showing expression of both *ABCB1* and *ABCG2* in breast, thyroid, pancreas, liver and kidney tumors as well as glioblastomas.

Figure 1.23: Expression of *ABCB1* and *ABCG2* in patient tumor samples

Figure 1.24 and Figure 1.25 illustrate secondary and high-resolution 3D structure, respectively, and mechanism of ABCG2 (BCRP), ABCB1 (MDR1/P-gp) and ABCC1 (MRP1) [393,396].

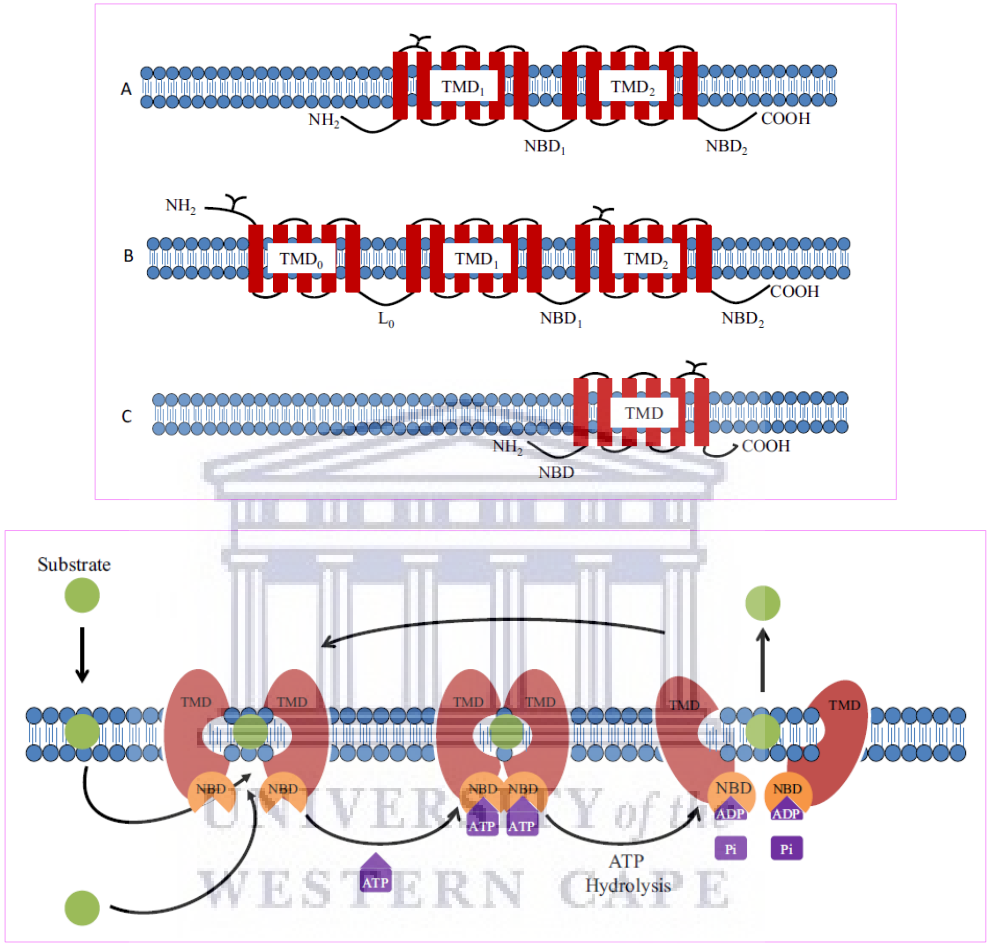

Source: [393]. Secondary structure models of drug efflux transporters of the ATP-binding cassette family. **(A)** P-gp/ABCB1, **(B)** MRP2/ABCC2, **(C)** BCRP/ABCG2. TMD – transmembrane domain; NBD – nucleotide-binding domain; L0 – loop 0. ABC transporters are energy-dependent transporters; they exhibit a conformational change upon substrate binding and ATP hydrolysis which drives the transport process of the substrate.

Figure 1.24: Secondary structure models of drug efflux transporters of the ATP-binding cassette family

However, increasing evidence for a role in MDR *in vivo* are emerging for other family members [401], even though sporadic literature accounts have appeared that multiple members of the ABCA [402] and ABCB [403] subfamilies, and the majority of the ABCC subfamily, are also able to efflux chemotherapeutics *in vitro* [398,399].

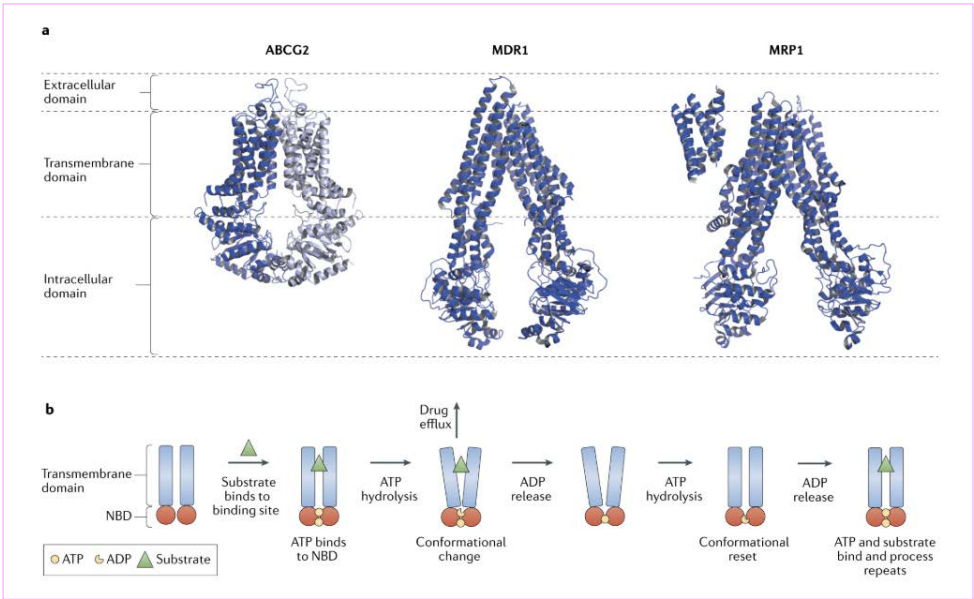

Source: [396]. **a** | High-resolution 3D structures of ATP-binding cassette (ABC) subfamily G member 2 (ABCG2) [404], multidrug resistance protein 1 (ABCB1/MDR1) [405] and multidrug resistance-associated protein 1 (MRP1). Although the structure for MRP1 is that of *Bos taurus*, the protein identity is 91%, and the structure is likely similar to that of human MRP1. Structures were generated using the PyMOL Molecular Graphics System (DeLano Scientific, Palo Alto, CA, USA with data from the Research Collaboratory for Structural Bioinformatics Protein Data Bank (RCSB PDB). **b** | Schematic representation of the proposed pumping action of MDR1. The substrate binds to the binding pocket, and ATP binds to the two binding sites in the nucleotide-binding domains (NBDs). This is followed by the hydrolysis of ATP, which generates a conformational change, allowing the substrate to be released from the protein [406]. The second molecule of ATP is hydrolyzed, allowing for a conformational reset where substrate and ATP can bind again so the process can repeat.

Figure 1.25: High resolution structure and mechanism of ABCG2 (BCRP), ABCB1 (MDR1/P-gp) and ABCC1 (MRP1)

In the subsections that follow, the *bona fide* ABC transporters in breast cancer drug resistance, i.e., P-gp/ABCB1/MDR1, BCRP/ABCG2 and MRP1/ABCC1 are briefly described.

B.2 Permeability-Glycoprotein (P-Glycoprotein/ABCB1/MDR1)

P-glycoprotein (P-gp/ABCB1/MDR1) and breast cancer resistance protein (BCRP/ABCG2) are among the most important and best characterized ABC transporters involved in drug mobilization, with the MDR phenotype being expressed in tumor cells [392,393,395,396]. P-gp, encoded by two multidrug resistant genes (*MDR1*/*ABCB1* and *MDR3*/*ABCB4* (also designated *MDR2*) [407,408], acts as an

ATP-dependent drug efflux pump (Figure 1.24) in many cancer cells [394,395,397]. In its mature form, P-gp is a 170-kDa transmembrane glycosylated protein (consisting of 1280 amino acids) [409] with ATP binding sites [410,411]. P-gp/ABCB1/MDR1, like BCRP/ABCG2 and MRP1/ABCC1, functions as an ATP-driven efflux pump [406] with poly-specificity for a large number of substrates, inhibitors and chemosensitizers (Table 1.10) [392,393,395,412-415], including neutral or positively charged hydrophobic compounds as well as investigative and clinically approved chemotherapeutic agents such as doxorubicin (adriamycin), etoposide, taxol, paclitaxel, vincristine, daunorubicin and irinotecan [392,393,395-397,406]. Several lines of evidence have demonstrated correlations between tumor P-gp expression and patient response rates or survival rates, or have reported observations of elevated P-gp expression following chemotherapy.

Table 1.10: Selected substrates of P-gp/ABCB1, MRP2/ABCC2 and BCRP/ABCG2

P-gp/ABCB1	**Analgesics**: asimadoline, fentanyl, morphine, pentazocine **Antiarrhythmics**: amiodarone, digoxin, lidocaine, propafenone, quinidine, verapamil **Antibiotics**: cefoperazone, ceftriaxone, clarithromycin, doxycycline, erythromycin, gramicidin A, gramicidin D, grepafloxacin, itraconazole, ketoconazole, levofloxacin, rifampicin, sparfloxacin, tetracycline, valinomycin **Anticancer drugs**: 5-fluorouracil, actinomycin D, bisantrene, chlorambucil, colchicine, cisplatin, cytarabine, daunorubicin, docetaxel, doxorubicin, epirubicin, etoposide, gefitinib, hydroxyurea, irinotecan (CPT-11), methotrexate, mitomycin C, mitoxantrone, paclitaxel, tamoxifen, teniposide, topotecan, vinblastine, vincristine **Antihistamines**: cimetidine, fexofenadine, ranitidine, terfenadine **Antilipidemic**: lovastatin, simvastatin **Calcium channel blockers**: azidopine, bepridil, diltiazem, felodipine, nifedipine, nisoldipine, nitrendipine, tiapamil, verapamil **Fluorescent dyes**: calcein AM (calcein acetoxymethylester), Hoechst 33342, rhodamine 123 **HIV-protease inhibitors**: amprenavir, indinavir, lopinavir, nelfinavir, saquinavir, ritonavir **Immunosuppressive agents**: cyclosporin A, cyclosporin H, FK506, sirolimus, tacrolimus, valspodar (PSC-833) **Natural products**: curcuminoids, flavonoids **Neuroleptics**: chlorpromazine, phenothiazine **Others**: BCECF-AM, bepridil, calcein-AM, diltiazem, endosulfan, leupeptin, methyl parathion, paraquat, pepstatin A, trifluoperazine, trans-flupentixol
MRP2/ABCC2	**Antibiotics:** ampicillin, azithromycin, cefodizime, ceftriaxone, grepafloxacine, irinotecan **Anticancer drugs**: cisplatin, doxorubicin, epirubicin, etoposide, irinotecan, mitoxantrone, methotrexate, SN-38, vinblastine, vincristine **Antihypertensives:** olmesartan, temocaprilate **HIV drugs**: adevovir, cidofovir, indinavir, lopinavir, nelfinavir, ritonavir, saquinavir **Others:** ethinylestradiol-3-O-glucuronide, genistein-7-glucoside, p-Aminohippurate, phloridzin, quercetin 4′-β-glucoside, *vinca* alkaloids
BCRP/ABCG2	**Antibiotics**: ciprofloxacin, norfloxacin, ofloxacin **Anticancer drugs**: daunorubicin, doxorubicin, epirubicin, etoposide, gefitinib, imatinib, irinotecan, mitoxantrone, methotrexate, SN-38, teniposide, topotecan, **Antivirals**: delavirdine, lopinavir, lamivudine, nelfinavir, zidovudine **Antihypertensives**: reserpine **Calcium channel blockers:** nicardipine **Lipid lowering drugs:** cerivastatin, pravastatin, rosuvastatin **Others**: azidothymidine, chrysin, cyclosporin A, lamivudine, ortataxel, quercetin

Source: [393].

For example, an extensive meta-analysis adjudicated that breast cancer patients with P-gp expressing tumors were 3-fold more likely to be unresponsive to chemotherapy

than those without P-gp expression and that chemotherapy/and or hormonal therapy increased the proportion of patients with P-gp expressing tumors [416]. Interestingly, a recent study has substantiated that overexpression of P-gp induced by neoadjuvant chemotherapy (NACT) in locally advanced breast cancer patients is a proof-of-concept of acquired chemoresistance and may thus aid as an intermediate checkpoint in monitoring chemosensitivity for personalized treatment options so that further doses of ineffective chemotherapy may be minimized in non-responders, translating into better patient safety [417]. Moreover, HIF-1α and erythropoietin (EPO) expression is significantly associated with P-gp expression in invasive breast cancer with lymph node metastases, demonstrating a correlation between P-gp expression and patients with $HER2^+$ breast tumors that do not express steroid receptors [418].

It has been noted that in some breast tumors, *ABCB1* expression is found primarily in tumor-associated macrophages (TAMs) and not in the tumor cells *per se* [419], further complicating generalizations about the transporter's association with heterogeneous breast cancers [416,420]. Furthermore, analysis of *ABCB1* expression in human TNBC samples procured from a previous study [421], illuminated that tumors with an EMT phenotype (low expression of the EMT marker claudin) had high basal levels of *ABCB1* expression compared with basal-like tumors [422]. These characteristics, as we have seen in Section A.4.5, likely contribute to the poor outcomes of MBC.

The expression levels as well as genetic variations in *ABCB1* are associated with conflicting altered therapeutic responses in primary breast tumors [423-425]. A recent combination of a prospective and retrospective cohort study involving patients with advanced stage invasive breast cancer who received neoadjuvant chemotherapy showed that the expression of P-gp has no significant statistical correlation to metastases, recurrence and survival [383]. Therefore, further pharmacogenetic

evaluation of the *ABCB1* gene is necessary to correlate it with breast cancer treatment outcomes and optimization of individualized therapy [396,424,426].

B.3 Breast Cancer Resistance Protein (BCRP/ABCG2)

Another member of the ABC transporter family involved in MDR development, i.e., ABCG2 (also known as breast cancer resistance protein, BCRP), is encoded by the *ABCG2* gene [393,427,428]. ABCG2 is a half-transporter composed of one TMD and one NBD domain (Figure 1.24) [429,430]. Notwithstanding certain substrate specificity variations, BCRP's repertoire substantially overlaps with that of MDR1/P-gp or MRP2 (Table 1.10). ABCG2 is able to transport a particularly wide range of substrates, including important anticancer drugs—mitoxantrone, methotrexate, the camptothecins topotecan and irinotecan, epipodophyllotoxins, imidazoacridinones and the anthracycline doxorubicin [428].

Indeed, many tyrosine kinase inhibitors (TKIs) (Section C) that are ABCG2 substrates (e.g., imatinib, gefitinib, nilotinib, vandetanib, pelitinib and neratinib) [431-433] perturb the functions of both P-gp and BCRP, and may prove useful in the design of novel drug-combination therapeutic strategies. Nilotinib inhibits efflux mediated by P-gp/ABCB1 and BCRP/ABCG2 *in vitro* [434]. In addition, *in vivo* studies performed by the same authors demonstrated that nilotinib, in combination with paclitaxel or doxorubicin, significantly caused regression of tumors overexpressing the ABCB1 or ABCG2 transporter [435]. Likewise, telatinib, a vascular endothelial growth factor receptor (VEGFR) TKI, enhances the anticancer activity of ABCG2 substrate anticancer drugs by inhibiting ABCG2 efflux transporter activity in drug-resistant cell lines [436]. Curcumin has been shown to synergistically increase the sensitivity of ABCG2-overexpressing cells to mitoxantrone, topotecan, SN-38 and doxorubicin, which are substrates of the transporter [437].

Several similar studies have provided experimental evidence for the use of microRNA (miRNA) as a potential target for preventing and reversing drug resistance in breast cancer by restraining the expression levels of ABCG2 [438-440]. ABCG2 expression has been frequently linked with poorer outcomes in acute myelogenous leukemia (AML) as well as acute lymphoblastic leukemia (ALL), breast and lung cancer [428,441,442]. Therefore, a better understanding of ABCG2 in cancer biology is warranted to design novel compounds to suppress its mediation of drug resistant tumors.

B.4 Multidrug Resistance Protein 1 (MRP1/ABCC1)

MRP1 is also a mediator of acquired drug resistance and has been extensively studied in lung cancer [392] and neuroblastoma [397]. Mammalian MRP1 has a MW of 190 kDa and is both N-glycosylated and phosphorylated. Human MRP1 contains 1531 amino acids with 2 NBDs and 17 TMs in 3 TMDs (TMD0, TMD1 and TMD2). MRP1 mRNA and/or protein is frequently detected in patient tumor samples and is currently considered to be the most clinically relevant of the MRPs with respect to drug resistance in cancer [392]. MRP1-mediated drug efflux has a chemoprotective role in multiple tissues, which is corroborated by reports that the occurrence of anthracycline-induced cardiotoxicity is associated with certain ABCC1 single nucleotide polymorphisms (SNPs) in breast cancer [443] and childhood acute lymphoblastic leukaemia [444].

Several studies have supported a role for MRP1 in the drug resistance expressed in solid tumors such as non-small-cell lung cancer, prostate cancer, and some types of breast cancer [445,446]. MicroRNAs (miRNAs) are endogenous small noncoding RNAs (~ 22 nucleotides long) that target complementary sequences within an mRNA molecule and cause gene silencing via translational repression or target degradation

[445]. Indeed, ABCC1 (MRP1) mRNA levels can be modulated by several mi-RNAs congruent with extrapolations from several miRNA databases, e.g., downregulation of miR-326 (which targets ABCC1 mRNA) and downregulation of miR-134 have been implicated in the drug resistance phenotypes of MRP1-overexpressing breast and lung cancer cell lines, respectively [447,448]. These miRNAs should be explored further to expand the armamentarium of available therapies that target ABC transporter-mediated MDR in breast cancer [204,449].

SECTION C: RECEPTOR TYROSINE KINASES (RTKS)

C.1 Receptor Tyrosine Kinases (RTKs) and Cancer Signaling Pathways

Tyrosine kinases (TKs, also referred to as tyrosine-specific protein kinases, TPKs) constitute a large and diverse group of enzymes that catalyze the transfer of a phosphate group from adenosine triphosphate (ATP) to a tyrosine residue on target proteins. Once phosphorylated, these target proteins become activated and, in turn, transactivate a plethora of effectors in a large network of signal transduction pathways that regulate cell proliferation, differentiation, survival (anti-apoptotic signaling and programmed cell death) and metabolism [450]. Mutations in kinase genes can cause aberrant phosphorylation in eukaryotes, which is associated with a multiplicity of clinicopathological conditions ranging from cancer to inflammatory diseases, diabetes, infectious diseases, cardiovascular disorders, cell growth and survival [451]. The significance of tyrosine phosphorylation is exemplified by the countless genomic alterations/mutations, rearrangements and autocrine activation events that are associated with TPKs.

These alterations include gain of function (GOF, i.e., upregulation / insertion / overexpression / amplification) and/or loss of function (LOF, downregulation/deletion) mutations [450-453]. The two main classes of kinase are tyrosine kinases (TKs) and serine–threonine kinases (STKs) [451]. TPKs can further be subdivided into two main classes: receptor TPKs (hereinafter referred to as receptor tyrosine kinases or RTKs), and non-receptor TPKs (NRTKs) [454]. The STKs and NRTKs will not be considered further for the purpose of this thesis' literature review, but recent reports abound [455-459]. RTKs play central roles in a wide range of cellular processes, including differentiation, proliferation, migration, angiogenesis, tumor progression and survival [452]. In humans, ~60 RTKs have been identified based on sequence homology and structure. These RTKs are clustered into 20 families: EGFR, PDGFR, VEGFR, FGFR, InsR, PTK7, TRK, ROR, MuSK, MET, TAM, TIE, EPH, RET, RYK, DDR, ROS, LMR, ALK and STYK1 [460,461].

Activation of RTKs is triggered by binding of receptor-specific ligands (e.g., growth factors) to their extracellular domains, which sets off ligand-induced receptor dimerization and/or oligomerization [452,462] as illustrated in Figure 1.26. The successive conformational changes culminate in *trans*-autophosphorylation of each tyrosine kinase domain (TKD), thus unlocking the *cis*-autoinhibition and rendering the TKD to assume an active conformation [462]. Autophosphorylation of RTKs also recruits and activates several downstream signaling proteins which contain Src homology-2 (SH2) or phosphotyrosine binding (PTB) domains which then bind to specific phosphotyrosine residues within the receptor and engage downstream mediators that propagate critical cellular signalling pathways [452]. Normal physiological levels of RTK activity are tightly regulated by homeostatic controls, however, RTKs acquire transforming abilities through several processes, and the ultimate outcome is the disturbance of the dynamic equilibrium between cell

growth/proliferation and cell death [462]. A gain-of-function (GOF) mutation (amplification) in an RTK leads to aberrant downstream signal transduction, not subjected to the normal 'checks and balances' that occur with physiological signaling. Of particular interest, is the uncontrolled and sustained proliferation caused by 'driver mutations' – defined as mutations that can confer a selective growth advantage hallmark on tumor cells [463].

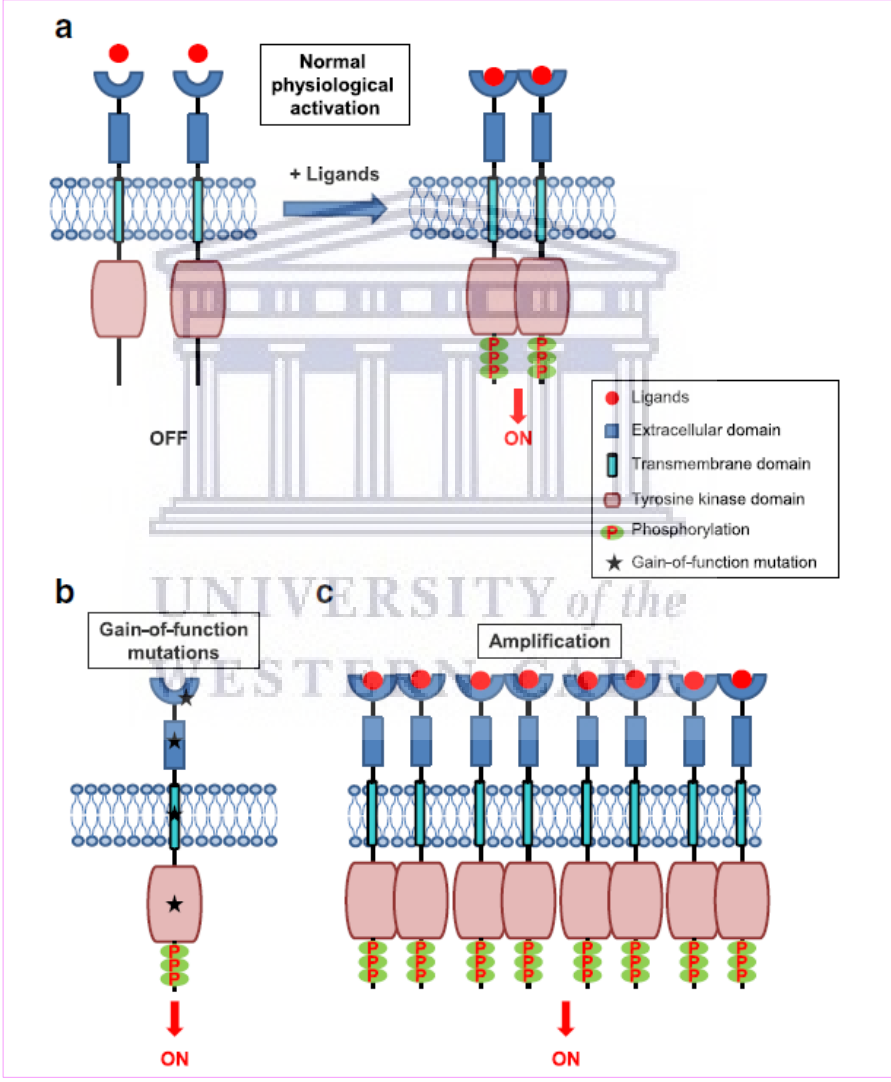

Source: [452]. **a** | Schematic representation of RTK activation in normal physiology. RTKs are activated through formation of inter-molecular dimerization in the presence of ligands, resulting in kinase activation and phosphorylation of the receptor C-terminal tail. **b** | Schematic representation of potential gain-of-function mutations in the various subdomains of an RTK. The mutations lead to constitutive activation of the RTK, typically in the absence of ligand. **c** | Overexpression of RTKs – often as a result of genomic amplification of the RTK gene - leads to increased local concentration of receptors.

Figure 1.26: Mechanisms of physiological and oncogenic RTK activation

The phosphoinositide 3-kinase (PI3K)/AKT signal transduction pathway (PI3K/AKT) is a paradigm of a critical signaling network correlated with essential cellular functions (e.g., cell survival, proliferation and differentiation) and aberrant processes that promote tumorigenesis in different types of cancer [464,465]. Aberrant activation of RTKs and somatic mutations at key nodes of the PI3K/AKT pathway represent two of the most pivotal mechanisms that activate the PI3K/AKT network system in human cancers [466]. Activation of classical PI3K/AKT signalling by RTKs is depicted in Figure 1.27 [453].

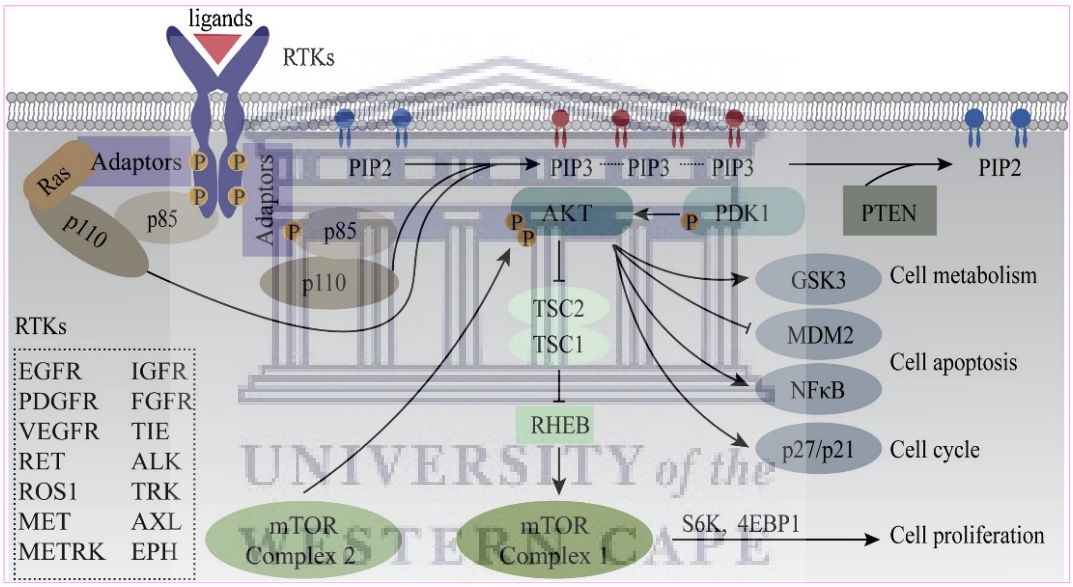

Source: [453]. Growth factors (e.g., EGF, VEGF, FGF, etc.) bind to extracellular regions of RTKs, cross-linking RTK into a dimeric complex. Following dimerization, conformation change leads to the release of *cis*-autoinhibition, while some special tyrosine residues in TKD domain are phosphorylated in cis or in a trans manner. Phosphorylation of RTKs enables recruitment of PI3K to the plasma membrane via direct binding of p85 to the intracellular domain of RTK (e.g., PDGFR) or indirect binding through adaptors (e.g., GRB2/GAB for EGFR, IRS1/IRS2 for IR). This results in depression of p110 kinase activity and therefore phosphorylate phosphatidylinositol-4,5-bisphosphate (PIP2) on the plasma membrane to generate the phosphatidylinositol-3,4,5-trisphosphate (PIP3). Accumulation of PIP3 on the cell membrane leads to AKT and phosphoinositide-dependent protein kinase 1 (PDK1) co-localization on membrane and AKT is phosphorylated by both PDK1 and mTOR complex 2 (mTORC2). Consequently, several downstream critical cellular effector proteins (e.g., MDM2, GSK3, p27, and p21) are phosphorylated, through which multiple cell functions, such as cell metabolism, cell apoptosis, cell proliferation and cell cycle, are regulated. Finally, the 3′-phosphatase PTEN dephosphorylates PIP3 and thus terminates PI3K signaling. GSK3, glycogen synthase kinase 3 (GSK3); MDM2, murine double minute 2; TSC1/2, tuberous sclerosis 1/2; RHEB, ras homologue enriched in brain; NFκB, nuclear factor κB; mTOR, mammalian target of rapamycin; S6K, ribosomal protein S6 kinase; 4EBP1, 4E binding protein 1; GRB2, growth factor receptor binding protein 2; GAB, GRB2-associated binder-1; IRS1/2, Insulin receptor substrate 1/2.

Figure 1.27: Activation of the classical PI3K signaling pathway by RTKs

Thus, mutations in the RTK-PI3K/AKT axis may be explored as novel predictive biomarkers of tumor responses to targeted therapies [453,467]. *EGFR* mutations serve as a paradigm to appreciate the spectrum and functional dimensions of mutations in RTKs. Section C.2, Section C.3 and Section C.4 review the respective systems integration of the EGFR/ERBB/HER family of RTKs and the ABC transporters in breast cancer, which is the focal point of the research undertaken in this thesis.

C.2 The Human EGFR/ERBB/HER Family in Breast Cancer

The human epidermal growth factor receptor (EGFR/ERBB/HER) family, also known as HER receptors, consists of four members: ERBB1 (EGFR/HER1), ERBB2 (HER2), ERBB3 (HER3) and ERBB4 (HER4) [453,468-470]. The *ERBB* gene symbol stems from the avian viral erythroblastosis oncogene to which these receptors are related. By convention, human *EGFR* gene symbols are indicated in uppercase italics. Thus, the four members of the *EGFR* gene family include: (i) *EGFR/ERBB1/HER1*, (ii) *ERBB2/HER2/NEU*, (iii) *ERBB3/HER3*, and (iv) *ERBB4/HER4*.

The EGFR/ERBB/HER receptors form homo-/hetero dimers in response to ligand binding and each shows distinct specificity and affinity to its ligand: epidermal growth factor (EGF), transforming growth factor-α (TGF-α) and amphiregulin specifically bind to EGFR, whereas heparin-binding EGF, betacellulin and epiregulin bind both HER4 and EGFR. By contrast, neuregulin consist of spliced isoforms that binds HER4 and HER3. HER-2 has no known ligands, but is a preferred heterodimerization partner for EGFR and other members of the ErbB receptor family [471].

Moreover, the transforming potential and signal pathways that are activated by the receptor binding are exclusive. For example, heterodimers EGFR-HER2 are associated with a more vigorous signal than that of homodimers EGFR-EGFR [469].

The signal transduction pathways associated with the activated EGFR/ERBB/HER includes mitogen-activated protein kinase (MAPK) which is responsible for cell proliferation, and phosphatidylinositol-3-kinase (PI3K/Akt) which regulates cell survival. Recruitment and activation of Akt triggers phosphorylation and inactivation of pro-apoptotic signals, and increases expression of anti-apoptotic signals [472].

These RTKs, along with other members, are significantly correlated with breast cancer progression and metastases Figure 1.28 [461]. EGFR is overexpressed in breast cancer and is associated with increased aggressiveness and poor clinical outcomes [473-475]. The EGFR/ERBB/HER family of RTKs is an archetypal proof-of-concept for breast cancer therapeutic exploitation and innovation (Figure 1.29) [476].

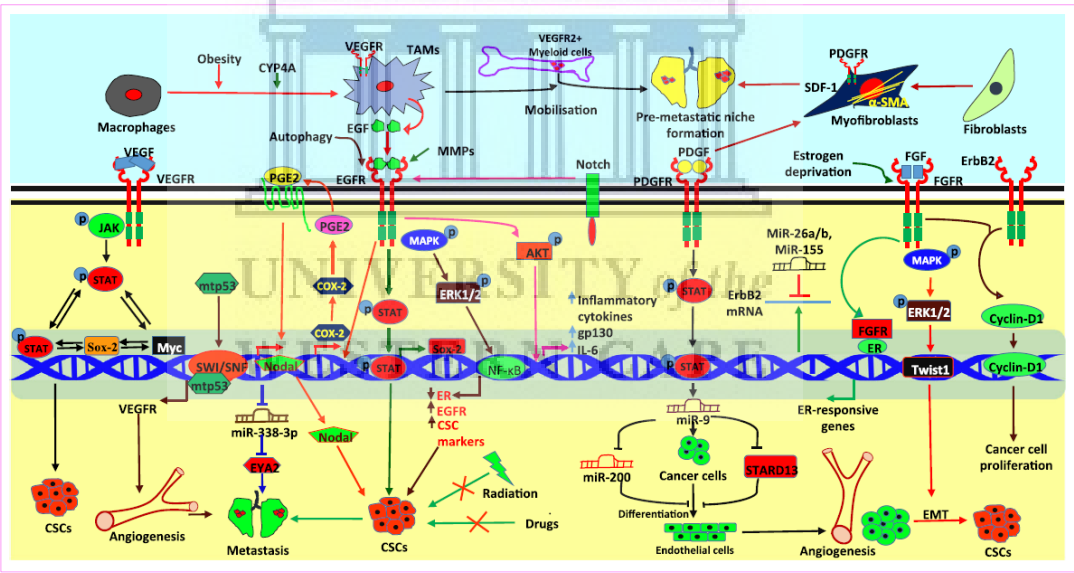

Source: [461]. VEGFR activates JAK/STAT signaling pathway to induce cancer stem cell phenotype through Myc and Sox2 expression. Mutant p53 induces the expression of VEGFR through the interaction with SWI/SNF complex. EGFR-regulated signaling also plays pivotal role in angiogenesis and metastasis. EGFR regulates the activation of JAK/STAT and MAPK signaling pathway to induce expression of Sox2 and other stem cell markers leading to enrichment of cancer stem cells. EGFR induces Akt phosphorylation to promote inflammation. PDGFR is expressed on stromal cells such as fibroblasts and is a marker of fibroblast activation. PDGFR-regulated STAT activation is involved in regulation of miR-9-mediated differentiation of cancer cells to endothelial cells leading to angiogenesis. FGFR-activated MAPK pathway induces EMT and CSC phenotype. Cooperation between the FGFR and HER2 regulates nuclear translocation of Cyclin D1 leading to enhanced cancer cell proliferation.

Figure 1.28: RTK-regulated signaling in breast cancer progression

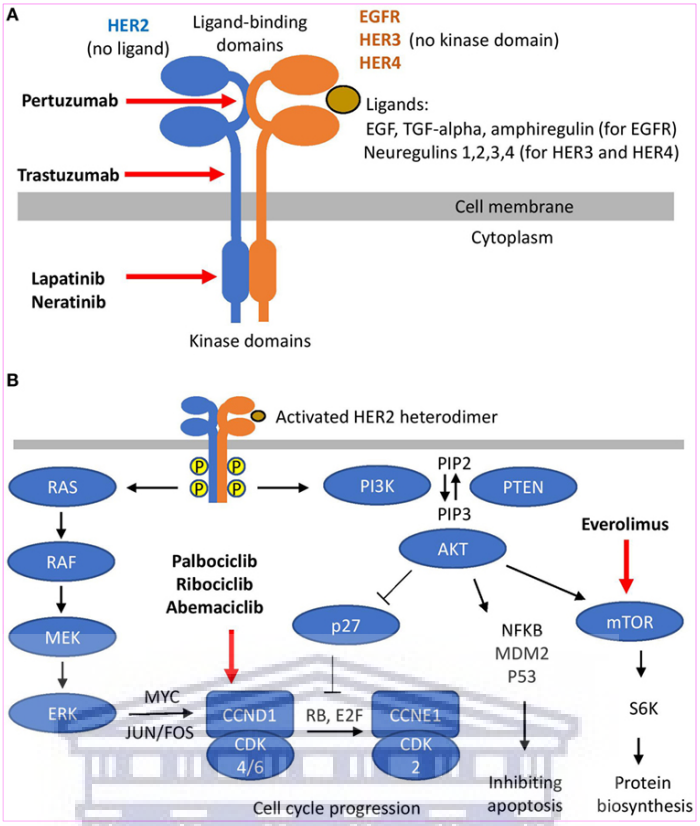

Source: [476]. **(A)** HER2 hetero-dimerization and HER2 targeting. **(B)** Signaling downstream of HER2 and its targeting.

Figure 1.29: Human epidermal growth factor receptor 2 (HER2) signaling and targeting

EGFR is the most extensively researched receptor of its family. To this end, several small molecule tyrosine kinase inhibitors (TKIs) and monoclonal antibodies (mAbs) have already been developed, undergone clinical trials, approved and applied as effective agents against MDR and metastatic breast tumors, but acquired resistance to these agents remain a constant clinical obstacle that needs to be circumvented [414,476-482]. Section C.3 provides an overview of TKIs in breast cancer, whereas Section C.4 focuses on the extensive repertoire of interactions between clinical TKIs (e.g., BCR-ABL, EGFR, VEGFR inhibitors) with the main ABC transporters implicated in MDR [483].

C.3 Tyrosine Kinase Inhibitors (TKIs) in Breast Cancer

Sustained cell proliferation is a hallmark of cancer that is modulated by the various components of the TME [11,46,122,275,278,281]. Drugs that target the kinase sites of RTKs to inhibit the phosphorylation of intracellular signaling hubs driving cell proliferation, metastases and angiogenesis are referred to as receptor tyrosine kinase inhibitors (RTKIs) or TKIs [484,485]. Since August 2019, 43 TKIs were approved by the Food and Drug Administration (FDA) as oncological agents [486]. Table 1.11 is a representative list of TKIs approved by the FDA for the treatment of various cancers [487].

The role of EGFR in cancer progression and as a prognostic biomarker is widely documented. It is also seen as a molecular target in TNBC [4,488]. Indeed, the EGFR signaling network encompasses more than 211 biochemical reactions and 322 signaling molecules [462,469,489]. EGFR is overexpressed in a number of cancers, including breast and non-small cell lung cancer [477]. HER2 overexpression is associated with a more aggressive type of disease and occurs in 20% of invasive cancers, with resistance to conventional chemotherapeutic agents [490]. The development of the well-known trastuzumab (Herceptin®, Genentech; South San Francisco, California, USA), a humanized mAb against HER2/EGFR2, paved the way for improved anti-EGFR treatment regimens [491].

Trastuzumab was approved in 1998 by the FDA for the adjuvant treatment of $HER2^+$ MBC and as monotherapy in chemotherapeutic-pre-treated MBC [492]. However, the emergence of trastuzumab-treatment resistance as well as the cardiotoxic effects has hampered the prognosis of MBC patients. Current alternative treatments in trastuzamab-resistant MBC involve the use of lapatinib, a tyrosine kinase inhibitor of EGFR and HER2, in conjunction with capecitabine [468,493].

Table 1.11: Representative list of TKIs approved by the US Food and Drug Administration (FDA) for the treatment of various cancers

Tyrosine Kinase Inhibitor	Approved	Pharmaceutical Company	Molecular Target	Cancer Targeted
Imatinib	2001	Novartis	Abl, PDGFR, SCFR	CML, GIST
Gefitinib	2003	AstraZeneca	EGFR	NSCLC
Nilotinib	2004	Novartis	Bcr-Abl, PDGFR	CML
Sorafenib	2005	Bayer	Raf, VEGFR, PDGER	Advanced RCC
Sunitinib	2006	Pfizer	PDGFR, VEGFR,	GIST, Advanced RCC
Dasatinib	2006	Bristol-Myers Squibb	Bcr-Abl, SRC, PDGFR	CML
Lapatinib	2007	GlaxoSmithKline	EGFR	Breast cancer
Pazopanib	2009	GlaxoSmithKline	VEGFR, PDGFR, FGFR	Advanced RCC, STS, NSCLC
Crizotinib	2011	Pfizer	ALK	NSCLC
Ruxolitinib	2011	Novartis	JAK1, JAK2	Myelofibrosis
Vandetanib	2011	AstraZeneca	VEGFR, EGFR	Advanced thyroid cancer
Axitinib	2012	Pfizer	VEGFR	Advanced RCC
Bosutinib	2012	Wyeth	Abl, SRC	CML
Afatinib	2013	Boehringer Ingelheim	EGFR	NSCLC
Erlotinib	2013	Roche	EGFR	NSCLC
Ceritinib	2014	Novartis	ALK	NSCLC
Osimertinib	2015	AstraZeneca	EGFR	NSCLC
Lenvatinib	2015	Eisai	VEGFR	DTC
Alectinib	2015	Roche	ALK	NSCLC
Regorafenib	2017	Bayer	VEGFR, EGFR	HCC, CRC, GIST
Neratinib	2017	Puma	HER2	Breast cancer
Brigatinib	2017	Ariad	ALK	NSCLC

Adapted from Jiao et al. [487]. tyrosine kinase inhibitor (TKI); chronic myeloid leukemia (CML); gastrointestinal stromal tumors (GIST); non-small cell lung cancer (NSCLC); renal cell carcinoma (RCC); soft tissue sarcoma (STS); differential thyroid carcinoma (DTC); hepatic cellular carcinoma (HCC); colorectal carcinoma (CRC); Abelson murine leukemia viral oncogene (Abl); platelet-derived growth factor receptor (PDGFR); mast/stem cell growth factor receptor (SCFR); epidermal growth factor receptor (EGFR); breakpoint cluster region-abelson oncogene (Bcr-Abl); rapidly accelerated fibrosarcoma (Raf)-retroviral oncogene possessing a serine/threonine kinase activity; vascular endothelial growth factor receptor (VEGFR); fibroblast growth factor receptor (FGFR); anaplastic lymphoma kinase (ALK); Janus kinase (JAK)–signal transducer and activator of transcription; Rous sarcoma viral oncogene non-receptor tyrosine kinase (NRTK) involved in cellular proliferation, survival, migration, and angiogenesis (SRC); human epidermal growth factor receptor 2 (HER2).

Furthermore, aberrations in the normal expression and functioning of EGFR due to mutations and implication in MDR cancers [454,494,495], including breast cancer, further underscores the significance of anti-EGFR therapies [450,484,496]. HER2 is overexpressed in ~20% of all breast cancers through the conversion of the HER2 proto-oncogene into the HER2 oncogene [497,498]. This biomarker correlates with more aggressive cancers compared to $HER2^-$ breast cancers with features like drug resistance, rapid spread and higher metastasis [499]. The primary HER2 aberration is gene amplification. Essentially, HER2 fulfils a crucial role in breast cancer as a driver mutation. Approximately 20% of patients with breast cancer harbor HER2 amplification; therefore, anti-HER2 drugs such as trastuzumab and lapatinib exhibit significant efficacy in patients with HER2-positive breast cancer [500]. Lapatinib and neratinib are small molecule TKIs approved for $HER2^+$ breast cancer—these drugs, reversibly and irreversibly inhibit both EGFR1 and HER2, respectively, by blocking ATP-binding to the receptors [485], but acquired resistance to neratinib has been demonstrated to occur via a $HER2^{T798I}$ gatekeeper mutation in a patient with $HER2^{L869R}$-mutant driven breast cancer [501].

HER3 is often co-expressed with HER2 and plays a pivotal role in cell growth and survival in HER2-dependent breast cancers [502]. Moreover, HER3 mutations are not only coupled with resistance to ER-targeted therapies, but also with resistance to EGFR1- and HER2-indicated treatments [503]. By contrast to the rest of EGFRs, membranous HER4 homodimerization generally correlates with an increase in survival rate and a reduction of proliferation indices, and thus good prognosis, whereas nuclear HER4 is associated with lower survival rates [490]. Recent advances in genomics analyses have paved the way for more promising EGFR/ERBB TKI candidates (Figure 1.30) [461,468,504,505] and mAbs (Table 1.12) to be evaluated in many clinical trials [490].

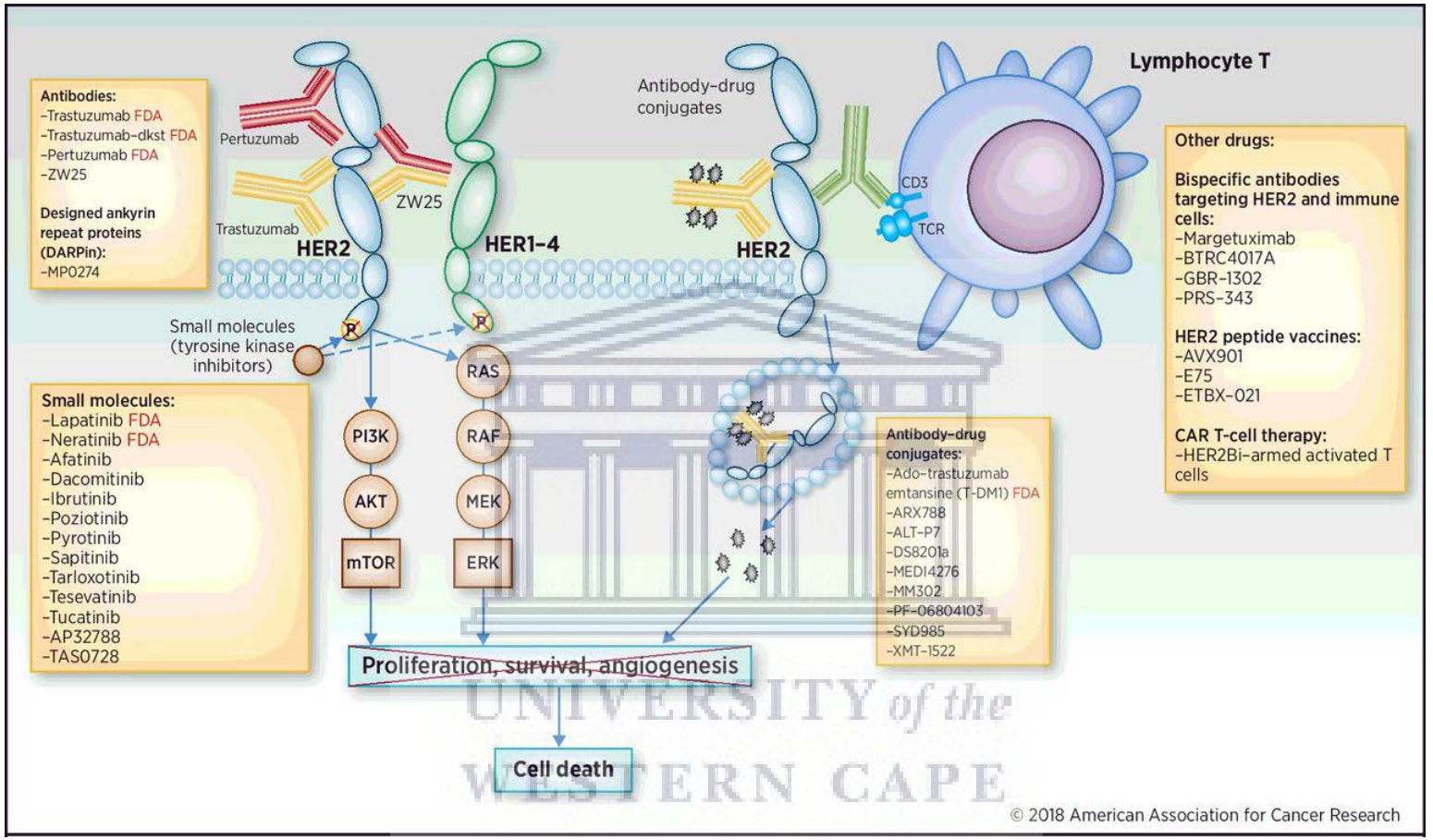

Source: [504]. HER2-targeted therapies approved by the FDA for HER2-positive cancer or currently in clinical trials (from www.clinicaltrials.gov, last accessed July 11, 2018). Therapies followed by FDA in red font indicate that the drug is FDA approved. CAR, chimeric antigen receptor.

Figure 1.30: Approved and emerging HER2-targeted therapies in clinical development

Table 1.12: Targeting therapy against EGFR family in breast cancer under investigation for treatment of breast cancer

Drug	Format	Target	Clinical Phase	Literature
Cetuximab	Chimeric MAb	EGFR1	I, II	[44,55]
Panitumumab	Humanized MAb	EGFR1	II	[56,57]
Zalutumumab	Human MAb	EGFR1	I, II	[60,61]
Trastuzumab	Humanized MAb	HER2	approved	[64,65,66]
Pertuzumab	Humanized MAb	HER2	approved	[70,71,72,73]
Trastuzumab Emtansin	Antibody-drug conjugate	HER2	approved	[75,76]
Trastuzumab Deruxtecan	Antibody-drug conjugate	HER2/Tubulin	I, II	[78]
MEDI4276	Bispecific antibody	HER2	I, II	[79]
Seribantumab	Humanized MAb	HER3	I, II	[80,81,82]
Lumretuzumab	Humanized MAb	HER3	I	[83,84]
MM-111	Bispecific antibody	HER3	I, II	[85,86]
MCL-128	Bispecific antibody	HER2/3	I, II	[87]
Gefitinib	Small-molecule tyrosine kinase inhibitor	EGFR1	approved	[91,92]
Erlotinib	Small-molecule tyrosine kinase inhibitor	EGFR1	approved	[94,95,98,99]
Lapatinib	Small-molecule tyrosine kinase inhibitor	EGFR1/HER2	approved	[70,100,101]
Neratinib	Small-molecule tyrosine kinase inhibitor	HER2	approved	[105,106,108]
Canertinib	Small-molecule tyrosine kinase inhibitor	pan-ERB	I, II	[113]
Afatinib	Small-molecule tyrosine kinase inhibitor	EGFR1, HER2, HER4	approved	[114,115,116]

In addition to the small molecule TKIs, several mAbs that bind specifically to the extracellular domain of EGFRs were designed to attack cancer via two mechanisms, i.e., (i) by binding the extracellular domain ideally to inhibit ligand binding and thus block receptor dimerization, auto-phosphorylation and downstream signaling as well as inducing receptor internalization, degradation and stable downregulation; (ii) alternatively, mABs have been coupled to cytotoxic agents. Thus, if they are co-internalized with the receptor, they induce cell death and impart cancer treatments with high selectivity, toxicity and improved therapeutic windows (Table 1.12) [453,490].

C.4 Tyrosine Kinase Inhibitors (TKIs) and ABC Transporters

In Section C.3, the use of TKIs and mAbs in the suppression of RTK-mediated tumor progression and uncontrolled cancer cell proliferation have been described. In this section, the specific role of ABC transporters in the development of resistance to TKIs will be discussed with a view to delineating the key determinants that can be targeted to overcome such drug resistance mechanisms. RTK overexpression correlates with poor patient outcomes, e.g., not only HER2 levels, but also the profusion of EGFR and HER3 have been associated with poor prognosis of breast cancer patients [503].

Amplification of RTKs confers on tumor cells the ability to evade cytotoxic stress. For example, mesenchymal-epithelial transition factor (MET) and HER2 amplification frequently accompanies the emergence of chemoresistance in cancer patients with EGFR-mutations [506,507]. MDR is principally mediated by an increased rate of drug efflux, alterations in drug metabolism, or activation of DNA repair systems [336,508]. An increase in drug efflux leads to decreased intracellular accumulation of the drug, limiting successful treatment outcome [396]. The ABC family of transporters, mainly P-glycoprotein (P-gp/MDR1/ABCB1), MRP1/ABCC1 and BCRP/ABCG2 have been

implicated in the energy-dependent efflux of a multitude of structurally and functionally diverse substrates (Section B). The TKIs have proven to effectively and specifically inhibit malignant cell growth and metastasis in most tumor types, including head and neck, gastric, prostate and breast cancer and several types of leukemia [468,484,507]. It is hardly surprising that the MDR transporters have been recognized as important mediators of the general ADME-Tox (absorption, distribution, metabolism, excretion, toxicity) properties of small molecule TKIs, as well as key factors of resistance against targeted anticancer therapeutics [431,432,454,483,509-516].

The therapeutic efficacy of TKIs depends on their access to intracellular targets, which may be altered by RTK mutations. However, ABCG2 and ABCB1 have a selectively high affinity for some of these kinase inhibitors (imatinib, nilotinib and dasatinib), but not for others (bosutinib) [432,513]. Therefore, both ABCG2 and ABCB1 efflux pumps modulate tumor cell resistance to certain TKIs, which stimulate their ATPase activity [516]. Imatinib was shown to be a substrate for ABCC1/MRP1 and it could amplify the expression of ABCC1/MRP1, which conferred imatinib resistance [517].

Likewise, sorafenib, as a substrate for ABCC2/MRP2, might contribute to sorafenib resistance [518], and so on. A list of selected TKIs and their interactions with ABC transporters appears in Table 1.13 [519]. Therefore, the combination of TKIs and cytotoxic agents may enhance the effectiveness of anticancer therapies since TKIs compete for ABC transporter binding and subsequent efflux and so reverse MDR to cytotoxic drugs (Figure 1.31; Figure 1.32; Table 1.14) [515,519]. It has been noted that ABCG2 has several polymorphic variants with altered substrate specificities and activities which may be clinically relevant for personalized TKI therapeutic considerations [454,516,520].

Table 1.13: Interactions of selected TKIs with ABC transporters

ABC Transporter	Substrate	Inhibitor	Substrate/Inhibitor
ABCA3	dasatinib [7]; imatinib [7]; nilotinib [7]	–	–
ABCB1 (P-glycoprotein, MDR1)	brigatinib [9]; crizotinib [35]	cabozantinib [36]; canertinib * [31]; cediranib * [37]; ceritinib [38]; erlotinib [34]; gefitinib [14]; motesanib * [39]; neratinib [29]; osimertinib [40]; regorafenib [34]; saracatinib * [41]; sorafenib [34]; sunitinib [21]; vandetanib [42]; vatalanib * [43]	afatinib [44]; alectinib [33]; apatinib * [17]; bosutinib [45]; dasatinib [45]; ibrutinib [27]; imatinib [46]; lapatinib [47,48]; nilotinib [45]; nintedanib [22]; pazopanib [31,34]; ponatinib [19]
ABCC1 (MRP1)	–	cediranib * [37]; ibrutinib [49]; sunitinib [21]; vandetanib [42]	–
ABCC2 (MRP2)	sorafenib [50]	sunitinib [51]	–
ABCC3 (MRP3)	imatinib [52]; sorafenib [53]	–	–
ABCC4 (MRP4)	imatinib [8]	erlotinib [54]; gefitinib [54]; sorafenib [55]; sunitinib [51]	–
ABCC6 (MRP6)	dasatinib [10]; nilotinib [10]	–	–
ABCC10 (MRP7)	gefitinib [11]	erlotinib [16]; ibrutinib [27]; imatinib [56]; lapatinib [16]; linsitinib * [13]; masitinib * [30]; nilotinib [20]; ponatinib [57]; sorafenib [24]	–
ABCC11 (MRP8)	–	sorafenib [24]	–
ABCG2 (BRCP)	brigatinib [9]; gefitinib [58]	axitinib [34]; cabozantinib [15]; canertinib * [31]; ceritinib [38]; erlotinib [34]; icotinib * [59]; linsitinib * [13]; masitinib * [60]; osimertinib [40]; quizartinib * [61]; regorafenib [34]; sorafenib [24]; sunitinib [21]; tandutinib * [15]; vandetanib [42]; vatalanib * [43]	afatinib [32]; alectinib [33]; apatinib * [17]; bosutinib [45]; dasatinib [45]; imatinib [46]; lapatinib [47]; nilotinib [45]; pazopanib [31,34]; ponatinib [19]; telatinib * [25]

* experimental TKIs.

Source and cross-references: [519].

Table 1.14: TKIs as inhibitors of ABC transporters implicated in MDR and corresponding substrate drugs

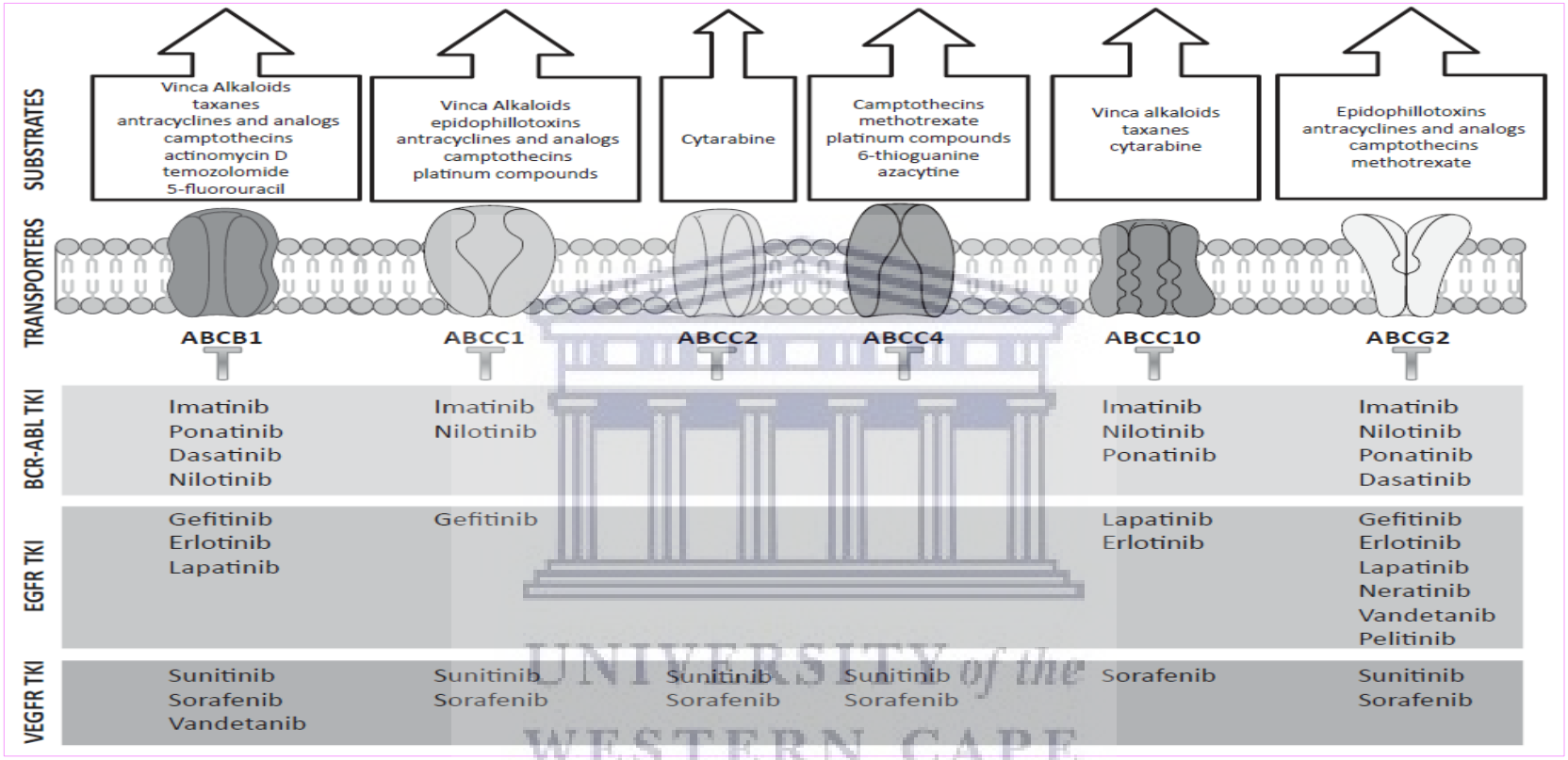

Source: [483]. paradigmatic examples of TKIs functionally demonstrated to act as inhibitors of specific ABC transporters and their potential capability to impact on the tumor cell efflux and subsequently on cytotoxicity of antitumor drugs recognized by the pumps.

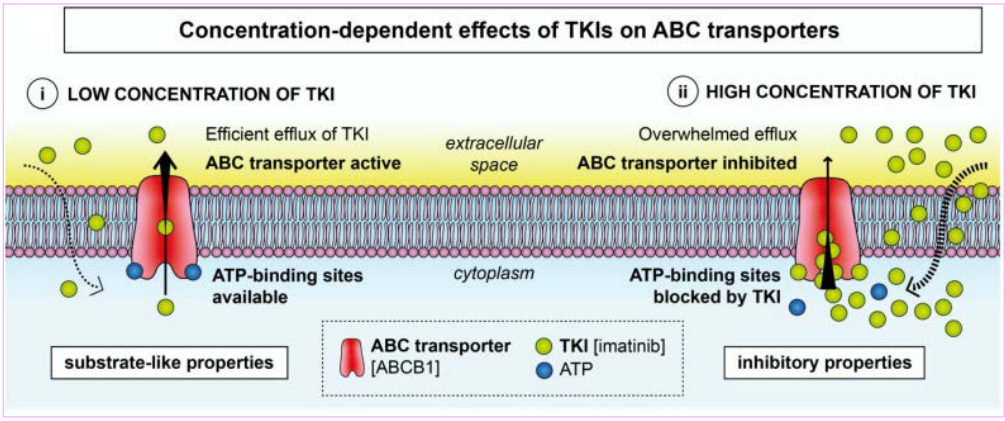

Source: [519]. At low concentrations (i), some TKIs exhibit substrate-like properties and are exported out of the cell by the respective ABC transporters. A high concentration of TKIs (ii) leads to blockage of the ATP-binding sites of ABC transporters, which results in inhibited efflux of the TKI. Examples of TKIs and specific transporters are given in square brackets.

Figure 1.31: Transport of TKIs by ABC transporters

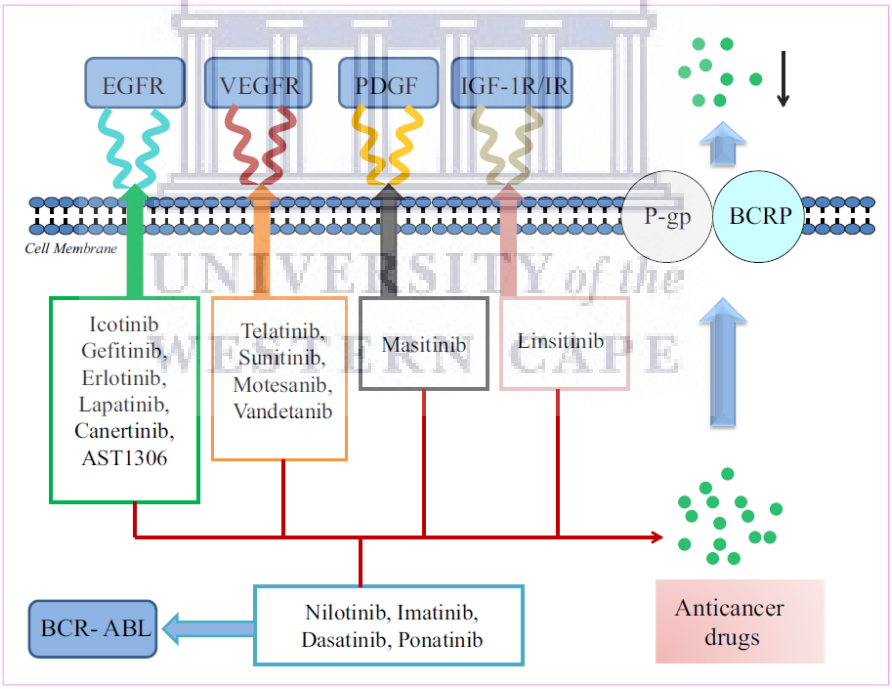

Source: [393]. BRAF TKI, breakpoint cluster region-Abelson (BCR-ABL) TKIs, epidermal growth factor receptor (EGFR) TKIs, vascular endothelial growth factor receptor (VEGFR) TKIs, platelet-derived growth factor (PDGF) inhibitors, insulin-like growth factor 1 (IGF-1R)/insulin receptor (IR) TKI either block the function of or down-regulate MDR-ABC transporters such as P-gp/ABCB1 and BCRP/ABCG2. Black solid arrows indicate a reduction on the efflux of various anticancer drugs.

Figure 1.32: Overview of TKIs as antagonists in the regulation of ABC transporters

In addition, other transporters, such as ABCC10/MRP7 or ABCC4/MRP4, may also play roles in MDR and its reversal by TKIs [514,519]. Several clinical studies of RTK-targeted therapeutics in breast cancer have recently been reviewed, underscoring the revolutionary impact of RTKIs on the practice of oncology [461,483-485]. Clearly, TKIs play a crucial role in overcoming chemotherapy resistance, thus opening vistas for further exploitation of their repurposing and combination with other anticancer drugs, particularly conventional substrates of the ABC transporters, to identify safer and more effective clinical chemotherapeutic indications (Table 1.23 and Figure 1.32) [393,483,519].

SECTION D: DRUGS SELECTED FOR THIS STUDY

D.1 EGFR Inhibitor I (EGFRi)

EGFR Inhibitor I (CAS 879127-07) (cyclopropanecarboxylic acid-(3-(6-(3-trifluoro-methyl-phenylamino)-pyrimidin-4-ylamino)-phenyl)-amide) is a 4,6-dianilinopyrimidine compound, predominantly used for research, but less effective when compared to 2,4-dianilinopyrimidine compounds. Ceritinib is a 2,4-dianilinopyrimidine compound which received FDA approval for the treatment of patients with anaplastic lymphoma kinase (ALK)-positive non-small cell lung cancer (NSCLC) who have developed resistance to crizotinib, an ALK TKI [486,521]. The 4,6-dianilinopyrimidine compound has a higher affinity for EGFR when tested against 55 recombinant kinases and demonstrated potency against EGFR mutations L858R and L861Q [522]. EGFR Inhibitor I's selectivity for the protein kinase EGFR was further demonstrated in a study that involved investigations of selectivity of 178 kinase inhibitors against 300 human

protein kinases, in the presence of ATP molecules. EGFR Inhibitor I scored 0.78 using the Gini coefficient, which measures the selectivity of an inhibitor against a single target [523].

D.2 Doxorubicin (DOX)

Doxorubicin is an anthracycline antibiotic that is used as an effective chemotherapeutic agent in the treatment of many solid tumors [524]. It was first isolated in 1967 from a mutagenic strain of *Streptomyces* bacterium, a gram-positive *Actinomycete* [525-527]. Its anticancer activity was first demonstrated in mice and rats with Oberling-Guerin myeloma, leukemia and Ehrlich ascites carcinoma [528]. Doxorubicin causes DNA intercalation of double-stranded DNA, but the major target is considered topoisomerase II which results in inhibition of cell proliferation and induction of apoptosis [524]. Furthermore, doxorubicin has the ability to arrest cell cycle progression and induce the release of free radicals of ROS *in vitro* [529]. As effective as doxorubicin appeared to be as a neoplastic agent, the side effects associated with its dose administration overshadow these contributions [530,531].

Cardiotoxicity, the major side effect induced by doxorubicin, has hampered its clinical significance as well as patient survival. DNA damage, senescence and oxidative stress in cardiomyocytes are associated with the cardiotoxicity [532]. Moreover, doxorubicin drug resistance has been reported in MCF-7 breast cancer cells overexpressing the ABC transporter, P-glycoprotein (P-gp) [533]. The transport of doxorubicin by P-gp was recently confirmed using targeted molecular dynamics (MD) simulations and molecular mechanics, i.e., Poisson-Boltzmann surface area (MM-PBSA) analysis [534]. To address the clinical implications of drug toxicity and drug resistance, more recent studies demonstrated an effective reduction of toxic side effects of doxorubicin when combined with a plant derived flavonoid, quercetin, as well

as the potential of decreasing the expression of P-gp in cancer cells [535,536]. This was further supported by a laboratory study that highlighted the synergistic interactions between metformin and doxorubicin with inhibition of P-gp and reversal of drug resistance in doxorubicin-resistant MCF-7 breast cancer cells [537,538].

D.3 Cisplatin (Cis-Diammine-Dichloro-Platinum)

The effects of cisplatin (cis-diamminedichloroplatinum) (CDDP) were first observed in 1965, whereby the presence of this platinum metal compound was associated with inhibition in bacterial cell growth [539]. What was also observed at this early stage of experimentation, was cisplatin's efficacy against a range of solid tumors, particularly testicular cancer [539]. This was followed by the FDA's approval of cisplatin as clinical treatment against testicular and bladder cancer in 1978. In tumor cells, cisplatin's major target is DNA. The anticancer drug functions by forming interstrand crosslinks between the base pairs of DNA that form adducts, causing DNA damage that arrests cell cycle progression and DNA replication, and inhibition of transcription which ultimately leads to apoptosis [540].

Notwithstanding the effectiveness of cisplatin as an antineoplastic agent in a myriad of cancers, its toxic side effects as well as resistance in certain cancers were observed in early research [539,541]. One of the major side effects associated with cisplatin is nephrotoxicity. Cisplatin is absorbed and excreted by the kidneys which causes damage to the proximal tubular cells through pathways associated with oxidative stress, inflammation and fibrogenesis [542]. Numerous platinum analogues were synthesized in an attempt to overcome cisplatin toxicity, with carboplatin being successful in lowering toxicity, but drug resistance still remained a major concern for patient survival outcome [543,544]. Cisplatin resistance is associated with a number of mechanisms, including amplified DNA repair, increased drug inactivation and

altered intracellular drug accumulation [545-547]. At the cellular level, copper transporters facilitate uptake of cisplatin whereas ABC transporters (P-gp) are responsible for its drug efflux. In tumor cells, upregulation of P-gp confers cisplatin resistance [548]. Numerous studies have been conducted over the years that focused on reversing or eliminating cisplatin drug resistance. An decoction extract of *Taxux chinensis*, a tree indigenous to China, has shown significant results in reducing chemotherapeutic resistance to cisplatin in NSCLC stem cells by effectively inhibiting the ABC transporters [549]. Similarly, cepharantine, an anticancer compound extracted from the plant *Stephania cepharantha*, effectively reversed P-gp-mediated cisplatin resistance in oesophageal squamous carcinoma cells [550]. More recently, a study involving the use of phytochemicals to overcome cisplatin drug resistance by directly targeting P-gp has yielded encouraging results and further highlighted the need to explore alternative treatment options in the clinical setting [548].

SECTION E: RESEARCH CONTEXT AND SIGNIFICANCE

E.1. Problem Statement

Worldwide, breast cancer is the most frequent type of cancer diagnosed in females, besides being the leading cause of death amongst females in underdeveloped countries [38,39,78,80,82]. Breast cancer deaths are generally higher in many low- and middle-income countries, such as those in sub-Saharan Africa [375] and developing Asian countries [376]. According to the CONCORD cancer survival program, e.g., 5-year survival rates (between 2000 and 2014) for breast cancer was 90% in the United States, but 40% in South Africa, further suggestive of the global

disparities in the effective delivery of oncology services allied to breast and other cancers [377,378]. Breast cancer heterogeneity and the corresponding disparate patient responses to current evidence-based drug regimens have become an important exploratory concept of multidisciplinary disease management, consistently highlighting trends for cutting-edge multitargeted personalized therapies and treatment de-escalation (dose-reduction) to curb adverse events in ~70–80% of patients with early-stage, non-metastatic disease [147]. In recent years, the hallmarks and co-expression networks of breast cancer drivers, especially the interrelationships among the signature genes/biomarkers encoding self-sufficiency in growth signalling and insensitivity to anticancer drugs (chemoresistance) as mediated by the amplification or mutation of growth factor receptor tyrosine kinases (RTKs) and ABC multidrug transporters, respectively, have received a renewed surge of optimism for their translational potential [28,241,551].

Moreover, the therapeutic combination of different TKIs with other compounds or standard anticancer drugs for repurposing and more efficacious personalized treatments with reduced toxic side effects has not only become a leading investigative paradigm of targeting oncogenic RTK signaling, but also for circumventing intrinsic or acquired MDR for successful patient survival outcomes [393,396,454,483,484,509-511,514,552].

In this study, we have investigated various combinations of different classes of anticancer drugs (doxorubicin and cisplatin) and a tyrosine kinase inhibitor (EGFR Inhibitor I) on the human MCF-7 wild-type and triple-negative MDA-MB231 breast carcinoma cell lines, in terms of their cytotoxic and apoptotic potential, drug-drug (combinatorial) interactions, ABCB1/P-gp drug efflux perturbation, and *ABCB1* and *EGFR* gene expression profiles.

E.2 Hypothesis

We hypothesize that the EGFR Inhibitor I will significantly downregulate the function of P-gp as an efflux pump, thereby sensitizing the ABC transporter whilst the combinations with conventional antineoplastic agents (doxorubicin and cisplatin) will yield greater anticancer efficacy at lower concentrations than those predicted by their individual toxicities against MCF-7 wild-type breast cancer cells and triple-negative MDA-MB 231 breast cancer cells *in vitro*.

E.3 Aims and Objectives of the Study

E.3.1 Purpose of Study

The purpose of this study was to explore methods to address drug resistance through a multitargeted approach with the aim of informing current knowledge and best practices of anticancer treatment regimens that will ultimately be beneficial to breast cancer patients in improving patient prognosis by enhancing the efficacy of drug treatment by chemosensitization of P-gp and, at the same time, reducing drug toxicities by lowering the drug doses in combination regimens.

E.3.2 Aim of the Study

The aim of this specific study was two-fold. Firstly, we focused on exploring the use of a small molecule ATP-competitive tyrosine kinase inhibitor (TKI) individually as well as in combination with current chemotherapeutic drugs used clinically, i.e., doxorubicin and cisplatin, in order to target P-gp expression in two human breast carcinoma cell lines, namely, MCF-7 (ER^+ positive) and MDA-MB 231 (TNBC) with the aim to increase chemotherapeutic drug efficacy with a lower toxicity. Secondly, we investigated the effects of the doxorubicin-cisplatin-TKI drug interactions on the EGFR which plays a significant role in cancer cell survival and progression. In addition, *ABCB1* and *EGFR* gene expression profiles in these cell lines were also evaluated.

E.3.3 Objectives of the Study

The objectives of this study were to:

1. Evaluate combinations of a TKI (EGFR Inhibitor I) with conventional molecularly-targeted antineoplastic agents (doxorubicin and cisplatin) for enhanced efficacy towards MCF-7 and MDA-MB 231 TNBC breast cancer cell killing *in vitro*.

2. Assess the apoptosis-inducing effects of EGFR Inhibitor I, doxorubicin and cisplatin on MCF-7 and MDA-MB-231 TNBC breast carcinoma cells.

3. Correlate the *in vitro* effects of the various drug treatments individually and in combination with the molecular sensitivity of *EGFR* and *ABCB1* expression in MCF-7 and MDA-MB-231 TNBC breast carcinoma cells.

4. Assess the effects of single and pairwise combinations EGFR Inhibitor I, doxorubicin and cisplatin on the function of the ABC transporter (ABCB1, MDR1, P-gp) in MCF-7 and MDA-MB-231 TNBC breast carcinoma cells.

SECTION F: OUTLINE OF THESIS CHAPTERS

This study is presented in 7 chapters arranged as follows:

F.1 Chapter 1: Introduction and Literature Review

Chapter 1 is an introduction the study. It provides a literature review of the hallmarks

of cancer and how these can be exploited for cancer therapy. The literature review further encompasses various aspects of breast cancer, including epidemiology, etiology and prevention, molecular pathogenesis, classification of molecular subtypes and staging, current evidence-based breast cancer therapeutics, breast cancer survival, clinical drug resistance, disease recurrence and adverse events.

Special sections are devoted to the impact of drug combinations, multidrug transporters and receptor tyrosine kinases on the current breast cancer landscape. The chapter also comprises the research context, problem statement, hypothesis, aims and objectives, context and significance of the study.

F.2 Chapter 2: Research Methodology and Experimental Design

This chapter covers the research methodology applied in the execution of the study, namely experimental design, drugs and chemicals used, culture and maintenance of the MCF-7 and MDA-MB-231 breast cancer cell lines, drug preparations, drug cytotoxicity and drug combination response surface analysis, apoptosis (caspase-3/7) assays, P-glycoprotein drug efflux measurements, and *ABCB1* and *EGFR* gene expression analysis using Real-Time qPCR.

F.3 Chapter 3: Results and Discussion of the Analyses of Single Agent and Combination Drug Responses

The chapter presents the results and discussion of the dose-response curve analysis of MCF-7 and MDA-MB-231 breast cancer cell lines exposed for various time intervals to EGFRi, DOX and CDDP, either alone or in dual equimolar concentrations. In addition, detailed analyses of the drug combinations are described and discussed in relation to drug potency and dose-response surfaces based on the Bliss independence and Loewe additivity synergy models.

F.4 Chapter 4: Results and Discussion of the Analysis of Caspase-3/7 Activity for Apoptosis Detection

In this chapter, programmed cell death (apoptosis) induced in MDA-MB-231 and MCF-7 breast carcinoma cells by the different drug treatments (EGFRi, DOX and CDDP) as assessed by the CellEvent™ Caspase-3/7 assay is appraised.

F.5 Chapter 5: Results and Discussion of the Analysis of P-Glycoprotein-Mediated Drug Efflux Function

In this chapter, P-gp efflux pump function as assessed by means of the intracellular retention Calcein-AM assay following exposure of MDA-MB-231 and MCF-7 breast carcinoma cells to 10-fold increments of EGFRi, DOX and CDDP, is presented and discussed.

F.6 Chapter 6: Results and Discussion of RT-qPCR Gene Expression Analysis of *EGFR* and *ABCB1*

This chapter deals with the expression of the *EGFR* and *ABCB1* genes in MDA-MB-231 and MCF-7 breast carcinoma cells in the presence of single agent $\log_{10}$ concentrations (range 0.1 to 100 µM) of EGFRi, DOX and CDDP.

F.7 Chapter 7: Final Perspectives

This chapter contexualizes the study's findings in terms of the current breast cancer landscape.

CHAPTER 2

RESEARCH METHODOLOGY AND EXPERIMENTAL DESIGN

2.1 Introduction

This chapter focuses on the research methodology and the design that has been chosen for the study. The research context and significance—problem statement, hypothesis, aims and objectives of the study were described in Chapter 1. This chapter summarizes the materials and methods used such as the drugs tested and chemicals required for the maintenance of the MCF-7 and MDA-MB 231 breast carcinoma cell cultures. Analyses of carcinoma cells exposed to EGFR I inhibitor (EGFRi), doxorubicin (DOX) and cisplatin (CDDP), alone and in combination, included growth and dose-response curves (cytotoxicity assays), drug synergy analysis, apoptosis evaluation using caspase-3/7 assays, P-gp drug efflux pump function evaluation as using Cayman's calcein-AM multidrug resistance assay and gene expression analysis of *ABCB1* and *EGFR* using Real-Time PCR. The statistical methods used for data analysis are also described.

2.2 Drugs and Chemicals

Drugs and chemicals used in this study included EGFR Inhibitor I [cyclopropane carboxylic acid-(3-(6-(3-trifluoro-methyl-pheny-lamino)-pyrimidin-4-yl) amino)-phenyl-amide) (CAS879127-07-8 Calbiochem, Merck, Darmstadt, Germany), Doxorubicin Hydrochloride (CAS 25316-40-9, Sigma-Aldrich, St Louis, MO, USA), Cisplatin (Cis-Diammineplatinum (II) Dichloride) (CAS 15663-27-1, Sigma-Aldrich St Louis, MO, USA), heat-inactivated fetal bovine serum (HIFBS) (Biochrome, The Scientific Group),

Phosphate-buffered saline (PBS) (Gibco, Life Technologies), Dulbecco's Modified Eagles Medium supplemented with F-12 Glutamax (Gibco Life Technologies), Penicillin/Streptomycin (Gibco Life Technologies), Trypsin-EDTA (Gibco Life Technologies), 0.9% NaCl, Dimethyl sulfoxide (DMSO) (Sigma-Aldrich, St Louis, MO, USA), Calcein-AM Multidrug Resistance kit (Cayman Chemicals, Item no. 600370), CellEvent™ Caspase-3/7 Green Detection Reagent (Cat. No. C10423, Invitrogen, ThermoFisher Scientific), MTT-thiazolyl blue tetrazolium bromide (CAS 298-93-1, Sigma-Aldrich), CTS™ (Cell Therapy Systems) Synth-a-Freeze® medium (ThermoFisher Scientific) Maxima First Strand cDNA Synthesis Kit for RT-qPCR (ThermoFisher Scientific), RNeasy Mini QIAcube Kit (QIAGEN, ThermoFisher Scientific)

2.3 Culture of MCF-7 and MDA-MB-231 Breast Carcinoma Cells

Cell lines were acquired from the American Type Culture Collection (ATCC) and included an estrogen receptor-positive (ER^+) breast carcinoma cell line, MCF-7, catalogue number (ATCC HTB-22) and a triple-negative breast cancer cell line (TNBC), MDA-MB-231, catalogue number (ATCC HTB-26). All tissue culture operations were carried out in a model NU-5510E NuAire DHD Autoflow automatic CO_2 air-jacketed incubator (and an AireGard NU-201-430E Horizontal Laminar Airflow table top workstation that provides a HEPA filtered clean work area (NuAire). Frozen 2-ml vials of both cells lines were suspended and maintained in pre-warmed Dulbecco's Modified Eagle Medium (DMEM) supplemented with 10% heat-inactivated fetal bovine serum (HIFBS), 0.2% penicillin/streptomycin (100 U/ml penicillin and 100 µg/ml streptomycin) and grown as monolayer cultures at 37°C in T-25 cm^3 sterile cell culture flasks and transferred into a humidified incubator (Relative Humidity/RH 80%) in an atmosphere of 5% CO_2:95% air. The cells were allowed to attach to the culture substratum overnight. Once 80% confluency was reached, the media was aspirated

and the cell monolayer washed with PBS to remove all traces of media. Then, cells were trypsinized using 2 ml of 0.25% Trypsin-EDTA. This was followed by placing the Trypsin-EDTA containing flasks into the incubator for 2 min intervals until the monolayer of the cells were starting to detach from the substratum of the flask. Equal amounts (2 ml) of culture media were added to the flasks to neutralize the enzymic effect of Trypsin-EDTA. The cells were gently mixed using an electronic pipette aid and detached cells aspirated and transferred to a 15-ml conical centrifuge tube, placed in a centrifuge and spun for 5 min at 2500 rpm to separate the cells from the medium-trypsin solution. After centrifugation, the supernatant was discarded and the cell pellet resuspended in 5 ml complete medium. The cells were mixed thoroughly to ensure a homogeneous cell suspension, 1 ml of which was transferred to T-75 cm^3 culture flask containing 9 ml complete medium to maintain stock cultures.

2.4 Drug Preparation

Cisplatin (CDDP), Doxorubicin (DOX) and EGFR Inhibitor I (EGFRi) were prepared according to the manufacturers' instructions. DOX and EGFRi were dissolved in DMSO whereas CDDP was dissolved in 0.9% NaCl to ensure biological activity [553]. The compounds were prepared in a log_{10} dose/concentration range of 0.001, 0.01, 0.1, 1, 10 and 100 µM in neat medium and administered to cell cultures. The 50% inhibitory concentration of cellular population (IC_{50}) was calculated in subsequent experiments.

2.5 Cellular Proliferation Assays

Cell viability of the MDA-MB-231 and MCF-7 cell lines was periodically checked by adding 15 µl of 0.4% trypan blue to 15 µl cell suspension in an Eppendorf tube and mixed. This was done with every subculture and seeding of cells. Trypan blue is a dye that differentiates between viable and non-viable cells by only staining non-viable cells

and being excluded from viable cells. Viable cells were counted using a Countess II automated cell counter (Invitrogen, ThermoFisher Scientific).

2.6 Cytotoxicity Assays

MTT (3-[4, 5-dimethylthiazol-2-yl]-2, 5-diphenyl tetrazolium bromide), a yellow tetrazolium salt is reduced to purple formazan, following cleavage of the tetrazolium ring by succinate dehydrogenase within the mitochondria of metabolically active cells [554]. The inability of formazan to diffuse through the cell membrane allows its accumulation within healthy living cells. The insoluble formazan crystals that form within the cell can be dissolved in acidified isopropanol, DMSO or sodium dodecyl sulphate (SDS). MCF-7 and MDA-MB 231 breast cancer cells were seeded at a density of 5 x 10^4 cells/ml per well into sterile 96-well flat-bottom microtiter plates. A 100-µl cell suspension was added to each well and cells allowed to attach for 24h under normal incubation conditions. After 24h, culture medium was aspirated and replaced with 100 µl of medium containing increasing $\log_{10}$ dose concentrations (0.001, 0.01, 0.1, 1, 10 and 100 µM) of EGFRi, DOX and CDDP.

MDA-MB-231 cultures were also exposed to DOX and CDDP in combination at equimolar concentrations ratio 1:1 over the respective time intervals. All experiments were repeated in triplicate. Plates were subsequently incubated for 24, 48 and 72 hours respectively. After the incubation period, 20 µl MTT solution (5 mg/ml MTT in PBS) was added to each well, the plate covered with aluminium foil and incubated for 2h. Thereafter, the supernatant was aspirated and 200 µl neat isopropanol was added to each well and incubated at room temperature on a vortex shaker for 25 min, still enclosed in foil. Plates were read at 560 nm using the Titertek Multiskan GO model MCC/340 microplate reader.

2.8 CellEvent™ Caspase-3/7 Assay

CellEvent™ Caspase-3/7 green detection reagent is a fluorogenic substrate used to detect activated caspase-3 and -7. The substrate, a four-amino acid peptide—Asp (D)–Glu(E)–Val(V)–Asp(D), i.e., DEVD, is cell permeable, but intrinsically non-fluorescent, and conjugated to a nucleic acid binding dye. After caspase-3 or -7 is activated in apoptotic cells, the DEVD substrate is cleaved, which allows the binding dye to attach to the DNA and produce a bright fluorogenic response that is detected at absorption and emission wavelengths of 502 nm and 530 nm, respectively.

MCF-7 and MDA-MB 231 cells were seeded into sterile flat bottom 96-well black plates at a density of 5 x10^4 cells/ml and incubated overnight at 37°C. This was followed by preparing the compounds and exposing the cells to EGFRi, DOX and CDDP individually at log_{10} dose/concentration ranges 0.1-100 µM. Cells were incubated for 24h. The caspase-3/7 was prepared by dilution in complete medium to a final concentration of 6 µM. The culture medium was aspirated from each well and 100 µl of the prepared reagent added to the respective wells and incubated at 37°C for 30 min. After incubation, the plates were removed and the cells imaged using a fluorescent plate reader at 502/530 nm excitation and emission spectrum.

2.8 ABCB1/P-Glycoprotein (P-gp) Drug-Efflux Measurement

ABCB1/P-gp's function as a drug efflux pump was evaluated using the Calcein-AM Multidrug Resistance Assay Kit. The assay incorporates the use of Calcein-AM, a non-fluorescent cell-permeable dye. The Calcein-AM assay has been shown to identify both substrates and inhibitors of MDR proteins, and therefore offer an advantage over other assays [555-558]. Upon transport of Calcein-AM into viable cells, intracellular esterases bind and trap the compound where it exhibits green fluorescence. Calcein-AM is a substrate of P-gp and is rapidly excluded in cells overexpressing the protein

thereby reducing the fluorescence in those cells. Cyclosporin A (a competitive inhibitor) and Verapamil (a non-competitive inhibitor) are used as positive controls in acting as inhibitors of P-gp in the assay. MCF-7 and MDA-MB-231 cells were seeded into sterile 96-well flat bottom plates at a density of 5 $x10^4$ cells/ml per well and incubated overnight at 37°C. This was followed by exposing the cells to EGFRi individually at log10 dose/concentration ranges 0.01-100 µM and in combination with DOX and CDDP at equimolar dose ranges. Cells were incubated for 24h and 48h, respectively. On the respective days of the experiment (24h or 48h), the medium containing the compounds were aspirated from the wells and 100 µl of each positive control (Cyclosporin A and Verapimil) added to the untreated wells and incubated for 30 min. After incubation, 100 µl of Calcein-AM solution were added to all the wells and incubated for a further 30 min at 37°C. After incubation, the plates were removed and centrifuged at 400 x g at room temperature for 5 min. The supernatant was aspirated and 200 µl of ice-cold medium added to each well. Plates were again centrifuged at 400 x g at room temperature for 5 min followed by aspiration of the supernatant and another addition of 200 µl of ice-cold medium to each well. The plates were immediately analyzed using a fluorescent plate reader at excitation wavelength of 485 nm and emission wavelength of 535 nm.

2.9 Real-Time PCR and *ABCB1* and *EGFR* Gene Expression Analysis

2.9.1 Sample Preparation

MCF-7 and MDA-MB 231 cells were seeded at a density of 5 x 10^4 cells/ml into sterile 48-well plates. A 100-µl cell suspension was added to each well and cells allowed to attach for 24h under normal incubation conditions. After 24h, culture medium on all cell cultures were aspirated and replaced with 100 µl of medium containing increasing log_{10} dose/concentrations (0.001, 0.01, 0.1, 1, 10 and 100 µM) of EGFRi, DOX and CDDP. The cells were also exposed to the three compounds in combination (EGFRi

-DOX, EGFRi-CDDP and DOX-CDDP) at equimolar concentration ratios 1:1 for 48h. After 48h, the medium containing compound was removed and washed with 1 ml PBS to remove all traces of drug. The PBS was aspirated and 500 µl Trypsin-EDTA was added to each well and incubated for 3 min to allow cells to detach. After detachment of the cells, the cells were centrifuge and resuspended in neat medium.

2.9.2 RNA Extraction

Total RNA were extracted from the treated and untreated MCF-7 and MDA-MB-231 cell cultures using an automated RNA extraction RNeasy Mini QIAcube Kit (QIAGEN) on the QIAcube instrument according to the manufacturer's instructions. The extracted RNAs were then quantified using the Nanodrop 8000 spectrophotometer and the absorbance ratios at 260/280 and 260/230 measured to assure RNA purity. The integrity of each RNA sample was assessed with a RNA 6000 NanoChip kit (Agilent Technologies) using the Agilent 2100 electrophoresis Bioanalyzer (Agilent Technologies).

2.9.3 cDNA Synthesis

The concentration of RNA samples was normalized to 0.5 ng/µl and 8 µl was reverse-transcribed using the Maxima First Strand cDNA Synthesis Kit for RT-qPCR with dsDNase (ThermoScientific) in a total volume of 20 µl according to the manufacturer's instructions. The reaction temperature was set at 60°C for 30 min followed by heat denaturation at 85°C for 5 min. No reverse transcriptase control (NRT) reactions (one sample from each biological replicate) were performed alongside to assess for genomic DNA contamination of the RNA sample. A No template control (NTC) reaction was also included to assess for reagent contamination. The primers used for the study were selected from literature (Table 6.1). Two sets of primers for the target genes and one of each of the reference genes were selected. The efficiency of each

primer pair was determined by means of standard curves and the specificity of each primer pair was evaluated and confirmed by BLAST analysis. The target genes *ABCB1* and *EGFR* each had two sets of primers 105 bp, 253 bp and 125 bp, 166 bp, respectively, to determine the pair with the highest specificity and efficiency. Primer set specificity for *ABCB1* and *EGFR* and the selected reference genes were assessed by generation of respective melting curves.

2.9.4 cDNA Pre-Amplification

To increase sensitivity for the samples at low concentration, a pre-amplification protocol was applied. Aliquots of primers for *ABCB1* (105 bp), *EGFR1* (125 bp), *ACTB, GAPDH, HPRT1* and *HSPCB* were pooled to a final concentration of 500 nM each. Two µl (2 µl) of each reverse transcription reaction was mixed with 1.0 µl of the primer pool, 5.0 µl TaqMan Pre-Amplification MasterMix (Applied Biosystems) and nuclease-free water to a final volume of 10 µl. The pre-amplification reaction was performed on ABI9700 (Applied Biosystems) using the following cycling conditions: single cycle at 95°C for 10 minutes; 14 cycles at 95°C for 15 seconds, 60°C for 4 minutes; single cycle at 99°C for 10 minutes. Pre-amplification products were diluted 1:20 in 1× Tris-EDTA (TE) buffer.

2.9.5 RT-qPCR Assay

RTR-qPCR was performed in a total volume of 10 µl reactions utilizing 2 µl diluted pre-amplification product as template, 5 µl of 2x PowerUp SYBR Green I MasterMix (ThermoFisher Scientific), and both the forward and reverse primers at the optimized final concentrations. NTC and NRT were included in all assays as negative controls. Each reaction was run in triplicate. Reactions were performed on the QuantStudio 12K Flex Real-Time PCR System (Applied Biosystems) using the following cycling parameters: UDG activation at 50°C for 2 min; initial denaturation at 95°C for 2 min

followed by 40 cycles of 95°C for 15 sec, 15 sec at the optimized annealing temperature and 72°C for 1 min. Melting curve analysis was performed on all reactions at the end of the PCR run using default parameters. Amplification data were analyzed with the Life Technologies QuantStudio 12K Flex Software v1.2.4, applying user-defined thresholds to obtain Cq-values. Outliers in technical replicate reactions, reactions that showed no amplification and reactions that showed multiple Tm peaks during melt curve analysis were removed before analysis.

2.10 Data Analysis

Statistical analysis for the cytotoxicity assays were performed by non-linear regression analysis to determine the best-fit IC_{50} estimates and corresponding 95% confidence intervals (95% CI) for EGFR Inhibitor I (EGFRi), Doxorubicin (DOX) and Cisplatin (CDDP), using the [Inhibitor] vs. normalized response - variable slope template of GraphPad Prism (GraphPad Prism version 8.43 for Windows, GraphPad Software, San Diego California USA, http://www.graphpad.com).

$$y = \frac{100\%}{1 + \left(\frac{x}{IC_{50}}\right)^{s}}$$

In this equation, *s* is a slope factor. The equation assumes that *y* falls with increasing *x*. In this study, *y* represents cell survival and *x* the concentration of drug. Many inhibitory dose-response curves have a standard slope of -1.0. The variable slope model does not assume a standard slope, but rather fits the Hill slope from the data [559-561]. The IC_{50} is a measure of the potency of a drug and is thus the concentration of drug required to achieve the half-maximal effect ($E_{max}/2$), and assumes a minimum (E_0) and a maximum (E_{max}) effect [561-569]. The Potency Ratio (PR), also referred to as the Dose-Reduction Index (DRI) [315,324], for each drug used in equimolar dual

combinations with the other drugs was computed according to Fieller's theorem [570-572] as simplified by Bliss [317,573,574], often designated as the Ratio of Means Test [568,575-580].

$$(PR = DRI)_{1=} \frac{(D_x)_1}{(D_1)}$$

$$(PR = DRI)_{2=} \frac{(D_x)_2}{(D_2)}$$

Where $(D_x)_1$ is the concentration of Drug 1 [$(D_x)_1$] that induces 50% inhibition of cell growth, and $(D)_1$ the concentration of the dual agent combination $(D_x)_1$ + $(D_x)_2$ that induces 50% inhibition of cell growth. Likewise, $(D_x)_2$ is the concentration of Drug 2 [$(D_x)_2$] that induces 50% inhibition of cell growth, and $(D)_2$ the concentration of the dual agent combination $(D_x)_1$ + $(D_x)_2$ that induces 50% inhibition of cell growth The PR or DRI is a measure of how many fold the dose of each drug in a synergistic combination may be reduced, at a given effect level, compared with the doses of each drug alone [327]. The reduced dose which will reduce toxicity at the increased effect should lead to beneficial clinical consequences. DRI = 1 indicates no dose reduction, whereas DRI>1 and <1 indicate favorable and unfavorable dose-reduction, respectively [315]. In our system, the PRs were calculated from the IC_{50}s of the drug alone and the drug in combination and tabulated (Table 3.2).

Dose-reduction (DR) plots for the entire range of drug concentrations used to induce different effect levels are shown in the results. Drug synergy and combination analysis was performed based on the Dose Equivalence Principle (DEP) or Loewe Additivity model [342-344] expanded as the Chou-Talalay Combination Index (CI) theorem and algorithm [314,327,346,581], and the Multiplicative Survival Principle (MSP), introduced as the Bliss Independence model [317].

All these models of synergy have been reviewed extensively over the years towards a consensus framework for the determination and reporting of drug combination synergy metrics [288,290-292,314,318-321,323,350,561,582,583].

In this study, we have limited our dose-response surface analysis to the Loewe Additivity and Bliss Independence models as illustrated in Figure 2.1.

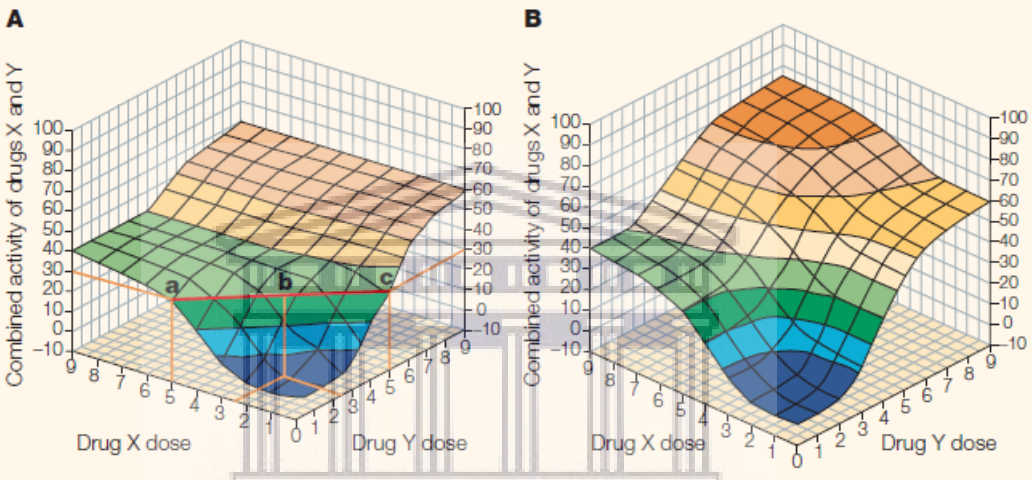

| **Response surfaces for combination effect reference models.** Synergy or antagonism is determined by comparing a measured response to a chosen combination effect reference model. Different reference models are used to represent different types of underlying connectivity, and no one model is preferred in all circumstances. **A** | Loewe additivity is the expected response for compounds that act similarly on the same molecular target. The combined effect is determined by adding specific doses, after correcting for the relative potency of each compound at a particular effect level. So, according to this model, the combined activity of two compounds X and Y at concentrations C_X and C_Y is the activity level I_{XY} that satisfies the equation $C_X/C(I_X = I_{XY}) + C_Y/C(I_Y = I_{XY}) = 1$ (where C_X and C_Y are the single-agent concentrations for X and Y that individually produce an activity of I_{XY}). Therefore, in the example shown, 30% inhibition (shown by the red line) can be achieved with 5 dose units of X (point **a**) or 5 dose units of Y (point **c**), or with 2.5 dose units of X plus 2.5 units of Y (point **b**). Note that the response surface has linear iso-effect contours for effect levels that both single agents can achieve, and that the combined activity never exceeds that of the most effective single agent. **B** | Bliss Independence is the expected combination response when both single agents act on targets interacting through independent probability events, like bullets emanating from separate guns in target practice. Here, the combined activity I_{XY} at concentrations C_X and C_Y satisfies the equation $I_{XY} = I_X + I_Y - I_X I_Y$ (where I_X and I_Y are the single-agent activity levels at C_X and C_Y). This much simpler expression depends only on the single-agent effect levels at corresponding concentrations, so Bliss Independence can be experimentally determined even if the single-agent curves have not been well sampled. In the example, note that the same single-agent curves as in (**A**) produce nonlinear iso-effect contours, and the combination reaches higher effect levels than the single agents ever do.

Source: [311]

Figure 2.1: Response surfaces for combination effect reference models

For this purpose, we have utilized the new Combenefit™ software tool (licensed under the MIT Licence, https://sourceforge.net/p/combenefit/) that enables the visualization, analysis and quantification of drug combination effects in terms of synergy and/or antagonism. Data from combination assays were processed using classical synergy models (Loewe and Bliss) and presented as dose-response surfaces (plotted as either a heat map or 3D surface plot where the *x* and *y* axes are drug concentration and the color or *z* axis is the measured effect, respectively), contour plots of isoboles (linear iso-effect lines), synergy/antagonism matrix distributions and dose-reduction (DR) plots [584]. Deviations between observed and expected responses with positive and negative values denote synergy and antagonism, respectively.

Apoptosis (Caspase-3/7) and P-gp efflux activity (Calcein-AM) assays, as well as results of RT-qPCR *EGFR* and *ABCB1* gene expression analysis in MCF-7 and MDA-MB-231 breast carcinoma cells were analyzed by One-Way Analysis of Variance (ANOVA) followed by Dunnett's multiple comparisons *post hoc* test for pairwise analysis between a set of treatments against a single control mean), at a significance level of $p<0.05$. All ANOVA tests were performed using SigmaPlot version 14 from Systat Software, Inc., San Jose California USA, www.systatsoftware.com).

CHAPTER 3

RESULTS AND DISCUSSION OF THE ANALYSES OF SINGLE AGENT AND COMBINATION DRUG RESPONSES

3.1 Introduction

In this study, MDA-MB-231 TNBC and MCF-7 breast carcinoma cells were exposed to a $\log_{10}$ concentration range of 0.001-100 µM of EGFR Inhibitor I (EGFRi), doxorubicin (DOX) and cisplatin (CDDP), individually or in dual equimolar combinations with the other drugs over a period of 24-72h. Cells were seeded at a density of $5x10^4$ cells/ml per well and cytotoxicity was determined at 24h, 48h and 72h intervals using the MTT assay as described in Section 2.6. The best-fit IC_{50} estimates and corresponding 95% confidence intervals (95% CI) for EGFRi, DOX and CDDP were determined by non-linear regression analysis of dose-response data using the variable slope model of GraphPad Prism v8 (http://www.graphpad.com) as detailed in Section 2.10. The same drug concentrations were utilized in subsequent experiments or were slightly modified, where indicated.

3.2 Effects of EGFRi, DOX and CDDP on MDA-MB-231 TNBC Cell Survival

The dose-response curves of the effects of exposure of MDA-MB-231 TNBC cells to EGFRi, DOX and CDDP for 24-72h are presented in Figure 3.1 and Figure 3.2. The estimated IC_{50}s of the drugs, i.e., the concentrations that produced half-maximal responses ($E_{max}/2$) in MDA-MB-231 TNBC cells are depicted in Table 3.1. The dose-response curves exhibited the classical hyperbolic or sigmoidal shape. The potency (IC_{50}) of EGFRi after 48h and 72h was approximately 3-4-fold greater than that of the

24h exposure, i.e., 7.05 µM (95% CI: 5.244 to 9.486) and 6.03 µM (95% CI: 4.566 to 7.965), respectively, compared to 23.60 µM (95% CI: 14.35 to 39.88; Table 3.1). Thus, the lower the IC_{50} of a drug, the greater its potency [350,561,585]. EGFRi also has a greater single-agent time-dependent potency than either DOX or CDDP, particularly after 24 and 48h exposure intervals, whereas the cytotoxic effects after 72h treatment of the cells with DOX and CDDP were almost identical, judging by the IC_{50}s and their associated 95% CIs that overlapped, i.e., 9.67 µM (95% CI: 3.35 to 32.71) and 49.29 µM (95% CI: 6.656 to 285.9; Table 3.1).

3.3 Effects of EGFRi, DOX and CDDP on MCF-7 Cell Survival

MCF-7 (ER^+) breast carcinoma cells were exposed to the same drugs under the same conditions as the MDA-MB-231 TNBC cells. The results are summarized in Figure 3.3, Figure 3.4 and Table 3.1. In MCF-7 breast carcinoma cells, the half-maximal inhibitory concentrations (IC_{50}s) for EGFRi at 24, 48 and 24h closely resemble those observed for MDA-MB-231 TNBC cells (Table 3.1). The IC_{50} for DOX in MCF-7 breast carcinoma cells at 24h was estimated to be 6315 µM (95% CI: 1178 to 107487), which suggests a high level of resistance to the anthracycline antibiotic, but after 48 and 72h of exposure, these cells were 760-fold and 4511-fold more sensitive to DOX, based on IC_{50}s of 8.3 µM (95%CI: 3.759 to 20.97) and 1.40 µM (95% CI: 0.593 to 3.631), respectively. In MCF-7 breast carcinoma cells, the IC_{50} for CDDP after 24h exposure, i.e., 256 µM (95% CI: 142.4 to 632.8) was equivalent to that estimated for MDA-MB-231 TNBC cells after 24h exposure, i.e., 144 µM, but this was not significant as the non-linear regression did not converge (R^2=-0.57). Similarly, no significant differences (p=0.528) between the IC_{50}s of CDDP were noted for the cell lines after 48 and 72h exposure, based on values of 27.79 µM (95% CI: 19.57 to 39.47) vs 60.49 µM (95% CI: 27.34 to 137.9) and 71.15 µM (95% CI: ND) vs 49.29 µM (95% CI: 6.656 to 285.9), respectively.

3.4 Analysis of Drug Potencies in MDA-MB-231 TNBC Cells Exposed to Dual Agent Combinations of EGFRi, DOX and CDDP

MDA-MB-231 TNBC cells were exposed to EGFRi, DOX and CDDP for 24, 48 and 72h time intervals in combination using equimolar dose ratios in the concentration range of 0.001-100 µM. The results are summarized in Table 3.1, Table 3.2 and Figure 3.5. The hierarchy of time-dependent potency of the various combinations were as follows: 72h (EGFRi + DOX—IC_{50} of 0.46 µM; 95% CI: 0.166 to 1.138) > EGFRi + CDDP—IC_{50} of 2.87 µM; 95% CI: 1.451 to 5.870) > DOX + CDDP—IC_{50} of 27.73 µM; 95% CI ND). In terms of the same hierarchical system, EGFRi + CDDP at 24 and 48h were more potent than either EGRi + DOX and DOX + CDDP.

The potency of EGFRi in the EGFRi + DOX dual drug combination regimen was enhanced 13-fold (95% CI: 6.304 to 239.532) after 72h exposure—implying favorable dose reduction and efficacy [315], whereas no enhancement occurred after 24 and 48h (PR < 1 at both time intervals), indicating unfavorable dose reduction (Table 3.2). By analogy, the potency of DOX in the EGFRi + DOX two-drug combination was increased 4- and 21-fold, respectively, for the 48 and 72h exposure times, but no favorable dose reduction was observed after 24h.

In MDA-MB-231 TNBC cells, the potency of CDDP eclipsed that of EGFRi in the combination of EGFRi and CDDP, after both the 48 and 72h exposure times, i.e., 75-fold (95% CI: ND) vs ~9-fold (95% CI: ND) and 17-fold (95% CI: -49.82 to 161.56) vs 2-fold (95% CI: 1.031 to 12.643). Nonetheless, both EGFRi and CDDP produced favorable time-dependent dose-reductions (or potencies) in the two-drug combination regimen. In the case of the DOX + CDDP equimolar mixture, DOX ranks 10-fold higher in potency than CDDP, particularly after 48h exposure of MDA-MB-231 TNBC cells to the combination.

3.5 Analysis of Drug Potencies in MCF-7 Breast Carcinoma Cells Exposed to Dual Agent Combinations of EGFRi, DOX and CDDP

As with MDA-MB-231 TNBC cells, the MCF-7 breast carcinoma cells were exposed to concurrent two-drug combinations in equimolar $\log_{10}$ concentrations in the range of 0.001-100 µM, viz., EGFRi + DOX, EGFRi + CDDP and DOX + CDDP for 24, 48 and 72h time intervals (Figure 3.6, Table 3.1 and Table 3.2). EGFRi + DOX and DOX + CDDP yielded similar high potencies after 48h [i.e., IC_{50} of 0.85 µM (95% CI: 0.441 to 1.578) and IC_{50} of 0.93 µM (95% CI: 0.177 to 5.275)] and 72h [i.e., IC_{50} of 0.01 µM (95% CI: 0.0003 to 0.027) and IC_{50} of 0.61 µM (95% CI: 0.02 to 0.143)].

The potencies of all the concurrent drug combinations at 24h were extremely lower by comparison (Table 3.1). Table 3.2 summarizes the relative potency ratios (PRs) at various time intervals of exposure of MCF-7 breast carcinoma cell lines to EGFRi, DOX and CDDP combinations. The greatest PR or DRI (1186 at 72h) was observed for CDDP in the DOX + CDDP combination, but the significance of this could not be established because the 95% CI could not be determined by the regression analysis.

The same argument holds true for the PR of 396 for EGFR in the EGFRi + DOX combination at 72h. The most reliable DRIs (i.e., PR) were in order of rank: 23-fold (90% CI: 0.81 to 481) for DOX in the DOX + CDDP combination at 72h > 10-fold (90% CI: 0.74 to 29.52) for DOX in the EGFRi + DOX combination at 48h > 7-fold (95% CI: 3.34 to 24.11) for EGFRi in the EGFRi + DOX combination at 48h. Thus, synergistic cytotoxic effects on MCF-7 cells were exerted by the various drug combinations in a time-dependent manner.

The findings presented in Section 3.4 and Section 3.5 demonstrated that EGFRi, DOX and CDDP in various combinations synergistically inhibited the growth of both MDA-MB-231 TNBC cells and MCF-7 cells in vitro.

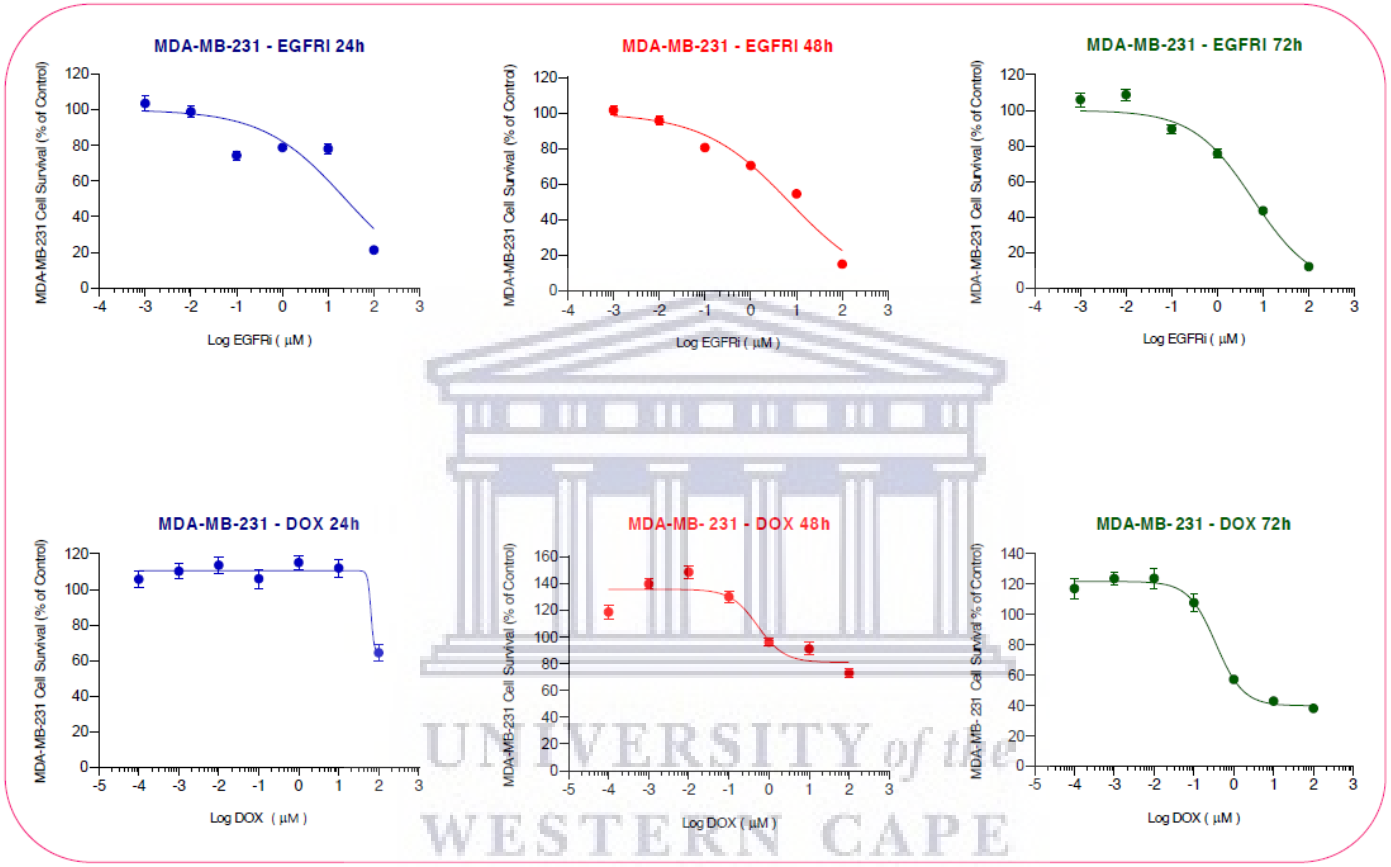

Figure 3.1: Dose response curves obtained by non-linear regression analysis of cell survival data of MDA-MB-231 TNBC cells exposed to EGFRi for 24, 48 and 72h, respectively (top panel), and DOX for 24, 48 and 72h, respectively (bottom panel). Data are means ± SEM. (n=12).

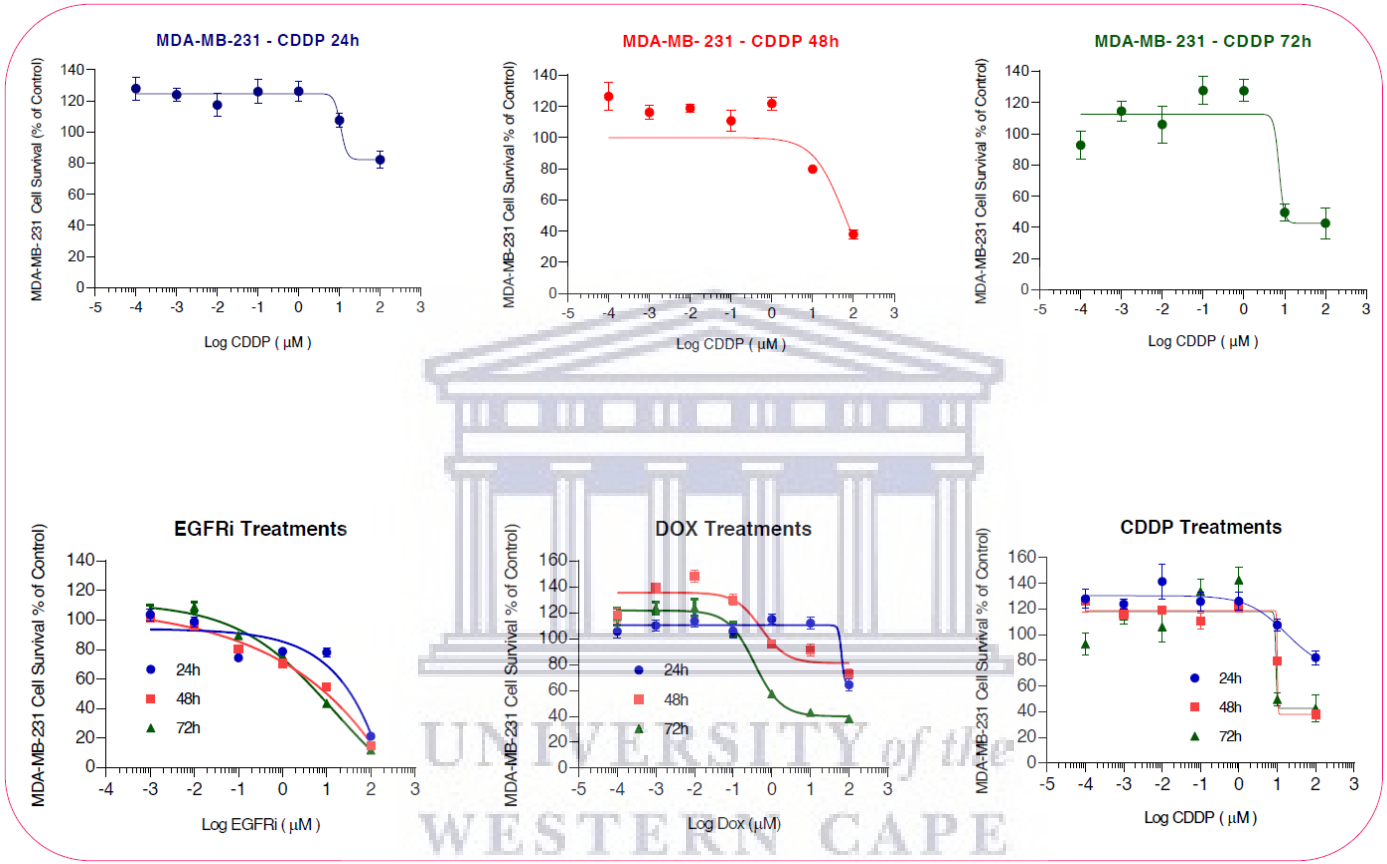

Figure 3.2: Dose response curves obtained by non-linear regression analysis of cell survival data of MDA-MB-231 TNBC cells exposed to CDDP for 24, 48 and 72h, respectively (top panel) and composite dose-response profiles for EGFRi, DOX and CDDP at 24, 48 and 72h, respectively (bottom panel). Data are means ± SEM. (n=12).

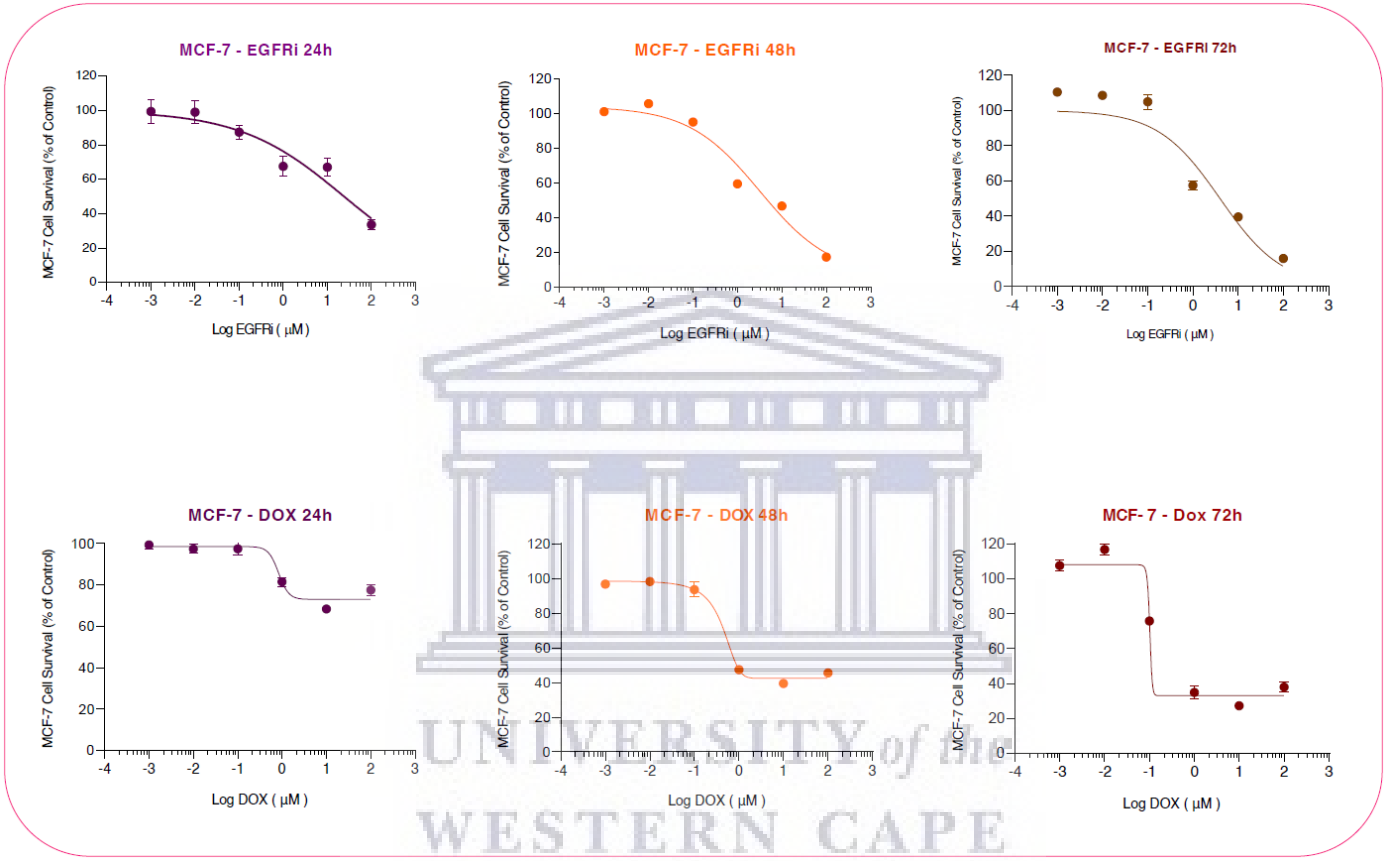

Figure 3.3: Dose response curves obtained by non-linear regression analysis of cell survival data of MCF-7 breast carcinoma cells exposed to EGFRi for 24, 48 and 72h, respectively (top panel), and DOX for 24, 48 and 72h, respectively (bottom panel). Data are means ± SEM. (n=8).

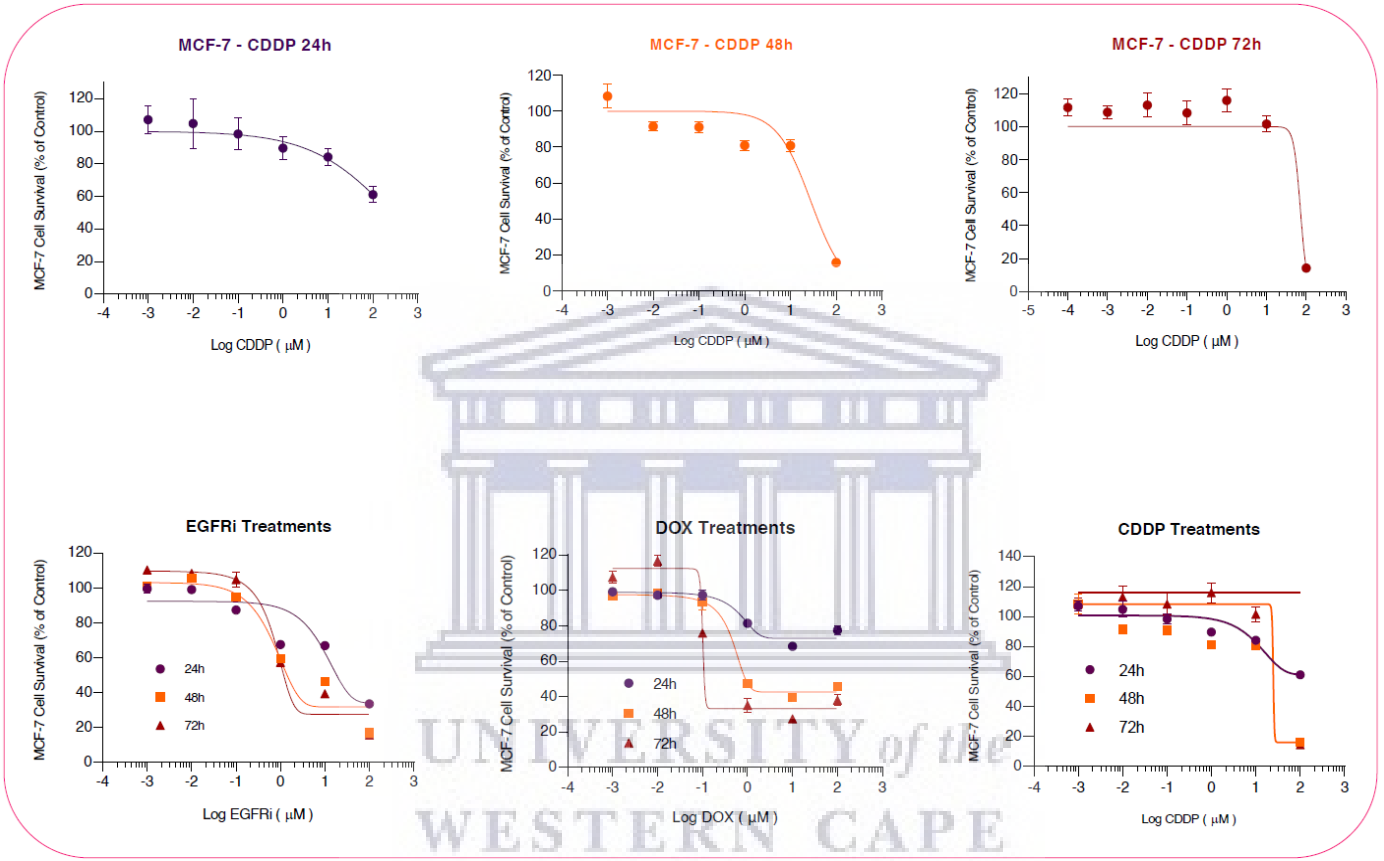

Figure 3.4: Dose response curves obtained by non-linear regression analysis of cell survival data of MCF-7 breast carcinoma cells exposed to CDDP for 24, 48 and 72h, respectively (top panel), and composite dose-response profiles for EGFRi, DOX and CDDP at 24, 48 and 72h, respectively (bottom panel). Data are means ± SEM. (n=8).

Table 3.1: Estimated concentrations (IC_{50}s) that produced half-maximal responses in MDA-MB-231 and MCF-7 breast carcinoma cell lines to EGFRi, DOX and CDDP after various time intervals of exposure

		MDA-MB-231 Triple Negative Breast Carcinoma Cells			MCF-7 Breast Carcinoma Cells			
Single Agent		Time	24h	48h	72h	24h	48h	72h
	EGFRi	IC_{50} (μM)	23.60	7.05	6.03	24.11	5.57	3.96
		95% CI	14.35 to 39.88	5.244 to 9.486	4.566 to 7.965	16.77 to 35.88	4.146 to 7.478	2.593 to 6.095
		R^2	0.71	0.91	0.91	0.91	0.95	0.90
	DOX	IC_{50} (μM)	111.40	344.40	9.67	6315.00	8.30	1.40
		95% CI	ND	ND	3.35 to 32.71	1178 to 107847	3.759 to 20.97	0.5926 to 3.631
		R^2	0.43	-0.11	0.67	0.61	0.76	0.74
	CDDP	IC_{50} (μM)	144.00	60.49	49.29	255.80	27.79	71.15
		95% CI	ND	27.34 to 137.9	6.656 to 285.9	142.4 to 632.8	19.57 to 39.47	ND
		R^2	-0.57	0.29	0.18	0.72	0.81	0.79
		MDA-MB-231 Triple Negative Breast Carcinoma Cells			MCF-7 Breast Carcinoma Cells			
Combinations		Time	24h	48h	72h	24h	48h	72h
	EGFRi + DOX	IC_{50} (μM)	440.10	82.83	0.46	5117.00	0.85	0.01
		95% CI	ND	53.74 to 140.4	0.1655 to 1.138	ND	0.4406 to 1.578	0.0002703 to 0.027
		R^2	0.39	0.79	0.59	0.42	0.84	0.64
	EGFRi + CDDP	IC_{50} (μM)	130.30	0.81	2.87	130.00	246.00	2.87
		95% CI	ND	0.2741 to 2.305	1.451 to 5.870	ND	ND	1.451 to 5.870
		R^2	-0.25	0.80	0.87	-0.25	0.07	0.87
	DOX + CDDP	IC_{50} (μM)	655.00	34.21	27.73	1865.00	0.93	0.06
		95% CI	89.23 to 46748	ND	ND	ND	0.1774 to 5.275	0.01992 to 0.1493
		R^2	0.70	0.90	0.38	0.22	0.62	0.72

IC_{50} values are best-fit estimates of non-linear regression analysis of drug vs normalized responses (inhibition, variable slope). The variable slope model does not assume a standard slope of -1.0, but fits the Hill slope from the data (https://www.graphpad.com/guides/prism/8/curve-fitting/REG_DR_inhibit_normalized_variable_2.htm). 95% CI = 95% confidence interval; ND = the regression did not converge and, as such, the associated 95%CI values were not determinable. In such cases, the IC_{50} estimates are ambiguous and should thus be interpreted with caution.

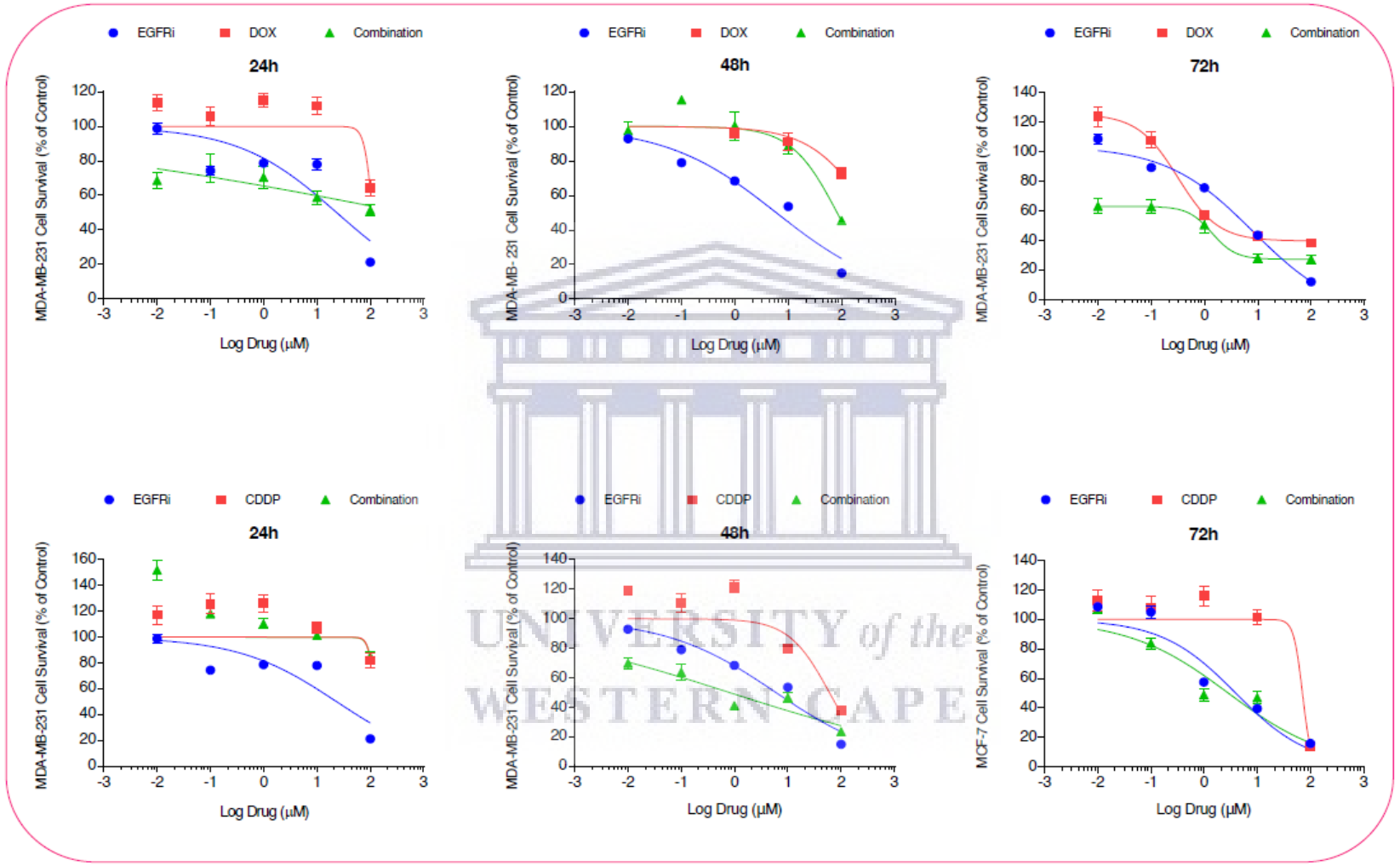

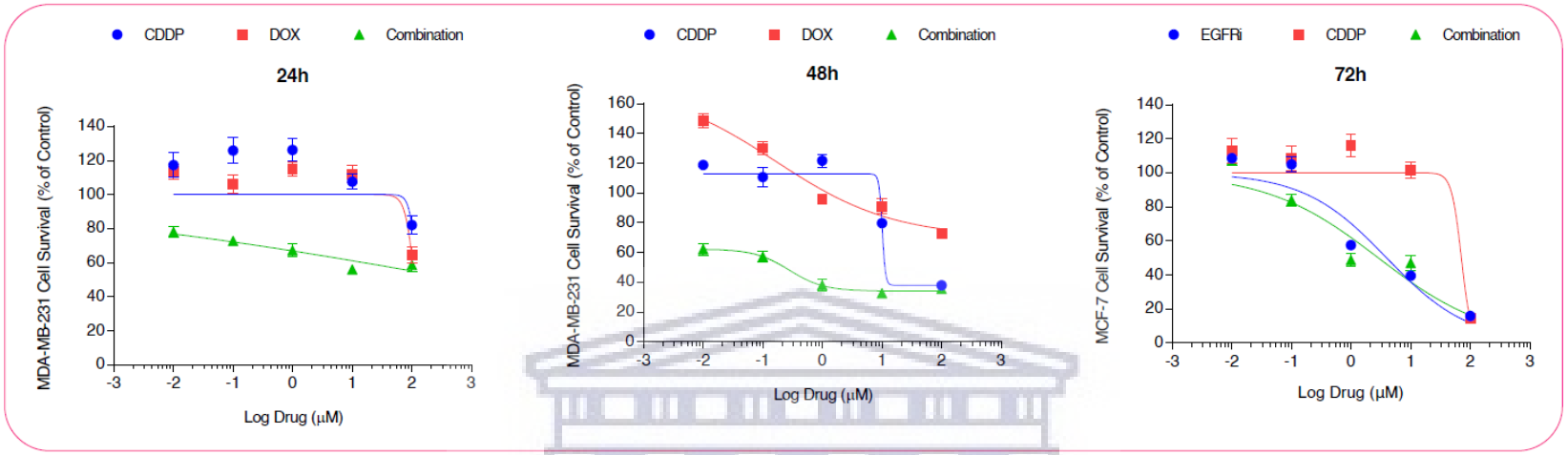

Figure 3.5: Effects of EGFRi, DOX and CDDP, alone and in equimolar combinations with each other at various time intervals (24, 48 and 72h) on the growth and survival of MDA-MB-231 TNBC cells. Cell survival was assessed by the MTT assay and Hill-type dose-response curves generated by non-linear regression as described in Chapter 2: Section 2.6 and Section 2.10, respectively. Values are Means ± SEM (n=12). The respective IC_{50} values are listed Table 3.1.

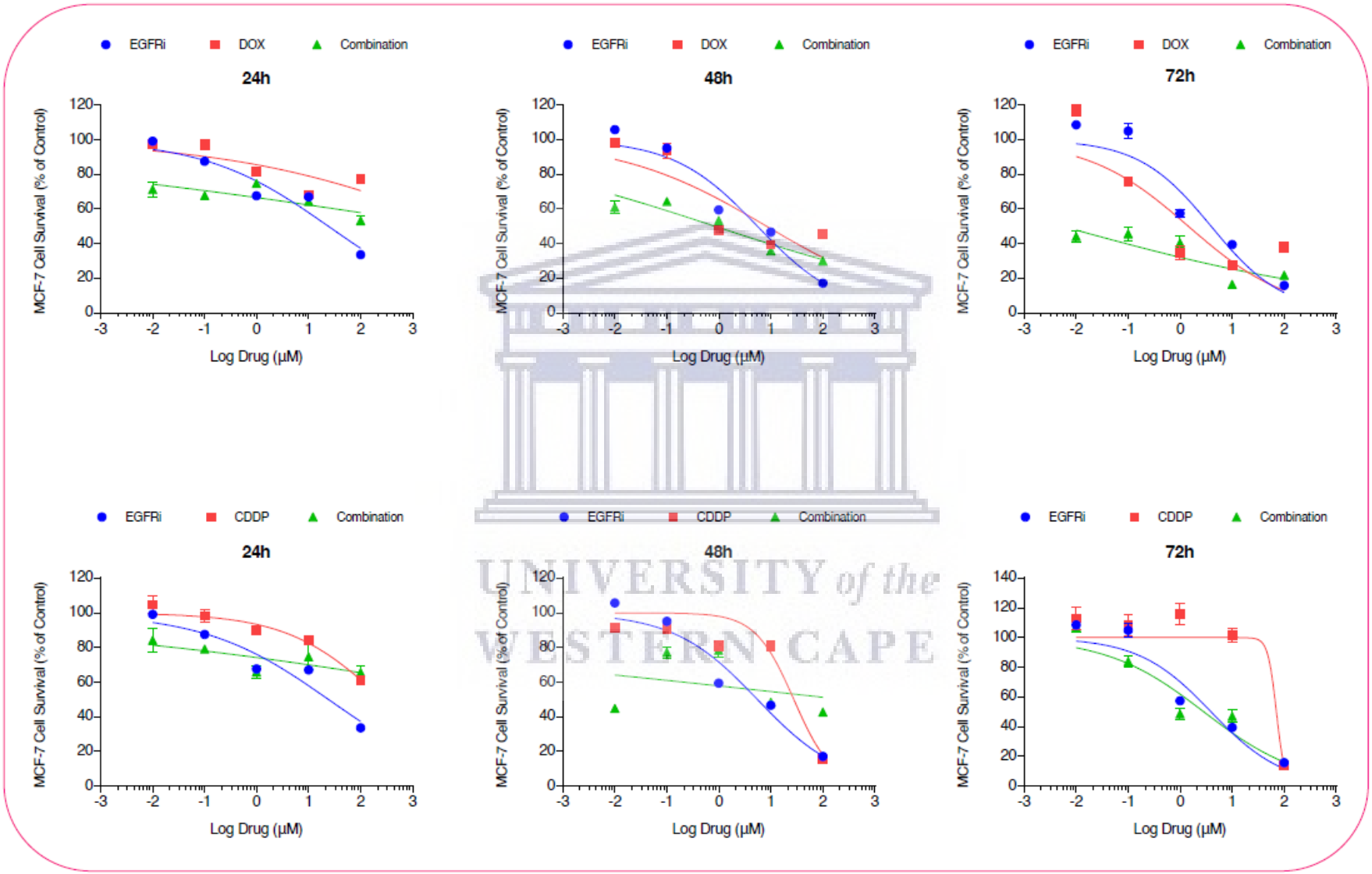

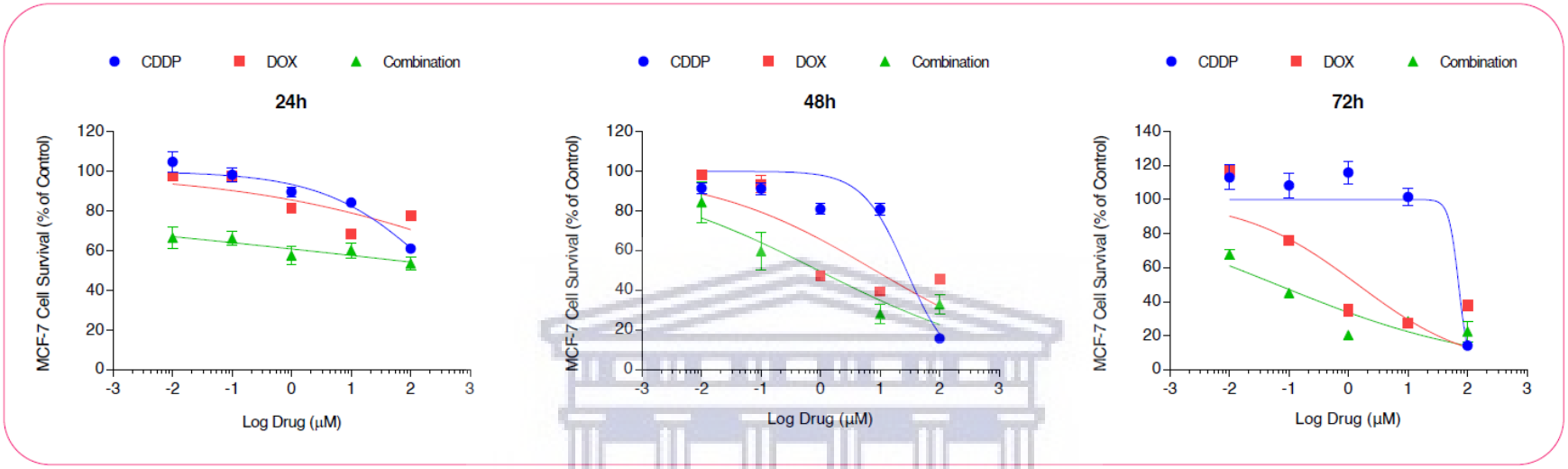

Figure 3.6: Effects of EGFRi, DOX and CDDP, alone and in equimolar combinations with each other at various time intervals (24, 48 and 72h) on the growth and survival of MCF-7 breast carcinoma cells. Cell survival was assessed by the MTT assay and Hill-type dose-response curves generated by non-linear regression as described in Chapter 2: Section 2.6 and Section 2.10, respectively. Values are Means ± SEM (n=12). The respective IC_{50} values are listed Table 3.1.

Table 3.2: Relative potency ratios at various time intervals of exposure of MDA-MB-231 and MCF-7 breast carcinoma cell lines to EGFRi, DOX and CDDP combinations

MDA-MB-231: Potency Ratios of Drugs Calculated According to Fieller's Ratio of Means Test as Modified by Bliss			
Potency Ratio (PR)	**Time (h)**	**PR**	**95% CI¶; 90% CI§**
PR of EGFRi in EGFRi + DOX	24	0.05	ND
	48	0.29	0.107 to 0.731¶
	72	13.11	6.304 to 239.532*
PR of DOX in EGFRi + DOX	24	0.25	ND
	48	4.16	ND
	72	21.02	-8.531 to 402.766¶
PR of EGFRi in EGFRi + CDDP	24	0.18	ND
	48	8.71	ND
	72	2.10	1.031 to 12.643¶; 1.152 to 6.774§
PR of CDDP in EGFRi + CDDP	24	1.11	ND
	48	74.68	ND
	72	17.17	-49.816 to 161.585¶; -31.128 to 95.915§
PR of DOX in DOX + CDDP	24	0.17	ND
	48	10.07	ND
	72	0.35	-49.816 to 161.585¶; -31.128 to 95.915§
PR of CDDP in DOX + CDDP	24	0.22	ND
	48	1.77	ND
	72	1.78	-49.816 to 161.585¶; -31.128 to 95.915§
MCF-7: Potency Ratios of Drugs Calculated According to Fieller's Ratio of Means Test as Modified by Bliss			
	Time (h)	**PR**	**95% CI¶; 90% CI§**
PR of EGFRi in EGFRi + DOX	24	0.01	ND
	48	6.55	3.341 to 24.111¶; 3.730 to 16.572§
	72	396	ND
PR of DOX in EGFRi + DOX	24	1.23	ND
	48	9.77	0.736 to 29.517§
	72	140	ND
PR of EGFRi in EGFRi + CDDP	24	0.19	ND
	48	0.03	ND
	72	1.38	0.569 to 8.411¶; 0.669 to 4.536§
PR of CDDP in EGFRi + CDDP	24	1.97	ND
	48	0.11	ND
	72	24.79	ND
PR of DOX in DOX + CDDP	24	3.39	ND
	48	8.93	ND
	72	23.33	0.809 to 481.010§
PR of CDDP in DOX + CDDP	24	0.14	ND
	48	29.88	ND
	72	1186	ND

PR: Potency Ratio, also referred to as the **Dose-Reduction Index (DRI)** which indicates the fold increase in potency of a drug in a combination regimen or the fold reduction in concentration of that drug to produce the maximal effect achieved by the drug as a single agent. **CI:** Confidence Interval calculated for the ratio (quotient) of drug alone and the drug in a combination according to Fieller's Theorem [Fieller EC (1944) A fundamental formula in the statistics of biological assay, and some applications. *Quarterly Journal of Pharmacy and Pharmacology* 17:117-123] and simplified by Bliss [Bliss CI (1956) Confidence limits for measuring the precision of bioassays. *Biometrics* 12(4):491-526]. **ND:** Since the confidence interval of the denominator includes zero, it is not possible to compute the CI of the quotient.

3.6 Drug Combination Response Surface Analysis of EGFRi, DOX and CDDP Interaction Effects

3.6.1 Introduction

The literature abounds with zero interaction response surface models (RSMs) that present data as three-dimensional (3D) concentration effect curves [288,320,350,561,586]. The concentrations of drugs A and B are generally plotted on the *x*-axis and *y*-axis, and the fraction affected (F_a) or other observed effect (e.g., Survival as a % of Control) is plotted on the *z*-axis. The 3D surface so generated usually derives from Loewe additivity [316] and/or Bliss independence [317] principles that define the predicted results of no interaction (zero effect or additivity) for the drug combination as expounded in Section A.4.6 and Section 2.10. In this study, we have evaluated the combination effects of 24-72h exposure of EGFRi, DOX and CDDP in a fixed 1:1 ratio, i.e., at equimolar concentrations in a concurrent dual agent regimen, on MDA-MB-231 TNBC cells and MCF-7 breast carcinoma cells. The survival data obtained from MTT cytotoxicity assays (Section 2.6) were assessed to identify synergistic and/or antagonistic interactions among the different drug combinations.

In order to achieve this objective, we have utilized the Combenefit software tool [584] that permits the visualization, analysis and quantification of drug combination effects in terms of synergy and/or antagonism, according to classical Synergy models such as Loewe [342], Bliss [317] and Highest Single Agent (HSA) [587]. A drug combination is usually classified as synergistic, antagonistic, or non-interactive. This classification is based on the deviation of the observed drug combination response from the expected effect of non-interaction (the null hypothesis) [588]. We have limited our analysis to the Loewe additivity and Bliss independence models, albeit HSA datasets have as well been generated. The experimental dose-response surface that renders combination effects in concentration space, is first scanned by the software as a matrix

of % of the control value across concentrations. Single-agent effects are mined from the data and fitted with a dose-response curve. Based on the two single agent dose response curves, a model-based combination dose-response surface is derived. This surface gives a 'reference' dose-response surface for a non-synergistic (additive/independent) combination, whose properties are shaped by the selected model (Loewe or Bliss). The experimental combination dose-response surface is then contrasted to that generated by the model, rendering a synergy distribution in concentration space. This synergy distribution can be further summarized via metrics such as synergy matrices and dose-reduction plots as well as isobole contours. The synergy score for a drug combination is the average of all dose combination measurements. However, in this study, we have reported highest Bliss and Loewe scores of synergism and antagonism.

The 2D and 3D synergy maps highlight synergistic and antagonistic dose regions in blue and red colors, respectively. By comparing the Bliss and Loewe synergy and antagonism scores one can ascertain the relative contribution of each drug in a cocktail to the joint combination response. The synergy scores can be interpreted as the relative excess response due to drug interactions (i.e., a synergy score of 20 corresponds to 20% of response beyond expectation). There is no particular threshold to define a good synergy score. Nevertheless, based on unified principles, a synergy scores near 0 gives limited confidence on synergy or antagonism. So, when the synergy score is:

- Less than -10: the interaction between two drugs is likely to be *antagonistic*;
- From -10 to 10: the interaction between two drugs is likely to be *additive*;
- Larger than 10: the interaction between two drugs is likely to be *synergistic*.

Combenefit analysis of the interaction effects of three pairwise drug (D) combinations (D_A+D_B, D_A+D_C, D_B+D_C) of EGFRi (D_A), DOX (D_B) and CDDP (D_C) on MDA-MB-231 TNBC and MCF-7 breast carcinoma cells are shown in a series of 3D dose-response surface plots, synergy and antagonism heat maps or matrices, contour and dose-reduction plots, according to the Bliss independence and Loewe additivity reference models in a time-dependent array. The strength of the interaction is indicated by the colors (blue, strong synergistic; red, strong antagonistic). Thus, the most notable effects (i.e., highest Bliss and Loewe scores of synergism and antagonism) of the 24, 48 and 72h exposure times of MDA-MB-231 TNBC and MCF-7 breast carcinoma cells to the various two-drug combinations corresponding to the Bliss and Loewe models are summarized sequentially as shown in Table 3.3 and Table 3.4, respectively. Hyperlinks to the corresponding figures are also indicated.

3.6.2 Interaction Effects of Combinations of EGFRi, DOX and CDDP in MDA-MB-231 TNBC Cells

The highest Bliss synergism score (44) was noted at 72h of exposure of MDA-MB-231 TNBC cells to the EGFRi + DOX combination for doses of 0.01 µM EGFRi and 0.1 µM DOX (Table 3.3 and Figure 3.9A). This implies that at this dose ratio, the potency of EGFRi is 10-fold greater than that of DOX in the combination and EGFRi enhances the effect produced by DOX. In EGFRi + DOX combination of equal dose (equimolar) ratio of 1:1 (i.e., 0.1 µM EGFRi + 0.1 µM DOX combination), the concentration of EGFRi can be reduced 10-fold (i.e., to 0.01 µM) to elicit the same maximal effect (E_{max}) by either drug alone. The second highest Bliss synergism score (37) for the same dose ratio was attained after 24h (Table 3.3 and Figure 3.7A), but not after 48h, suggesting that at this time the interaction between two drugs is likely to be additive. The highest Bliss antagonism score (-60) for doses of 10 µM EGFRi and 0.01 µM DOX after 48h exposure to the combination indicates that the lower

concentration of DOX decreases the joint effect of the EGFRi + DOX combination (Table 3.3 and Figure 3.8A). Similar Bliss and Loewe synergism and antagonism scores were obtained for the EGFRi + DOX combination at the same dose ratios after 24, 48 and 72h (Table 3.3 and respective figure hyperlinks). In terms of Bliss and Loewe synergism, the EGFRi + CDDP combination yielded an effect of non-interaction in MDA-MB-231 TNBC cells after 24h exposure (Figure 3.10A and Figure 3.10C, respectively), but equivalent Bliss and Loewe antagonism scores (-67) were observed at a ratio of 0.01 µM EGFRi:0.1 µM DOX). Likewise, equivalent Bliss and Loewe synergism and antagonism scores were observed after 48 and 72h exposure to the combination at the corresponding dose ratios indicated, the highest synergism score being 56 and the highest antagonism score being -160 (Table 3.3 and respective figure hyperlinks).

In MDA-MB-231 TNBC cells, exposure to DOX + CDDP yielded similar Bliss and Loewe synergism and antagonism scores for all the times of exposure, except at 24h for which the two drugs were non-interactive (Table 3.3 and respective figure hyperlinks). The highest synergism score was 75 and the highest antagonism score was -257 as determined by both response surface models. In summary, in the pairwise drug combination with DOX, EGFRi was the most potent contributor to Bliss and Loewe synergism at 10-fold lower doses (0.01 µM) relative to DOX (0.1 µM), whereas heterogeneous dose ratios were observed for both EGFRi and DOX in the combination to yield Bliss and Loewe antagonistic drug interactions (Table 3.3).

In the figures for each time point (24, 48, 72h), for both Bliss and Loewe drug interaction models, the top panels depict the effects (% of Control, *top panel left*) of the three pairwise drug (D) combinations (D_A+D_B, D_A+D_C, D_B+D_C) of EGFRi (D_A), DOX (D_B) and CDDP (D_C), whereas the dose-response shifts for each of the drugs in

combination with the partner drug are shown in the *top panel center* and *top panel right.* Thus, drug interaction simulations of both Bliss and Loewe models, shown in Figure 3.7B and Figure 3.7D, respectively, summarize the effects (% of Control, *top panel left*) and dose-response shifts for DOX (*top panel center*) and EGFRi (*top panel* right) in the EGFRi + DOX combination for MDA-MB-231 TNBC cells after 24h exposure, while Figure 3.8B and Figure 3.8D represent the same for the 48h time point, and Figure 3.9B and Figure 3.9D that for the 72h time point. This order of arrangement is repeated for all the drug combination effects at the corresponding time intervals for both MDA-MB-231 TNBC cells (Table 3.3 and figure hyperlinks) and MCF-7 breast carcinoma cells (Table 3.4 and figure hyperlinks).

3.6.3. Interaction Effects of Combinations of EGFRi, DOX and CDDP in MCF-7 Breast Carcinoma Cells

Exposure of MCF-7 breast carcinoma cells to three pairwise drug (D) combinations (D_A+D_B, D_A+D_C, D_B+D_C) of EGFRi (D_A), DOX (D_B) and CDDP (D_C) yielded equivalent Bliss and Loewe synergism and antagonism scores at corresponding dose ratios (Table 3.4 and respective figure hyperlinks). Interestingly, in the EGFRi + DOX combination, Bliss and Loewe synergy scores were effected by the equal interaction of EGRRi and DOX at a 1:1 ratio (i.e., 0.01 µM EGFRi + 0.01 µM DOX) at all the exposure times (24, 48 and 72h; Table 3.4, Figure 3.16A, Figure 3.16C, Figure 3.17A, Figure 3.17C, Figure 3.18A, Figure 3.18C), whereas the corresponding antagonism scores for the selected models were effected by a heterogeneous drug concentration space.

Likewise, in the DOX + CDDP combination regimen, both Bliss and Loewe synergism scores of 32 were effected at a dose ratio of 1:1, i.e., at 0.1 µM DOX + 0.1 µM CDDP, after 24h incubation (Table 3.4, Figure 3.22A and Figure 3.22C), a response identical

to that observed for the same drug combination and dose ratios in MDA-MB-231 TNBC cells (Table 3.3, Figure 3.13A, Figure 3.13C). In the case of synergistic drug interactions between DOX and CDDP, DOX was the more potent drug partner to the effect at all the times indicated, but the potency of DOX was antagonized when combined with very high concentrations of CDDP. Remarkably, after 72h, a 10-fold lower concentration of DOX and 100-fold higher concentration of CDDP, relative to the 24h exposure time, effected a slightly greater synergistic drug interaction (scores of 32 vs 37) as dictated by both the Bliss and Loewe models (Table 3.4; and Figure 3.22A, Figure 3.22 vs Figure 3.24A, Figure 3.24C), corroborating the evidence that DOX is the more potent drug in the DOX + CDDP combination.

3.7 Discussion

Globally, breast cancer is the most frequently diagnosed cancer and the primary cause of cancer deaths among women [78]. In this study, we have used the estrogen receptor positive (ER^+) MCF-7 breast carcinoma cell line [589-592] and the triple-negative breast cancer (TNBC) MDA-MB-231 cell line [593-596] as they are prototype cell lines that provide contextual relevance in researching breast cancer pathology and drug development [597]. TNBC refers to breast cancers without ERBB2 amplification or overexpression, and lacking estrogen and progesterone receptors. In the multidisciplinary breast cancer therapeutic landscape, a dire need exists to define mechanistic drug interactions and find potent multidrug combinations that are safe and efficacious at low concentrations to improve overall survival and minimize side effects [147,365,388,598-600].

The EGFR/ERBB/HER family of receptor tyrosine kinases (RTKs) is a proof-of-concept for breast cancer therapeutic exploitation and innovation [468,472,476,490]. There are two classes of inhibitors of EGFR, namely, *monoclonal antibodies* (e.g.,

cetuximab and trastuzamab), which target the extracellular domain and impede binding of native EGF ligand to the receptor and *small molecule inhibitors* (e.g., gefitinib and erlotinib) that compete with ATP in the intracellular tyrosine kinase domain and block activity, irrespective of endogenous ligand binding [461,504]. Recently, it has been shown that the majority of the 4,6-pyrimidinediamine derivatives exert potent inhibition against gain-of-function *EGFR* mutations [601]. EGFR Inhibitor [cyclopropane carboxylic acid-(3-(6-(3-trifluoro-methyl-pheny-lamino)-pyrimidin-4-yl)-amino)-phenyl-amide), abbreviated as EGFRi in this study, is a small molecule receptor tyrosine kinase inhibitor (RTKI) or TKI that is highly selective for the epidermal growth factor receptor 1 (HER1, ERBB1, EGFR1) [522]. EGFRi is an investigational agent that specifically blocks EGFR autophosphorylation, hampering downstream growth signaling pathways [505,602].

In this study, dose-response curve analysis indicated that EGFRi decreased growth and survival in both MDA-MB-231 TNBC and MCF-7 breast carcinoma cells, either as a single agent or in pairwise ratiometric combinations with DOX and CDDP. Moreover, the three pairwise drug (D) combinations (D_A+D_B, D_A+D_C, D_B+D_C) of EGFRi (D_A), DOX (D_B) and CDDP (D_C) yielded equivalent highest Bliss and Loewe synergism and antagonism scores at corresponding dose ratios in a time-dependent manner. Consistent with these models, the hierarchy of potency between the drugs in the dual agent combination was apparent, i.e., EGFRi > DOX > CDDP.

Drug combinations that produce synergistic effects to enhance cancer cell killing have become increasingly important in cancer chemotherapy as a tactic for overcoming recurrent drug-resistant disease. Several TKIs have been shown to enhance the efficacy of chemotherapeutic agents and many have been screened for their efficacy in clinical trials [414]. Some TKIs such as lapatinib, trastuzumab and bevacizumab

have been approved by the FDA for clinical management of breast cancer. Interestingly, TKIs revert conventional therapy-induced multidrug resistance (MDR) and improve the disease-free survival (DFS) in metastatic breast cancer (MBC) patients [461,514]. Lapatinib, a reversible chlorophenyl-quinazoline ErbB2/HER2 inhibitor, is FDA-approved for use in combination treatment with capecitabine and/or letrozole against MBC [476]. Early preclinical models showed synergistic and additive interactions of trastuzumab with chemotherapeutic agents used in MBC (including, platinum agents such as CDDP and carboplatin, taxanes, and anthracyclines such as DOX) [603]. The synergy of trastuzumab with DNA-damaging chemotherapy, such as DNA cross-linking platinum agents, may be induced by the inhibition of HER2-stimulated DNA-repair genes [604].

In combination therapy of MBC, a single cytotoxic agent is usually added to HER2-targeted treatment. The efficacy of anthracyclines in HER2-positive MBC is limited because patients who are exposed to anthracycline antibiotics in the adjuvant setting develop cumulative cardiotoxicity which overlaps with the toxicity of trastuzumab causing high rates of heart failure in such a combination [605]. Minimization of cardiotoxicity is achieved by combination of HER2-targeted agents with taxanes instead of anthracyclines. This made taxanes such as paclitaxel or docetaxel the first line of choice for the cytotoxic component of combination therapies. Addition of a second cytotoxic agent has provided no survival benefit in these clinical trials [531,532,534].

Breast cancer treatment option plans are determined by the type of cancer as well as hormone status [146]. Besides surgery and radiation, which is often the first line of treatment for many breast cancers, HR^+-breast cancer treatment options involve the use of endocrine therapy, and $HER2^+$ breast cancer the use of targeted therapy.

However, chemotherapy still remains the number one choice for the treatment of TNBC [146,182,239]. MBC treatment strategies involve the incorporation of hormone therapy, immune therapy, chemotherapy as well as gene therapy [7]. In many cases, combinations of different therapies have been used successfully as treatment options in advanced stages of breast cancer [606,607]. However, failure of conventional treatment strategies against TNBC highlights the importance for the discovery and development of more successful combination therapeutic treatment regimens [608]. The administration of chemotherapy in triple-negative versus non-triple negative patients, demonstrated a decrease in overall DFS in TNBC patients, compared to non-triple negative breast cancer patients [191].

Furthermore, the development of drug resistance to many of these treatment plans, particularly chemotherapy that incorporates the use of anthracyclines such as DOX and alkylating agents such as carboplatin and CDDP, have become a common occurrence. In our study we combined the *in vitro* use of three different classes of anticancer compounds, two of which share a molecular target (DNA), but with independent modes of action, and one targeting the EGFR overexpressed in cancer cells, that is responsible for the activation of growth and survival signaling pathways as well as apoptosis evasion [470,472].

In another study, the combination of a histone deacetylase (HDAC) inhibitor (vorinostat) with a TKI (dasatinib) exerted synergistic anticancer effects on MCF-7 cells by inducing cell cycle arrest, ROS production, and apoptosis through the mitochondria-mediated intrinsic pathway [609]. Our study demonstrated that the EGFR Inhibitor was more effective, when administered individually, in inhibiting cell growth in both MCF-7 and MDA-MB-231 cells compared to DOX and CDDP. DOX is a topoisomerase-2 inhibitor that interacts with a nicked DNA strand linked to the

enzyme leads to irreversible DNA damage and thus apoptosis in proliferating cells [610]. The combined interaction of CDDP with DOX has previously been shown to produce synergistic drug interactions [611-613]. This type of cell death was confirmed by our caspase-3/7 markers for apoptosis, when MDA-MB-231 TNBC and MCF-7 breast carcinoma cells were exposed to EGFRi, DOX and CDDP for 24h at various concentrations (Chapter 4). However, the use of both DOX and CDDP as monotherapy is discouraged due to its associated drug resistance in cancer, as well as toxic side effects when used at high concentrations. CDDP induces nephrotoxicity at high concentrations [542,614,615]. The clinical administration of DOX at high dosages has been associated with cardiotoxicity as a result of accrual of ROS that causes induction of oxidative stress that sets off pathways that result in DNA damage, senescence, necrosis and apoptosis in cardiomyocytes, fibroblasts, vascular cells, endothelial progenitor cells, bone marrow cells and many other organ systems [531,532]. Both DOX and CDDP treatment are associated with MDR development in cancer patients.

By analogy, even though significant clinical benefits derive from treatment with EGFR tyrosine kinase inhibitors (TKIs, e.g., erlotinib, gefitinib, and afatinib), acquired therapeutic resistance, driven by *EGFR* mutations, to these agents invariably develops, underscoring the need for novel strategies for identifying and confronting TKI drug resistance to alter the treatment landscape for cancers with EGFR-mutants [328,477,484,487,519]. The results in this study showed that the application of the Bliss independence and Loewe additivity models in the Combenefit software was appropriate to navigate the concentration and effect spaces of equimolar two-drug combinations that may prove interesting and useful for further exploration of potent and efficacious EGFR, DOX and CDDP combinations.

Table 3.3: Summary of highest synergy/antagonism scores in MDA-MB-231 TNBC cells

MDA-MB-231 TNBC Cells									
Figure Hyperlinks					Time (h)	Highest Bliss Score		Highest Loewe Score	
Combination	Bliss		Loewe			Synergism	Antagonism	Synergism	Antagonism
EGFRi (D_A) + DOX (D_B)	3.7A	3.7B	3.7C	3.7D	24	**37** (0.01:0.1)	**-25** (10:100 | 100:0.01)	**37** (0.01:0.1)	**-25** (10:100 | 100:0.01)
	3.8A	3.8B	3.8C	3.8D	48	**9** (0.01:0.1)	**-60** (10:0.01)	**9** (0.01:0.1)	**-60** (10:0.01)
	3.9A	3.9B	3.9C	3.9D	72	**44** (0.01:0.1)	**-23** (0.1:10)	**43** (0.01:0.1 | 0.1:0.1)	**-22** (100:0.01)
EGFRi (D_A) + CDDP (D_C)	3.10A	3.10B	3.10C	3.10D	24	None	**-67** (0.01:0.1)	None	**-67** (0.01:0.1)
	3.11A	3.11B	3.11C	3.11D	48	**32** (1:0.01)	**-40** (0.01:100)	**32** (1:0.01)	**-38** (0.01:100)
	3.12A	3.12B	3.12C	3.12D	72	**56** (0.01:1 | 1:0.1)	**-160** (0.1:0.01)	**56** (0.01:1 | 1:0.1)	**-160** (0.1:0.01)
DOX (D_B)+ CDDP (D_C)	3.13A	3.13B	3.13C	3.13D	24	**32** (0.1:0.1)	**-2** (10:100)	**32** (0.1:0.1)	None
	3.14A	3.14B	3.14C	3.14D	48	**70** (0.1:1)	**-256** (0.01:10)	**68** (0.1:1)	**-257** (0.01:10)
	3.15A	3.15B	3.15C	3.15D	72	**75** (0.1:0.1)	**-84** (10:1)	**75** (0.1:0.1)	**-84** (10:1)

Drug combination effects were determined as described in Data Analysis, Section 2.10, using the Combenefit™ software (licensed under the MIT Licence, https://sourceforge.net/p/combenefit/) that incorporates the three classical mathematical models of dose-responses for synergy analysis, viz., *Loewe Additivity*, *Bliss Independence* and *Highest Single Agent* [584]. In the present study, the first two models were selected for the analysis of the drug combinations indicated.

Table 3.4: Summary of highest synergy/antagonism scores in MCF-7 breast carcinoma cells

MCF-7 Breast Carcinoma Cells									
Figure Hyperlinks					Time (h)	Highest Bliss Score		Highest Loewe Score	
Combination (D_A + D_B)	Bliss		Loewe			Synergism	Antagonism	Synergism	Antagonism
EGFRi (D_A) + DOX (D_B)	3.16A	3.16B	3.16C	3.16D	24	**33** (0.01:0.01)	**-28** (100:100)	**33** (0.01:0.01)	**-21** (100:100)
	3.17A	3.17B	3.17C	3.17D	48	**47** (0.01:0.01)	**-30** (0.01:100)	**47** (0.01:0.01)	**-29** (0.01:100)
	3.18A	3.18B	3.18C	3.18D	72	**67** (0.01:0.01)	**-33** (1:1)	**67** (0.01:0.01)	**-19** (1:1)
EGFRi (D_A) + CDDP (D_C)	3.19A	3.19B	3.19C	3.19D	24	**17** (1:0.01)	**-49** (100:10)	**18** (1:0.01)	**-45** (10:0.1)
	3.20A	3.20B	3.20C	3.20D	48	**54** (0.01:1)	**-59** (1:100)	**54** (0.01:1)	**-56** (0.1:100)
	3.21A	3.21B	3.21C	3.21D	72	**27** (0.1:0.01)	**-82** (0.01:100)	**27** (0.1:0.01)	**-82** (0.01:100)
DOX (D_B) + CDDP (D_C)	3.22A	3.22B	3.22C	3.22D	24	**32** (0.1:0.1)	**-2** (10:100)	**32** (0.1:0.1)	None
	3.23A	3.23B	3.23C	3.23D	48	**70** (0.1:1)	**-51** (0.1:100)	**68** (0.1:1)	**-50** (0.1:100)
	3.24A	3.24B	3.24C	3.24D	72	**37** (0.01:10)	**-49** (0.01:100)	**37** (0.01:10)	**-49** (0.01:100)

Drug combination effects were determined as described in Data Analysis, Section 2.10, using the Combenefit™ software (licensed under the MIT Licence, https://sourceforge.net/p/combenefit/) that incorporates the three classical mathematical models of dose-responses for synergy analysis, viz., *Loewe Additivity*, *Bliss Independence* and *Highest Single Agent* [584]. In the present study, the first two models were selected for the analysis of the drug combinations indicated.

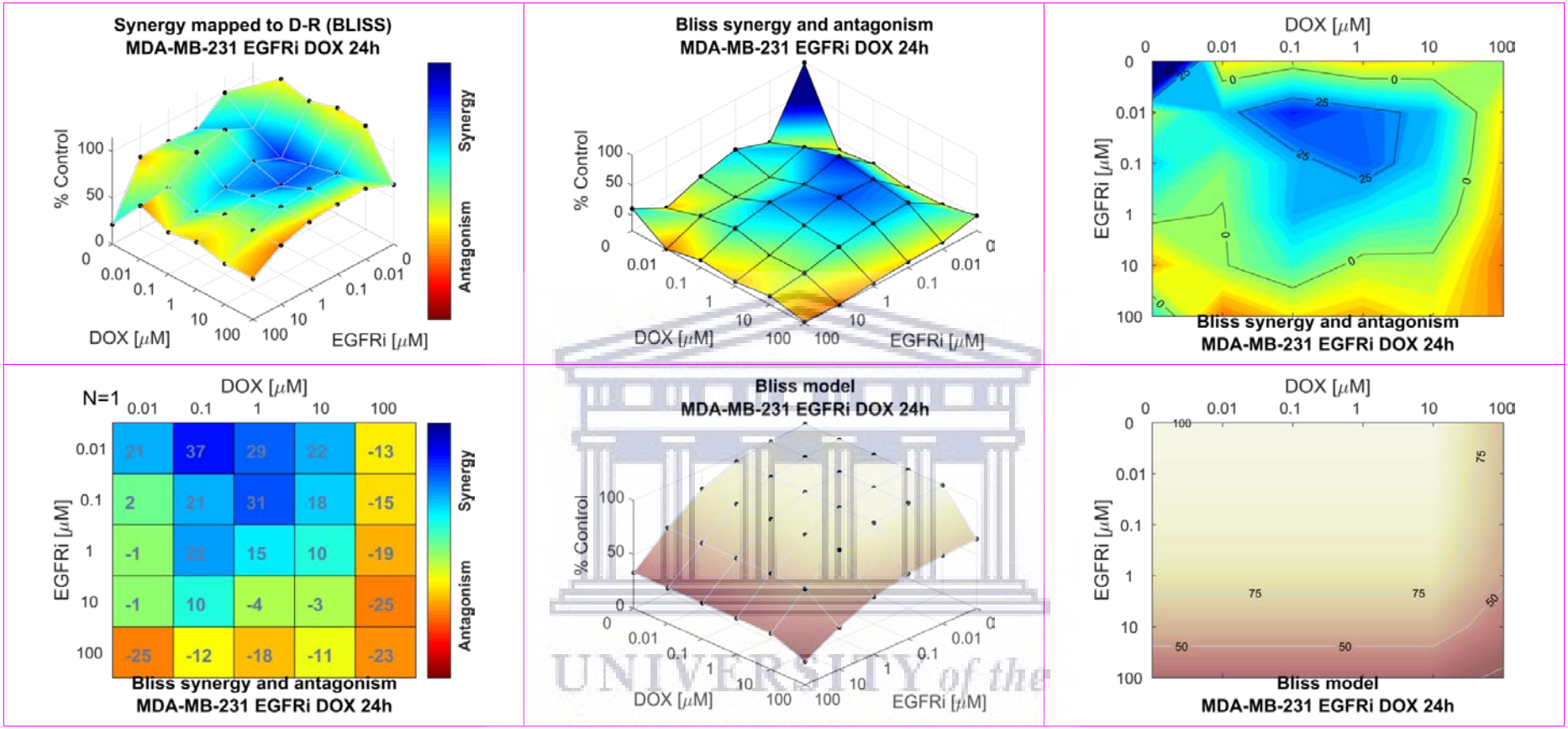

Figure 3.7A: Bliss independence response surface reference model for the dual agent combination effects of 24h treatment of MDA-MB-231 TNBC cells with EGFRi and DOX. **Top panel left:** Bliss independence mapping of the synergy levels on the experimental combination dose-response surface | **Top panel center:** Bliss synergy and antagonism levels visualized as a surface | **Top panel right:** Contour map of isoboles (iso-effect lines) of Bliss synergy and/or antagonism | **Bottom panel left:** Bliss synergy and antagonism matrix | **Bottom panel center**: Bliss model reference dose-response surface | **Bottom panel right:** Bliss model reference dose-response contour map.

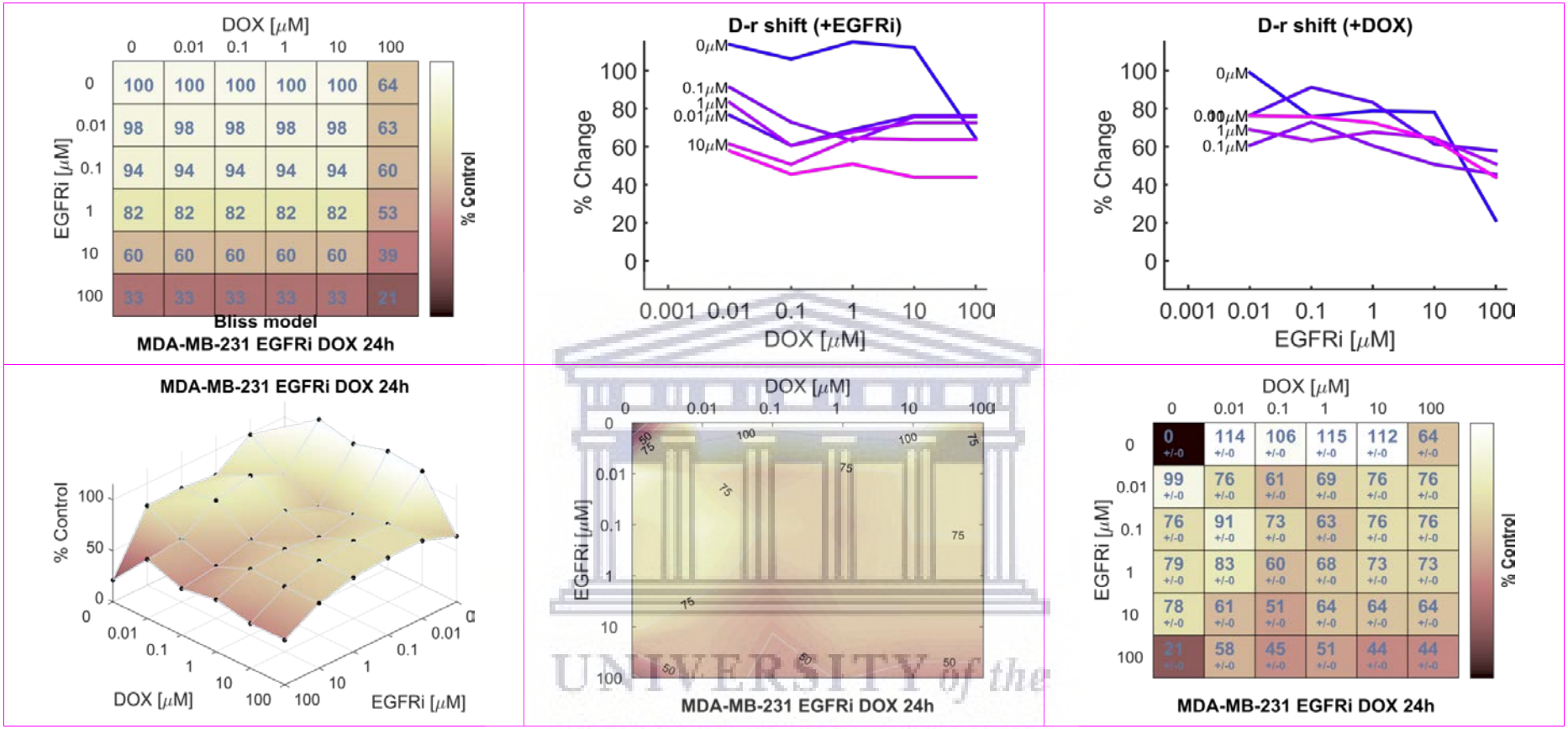

Figure 3.7B: Bliss reference model graphical presentation of the combination effects of 24h treatment of MDA-MB-231 TNBC cells with EGFRi and DOX. **Top panel left:** Bliss model reference dose-response matrix. | **Top panel center:** EGFRi dose-response shift in presence of increasing concentrations of DOX | **Top panel right:** DOX dose-response shift in presence of increasing concentrations of EGFRi | **Bottom panel left:** EGFRi and DOX combination dose-response surface | **Bottom panel center**: EGFRi and DOX combination dose-response contour map | **Bottom panel right:** EGFRi and DOX combination dose-response matrix.

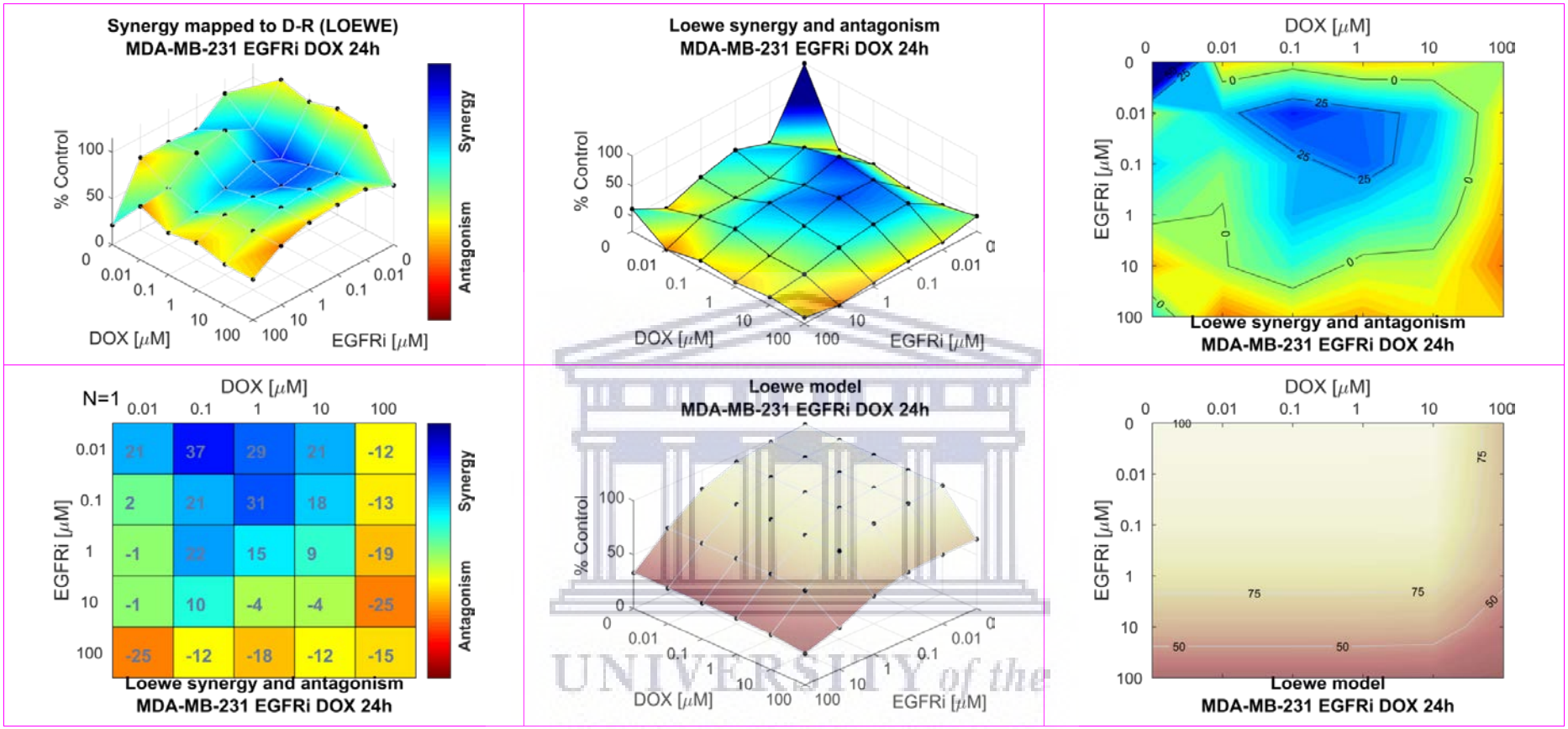

Figure 3.7C: Loewe additivity response surface reference model for the dual agent combination effects of 24h treatment of MDA-MB-231 TNBC cells with EGFRi and DOX. **Top panel left:** Loewe additivity mapping of the synergy levels on the experimental combination dose-response surface | **Top panel center:** Loewe synergy and antagonism levels visualized as a surface | **Top panel right:** Contour map of isoboles (iso-effect) of Loewe synergy and/or antagonism | **Bottom panel left:** Loewe synergy and antagonism matrix | **Bottom panel center**: Loewe model reference dose-response surface | **Bottom panel right:** Loewe model reference dose-response contour map.

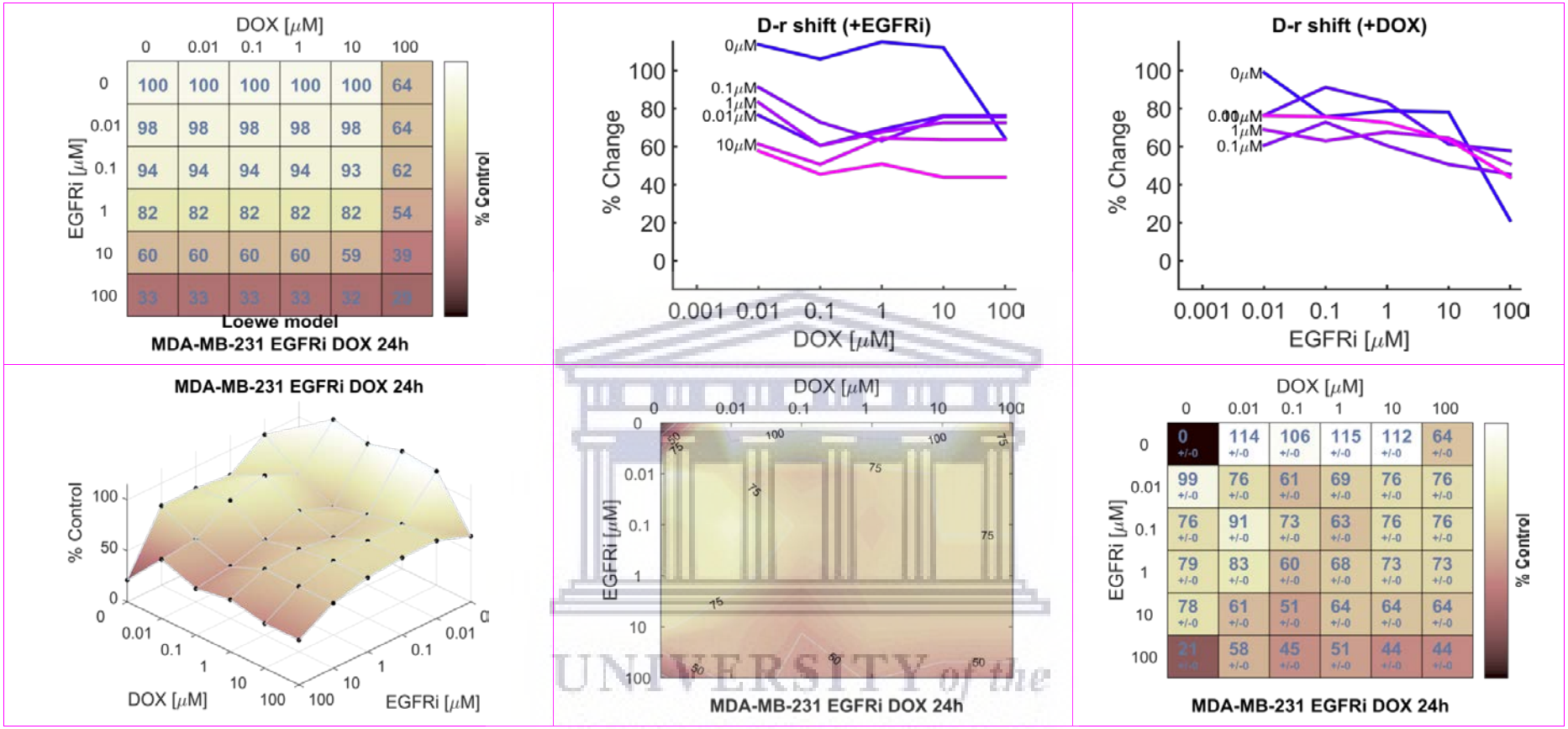

Figure 3.7D: Loewe reference model graphical presentation of the combination effects of 24h treatment of MDA-MB-231 TNBC cells with EGFRi and DOX. **Top panel left:** Loewe additivity model reference dose-response matrix. | **Top panel center:** EGFRi dose-response shift in presence of increasing concentrations of DOX | **Top panel right:** DOX dose-response shift in presence of increasing concentrations of EGFRi | **Bottom panel left:** EGFRi and DOX combination dose-response surface | **Bottom panel center**: EGFRi and DOX combination dose-response contour map | **Bottom panel right:** EGFRi and DOX combination dose-response matrix.

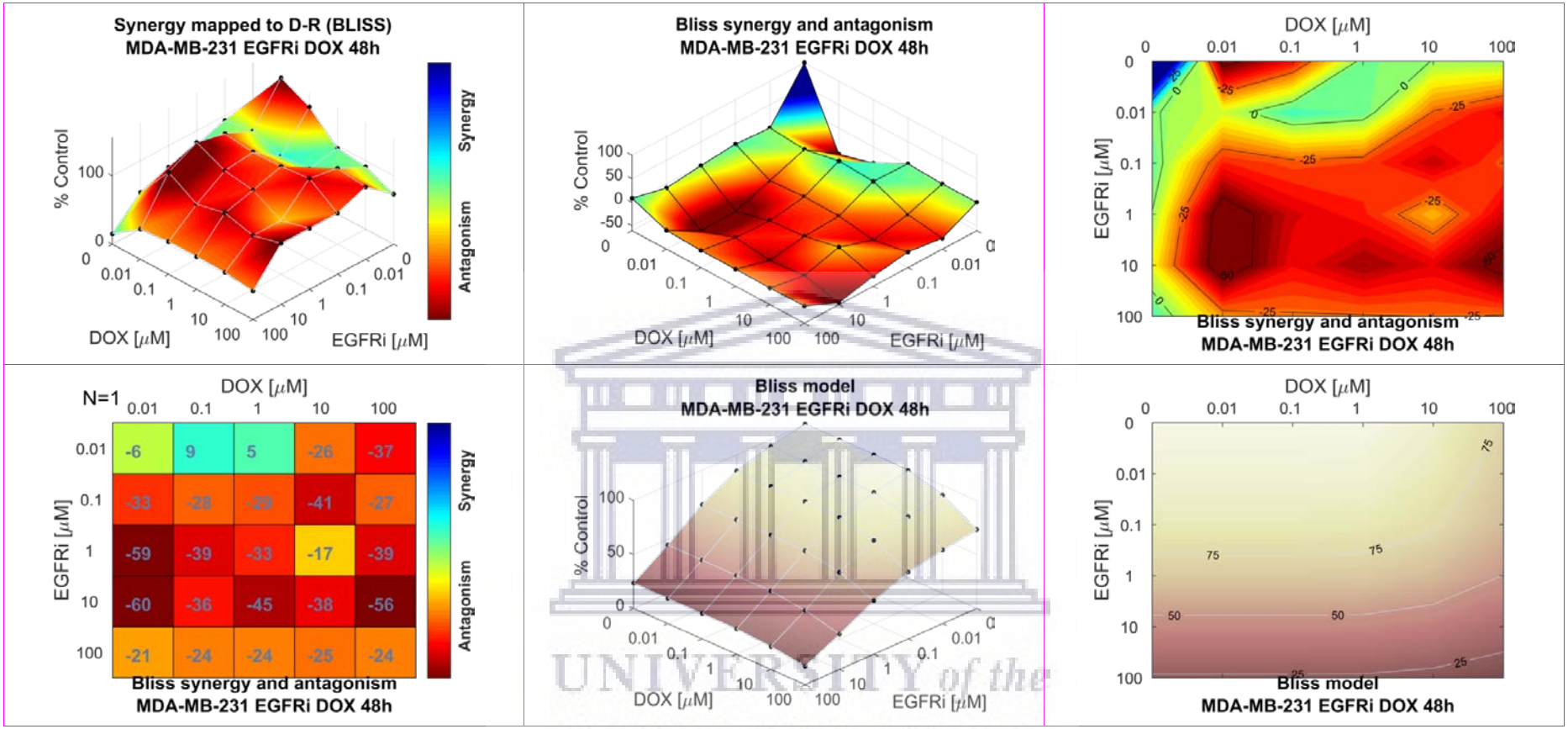

Figure 3.8A: Bliss independence response surface reference model for the dual agent combination effects of 48h treatment of MDA-MB-231 TNBC cells with EGFRi and DOX. **Top panel left:** Bliss independence mapping of the synergy levels on the experimental combination dose-response surface | **Top panel center:** Bliss synergy and antagonism levels visualized as a surface | **Top panel right:** Contour map of isoboles (iso-effect) of Bliss synergy and/or antagonism | **Bottom panel left:** Bliss synergy and antagonism matrix | **Bottom panel center**: Bliss model reference dose-response surface | **Bottom panel right:** Bliss model reference dose-response contour map.

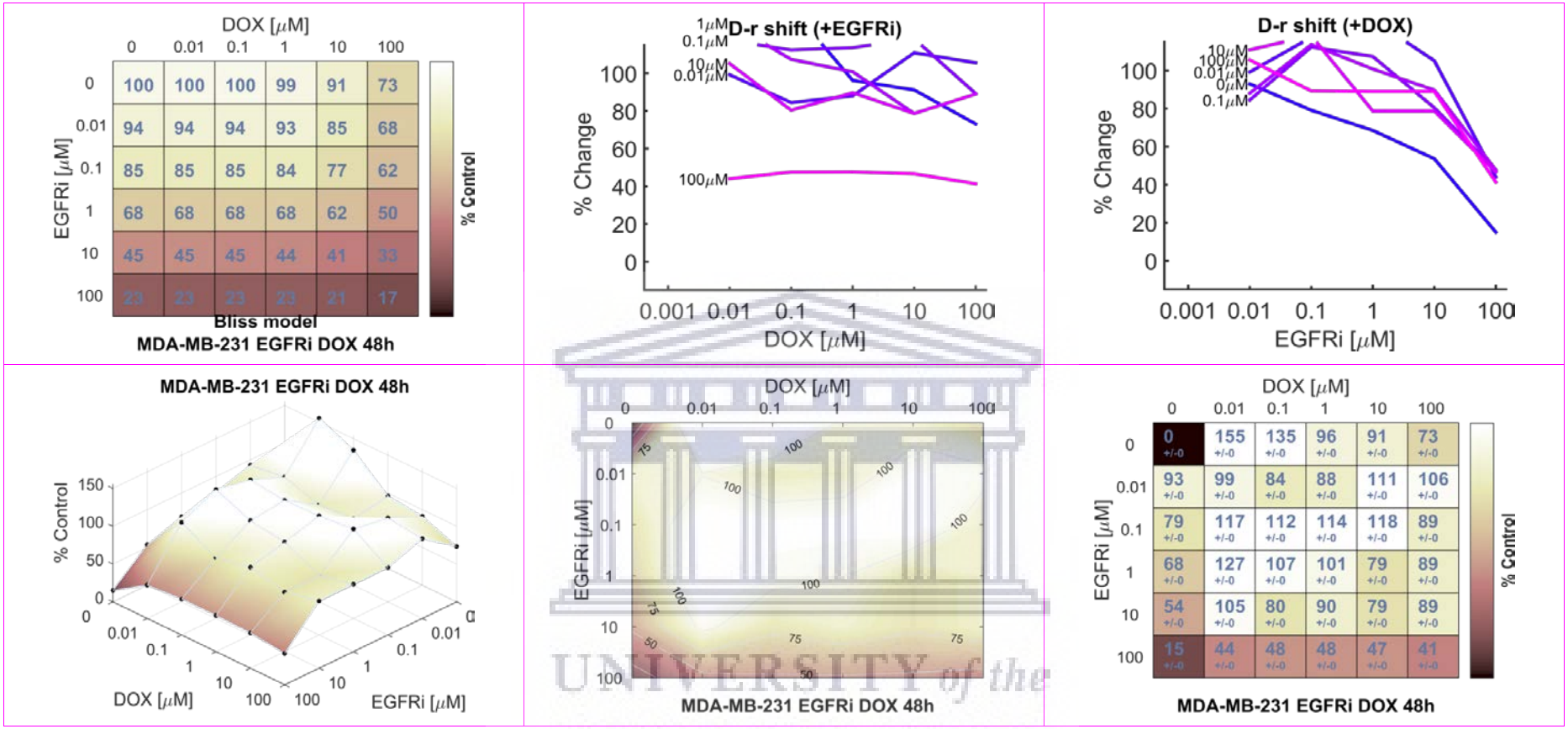

Figure 3.8B: Bliss reference model graphical presentation of the combination effects of 48h treatment of MDA-MB-231 TNBC cells with EGFRi and DOX. **Top panel left:** Bliss model reference dose-response matrix. | **Top panel center:** EGFRi dose-response shift in presence of increasing concentrations of DOX | **Top panel right:** DOX dose-response shift in presence of increasing concentrations of EGFRi | **Bottom panel left:** EGFRi and DOX combination dose-response surface | **Bottom panel center**: EGFRi and DOX combination dose-response contour map | **Bottom panel right:** EGFRi and DOX combination dose-response matrix.

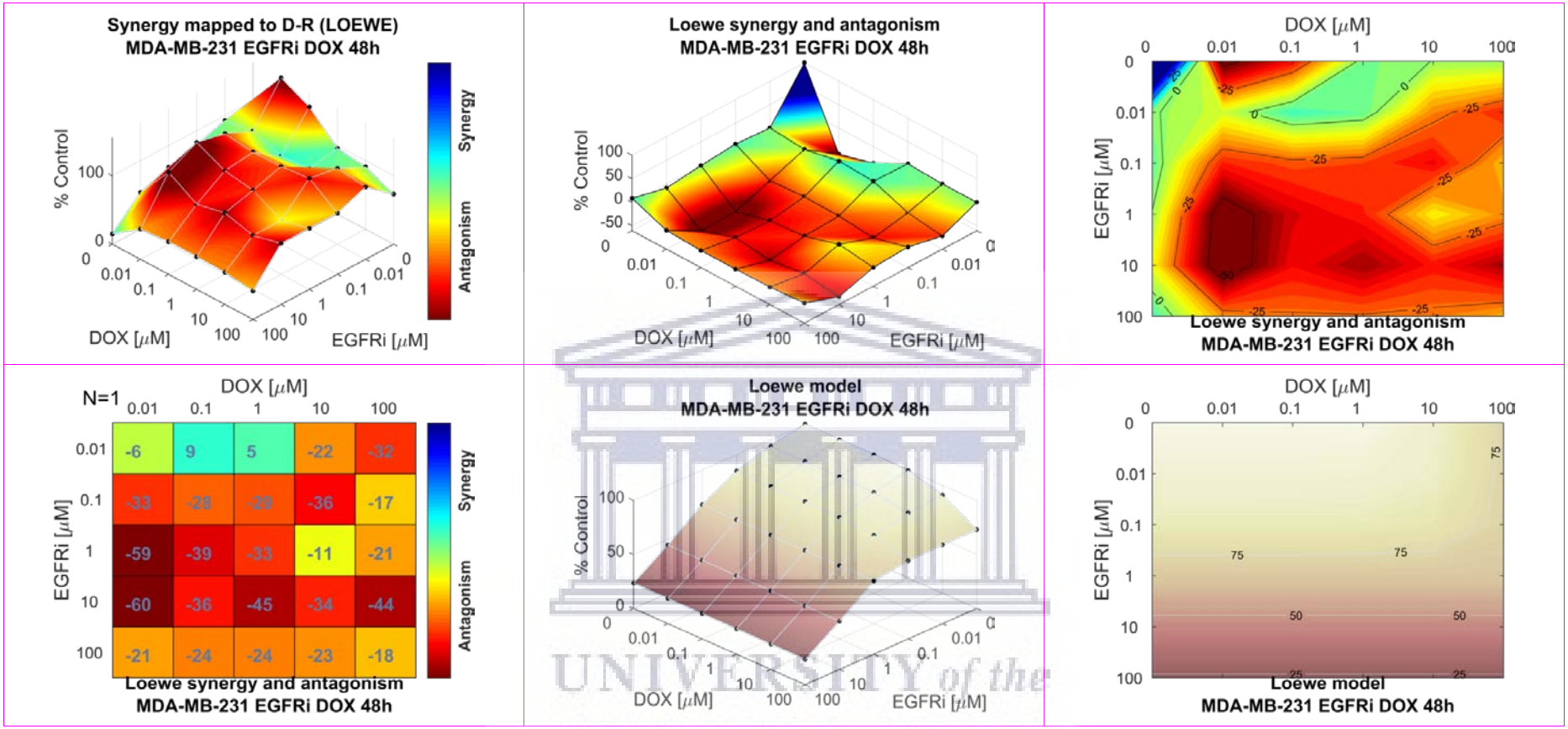

Figure 3.8C: Loewe additivity response surface reference model for the dual agent combination effects of 48h treatment of MDA-MB-231 TNBC cells with EGFRi and DOX. **Top panel left:** Loewe additivity mapping of the synergy levels on the experimental combination dose-response surface | **Top panel center:** Loewe synergy and antagonism levels visualized as a surface | **Top panel right:** Contour map of isoboles (iso-effect) of Loewe synergy and/or antagonism | **Bottom panel left:** Loewe synergy and antagonism matrix | **Bottom panel center**: Loewe model reference dose-response surface | **Bottom panel right:** Loewe model reference dose-response contour map.

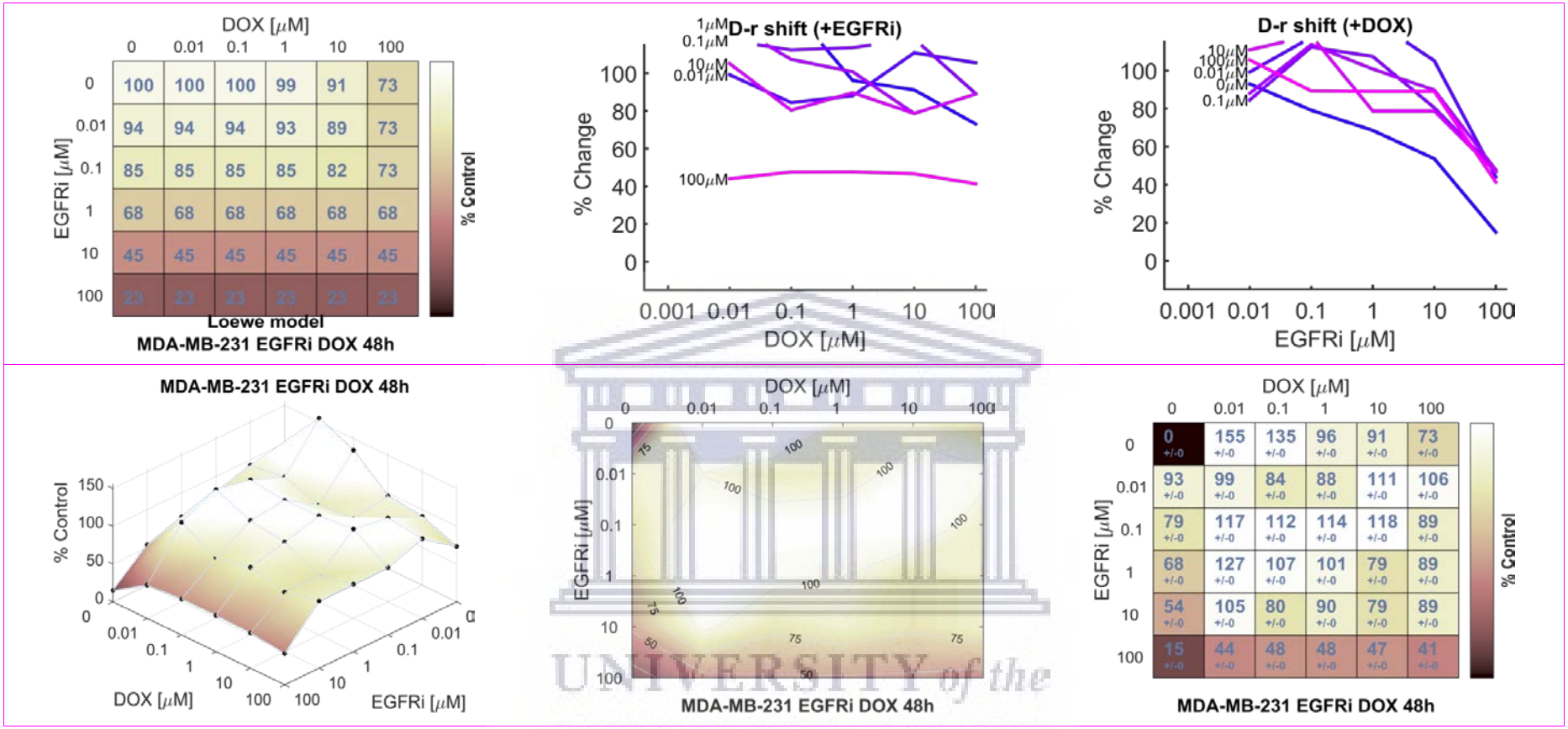

Figure 3.8D: Loewe reference model graphical presentation of the combination effects of 48h treatment of MDA-MB-231 TNBC cells with EGFRi and DOX. **Top panel left:** Loewe additivity model reference dose-response matrix. | **Top panel center:** EGFRi dose-response shift in presence of increasing concentrations of DOX | **Top panel right:** DOX dose-response shift in presence of increasing concentrations of EGFRi | **Bottom panel left:** EGFRi and DOX combination dose-response surface | **Bottom panel center**: EGFRi and DOX combination dose-response contour map | **Bottom panel right:** EGFRi and DOX combination dose-response matrix.

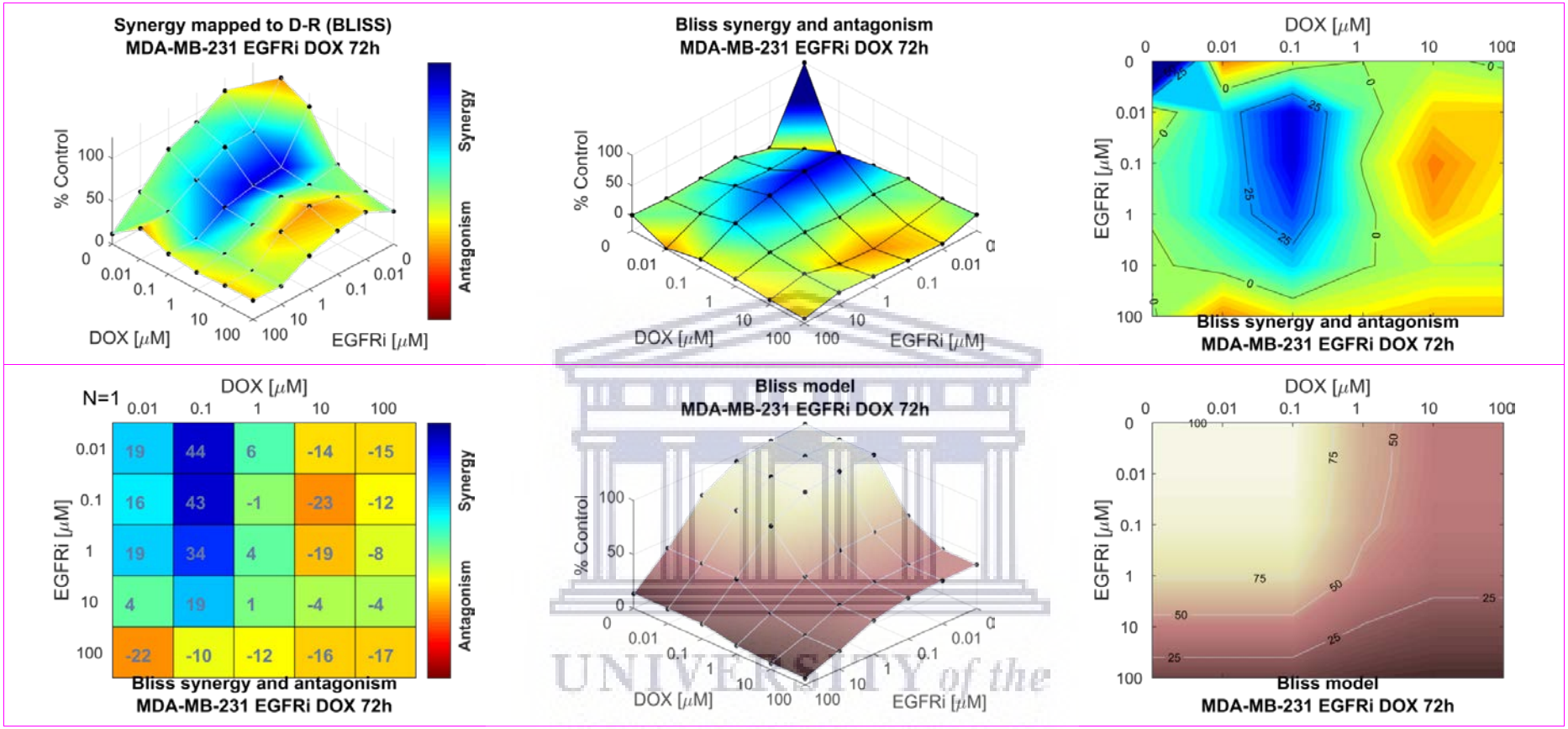

Figure 3.9A: Bliss independence response surface reference model for the dual agent combination effects of 72h treatment of MDA-MB-231 TNBC cells with EGFRi and DOX. **Top panel left:** Bliss independence mapping of the synergy levels on the experimental combination dose-response surface | **Top panel center:** Bliss synergy and antagonism levels visualized as a surface | **Top panel right:** Contour map of isoboles (iso-effect) of Bliss synergy and/or antagonism | **Bottom panel left:** Bliss synergy and antagonism matrix | **Bottom panel center**: Bliss model reference dose-response surface | **Bottom panel right:** Bliss model reference dose-response contour map.

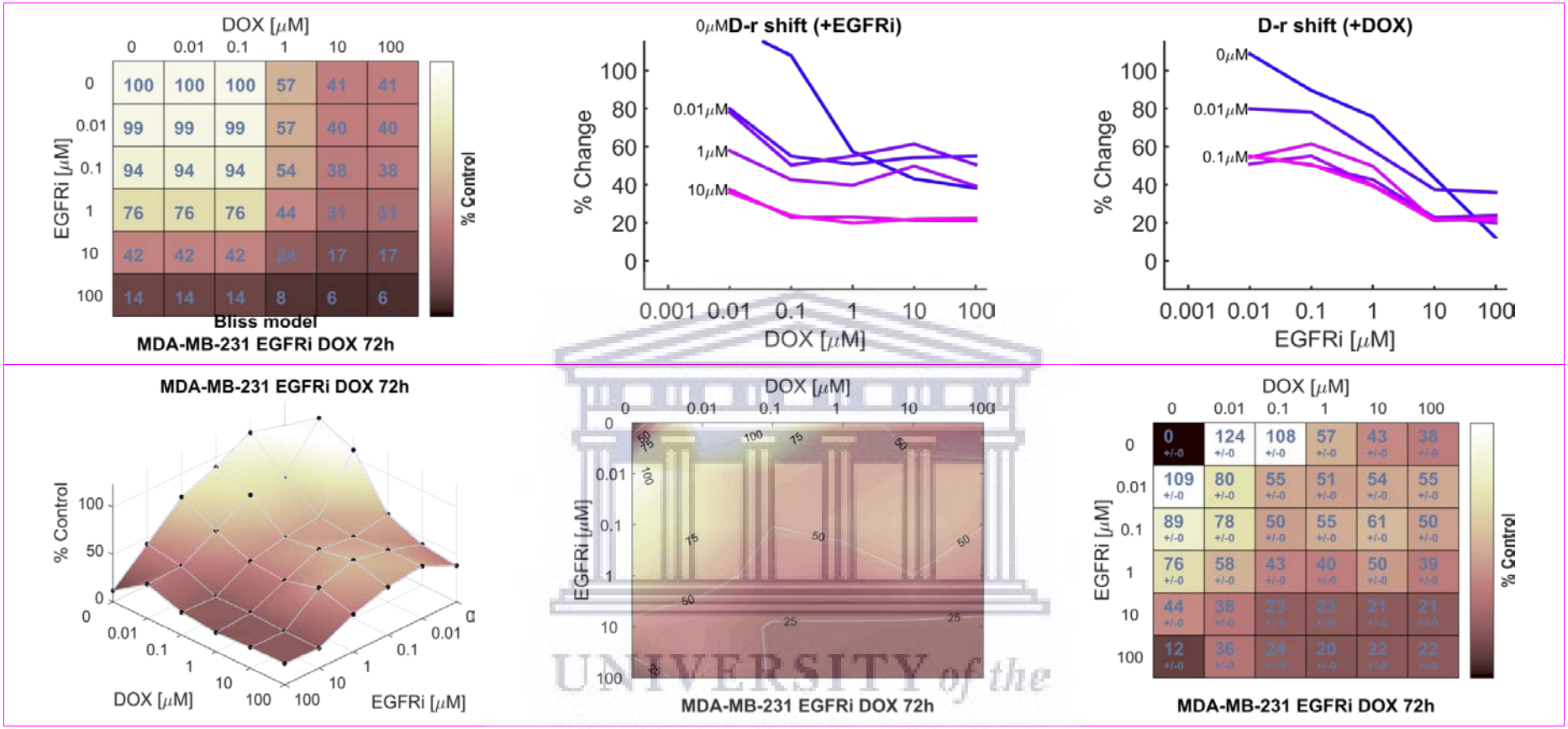

Figure 3.9B: Bliss reference model graphical presentation of the combination effects of 72h treatment of MDA-MB-231 TNBC cells with EGFRi and DOX. **Top panel left:** Bliss model reference dose-response matrix. | **Top panel center:** EGFRi dose-response shift in presence of increasing concentrations of DOX | **Top panel right:** DOX dose-response shift in presence of increasing concentrations of EGFRi | **Bottom panel left:** EGFRi and DOX combination dose-response surface | **Bottom panel center**: EGFRi and DOX combination dose-response contour map | **Bottom panel right:** EGFRi and DOX combination dose-response matrix.

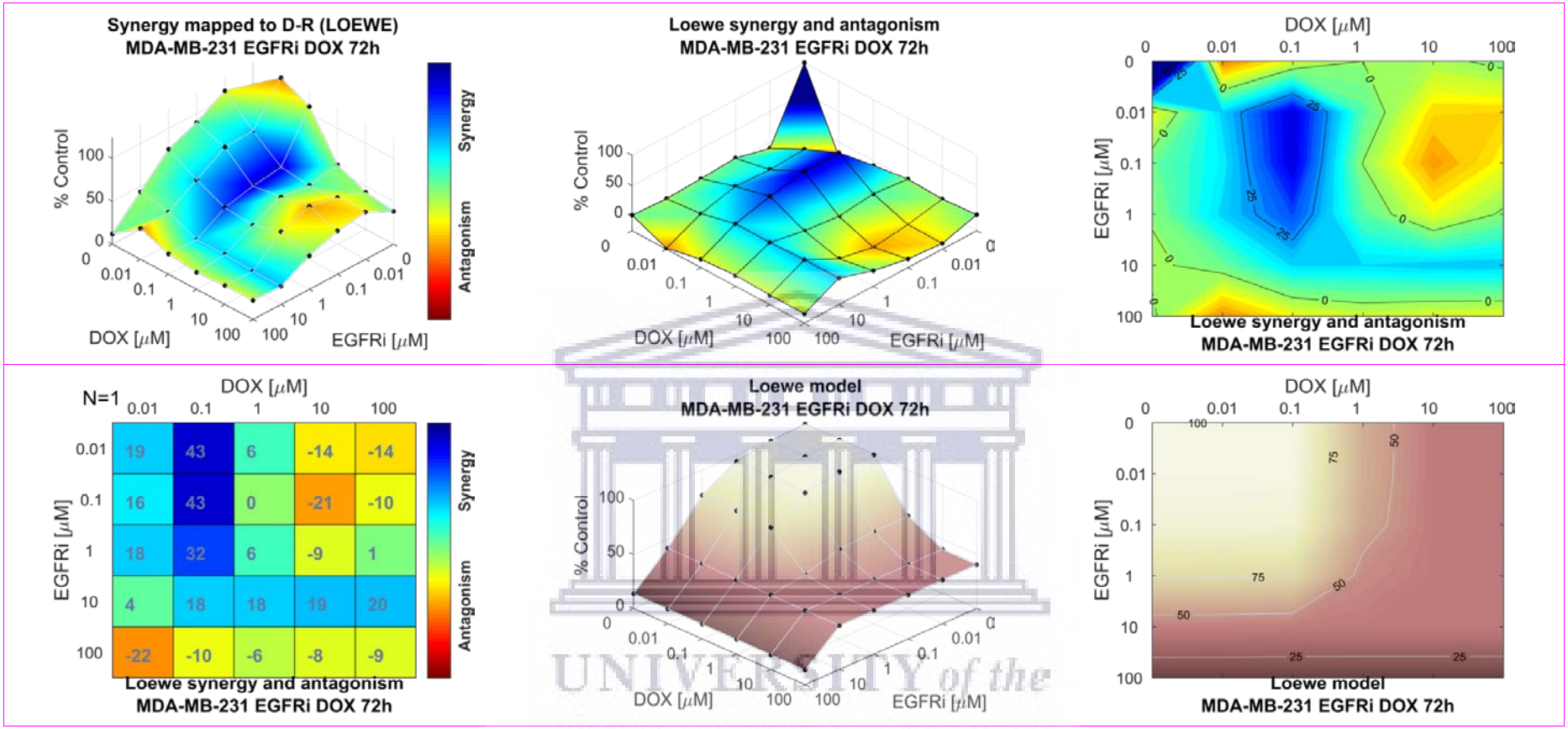

Figure 3.9C: Loewe additivity response surface reference model for the dual agent combination effects of 72h treatment of MDA-MB-231 TNBC cells with EGFRi and DOX. **Top panel left:** Loewe additivity mapping of the synergy levels on the experimental combination dose-response surface | **Top panel center:** Loewe synergy and antagonism levels visualized as a surface | **Top panel right:** Contour map of isoboles (iso-effect) of Loewe synergy and/or antagonism | **Bottom panel left:** Loewe synergy and antagonism matrix | **Bottom panel center**: Loewe model reference dose-response surface | **Bottom panel right:** Loewe model reference dose-response contour map.

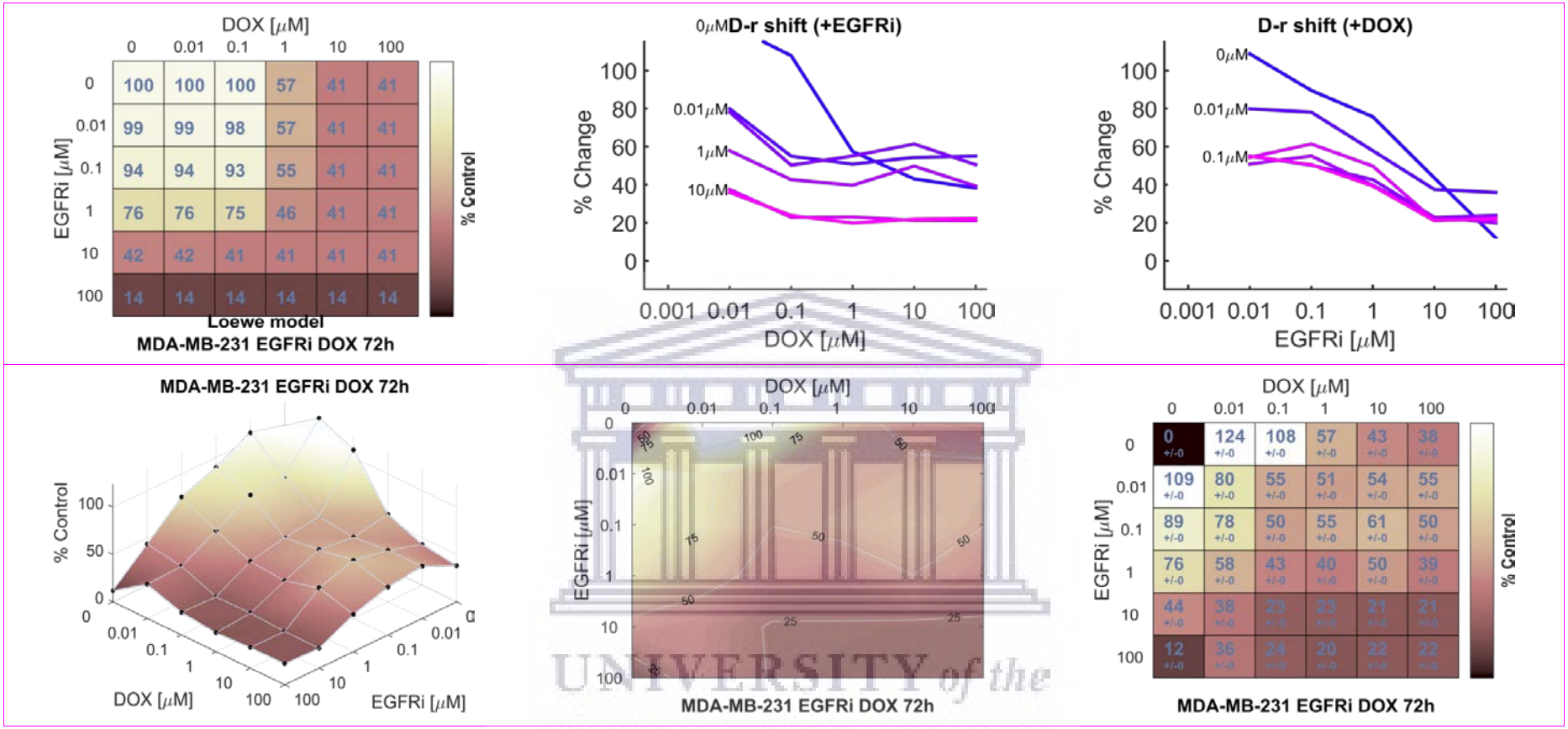

Figure 3.9D: Loewe reference model graphical presentation of the combination effects of 72h treatment of MDA-MB-231 TNBC cells with EGFRi and DOX. **Top panel left:** Loewe additivity model reference dose-response matrix. | **Top panel center:** EGFRi dose-response shift in presence of increasing concentrations of DOX | **Top panel right:** DOX dose-response shift in presence of increasing concentrations of EGFRi | **Bottom panel left:** EGFRi and DOX combination dose-response surface | **Bottom panel center**: EGFRi and DOX combination dose-response contour map | **Bottom panel right:** EGFRi and DOX combination dose-response matrix.

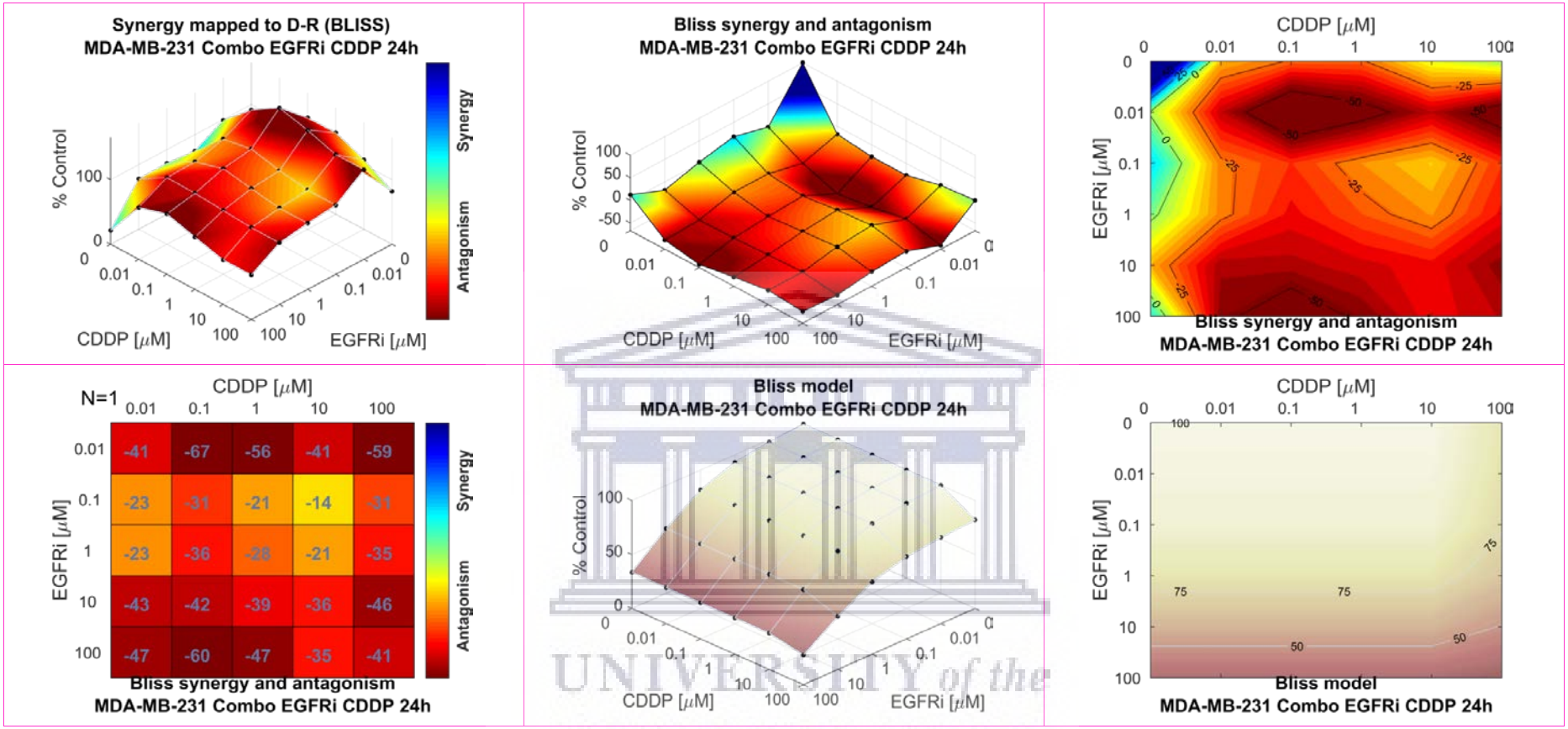

Figure 3.10A: Bliss independence response surface reference model for the dual agent combination effects of 24h treatment of MDA-MB-231 TNBC cells with EGFRi and CDDP. **Top panel left:** Bliss independence mapping of the synergy levels on the experimental combination dose-response surface | **Top panel center:** Bliss synergy and antagonism levels visualized as a surface | **Top panel right:** Contour map of isoboles (iso-effect) of Bliss synergy and/or antagonism | **Bottom panel left:** Bliss synergy and antagonism matrix | **Bottom panel center**: Bliss model reference dose-response surface | **Bottom panel right:** Bliss model reference dose-response contour map.

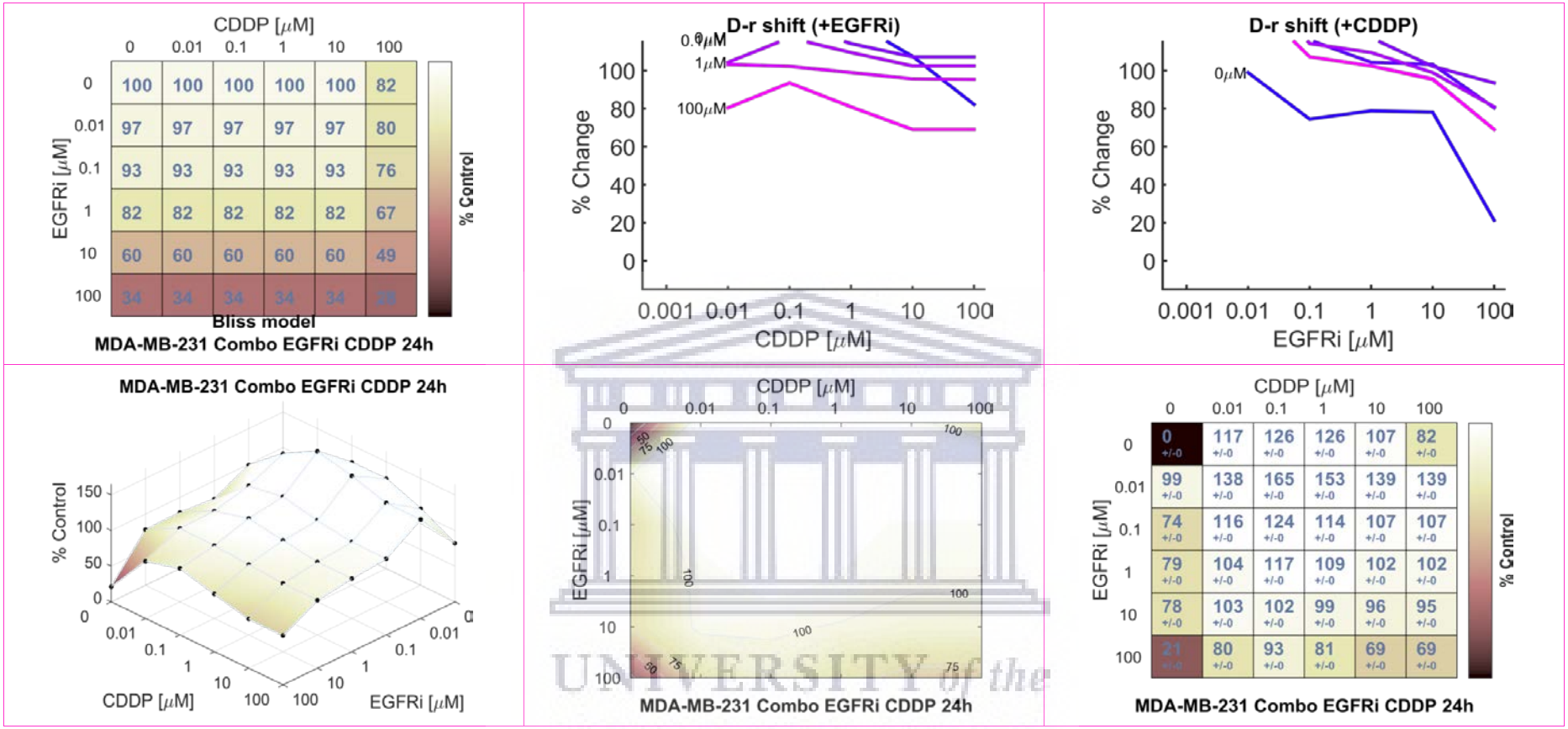

Figure 3.10B: Bliss reference model graphical presentation of the combination effects of 24h treatment of MDA-MB-231 TNBC cells with EGFRi and CDDP. **Top panel left:** Bliss model reference dose-response matrix. | **Top panel center:** EGFRi dose-response shift in presence of increasing concentrations of CDDP | **Top panel right:** CDDP dose-response shift in presence of increasing concentrations of EGFRi | **Bottom panel left:** EGFRi and CDDP combination dose-response surface | **Bottom panel center**: EGFRi and CDDP combination dose-response contour map | **Bottom panel right:** EGFRi and CDDP combination dose-response matrix.

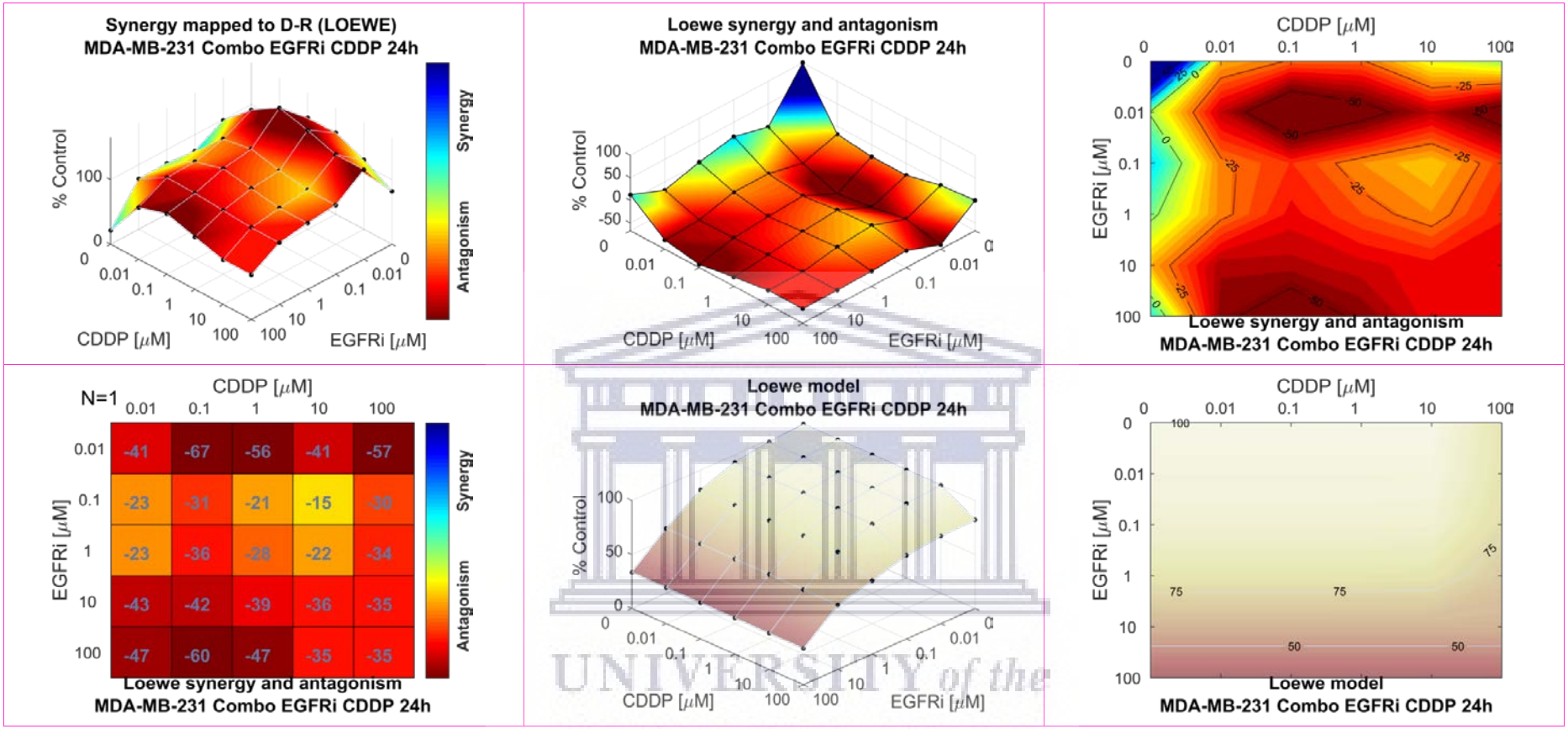

Figure 3.10C: Loewe additivity response surface reference model for the dual agent combination effects of 24h treatment of MDA-MB-231 TNBC cells with EGFRi and CDDP. **Top panel left:** Loewe additivity mapping of the synergy levels on the experimental combination dose-response surface | **Top panel center:** Loewe synergy and antagonism levels visualized as a surface | **Top panel right:** Contour map of isoboles (iso-effect) of Loewe synergy and/or antagonism | **Bottom panel left:** Loewe synergy and antagonism matrix | **Bottom panel center**: Loewe model reference dose-response surface | **Bottom panel right:** Loewe model reference dose-response contour map.

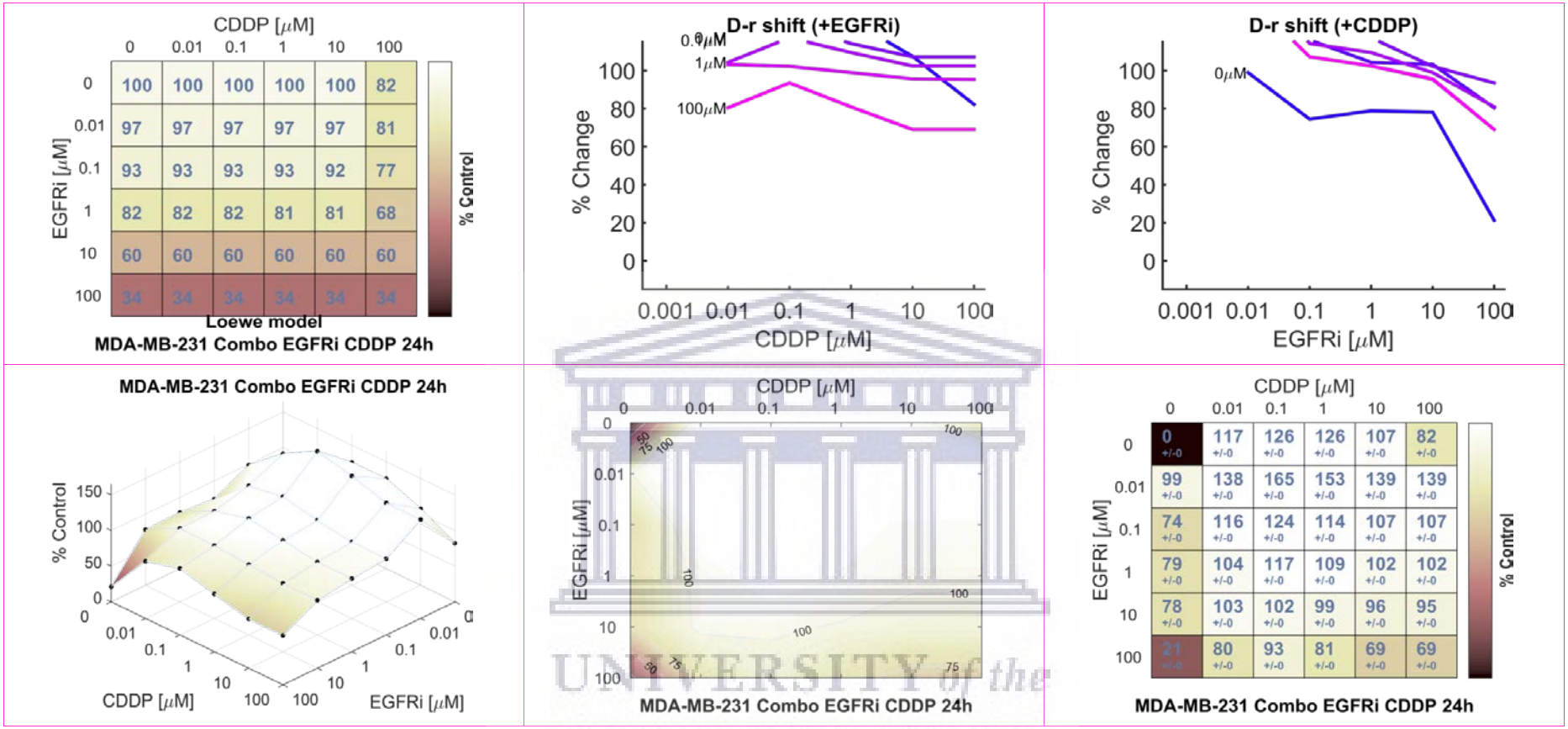

Figure 3.10D: Loewe reference model graphical presentation of the combination effects of 24h treatment of MDA-MB-231 TNBC cells with EGFRi and CDDP. **Top panel left:** Loewe additivity model reference dose-response matrix. | **Top panel center:** EGFRi dose-response shift in presence of increasing concentrations of CDDP | **Top panel right:** CDDP dose-response shift in presence of increasing concentrations of EGFRi | **Bottom panel left:** EGFRi and CDDP combination dose-response surface | **Bottom panel center**: EGFRi and CDDP combination dose-response contour map | **Bottom panel right:** EGFRi and CDDP combination dose-response matrix.

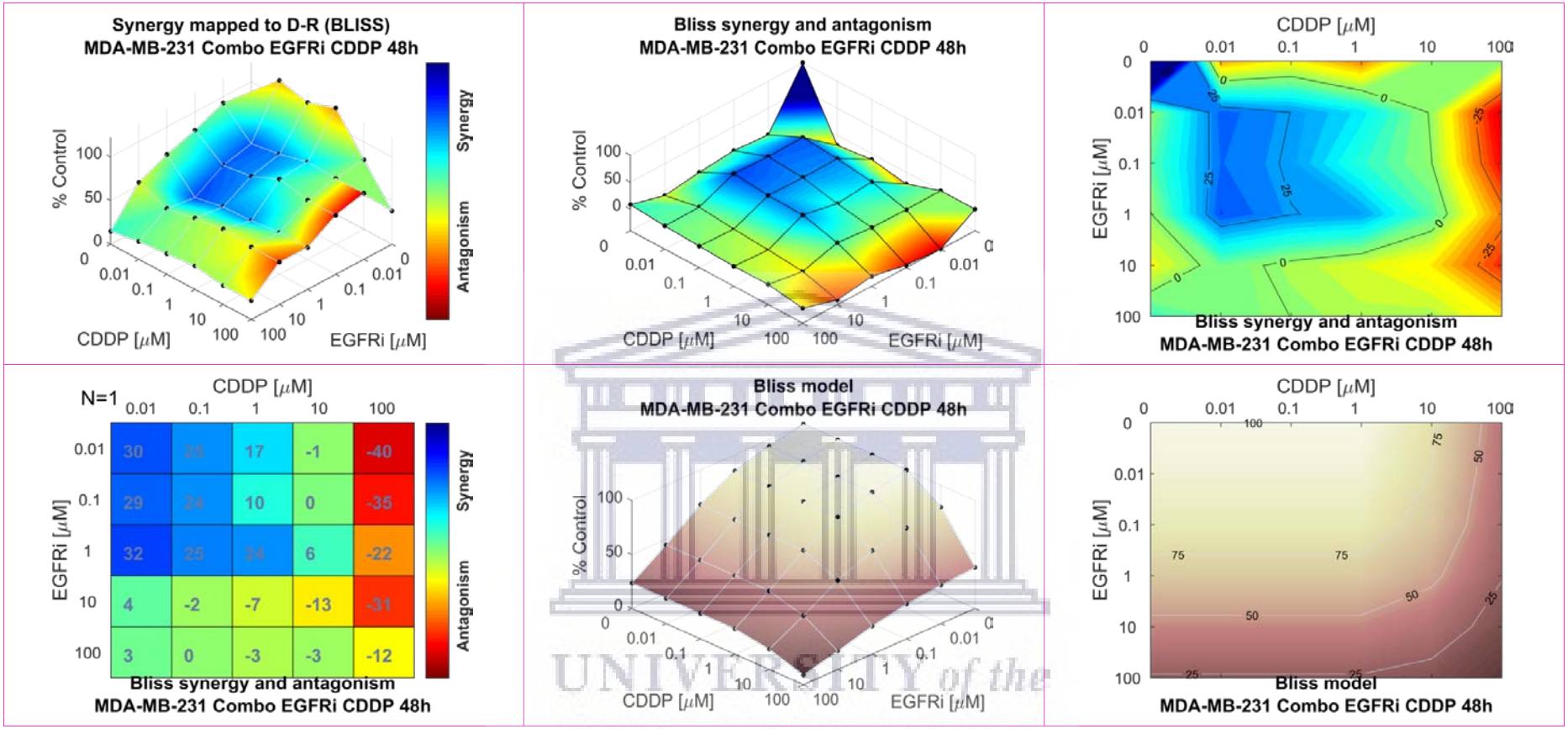

Figure 3.11A: Bliss independence response surface reference model for the dual agent combination effects of 48h treatment of MDA-MB-231 TNBC cells with EGFRi and CDDP. **Top panel left:** Bliss independence mapping of the synergy levels on the experimental combination dose-response surface | **Top panel center:** Bliss synergy and antagonism levels visualized as a surface | **Top panel right:** Contour map of isoboles (iso-effect) of Bliss synergy and/or antagonism | **Bottom panel left:** Bliss synergy and antagonism matrix | **Bottom panel center**: Bliss model reference dose-response surface | **Bottom panel right:** Bliss model reference dose-response contour map.

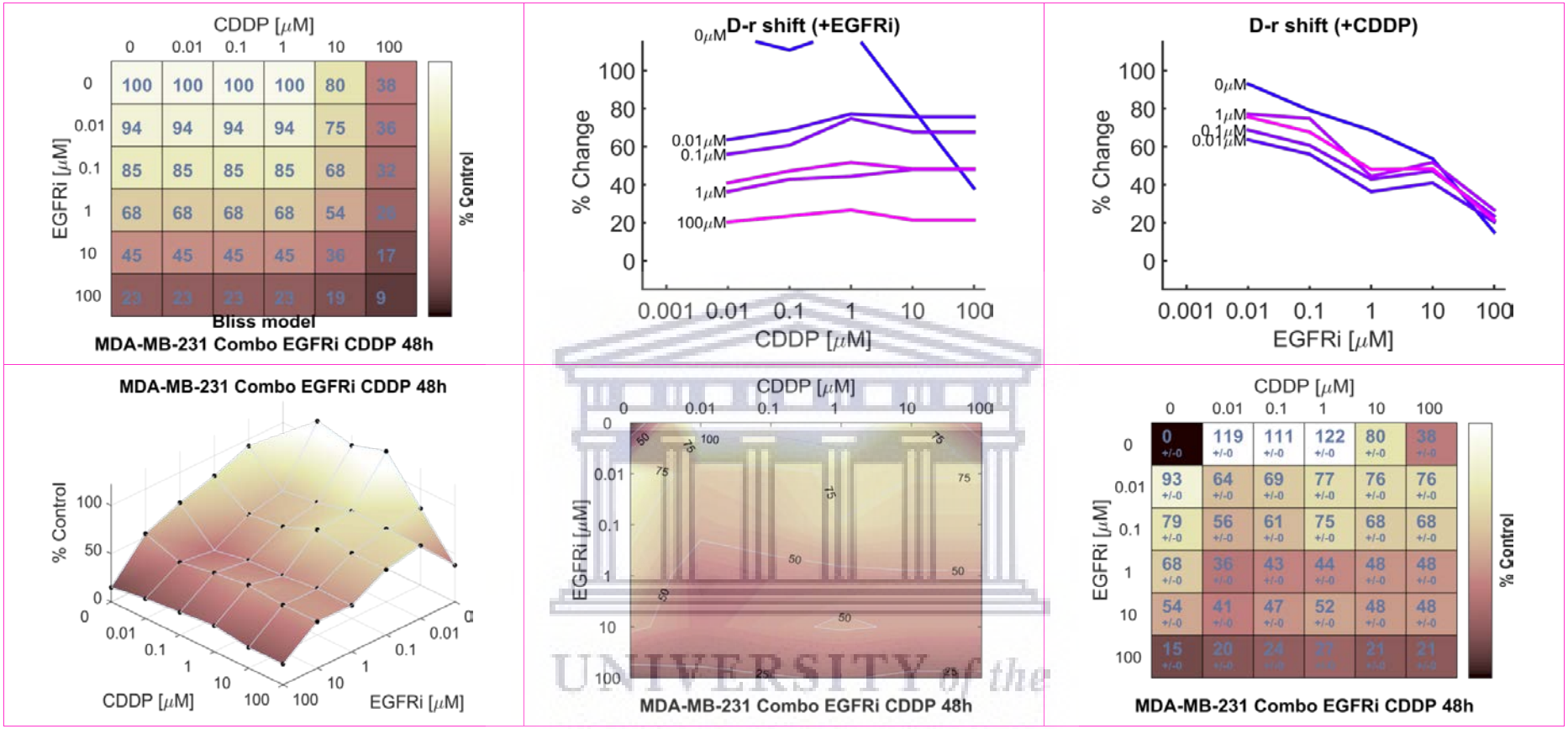

Figure 3.11B: Bliss reference model graphical presentation of the combination effects of 48h treatment of MDA-MB-231 TNBC cells with EGFRi and CDDP. **Top panel left:** Bliss model reference dose-response matrix. | **Top panel center:** EGFRi dose-response shift in presence of increasing concentrations of CDDP | **Top panel right:** CDDP dose-response shift in presence of increasing concentrations of EGFRi | **Bottom panel left:** EGFRi and CDDP combination dose-response surface | **Bottom panel center**: EGFRi and CDDP combination dose-response contour map | **Bottom panel right:** EGFRi and CDDP combination dose-response matrix.

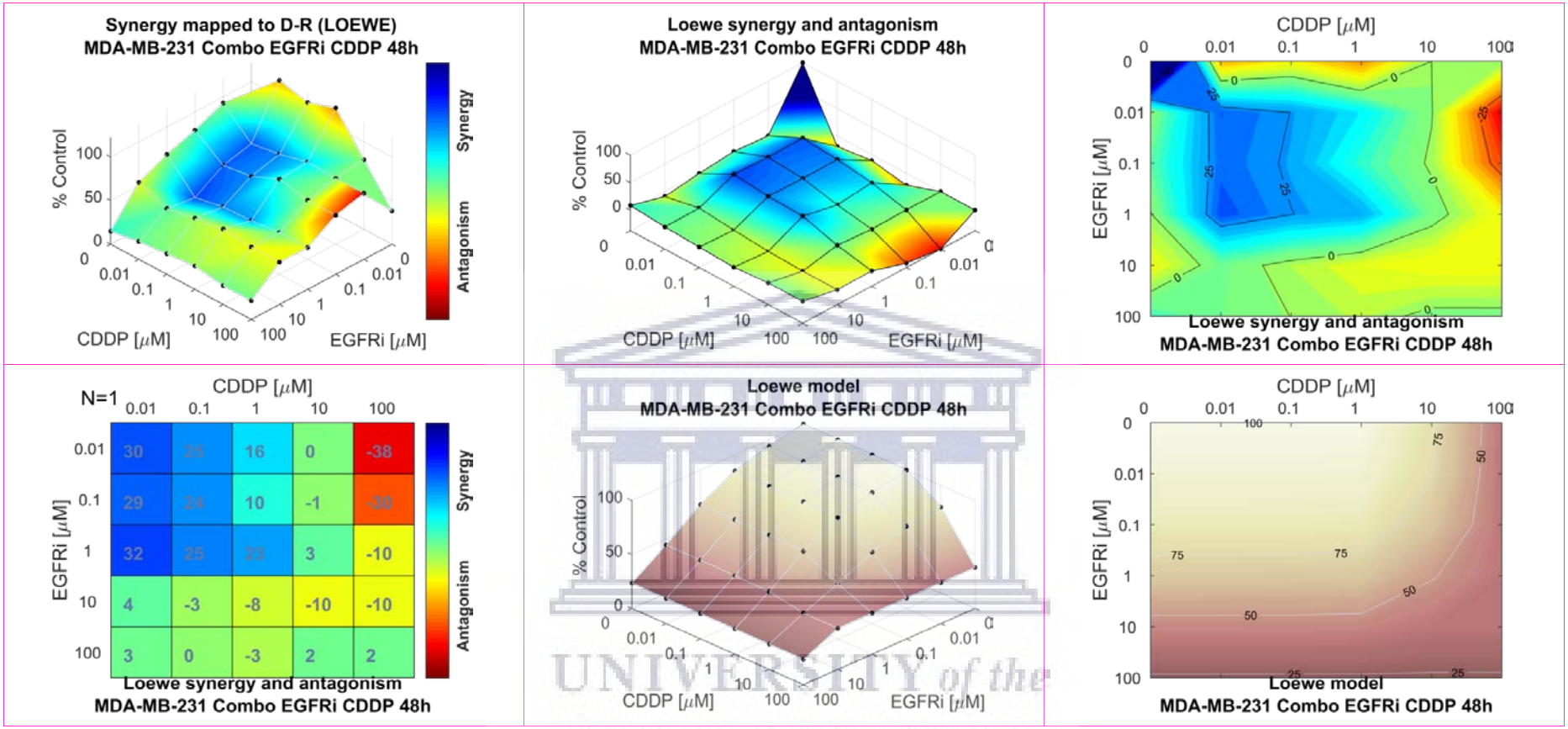

Figure 3.11C: Loewe additivity response surface reference model for the dual agent combination effects of 48h treatment of MDA-MB-231 TNBC cells with EGFRi and CDDP. **Top panel left:** Loewe additivity mapping of the synergy levels on the experimental combination dose-response surface | **Top panel center:** Loewe synergy and antagonism levels visualized as a surface | **Top panel right:** Contour map of isoboles (iso-effect) of Loewe synergy and/or antagonism | **Bottom panel left:** Loewe synergy and antagonism matrix | **Bottom panel center**: Loewe model reference dose-response surface | **Bottom panel right:** Loewe model reference dose-response contour map.

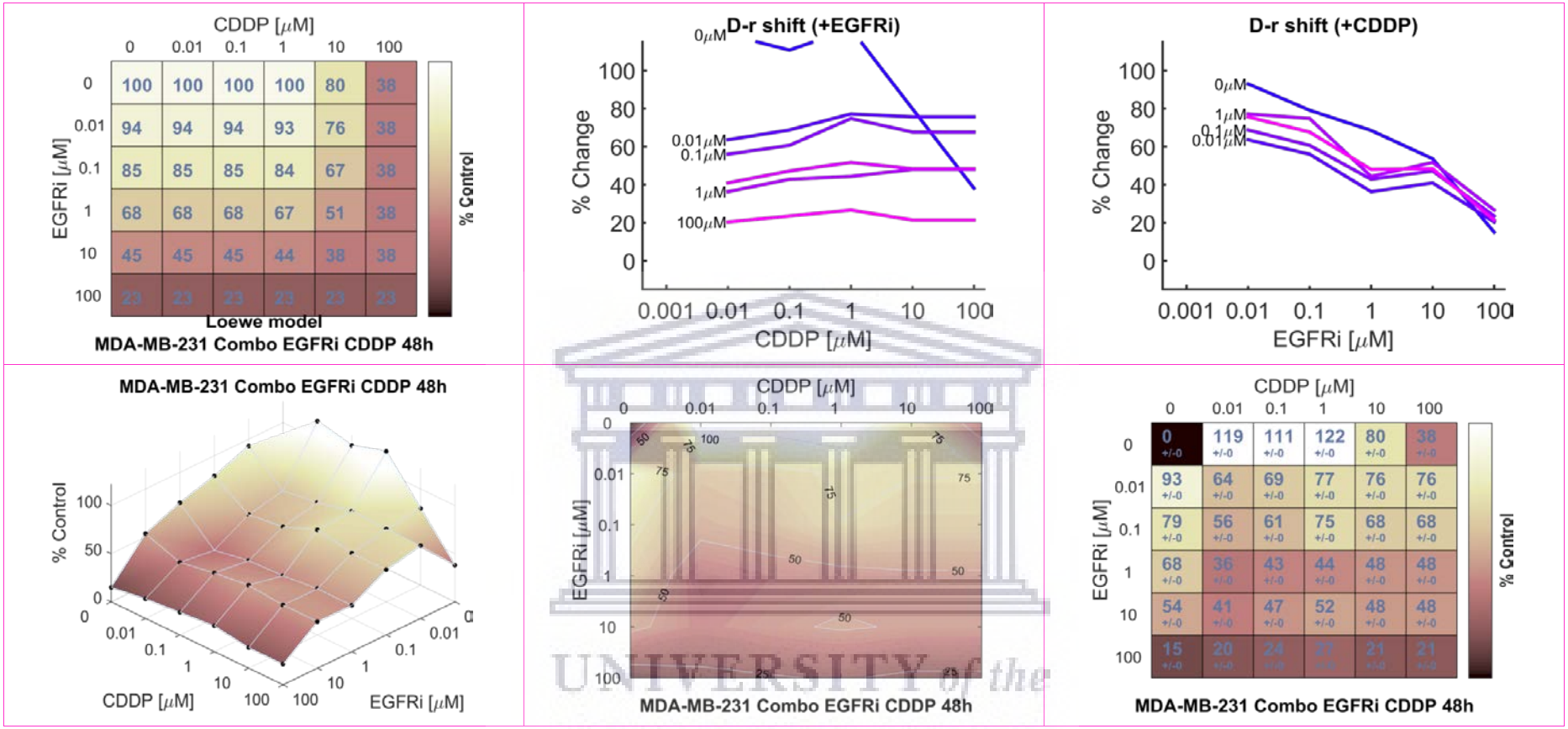

Figure 3.11D: Loewe reference model graphical presentation of the combination effects of 48h treatment of MDA-MB-231 TNBC cells with EGFRi and CDDP. **Top panel left:** Loewe additivity model reference dose-response matrix. | **Top panel center:** EGFRi dose-response shift in presence of increasing concentrations of CDDP | **Top panel right:** CDDP dose-response shift in presence of increasing concentrations of EGFRi | **Bottom panel left:** EGFRi and CDDP combination dose-response surface | **Bottom panel center**: EGFRi and CDDP combination dose-response contour map | **Bottom panel right:** EGFRi and CDDP combination dose-response matrix.

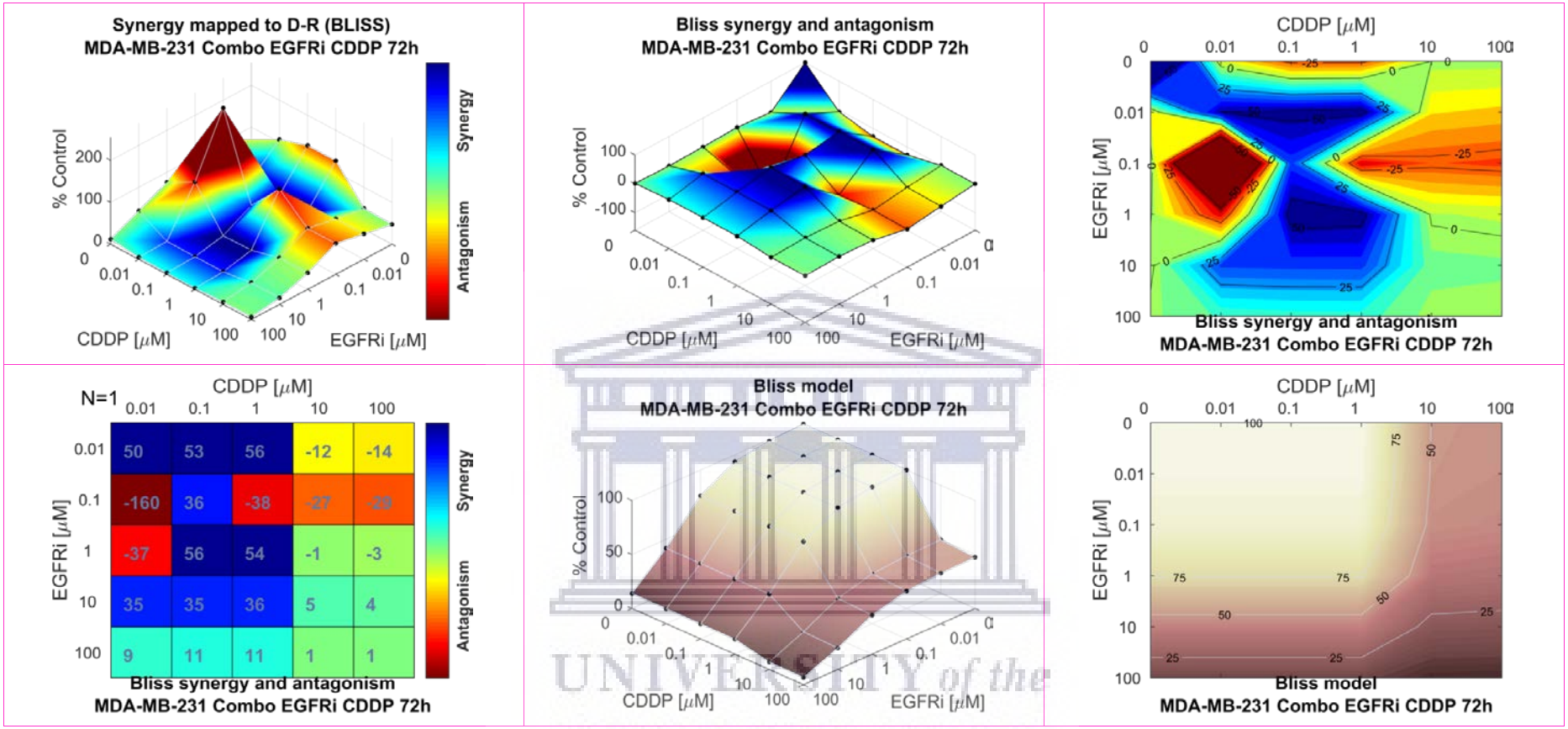

Figure 3.12A: Bliss independence response surface reference model for the dual agent combination effects of 72h treatment of MDA-MB-231 TNBC cells with EGFRi and CDDP. **Top panel left:** Bliss independence mapping of the synergy levels on the experimental combination dose-response surface | **Top panel center:** Bliss synergy and antagonism levels visualized as a surface | **Top panel right:** Contour map of isoboles (iso-effect) of Bliss synergy and/or antagonism | **Bottom panel left:** Bliss synergy and antagonism matrix | **Bottom panel center**: Bliss model reference dose-response surface | **Bottom panel right:** Bliss model reference dose-response contour map.

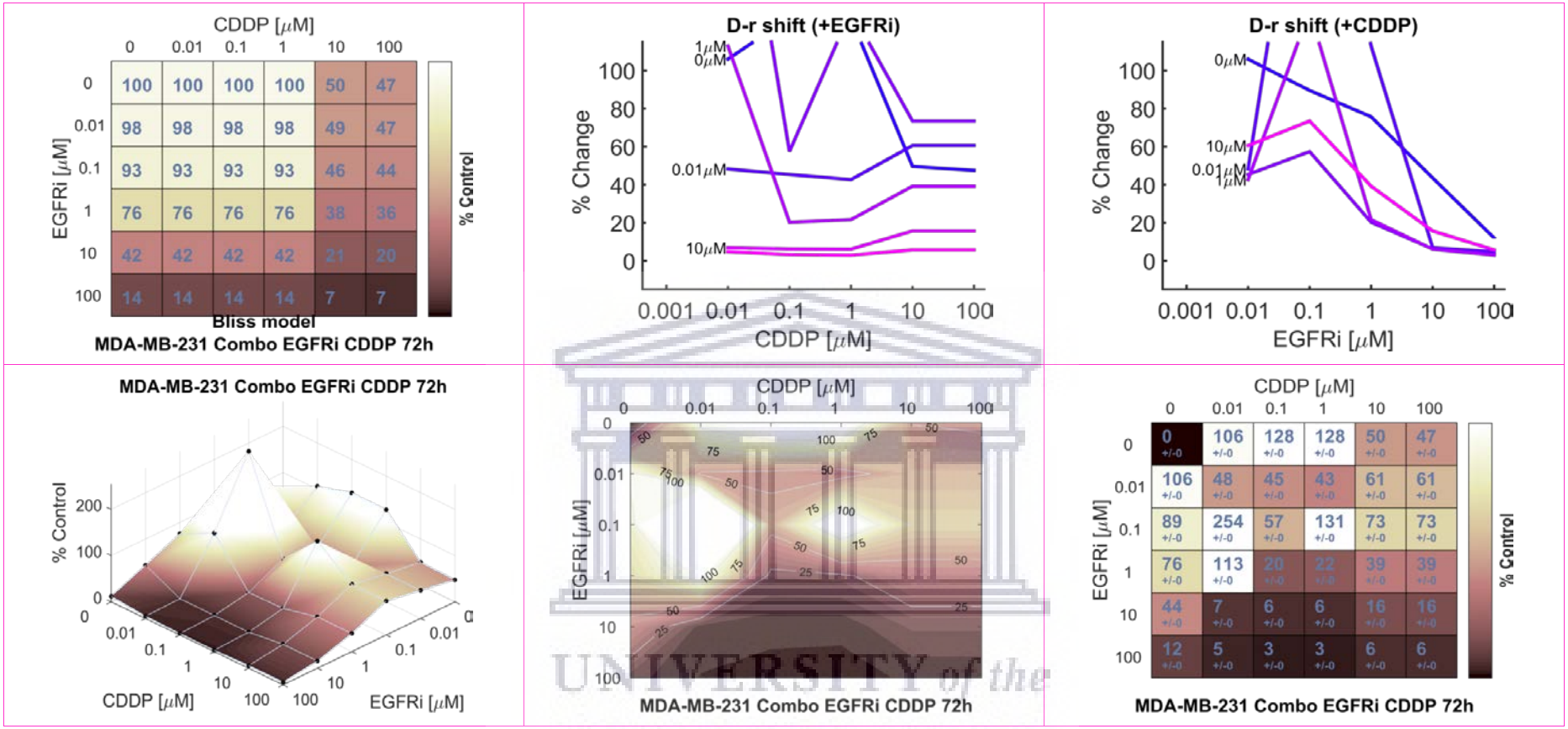

Figure 3.12B: Bliss reference model graphical presentation of the combination effects of 72h treatment of MDA-MB-231 TNBC cells with EGFRi and CDDP. **Top panel left:** Bliss model reference dose-response matrix. | **Top panel center:** EGFRi dose-response shift in presence of increasing concentrations of CDDP | **Top panel right:** CDDP dose-response shift in presence of increasing concentrations of EGFRi | **Bottom panel left:** EGFRi and CDDP combination dose-response surface | **Bottom panel center**: EGFRi and CDDP combination dose-response contour map | **Bottom panel right:** EGFRi and CDDP combination dose-response matrix.

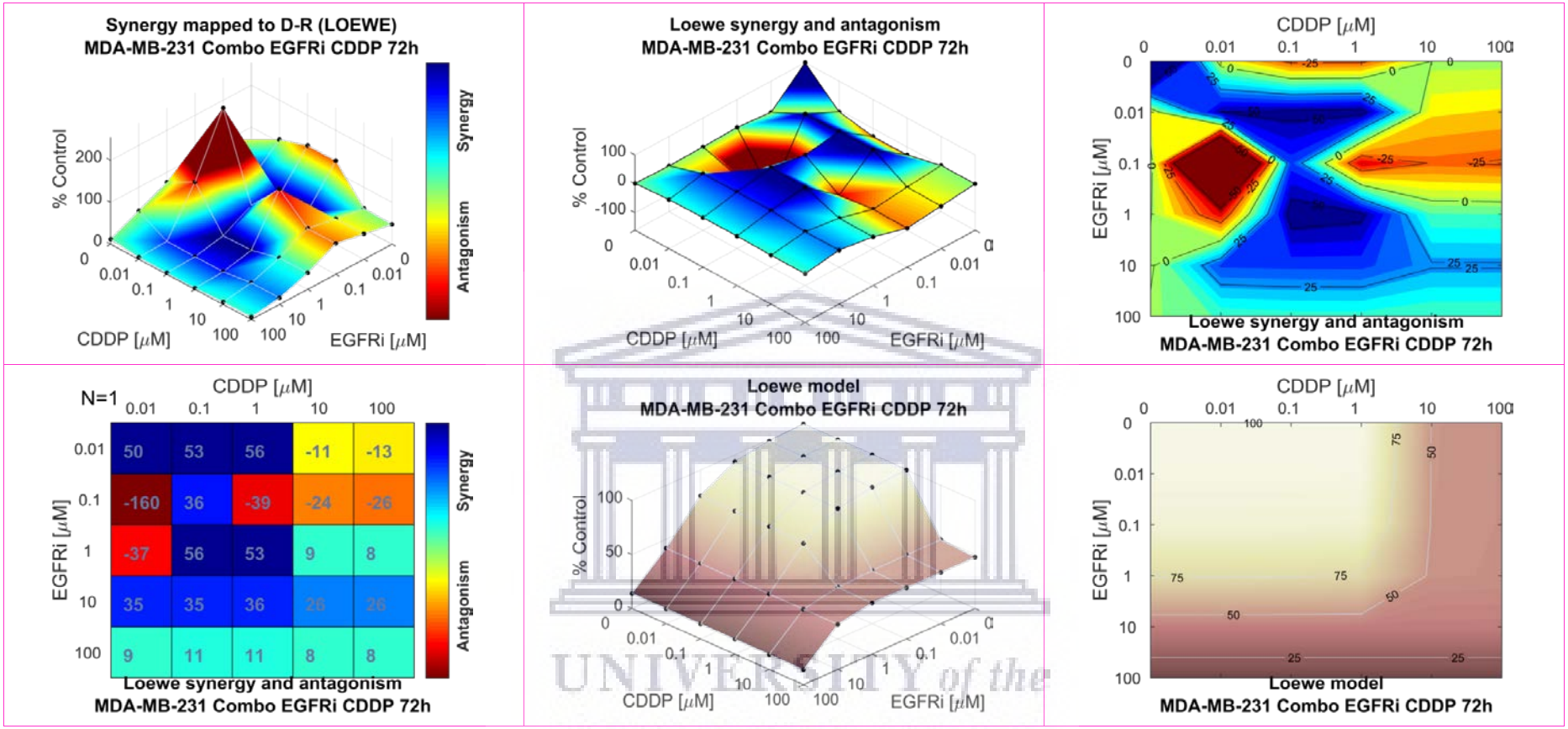

Figure 3.12C: Loewe additivity response surface reference model for the dual agent combination effects of 72h treatment of MDA-MB-231 TNBC cells with EGFRi and CDDP. **Top panel left:** Loewe additivity mapping of the synergy levels on the experimental combination dose-response surface | **Top panel center:** Loewe synergy and antagonism levels visualized as a surface | **Top panel right:** Contour map of isoboles (iso-effect) of Loewe synergy and/or antagonism | **Bottom panel left:** Loewe synergy and antagonism matrix | **Bottom panel center**: Loewe model reference dose-response surface | **Bottom panel right:** Loewe model reference dose-response contour map.

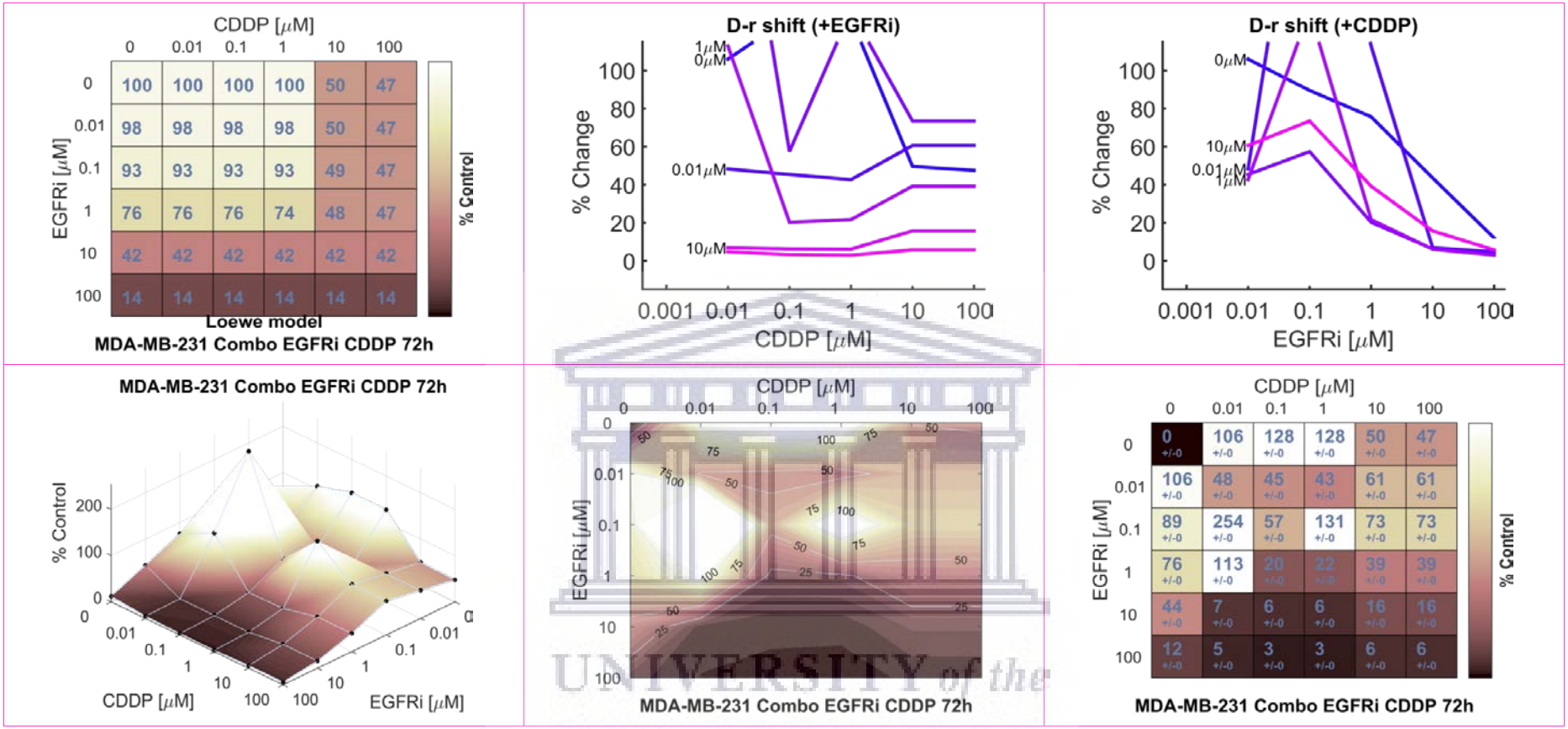

Figure 3.12D: Loewe reference model graphical presentation of the combination effects of 72h treatment of MDA-MB-231 TNBC cells with EGFRi and CDDP. **Top panel left:** Loewe additivity model reference dose-response matrix. | **Top panel center:** EGFRi dose-response shift in presence of increasing concentrations of CDDP | **Top panel right:** CDDP dose-response shift in presence of increasing concentrations of EGFRi | **Bottom panel left:** EGFRi and CDDP combination dose-response surface | **Bottom panel center**: EGFRi and CDDP combination dose-response contour map | **Bottom panel right:** EGFRi and CDDP combination dose-response matrix.

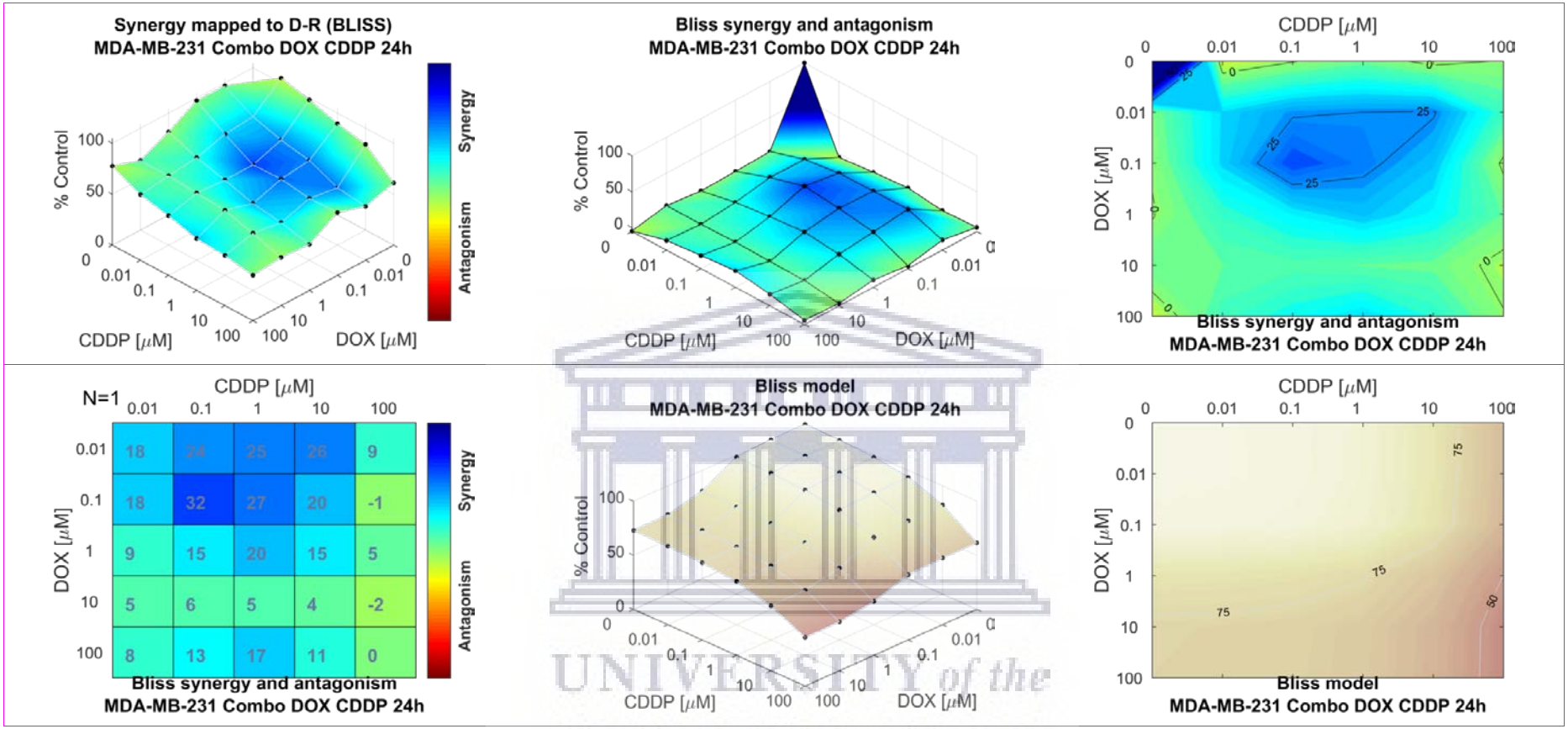

Figure 3.13A: Bliss independence response surface reference model for the dual agent combination effects of 24h treatment of MDA-MB-231 TNBC cells with DOX and CDDP. **Top panel left:** Bliss independence mapping of the synergy levels on the experimental combination dose-response surface | **Top panel center:** Bliss synergy and antagonism levels visualized as a surface | **Top panel right:** Contour map of isoboles (iso-effect) of Bliss synergy and/or antagonism | **Bottom panel left:** Bliss synergy and antagonism matrix | **Bottom panel center**: Bliss model reference dose-response surface | **Bottom panel right:** Bliss model reference dose-response contour map.

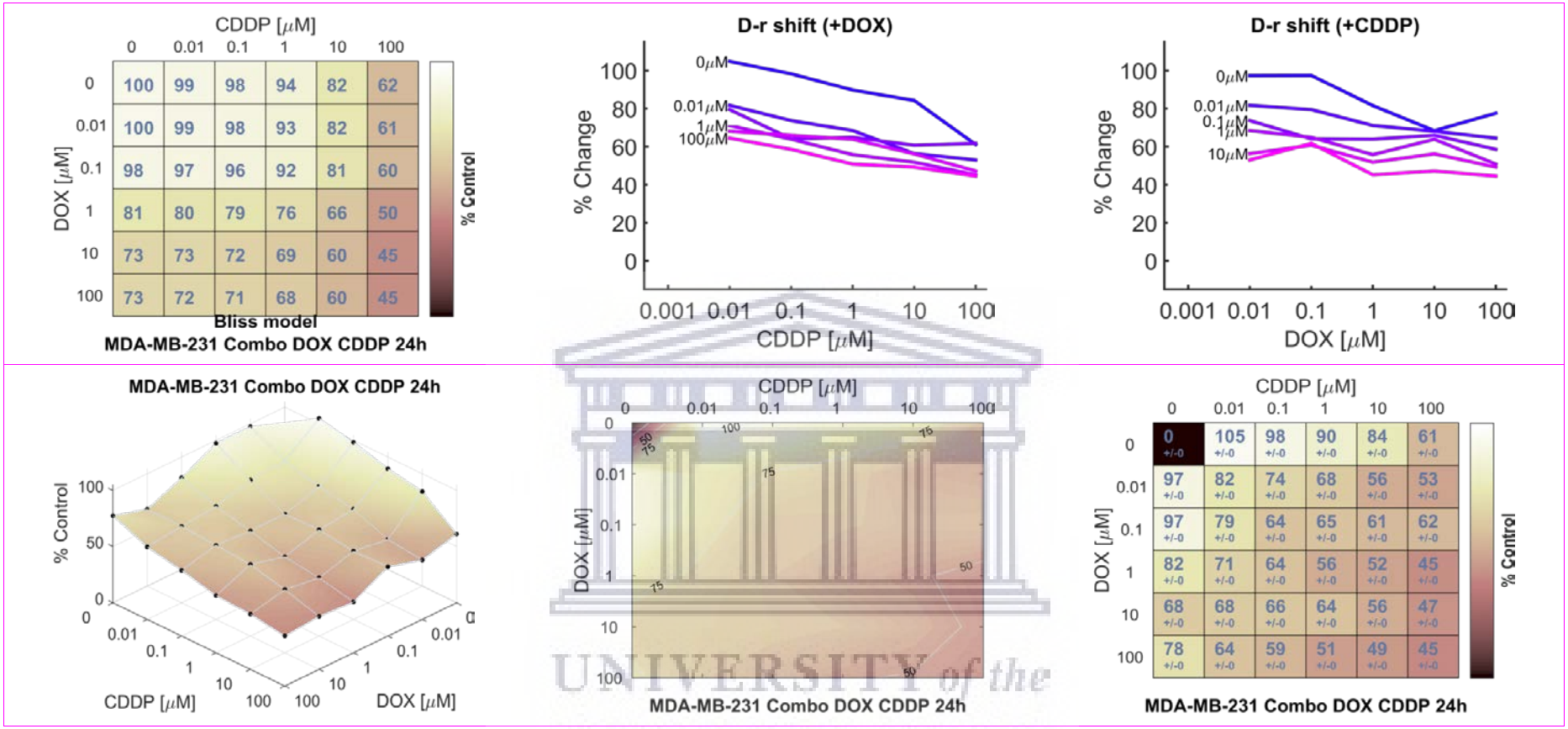

Figure 3.13B: Bliss reference model graphical presentation of the combination effects of 24h treatment of MDA-MB-231 TNBC cells with DOX and CDDP. **Top panel left:** Bliss model reference dose-response matrix. | **Top panel center:** DOX dose-response shift in presence of increasing concentrations of CDDP | **Top panel right:** CDDP dose-response shift in presence of increasing concentrations of DOX | **Bottom panel left:** DOX and CDDP combination dose-response surface | **Bottom panel center**: DOX and CDDP combination dose-response contour map | **Bottom panel right:** DOX and CDDP combination dose-response matrix.

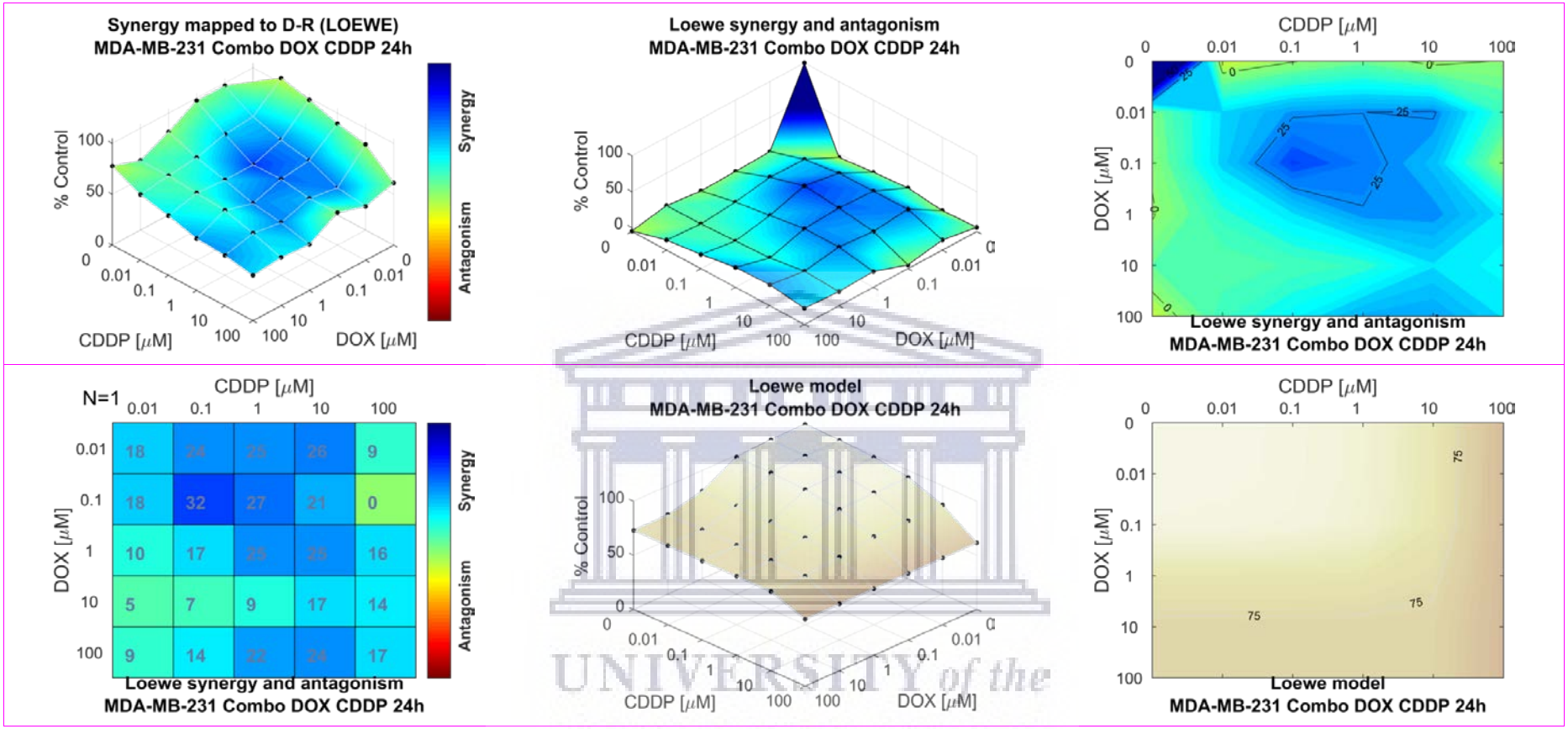

Figure 3.13C: Loewe additivity response surface reference model for the dual agent combination effects of 24h treatment of MDA-MB-231 TNBC cells with DOX and CDDP. **Top panel left:** Loewe additivity mapping of the synergy levels on the experimental combination dose-response surface | **Top panel center:** Loewe synergy and antagonism levels visualized as a surface | **Top panel right:** Contour map of isoboles (iso-effect) of Loewe synergy and/or antagonism | **Bottom panel left:** Loewe synergy and antagonism matrix | **Bottom panel center**: Loewe model reference dose-response surface | **Bottom panel right:** Loewe model reference dose-response contour map.

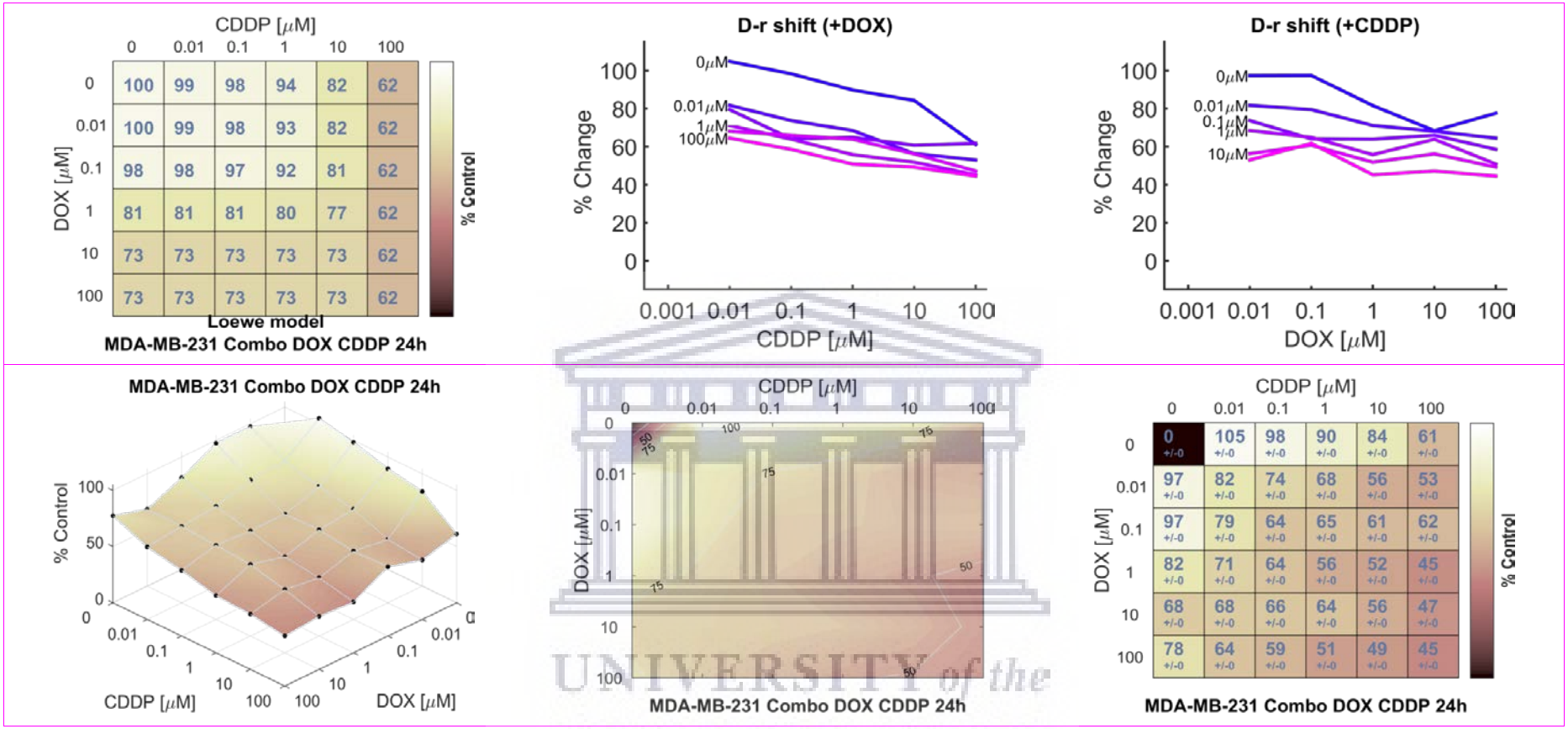

Figure 3.13D: Loewe reference model graphical presentation of the combination effects of 24h treatment of MDA-MB-231 TNBC cells with DOX and CDDP. **Top panel left:** Loewe additivity model reference dose-response matrix. | **Top panel center:** DOX dose-response shift in presence of increasing concentrations of CDDP | **Top panel right:** CDDP dose-response shift in presence of increasing concentrations of DOX | **Bottom panel left:** DOX and CDDP combination dose-response surface | **Bottom panel center**: DOX and CDDP combination dose-response contour map | **Bottom panel right:** DOX and CDDP combination dose-response matrix.

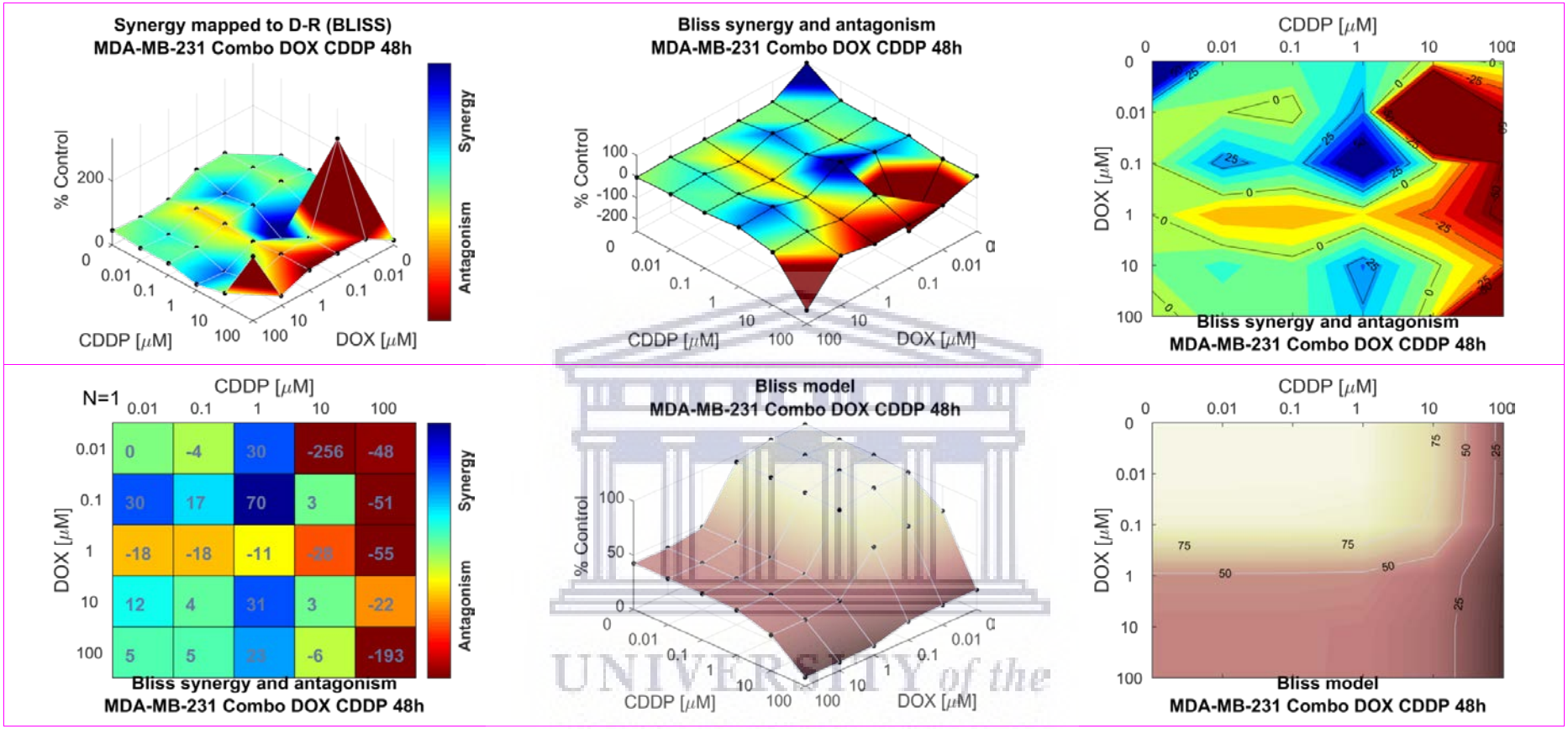

Figure 3.14A: Bliss independence response surface reference model for the dual agent combination effects of 48h treatment of MDA-MB-231 TNBC cells with DOX and CDDP. **Top panel left:** Bliss independence mapping of the synergy levels on the experimental combination dose-response surface | **Top panel center:** Bliss synergy and antagonism levels visualized as a surface | **Top panel right:** Contour map of isoboles (iso-effect) of Bliss synergy and/or antagonism | **Bottom panel left:** Bliss synergy and antagonism matrix | **Bottom panel center**: Bliss model reference dose-response surface | **Bottom panel right:** Bliss model reference dose-response contour map.

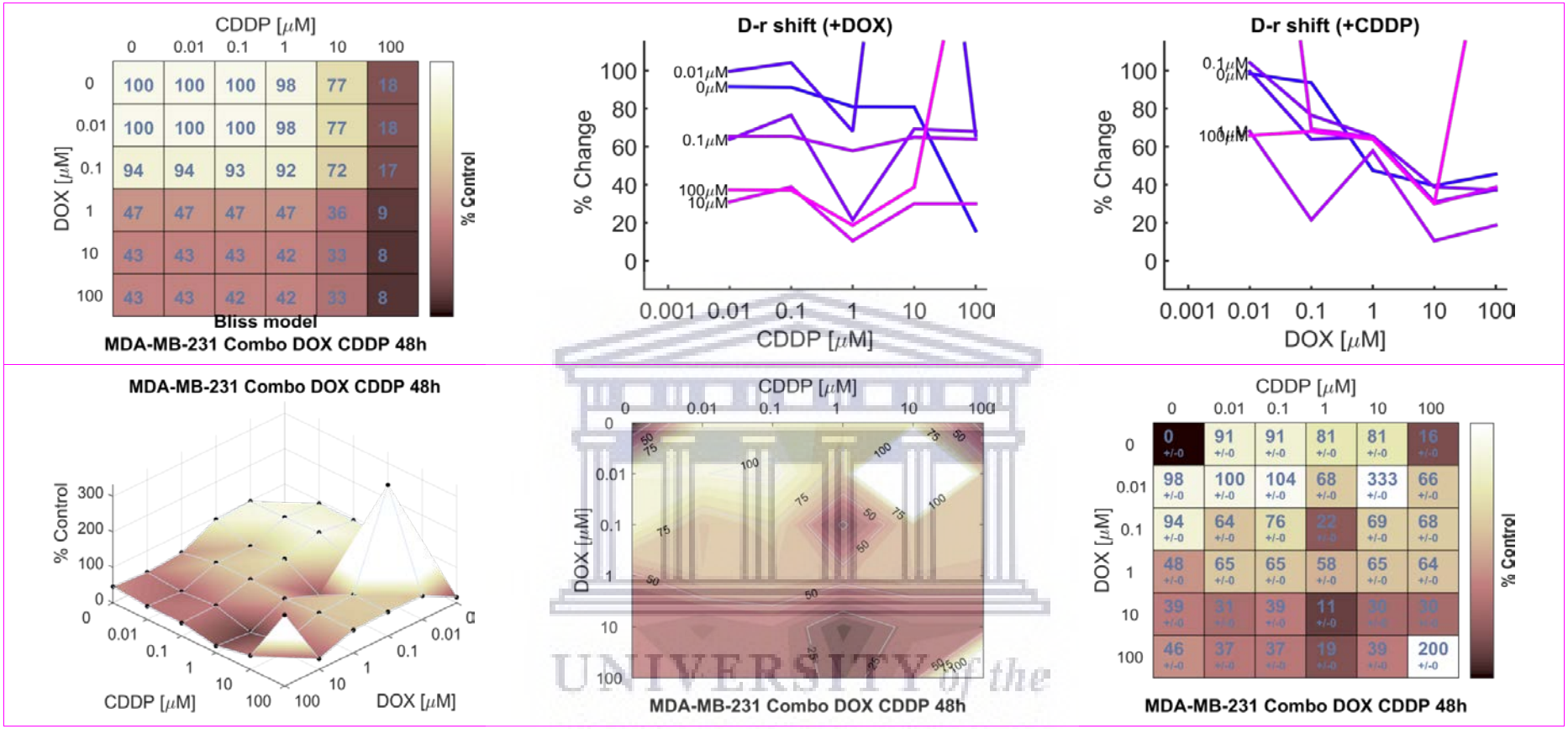

Figure 3.14B: Bliss reference model graphical presentation of the combination effects of 48h treatment of MDA-MB-231 TNBC cells with DOX and CDDP. **Top panel left:** Bliss model reference dose-response matrix. | **Top panel center:** DOX dose-response shift in presence of increasing concentrations of CDDP | **Top panel right:** CDDP dose-response shift in presence of increasing concentrations of DOX | **Bottom panel left:** DOX and CDDP combination dose-response surface | **Bottom panel center**: DOX and CDDP combination dose-response contour map | **Bottom panel right:** DOX and CDDP combination dose-response matrix.

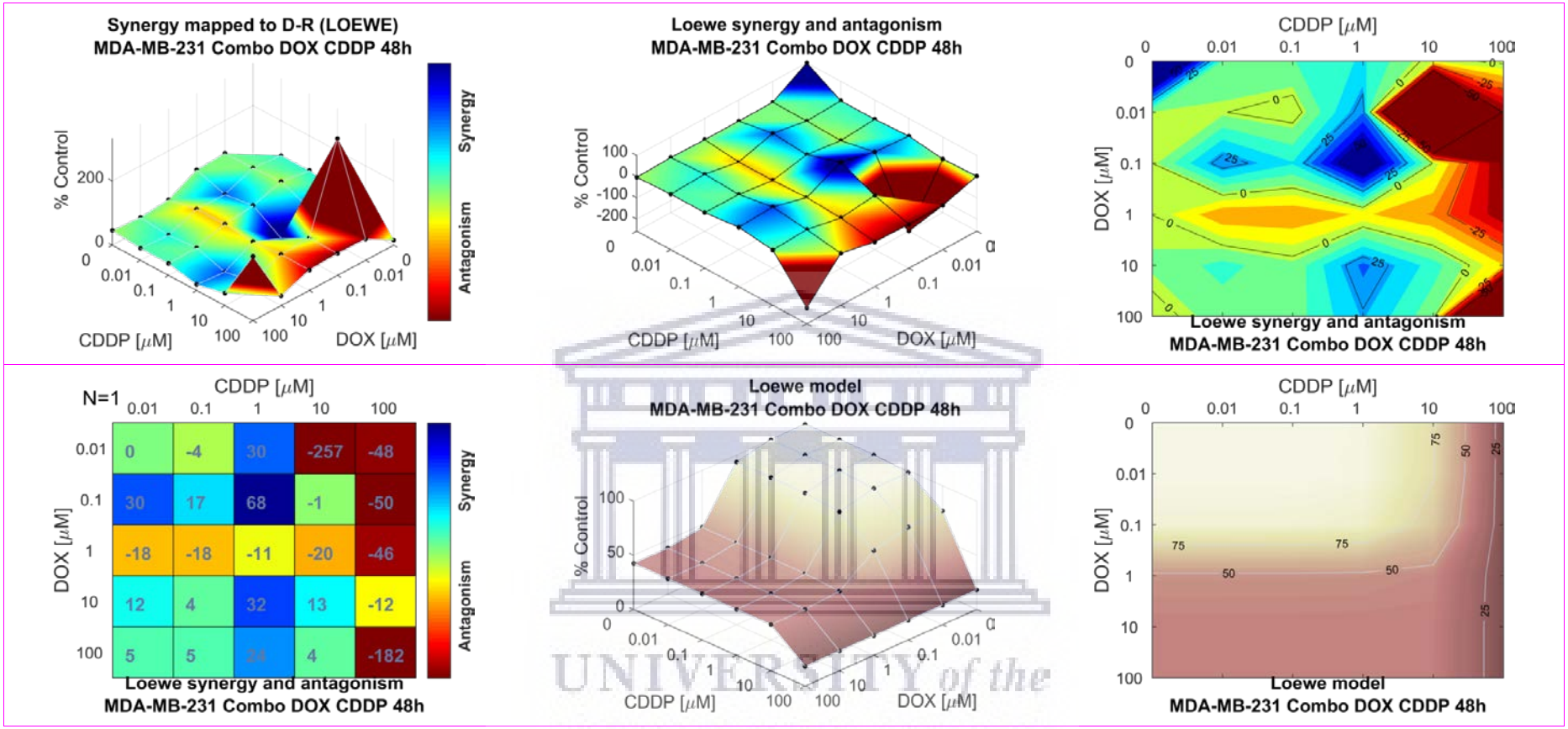

Figure 3.14C: Loewe additivity response surface reference model for the dual agent combination effects of 48h treatment of MDA-MB-231 TNBC cells with DOX and CDDP. **Top panel left:** Loewe additivity mapping of the synergy levels on the experimental combination dose-response surface | **Top panel center:** Loewe synergy and antagonism levels visualized as a surface | **Top panel right:** Contour map of isoboles (iso-effect) of Loewe synergy and/or antagonism | **Bottom panel left:** Loewe synergy and antagonism matrix | **Bottom panel center**: Loewe model reference dose-response surface | **Bottom panel right:** Loewe model reference dose-response contour map.

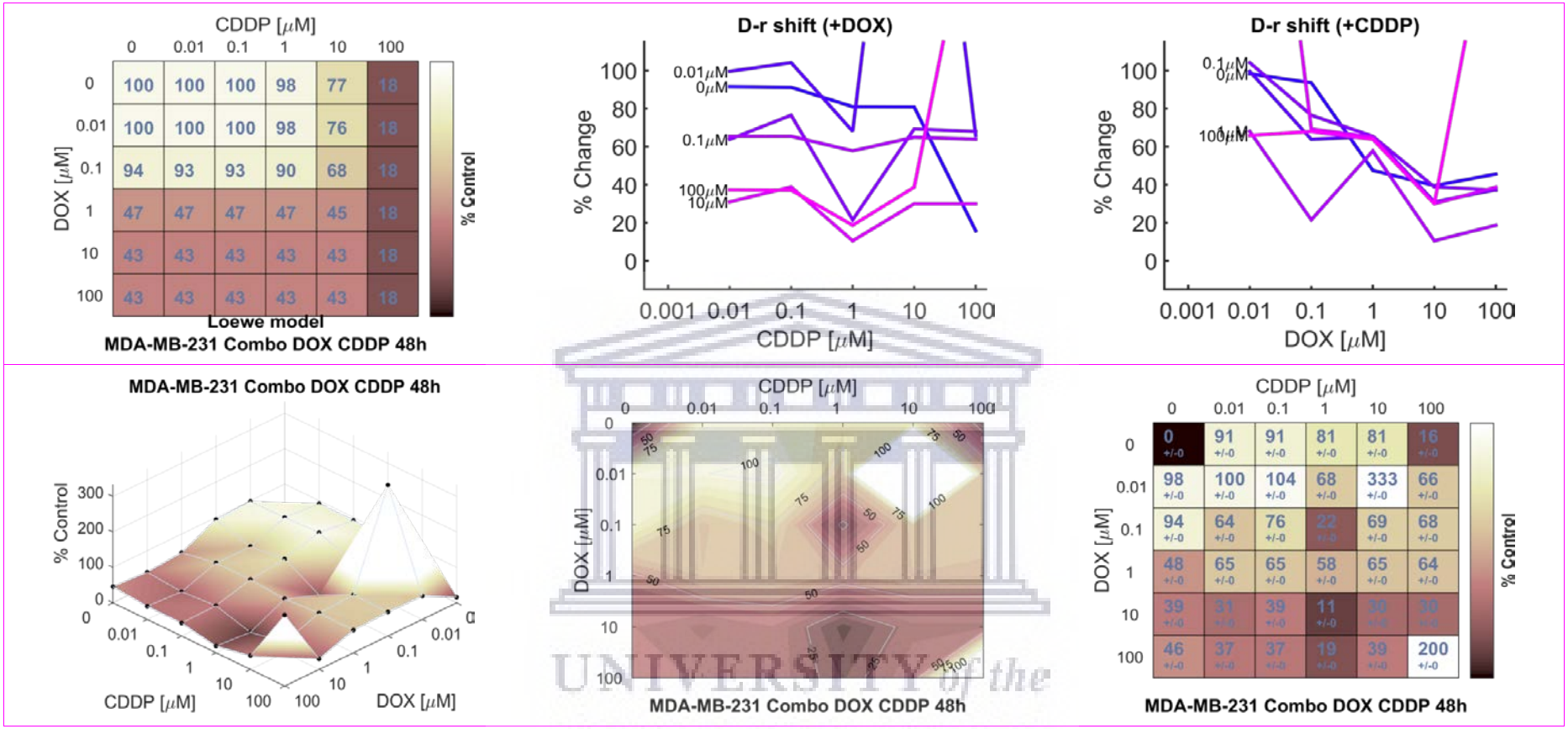

Figure 3.14D: Loewe reference model graphical presentation of the combination effects of 48h treatment of MDA-MB-231 TNBC cells with DOX and CDDP. **Top panel left:** Loewe additivity model reference dose-response matrix. | **Top panel center:** DOX dose-response shift in presence of increasing concentrations of CDDP | **Top panel right:** CDDP dose-response shift in presence of increasing concentrations of DOX | **Bottom panel left:** DOX and CDDP combination dose-response surface | **Bottom panel center**: DOX and CDDP combination dose-response contour map | **Bottom panel right:** DOX and CDDP combination dose-response matrix.

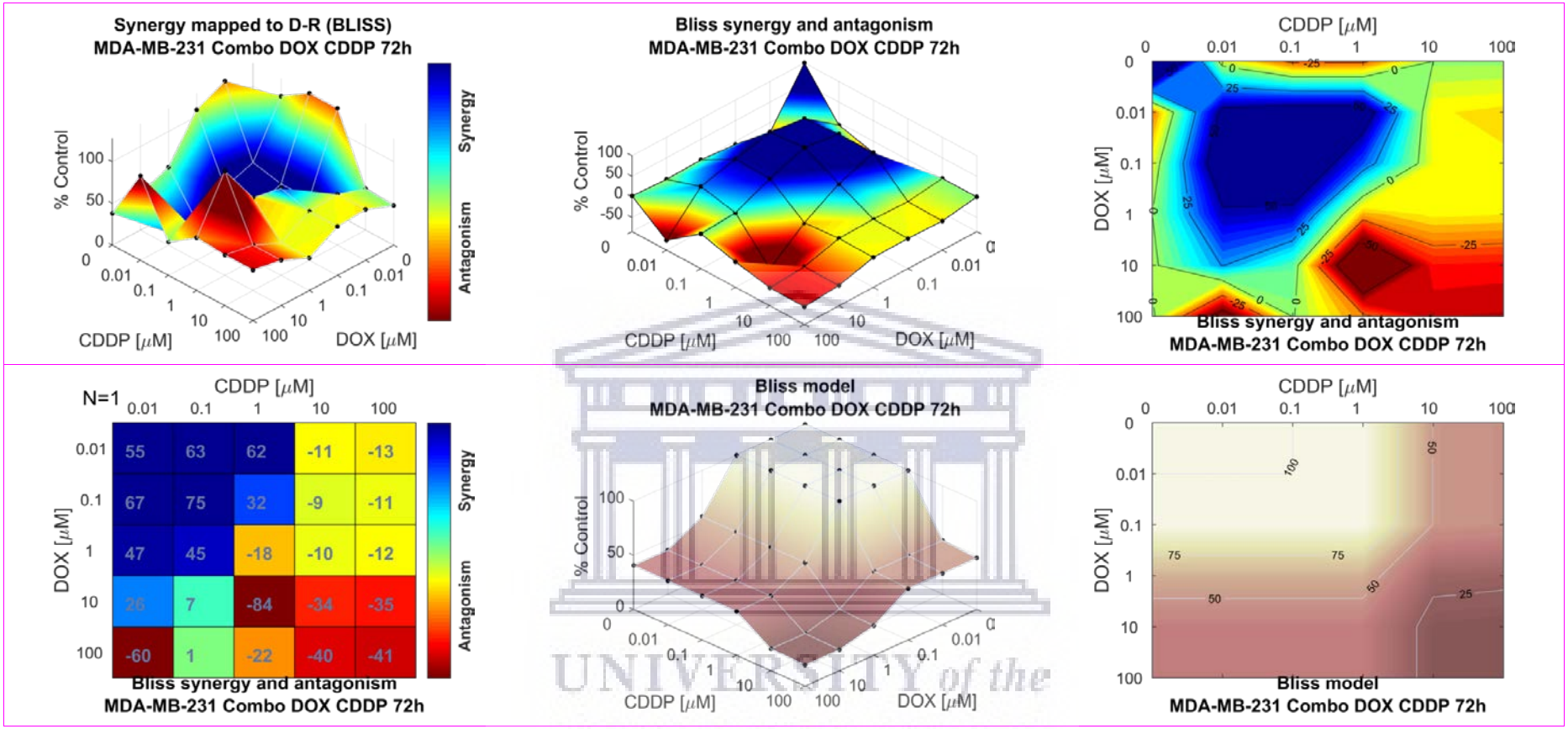

Figure 3.15A: Bliss independence response surface reference model for the dual agent combination effects of 72h treatment of MDA-MB-231 TNBC cells with DOX and CDDP. **Top panel left:** Bliss independence mapping of the synergy levels on the experimental combination dose-response surface | **Top panel center:** Bliss synergy and antagonism levels visualized as a surface | **Top panel right:** Contour map of isoboles (iso-effect) of Bliss synergy and/or antagonism | **Bottom panel left:** Bliss synergy and antagonism matrix | **Bottom panel center**: Bliss model reference dose-response surface | **Bottom panel right:** Bliss model reference dose-response contour map.

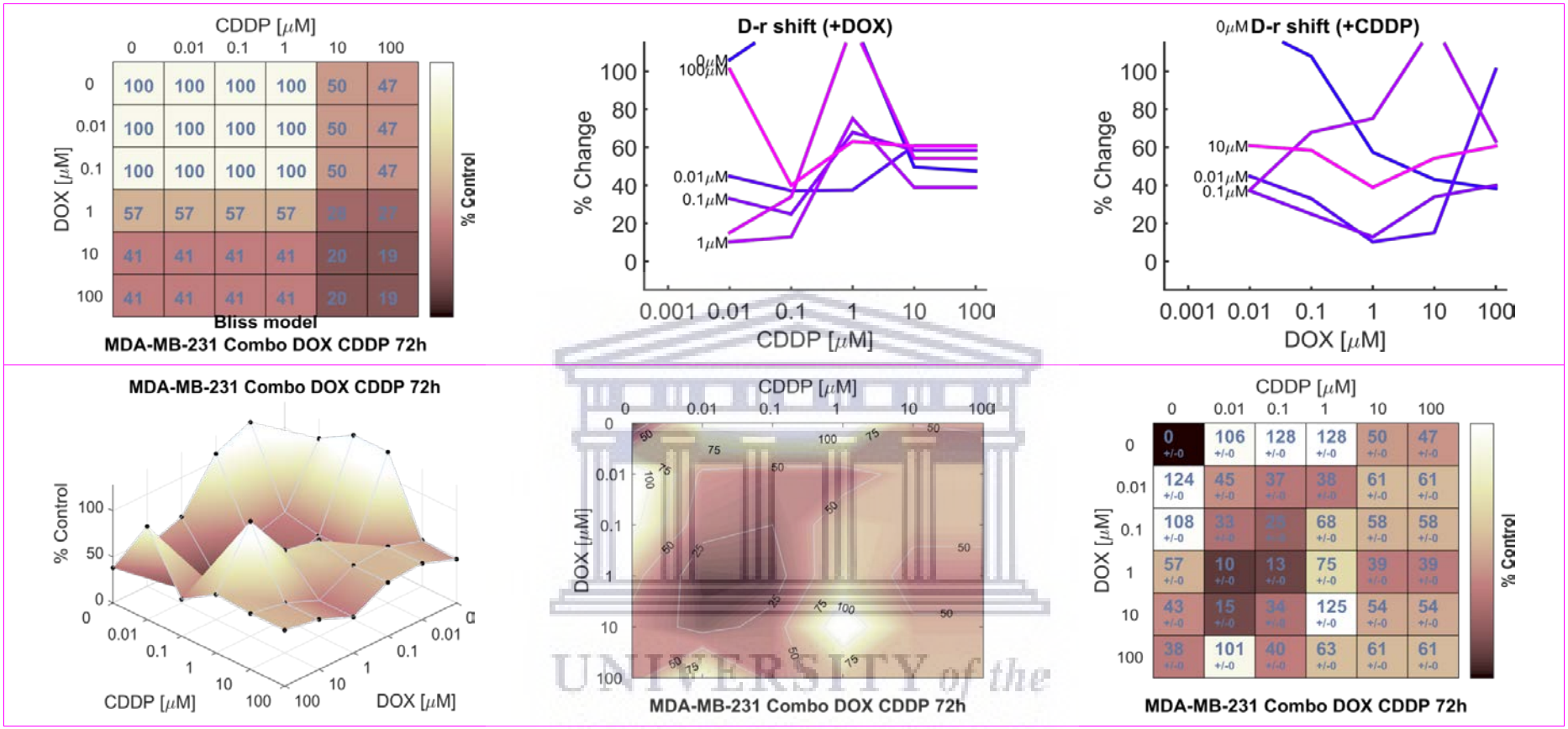

Figure 3.15B: Bliss reference model graphical presentation of the combination effects of 72h treatment of MDA-MB-231 TNBC cells with DOX and CDDP. **Top panel left:** Bliss model reference dose-response matrix. | **Top panel center:** DOX dose-response shift in presence of increasing concentrations of CDDP | **Top panel right:** CDDP dose-response shift in presence of increasing concentrations of DOX | **Bottom panel left:** DOX and CDDP combination dose-response surface | **Bottom panel center**: DOX and CDDP combination dose-response contour map | **Bottom panel right:** DOX and CDDP combination dose-response matrix.

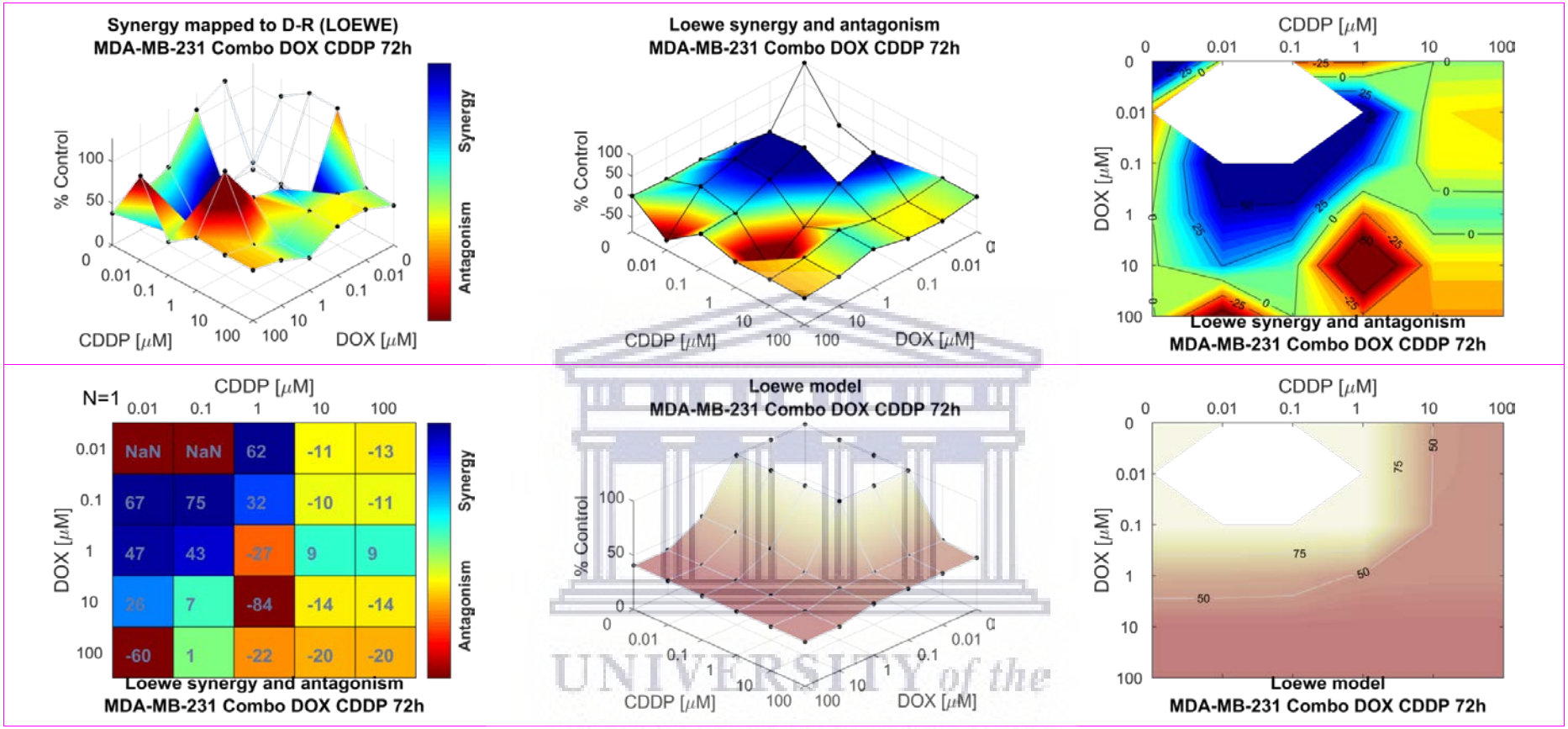

Figure 3.15C: Loewe additivity response surface reference model for the dual agent combination effects of 72h treatment of MDA-MB-231 TNBC cells with DOX and CDDP. **Top panel left:** Loewe additivity mapping of the synergy levels on the experimental combination dose-response surface | **Top panel center:** Loewe synergy and antagonism levels visualized as a surface | **Top panel right:** Contour map of isoboles (iso-effect) of Loewe synergy and/or antagonism | **Bottom panel left:** Loewe synergy and antagonism matrix | **Bottom panel center**: Loewe model reference dose-response surface | **Bottom panel right:** Loewe model reference dose-response contour map.

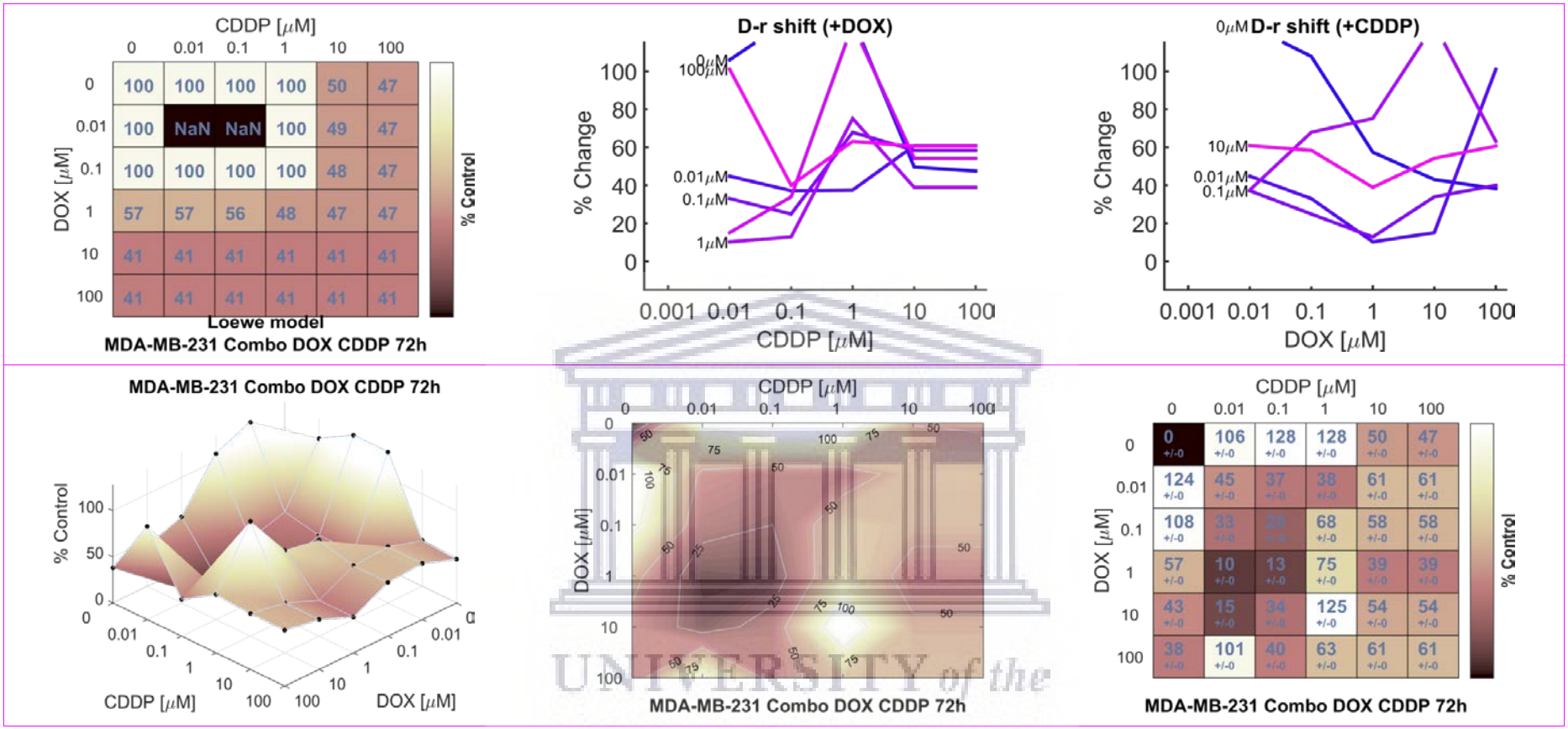

Figure 3.15D: Loewe reference model graphical presentation of the combination effects of 72h treatment of MDA-MB-231 TNBC cells with DOX and CDDP. **Top panel left:** Loewe additivity model reference dose-response matrix. | **Top panel center:** DOX dose-response shift in presence of increasing concentrations of CDDP | **Top panel right:** DOX dose-response shift in presence of increasing concentrations of CDDP | **Bottom panel left:** DOX and CDDP combination dose-response surface | **Bottom panel center:** DOX and CDDP combination dose-response contour map | **Bottom panel right:** DOX and CDDP combination dose-response matrix. NaN: not a number, i.e., data point not determined.

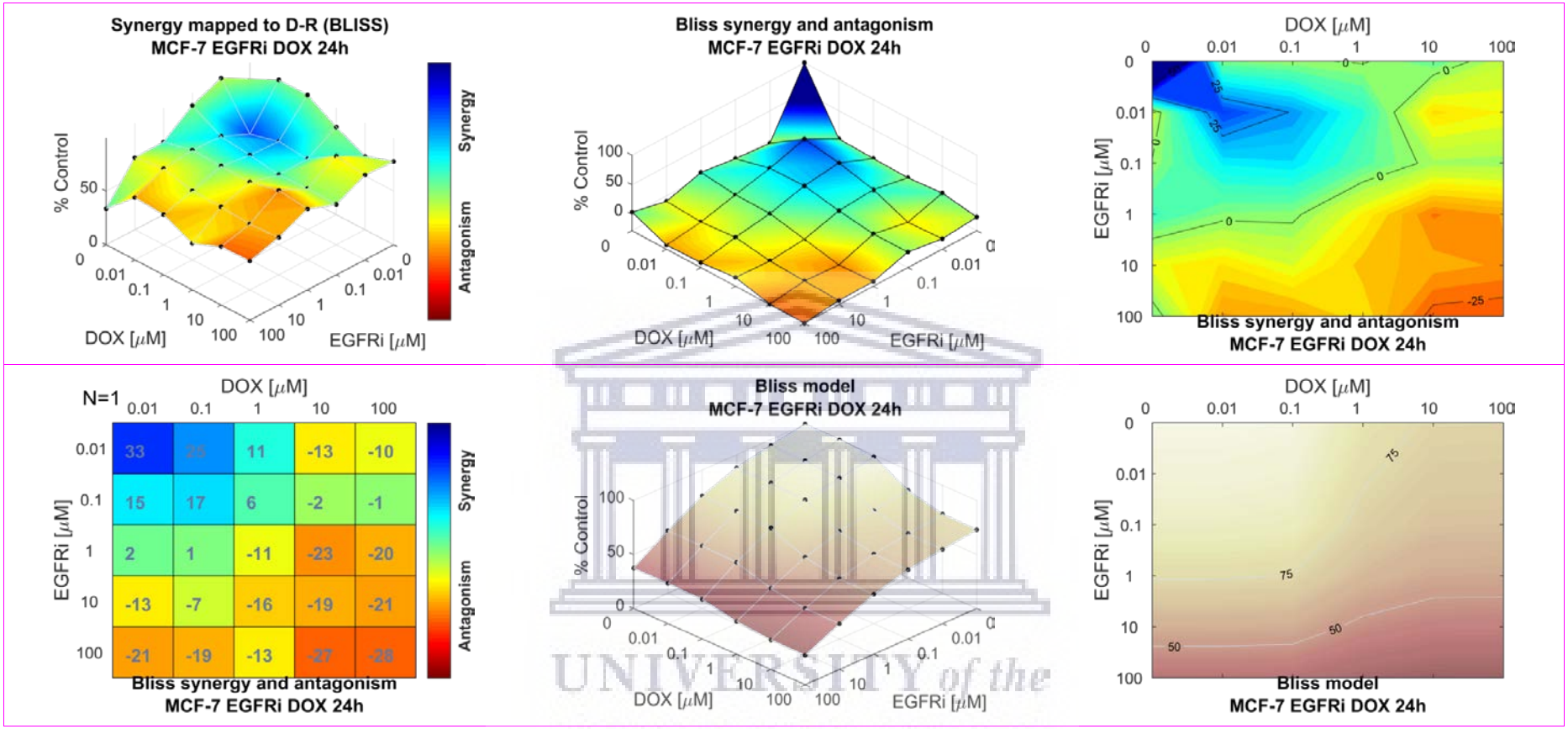

Figure 3.16A: Bliss independence response surface reference model for the dual agent combination effects of 24h treatment of MCF-7 breast carcinoma cells with EGFRi and DOX. **Top panel left:** Bliss independence mapping of the synergy levels on the experimental combination dose-response surface | **Top panel center:** Bliss synergy and antagonism levels visualized as a surface | **Top panel right:** Contour map of isoboles (iso-effect lines) of Bliss synergy and/or antagonism | **Bottom panel left:** Bliss synergy and antagonism matrix | **Bottom panel center**: Bliss model reference dose-response surface | **Bottom panel right:** Bliss model reference dose-response contour map.

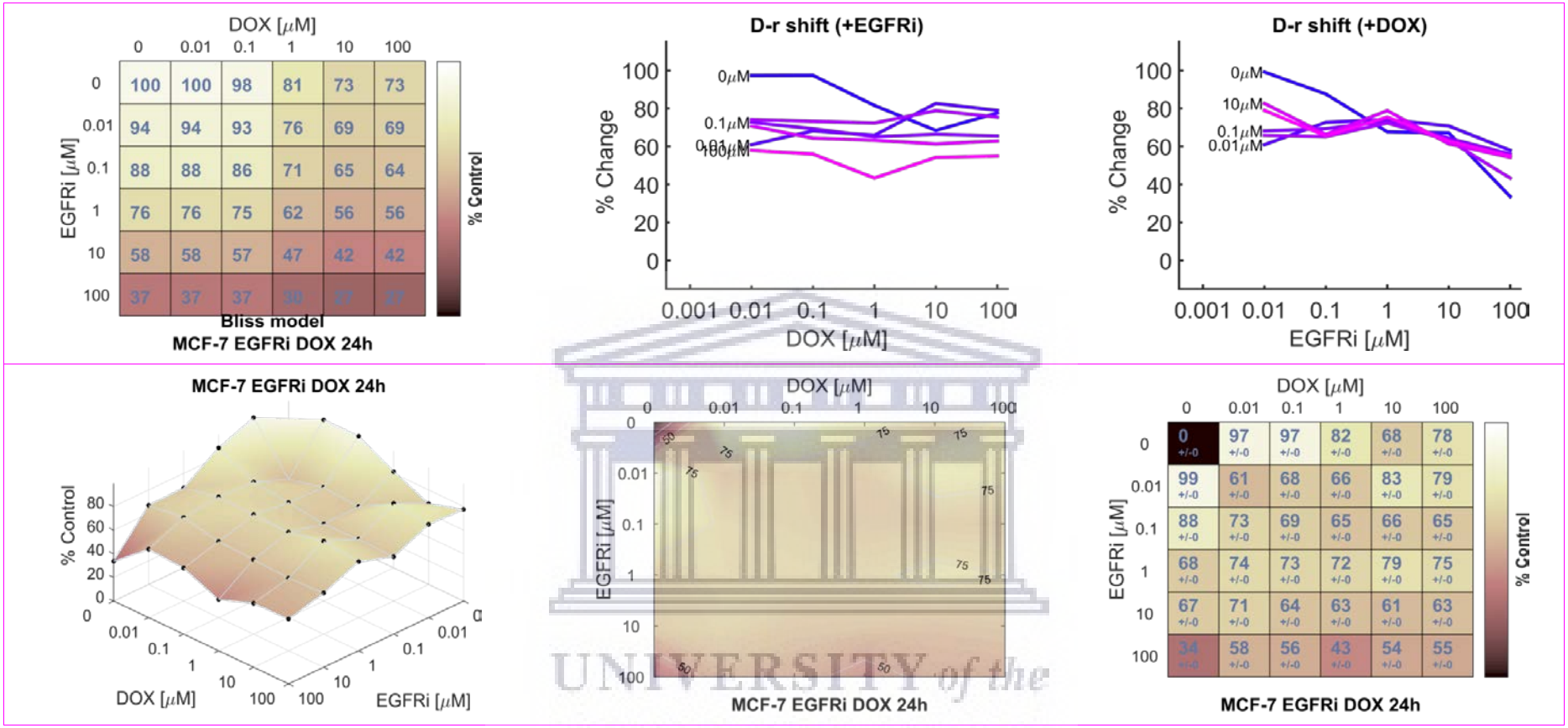

Figure 3.16B: Bliss reference model graphical presentation of the combination effects of 24h treatment of MCF-7 breast carcinoma cells with EGFRi and DOX. **Top panel left:** Bliss model reference dose-response matrix. | **Top panel center:** EGFRi dose-response shift in presence of increasing concentrations of DOX | **Top panel right:** DOX dose-response shift in presence of increasing concentrations of EGFRi | **Bottom panel left:** EGFRi and DOX combination dose-response surface | **Bottom panel center**: EGFRi and DOX combination dose-response contour map | **Bottom panel right:** EGFRi and DOX combination dose-response matrix.

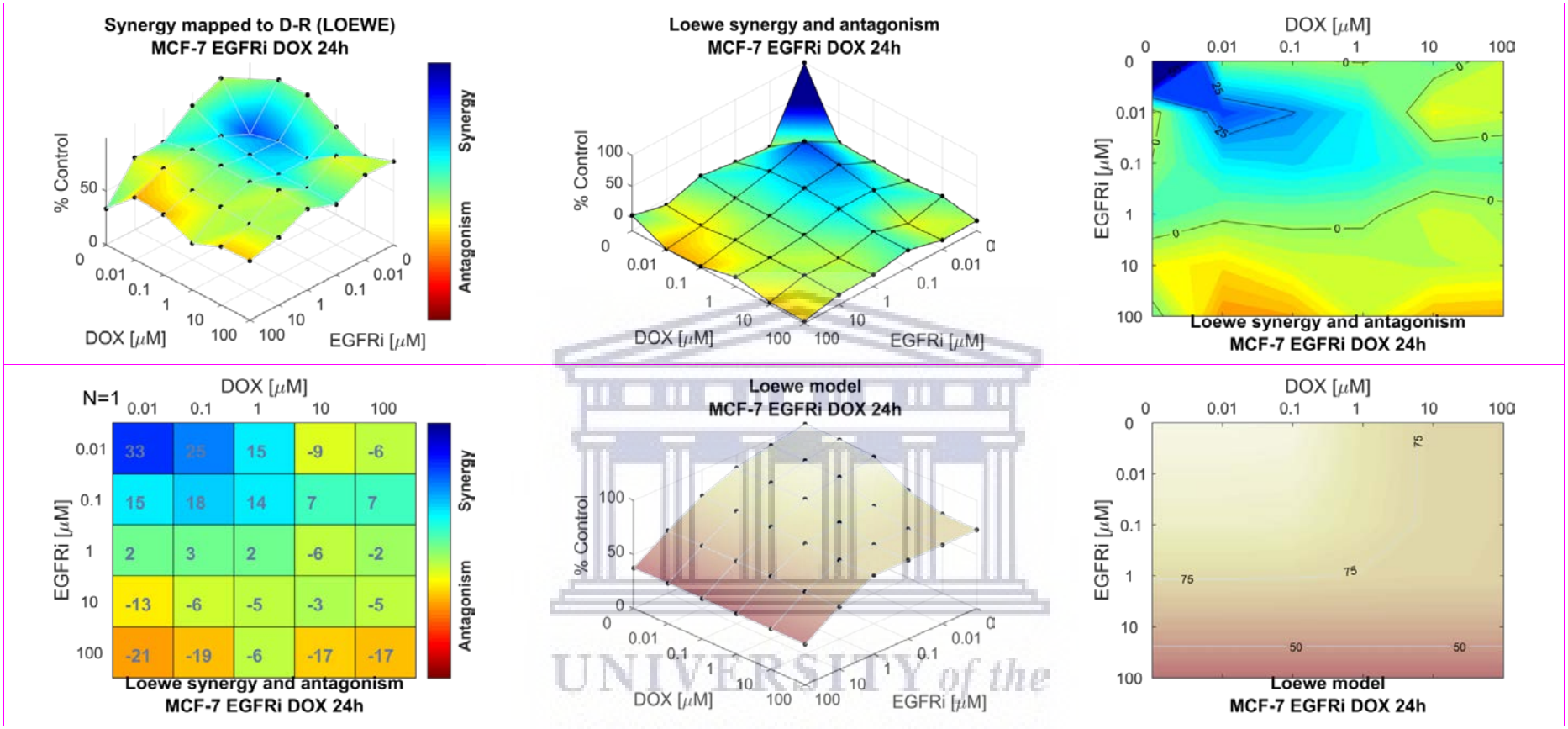

Figure 3.16C: Loewe additivity response surface reference model for the dual agent combination effects of 24h treatment of MCF-7 breast carcinoma cells with EGFRi and DOX. **Top panel left:** Loewe additivity mapping of the synergy levels on the experimental combination dose-response surface | **Top panel center:** Loewe synergy and antagonism levels visualized as a surface | **Top panel right:** Contour map of isoboles (iso-effect) of Loewe synergy and/or antagonism | **Bottom panel left:** Loewe synergy and antagonism matrix | **Bottom panel center**: Loewe model reference dose-response surface | **Bottom panel right:** Loewe model reference dose-response contour map.

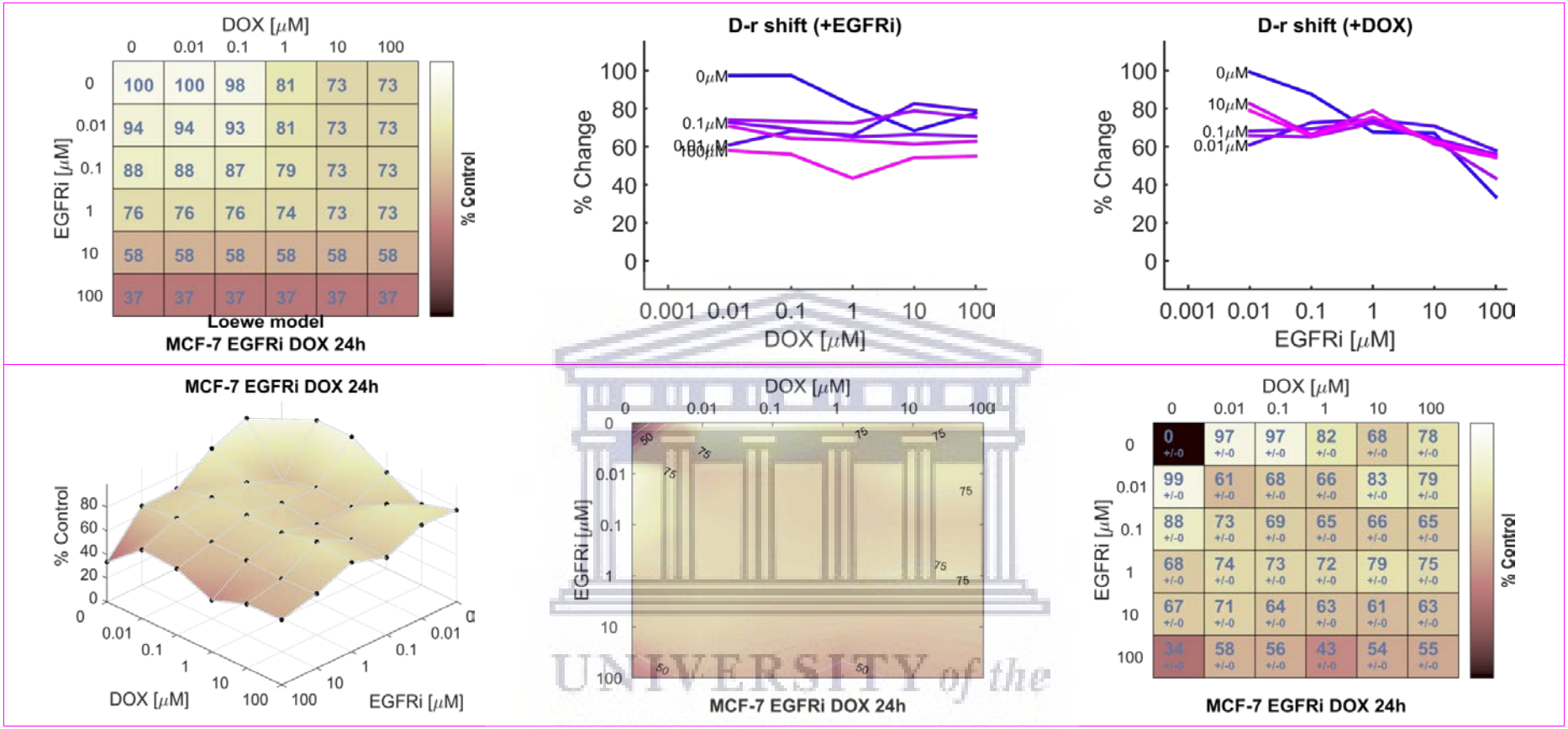

Figure 3.16D: Loewe reference model graphical presentation of the combination effects of 24h treatment of MCF-7 breast carcinoma cells with EGFRi and DOX. **Top panel left:** Loewe additivity model reference dose-response matrix. | **Top panel center:** EGFRi dose-response shift in presence of increasing concentrations of DOX | **Top panel right:** DOX dose-response shift in presence of increasing concentrations of EGFRi | **Bottom panel left:** EGFRi and DOX combination dose-response surface | **Bottom panel center**: EGFRi and DOX combination dose-response contour map | **Bottom panel right:** EGFRi and DOX combination dose-response matrix.

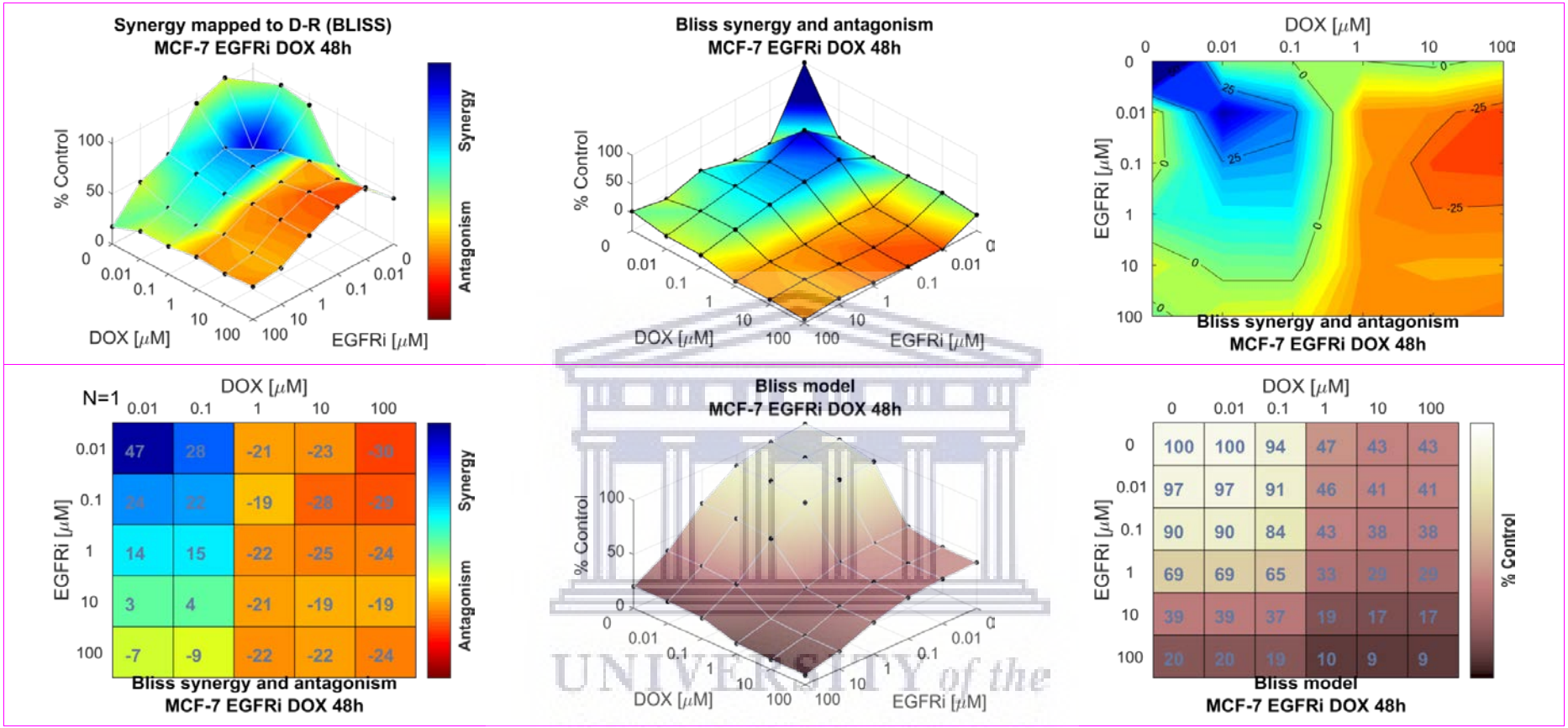

Figure 3.17A: Bliss independence response surface reference model for the dual agent combination effects of 48h treatment of MCF-7 breast carcinoma cells with EGFRi and DOX. **Top panel left:** Bliss independence mapping of the synergy levels on the experimental combination dose-response surface | **Top panel center:** Bliss synergy and antagonism levels visualized as a surface | **Top panel right:** Contour map of isoboles (iso-effect lines) of Bliss synergy and/or antagonism | **Bottom panel left:** Bliss synergy and antagonism matrix | **Bottom panel center**: Bliss model reference dose-response surface | **Bottom panel right:** Bliss model reference dose-response contour map.

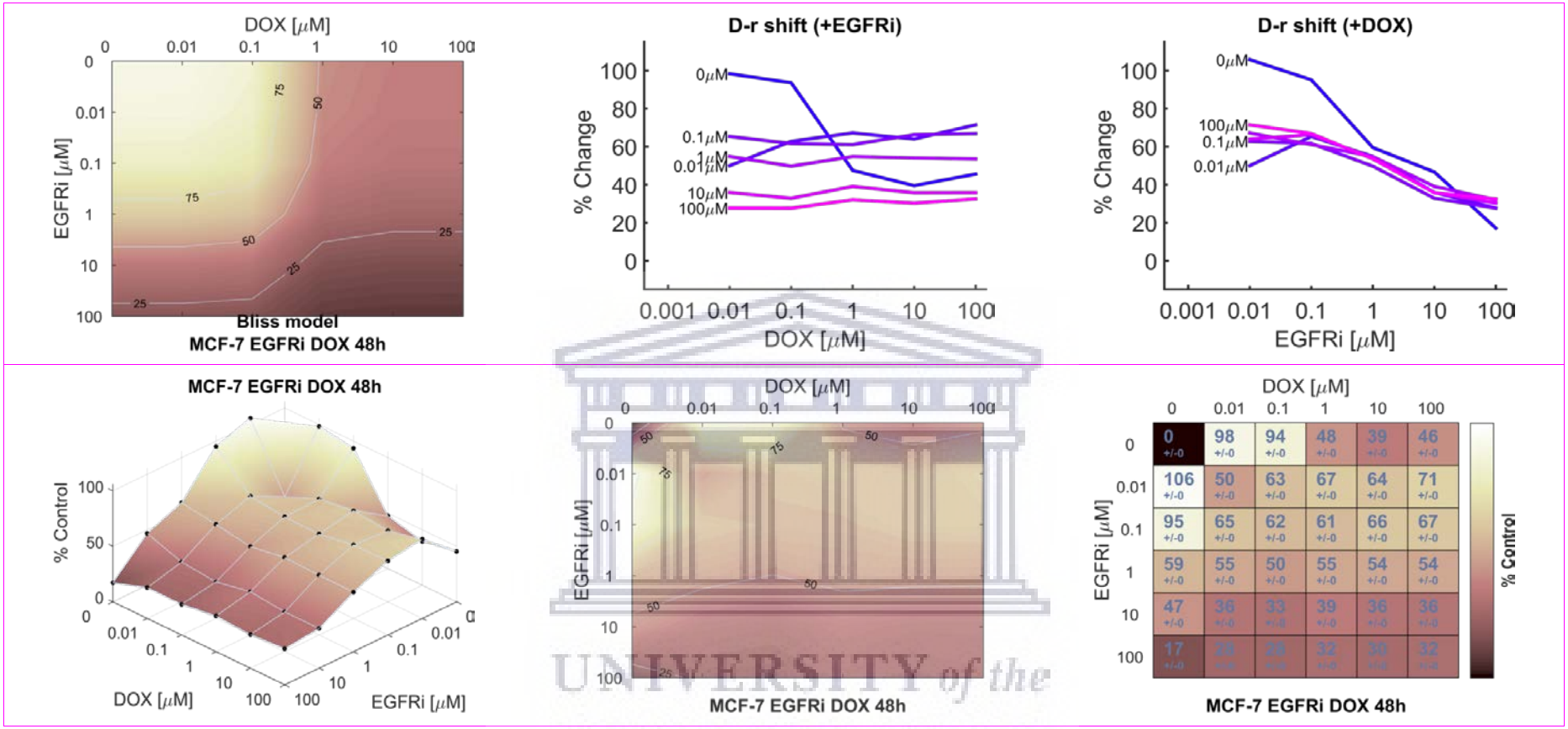

Figure 3.17B: Bliss reference model graphical presentation of the combination effects of 48h treatment of MCF-7 breast carcinoma cells with EGFRi and DOX. **Top panel left:** Bliss model reference dose-response matrix. | **Top panel center:** EGFRi dose-response shift in presence of increasing concentrations of DOX | **Top panel right:** DOX dose-response shift in presence of increasing concentrations of EGFRi | **Bottom panel left:** EGFRi and DOX combination dose-response surface | **Bottom panel center**: EGFRi and DOX combination dose-response contour map | **Bottom panel right:** EGFRi and DOX combination dose-response matrix.

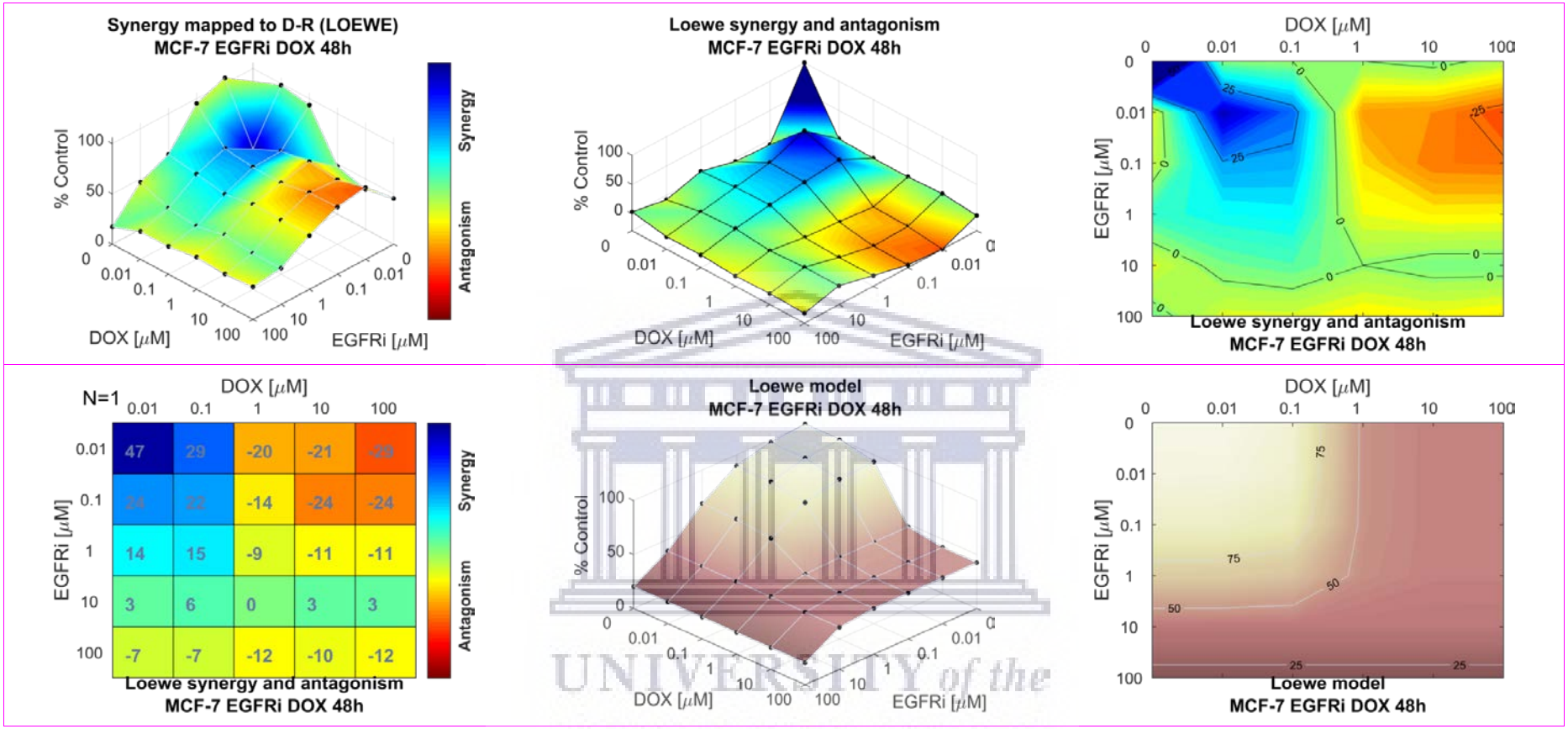

Figure 3.17C: Loewe additivity response surface reference model for the dual agent combination effects of 48h treatment of MCF-7 breast carcinoma cells with EGFRi and DOX. **Top panel left:** Loewe additivity mapping of the synergy levels on the experimental combination dose-response surface | **Top panel center:** Loewe synergy and antagonism levels visualized as a surface | **Top panel right:** Contour map of isoboles (iso-effect) of Loewe synergy and/or antagonism | **Bottom panel left:** Loewe synergy and antagonism matrix | **Bottom panel center**: Loewe model reference dose-response surface | **Bottom panel right:** Loewe model reference dose-response contour map.

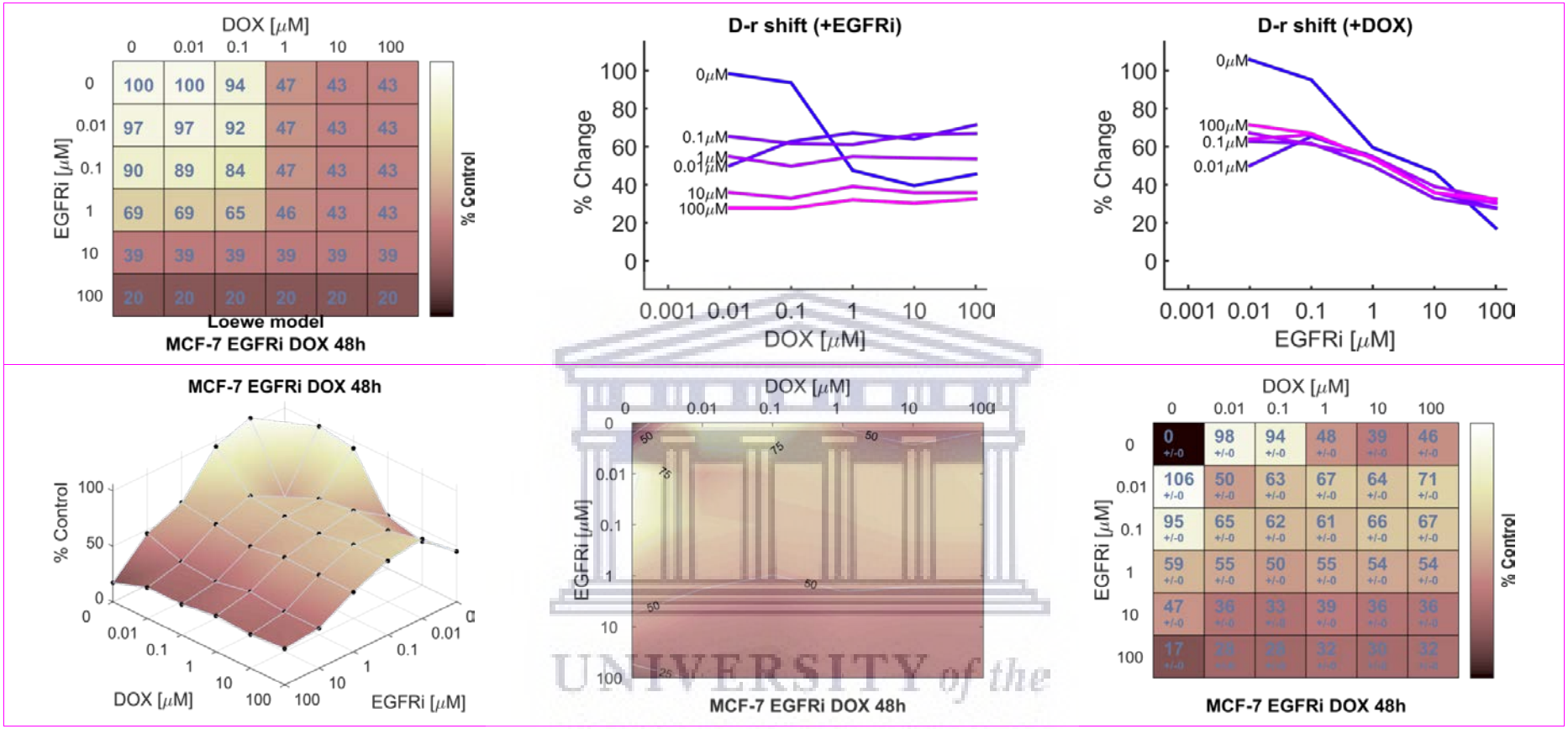

Figure 3.17D: Loewe reference model graphical presentation of the combination effects of 48h treatment of MCF-7 breast carcinoma cells with EGFRi and DOX. **Top panel left:** Loewe additivity model reference dose-response matrix. | **Top panel center:** EGFRi dose-response shift in presence of increasing concentrations of DOX | **Top panel right:** DOX dose-response shift in presence of increasing concentrations of EGFRi | **Bottom panel left:** EGFRi and DOX combination dose-response surface | **Bottom panel center**: EGFRi and DOX combination dose-response contour map | **Bottom panel right:** EGFRi and DOX combination dose-response matrix.

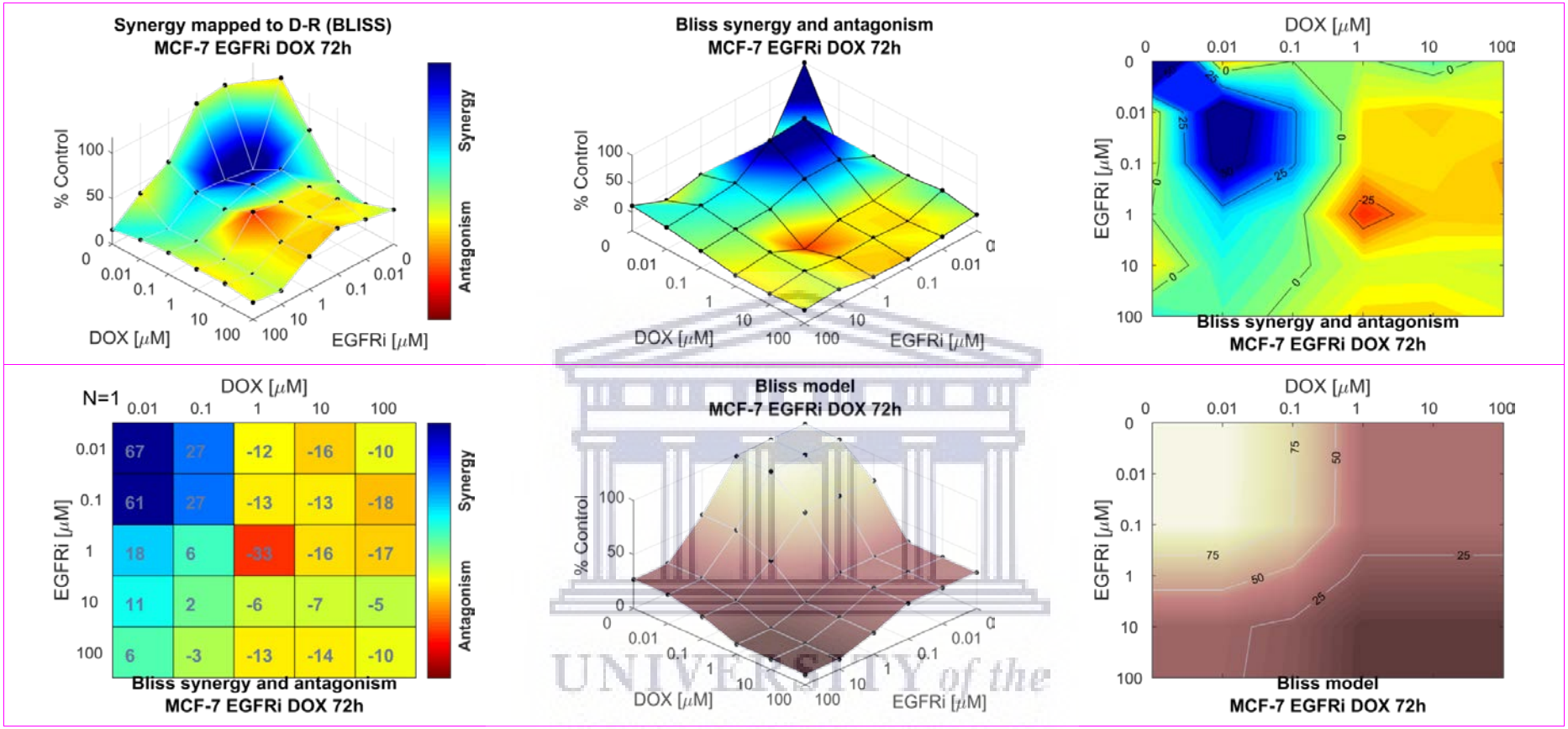

Figure 3.18A: Bliss independence response surface reference model for the dual agent combination effects of 72h treatment of MCF-7 breast carcinoma cells with EGFRi and DOX. **Top panel left:** Bliss independence mapping of the synergy levels on the experimental combination dose-response surface | **Top panel center:** Bliss synergy and antagonism levels visualized as a surface | **Top panel right:** Contour map of isoboles (iso-effect lines) of Bliss synergy and/or antagonism | **Bottom panel left:** Bliss synergy and antagonism matrix | **Bottom panel center**: Bliss model reference dose-response surface | **Bottom panel right:** Bliss model reference dose-response contour map.

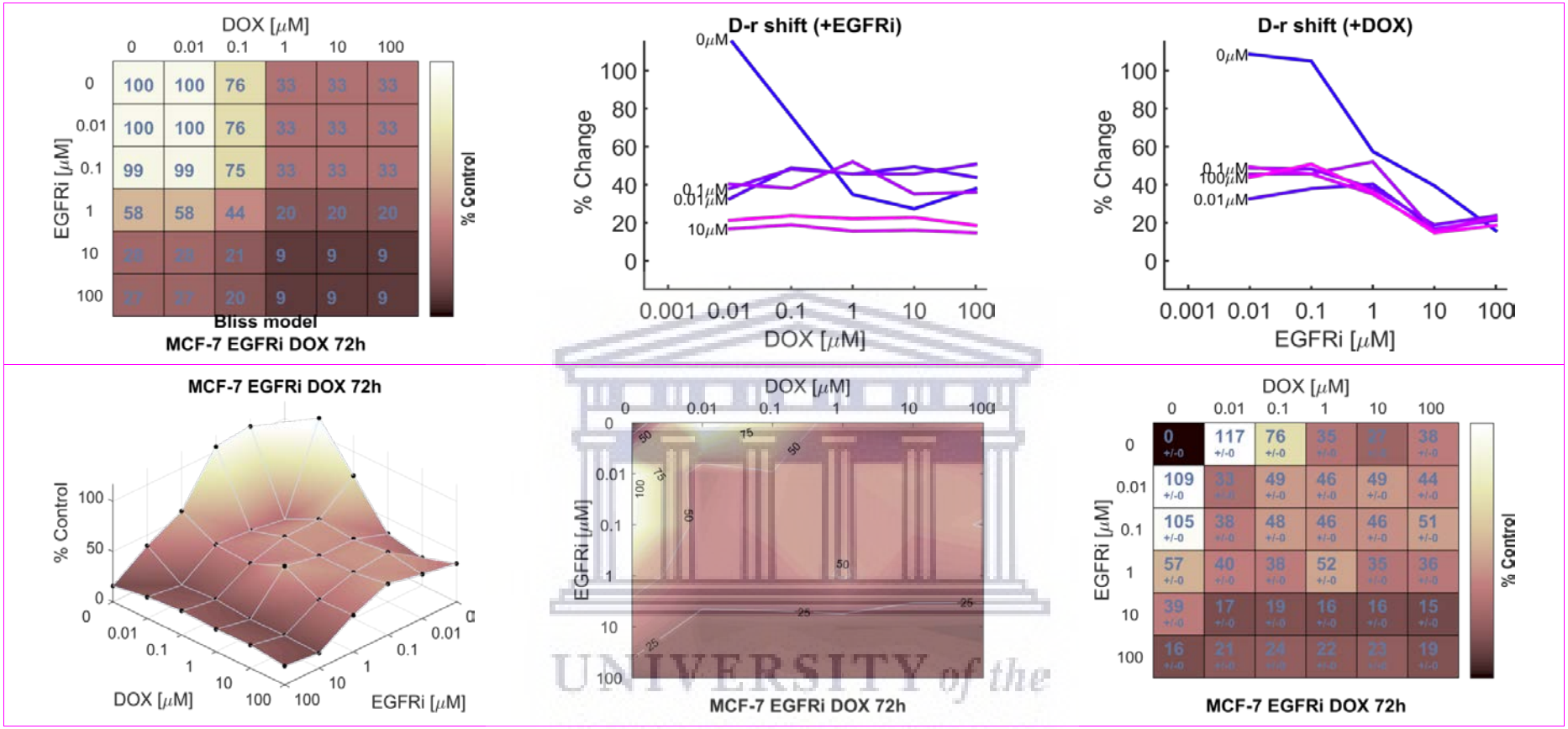

Figure 3.18B: Bliss reference model graphical presentation of the combination effects of 72h treatment of MCF-7 breast carcinoma cells with EGFRi and DOX. **Top panel left:** Bliss model reference dose-response matrix. | **Top panel center:** EGFRi dose-response shift in presence of increasing concentrations of DOX | **Top panel right:** DOX dose-response shift in presence of increasing concentrations of EGFRi | **Bottom panel left:** EGFRi and DOX combination dose-response surface | **Bottom panel center**: EGFRi and DOX combination dose-response contour map | **Bottom panel right:** EGFRi and DOX combination dose-response matrix.

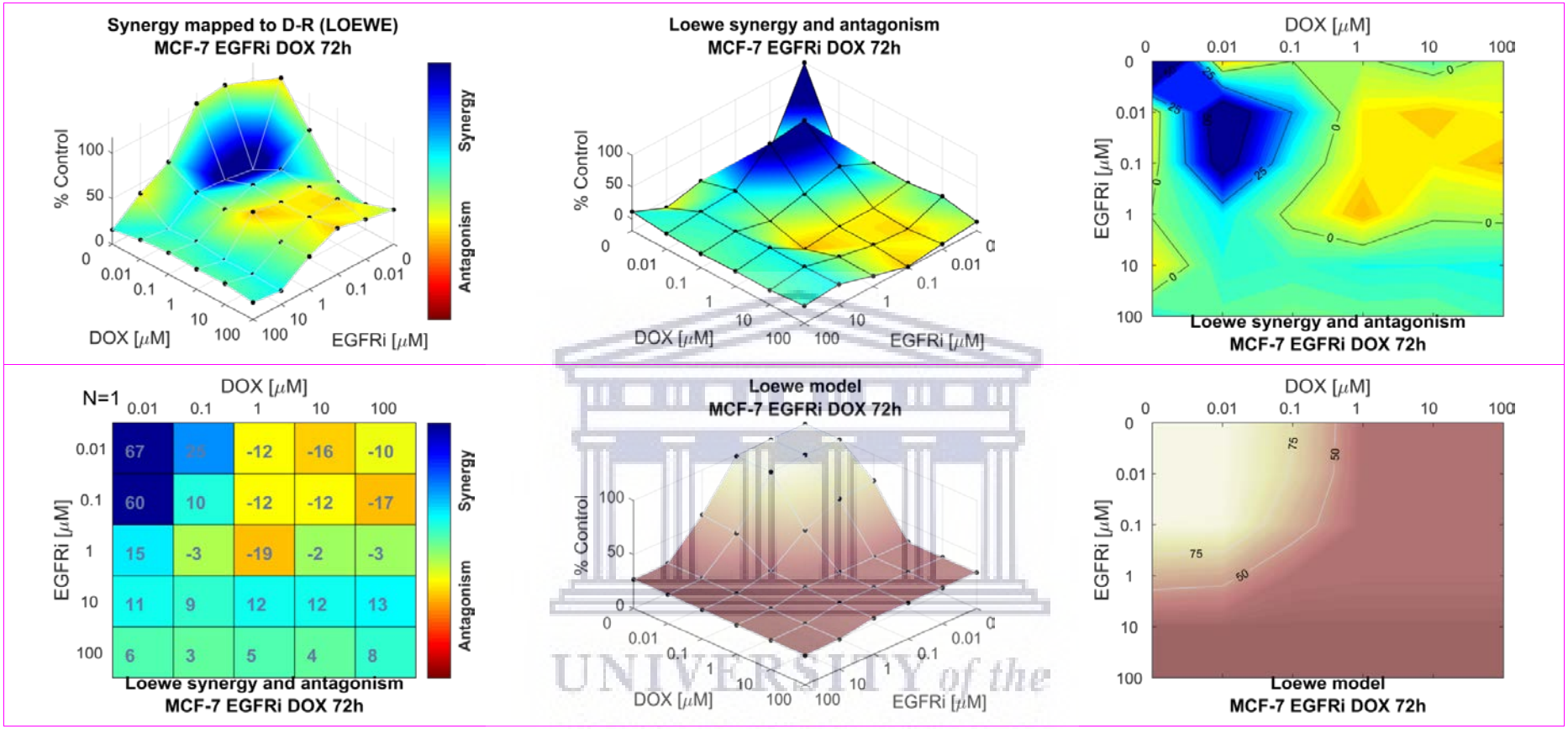

Figure 3.18C: Loewe additivity response surface reference model for the dual agent combination effects of 72h treatment of MCF-7 breast carcinoma cells with EGFRi and DOX. **Top panel left:** Loewe additivity mapping of the synergy levels on the experimental combination dose-response surface | **Top panel center:** Loewe synergy and antagonism levels visualized as a surface | **Top panel right:** Contour map of isoboles (iso-effect) of Loewe synergy and/or antagonism | **Bottom panel left:** Loewe synergy and antagonism matrix | **Bottom panel center**: Loewe model reference dose-response surface | **Bottom panel right:** Loewe model reference dose-response contour map.

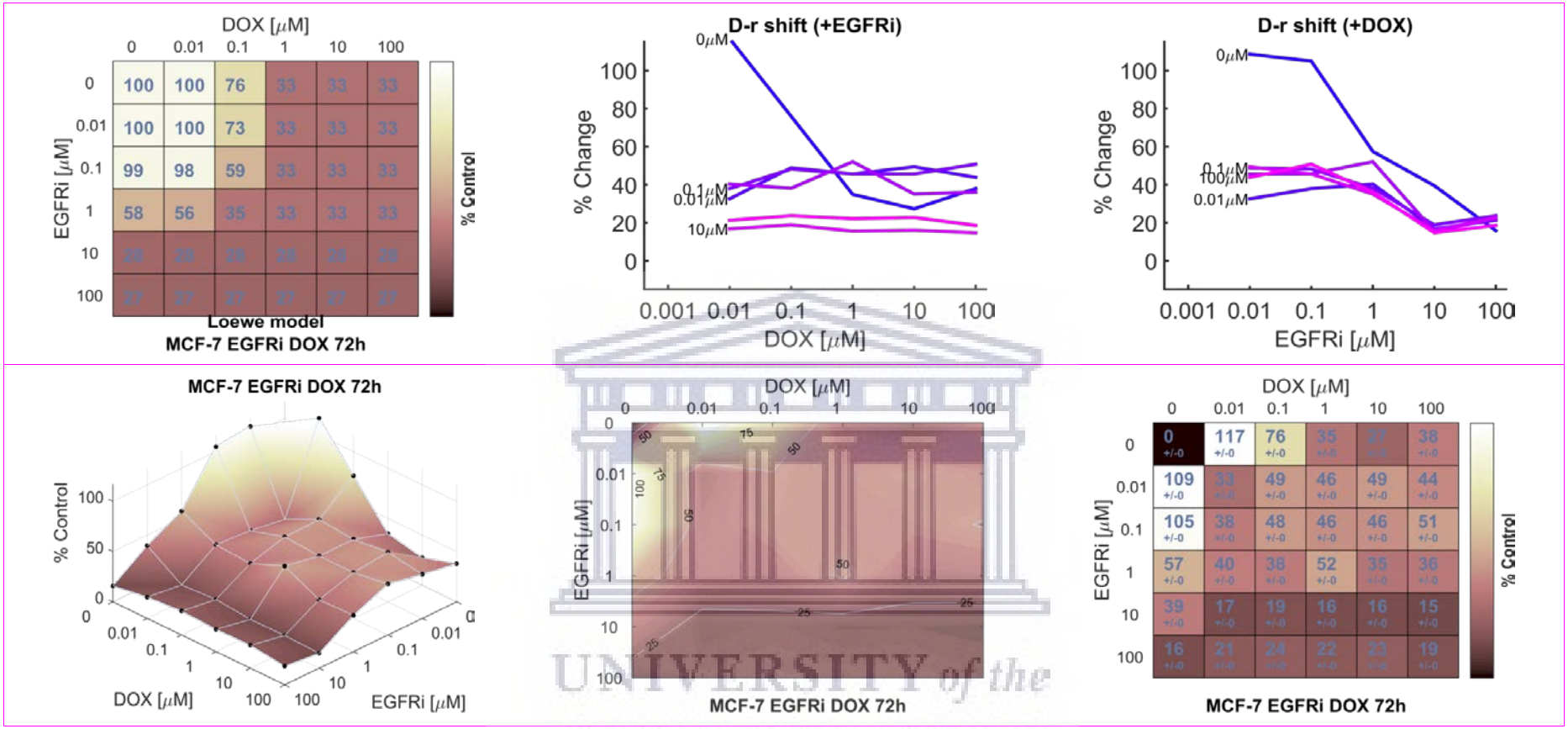

Figure 3.18D: Loewe reference model graphical presentation of the combination effects of 72h treatment of MCF-7 breast carcinoma cells with EGFRi and DOX. **Top panel left:** Loewe additivity model reference dose-response matrix. | **Top panel center:** EGFRi dose-response shift in presence of increasing concentrations of DOX | **Top panel right:** DOX dose-response shift in presence of increasing concentrations of EGFRi | **Bottom panel left:** EGFRi and DOX combination dose-response surface | **Bottom panel center**: EGFRi and DOX combination dose-response contour map | **Bottom panel right:** EGFRi and DOX combination dose-response matrix.

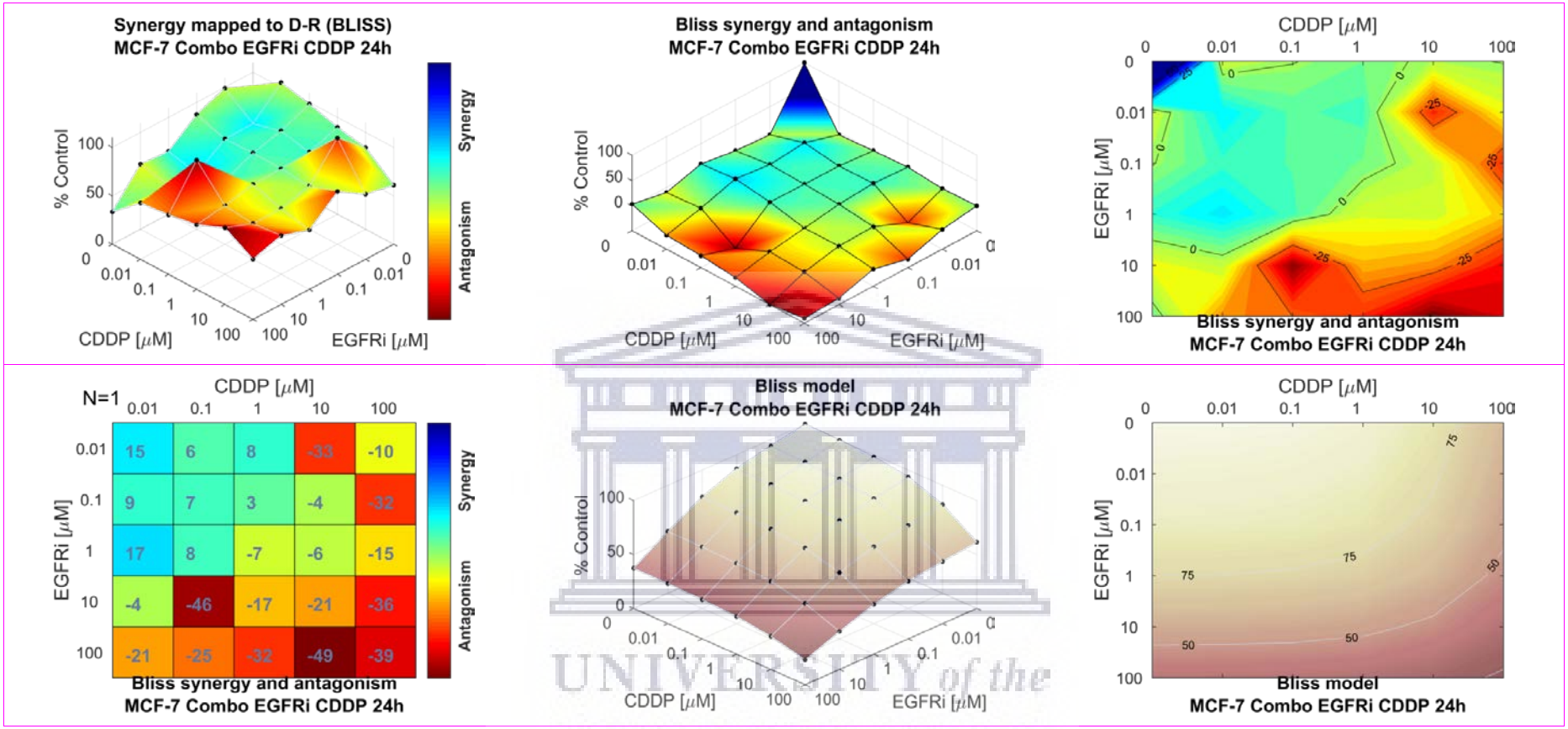

Figure 3.19A: Bliss independence response surface reference model for the dual agent combination effects of 24h treatment of MCF-7 breast carcinoma cells with EGFRi and CDDP. **Top panel left:** Bliss independence mapping of the synergy levels on the experimental combination dose-response surface | **Top panel center:** Bliss synergy and antagonism levels visualized as a surface | **Top panel right:** Contour map of isoboles (iso-effect lines) of Bliss synergy and/or antagonism | **Bottom panel left:** Bliss synergy and antagonism matrix | **Bottom panel center**: Bliss model reference dose-response surface | **Bottom panel right:** Bliss model reference dose-response contour map.

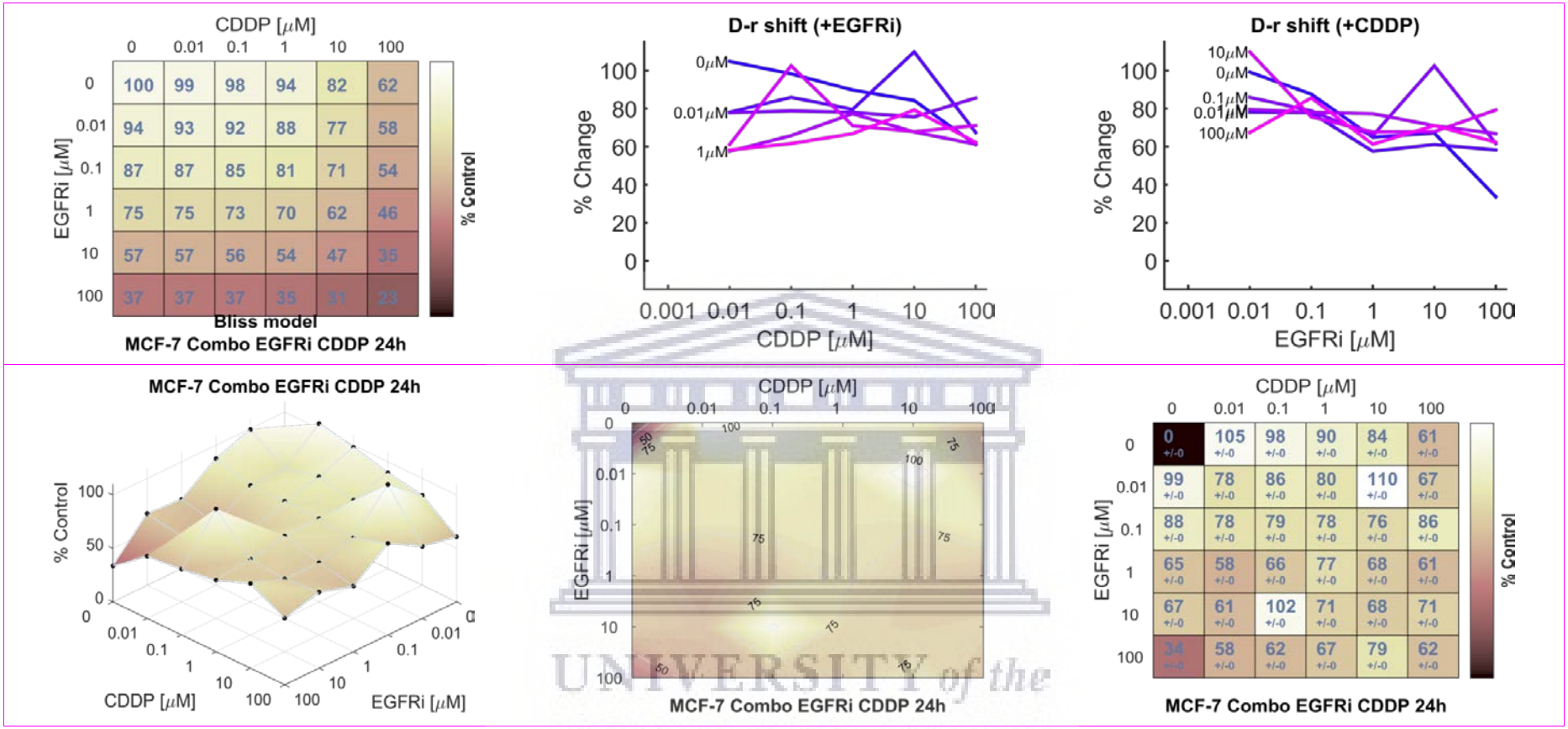

Figure 3.19B: Bliss reference model graphical presentation of the combination effects of 24h treatment of MCF-7 breast carcinoma cells with EGFRi and CDDP. **Top panel left:** Bliss model reference dose-response matrix. | **Top panel center:** EGFRi dose-response shift in presence of increasing concentrations of CDDP | **Top panel right:** CDDP dose-response shift in presence of increasing concentrations of EGFRi | **Bottom panel left:** EGFRi and CDDP combination dose-response surface | **Bottom panel center**: EGFRi and CDDP combination dose-response contour map | **Bottom panel right:** EGFRi and CDDP combination dose-response matrix.

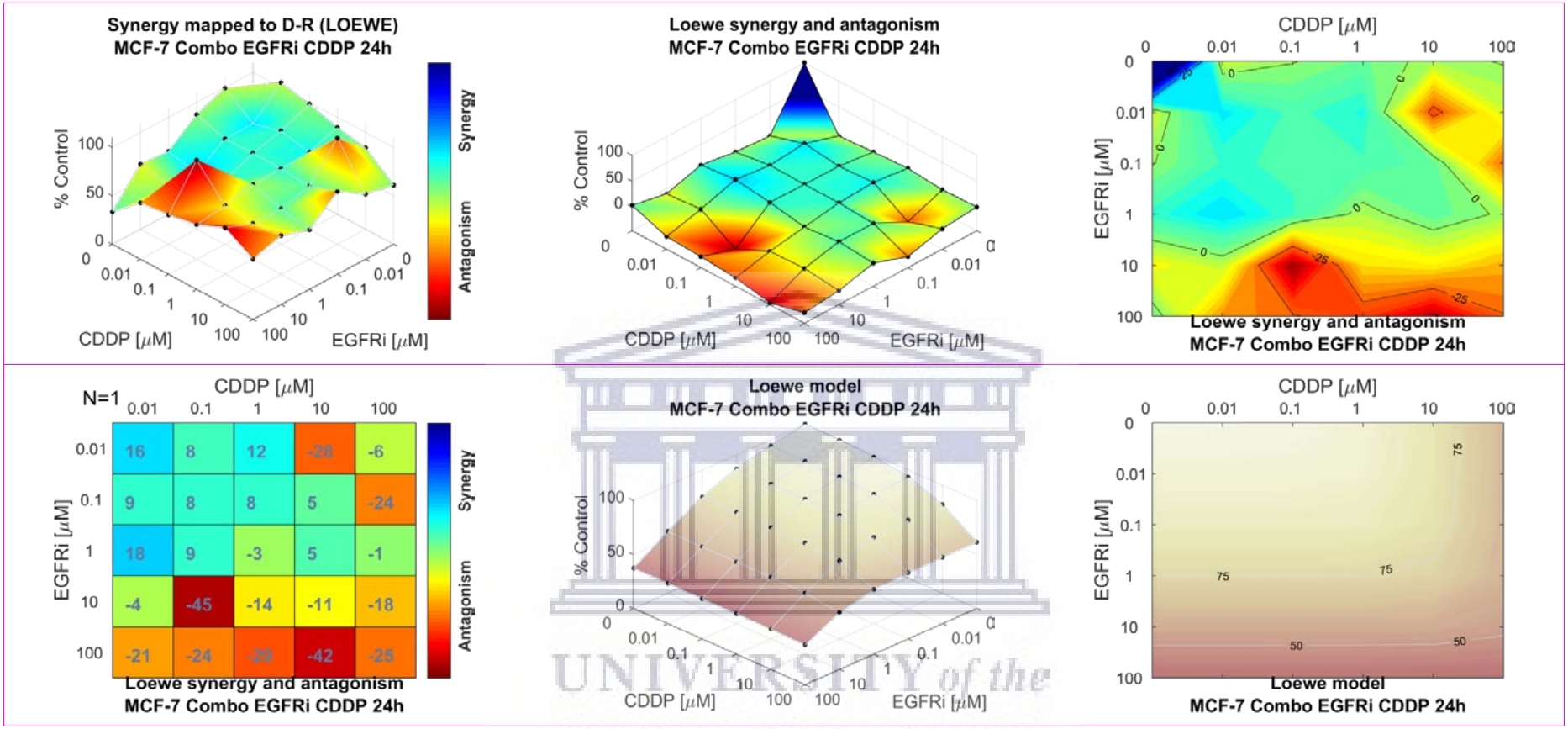

Figure 3.19C: Loewe additivity response surface reference model for the dual agent combination effects of 24h treatment of MCF-7 breast carcinoma cells with EGFRi and CDDP. **Top panel left:** Loewe additivity mapping of the synergy levels on the experimental combination dose-response surface | **Top panel center:** Loewe synergy and antagonism levels visualized as a surface | **Top panel right:** Contour map of isoboles (iso-effect) of Loewe synergy and/or antagonism | **Bottom panel left:** Loewe synergy and antagonism matrix | **Bottom panel center**: Loewe model reference dose-response surface | **Bottom panel right:** Loewe model reference dose-response contour map.

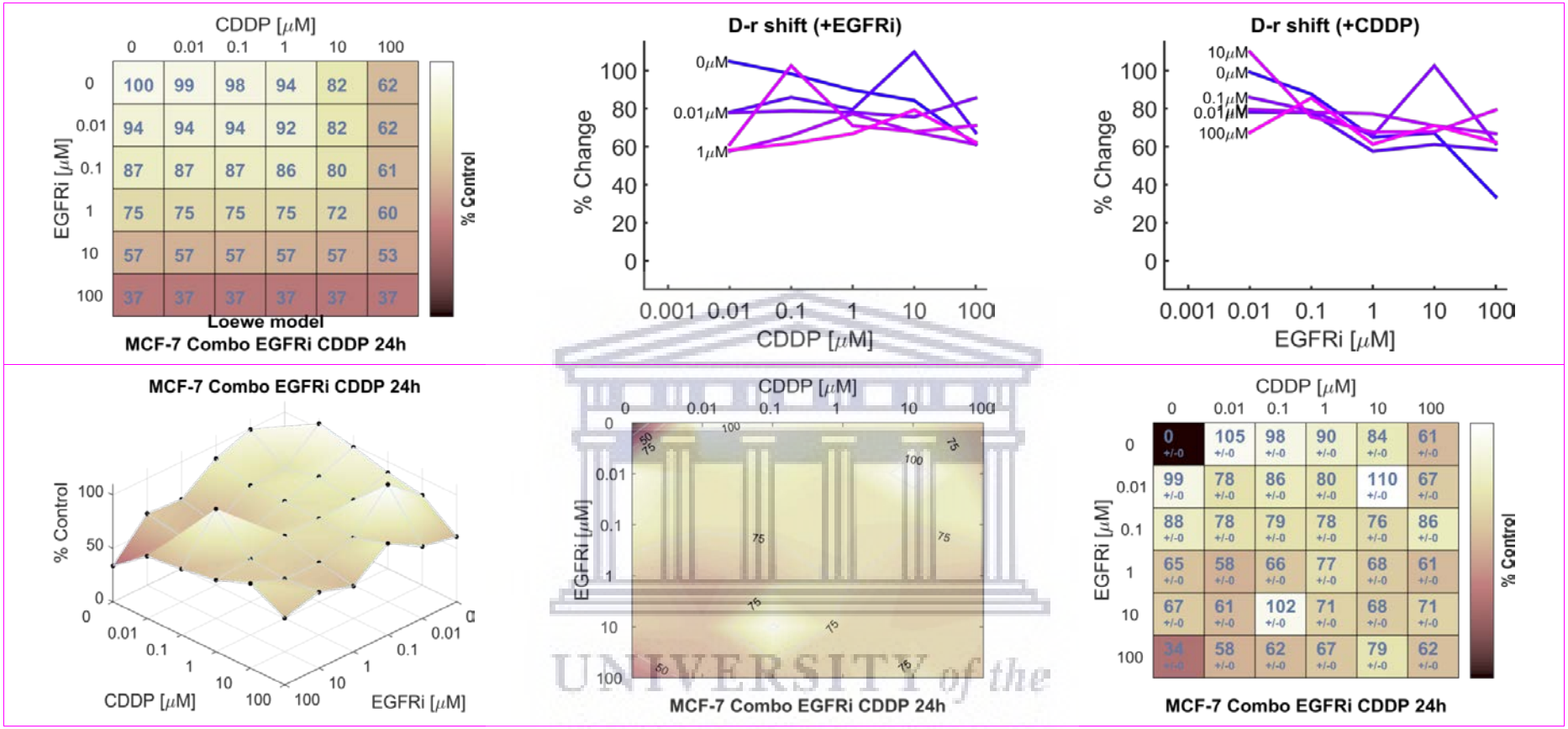

Figure 3.19D: Loewe reference model graphical presentation of the combination effects of 24h treatment of MCF-7 breast carcinoma cells with EGFRi and CDDP. **Top panel left:** Loewe additivity model reference dose-response matrix. | **Top panel center:** EGFRi dose-response shift in presence of increasing concentrations of CDDP | **Top panel right:** CDDP dose-response shift in presence of increasing concentrations of CDDP | **Bottom panel left:** EGFRi and CDDP combination dose-response surface | **Bottom panel center**: EGFRi and CDDP combination dose-response contour map | **Bottom panel right:** EGFRi and CDDP combination dose-response matrix.

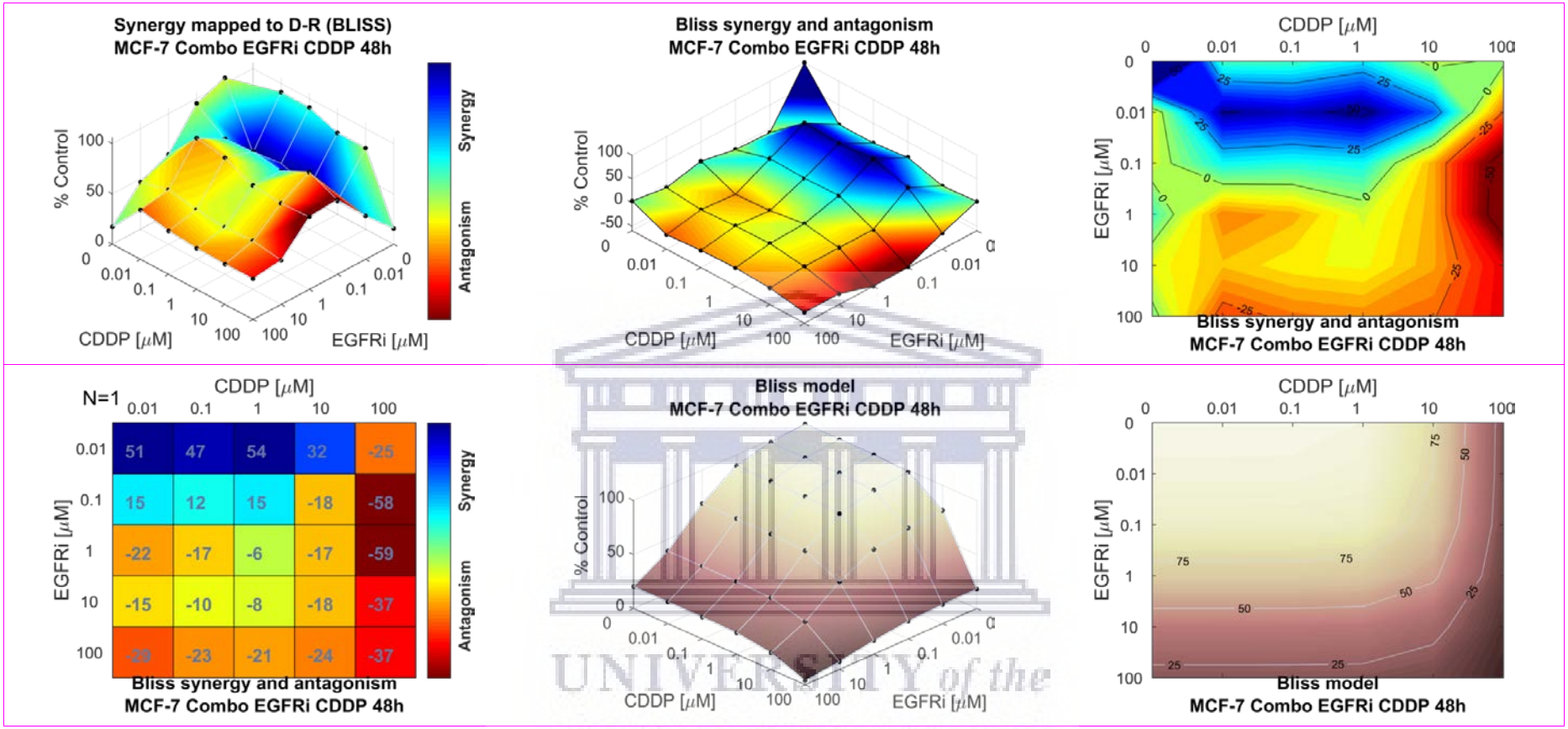

Figure 3.20A: Bliss independence response surface reference model for the dual agent combination effects of 48h treatment of MCF-7 breast carcinoma cells with EGFRi and CDDP. **Top panel left:** Bliss independence mapping of the synergy levels on the experimental combination dose-response surface | **Top panel center:** Bliss synergy and antagonism levels visualized as a surface | **Top panel right:** Contour map of isoboles (iso-effect lines) of Bliss synergy and/or antagonism | **Bottom panel left:** Bliss synergy and antagonism matrix | **Bottom panel center**: Bliss model reference dose-response surface | **Bottom panel right:** Bliss model reference dose-response contour map.

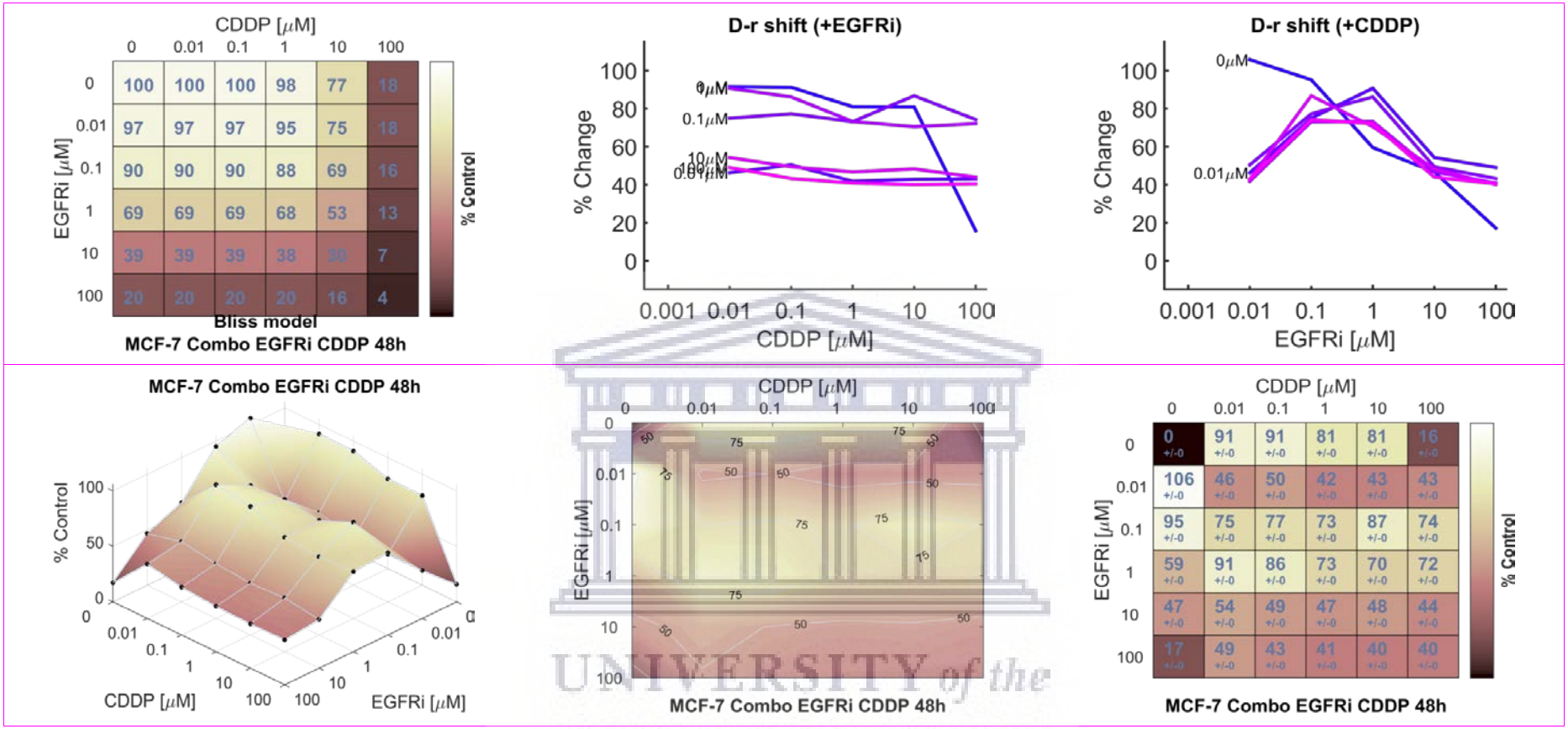

Figure 3.20B: Bliss reference model graphical presentation of the combination effects of 48h treatment of MCF-7 breast carcinoma cells with EGFRi and CDDP. **Top panel left:** Bliss model reference dose-response matrix. | **Top panel center:** EGFRi dose-response shift in presence of increasing concentrations of CDDP | **Top panel right:** CDDP dose-response shift in presence of increasing concentrations of EGFRi | **Bottom panel left:** EGFRi and CDDP combination dose-response surface | **Bottom panel center**: EGFRi and CDDP combination dose-response contour map | **Bottom panel right:** EGFRi and CDDP combination dose-response matrix.

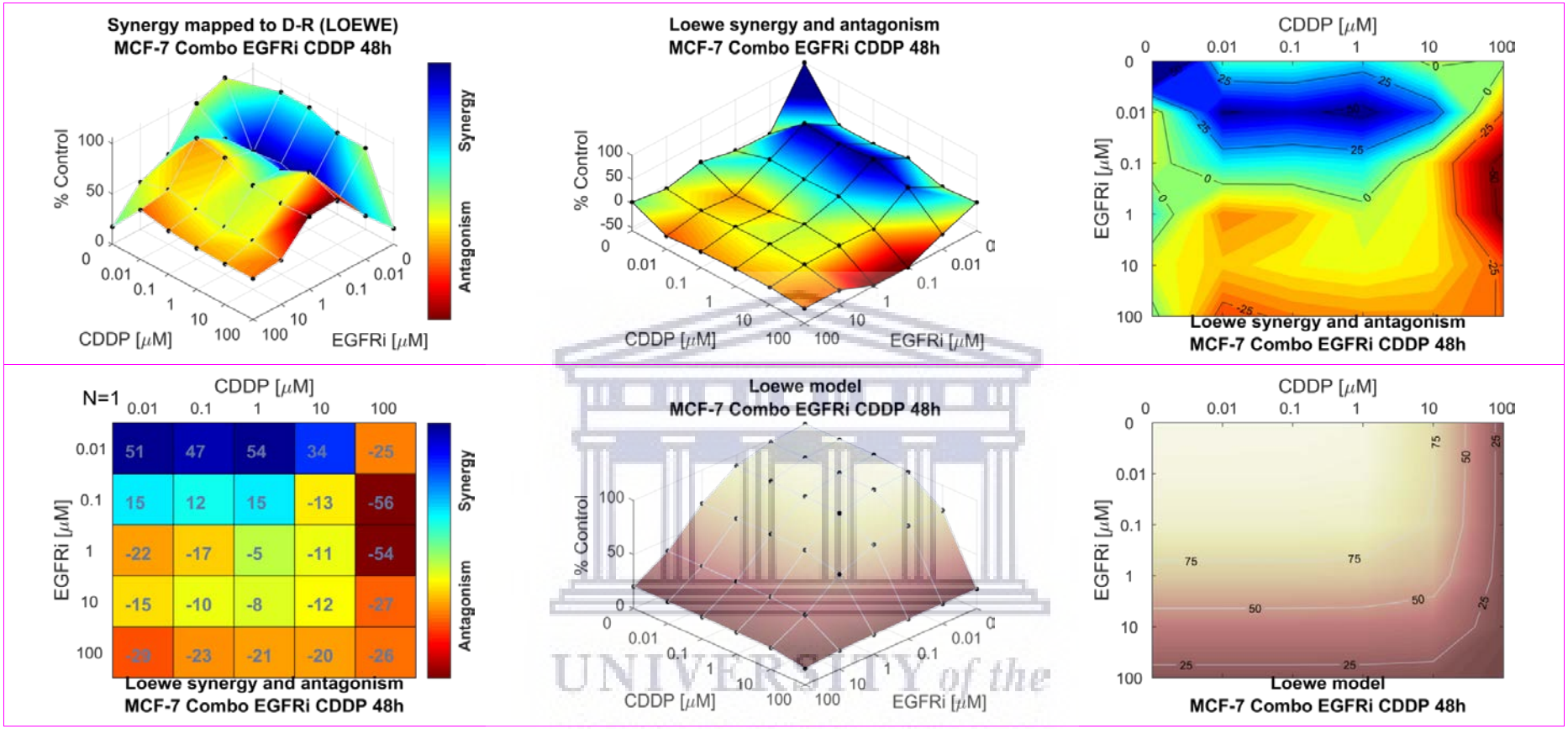

Figure 3.20C: Loewe additivity response surface reference model for the dual agent combination effects of 48h treatment of MCF-7 breast carcinoma cells with EGFRi and CDDP. **Top panel left:** Loewe additivity mapping of the synergy levels on the experimental combination dose-response surface | **Top panel center:** Loewe synergy and antagonism levels visualized as a surface | **Top panel right:** Contour map of isoboles (iso-effect) of Loewe synergy and/or antagonism | **Bottom panel left:** Loewe synergy and antagonism matrix | **Bottom panel center**: Loewe model reference dose-response surface | **Bottom panel right:** Loewe model reference dose-response contour map.

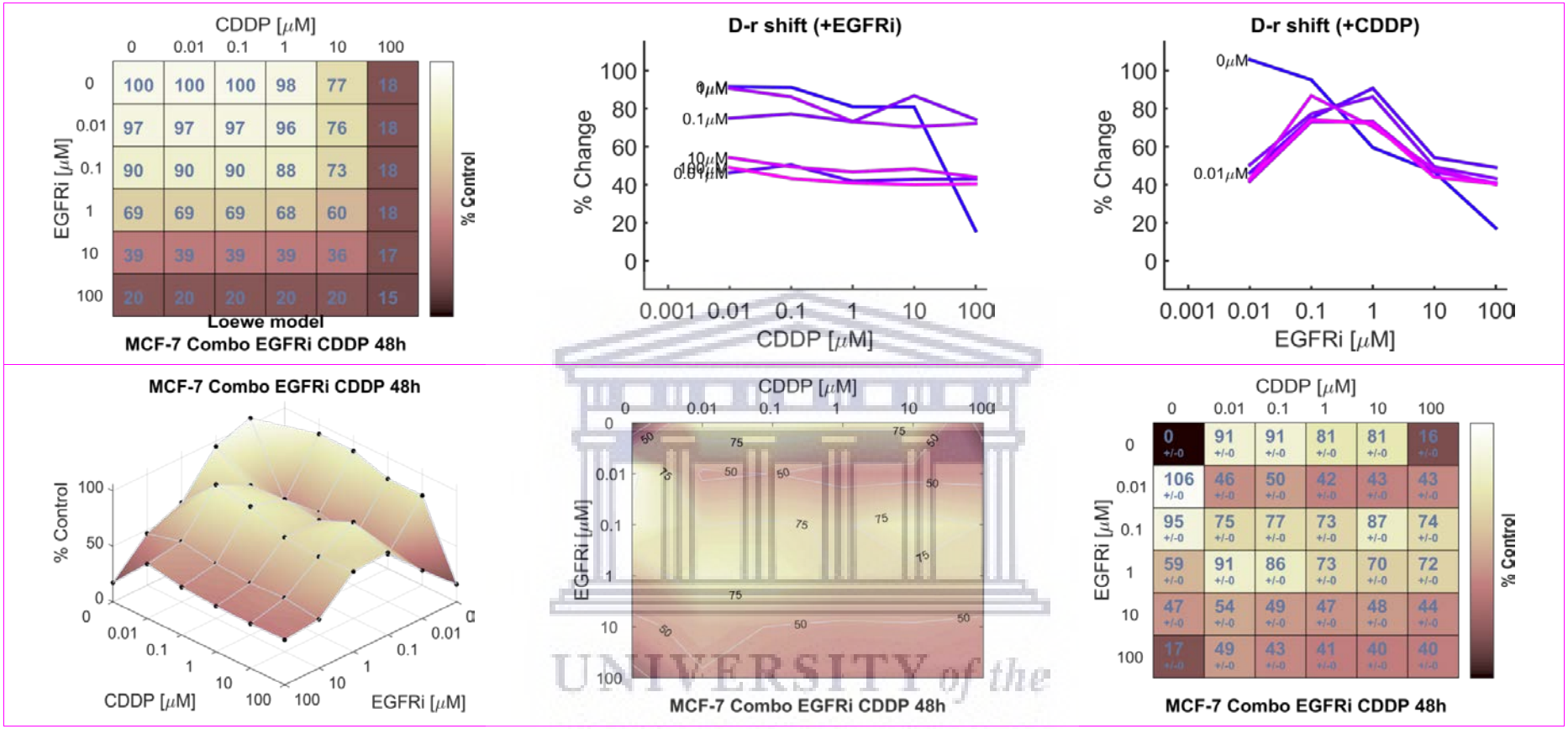

Figure 3.20D: Loewe reference model graphical presentation of the combination effects of 48h treatment of MCF-7 breast carcinoma cells with EGFRi and CDDP. **Top panel left:** Loewe additivity model reference dose-response matrix. | **Top panel center:** EGFRi dose-response shift in presence of increasing concentrations of CDDP | **Top panel right:** CDDP dose-response shift in presence of increasing concentrations of EGFRi | **Bottom panel left:** EGFRi and CDDP combination dose-response surface | **Bottom panel center**: EGFRi and CDDP combination dose-response contour map | **Bottom panel right:** EGFRi and CDDP combination dose-response matrix.

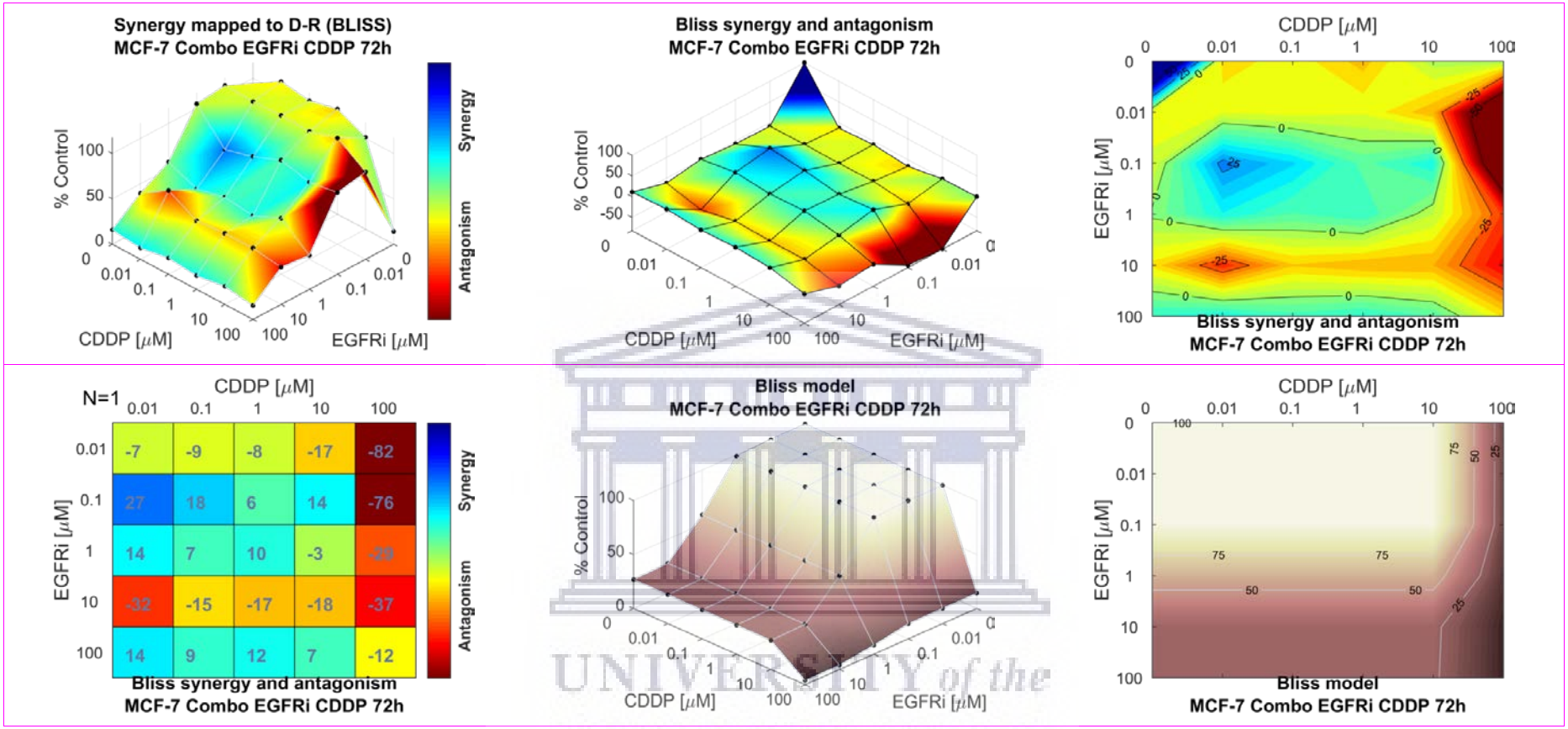

Figure 3.21A: Bliss independence response surface reference model for the dual agent combination effects of 72h treatment of MCF-7 breast carcinoma cells with EGFRi and CDDP. **Top panel left:** Bliss independence mapping of the synergy levels on the experimental combination dose-response surface | **Top panel center:** Bliss synergy and antagonism levels visualized as a surface | **Top panel right:** Contour map of isoboles (iso-effect lines) of Bliss synergy and/or antagonism | **Bottom panel left:** Bliss synergy and antagonism matrix | **Bottom panel center**: Bliss model reference dose-response surface | **Bottom panel right:** Bliss model reference dose-response contour map.

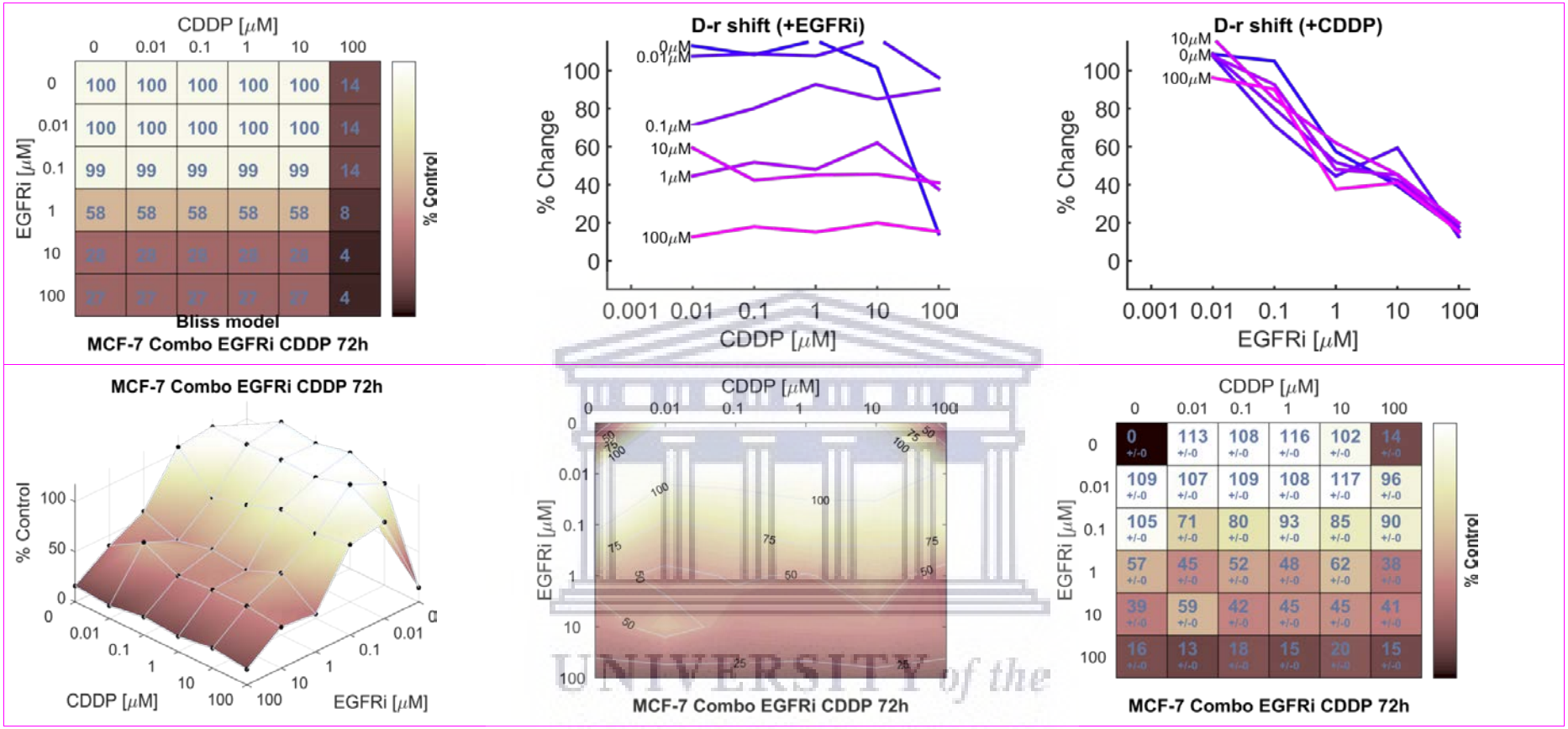

Figure 3.21B: Bliss reference model graphical presentation of the combination effects of 72h treatment of MCF-7 breast carcinoma cells with EGFRi and CDDP. **Top panel left:** Bliss model reference dose-response matrix. | **Top panel center:** EGFRi dose-response shift in presence of increasing concentrations of CDDP | **Top panel right:** CDDP dose-response shift in presence of increasing concentrations of EGFRi | **Bottom panel left:** EGFRi and CDDP combination dose-response surface | **Bottom panel center**: EGFRi and CDDP combination dose-response contour map | **Bottom panel right:** EGFRi and CDDP combination dose-response matrix.

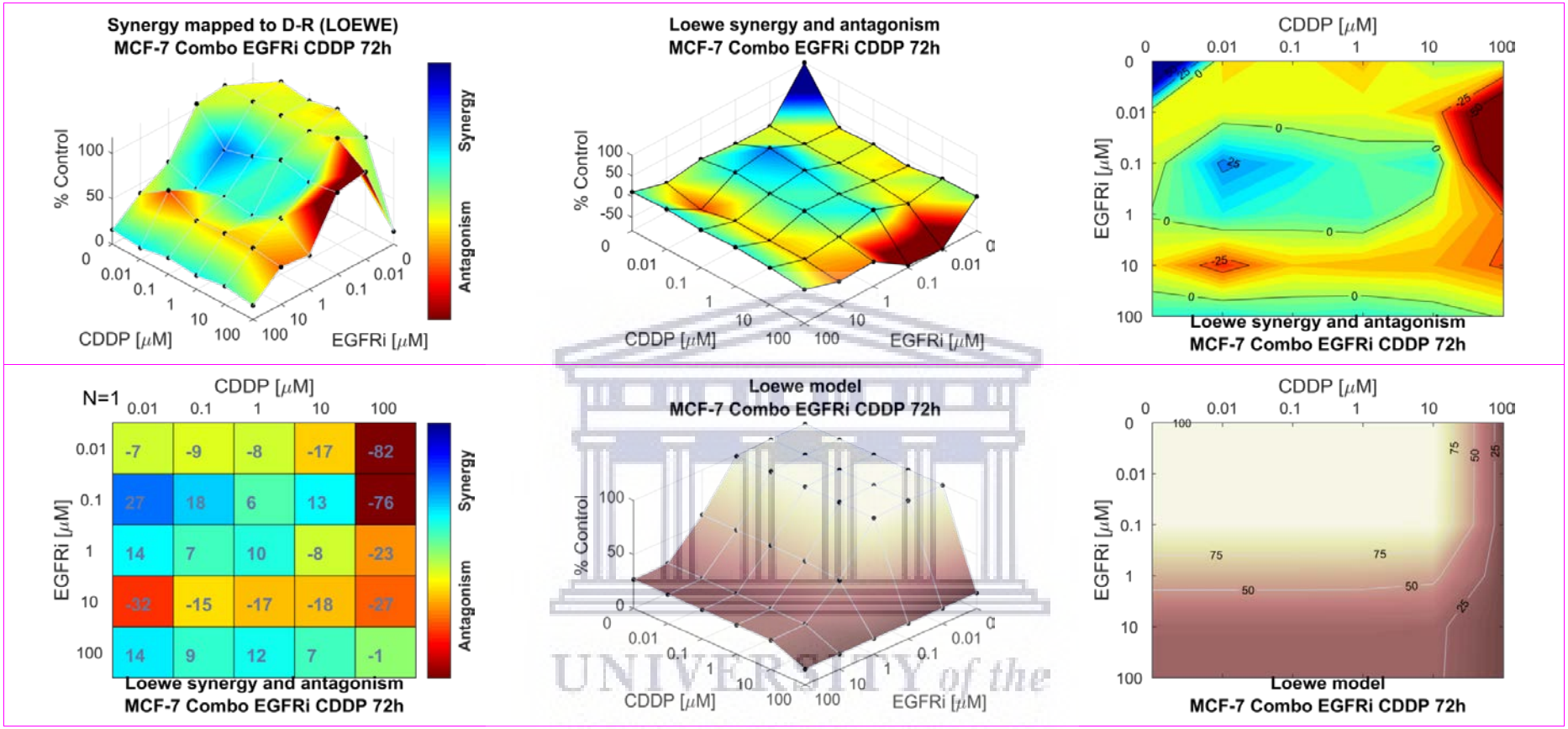

Figure 3.21C: Loewe additivity response surface reference model for the dual agent combination effects of 72h treatment of MCF-7 breast carcinoma cells with EGFRi and CDDP. **Top panel left:** Loewe additivity mapping of the synergy levels on the experimental combination dose-response surface | **Top panel center:** Loewe synergy and antagonism levels visualized as a surface | **Top panel right:** Contour map of isoboles (iso-effect) of Loewe synergy and/or antagonism | **Bottom panel left:** Loewe synergy and antagonism matrix | **Bottom panel center**: Loewe model reference dose-response surface | **Bottom panel right:** Loewe model reference dose-response contour map.

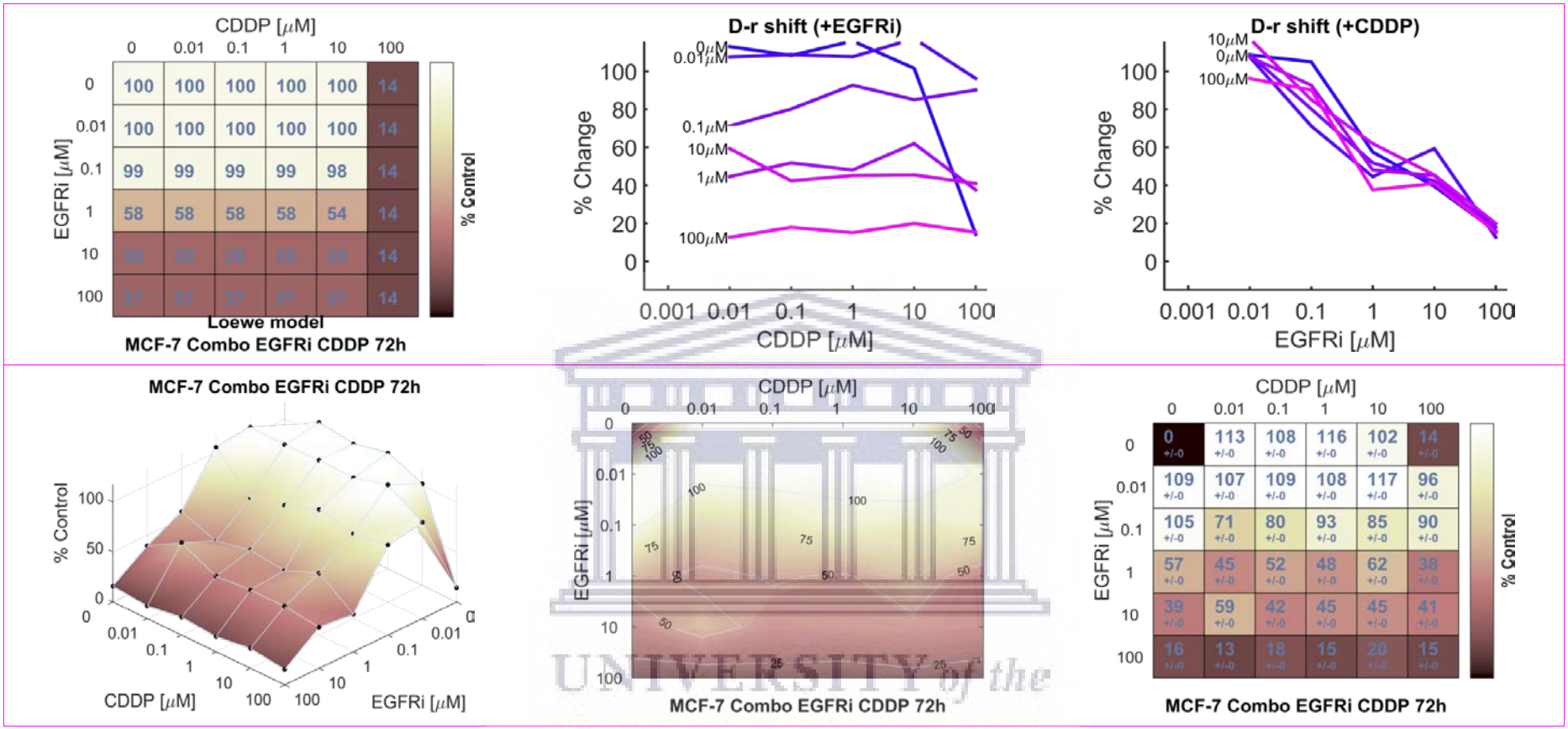

Figure 3.21D: Loewe reference model graphical presentation of the combination effects of 72h treatment of MCF-7 breast carcinoma cells with EGFRi and CDDP. **Top panel left:** Loewe additivity model reference dose-response matrix. | **Top panel center:** EGFRi dose-response shift in presence of increasing concentrations of CDDP | **Top panel right:** CDDP dose-response shift in presence of increasing concentrations of EGFRi | **Bottom panel left:** EGFRi and CDDP combination dose-response surface | **Bottom panel center**: EGFRi and CDDP combination dose-response contour map | **Bottom panel right:** EGFRi and CDDP combination dose-response matrix.

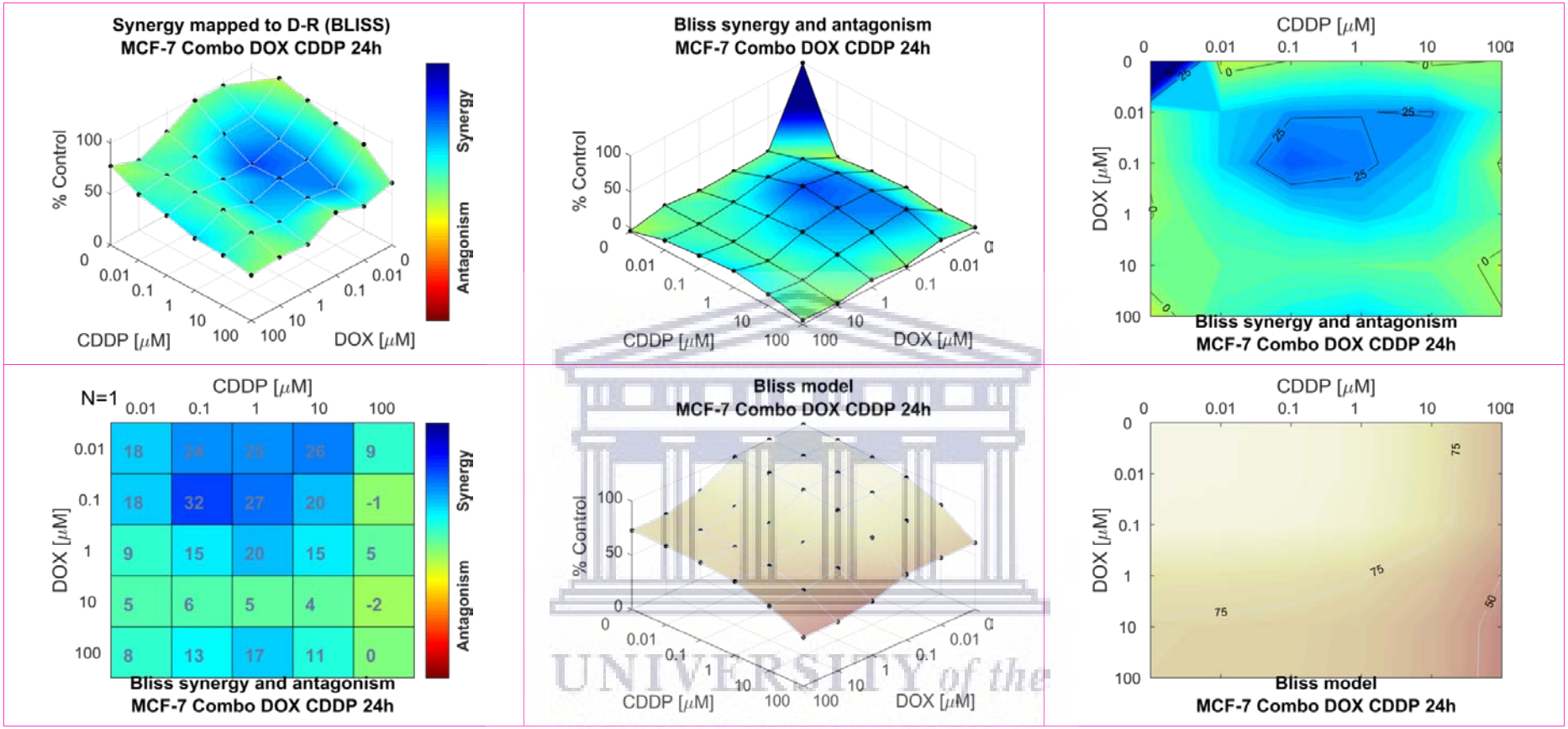

Figure 3.22A: Bliss independence response surface reference model for the dual agent combination effects of 24h treatment of MCF-7 breast carcinoma cells with DOX and CDDP. **Top panel left:** Bliss independence mapping of the synergy levels on the experimental combination dose-response surface | **Top panel center:** Bliss synergy and antagonism levels visualized as a surface | **Top panel right:** Contour map of isoboles (iso-effect) of Bliss synergy and/or antagonism | **Bottom panel left:** Bliss synergy and antagonism matrix | **Bottom panel center**: Bliss model reference dose-response surface | **Bottom panel right:** Bliss model reference dose-response contour map.

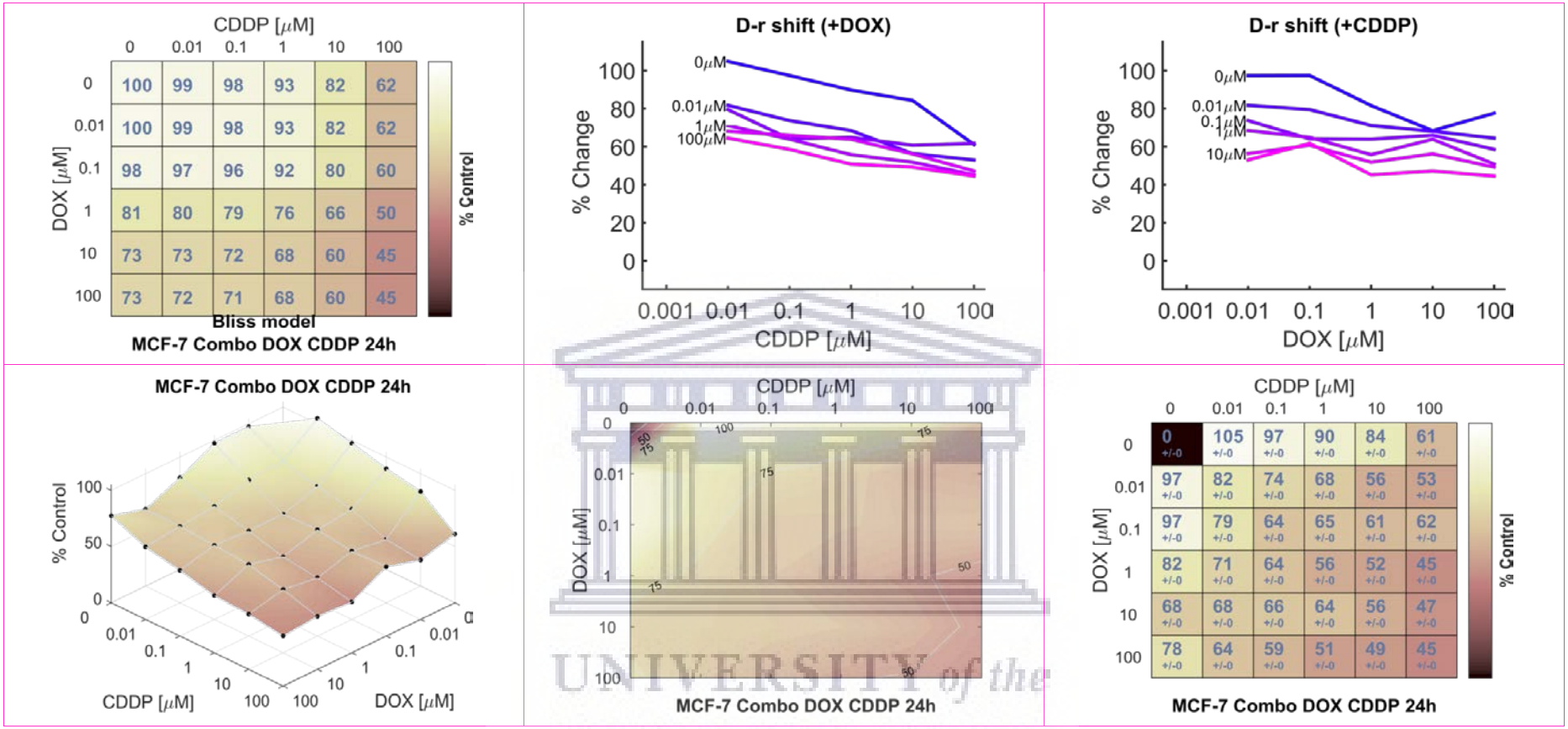

Figure 3.22B: Bliss reference model graphical presentation of the combination effects of 24h treatment of MCF-7 breast carcinoma cells with DOX and CDDP. **Top panel left:** Bliss model reference dose-response matrix. | **Top panel center:** DOX dose-response shift in presence of increasing concentrations of CDDP | **Top panel right:** CDDP dose-response shift in presence of increasing concentrations of DOX | **Bottom panel left:** DOX and CDDP combination dose-response surface | **Bottom panel center**: DOX and CDDP combination dose-response contour map | **Bottom panel right:** DOX and CDDP combination dose-response matrix.

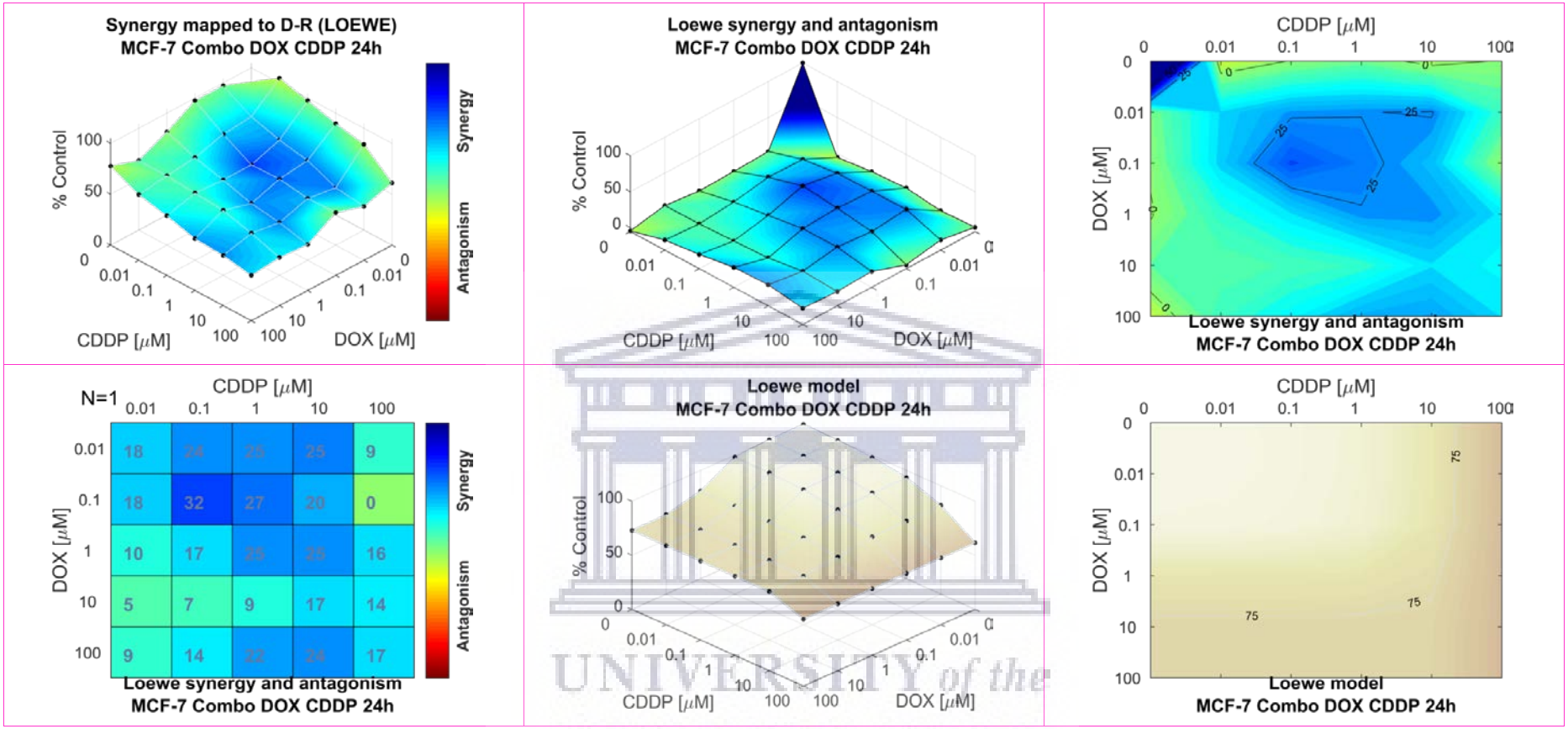

Figure 3.22C: Loewe additivity response surface reference model for the dual agent combination effects of 24h treatment of MCF-7 breast carcinoma cells with DOX and CDDP. **Top panel left:** Loewe additivity mapping of the synergy levels on the experimental combination dose-response surface | **Top panel center:** Loewe synergy and antagonism levels visualized as a surface | **Top panel right:** Contour map of isoboles (iso-effect) of Loewe synergy and/or antagonism | **Bottom panel left:** Loewe synergy and antagonism matrix | **Bottom panel center**: Loewe model reference dose-response surface | **Bottom panel right:** Loewe model reference dose-response contour map.

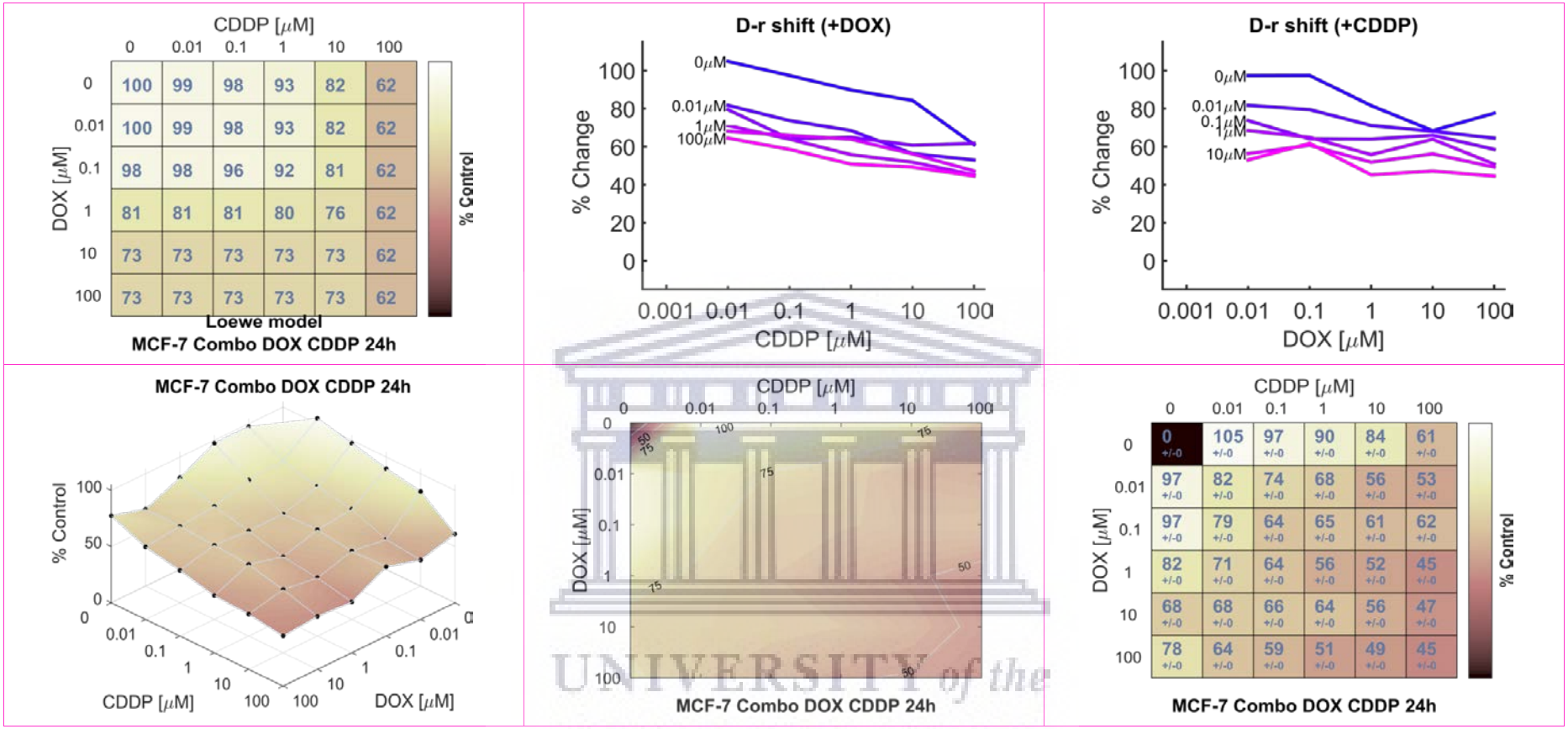

Figure 3.22D: Loewe reference model graphical presentation of the combination effects of 24h treatment of MCF-7 breast carcinoma cells with DOX and CDDP. **Top panel left:** Loewe additivity model reference dose-response matrix. | **Top panel center:** DOX dose-response shift in presence of increasing concentrations of CDDP | **Top panel right:** CDDP dose-response shift in presence of increasing concentrations of DOX | **Bottom panel left:** DOX and CDDP combination dose-response surface | **Bottom panel center**: DOX and CDDP combination dose-response contour map | **Bottom panel right:** DOX and CDDP combination dose-response matrix.

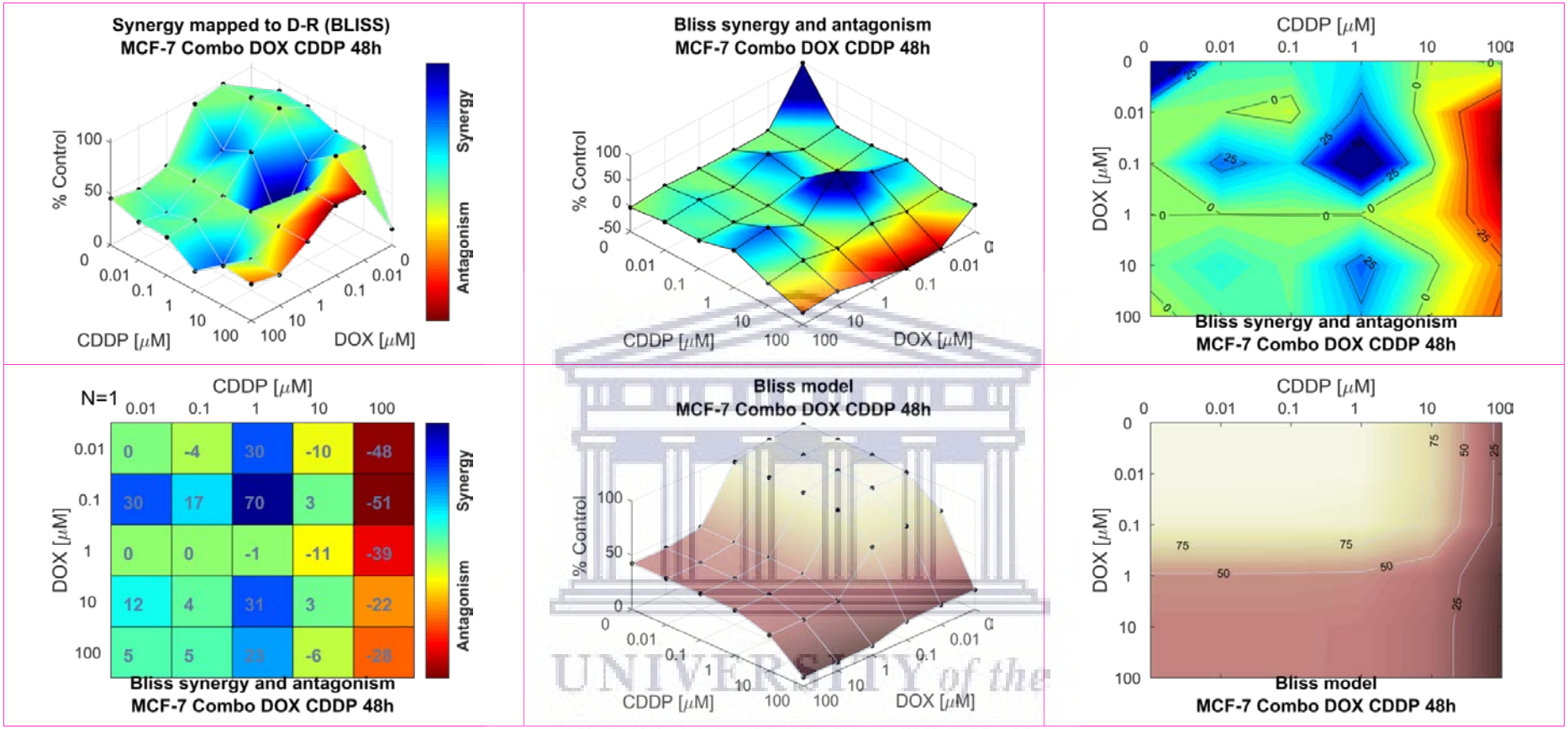

Figure 3.23A: Bliss independence response surface reference model for the dual agent combination effects of 48h treatment of MCF-7 breast carcinoma cells with DOX and CDDP. **Top panel left:** Bliss independence mapping of the synergy levels on the experimental combination dose-response surface | **Top panel center:** Bliss synergy and antagonism levels visualized as a surface | **Top panel right:** Contour map of isoboles (iso-effect) of Bliss synergy and/or antagonism | **Bottom panel left:** Bliss synergy and antagonism matrix | **Bottom panel center**: Bliss model reference dose-response surface | **Bottom panel right:** Bliss model reference dose-response contour map.

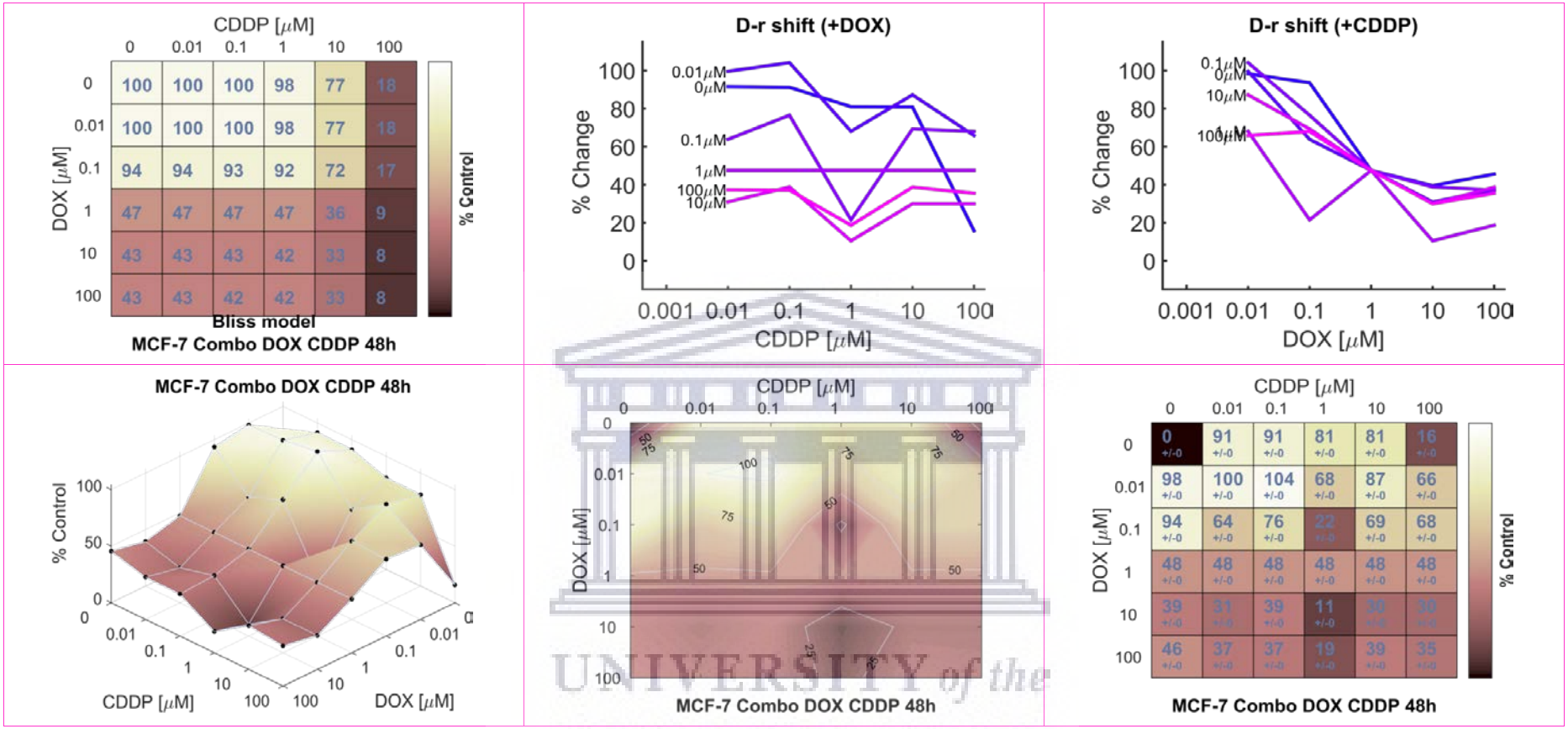

Figure 3.23B: Bliss reference model graphical presentation of the combination effects of 48h treatment of MCF-7 breast carcinoma cells with DOX and CDDP. **Top panel left:** Bliss model reference dose-response matrix. | **Top panel center:** DOX dose-response shift in presence of increasing concentrations of CDDP | **Top panel right:** CDDP dose-response shift in presence of increasing concentrations of DOX | **Bottom panel left:** DOX and CDDP combination dose-response surface | **Bottom panel center**: DOX and CDDP combination dose-response contour map | **Bottom panel right:** DOX and CDDP combination dose-response matrix.

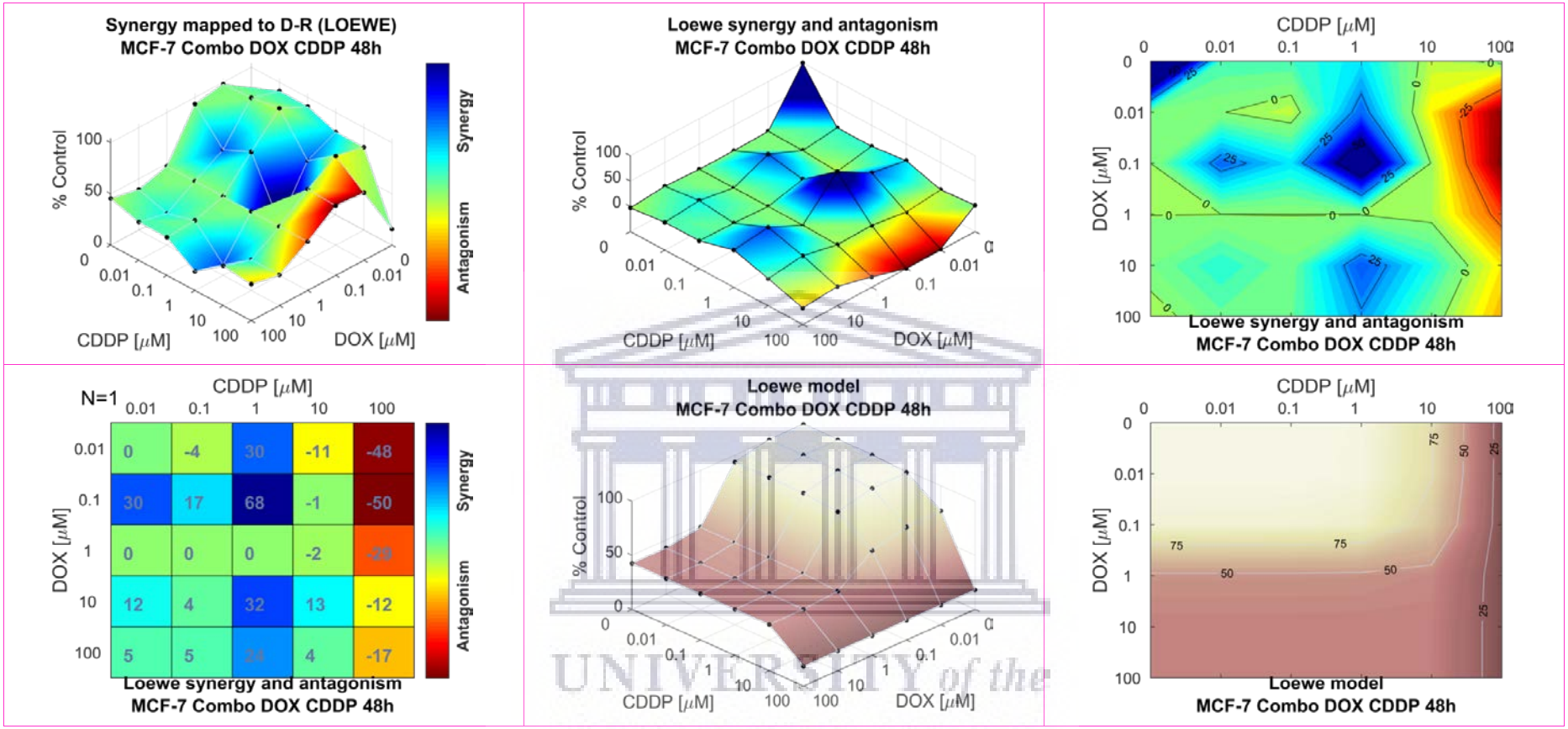

Figure 3.23C: Loewe additivity response surface reference model for the dual agent combination effects of 48h treatment of MCF-7 breast carcinoma cells with DOX and CDDP. **Top panel left:** Loewe additivity mapping of the synergy levels on the experimental combination dose-response surface | **Top panel center:** Loewe synergy and antagonism levels visualized as a surface | **Top panel right:** Contour map of isoboles (iso-effect) of Loewe synergy and/or antagonism | **Bottom panel left:** Loewe synergy and antagonism matrix | **Bottom panel center**: Loewe model reference dose-response surface | **Bottom panel right:** Loewe model reference dose-response contour map.

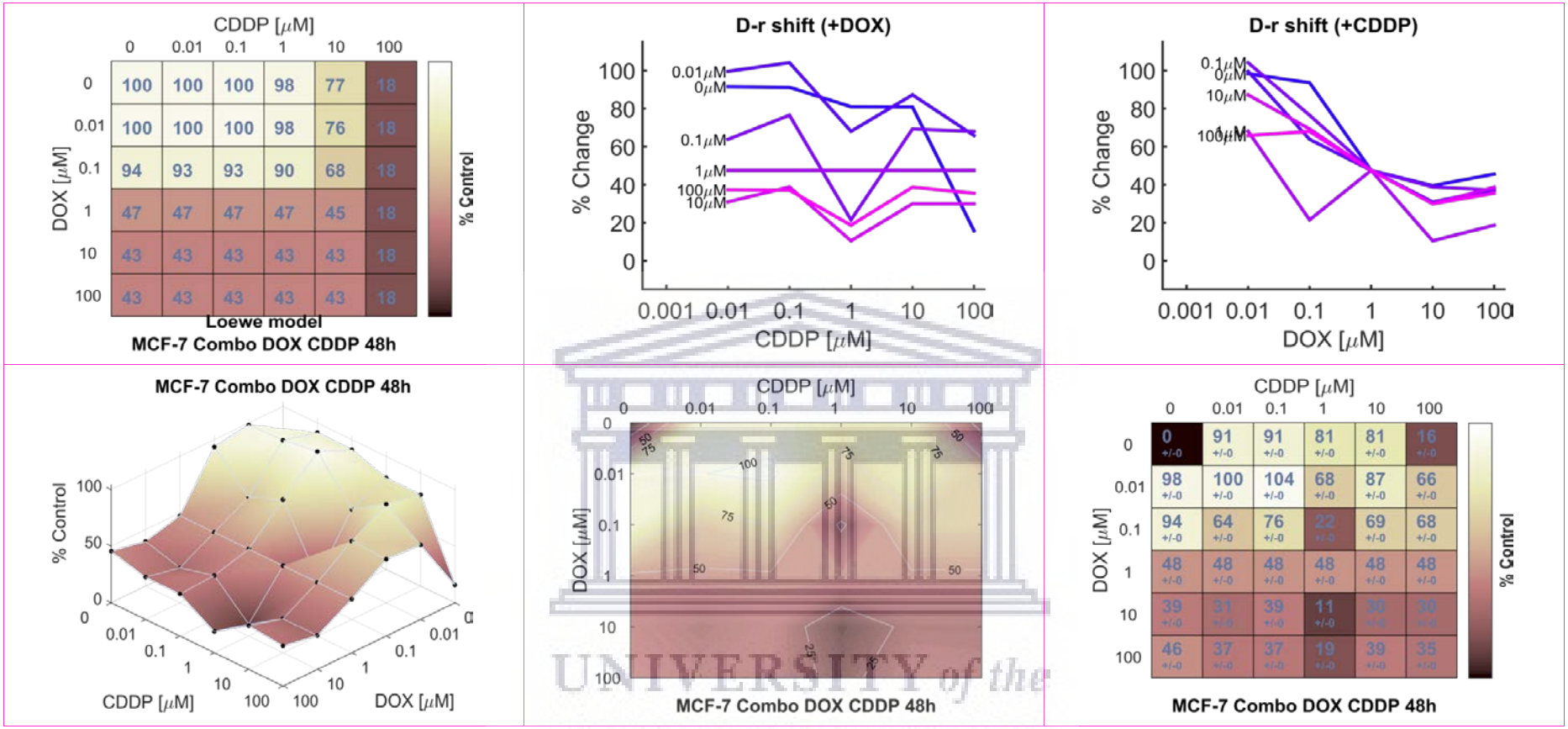

Figure 3.23D: Loewe reference model graphical presentation of the combination effects of 48h treatment of MCF-7 breast carcinoma cells with DOX and CDDP. **Top panel left:** Loewe additivity model reference dose-response matrix. | **Top panel center:** DOX dose-response shift in presence of increasing concentrations of CDDP | **Top panel right:** CDDP dose-response shift in presence of increasing concentrations of DOX | **Bottom panel left:** DOX and CDDP combination dose-response surface | **Bottom panel center**: DOX and CDDP combination dose-response contour map | **Bottom panel right:** DOX and CDDP combination dose-response matrix.

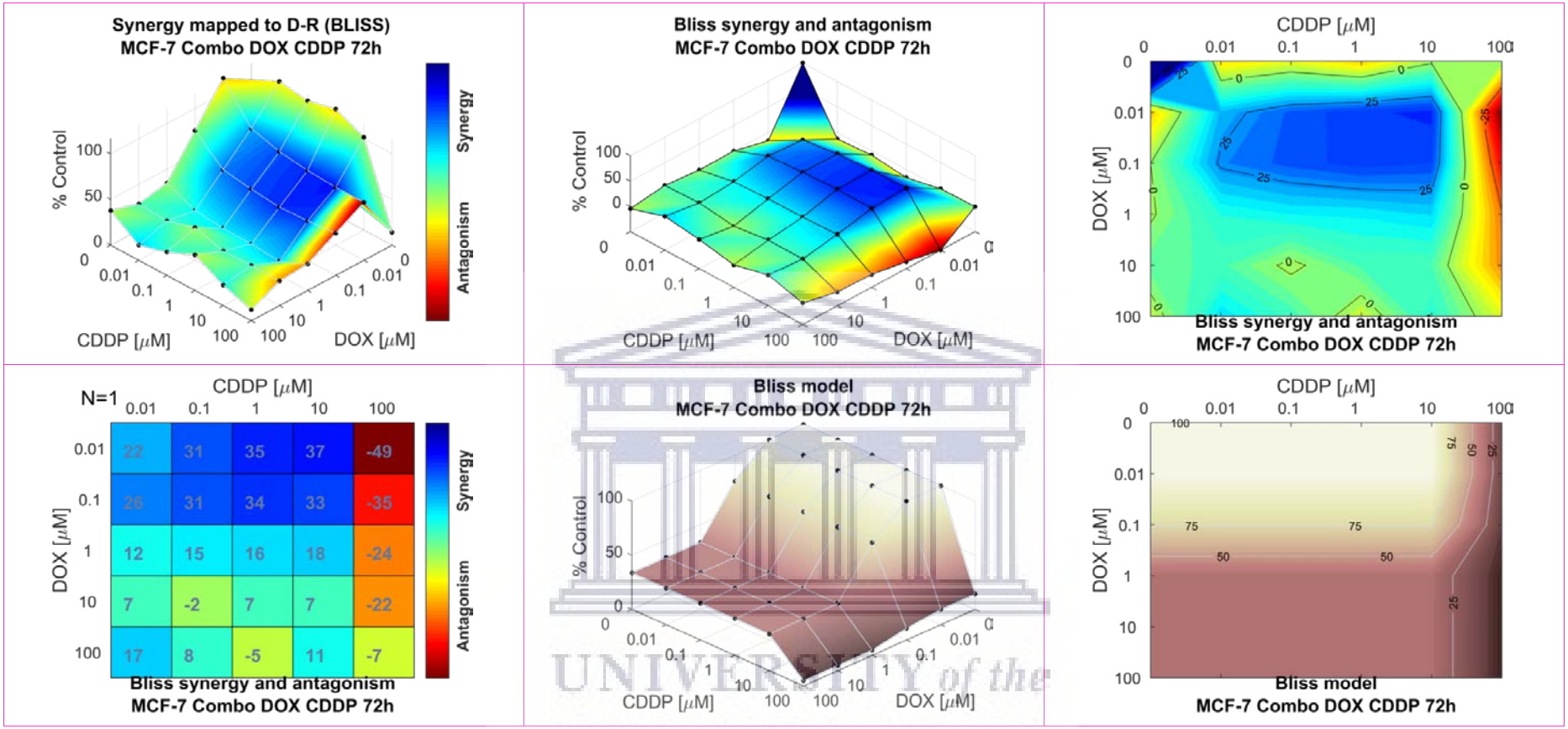

Figure 3.24A: Bliss independence response surface reference model for the dual agent combination effects of 72h treatment of MCF-7 breast carcinoma cells with DOX and CDDP. **Top panel left:** Bliss independence mapping of the synergy levels on the experimental combination dose-response surface | **Top panel center:** Bliss synergy and antagonism levels visualized as a surface | **Top panel right:** Contour map of isoboles (iso-effect) of Bliss synergy and/or antagonism | **Bottom panel left:** Bliss synergy and antagonism matrix | **Bottom panel center**: Bliss model reference dose-response surface | **Bottom panel right:** Bliss model reference dose-response contour map.

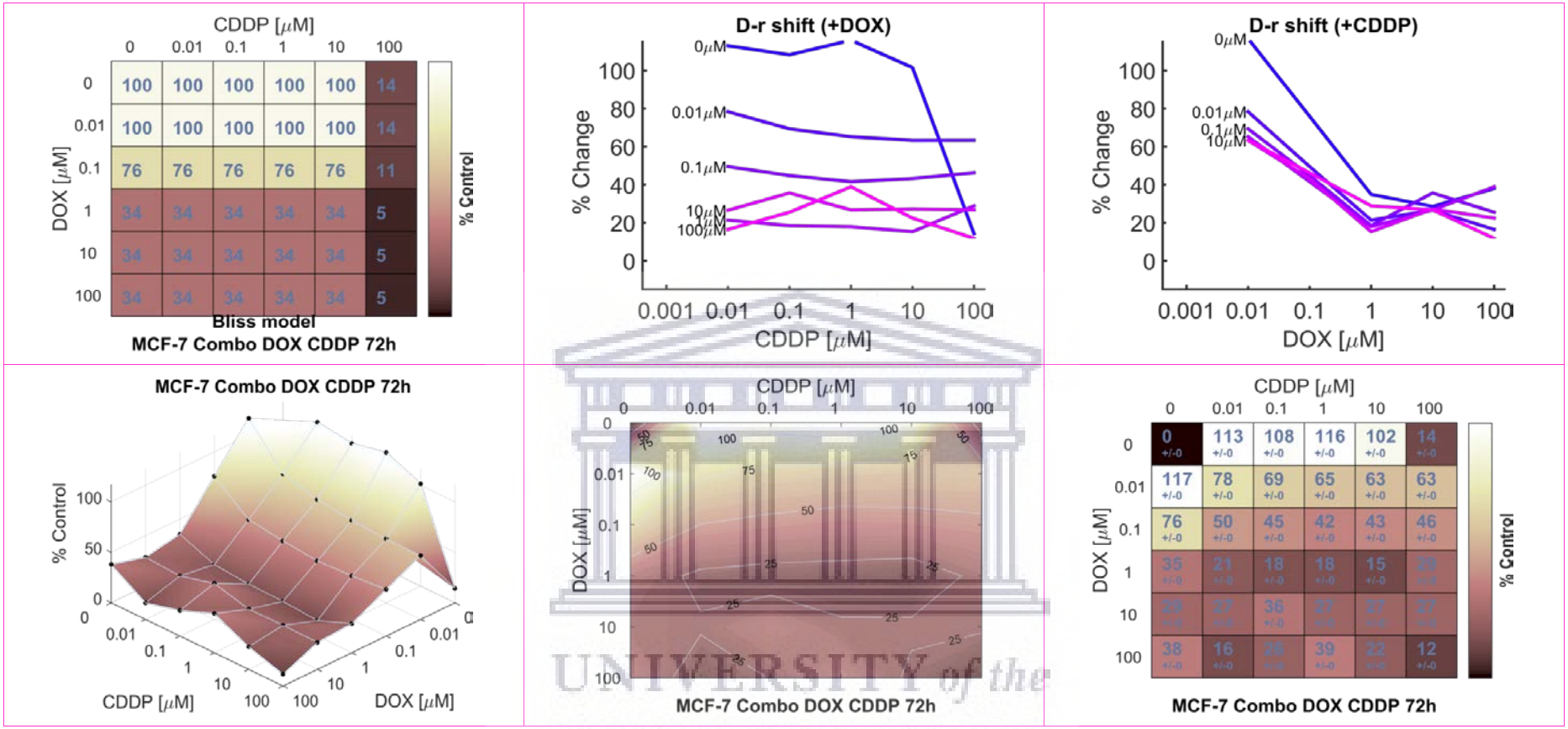

Figure 3.24B: Bliss reference model graphical presentation of the combination effects of 72h treatment of MCF-7 breast carcinoma cells with DOX and CDDP. **Top panel left:** Bliss model reference dose-response matrix. | **Top panel center:** DOX dose-response shift in presence of increasing concentrations of CDDP | **Top panel right:** CDDP dose-response shift in presence of increasing concentrations of DOX | **Bottom panel left:** DOX and CDDP combination dose-response surface | **Bottom panel center**: DOX and CDDP combination dose-response contour map | **Bottom panel right:** DOX and CDDP combination dose-response matrix.

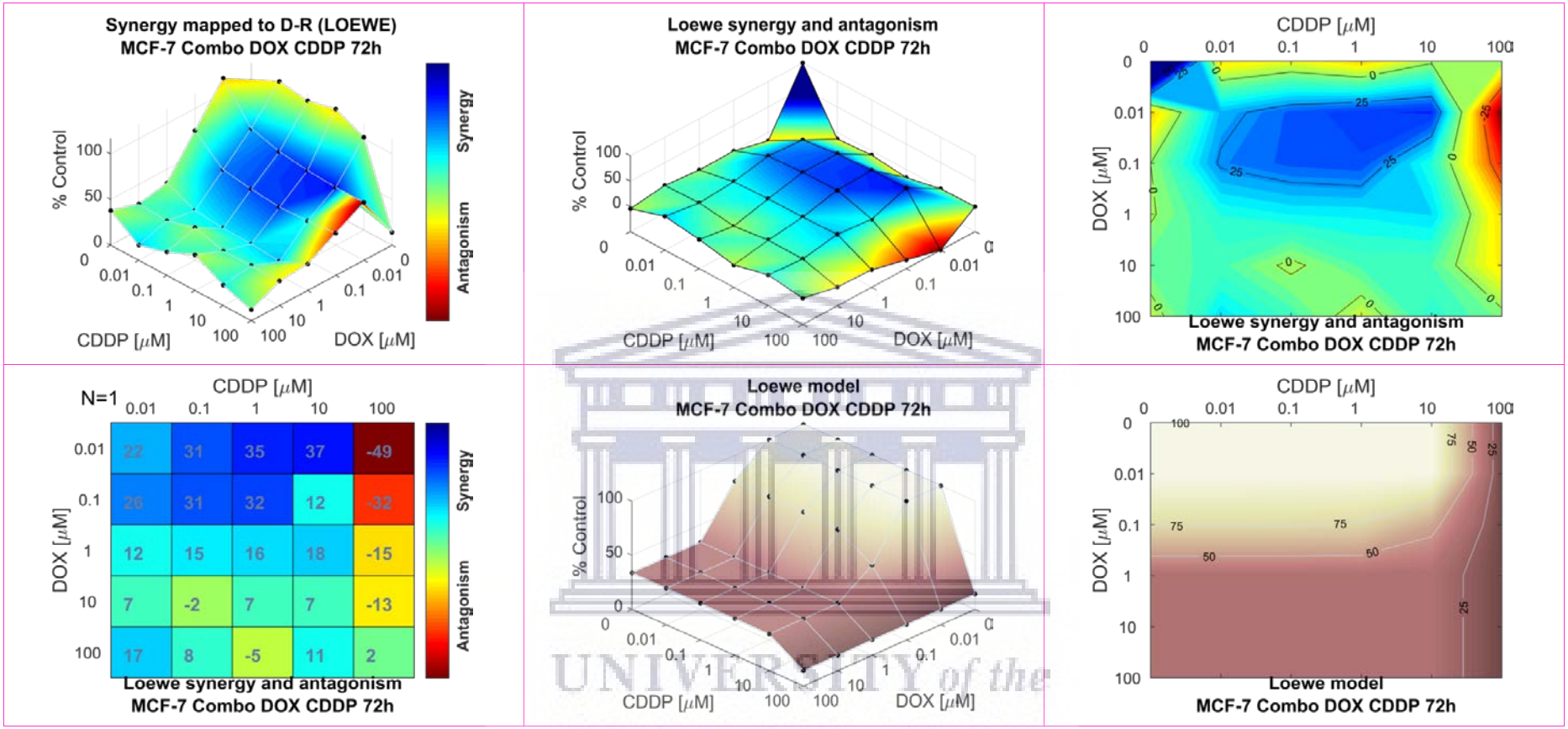

Figure 3.24C: Loewe additivity response surface reference model for the dual agent combination effects of 72h treatment of MCF-7 breast carcinoma cells with DOX and CDDP. **Top panel left:** Loewe additivity mapping of the synergy levels on the experimental combination dose-response surface | **Top panel center:** Loewe synergy and antagonism levels visualized as a surface | **Top panel right:** Contour map of isoboles (iso-effect) of Loewe synergy and/or antagonism | **Bottom panel left:** Loewe synergy and antagonism matrix | **Bottom panel center**: Loewe model reference dose-response surface | **Bottom panel right:** Loewe model reference dose-response contour map.

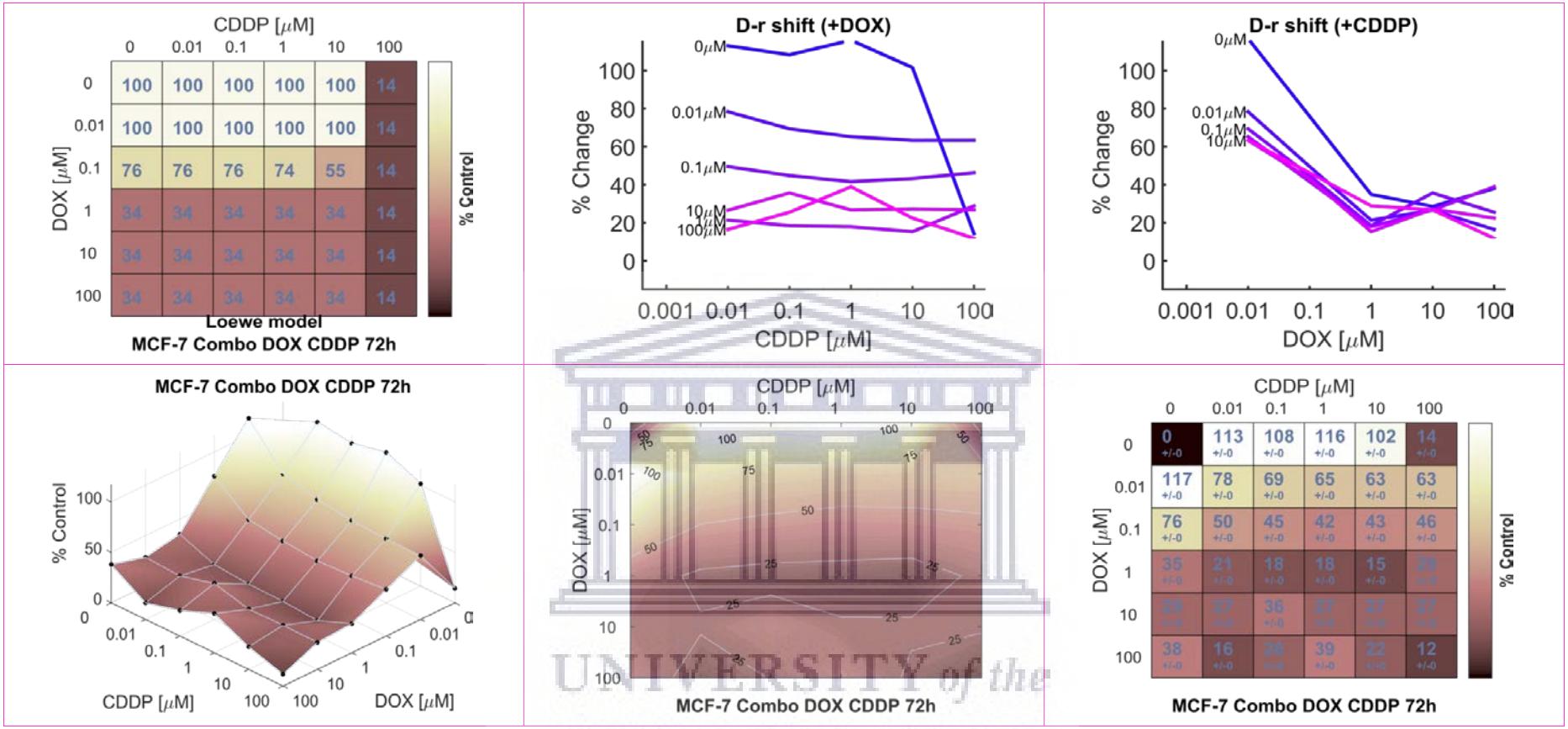

Figure 3.24D: Loewe reference model graphical presentation of the combination effects of 72h treatment of MCF-7 breast carcinoma cells with DOX and CDDP. **Top panel left:** Loewe additivity model reference dose-response matrix. | **Top panel center:** DOX dose-response shift in presence of increasing concentrations of CDDP | **Top panel right:** CDDP dose-response shift in presence of increasing concentrations of DOX | **Bottom panel left:** DOX and CDDP combination dose-response surface | **Bottom panel center**: DOX and CDDP combination dose-response contour map | **Bottom panel right:** DOX and CDDP combination dose-response matrix.

CHAPTER 4

RESULTS AND DISCUSSION OF THE ANALYSIS OF CASPASE-3/7 ACTIVITY FOR APOPTOSIS DETECTION

4.1 Introduction

In this chapter, MCF-7 and MDA-MB-231 TNBC breast carcinoma cells were exposed to $\log_{10}$ single-drug increments of EGFRi, DOX and CDDP for 24h and programmed cell death (PCD, also referred to as apoptosis) examined thereafter using the CellEvent™ Caspase-3/7 assay as described Chapter 2, Section 2.8.

4.2 Caspase-3/7 Activity in MCF-7 and MDA-MB-231 Cells as Indicator of Apoptosis

The MCF-7 cell cultures were more sensitive to CDDP which induced early apoptosis at some of the concentrations tested. Significant levels of caspase 3/7 activity were induced by 1 µM (p=0.016), 10 µM (p=0.023) and 100 µM (p=0.016) CDDP, whereas DOX was effective at inducing apoptosis at the highest concentration, i.e., 100 µM (p=0.003). EGFRi treatment did not induce significant levels of apoptosis Figure 4.1.

In MDA-MB-231 TNBC cells, EGFRi treatment significantly induced caspase activity at all concentrations tested, i.e., at 1 µM (p=0.007), 10 µM (p=0.004), 100 µM (p=0.032), except at 0.1 µM (p=0.059, marginally significant). DOX induced apoptosis in MDA-MB-231 TNBC cells at low concentrations, i.e., 0.1 µM (p=0.008) and 1 µM (p=0.024). However, significant levels of apoptosis with caspase activation were induced by CDDP at 0.1 µM, 1 µM and 100 µM ($p<0.0001$ in all cases), but not at 10 µM (p=0.066) Figure 4.2.

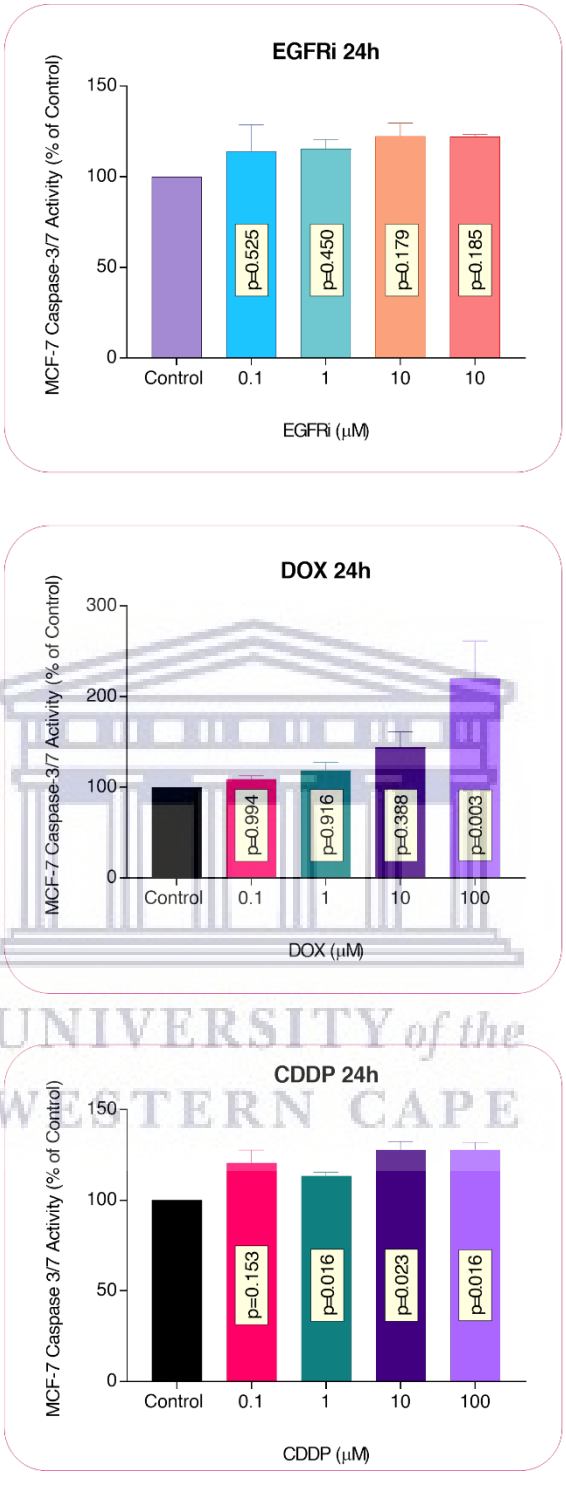

Figure 4.1: Caspase-3/7 activity following 24h exposure of MCF-7 breast carcinoma cells to EGFRi, DOX and CDDP. Data were analyzed by one-way ANOVA. All multiple comparisons were performed according to the Dunnet's method and the overall significance level was set at $p<0.05$. Actual p-values are indicated within bars. Values are means ± SEM (n=4).

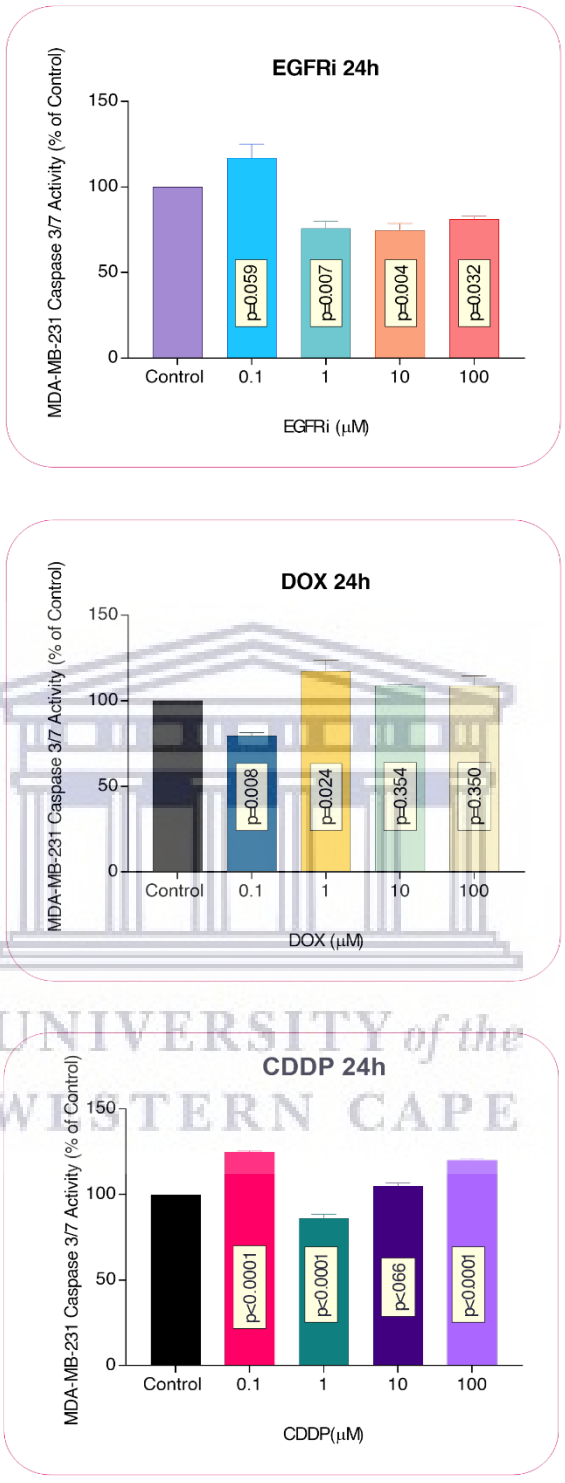

Figure 4.2: Caspase-3/7 activity following 24h exposure of MDA-MB-231 TNBC cells to EGFRi, DOX and CDDP. Data were analyzed by one-way ANOVA. All multiple comparisons were performed according to the Dunnet's method and the overall significance level was set at $p<0.05$. Actual p-values are indicated within bars. Values are means ± SEM (n=4).

4.3 Discussion

In this study, 24h treatment of MCF-7 and MDA-MB-231 TNBC breast carcinoma cells with DOX and CDDP induced significant levels of caspase activity, and thus apoptosis, in a concentration-dependent manner. EGFRi did not induce apoptosis in MCF-7 breast carcinoma cells, but effected apoptosis in MDA-MB-231 TNBC cells. The latter cell line was resistant to the apoptosis-inducing effects of DOX at high concentrations (i.e., 10 and 100 µM), and CDDP at 10 µM, whereas MCF-7 breast carcinoma cells displayed apoptosis resistance to the entire concentration range of EGFRi (i.e., 0.1 to 100 µM), and DOX at 0.1 to 10 µM), but not to 100 µM DOX. Anthracyclines can exert cytostatic effects and steer cells towards an apoptotic mode, but cellular senescence and other types of cell death programs, including immunogenic death, are also probable [531,532,534]. Besides, anthracycline-containing chemotherapies were traditionally assumed to kill proliferating tumor cells only via apoptosis or necrosis, in a manner independent from the immune system of patients. Yet, anthracyclines can also elicit an effective antitumor immune response that suppresses the growth of inoculated tumors or leads to the regression of established neoplasia [616]. MDR is a major cause of recurrence and poor prognosis in TNBC patients, which may explain the relative resistance to DOX in the MDA-MB-231 TNBC cells.

A recent drug combination study showed that curcumol enhanced the sensitivity of MDA-MB-231 TNBC cells to DOX *in vitro* and *in vivo* via suppression of ABCC3, a member of the ABC multidrug transporters [617]. This study was corroborated by the observation that a combination of the dual-target MDM2/MDMX inhibitor with DOX not only suppressed proliferation, promoted cell cycle arrest and induced apoptosis, but also reduced drug efflux in DOX-resistant breast cancer cell lines [618]. MCF-7/DOX-resistant cells are much more sensitive to apoptotic stimuli than previously thought [619]. Our own laboratory established that a combination of fucoidan with the standard

chemotherapeutic agents—CDDP, DOX and taxol, significantly enhanced the cytotoxicity of these drugs and accumulation of MCF-7 breast carcinoma cells in the G_2/M and sub-G_1 phases of the cell cycle, and induction of apoptosis [620]. Significant emphasis is currently being placed on combination chemotherapy of cancer using conventional cytotoxic agents and naturally occurring antitumor agents, displaying distinctive mechanisms of action with non-overlapping toxicity. The chemopreventive agent silibinin, e.g., synergizes the therapeutic potential of DOX, CDDP or carboplatin in both estrogen-dependent and -independent human breast carcinoma representative cell lines, MCF-7 and MDA-MB468, respectively [621].

Combination of vorinostat, a HDAC inhibitor, with dasatinib, a small molecule TKI, produced synergistic effects on MCF-7 breast carcinoma cells by inducing cell cycle arrest, ROS production, and apoptosis [609]. As indicated in Section C (Chapter 1) EGFR (ERBB1) and HER-2/neu (ERBB2) are members of the ERBB family of RTKs that are associated with poor prognosis and decreased survival in cancer patients. A previous study assessed the effects of combining ERBB and Bcl-2 inhibitors (lapatinib and GW2974, respectively) on the growth of human breast cancer cell lines [MCF-7 human breast cancer cells, a HER-2/neu transfected MCF-7 cell line (MCF/18), and a tamoxifen-resistant MCF-7 cell line (MTR-3)] and reported a synergistic growth inhibitory effect on all cell lines, thus accentuating the beneficial effects of Bcl-2 inhibitors to induce apoptosis whilst at the same time blocking the ERBB family of RTKs [622]. The results of this study indicate that the drugs tested may shed light on apoptosis mechanisms in the MDA-MB-231 TNBC and MCF-7 breast carcinoma cell lines. However, a major drawback of our study is that no drug combinations were analysed. Drug combinations are critical to delineating and overcoming drug resistance, and minimizing side effects with optimal delivery systems as has been reviewed for DOX as a first line agent for breast cancer, among other cancers [530].

CHAPTER 5

RESULTS AND DISCUSSION OF THE ANALYSIS OF P-GLYCOPROTEIN-MEDIATED DRUG EFFLUX FUNCTION

5.1 Introduction

The roles of overexpression of ABC drug transporters in cancer, including breast cancer, MDR development and poor patient response rates or survival rates have been discussed in Chapter 1 (Section B). In this study, the function of P-glycoprotein (P-gp/ABCB1/MDR1) as a drug efflux pump was determined using the Calcein-AM retention assay as described in Chapter 2 (Section 2.8). This assay discriminates between the effects of substrates and inhibitors on P-gp function. Calcein-AM is a fluorescent dye and substrate of P-gp, and is readily excluded in cells expressing the drug transporter. Cyclosporin A and Verapamil are competitive and non-competitive inhibitors of P-gp, respectively, and were included in the assay as positive controls. The effects of 48h exposure of MCF-7 and MDA-MB-231 TNBC breast carcinoma cells to EGFRi, DOX and CDDP, alone and in combination with the other drugs, on intracellular Calcein-AM retention were measured quantitatively and compared as depicted in Figure 5.1 and Figure 5.2, respectively.

5.2 Calcein-AM Retention in MCF-7 and MDA-MB-231 Cells as an Indicator of P-Glycoprotein Drug Efflux Pump Functional Activity

Calcein-AM retention in MCF-7 breast carcinoma cells was significantly increased following single-agent treatment with a high concentration of EGFRi (100 µM; $p=0.0004$). However, both DOX and CDDP significantly reduced Calcein-AM retention at concentrations of 1 and 10 µM ($p<0.005$ in all cases) Figure 5.1 (*top panel*).

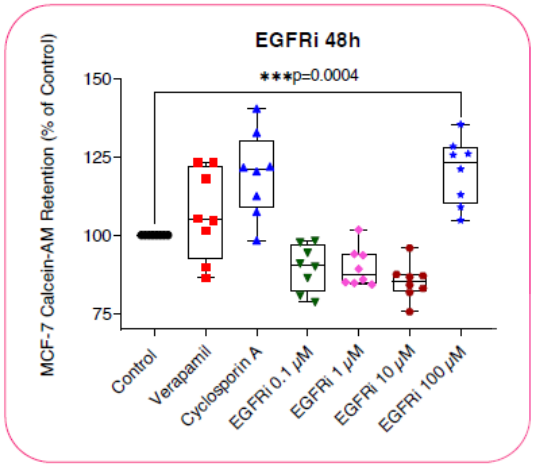

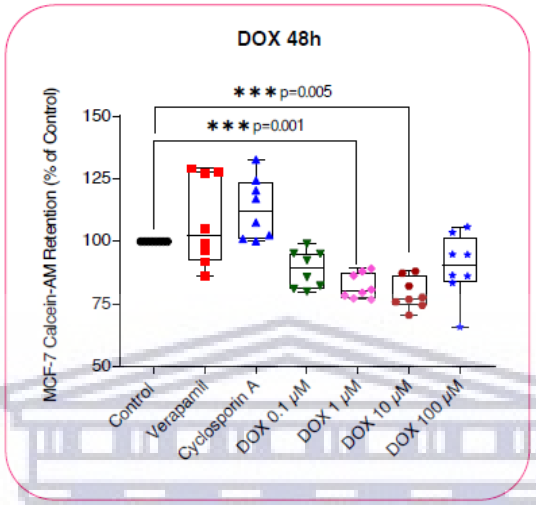

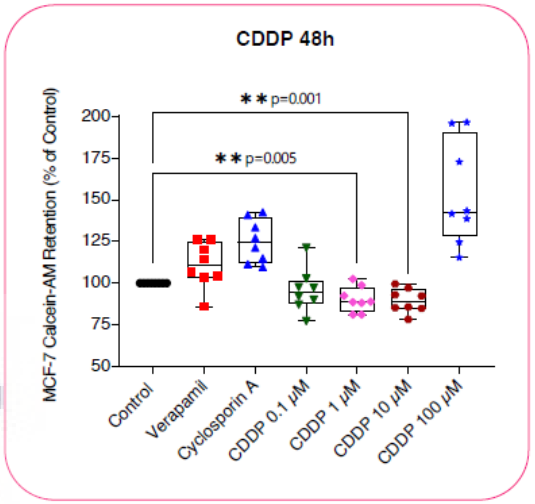

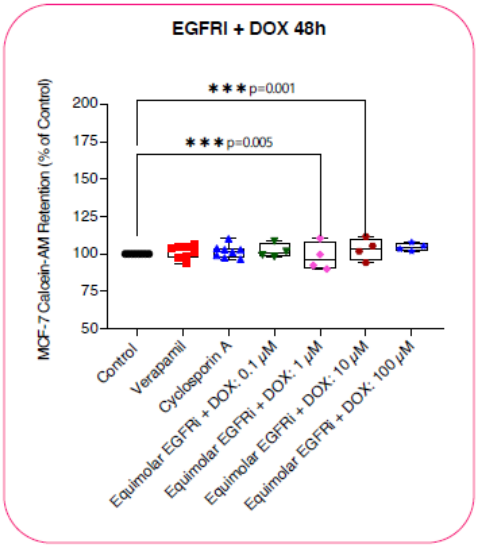

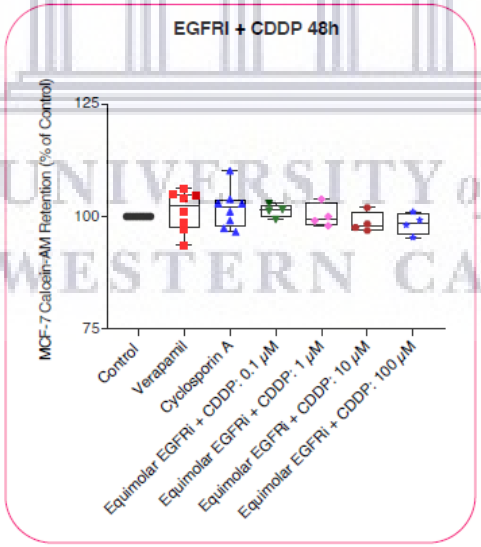

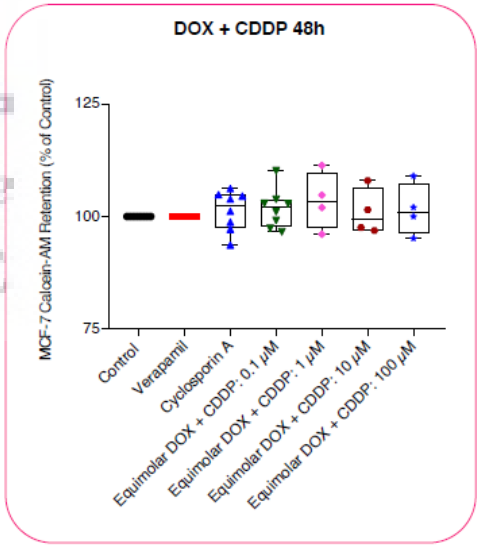

Figure 5.1: Intracellular Calcein-AM retention in MCF-7 breast carcinoma cells after 48h exposure to EGFRi, DOX and CDDP, alone (*top panel*), and in combination (*bottom panel*) with the other drugs. Data were analyzed by one-way ANOVA. Multiple comparisons were performed according to Dunnet's method and the overall significance level was set at $p<0.05$. Actual p-values are indicated on the graphs. Values are means ± SEM (n=4).

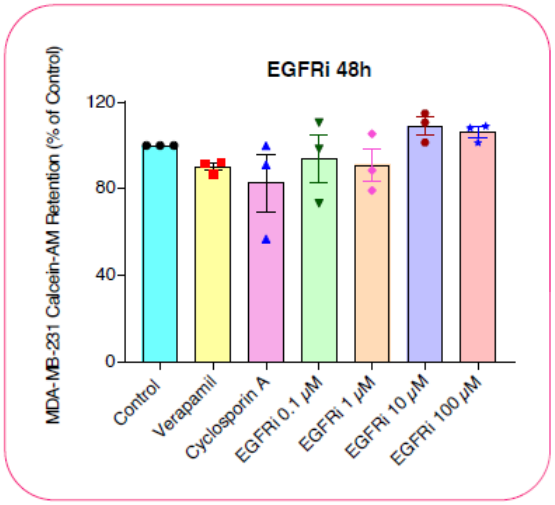

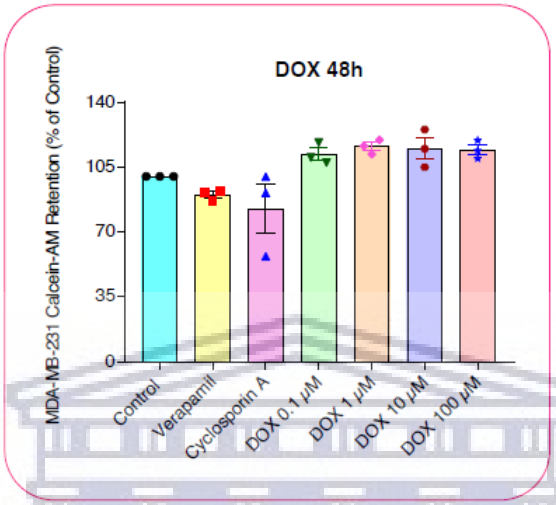

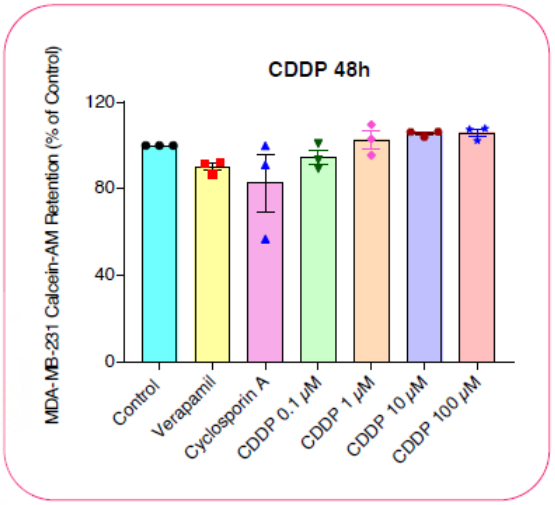

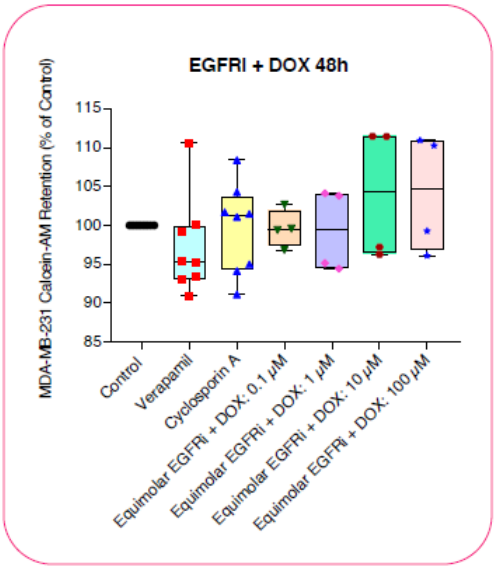

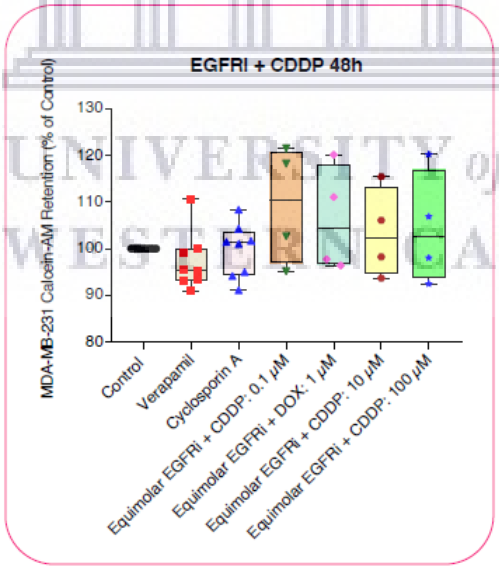

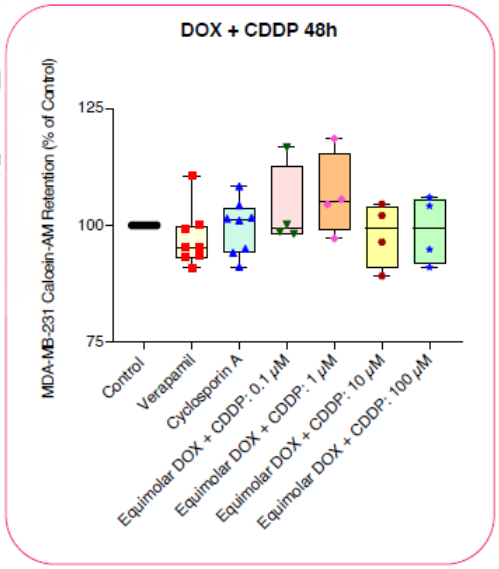

Figure 5.2: Intracellular Calcein-AM retention in MDA-MB-231 TNBC cells after 48h exposure to EGFRi, DOX and CDDP, alone (*top panel*), and in combination (*bottom panel*) with the other drugs. Data were analyzed by one-way ANOVA. Multiple comparisons were performed according to Dunnet's method and the overall significance level was set at $p<0.05$. Actual p-values are indicated on the graphs. Values are means ± SEM (n=4).

Only equimolar combinations of EGFRi and DOX at 1 and 10 µM significantly increased (p=0.005 and p=0.001, respectively) Calcein-AM retention, whereas the combinations of EGFRi with CDDP and DOX with CDDP did not affect Calcein-AM relative to control. Increased Calcein-AM indicates inhibition of P-gp-mediated drug efflux and decreased retention signifies no effect or stimulation of the transporter's function. In MDA-MB-231 TNBC cells, individual as well as combinations EGFRi, DOX and CDDP had no significant effects on Calcein-AM retention, which likely suggests that these cells do not express P-gp.

5.3 Discussion

Resistance to chemotherapeutic agents in cancer may occur through a number of mechanisms, including reduced uptake and increased efflux of antineoplastic compounds in cancer cells [392,393,396,508,623]. P-gp's function as an efflux pump and its role in drug resistance is well documented [395,396,552]. Some studies have also described a link between EGFR and P-gp and how the cellular activation and phosphorylation of EGFR is associated with the expression and overexpression of P-gp [414]. Interestingly, several TKIs (e.g., imatinib, nilotinib, dasatinib, ponatinib, gefitinib, erlotinib, lapatinib, vandetanib, sunitinib, sorafenib) have been reported to interact with ABC transporters (e.g., ABCB1, ABCC1, ABCG2, ABCC10), and may have dual roles as substrates or inhibitors, depending on the expression of specific pumps, drug concentration, affinity for transporters and types of co-administered agents [483].

Dacomitinib, a second generation, irreversible TKI, for example, has shown positive anticancer activities in some preclinical and clinical trials and antagonizes MDR in cancer cells by inhibiting the efflux activity of ABCB1 and ABCG2 transporters [624]. This effect has also been observed in the present study in that EGFRi alone and in combination with DOX increased Calcein-AM retention in MCF-7 breast carcinoma cells. Therefore, these studies corroborate the tenet of combination therapeutic strategies with TKIs and substrates of ABCB1 and/or ABCG2 transporters in ABCB1- or ABCG2-overexpressing cancers [414].

An earlier study demonstrated that P-gp stability was regulated by the MEK-ERK-RSK pathway which is activated by the EGFR. Signal transduction inhibitor, U0126, successfully blocked the MEK-ERK-RSK pathway and supressed P-gp expression by facilitating its degradation, in *ABCB1* gene transfected MCF-7 MDA-MB-231 TNBC human breast cancer cells [625]. Our findings revealed that the individual treatment of MCF-7 breast carcinoma cells with 100 µM EGFRi resulted in a significant increase in intracellular Calcein-AM retention, thus successfully inhibiting P-gp drug efflux, whereas exposure to concentrations of 1 and 10 µM DOX and decreased Calcein-AM retention, consistent with increased drug efflux. The combinations, however, delivered no enhanced drug accumulation, except for equimolar combinations of EGFRi and DOX at 1 and 10 µM. DOX is a known substrate of the P-gp [626] which explains its ineffectiveness at inhibiting P-gp in the MCF-7 breast carcinoma cells. The individual compounds demonstrated no significant level of Calcein-AM retention in the MDA-MB-231 TNBC cells. This may be attributed to the low levels of the *ABCB1* gene expression detected in our treated samples which encodes the expression of the P-gp (Chapter 6).

Over the past 10 years, there has been renewed efforts in the field of drug discovery and development in identifying more efficient cancer therapeutic mechanisms to overcome drug resistance in cancer. Quercetin a plant derived flavonoid, with antitumor activity has been shown to enhance the cytotoxicity of DOX when used in combination, at the same time reducing the toxicity in non-cancerous and myocardial cells (AC16) as well as downregulating the expression of P-gp, BCRP and MRP1 in MCF-7 and MDA-MB-231 TNBC breast carcinoma cells [535]. The combined treatment of metformin with DOX not only synergistically enhanced the growth inhibitory effect in MCF-7 DOX-resistant cell lines, but also reversed drug resistance in the cells by inhibiting the function of P-gp by reducing ATP production [537,538]. The utilization of nanotechnology for drug delivery in tumor cells is a novel application in breast cancer therapy. Breast cancer treatments using nanocarriers involves the use of polymeric nanomicelles, polymer-conjugates, liposomes, dendrimers and inorganic nanoparticles [627].

The co-delivery of a number of anticancer agents using nucleic acids and chemotherapeutic agents, such as MDR-1 (P-gp) siRNA with DOX in polymers and liposomes and Verapamil and Cycolosporin A with DOX, has been employed to enhance toxic efficacy and overcome drug resistance induced by P-gp in MDA-MB-231 TNBC and MCF-7 and MCF-7Adr/DOX-drug resistant breast cancer cell lines [627]. To date there are no approved drugs available to use clinically to overcome MDR by specifically targeting P-gp [628]. MDR inhibitors have shown success *in vitro*, however, this has not translated clinically particularly due to the side effects of high dosage administration that results in suppressing the immune system and cardiovascular system. Verapamil, an anti-hypertensive agent, and Cyclosporin A for the treatment of rheumatoid arthritis, are amongst the well-known inhibitors of P-gp used clinically [629,630], and have been incorporated in our study as positive controls for P-gp inhibition. Notwithstanding the side effects and limitations associated with MDR inhibitors' reduced affinity and specificity [397], this does not detract from the potential offered by utilizing MDR inhibitors together with chemotherapeutic agents to enhanced their efficacy [628,631].

The use of small molecule ATP binding TKIs offers an alternative to MDR inhibitors. Not only are these molecules highly selective towards their target, but they also present limited to no side effects. The FDA, to date, has approved 48 small molecule protein kinases, 37 of which are used against solid tumors [468]. The most common drug targets for these compounds are EGFR, VEGFR and ALK. Six of the 48 approved drugs, target the EGFR family with the majority of the TKIs approved for the treatment of non-small cell lung cancer (NSCLC) [468]. Due to the homologous active cysteine sites on the different EGFR members, at least 38% of approved TKIs have the ability to cross-react and bind to more than one member extending their therapeutic efficacy [468,632]. In breast cancer, anti-EGFR TKIs, lapatinib, a dual inhibitor of EGFR and HER-2, and neratinib against HER-2, are the only TKIs approved specifically for the treatment of recurrent breast cancer overexpressing HER-2 in combination with capecitabine, and as an extended adjuvant following trastuzumab therapy, respectively [468,633,634].

Following its approval, lapatinib has subsequently been used in a number of studies beyond the spectrum of breast cancer and in different applications [635]. *In vitro* studies have demonstrated that lapatinib synergistically enhanced the cytotoxic effects of DOX in DOX-resistant MCF-7 cells as well as reversed DOX chemoresistance by increasing intracellular drug accumulation of DOX [626]. In esophageal squamous cancer, the combination of paclitaxel and lapatinib resulted in synergistic inhibition of cellular growth [636]. ATP competitive reversible and irreversible TKIs have made a significant contribution towards overcoming MDR in diverse panels of cancers. The combinatorial use of erlotinib with a select antioxidant, demonstrated a decrease in cellular viability in 4 human TNBC cell lines, viz., MDA-MB 468, SUM-149, SUM-159 and HCC-70 [637]. In drug resistant NSCLC cells, PD15303 a potent EGFR inhibitor structurally similar to dacomitinib, significantly reversed ABC transporter ABCG2-mediated drug resistance and synergistically enhanced cytotoxic effects when combined with antineoplastic agents and substrates of ABCG2, mitoxantrone, SN-38 and topotecan [624]. Furthermore, dacomitinib also successfully and significantly reversed drug resistance in the cells mediated by ABCB1 (P-gp) and ABCC1 (MRP1), but not ABCC1 members of the ABC transporter family [624].

In this study, EGFRi successfully and effectively inhibited the EGFR and P-gp function by reducing cell proliferation and survival and increasing intracellular Calcein-AM retention in our drug-treated MCF-7 and MDA-MB-231 TNBC breast carcinoma cells. Our findings suggest that EGFR Inhibitor [Cyclopropanecarboxylic acid-(3-(6-(3-trifluoromethyl-phenylamino)-pyrimidin-4-ylamino)-phenyl-amide (CAS879127-07-8 Calbiochem, Merck KGaA, Darmstadt, Germany) could possibly be classified as an inhibitor of P-gp, however, more tests need to be conducted to confirm the P-gp inhibitory repertoire of EGFR Inhibitor. Not all TKIs confer inhibition of ABC transporters and some TKIs may be classified as inhibitors, substrates, or even both [638]. TKI-associated ABC transporter substrate status may also be linked to drug resistance, the same as any other chemotherapeutic agent (e.g., DOX and paclitaxel), however, in TKI resistance it may be attributed to concentration administration (low dosage, high potential of being ineffective in

inhibition) and can potentially be overcome, as well as selectivity of TKIs for specific ABC transporters [483]. Furthermore, mutations of EGFR (T790M), particularly in NSCLC are quite a common occurrence of intrinsic resistance and render many approved first generation TKIs ineffective as a possible monotherapy strategy [477]. Nevertheless, the progress that has been made to date in the development of newer generations of more effective TKIs and the option to combine them with different classes of clinically approved antineoplastic agents still offers a better and more effective therapeutic treatment option with higher efficacy and little to no side effects. Thus, the clinical administration of TKIs needs to be considered only after molecular assessment and P-gp status of such TKIs and any common mutations in the EGFR has been detected.

The development of resistance to TKI therapy is a common occurrence and is a result of EGFR mutations, the overexpression and amplification of certain proteins (ABC transporters), receptors or genes [487]. Mutations in the EGFR kinase domain, is more prevalent in NSCLC. First generation TKIs, gefitinib and erlotinib were developed for the treatment of NSCLC associated with EGFR mutations in exon-19 and 21 L858R. This was shortly followed by the development of drug resistance in NSCLC due to an exon 20 T790M mutation in EGFR induced by TKI treatment [487]. In breast cancer, the most common mutation resulting in TKI resistance is that of the ERBB2 (HER-2), which renders lapatinib treatment ineffective in patient samples containing this mutation [468]. Other mechanisms involved in TKI resistance in cancer include compensatory pathways that involve RTK such as HER3, c-MET (hepatocyte growth factor receptor) and AXL and DNA repair pathways [483,487,639]. Our individual EGFRi and DOX, as well as combinations of drug treatments, demonstrated significant downregulation of the EGFR gene in both MCF-7 and MDA-MB-231 TNBC breast carcinoma cells (presented in Chapter 6). Our findings suggest that the combinatorial use of the EGFRi with DOX and CDDP has the potential as a therapeutic treatment strategy to enhance the level of growth inhibition and reverse the MDR phenotype in many cancers.

CHAPTER 6

RESULTS AND DISCUSSION OF RT-QPCR GENE EXPRESSION ANALYSIS OF EGFR AND ABCB1

6.1 Introduction

This chapter covers the gene expression profiles of *ABCB1* and *EGFR* that encode for the expression of P-gp and EGFR, respectively, as assessed using Real-Time qPCR (Chapter 2, Section 2.9) following 48h treatment of MCF-7 and MDA-MB-231 TNBC breast carcinoma cells with a series of single and pairwise equimolar drug combinations, as indicated.

6.2 RT-qPCR *EGFR* and *ABCB1* Gene Expression Analysis

Primer sequences for the two target genes, i.e., *EGFR1* and *ABCB1* (P-gp) and the five housekeeping (reference) genes are shown in Table 6.1. The reference genes selected were reported to be optimal for normalization in breast tumor and normal tissues [640]. All qPCR assays revealed amplification of a single amplicon as shown by single melting temperature peaks on melting curves (Figure 6.1 and Figure 6.2) and single PCR products of expected size on agarose gels (Figure 6.3).

No non-specific primer dimer binding was detected which illustrates the high specificity of the primer pairs. The 125 bp and 105 bp primers yielded efficiencies within the normal range for the *EGFR* and *ABCB1* genes, respectively. These primer sets were selected for the subsequent expression analysis. Expression of *EGFR* could be detected in both MCF-7 and MDA-MB-231 breast cancer cell samples with Ct (cycle threshold) values within the dynamic range of the standard curve (Figure 6.3).

Table 6.1: Primer sequences for the two target genes and the five housekeeping (reference) genes

Gene Symbol	Primer Name	Primer Sequence (5' 3')	Amplicon Size	Sources
ABCB1	abcb1F1	TTG CTG CTT ACA TTC AGG TTT CA	105 bp	[641]
	abcb1R1	AGC CTA TCT CCT GTC GCA TTA		
	abcb1F2	GCC TGG CAG CTG GAA GAC AAA TAC	253 bp	[642]
	abcb1R2	ATG GCC AAA ATC ACA AGG GTT AGC		
EGFR1	egfrF1	TCC CTC AGC CAC CCA TAT GTA C	125 bp	[643]
	egfrR1	GTC TCG GGC CAT TTT GGA GAA TTC		
	egfrF2	ATA GTC GCC CAA AGT TCC GTG AGT	166 bp	[644]
	egfrR2	ACC ACG TCG TCC ATG TCT TCT TCA		
18S rRNA	18SrRNA-F	GGA TGT AAA GGA TGG AAA ATA CA	72 bp	[640]
	18SrRNA-R	TCC AGG TCT TCA CGG AGC TTG TT		
ACTB	ACTBF	TGA CGT GGA CAT CCG CAA AG	205 bp	[640]
	ACTBR	CTG GAA GGT GGA CAG CGA GG		
GADPH	GAPDH-F	GAC AGT CAG CCG CAT CTT CT	127 bp	[640]
	GAPDH-R	TTA AAA GCA GCC CTG GTG AC		
HPRT1	HPRT1F	GAC CAG TCA ACA GGG GAC AT	132 bp	[640]
	HPRT1R	CCT GAC CAA GGA AAG CAA AG		
HSPCB	HSPCBF	TCT GGG TAT CGG AAA GCA AGC C	80 bp	[645]
	HSPCBR	GTG CAC TTC CTC AGG CAT CTT G		

ABCB1: P-glycoprotein (*MDR1*); *EGFR1*: Epidermal growth factor receptor-1; *ACTB*: ß-actin; *GADPH*: Glyceraldehyde 3 phosphate dehydrogenase 1; *HPRT1*: Hypoxanthine phosphoribosyl-transferase 1; *HSPCB*: Heat shock protein 90 family

6.3 Effects of EGFRi, DOX and CDDP on the Expression of *EGFR* in MCF-7 and MDA-MB-231 TNBC Breast Carcinoma Cells

EGFRi and DOX were the most effective of the three single drugs ($p<0.001$) in downregulating EGFR gene expression, in both MCF-7 (Figure 6.4, *top panel*) and MDA-MB-231 TNBC (Figure 6.4, *bottom panel*) breast carcinoma cells. CDDP did not perturb *EGFR* expression in MCF-7 breast carcinoma cells, but significantly decreased the RTK's expression in MDA-MB-231 TNBC cells.

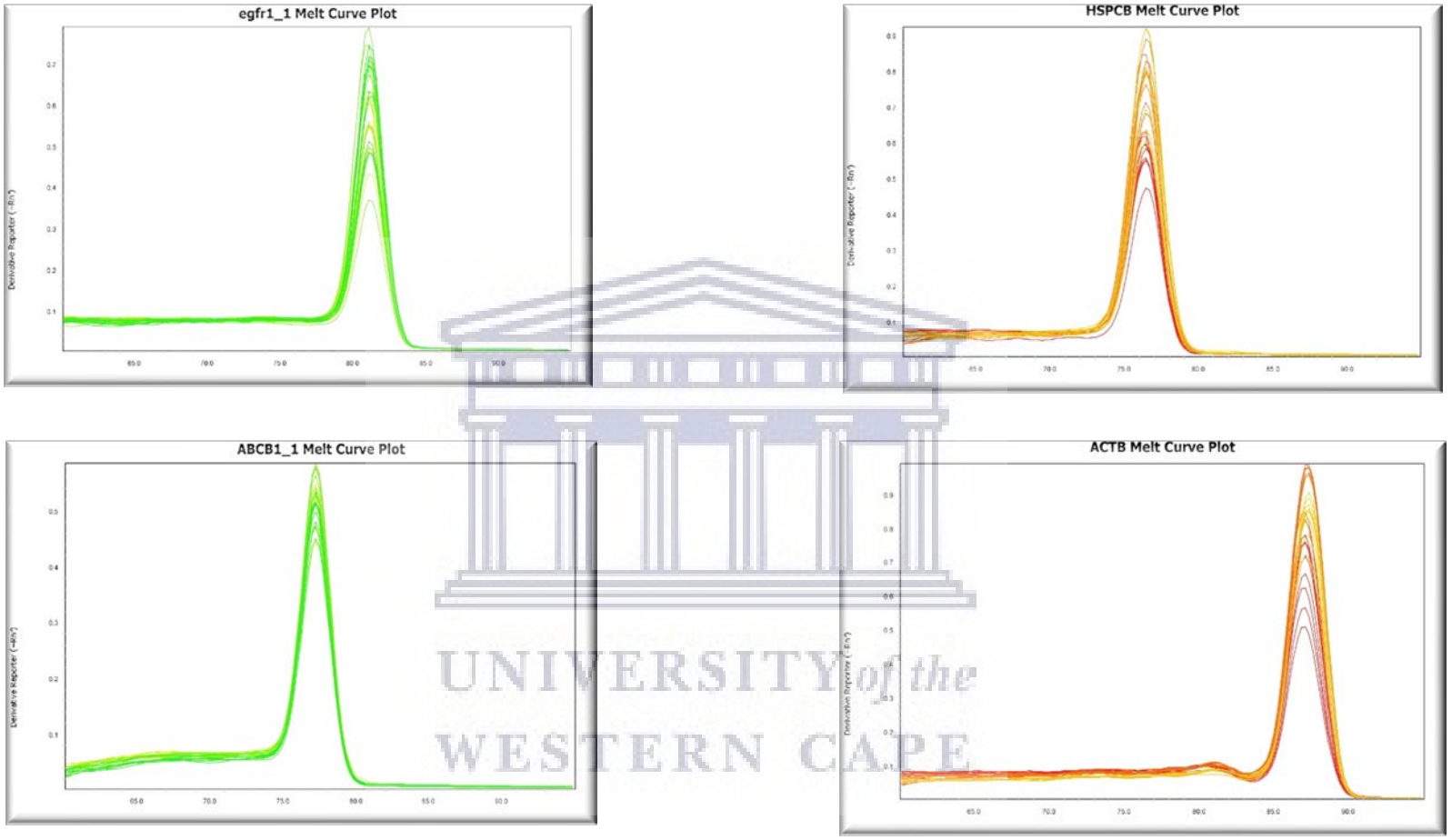

Figure 6.1: Melt curves of qPCR assays for *EGFR1*, *HSPCB*, *ABCB1* and *ACTB*. Single peaks on the melt curve analysis for the target and reference genes, indicate a single amplicon in each assay. The single melting curve describe the specificity of each primer pair.

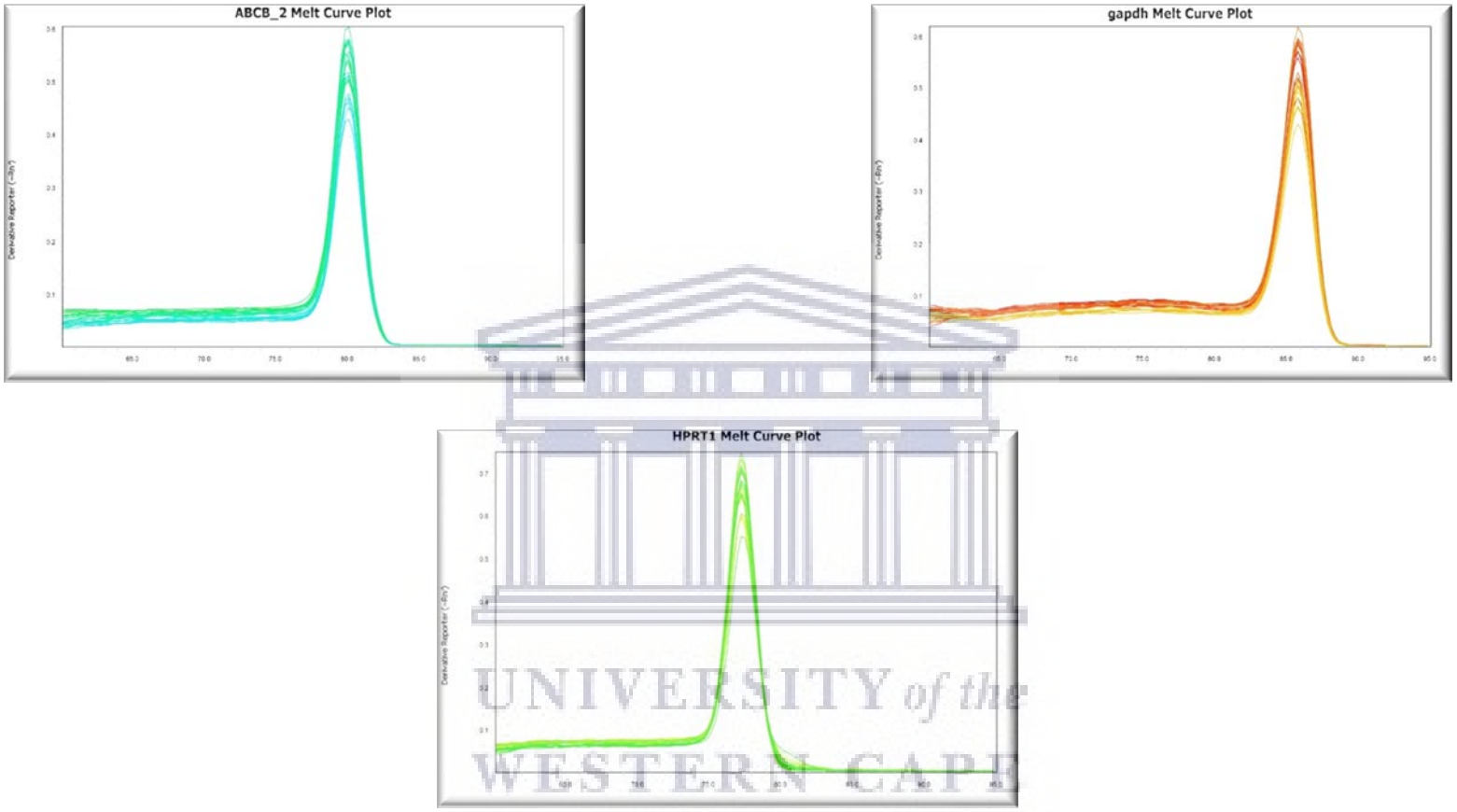

Figure 6.2: Melt curves of qPCR assays for *ABCB2*, *GAPDH* and *HPRT1*. Single peaks on the melt curve analysis for the target and reference genes, indicate a single amplicon in each assay. The single melting curve describe the specificity of each primer pair (continued).

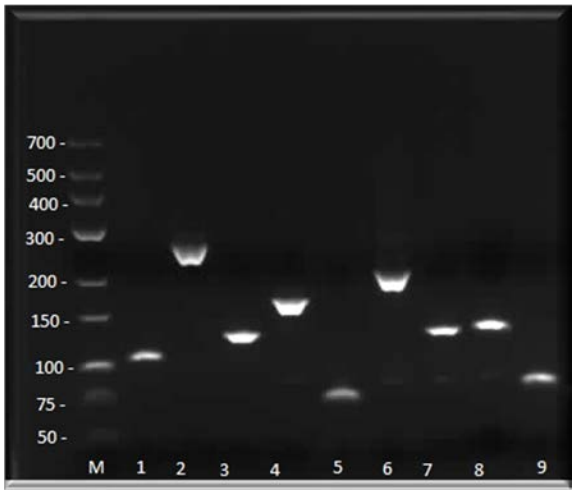

Figure 6.3: The various qPCR assays in 4% agarose gels confirms the presence of a single fragment of the expected size. **Lane M**: molecular weight marker (sizes are shown on the left); **Lane 1**: *ABCB1* (105 bp); **Lane 2**: *ABCB1* (253 bp); **Lane 3**: *EGFR1* (125 bp); **Lane 4**: *EGFR1* (166 bp); **Lane 5**: 18S rRNA (72 bp); **Lane 6**: *ACTB* (205 bp); **Lane 7**: *GAPDH* (127 bp); **Lane 8**: *HPRT1* (132 bp) and **Lane 9**: HSPCB (80 bp).

Except for the DOX + CDDP combination at 0.1 µM in MDA-MB-231 TNBC cells, the expression of *EGFR* was significantly ($p<0.001$ in all cases,) downregulated by 1:1 concentration ratiometric combinations of EGFRi + DOX, EGFRi + CDDP and DOX + CDDP in both MCF-7 and MDA-MB-231 TNBC breast carcinoma cells (Figure 6.5). These findings correlate with the level of growth inhibition for different cell lines, described in Chapter 3.

6.3 Discussion

In MCF-7 and MDA-MB-231 TNBC breast carcinoma cells, the combinations of EGFRi + DOX and DOX + CDDP had the most profound effects in downregulating the expression of the *EGFR* gene, in both cell lines. EGFRi in combination with DOX offers a better option to be used as therapeutic choice, considering the side effects associated with DOX [524,528,530-532] and CDDP [615].

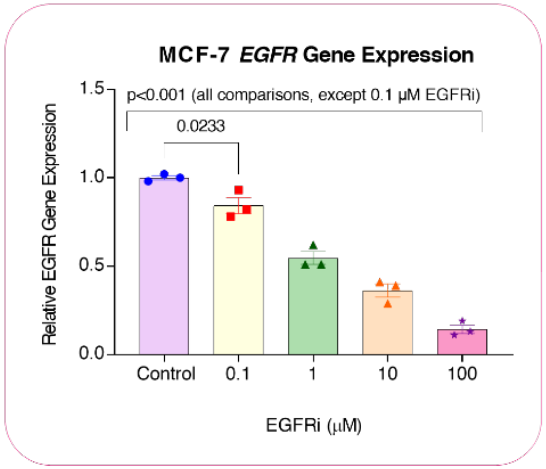

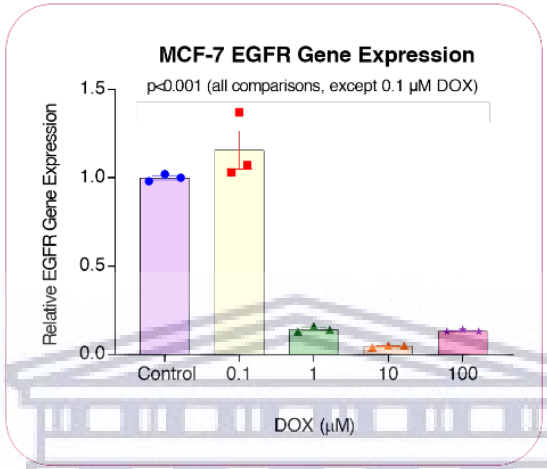

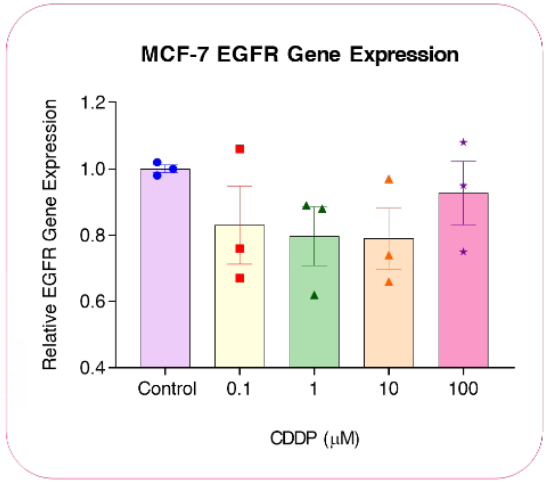

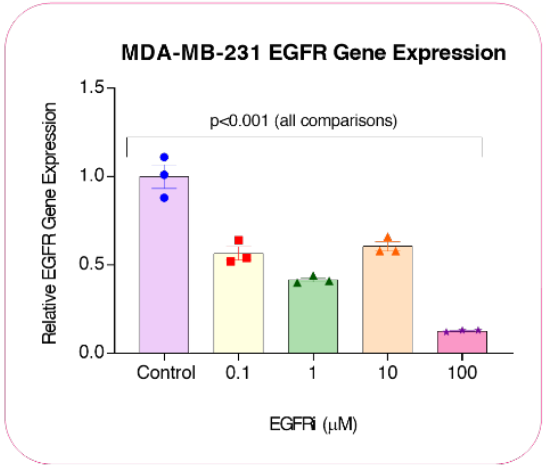

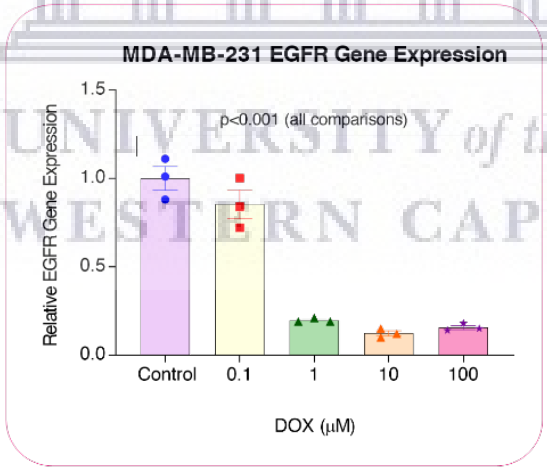

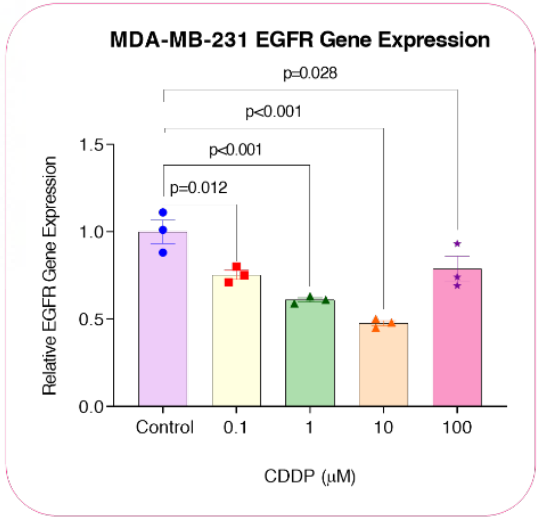

Figure 6.4: Effects of 48h single-agent EGFRi, DOX and CDDP treatments on the expression levels of the *EGFR* gene in MCF-7 (top panel) and MDA-MB-231 TNBC (bottom panel) breast carcinoma cells. All data are representative of at least three independent experiments and are presented as means ± SEM (n=3) for cells treated with single agent drugs as indicated. One-way ANOVA analysis was also used to determine significant differences among treatments compared with their respective untreated controls), followed by a Dunnett's *post hoc* test to compare all pairs of data sets. Data were considered statistically significant when $p<0.05$.

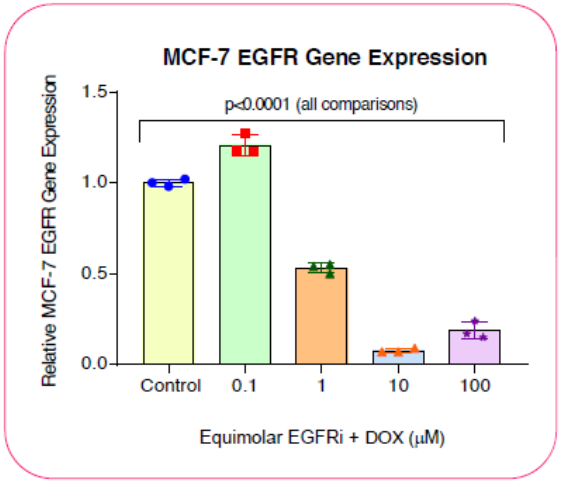

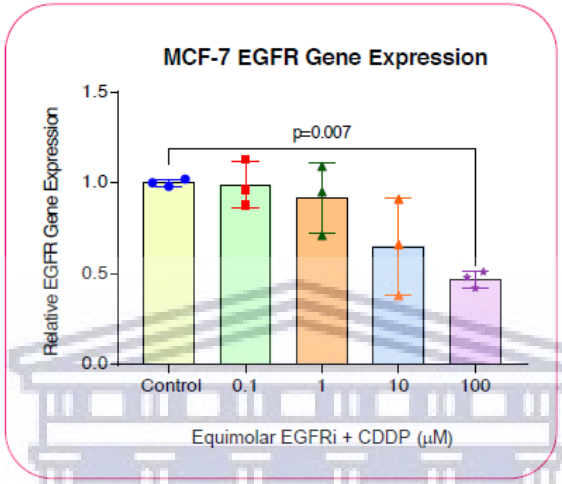

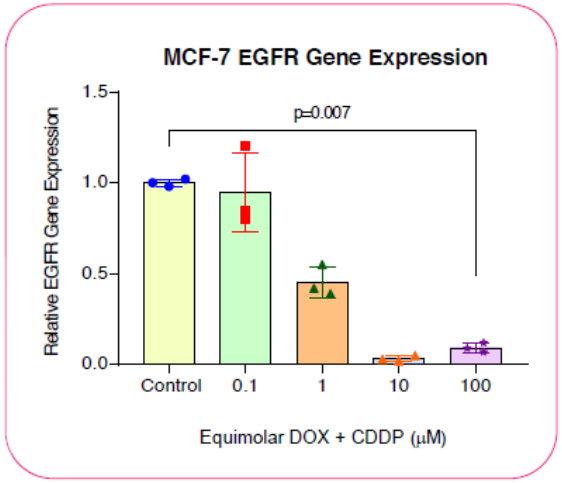

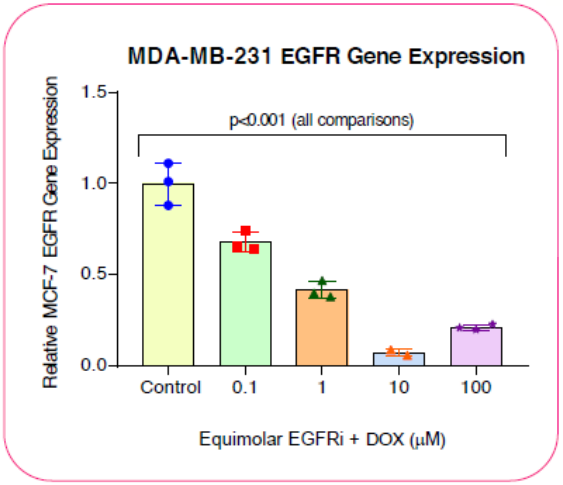

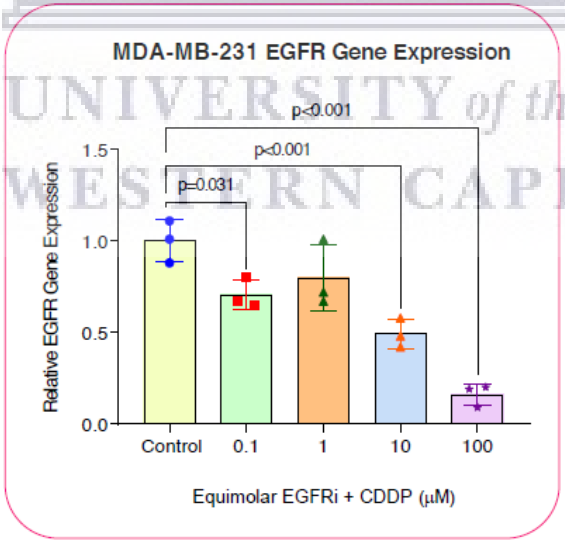

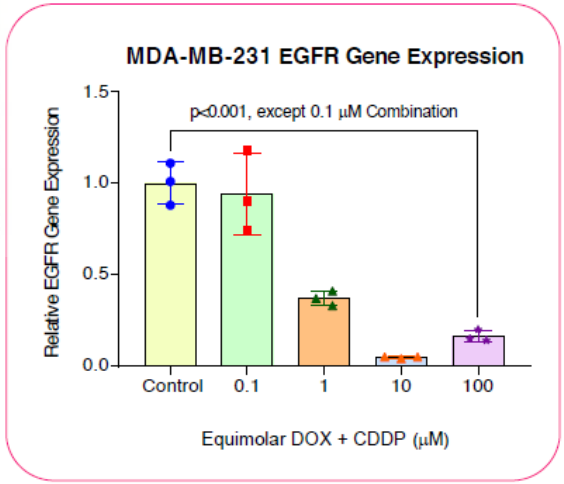

Figure 6.5: Effects of 48h pairwise EGFRi, DOX and CDDP treatments on the expression levels of the *EGFR* gene in MCF-7 (top panel) and MDA-MB-231 TNBC (bottom panel) breast carcinoma cells. All data are representative of at least three independent experiments and are presented as means ± SEM (n=3) for cells treated with single agent drugs as indicated. One-way ANOVA analysis was also used to determine significant differences among treatments compared with their respective untreated controls), followed by a Dunnett's post hoc test to compare all pairs of data sets. Data were considered statistically significant when $p<0.05$.

The expression of the *ABCB1* gene, however, was either undetectable in diluted samples of both MCF-7 and MDA-MB-231 TNBC breast carcinoma cells, or resulted in Ct values > 35 which was outside of the dynamic range of the qPCR assay, even after cDNA pre-amplification was employed to assist with the insufficient number of copies of *ABCB1* gene expression. Furthermore, the use of higher concentrations of sample had no response. In the majority of samples, no expression of the *ABCB1* gene was observed and, if there was any, there was a huge variation within replicates of the same experiment. These observations suggest that the *ABCB1* gene might be expressed at undetectable levels within these cells.

However, transcription factors such as CEBPb have been shown to play a role in the activation or repression of the endogenous, chromosomally embedded *ABCB1 (MDR1, P-gp)* gene in MCF-7 breast cancer cell lines [646]. In both MCF-7 and MDA-MB-231 TNBC breast cancer cells, enhanced intracellular calcium mobilized from endoplasmic reticulum stores led to hypertonic stress which induced P-gp expression-mediated paclitaxel drug resistance in these breast cancer cells [647]. Likewise, elevated ROS, i.e., oxidative stress, was found to be the underlying mechanism contributing to P-gp overexpression induced by DOX in MCF-7 breast carcinoma cells [648].

It is therefore likely that in our system, *ABCB1* expression in MCF-7 and MDA-MB-231 TNBC breast carcinoma cells would have been detected had we sustained the selection pressure of the cytotoxic agents for longer than 48h. Also, low or non-P-gp expressing drug-sensitive MCF-7 breast carcinoma cells can become resistant by an additional mechanism involving a non-genomic acquisition of functional P-glycoproteins transmitted by donor cells in the medium [649,650]. Furthermore, several studies have correlated the clinical impact of *ABCB1* polymorphisms in breast

cancer treatment outcomes such as therapeutic response, chemotoxicity, and overall survival [424,651,652]. Therefore, evaluation of the effects of *ABCB1* polymorphisms on the outcome of breast cancer treatment is an important paradigm for tailoring individualized anticancer therapy.

CHAPTER 7

FINAL PERSPECTIVES

7.1 Introduction

According to GLOBOCAN estimates of incidence and mortality worldwide for 36 cancers in 185 countries, an estimated 2.1 million women were newly diagnosed with breast cancer (BC) in 2018 [78,80]. BC is also the leading cause of cancer in sub-Saharan Africa [83,653]. BC can be described as a highly heterogeneous group of diseases in terms of histology and clinical behavior and can be classified into 3 basic types based on their immunohistochemical properties (hormone status). They are HR^+, human epidermal growth factor receptor 2 positive ($HER2^+$), and triple-negative breast cancers (TNBC) [146]. HR^+-positive BCs are estrogen receptor (ER) and progesterone receptor (PR) positive. Approximately 85% of all breast cancers are HR^+.

TNBC, a subtype of BC, comprises 10–15% of all BCs and is distinguished by the absence of ER, PR, as well as HER2 [32,200]. TNBC is correlated with extreme aggressiveness and poor prognosis and remains the most difficult BC subtype to treat, presumably because it lacks effective endocrine therapy and molecular targeted therapy compared to other BC subtypes [111,147,654]. The major global challenge in BC continues to be the search for new therapeutic modalities and personalized medicines to cover the enormous spectrum of genetic signatures and hallmarks that present obstacles to BC prevention and eradication [113]. This chapter will briefly explore the significance of the study findings and prospects for further research.

7.2 Context and Significance of the Research

In this study, we have used two BC cell lines, the ER^+ MCF-7 breast carcinoma cell line [589-592] and the TNBC MDA-MB-231 cell line [593-596]. The MCF-7 cell line is named after the Michigan Cancer Foundation and represents Herbert D. Soule's 7th attempt to establish a cell line from a patient who underwent a mastectomy for an adenocarcinoma in her left breast [655]. Despite some limitations, the MCF-7 cell line expresses significant levels of ER and serves as a model of many invasive human breast cancers [589,590,656,657].

Likewise, the MDA-MB-231 TNBC cell line was established from a pleural effusion obtained from a 51-year-old woman who had had a right radical mastectomy in January 1969 for a poorly differentiated tumor tending toward papillary configuration and tubule formation. This patient also had an intraductal carcinoma. A pericardial effusion and a left pleural effusion appeared in June and July 1973, respectively, and both contained malignant cells compatible with a primary tumor of the breast [593]. Therefore, these prototype cell lines provide contextual relevance in researching breast cancer pathology and drug development [597].

Breast cancer is a multifaceted disease, with heterogeneous biological tumor subtypes and disparate responses to modern first-line treatment options which still overshadow the progress made in our understanding and practice to prevent and improve survival outcomes [82,123,147,150,152,196,210,238]. In recent years, a new paradigm in cancer treatment known as "adaptive therapy" has been advanced to maintain a controllable stable tumor burden by allowing a significant population of treatment-sensitive cells to survive [368]. Adaptive therapy is based on the tenet of competitive interactions between drug-sensitive and drug-resistant subclones [658-660].

In accordance with the hallmarks of cancer reviewed in Chapter 1 (Section A.1), tumor cell resistance may confer some fitness costs due to increased rates of DNA repair or other costly metabolic activities (e.g., ATP hydrolysis) required by ABC transporters to pump toxic drugs across cell membranes (Chapter 1, Section B.1) [329]. Cancer cell resistance mechanisms, whether mitigation, detoxification, or re-routing metabolic pathways, divert finite resources that would otherwise be available for normal cell proliferation or other avenues for cell survival and homeostasis [368,661]. Such evolutionary cancer modeling of adaptive therapies have been piloted and are currently being evaluated in several clinical trials for *EGFR*-mutant NSCLC [662,663], metastatic castrate-resistant prostate cancer [664] and metastatic breast cancer (MBC) [241,665].

Notwithstanding, the high initial efficacy of targeted therapies ultimately fail in advanced stage tumors that have developed resistance resulting in relapse. Our understanding of how resistance evolves pales in comparison to the substantial corpus of research on the molecular mechanisms of resistance (Chapter 1, Section B). In NSCLC, e.g., resistance can originate from heterogeneous, weakly resistant subpopulations of cells with variable sensitivity to different ALK inhibitors (recall that ALK is also a member of the receptor tyrosine kinase (RTK) family, as is EGFR; cf. Chapter 1, Section C).

Resistance to TKIs, or ALK inhibitors in this case, involves gradual, multifactorial adaptation to the inhibitors via acquisition of multiple cooperating genetic and epigenetic modifications. Such adaptation of tumor cells might present unique, temporally restricted collateral sensitivities, absent in therapy naïve or fully resistant cells, implying the potential for new therapeutic interventions, directed against evolving resistance [241,658-660,662-666].

Cancer cells upregulate P-gp expression as an adaptive response to evade chemotherapy-mediated cytotoxic onslaught or cell death [552]. While several P-gp inhibitors have been described, very few have successfully passed all phases of clinical trials. Studies show that application of P-gp inhibitors in cancer therapy regimens following development of MDR achieved limited beneficial outcomes. Moreover, the non-specific substrate binding of certain compounds to P-gp has made the drug-design landscape a major challenge [392,413,534,552,628,667-670].

The epidermal growth factor receptor (EGFR) is a member of the ERBB family of RTKs that plays pivotal roles in tumor cell survival and proliferation [452,487,490,507]. Since EGFR is frequently overexpressed in TNBC (>50%), it is a recognized biomarker and therapeutic target in breast cancer [162,200,671-674]. The ABC transporters are important mediators of the general ADME-Tox (absorption, distribution, metabolism, excretion, toxicity) properties of small molecule TKIs, as well as key regulators of resistance against targeted anticancer therapeutics [431,432,454,483,509-516]. ABCG2 and ABCB1 bind avidly to TKIs such as imatinib, nilotinib and dasatinib, thus modulating resistance to TKIs which stimulate ATP degradation and drug efflux [516,517].

Thus, combined MDR-ABC transporter and TKI effect targeting offers a major advantage in future drug development programs [414,675,676]. Combination therapy is central to modern medicine and provides the basis for selection of drug treatment of cancer [290,323,677]. In TNBC, an aggressive type of BC representing 15% of BC with limited treatment options [678], e.g., high throughput screening (HTS) of TNBC cell lines uncovered that overexpression of the *MYCN* oncogene was associated with increased sensitivity to BET inhibitors. The combination of BET and MEK inhibitors synergistically decreased tumor cell viability in MYCN-expressing TNBC cells and

patient-derived xenograft models [666,679]. This corroborates the proof-of-concept that carefully selected combination of therapeutic interventions affords patients with the prospect of maximum benefit from therapy while minimizing or eliminating recurrence, resistance and toxic adverse effects, as well as ensuring that patients enjoy a good quality of life [352].

Quantitative models of drug–drug interactions are also indispensable for judiciously navigating drug combination discovery and translation in the treatment of complex, multifactorial diseases [350,561]. Multiagent therapies, due to their ability to delay or overcome resistance or induce collateral sensitivity (Section A.4.6.1), are a hallmark of treatment in multiple myeloma (MM). The expanding number of therapeutic options in MM requires high-throughput combination screening tools to better allocate treatment, and facilitate personalized therapy [680]. Several drug-combination analysis websites and data portals have recently been introduced to mine huge amounts of pharmacological data with the aim of improving current combination chemotherapy strategies [348,561,582,584,588,677,681-687].

Clearly, the approach used in this study encompassed all the above elements for a guided translational approach to combining conventional anticancer drugs with TKIs for more efficacious treatment regimens that will minimize adverse events, overcome drug resistance and render useful future clinical paradigms. The research also offers new vistas for additional studies, including analysis of various drug combinations in relation to other ABC transporters, e.g., ABCG2 [688], and other members of the EGFR family commonly overexpressed in breast tumors, viz., ERBB2 (HER2), ERBB3 (HER3) and ERBB4 (HER4) (Section C.2). The results reported in this thesis will be published in accredited peer-reviewed journals.

7.3 Funding Disclosure

- This work is based on the research supported wholly by the National Research Foundation of South Africa (Grant Number: 114600).

- Financial support of the University of the Western Cape, the University of the Free State and the Ackerman Family Educational Trust is gratefully acknowledged.

- The British Council Newton Fund – generously sponsored Beynon Abrahams' 4-week visit to the Department of Pharmaceutical and Environmental Sciences at the University of Greenwich, Dublin, Ireland.

REFERENCES

1. Steward W, Thomas A. The burden of cancer. In: Pelengaris S, Khan M, eds. *The Molecular Biology of Cancer*. Oxford: Blackwell Publishing; 2006:36-60.

2. American Cancer Society. Cancer Facts & Figures 2019. Atlanta, 2019.

3. Lukong KE. Understanding breast cancer - the long and winding road. *BBA Clinical* 2017;7:64-77.

4. Costa R, Shah AN, Santa-Maria CA, Cruz MR, Mahalingam D, Carneiro BA, Chae YK, Cristofanilli M, Gradishar WJ, Giles FJ. Targeting epidermal growth factor receptor in triple negative breast cancer: New discoveries and practical insights for drug development. *Cancer Treatment Reviews* 2017;53:111-119.

5. Bayraktar S, Gluck S. Molecularly targeted therapies for metastatic triple-negative breast cancer. *Breast Cancer Research and Treatment* 2013;138(1):21-35.

6. Garrido-Castro AC, Lin NU, Polyak K. Insights into molecular classifications of triple-negative breast cancer: Improving patient selection for treatment. *Cancer Discovery* 2019;9(2):176-198.

7. Al-Mahmood S, Sapiezynski J, Garbuzenko OB, Minko T. Metastatic and triple-negative breast cancer: Challenges and treatment options. *Drug Delivery and Translational Research* 2018;8(5):1483-1507.

8. Hanahan D, Weinberg RA. The hallmarks of cancer. *Cell* 2000;100(1):57-70.

9. Hanahan D, Weinberg RA. Hallmarks of cancer: The next generation. *Cell* 2011;144(5):646-674.

10. Fares J, Fares MY, Khachfe HH, Salhab HA, Fares Y. Molecular principles of metastasis: A hallmark of cancer revisited. *Signal Transduction and Targeted Therapy* 2020;5:28.

11. Fouad YA, Aanei C. Revisiting the hallmarks of cancer. *American Journal of Cancer Research* 2017;7(5):1016-1036.

12. Das CK, Banerjee I, Mandal M. Pro-survival autophagy: An emerging candidate of tumor progression through maintaining hallmarks of cancer. *Seminars in Cancer Biology* 2019.

13. Brouxhon SM, Kyrkanides S, Teng X, Athar M, Ghazizadeh S, Simon M, O'Banion MK, Ma L. Soluble E-cadherin: A critical oncogene modulating receptor tyrosine kinases, MAPK and PI3K/Akt/mTOR signaling. *Oncogene* 2014;33(2):225-235.

14. Yasmeen A, Bismar TA, Al Moustafa AE. ErbB receptors and epithelial-cadherin-catenin complex in human carcinomas. *Future Oncology* 2006;2(6):765-781.

15. Kawaguchi T. Organ preference of cancer metastasis and metastasis-related cell adhesion molecules including carbohydrates. *Cardiovascular & Hematological Disorders-Drug Targets* 2016;15(3):164-186.

16. Caon I, Bartolini B, Parnigoni A, Carava E, Moretto P, Viola M, Karousou E, Vigetti D, Passi A. Revisiting the hallmarks of cancer: The role of hyaluronan. *Seminars in Cancer Biology* 2019.

17. Cree IA, Charlton P. Molecular chess? Hallmarks of anti-cancer drug resistance. *BMC Cancer* 2017;17(1):10.

18. Singh SS, Vats S, Chia AY, Tan TZ, Deng S, Ong MS, Arfuso F, Yap CT, Goh BC, Sethi G, Huang RY, Shen HM, Manjithaya R, Kumar AP. Dual role of autophagy in hallmarks of cancer. *Oncogene* 2018;37(9):1142-1158.

19. De Palma M, Hanahan D. The biology of personalized cancer medicine: Facing individual complexities underlying hallmark capabilities. *Molecular Oncology* 2012;6(2):111-127.

20. Iannuccelli M, Micarelli E, Surdo PL, Palma A, Perfetto L, Rozzo I, Castagnoli L, Licata L, Cesareni G. Cancergenenet: Linking driver genes to cancer hallmarks. *Nucleic Acids Research* 2020;48(D1):D416-D421.

21. Yu LH, Huang QW, Zhou XH. Identification of cancer hallmarks based on the gene co-expression networks of seven cancers. *Frontiers in Genetics* 2019;10:99.

22. Souho T, Lamboni L, Xiao L, Yang G. Cancer hallmarks and malignancy features: Gateway for improved targeted drug delivery. *Biotechnology Advances* 2018;36(7):1928-1945.

23. Moses C, Garcia-Bloj B, Harvey AR, Blancafort P. Hallmarks of cancer: The CRISPR generation. *European Journal of Cancer* 2018;93:10-18.

24. Negrini S, Gorgoulis VG, Halazonetis TD. Genomic instability — an evolving hallmark of cancer. *Nature Reviews Molecular Cell Biology* 2010;11(3):220-228.

25. Luo J, Solimini NL, Elledge SJ. Principles of cancer therapy: Oncogene and non-oncogene addiction. *Cell* 2009;136(5):823-837.

26. Kroemer G, Pouyssegur J. Tumor cell metabolism: Cancer's Achilles' heel. *Cancer Cell* 2008;13(6):472-482.

27. Vaklavas C, Blume SW, Grizzle WE. Hallmarks and determinants of oncogenic translation revealed by ribosome profiling in models of breast cancer. *Translational Oncology* 2020;13(2):452-470.

28. Dai X, Hua T, Hong T. Integrated diagnostic network construction reveals a 4-gene panel and 5 cancer hallmarks driving breast cancer heterogeneity. *Scientific Reports* 2017;7(1):6827.

29. Singh M, Mukundan S, Jaramillo M, Oesterreich S, Sant S. Three-dimensional breast cancer models mimic hallmarks of size-induced tumor progression. *Cancer Research* 2016;76(13):3732-3743.

30. Dai X, Xiang L, Li T, Bai Z. Cancer hallmarks, biomarkers and breast cancer molecular subtypes. *Journal of Cancer* 2016;7(10):1281-1294.

31. Campoy EM, Laurito SR, Branham MT, Urrutia G, Mathison A, Gago F, Orozco J, Urrutia R, Mayorga LS, Roque M. Asymmetric cancer hallmarks in breast tumors on different sides of the body. *PloS One* 2016;11(7):e0157416.

32. Bernardi R, Gianni L. Hallmarks of triple negative breast cancer emerging at last? *Cell Research* 2014;24(8):904-905.

33. Jansen MP, Knijnenburg T, Reijm EA, Simon I, Kerkhoven R, Droog M, Velds A, van Laere S, Dirix L, Alexi X, Foekens JA, Wessels L, Linn SC, Berns EM, Zwart W. Hallmarks of aromatase inhibitor drug resistance revealed by epigenetic profiling in breast cancer. *Cancer Research* 2013;73(22):6632-6641.

34. Tian S, Roepman P, Van't Veer LJ, Bernards R, de Snoo F, Glas AM. Biological functions of the genes in the mammaprint breast cancer profile reflect the hallmarks of cancer. *Biomarker Insights* 2010;5:129-138.

35. Sledge GW, Jr., Miller KD. Exploiting the hallmarks of cancer: The future conquest of breast cancer. *European Journal of Cancer* 2003;39(12):1668-1675.

36. Doll R. The prevention of cancer: Pointers from epidemiology (e-Book). New York: Routledge; 2017.

37. Siegel RL, Miller KD, Jemal A. Cancer statistics, 2020. *CA: A Cancer Journal for Clinicians* 2020;70(1):7-30.

38. DeSantis CE, Ma J, Gaudet MM, Newman LA, Miller KD, Goding Sauer A, Jemal A, Siegel RL. Breast cancer statistics, 2019. *CA: A Cancer Journal for Clinicians* 2019;69(6):438-451.

39. Ahmad A. Breast cancer statistics: Recent trends. In: Ahmad A, ed. *Breast cancer metastasis and drug resistance*. Cham: Springer; 2019;1152:1-7.

40. Doll R, Peto R. The causes of cancer: Quantitative estimates of avoidable risks of cancer in the United States today. *JNCI: Journal of the National Cancer Institute* 1981;66(6):1192-1308.

41. World Health Organization Expert Committee on the Prevention of Cancer. Prevention of cancer. Report of a WHO expert committee. No. 276, 1964.

42. Tafani M, Russo A, Vito MD, Sale P, Pellegrini L, Schito L, Gentileschi S, Bracaglia R, Marandino F, Garaci E, Russo MA. Up-regulation of pro-inflammatory genes as adaptation to hypoxia in MCF-7 cells and in human mammary invasive carcinoma microenvironment. *Cancer Science* 2010;101(4):1014-1023.

43. Mittal S, Brown NJ, Holen I. The breast tumor microenvironment: Role in cancer development, progression and response to therapy. *Expert Review of Molecular Diagnostics* 2018;18(3):227-243.

44. Deshmukh SK, Srivastava SK, Poosarla T, Dyess DL, Holliday NP, Singh AP, Singh S. Inflammation, immunosuppressive microenvironment and breast cancer: Opportunities for cancer prevention and therapy. *Annals of Translational Medicine* 2019;7(20):593.

45. De Luca A, Carotenuto A, Rachiglio A, Gallo M, Maiello MR, Aldinucci D, Pinto A, Normanno N. The role of the EGFR signaling in tumor microenvironment. *Journal of Cellular Physiology* 2008;214(3):559-567.

46. Bhat V, Allan AL, Raouf A. Role of the microenvironment in regulating normal and cancer stem cell activity: Implications for breast cancer progression and therapy response. *Cancers (Basel)* 2019;11(9).

47. Colditz GA, Sellers TA, Trapido E. Epidemiology — identifying the causes and preventability of cancer? *Nature Reviews Cancer* 2006;6(1):75-83.

48. Yin J, Wu X, Li S, Li C, Guo Z. Impact of environmental factors on gastric cancer: A review of the scientific evidence, human prevention and adaptation. *Journal of Environmental Sciences* 2020;89:65-79.

49. Thoonen K, Osch LV, Vries H, Jongen S, Schneider F. Are environmental interventions targeting skin cancer prevention among children and adolescents effective? A systematic review. *International Journal of Environmental Research and Public Health* 2020;17(2).

50. Sundstrom K, Elfstrom KM. Advances in cervical cancer prevention: Efficacy, effectiveness, elimination? *PLos Medicine* 2020;17(1):e1003035.

51. Klein W, Rothman AJ, Suls J. Bridging behavioral science with cancer prevention and control: Contributions of an NCI working group (2009-2019). *Cancer Prevention Research* 2020.

52. Torre LA, Islami F, Siegel RL, Ward EM, Jemal A. Global cancer in women: Burden and trends. *Cancer Epidemiology Biomarkers & Prevention* 2017;26(4):444-457.

53. Xiao R, Pham Y, Ward MC, Houston N, Reddy CA, Joshi NP, Greskovich JF, Jr., Woody NM, Chute DJ, Lamarre ED, Prendes BL, Lorenz RR, Scharpf J, Burkey BB, Geiger JL, Adelstein DJ, Koyfman SA. Impact of active smoking on outcomes in HPV+ oropharyngeal cancer. *Head & Neck* 2020;42(2):269-280.

54. Ruano-Ravina A, Provencio-Pulla M, Fernandez-Villar JA. Promotion of anti-smoking strategies as the most effective and efficient way to reduce lung cancer (and other diseases). *Archivos de Bronconeumología* 2020;56(5):339.

55. Lipfert FW, Wyzga RE. Longitudinal relationships between lung cancer mortality rates, smoking, and ambient air quality: A comprehensive review and analysis. *Critical Reviews in Toxicology* 2019;49(9):790-818.

56. Kirby T. Reducing stigma around smoking would encourage more early lung cancer screening. *Lancet Respiratory Medicine* 2020;8(2):140.

57. Gram IT, Park SY, Wilkens LR, Haiman CA, Le Marchand L. Smoking and risk of colorectal cancer may differ by anatomical subsite and sex. *American Journal of Epidemiology* 2020.

58. Balata H, Traverse-Healy L, Blandin-Knight S, Armitage C, Barber P, Colligan D, Elton P, Kirwan M, Lyons J, McWilliams L, Novasio J, Sharman A, Slevin K, Taylor S, Tonge J, Waplington S, Yorke J, Evison M, Booton R, Crosbie PAJ. Attending community-based lung cancer screening influences smoking behaviour in deprived populations. *Lung Cancer* 2020;139:41-46.

59. Wee JT, Poh SS. The most important questions in cancer research and clinical oncology : Question 1. Could the vertical transmission of human papilloma virus (HPV) infection account for the cause, characteristics, and epidemiology of HPV-positive oropharyngeal carcinoma, non-smoking East Asian female lung adenocarcinoma, and/or East Asian triple-negative breast carcinoma? *Chinese Journal of Cancer* 2017;36(1):13.

60. Rigalli JP, Reichel M, Tocchetti GN, Reuter T, Dyckhoff G, Herold-Mende C, Weiss J. Human papilloma virus (HPV) 18 proteins E6 and E7 up-regulate ABC transporters in oropharyngeal carcinoma. Involvement of the nonsense-mediated decay (NMD) pathway. *Cancer Letters* 2018;428:69-76.

61. Yamauchi R, Takeyama Y, Takata K, Fukunaga A, Sakurai K, Tanaka T, Fukuda H, Fukuda S, Kunimoto H, Umeda K, Morihara D, Yokoyama K, Irie M, Shakado S, Sakisaka S, Hirai F. Hepatitis B virus reactivation after receiving cancer chemotherapy under administration of leuprorelin acetate. *Internal Medicine* 2020;59(9):1163-1166.

62. Su FH, Le TN, Muo CH, Te SA, Sung FC, Yeh CC. Chronic Hepatitis B virus infection associated with increased colorectal cancer risk in Taiwanese population. *Viruses* 2020;12(1).

63. Qin B, Zhao K, Wei J, Wang X, Xu M, Lang J, Sun H, Jin K. Novel evidence indicates the presence and replication of hepatitis B virus in breast cancer tissue. *Oncology Reports* 2020;43(1):296-305.

64. Batyrbekova N, Aleman S, Lybeck C, Montgomery S, Duberg AS. Hepatitis c virus infection and the temporal trends in the risk of liver cancer: A national register-based cohort study in Sweden. *Cancer Epidemiology Biomarkers & Prevention* 2020;29(1):63-70.

65. da Costa Nunes JF, Pires S, Chade DC. Human papillomavirus vaccination and prevention of intraepithelial neoplasia and penile cancer: Review article. *Current Opinion in Urology* 2020;30(2):208-212.

66. Huang Y, Xu S, Xu Y, Yao D, Wang L, Zhao Y, Wu Q. A new strategy for cervical cancer prevention among Chinese women: How much do they know and how do they react toward the HPV immunization? *Journal of Cancer Education* 2020.

67. Tomatis L. Etiologic evidence and primary prevention of cancer. *Drug Metabolism Reviews* 2000;32(2):129-137.

68. Esteban-Vasallo MD, Garcia-Riolobos C, Dominguez-Berjon MF, Zoni AC. Lifestyle interventions for cancer prevention in primary care: Differences between family physicians and nursing professionals. *Journal of Evaluation in Clinical Practice* 2020;26(1):326-334.

69. El-Bayoumy K, Manni A. Customized prevention trials could resolve the controversy of the effects of omega-3 fatty acids on cancer. *Nutrition and Cancer* 2020;72(2):183-186.

70. Fan F, Wang Z, Li B, Zhang H. Effects of eradicating Helicobacter pylori on metachronous gastric cancer prevention: A systematic review and meta-analysis. *Journal of Evaluation in Clinical Practice* 2020;26(1):308-315.

71. Dong P, Shi JF, Qiu WQ, Liu CC, Wang K, Huang HY, Wang DB, Liu GX, Liao XZ, Bai YN, Sun XJ, Ren JS, Yang L, Wei DH, Song BB, Lei HK, Liu YQ, Zhang YZ, Ren SY, Zhou JY, Wang JL, Gong JY, Yu LZ, Liu YY, Zhu L, Guo LW, Wang YQ, He YT, Lou PA, Cai B, Sun XH, Wu SL, Qi X, Zhang K, Li N, Dai M, Chen WQ, Mao AY, He J. [analysis on the health literacy of the cancer prevention and treatment and its related factors among urban residents in China from 2015 to 2017]. *Zhonghua Yu Fang Yi Xue Za Zhi* 2020;54(1):76-83.

72. Chinn J, Tewari KS. Multimodality screening and prevention of cervical cancer in sub-saharan Africa: A collaborative model. *Current Opinion in Obstetrics and Gynecology* 2020;32(1):28-35.

73. Graham DY, Tan MC. No Barrett's-no cancer: A proposed new paradigm for prevention of esophageal adenocarcinoma. *Journal of Clinical Gastroenterology* 2020;54(2):136-143.

74. Knerr S, West KM, Angelo FA. Organizational readiness to implement population-based screening and genetic service delivery for hereditary cancer prevention and control. *Journal of Genetic Counseling* 2020.

75. Muller C, Yurgelun M, Kupfer SS. Precision treatment and prevention of colorectal cancer-hope or hype? *Gastroenterology* 2020;158(2):441-446.

76. Maitin-Shepard M, McCullough ML, Bandera EV, Basen-Engquist K. U.S. Dietary guidelines and cancer prevention: Your input is needed! *Cancer Epidemiology Biomarkers & Prevention* 2020;29(1):257-259.

77. Global Burden of Disease Cancer Collaboration. Global, regional, and national cancer incidence, mortality, years of life lost, years lived with disability, and disability-adjusted life-years for 29 cancer groups, 1990 to 2016: A systematic analysis for the global burden of disease study. *JAMA Oncology* 2018;4(11):1553-1568.

78. Bray F, Ferlay J, Soerjomataram I, Siegel RL, Torre LA, Jemal A. Global cancer statistics 2018: Globocan estimates of incidence and mortality worldwide for 36 cancers in 185 countries. *CA: A Cancer Journal for Clinicians* 2018;68(6):394-424.

79. Global Burden of Disease Cancer Collaboration. Global, regional, and national cancer incidence, mortality, years of life lost, years lived with disability, and disability-adjusted life-years for 32 cancer groups, 1990 to 2015: A systematic analysis for the global burden of disease study. *JAMA Oncology* 2017;3(4):524-548.

80. Ferlay J, Colombet M, Soerjomataram I, Mathers C, Parkin DM, Pineros M, Znaor A, Bray F. Estimating the global cancer incidence and mortality in 2018: Globocan sources and methods. *International Journal of Cancer* 2019;144(8):1941-1953.

81. Koroltchouk V, Stanley K, Stjernsward J. The control of breast cancer. A World Health Organization perspective. *Cancer* 1990;65(12):2803-2810.

82. White MC, Kavanaugh-Lynch M, Davis-Patterson S, Buermeyer N. An expanded agenda for the primary prevention of breast cancer: Charting a course for the future. *International Journal of Environmental Research and Public Health* 2020;17(3).

83. Union for International Cancer Control. Cancer in Sub-Saharan Africa. Geneva: UICC; 2019.

84. Bray F, McCarron P, Parkin DM. The changing global patterns of female breast cancer incidence and mortality. *Breast Cancer Research* 2004;6(6):229-239.

85. Heng YJ, Wang J, Ahearn TU, Brown SB, Zhang X, Ambrosone CB, de Andrade VP, Brufsky AM, Couch FJ, King TA, Modugno F, Vachon CM, DuPre NC, Garcia-Closas M, Troester MA, Hunter DJ, Eliassen AH, Tamimi RM, Hankinson SE, Beck AH. Molecular mechanisms linking high body mass index to breast cancer etiology in post-menopausal breast tumor and tumor-adjacent tissues. *Breast Cancer Research and Treatment* 2019;173(3):667-677.

86. Hodis HN, Sarrel PM. Menopausal hormone therapy and breast cancer: What is the evidence from randomized trials? *Climacteric* 2018;21(6):521-528.

87. Mudhune GH, Armour M, McBride KA. Safety of menopausal hormone therapy in breast cancer survivors older than fifty at diagnosis: A systematic review and meta-analysis. *Breast* 2019;47:43-55.

88. Flaum LE, Gradishar WJ. Advances in endocrine therapy for postmenopausal metastatic breast cancer. *Cancer Treat Res* 2018;173:141-154.

89. Yang Z, Hu Y, Zhang J, Xu L, Zeng R, Kang D. Estradiol therapy and breast cancer risk in perimenopausal and postmenopausal women: A systematic review and meta-analysis. *Gynecological Endocrinology* 2017;33(2):87-92.

90. Carey LA, Perou CM, Livasy CA, Dressler LG, Cowan D, Conway K, Karaca G, Troester MA, Tse CK, Edmiston S, Deming SL, Geradts J, Cheang MC, Nielsen TO, Moorman PG, Earp HS, Millikan RC. Race, breast cancer subtypes, and survival in the Carolina Breast Cancer Study. *JAMA* 2006;295(21):2492-2502.

91. Malmgren JA, Calip GS, Atwood MK, Mayer M, Kaplan HG. Metastatic breast cancer survival improvement restricted by regional disparity: Surveillance, epidemiology, and end results and institutional analysis: 1990 to 2011. *Cancer* 2020;126(2):390-399.

92. Joyner SN. Quickstats: Breast cancer death rates* among women aged 50-74 years, by race/ethnicity - National Vital Statistics System, United States, 2006 and 2016. *Morbity and Mortality Weekly Report* 2018;67(21):614.

93. Scott LC, Mobley LR, Kuo TM, Il'yasova D. Update on triple-negative breast cancer disparities for the United States: A population-based study from the United States cancer statistics database, 2010 through 2014. *Cancer* 2019;125(19):3412-3417.

94. Pilavaki P, Giallouros G, Yiallourou AI, Pantavou K, Marcou Y, Demetriou A, Scoutellas V, Nikolopoulos GK. Epidemiology of breast cancer in Cyprus: Data on newly diagnosed cases and survival rates. *Data Brief* 2018;19:353-369.

95. Langa BC, Oliveira MM, Pereira SR, Lupicki K, Marian C, Govender D, Panieri E, Hiss D, Cavalli IJ, Abdul-Rasool S, Cavalli LR. Copy number analysis of the DLX4 and ERBB2 genes in South African breast cancer patients. *Cytogenetic and Genome Research* 2015;146(3):195-203.

96. Gao Y, Heller SL, Moy L. Male breast cancer in the age of genetic testing: An opportunity for early detection, tailored therapy, and surveillance. *Radiographics* 2018;38(5):1289-1311.

97. Mechanic LE, Lindstrom S, Daily KM, Sieberts SK, Amos CI, Chen HS, Cox NJ, Dathe M, Feuer EJ, Guertin MJ, Hoffman J, Liu Y, Moore JH, Myers CL, Ritchie MD, Schildkraut J, Schumacher F, Witte JS, Wang W, Williams SM, Participants UCC, Contributors UCCD, Gillanders EM. Up for a challenge (U4C): Stimulating innovation in breast cancer genetic epidemiology. *PLoS Genetics* 2017;13(9):e1006945.

98. Ki CS. From genetic testing to treatment and prevention of BRCA-related breast cancer. *Annals of Laboratory Medicine* 2020;40(2):99-100.

99. Zavala VA, Serrano-Gomez SJ, Dutil J, Fejerman L. Genetic epidemiology of breast cancer in Latin America. *Genes (Basel)* 2019;10(2).

100. Piccinin C, Panchal S, Watkins N, Kim RH. An update on genetic risk assessment and prevention: The role of genetic testing panels in breast cancer. *Expert Review of Anticancer Therapy* 2019;19(9):787-801.

101. Fasching PA, Ekici AB, Wachter DL, Hein A, Bayer CM, Haberle L, Loehberg CR, Schneider M, Jud SM, Heusinger K, Rubner M, Rauh C, Bani MR, Lux MP, Schulz-Wendtland R, Hartmann A, Beckmann MW. Breast cancer risk - from genetics to molecular understanding of pathogenesis. *Geburtshilfe Frauenheilkd* 2013;73(12):1228-1235.

102. Shiovitz S, Korde LA. Genetics of breast cancer: A topic in evolution. *Annals of Oncology* 2015;26(7):1291-1299.

103. Moslehi R, Freedman E, Zeinomar N, Veneroso C, Levine PH. Importance of hereditary and selected environmental risk factors in the etiology of inflammatory breast cancer: A case-comparison study. *BMC Cancer* 2016;16:334.

104. Zakhari S, Hoek JB. Epidemiology of moderate alcohol consumption and breast cancer: Association or causation? *Cancers (Basel)* 2018;10(10).

105. Dumitrescu RG, Shields PG. The etiology of alcohol-induced breast cancer. *Alcohol* 2005;35(3):213-225.

106. Dorchak JA, Maria S, Guarinoni JL, Duensing A, Somiari S, Cavanaugh J, Deyarmin B, Hu H, Iida J, Shriver CD, Witt-Enderby PA. The impact of hormonal contraceptives on breast cancer pathology. *Hormones and Cancer* 2018;9(4):240-253.

107. Liu YL, Wang DW, Yang ZC, Ma R, Li Z, Suo W, Zhao Z, Li ZW. Marital status is an independent prognostic factor in inflammatory breast cancer patients: An analysis of the surveillance, epidemiology, and end results database. *Breast Cancer Research and Treatment* 2019;178(2):379-388.

108. McCormack VA, Febvey-Combes O, Ginsburg O, dos-Santos-Silva I. Breast cancer in women living with HIV: A first global estimate. *International Journal of Cancer* 2018;143(11):2732-2740.

109. Coughlin SS. Epidemiology of breast cancer in women. *Advances in Experimental Medicine and Biology* 2019;1152:9-29.

110. Zhu X, Chen L, Huang B, Wang Y, Ji L, Wu J, Di G, Liu G, Yu K, Shao Z, Wang Z. The prognostic and predictive potential of Ki-67 in triple-negative breast cancer. *Scientific Reports* 2020;10(1):225.

111. Woodward WA. Building momentum for subsets of patients with advanced triple-negative breast cancer. *Lancet Oncology* 2020;21(1):3-5.

112. Shee K, Wells JD, Ung M, Hampsch RA, Traphagen NA, Yang W, Liu SC, Zeldenrust MA, Wang L, Kalari KR, Yu J, Boughey JC, Demidenko E, Kettenbach AN, Cheng C, Goetz MP, Miller TW. A transcriptionally definable subgroup of triple-negative breast and ovarian cancer samples shows sensitivity to hsp90 inhibition. *Clinical Cancer Research* 2020;26(1):159-170.

113. Azim HA, Ghosn M, Oualla K, Kassem L. Personalized treatment in metastatic triple-negative breast cancer: The outlook in 2020. *Breast Journal* 2020;26(1):69-80.

114. Poehls UG, Hack CC, Wunderle M, Renner SP, Lux MP, Beckmann MW, Fasching PA, Nabieva N. Awareness of breast cancer incidence and risk factors among healthy women in Germany: An update after 10 years. *European Journal of Cancer Prevention* 2019;28(6):515-521.

115. Rice MS, Tworoger SS, Hankinson SE, Tamimi RM, Eliassen AH, Willett WC, Colditz G, Rosner B. Breast cancer risk prediction: An update to the Rosner-Colditz breast cancer incidence model. *Breast Cancer Research and Treatment* 2017;166(1):227-240.

116. Ruiz R, Herrero C, Strasser-Weippl K, Touya D, St Louis J, Bukowski A, Goss PE. Epidemiology and pathophysiology of pregnancy-associated breast cancer: A review. *Breast* 2017;35:136-141.

117. Brinton LA, Gaudet MM, Gierach GL. Breast cancer. In: Thun MJ, Linet MS, Cerhan JR, Haiman CA, Schottenfeld D, eds. *Cancer epidemiology and prevention*. 4 ed. New York: Oxford University Press; 2018:861-888.

118. Hulka BS, Moorman PG. Breast cancer: Hormones and other risk factors. *Maturitas* 2008;61(1-2):203-213.

119. Ferlay J, Soerjomataram I, Dikshit R, Eser S, Mathers C, Rebelo M, Parkin DM, Forman D, Bray F. Cancer incidence and mortality worldwide: Sources, methods and major patterns in globocan 2012. *International Journal of Cancer* 2015;136(5):E359-386.

120. Martinson HA, Lyons TR, Giles ED, Borges VF, Schedin P. Developmental windows of breast cancer risk provide opportunities for targeted chemoprevention. *Experimental Cell Research* 2013;319(11):1671-1678.

121. Adami HO, Persson I, Ekbom A, Wolk A, Ponten J, Trichopoulos D. The aetiology and pathogenesis of human breast cancer. *Mutation Research* 1995;333(1-2):29-35.

122. Tharmapalan P, Mahendralingam M, Berman HK, Khokha R. Mammary stem cells and progenitors: Targeting the roots of breast cancer for prevention. *The EMBO Journal* 2019;38(14):e100852.

123. Feng Y, Spezia M, Huang S, Yuan C, Zeng Z, Zhang L, Ji X, Liu W, Huang B, Luo W, Liu B, Lei Y, Du S, Vuppalapati A, Luu HH, Haydon RC, He TC, Ren G. Breast cancer development and progression: Risk factors, cancer stem cells, signaling pathways, genomics, and molecular pathogenesis. *Genes & Diseases* 2018;5(2):77-106.

124. Sotgia F, Fiorillo M, Lisanti MP. Hallmarks of the cancer cell of origin: Comparisons with "energetic" cancer stem cells (e-CSCs). *Aging (Albany NY)* 2019;11(3):1065-1068.

125. Scioli MG, Storti G, D'Amico F, Gentile P, Fabbri G, Cervelli V, Orlandi A. The role of breast cancer stem cells as a prognostic marker and a target to improve the efficacy of breast cancer therapy. *Cancers (Basel)* 2019;11(7).

126. Shima H, Yamada A, Ishikawa T, Endo I. Are breast cancer stem cells the key to resolving clinical issues in breast cancer therapy? *Gland Surgery* 2017;6(1):82-88.

127. Rangel MC, Bertolette D, Castro NP, Klauzinska M, Cuttitta F, Salomon DS. Developmental signaling pathways regulating mammary stem cells and contributing to the etiology of triple-negative breast cancer. *Breast Cancer Research and Treatment* 2016;156(2):211-226.

128. Bombonati A, Sgroi DC. The molecular pathology of breast cancer progression. *Journal of Pathology* 2011;223(2):307-317.

129. Sin WC, Lim CL. Breast cancer stem cells-from origins to targeted therapy. *Stem Cell Investigation* 2017;4:96.

130. Wazer DE, Band V. Molecular and anatomic considerations in the pathogenesis of breast cancer. *Radiation Oncology Investigations* 1999;7(1):1-12.

131. Imyanitov EN, Hanson KP. Molecular pathogenesis of bilateral breast cancer. *Cancer Letters* 2003;191(1):1-7.

132. Bosch A, Eroles P, Zaragoza R, Vina JR, Lluch A. Triple-negative breast cancer: Molecular features, pathogenesis, treatment and current lines of research. *Cancer Treatment Reviews* 2010;36(3):206-215.

133. Badovinac-Crnjevic T, Jakic-Razumovic J, Podolski P, Plestina S, Sarcevic B, Munjas R, Vrbanec D. Significance of epidermal growth factor receptor expression in breast cancer. *Medical Oncology* 2011;28 Suppl 1:S121-128.

134. Perou CM. Comprehensive molecular portraits of human breast tumors. *Nature* 2012;490(7418):61-70.

135. Yarden Y, Pines G. The ERBB network: At last, cancer therapy meets systems biology. *Nature Reviews Cancer* 2012;12(8):553-563.

136. Zhang Z, Tang P. Genomic pathology and biomarkers in breast cancer. *Crit Rev Oncog* 2017;22(5-6):411-426.

137. Das D, Ghosh S, Maitra A, Biswas NK, Panda CK, Roy B, Sarin R, Majumder PP. Epigenomic dysregulation-mediated alterations of key biological pathways and tumor immune evasion are hallmarks of gingivo-buccal oral cancer. *Clinical Epigenetics* 2019;11(1):178.

138. Frost FG, Cherukuri PF, Milanovich S, Boerkoel CF. Pan-cancer RNA-seq data stratifies tumors by some hallmarks of cancer. *J Cell Mol Med* 2020;24(1):418-430.

139. Tate JG, Bamford S, Jubb HC, Sondka Z, Beare DM, Bindal N, Boutselakis H, Cole CG, Creatore C, Dawson E, Fish P, Harsha B, Hathaway C, Jupe SC, Kok CY, Noble K, Ponting L, Ramshaw CC, Rye CE, Speedy HE, Stefancsik R, Thompson SL, Wang S, Ward S, Campbell PJ, Forbes SA. Cosmic: The catalogue of somatic mutations in cancer. *Nucleic Acid Research* 2019;47(D1):D941-D947.

140. Diaz-Gay M, Vila-Casadesus M, Franch-Exposito S, Hernandez-Illan E, Lozano JJ, Castellvi-Bel S. Mutational signatures in cancer (MuSiCa): A web application to implement mutational signatures analysis in cancer samples. *BMC Bioinformatics* 2018;19(1):224.

141. ICGC/TCGA Pan-Cancer Analysis of Whole Genomes Consortium. Pan-cancer analysis of whole genomes. *Nature* 2020;578(7793):82-93.

142. Friedberg EC. A comprehensive catalogue of somatic mutations in cancer genomes. *DNA Repair (Amst)* 2010;9(4):468-469.

143. Pleasance ED, Cheetham RK, Stephens PJ, McBride DJ, Humphray SJ, Greenman CD, Varela I, Lin ML, Ordonez GR, Bignell GR, Ye K, Alipaz J, Bauer MJ, Beare D, Butler A, Carter RJ, Chen L, Cox AJ, Edkins S, Kokko-Gonzales PI, Gormley NA, Grocock RJ, Haudenschild CD, Hims MM, James T, Jia M, Kingsbury Z, Leroy C, Marshall J, Menzies A, Mudie LJ, Ning Z, Royce T, Schulz-Trieglaff OB, Spiridou A, Stebbings LA, Szajkowski L, Teague J, Williamson D, Chin L, Ross MT, Campbell PJ, Bentley DR, Futreal PA, Stratton MR. A comprehensive catalogue of somatic mutations from a human cancer genome. *Nature* 2010;463(7278):191-196.

144. Kessler MD, Bateman NW, Conrads TP, Maxwell GL, Dunning Hotopp JC, O'Connor TD. Ancestral characterization of 1018 cancer cell lines highlights disparities and reveals gene expression and mutational differences. *Cancer* 2019;125(12):2076-2088.

145. Almendro V, Fuster G. Heterogeneity of breast cancer: Etiology and clinical relevance. *Clinical and Translational Oncology* 2011;13(11):767-773.

146. Tang Y, Wang Y, Kiani MF, Wang B. Classification, treatment strategy, and associated drug resistance in breast cancer. *Clinical Breast Cancer* 2016;16(5):335-343.

147. Harbeck N, Penault-Llorca F, Cortes J, Gnant M, Houssami N, Poortmans P, Ruddy K, Tsang J, Cardoso F. Breast cancer. *Nature Reviews Disease Primers* 2019;5(1):66.

148. Tomao F, Papa A, Zaccarelli E, Rossi L, Caruso D, Minozzi M, Vici P, Frati L, Tomao S. Triple-negative breast cancer: New perspectives for targeted therapies. *OncoTargets and Therapy* 2015;8:177-193.

149. Perou CM, Sørlie T, Eisen MB, van de Rijn M, Jeffrey SS, Rees CA, Pollack JR, Ross DT, Johnsen H, Akslen LA, Fluge Ø, Pergamenschikov A, Williams C, Zhu SX, Lønning PE, Børresen-Dale A-L, Brown PO, Botstein D. Molecular portraits of human breast tumors. *Nature* 2000;406:747.

150. Russnes HG, Lingjaerde OC, Borresen-Dale AL, Caldas C. Breast cancer molecular stratification: From intrinsic subtypes to integrative clusters. *American Journal of Pathology* 2017;187(10):2152-2162.

151. Cedolini C, Bertozzi S, Londero AP, Bernardi S, Seriau L, Concina S, Cattin F, Risaliti A. Type of breast cancer diagnosis, screening, and survival. *Clinical Breast Cancer* 2014;14(4):235-240.

152. Yam C, Mani SA, Moulder SL. Targeting the molecular subtypes of triple negative breast cancer: Understanding the diversity to progress the field. *Oncologist* 2017;22(9):1086-1093.

153. Arpino G, Weiss H, Lee AV, Schiff R, De Placido S, Osborne CK, Elledge RM. Estrogen receptor-positive, progesterone receptor-negative breast cancer: Association with growth factor receptor expression and tamoxifen resistance. *Journal of the National Cancer Institute* 2005;97(17):1254-1261.

154. Baker E, Whiteoak N, Hall L, France J, Wilson D, Bhaskar P. Mammaglobin-a, vegfr3, and ki67 in human breast cancer pathology and five year survival. *Breast Cancer (Auckl)* 2019;13:1-8.

155. Konecny G, Pauletti G, Pegram M, Untch M, Dandekar S, Aguilar Z, Wilson C, Rong HM, Bauerfeind I, Felber M, Wang HJ, Beryt M, Seshadri R, Hepp H, Slamon DJ. Quantitative association between HER-2/neu and steroid hormone receptors in hormone receptor-positive primary breast cancer. *Journal of the National Cancer Institute* 2003;95(2):142-153.

156. Li Y, Zhang X, Qiu J, Pang T, Huang L, Zeng Q. Comparisons of p53, ki67 and BRCA1 expressions in patients with different molecular subtypes of breast cancer and their relationships with pathology and prognosis. *Journal of the Balkan Union of Oncology* 2019;24(6):2361-2368.

157. Penault-Llorca F, Radosevic-Robin N. Ki67 assessment in breast cancer: An update. *Pathology* 2017;49(2):166-171.

158. van Rooijen JM, Qiu SQ, Timmer-Bosscha H, van der Vegt B, Boers JE, Schroder CP, de Vries EGE. Androgen receptor expression inversely correlates with immune cell infiltration in human epidermal growth factor receptor 2-positive breast cancer. *European Journal of Cancer* 2018;103:52-60.

159. Nielsen KV, Ejlertsen B, Moller S, Jorgensen JT, Knoop A, Knudsen H, Mouridsen HT. The value of TOP2A gene copy number variation as a biomarker in breast cancer: Update of DBCG trial 89D. *Acta Oncologica* 2008;47(4):725-734.

160. Cardoso F, Durbecq V, Larsimont D, Paesmans M, Leroy JY, Rouas G, Sotiriou C, Renard N, Richard V, Piccart MJ, Di Leo A. Correlation between complete response to anthracycline-based chemotherapy and topoisomerase II-alpha gene amplification and protein overexpression in locally advanced/metastatic breast cancer. *International Journal of Oncology* 2004;24(1):201-209.

161. Press MF, Sauter G, Buyse M, Bernstein L, Guzman R, Santiago A, Villalobos IE, Eiermann W, Pienkowski T, Martin M, Robert N, Crown J, Bee V, Taupin H, Flom KJ, Tabah-Fisch I, Pauletti G, Lindsay MA, Riva A, Slamon DJ. Alteration of topoisomerase II-alpha gene in human breast cancer: Association with responsiveness to anthracycline-based chemotherapy. *Journal of Clinical Oncology* 2011;29(7):859-867.

162. Huang M, Wu J, Ling R, Li N. Quadruple negative breast cancer. *Breast Cancer* 2020;27(4):527-533.

163. West RB, Nuyten DS, Subramanian S, Nielsen TO, Corless CL, Rubin BP, Montgomery K, Zhu S, Patel R, Hernandez-Boussard T, Goldblum JR, Brown PO, van de Vijver M, van de Rijn M. Determination of stromal signatures in breast carcinoma. *PLoS Biology* 2005;3(6):e187.

164. Creighton CJ, Li XX, Landis M, Dixon JM, Neumeister VM, Sjolund A, Rimm DL, Wong H, Rodriguez A, Herschkowitz JI, Fan C, Zhang XM, He XP, Pavlick A, Gutierrez MC, Renshaw L, Larionov AA, Faratian D, Hilsenbeck SG, Perou CM, Lewis MT, Rosen JM, Chang JC. Residual breast cancers after conventional therapy display mesenchymal as well as tumor-initiating features. *Proceedings of the National Academy of Sciences of the United States of America* 2009;106(33):13820-13825.

165. Hu Z, Fan C, Oh DS, Marron JS, He X, Qaqish BF, Livasy C, Carey LA, Reynolds E, Dressler L, Nobel A, Parker J, Ewend MG, Sawyer LR, Wu J, Liu Y, Nanda R, Tretiakova M, Ruiz Orrico A, Dreher D, Palazzo JP, Perreard L, Nelson E, Mone M, Hansen H, Mullins M, Quackenbush JF, Ellis MJ, Olopade OI, Bernard PS, Perou CM. The molecular portraits of breast tumors are conserved across microarray platforms. *BMC Genomics* 2006;7:96.

166. Teschendorff AE, Miremadi A, Pinder SE, Ellis IO, Caldas C. An immune response gene expression module identifies a good prognosis subtype in estrogen receptor negative breast cancer. *Genome Biology* 2007;8(8):R157.

167. Joensuu H, Pylkkanen L, Toikkanen S. Bcl-2 protein expression and long-term survival in breast cancer. *American Journal of Pathology* 1994;145(5):1191-1198.

168. Zhang GJ, Kimijima I, Tsuchiya A, Abe R. The role of bcl-2 expression in breast carcinomas (review). *Oncology Reports* 1998;5(5):1211-1216.

169. Merino D, Lok SW, Visvader JE, Lindeman GJ. Targeting bcl-2 to enhance vulnerability to therapy in estrogen receptor-positive breast cancer. *Oncogene* 2016;35(15):1877-1887.

170. Levy MA, Claxton DF. Therapeutic inhibition of bcl-2 and related family members. *Expert Opinion on Investigational Drugs* 2017;26(3):293-301.

171. Hwang K-T, Woo JW, Shin HC, Kim HS, Ahn SK, Moon H-G, Han W, Park IA, Noh D-Y. Prognostic influence of bcl2 expression in breast cancer. *International Journal of Cancer* 2012;131(7):E1109-E1119.

172. Karimi-Busheri F, Rasouli-Nia A, Mackey JR, Weinfeld M. Senescence evasion by MCF-7 human breast tumor-initiating cells. *Breast Cancer Research* 2010;12(3):R31.

173. Olivier M, Langer√∏d A, Carrieri P, Bergh J, Klaar S, Eyfjord J, Theillet C, Rodriguez C, Lidereau R, Bi√®che I, Varley J, Bignon Y, Uhrhammer N, Winqvist R, Jukkola-Vuorinen A, Niederacher D, Kato S, Ishioka C, Hainaut P, B√∏rresen-Dale A-L. The clinical value of somatic tp53 gene mutations in 1,794 patients with breast cancer. *Clinical Cancer Research* 2006;12(4):1157-1167.

174. Langerød A, Zhao H, Borgan Ø, Nesland JM, Bukholm IRK, Ikdahl T, Kåresen R, Børresen-Dale A-L, Jeffrey SS. Tp53mutation status and gene expression profiles are powerful prognostic markers of breast cancer. *Breast Cancer Research* 2007;9(3):R30.

175. Bertone-Johnson ER, Chen WY, Holick MF, Hollis BW, Colditz GA, Willett WC, Hankinson SE. Plasma 25-hydroxyvitamin D and 1,25-dihydroxyvitamin D and risk of breast cancer. *Cancer Epidemiology Biomarkers & Prevention* 2005;14(8):1991-1997.

176. Lowe LC, Guy M, Mansi JL, Peckitt C, Bliss J, Wilson RG, Colston KW. Plasma 25-hydroxy vitamin D concentrations, vitamin D receptor genotype and breast cancer risk in a uk Caucasian population. *European Journal of Cancer* 2005;41(8):1164-1169.

177. Song D, Deng Y, Liu K, Zhou L, Li N, Zheng Y, Hao Q, Yang S, Wu Y, Zhai Z, Li H, Dai Z. Vitamin D intake, blood vitamin D levels, and the risk of breast cancer: A dose-response meta-analysis of observational studies. *Aging (Albany NY)* 2019;11(24):12708-12732.

178. Hu K, Callen DF, Li J, Zheng H. Circulating Vitamin D and overall survival in breast cancer patients: A dose-response meta-analysis of cohort studies. *Integrated Cancer Therapy* 2018;17(2):217-225.

179. Santagata S, Thakkar A, Ergonul A, Wang B, Woo T, Hu R, Harrell JC, McNamara G, Schwede M, Culhane AC, Kindelberger D, Rodig S, Richardson A, Schnitt SJ, Tamimi RM, Ince TA. Taxonomy of breast cancer based on normal cell phenotype predicts outcome. *Journal of Clinical Investigation* 2014;124(2):859-870.

180. Eroles P, Bosch A, Perez-Fidalgo JA, Lluch A. Molecular biology in breast cancer: Intrinsic subtypes and signaling pathways. *Cancer Treatment Reviews* 2012;38(6):698-707.

181. Lal S, McCart Reed AE, de Luca XM, Simpson PT. Molecular signatures in breast cancer. *Methods* 2017;131:135-146.

182. Harbeck N, Gnant M. Breast cancer. *Lancet* 2017;389(10074):1134-1150.

183. Veronesi U, Boyle P, Goldhirsch A, Orecchia R, Viale G. Breast cancer. *The Lancet* 2005;365(9472):1727-1741.

184. Polyak K. Breast cancer: Origins and evolution. *Journal of Clinical Investigation* 2007;117(11):3155-3163.

185. Allison KH. Molecular pathology of breast cancer: What a pathologist needs to know. *American Journal of Clinical Pathology* 2012;138(6):770-780.

186. Esebua M. Histopathology and grading of breast cancer. In: Schatten H, ed. *Cell and Molecular Biology of Breast Cancer*: Springer-Humana Press; 2013:1-27.

187. Shao N, Xie C, Shi Y, Ye R, Long J, Shi H, Shan Z, Thompson AM, Lin Y. Comparison of the 7th and 8th edition of American Joint Committee on Cancer (AJCC) staging systems for breast cancer patients: A Surveillance, Epidemiology and End Results (SEER) analysis. *Cancer Management and Research* 2019;11:1433-1442.

188. Tan GH, Bhoo-Pathy N, Taib NA, See MH, Jamaris S, Yip CH. The Will Rogers phenomenon in the staging of breast cancer - does it matter? *Cancer Epidemiology* 2015;39(1):115-117.

189. Stander M, Stander J. A simple method for correcting for the Will Rogers phenomenon with biometrical applications. *Biometrical Journal* 2020;2020:1-10.

190. Lester J. Local treatment of breast cancer. *Seminars in Oncology Nursing* 2015;31(2):122-133.

191. Joyce DP, Murphy D, Lowery AJ, Curran C, Barry K, Malone C, McLaughlin R, Kerin MJ. Prospective comparison of outcome after treatment for triple-negative and non-triple-negative breast cancer. *Surgeon* 2017;15(5):272-277.

192. Giuliano AE, Connolly JL, Edge SB, Mittendorf EA, Rugo HS, Solin LJ, Weaver DL, Winchester DJ, Hortobagyi GN. Breast cancer-major changes in the American Joint Committee on Cancer eighth edition cancer staging manual. *CA: A Cancer Journal for Clinicians* 2017;67(4):290-303.

193. He J, Tsang JY, Xu X, Li J, Li M, Chao X, Xu Y, Luo R, Tse GM, Sun P. AJCC 8th edition prognostic staging provides no better discriminatory ability in prognosis than anatomical staging in triple negative breast cancer. *BMC Cancer* 2020;20(1):18.

194. Lehmann BD, Bauer JA, Chen X, Sanders ME, Chakravarthy AB, Shyr Y, Pietenpol JA. Identification of human triple-negative breast cancer subtypes and preclinical models for selection of targeted therapies. *The Journal of Clinical Investigation* 2011;121(7):2750-2767.

195. Lehmann BD, Jovanovic B, Chen X, Estrada MV, Johnson KN, Shyr Y, Moses HL, Sanders ME, Pietenpol JA. Refinement of triple-negative breast cancer molecular subtypes: Implications for neoadjuvant chemotherapy selection. *PloS One* 2016;11(6):e0157368.

196. Pareja F, Reis-Filho JS. Triple-negative breast cancers - a panoply of cancer types. *Nature Reviews Clinical Oncology* 2018;15(6):347-348.

197. Kumar P, Aggarwal R. An overview of triple-negative breast cancer. *Archives of Gynecology and Obstetrics* 2016;293(2):247-269.

198. Prat A, Parker JS, Karginova O, Fan C, Livasy C, Herschkowitz JI, He X, Perou CM. Phenotypic and molecular characterization of the claudin-low intrinsic subtype of breast cancer. *Breast Cancer Research* 2010;12(5):R68.

199. Burstein MD, Tsimelzon A, Poage GM, Covington KR, Contreras A, Fuqua SA, Savage MI, Osborne CK, Hilsenbeck SG, Chang JC, Mills GB, Lau CC, Brown PH. Comprehensive genomic analysis identifies novel subtypes and targets of triple-negative breast cancer. *Clinical Cancer Research* 2015;21(7):1688-1698.

200. da Silva JL, Cardoso Nunes NC, Izetti P, de Mesquita GG, de Melo AC. Triple negative breast cancer: A thorough review of biomarkers. *Critical Reviews in Oncology/Hematology* 2020;145:102855.

201. Wu X, Ding M, Lin J. Three-microRNA expression signature predicts survival in triple-negative breast cancer. *Oncology Letters* 2020;19(1):301-308.

202. Toda H, Seki N, Kurozumi S, Shinden Y, Yamada Y, Nohata N, Moriya S, Idichi T, Maemura K, Fujii T, Horiguchi J, Kijima Y, Natsugoe S. RNA-sequence-based

microRNA expression signature in breast cancer: Tumor-suppressive mir-101-5p regulates molecular pathogenesis. *Molecular Oncology* 2020;14(2):426-446.

203. Wang Z, Wang X. Mir-122-5p promotes aggression and epithelial-mesenchymal transition in triple-negative breast cancer by suppressing charged multivesicular body protein 3 through mitogen-activated protein kinase signaling. *Journal of Cellular Physiology* 2020;235(3):2825-2835.

204. Amorim M, Lobo J, Fontes-Sousa M, Estevão-Pereira H, Salta S, Lopes P, Coimbra N, Antunes L, Palma de Sousa S, Henrique R, Jerónimo C. Predictive and prognostic value of selected micrornas in luminal breast cancer. *Frontiers in Genetics* 2019;10:815.

205. Rokudai S. High-throughput RNA interference screen targeting synthetic-lethal gain-of-function of oncogenic mutant tp53 in triple-negative breast cancer. *Methods in Molecular Biology* 2020;2108:297-303.

206. Synnott NC, O'Connell D, Crown J, Duffy MJ. COTI-2 reactivates mutant p53 and inhibits growth of triple-negative breast cancer cells. *Breast Cancer Research and Treatment* 2020;179(1):47-56.

207. Synnott NC, Murray A, McGowan PM, Kiely M, Kiely PA, O'Donovan N, O'Connor DP, Gallagher WM, Crown J, Duffy MJ. Mutant p53: A novel target for the treatment of patients with triple-negative breast cancer? *International Journal of Cancer* 2017;140(1):234-246.

208. Prajzendanc K, Domagala P, Hybiak J, Rys J, Huzarski T, Szwiec M, Tomiczek-Szwiec J, Redelbach W, Sejda A, Gronwald J, Kluz T, Wisniowski R, Cybulski C, Lukomska A, Bialkowska K, Sukiennicki G, Kulczycka K, Narod SA, Wojdacz TK, Lubinski J, Jakubowska A. BRCA1 promoter methylation in peripheral blood is associated with the risk of triple-negative breast cancer. *International Journal of Cancer* 2020;146(5):1293-1298.

209. Hon JD, Singh B, Sahin A, Du G, Wang J, Wang VY, Deng FM, Zhang DY, Monaco ME, Lee P. Breast cancer molecular subtypes: From TNBC to QNBC. *American Journal of Cancer Research* 2016;6(9):1864-1872.

210. Saini G, Bhattarai S, Gogineni K, Aneja R. Quadruple-negative breast cancer: An uneven playing field. *JCO Global Oncology* 2020;6:233-237.

211. Prado-Vázquez G, Gámez-Pozo A, Trilla-Fuertes L, Arevalillo JM, Zapater-Moros A, Ferrer-Gómez M, Díaz-Almirón M, López-Vacas R, Navarro H, Maín P, Feliú J, Zamora P, Espinosa E, Fresno Vara J. A novel approach to triple-negative breast cancer molecular classification reveals a luminal immune-positive subgroup with good prognoses. *Scientific Reports* 2019;9(1):1538.

212. Economopoulou P, Dimitriadis G, Psyrri A. Beyond BRCA: New hereditary breast cancer susceptibility genes. *Cancer Treatment Reviews* 2015;41(1):1-8.

213. Angeli D, Salvi S, Tedaldi G. Genetic predisposition to breast and ovarian cancers: How many and which genes to test? *International Journal of Molecular Sciences* 2020;21(3).

214. Margaritte P, Bonaiti-Pellie C, King MC, Clerget-Darpoux F. Linkage of familial breast cancer to chromosome 17q21 may not be restricted to early-onset disease. *American Journal of Human Genetics* 1992;50(6):1231-1234.

215. Hall JM, Lee MK, Newman B, Morrow JE, Anderson LA, Huey B, King MC. Linkage of early-onset familial breast cancer to chromosome 17q21. *Science* 1990;250(4988):1684-1689.

216. Wooster R, Neuhausen SL, Mangion J, Quirk Y, Ford D, Collins N, Nguyen K, Seal S, Tran T, Averill D, et al. Localization of a breast cancer susceptibility gene, BRCA2, to chromosome 13q12-13. *Science* 1994;265(5181):2088-2090.

217. Lee A, Moon BI, Kim TH. BRCA1/BRCA2 pathogenic variant breast cancer: Treatment and prevention strategies. *Annals of Laboratory Medicine* 2020;40(2):114-121.

218. Petrucelli N, Daly MB, Feldman GL. Hereditary breast and ovarian cancer due to mutations in BRCA1 and BRCA2. *Genetics in Medicine* 2010;12(5):245-259.

219. Keeney MG, Couch FJ, Visscher DW, Lindor NM. Non-BRCA familial breast cancer: Review of reported pathology and molecular findings. *Pathology* 2017;49(4):363-370.

220. Yiannakopoulou E. Etiology of familial breast cancer with undetected BRCA1 and BRCA2 mutations: Clinical implications. *Cellular Oncology* 2014;37(1):1-8.

221. Palacova M. Breast cancer in BRCA1/2 mutation carriers - do we treat it differently? Focus on systemic therapy for BRCA1/2 associated breast cancer. *Klinicka Onkologie* 2019;32(Supplementum2):24-30.

222. Stratton MR, Rahman N. The emerging landscape of breast cancer susceptibility. *Nature Genetics* 2008;40(1):17-22.

223. King M-C, Marks JH, Mandell JB. Breast and ovarian cancer risks due to inherited mutations in *BRCA1* and *BRCA2*. *Science* 2003;302(5645):643-646.

224. Liede A, Karlan BY, Narod SA. Cancer risks for male carriers of germline mutations in BRCA1 or BRCA2: A review of the literature. *Journal of Clinical Oncology* 2004;22(4):735-742.

225. Kuchenbaecker KB, Hopper JL, Barnes DR, Phillips KA, Mooij TM, Roos-Blom MJ, Jervis S, van Leeuwen FE, Milne RL, Andrieu N, Goldgar DE, Terry MB, Rookus MA, Easton DF, Antoniou AC, McGuffog L, Evans DG, Barrowdale D, Frost D, Adlard J, Ong KR, Izatt L, Tischkowitz M, Eeles R, Davidson R, Hodgson S, Ellis S, Nogues C, Lasset C, Stoppa-Lyonnet D, Fricker JP, Faivre L, Berthet P, Hooning MJ, van der Kolk LE, Kets CM, Adank MA, John EM, Chung WK, Andrulis IL, Southey M, Daly MB, Buys SS, Osorio A, Engel C, Kast K, Schmutzler RK, Caldes T, Jakubowska A, Simard J, Friedlander ML, McLachlan SA, Machackova E, Foretova L, Tan YY, Singer CF, Olah E, Gerdes AM, Arver B, Olsson H. Risks of breast, ovarian, and contralateral breast cancer for BRCA1 and BRCA2 mutation carriers. *JAMA* 2017;317(23):2402-2416.

226. Rosenberg SM, Ruddy KJ, Tamimi RM, Gelber S, Schapira L, Come S, Borges VF, Larsen B, Garber JE, Partridge AH. BRCA1 and BRCA2 mutation testing in young women with breast cancer. *JAMA Oncology* 2016;2(6):730-736.

227. Barton MK. Rates of testing for BRCA mutations in young women are on the rise. *CA: A Cancer Journal for Clinicians* 2016;66(4):269-270.

228. Liu Y, Ide Y, Inuzuka M, Tazawa S, Kanada Y, Matsunaga Y, Kuwayama T, Sawada T, Akashi-Tanaka S, Nakamura S. BRCA1/BRCA2 mutations in Japanese women with ductal carcinoma in situ. *Molecular Genetics & Genomic Medicine* 2019;7(3):e493.

229. Kemp Z, Turnbull A, Yost S, Seal S, Mahamdallie S, Poyastro-Pearson E, Warren-Perry M, Eccleston A, Tan MM, Teo SH, Turner N, Strydom A, George A, Rahman N.

Evaluation of cancer-based criteria for use in mainstream BRCA1 and BRCA2 genetic testing in patients with breast cancer. *JAMA Network Open* 2019;2(5):e194428.

230. Bobbili P, Olufade T, DerSarkissian M, Shenolikar R, Yu H, Duh MS, Tung N. Adherence to National Comprehensive Cancer Network Guidelines for BRCA testing among high risk breast cancer patients: A retrospective chart review study. *Hereditary Cancer in Clinical Practice* 2020;18:13.

231. Ngeow J, Sesock K, Eng C. Breast cancer risk and clinical implications for germline PTEN mutation carriers. *Breast Cancer Research and Treatment* 2017;165(1):1-8.

232. Bareche Y, Venet D, Ignatiadis M, Aftimos P, Piccart M, Rothe F, Sotiriou C. Unravelling triple-negative breast cancer molecular heterogeneity using an integrative multiomic analysis. *Annals of Oncology* 2018;29(4):895-902.

233. Yates LR, Desmedt C. Translational genomics: Practical applications of the genomic revolution in breast cancer. *Clinical Cancer Research* 2017;23(11):2630-2639.

234. Lehmann BD, Pietenpol JA. Clinical implications of molecular heterogeneity in triple negative breast cancer. *Breast* 2015;24 Suppl 2:S36-40.

235. Nik-Zainal S, Davies H, Staaf J, Ramakrishna M, Glodzik D, Zou X, Martincorena I, Alexandrov LB, Martin S, Wedge DC, Van Loo P, Ju YS, Smid M, Brinkman AB, Morganella S, Aure MR, Lingjærde OC, Langerød A, Ringnér M, Ahn S-M, Boyault S, Brock JE, Broeks A, Butler A, Desmedt C, Dirix L, Dronov S, Fatima A, Foekens JA, Gerstung M, Hooijer GKJ, Jang SJ, Jones DR, Kim H-Y, King TA, Krishnamurthy S, Lee HJ, Lee J-Y, Li Y, McLaren S, Menzies A, Mustonen V, O'Meara S, Pauporté I, Pivot X, Purdie CA, Raine K, Ramakrishnan K, Rodríguez-González FG, Romieu G, Sieuwerts AM, Simpson PT, Shepherd R, Stebbings L, Stefansson OA, Teague J, Tommasi S, Treilleux I, Van den Eynden GG, Vermeulen P, Vincent-Salomon A, Yates L, Caldas C, Veer Lvt, Tutt A, Knappskog S, Tan BKT, Jonkers J, Borg Å, Ueno NT, Sotiriou C, Viari A, Futreal PA, Campbell PJ, Span PN, Van Laere S, Lakhani SR, Eyfjord JE, Thompson AM, Birney E, Stunnenberg HG, van de Vijver MJ, Martens JWM, Børresen-Dale A-L, Richardson AL, Kong G, Thomas G, Stratton MR. Landscape of somatic mutations in 560 breast cancer whole-genome sequences. *Nature* 2016;534(7605):47-54.

236. Curtis C, Shah SP, Chin SF, Turashvili G, Rueda OM, Dunning MJ, Speed D, Lynch AG, Samarajiwa S, Yuan Y, Graf S, Ha G, Haffari G, Bashashati A, Russell R, McKinney S, Group M, Langerod A, Green A, Provenzano E, Wishart G, Pinder S, Watson P, Markowetz F, Murphy L, Ellis I, Purushotham A, Borresen-Dale AL, Brenton JD, Tavare S, Caldas C, Aparicio S. The genomic and transcriptomic architecture of 2,000 breast tumors reveals novel subgroups. *Nature* 2012;486(7403):346-352.

237. Cancer Genome Atlas N. Comprehensive molecular portraits of human breast tumors. *Nature* 2012;490(7418):61-70.

238. Provenzano E, Ulaner GA, Chin S-F. Molecular classification of breast cancer. *PET Clinics* 2018;13(3):325-338.

239. Waks AG, Winer EP. Breast cancer treatment: A review. *JAMA* 2019;321(3):288-300.

240. Szostakowska M, Trebinska-Stryjewska A, Grzybowska EA, Fabisiewicz A. Resistance to endocrine therapy in breast cancer: Molecular mechanisms and future goals. *Breast Cancer Research and Treatment* 2019;173(3):489-497.

241. Kam Y, Das T, Minton S, Gatenby RA. Evolutionary strategy for systemic therapy of metastatic breast cancer: Balancing response with suppression of resistance. *Womens Health (Lond)* 2014;10(4):423-430.

242. Moo TA, Sanford R, Dang C, Morrow M. Overview of breast cancer therapy. *PET Clinics* 2018;13(3):339-354.

243. Tremont A, Lu J, Cole JT. Endocrine therapy for early breast cancer: Updated review. *Ochsner Journal* 2017;17(4):405-411.

244. Abdel-Razeq H. Current frontline endocrine treatment options for women with hormone receptor-positive, human epidermal growth factor receptor 2 (HER2)-negative advanced-stage breast cancer. *Hematology/Oncology and Stem Cell Therapy* 2019;12(1):1-9.

245. Piotrzkowska-Wroblewska H, Dobruch-Sobczak K, Klimonda Z, Karwat P, Roszkowska-Purska K, Gumowska M, Litniewski J. Monitoring breast cancer response to neoadjuvant chemotherapy with ultrasound signal statistics and integrated backscatter. *PloS One* 2019;14(3):e0213749.

246. Muss HB, Polley MC, Berry DA, Liu H, Cirrincione CT, Theodoulou M, Mauer AM, Kornblith AB, Partridge AH, Dressler LG, Cohen HJ, Kartcheske PA, Perez EA, Wolff AC, Gralow JR, Burstein HJ, Mahmood AA, Sutton LM, Magrinat G, Parker BA, Hart RD, Grenier D, Hurria A, Jatoi A, Norton L, Hudis CA, Winer EP, Carey L. Randomized trial of standard adjuvant chemotherapy regimens versus capecitabine in older women with early breast cancer: 10-year update of the CALGB 49907 trial. *Journal of Clinical Oncology* 2019;37(26):2338-2348.

247. Oruc Z, Kaplan MA, Arslan C. An update on the currently available and future chemotherapy for treating bone metastases in breast cancer patients. *Expert Opinion on Pharmacotherapy* 2018;19(12):1305-1316.

248. Meric-Bernstam F, Johnson AM, Dumbrava EEI, Raghav K, Balaji K, Bhatt M, Murthy RK, Rodon J, Piha-Paul SA. Advances in HER2-targeted therapy: Novel agents and opportunities beyond breast and gastric cancer. *Clinical Cancer Research* 2019;25(7):2033-2041.

249. Laible M, Hartmann K, Gurtler C, Anzeneder T, Wirtz R, Weber S, Keller T, Sahin U, Rees M, Ramaswamy A. Impact of molecular subtypes on the prediction of distant recurrence in estrogen receptor (ER) positive, human epidermal growth factor receptor 2 (HER2) negative breast cancer upon five years of endocrine therapy. *BMC Cancer* 2019;19(1):694.

250. Nakashoji A, Hayashida T, Yokoe T, Maeda H, Toyota T, Kikuchi M, Watanuki R, Nagayama A, Seki T, Takahashi M, Abe T, Kitagawa Y. The updated network meta-analysis of neoadjuvant therapy for HER2-positive breast cancer. *Cancer Treatment Reviews* 2018;62:9-17.

251. Pareek A, Singh OP, Yogi V, Ghori HU, Tiwari V, Redhu P. Bone metastases incidence and its correlation with hormonal and human epidermal growth factor receptor 2 neu receptors in breast cancer. *Journal of Cancer Research and Therapeutics* 2019;15(5):971-975.

252. Zimmer AS, Gillard M, Lipkowitz S, Lee JM. Update on PARP inhibitors in breast cancer. *Current Treatment Options in Oncology* 2018;19(5):21.

253. McCann KE, Hurvitz SA. Advances in the use of PARP inhibitor therapy for breast cancer. *Drugs Context* 2018;7:212540.

254. Esteva FJ, Hubbard-Lucey VM, Tang J, Pusztai L. Immunotherapy and targeted therapy combinations in metastatic breast cancer. *Lancet Oncology* 2019;20(3):e175-e186.

255. Makhoul I, Atiq M, Alwbari A, Kieber-Emmons T. Breast cancer immunotherapy: An update. *Breast Cancer (Auckl)* 2018;12:1178223418774802.

256. Walstra C, Schipper RJ, Poodt IGM, van Riet YE, Voogd AC, van der Sangen MJC, Nieuwenhuijzen GAP. Repeat breast-conserving therapy for ipsilateral breast cancer recurrence: A systematic review. *European Journal of Surgical Oncology* 2019;45(8):1317-1327.

257. Karakatsanis A, Tasoulis MK, Warnberg F, Nilsson G, MacNeill F. Meta-analysis of neoadjuvant therapy and its impact in facilitating breast conservation in operable breast cancer. *British Journal of Surgery* 2018;105(5):469-481.

258. Zhong Y, Xu Y, Zhou Y, Mao F, Lin Y, Guan J, Shen S, Pan B, Wang C, Peng L, Huang X, Li Y, Wang X, Sun Q. Breast-conserving surgery without axillary lymph node surgery or radiotherapy is safe for HER2-positive and triple negative breast cancer patients over 70 years of age. *Breast Cancer Research and Treatment* 2020;182(1):117-126.

259. Ye F, Huang L, Lang G, Hu X, Di G, Shao Z, Cao A. Outcomes and risk of subsequent breast events in breast-conserving surgery patients with BRCA1 and BRCA2 mutation. *Cancer Med* 2020;9(5):1903-1910.

260. Albornoz CR, Matros E, Lee CN, Hudis CA, Pusic AL, Elkin E, Bach PB, Cordeiro PG, Morrow M. Bilateral mastectomy versus breast-conserving surgery for early-stage breast cancer: The role of breast reconstruction. *Plastic and Reconstructive Surgery* 2015;135(6):1518-1526.

261. Zehra S, Doyle F, Barry M, Walsh S, Kell MR. Health-related quality of life following breast reconstruction compared to total mastectomy and breast-conserving surgery among breast cancer survivors: A systematic review and meta-analysis. *Breast Cancer* 2020;27(4):534-566.

262. Zdravkovic D, Granic M, Crnokrak B. Proper treatment of breast angiosarcoma-mastectomy or breast conserving surgery? *Breast Cancer Research and Treatment* 2020;179(3):765.

263. Devane LA, Baban CK, O'Doherty A, Quinn C, McDermott EW, Prichard RS. The impact of neoadjuvant chemotherapy on margin re-excision in breast-conserving surgery. *World Journal of Surgery* 2020;44(5):1547-1551.

264. Jeon J, Kim SE, Lee DY, Choi D. Factors associated with endometrial pathology during tamoxifen therapy in women with breast cancer: A retrospective analysis of 821 biopsies. *Breast Cancer Research and Treatment* 2020;179(1):125-130.

265. Qian X, Li Z, Ruan G, Tu C, Ding W. Efficacy and toxicity of extended aromatase inhibitors after adjuvant aromatase inhibitors-containing therapy for hormone-receptor-positive breast cancer: A literature-based meta-analysis of randomized trials. *Breast Cancer Research and Treatment* 2019.

266. Rimawi M, Ferrero JM, de la Haba-Rodriguez J, Poole C, De Placido S, Osborne CK, Hegg R, Easton V, Wohlfarth C, Arpino G, Group PS. First-line trastuzumab plus an aromatase inhibitor, with or without pertuzumab, in human epidermal growth factor receptor 2-positive and hormone receptor-positive metastatic or locally advanced breast cancer (PERTAIN): A randomized, open-label Phase II trial. *Journal of Clinical Oncology* 2018;36(28):2826-2835.

267. Montagna E, Cancello G, Bagnardi V, Pastrello D, Dellapasqua S, Perri G, Viale G, Veronesi P, Luini A, Intra M, Calleri A, Rampinelli C, Goldhirsch A, Bertolini F, Colleoni M. Metronomic chemotherapy combined with bevacizumab and erlotinib in patients

with metastatic HER2-negative breast cancer: Clinical and biological activity. *Clinical Breast Cancer* 2012;12(3):207-214.

268. Montagna E, Cancello G, Dellapasqua S, Munzone E, Colleoni M. Metronomic therapy and breast cancer: A systematic review. *Cancer Treatment Reviews* 2014;40(8):942-950.

269. El-Arab LRE, Swellam M, El Mahdy MM. Metronomic chemotherapy in metastatic breast cancer: Impact on VEGF. *Journal of the Egyptian National Cancer Institute* 2012;24(1):15-22.

270. Barchiesi G, Krasniqi E, Barba M, Giulia MD, Pizzuti L, Massimiani G, Ciliberto G, Vici P. Highly durable response to capecitabine in patient with metastatic estrogen receptor positive breast cancer: A case report. *Medicine (Baltimore)* 2019;98(37):e17135.

271. Lu Q, Lee K, Xu F, Xia W, Zheng Q, Hong R, Jiang K, Zhai Q, Li Y, Shi Y, Yuan Z, Wang S. Metronomic chemotherapy of cyclophosphamide plus methotrexate for advanced breast cancer: Real-world data analyses and experience of one center. *Cancer Communications* 2020;40(5):222-233.

272. Denkert C, Liedtke C, Tutt A, von Minckwitz G. Molecular alterations in triple-negative breast cancer—the road to new treatment strategies. *The Lancet* 2017;389(10087):2430-2442.

273. Qiu SQ, Waaijer SJH, Zwager MC, de Vries EGE, van der Vegt B, Schroder CP. Tumor-associated macrophages in breast cancer: Innocent bystander or important player? *Cancer Treatment Reviews* 2018;70:178-189.

274. Place AE, Jin Huh S, Polyak K. The microenvironment in breast cancer progression: Biology and implications for treatment. *Breast Cancer Research* 2011;13(6):227.

275. Baghban R, Roshangar L, Jahanban-Esfahlan R, Seidi K, Ebrahimi-Kalan A, Jaymand M, Kolahian S, Javaheri T, Zare P. Tumor microenvironment complexity and therapeutic implications at a glance. *Cell Communication and Signaling* 2020;18(1):59.

276. Stakheyeva M, Riabov V, Mitrofanova I, Litviakov N, Choynzonov E, Cherdyntseva N, Kzhyshkowska J. Role of the immune component of tumor microenvironment in the efficiency of cancer treatment: Perspectives for the personalized therapy. *Current Pharmaceutical Design* 2017;23(32):4807-4826.

277. Datta M, Coussens LM, Nishikawa H, Hodi FS, Jain RK. Reprogramming the tumor microenvironment to improve immunotherapy: Emerging strategies and combination therapies. *American Society of Clinical Oncology Educational Book* 2019;39:165-174.

278. Shen S, Clairambault J. Cell plasticity in cancer cell populations. *F1000Research* 2020;9.

279. Noy R, Pollard JW. Tumor-associated macrophages: From mechanisms to therapy. *Immunity* 2014;41(1):49-61.

280. Qian B, Deng Y, Im JH, Muschel RJ, Zou Y, Li J, Lang RA, Pollard JW. A distinct macrophage population mediates metastatic breast cancer cell extravasation, establishment and growth. *PloS One* 2009;4(8):e6562.

281. Larionova I, Cherdyntseva N, Liu T, Patysheva M, Rakina M, Kzhyshkowska J. Interaction of tumor-associated macrophages and cancer chemotherapy. *Oncoimmunology* 2019;8(7):1596004.

282. Mantovani A, Marchesi F, Malesci A, Laghi L, Allavena P. Tumor-associated macrophages as treatment targets in oncology. *Nature Reviews Clinical Oncology* 2017;14(7):399-416.

283. Bendell JC, Tolcher AW, Jones SF, Beeram M, Infante JR, Larsen P, Rasor K, Garrus JE, Li J, Cable PL, Eberhardt C, Schreiber J, Rush S, Wood KW, Barrett E, Patnaik A. Abstract A252: A phase 1 study of ARRY-382, an oral inhibitor of colony-stimulating factor-1 receptor (CSF1R), in patients with advanced or metastatic cancers. *Molecular Cancer Therapeutics* 2013;12(11 Supplement):A252-A252.

284. Rogers TL, Holen I. Tumor macrophages as potential targets of bisphosphonates. *Journal of Translational Medicine* 2011;9(1):177.

285. Stasinopoulos I, Shah T, Penet M-F, Krishnamachary B, Bhujwalla Z. Cox-2 in cancer: Gordian knot or Achilles heel? *Frontiers in Pharmacology* 2013;4(34).

286. Goldstein LJ, Gurtler J, Del Prete SA, Tjulandin S, Semiglazov VF, Bayever E, Michiels B. Trabectedin as a single-agent treatment of advanced breast cancer after anthracycline and taxane treatment: A multicenter, randomized, Phase II study comparing 2 administration regimens. *Clinical Breast Cancer* 2014;14(6):396-404.

287. Blum JL, Gonçalves A, Efrat N, Debled M, Conte P, Richards PD, Richards D, Lardelli P, Nieto A, Cullell-Young M, Delaloge S. A phase II trial of trabectedin in triple-negative and HER2-overexpressing metastatic breast cancer. *Breast Cancer Research and Treatment* 2016;155(2):295-302.

288. Twarog NR, Connelly M, Shelat AA. A critical evaluation of methods to interpret drug combinations. *Scientific Reports* 2020;10(1):5144.

289. DeVita VT, Jr., Young RC, Canellos GP. Combination versus single agent chemotherapy: A review of the basis for selection of drug treatment of cancer. *Cancer* 1975;35(1):98-110.

290. van Hasselt JGC, Iyengar R. Systems pharmacology: Defining the interactions of drug combinations. *Annual Review of Pharmacology and Toxicology* 2019;59:21-40.

291. Vakil V, Trappe W. Drug combinations: Mathematical modeling and networking methods. *Pharmaceutics* 2019;11(5).

292. Weinstein ZB, Bender A, Cokol M. Prediction of synergistic drug combinations. *Current Opinion in Systems Biology* 2017;4:24-28.

293. Masood I, Kiani MH, Ahmad M, Masood MI, Sadaquat H. Major contributions towards finding a cure for cancer through chemotherapy: A historical review. *Tumori Journal* 2016;102(1):6-17.

294. Twarog NR, Stewart E, Hammill CV, Shelat AA. Braid: A unifying paradigm for the analysis of combined drug action. *Scientific Reports* 2016;6(1):25523.

295. Zimmer A, Katzir I, Dekel E, Mayo AE, Alon U. Prediction of multidimensional drug dose responses based on measurements of drug pairs. *Proceedings of the National Academy of Sciences* 2016;113(37):10442-10447.

296. Sauter ER. Cancer prevention and treatment using combination therapy with natural compounds. *Expert Review of Clinical Pharmacology* 2020;13(3):265-285.

297. Geldof T, Rawal S, Dyck WV, Huys I. Comparative and combined effectiveness of innovative therapies in cancer: A literature review. *Journal of Comparative Effectiveness Research* 2019;8(4):205-216.

298. Nair PR. Delivering combination chemotherapies and targeting oncogenic pathways via polymeric drug delivery systems. *Polymers (Basel)* 2019;11(4).

299. Madani Tonekaboni SA, Soltan Ghoraie L, Manem VSK, Haibe-Kains B. Predictive approaches for drug combination discovery in cancer. *Briefings in Bioinformatics* 2016;19(2):263-276.

300. Dry JR, Yang M, Saez-Rodriguez J. Looking beyond the cancer cell for effective drug combinations. *Genome Medicine* 2016;8(1):125.

301. Zheng W, Sun W, Simeonov A. Drug repurposing screens and synergistic drug-combinations for infectious diseases. *British journal of pharmacology* 2018;175(2):181-191.

302. Pál C, Papp B, Lázár V. Collateral sensitivity of antibiotic-resistant microbes. *Trends in Microbiology* 2015;23(7):401-407.

303. Darrason M. Mechanistic and topological explanations in medicine: The case of medical genetics and network medicine. *Synthese* 2018;195(1):147-173.

304. Loscalzo J, Kohane I, Barabasi AL. Human disease classification in the postgenomic era: A complex systems approach to human pathobiology. *Molecular Systems Biology* 2007;3:124.

305. Marusyk A, Janiszewska M, Polyak K. Intratumor heterogeneity: The Rosetta stone of therapy resistance. *Cancer Cell* 2020;37(4):471-484.

306. Acar A, Nichol D, Fernandez-Mateos J, Cresswell GD, Barozzi I, Hong SP, Trahearn N, Spiteri I, Stubbs M, Burke R, Stewart A, Caravagna G, Werner B, Vlachogiannis G, Maley CC, Magnani L, Valeri N, Banerji U, Sottoriva A. Exploiting evolutionary steering to induce collateral drug sensitivity in cancer. *Nature Communications* 2020;11(1):1923.

307. Ginsburg GS, McCarthy JJ. Personalized medicine: Revolutionizing drug discovery and patient care. *Trends in Biotechnology* 2001;19(12):491-496.

308. Meyer JM, Ginsburg GS. The path to personalized medicine. *Current Opinion in Chemical Biology* 2002;6(4):434-438.

309. Apellaniz-Ruiz M, Gallego C, Ruiz-Pinto S, Carracedo A, Rodríguez-Antona C. Human genetics: International projects and personalized medicine. *Drug Metabolism and Personalized Therapy* 2016;31(1):3-8.

310. Iyengar R. Complex diseases require complex therapies. *EMBO Reports* 2013;14(12):1039-1042.

311. Keith CT, Borisy AA, Stockwell BR. Multicomponent therapeutics for networked systems. *Nature Reviews Drug Discovery* 2005;4(1):71-78.

312. Al-Lazikani B, Banerji U, Workman P. Combinatorial drug therapy for cancer in the post-genomic era. *Nature Biotechnology* 2012;30(7):679-692.

313. Zhao B, Sedlak JC, Srinivas R, Creixell P, Pritchard JR, Tidor B, Lauffenburger DA, Hemann MT. Exploiting temporal collateral sensitivity in tumor clonal evolution. *Cell* 2016;165(1):234-246.

314. Chou T-C. The combination index (CI < 1) as the definition of synergism and of synergy claims. *Synergy* 2018;7:49-50.

315. Chou TC. Drug combination studies and their synergy quantification using the Chou-Talalay method. *Cancer Research* 2010;70(2):440-446.

316. Loewe S. The problem of synergism and antagonism of combined drugs. *Arzneimittel-Forschung* 1953;3(6):285-290.

317. Bliss CI. The toxicity of poisons applied jointly1. *Annals of Applied Biology* 1939;26(3):585-615.

318. Greco WR, Bravo G, Parsons JC. The search for synergy: A critical review from a response surface perspective. *Pharmacological Reviews* 1995;47(2):331-385.

319. Berenbaum MC. Synergy, additivism and antagonism in immunosuppression. A critical review. *Clinical and Experimental Immunology* 1977;28(1):1-18.

320. Lederer S, Dijkstra TMH, Heskes T. Additive dose response models: Defining synergy. *Frontiers in Pharmacology* 2019;10:1384.

321. Schindler M. Theory of synergistic effects: Hill-type response surfaces as 'null-interaction' models for mixtures. *Theoretical Biology & Medical Modelling* 2017;14(1):15.

322. Goldoni M, Johansson C. A mathematical approach to study combined effects of toxicants in vitro: Evaluation of the Bliss independence criterion and the Loewe additivity model. *Toxicology In Vitro* 2007;21(5):759-769.

323. Saputra EC, Huang L, Chen Y, Tucker-Kellogg L. Combination therapy and the evolution of resistance: The theoretical merits of synergism and antagonism in cancer. *Cancer Research* 2018;78(9):2419-2431.

324. Chou TC. Theoretical basis, experimental design, and computerized simulation of synergism and antagonism in drug combination studies. *Pharmacological Reviews* 2006;58(3):621-681.

325. Kashif M, Andersson C, Mansoori S, Larsson R, Nygren P, Gustafsson MG. Bliss and Loewe interaction analyses of clinically relevant drug combinations in human colon cancer cell lines reveal complex patterns of synergy and antagonism. *Oncotarget* 2017;8(61):103952-103967.

326. Demidenko E, Miller TW. Statistical determination of synergy based on Bliss definition of drugs independence. *PloS One* 2019;14(11):e0224137.

327. Chou TC, Talalay P. Quantitative analysis of dose-effect relationships: The combined effects of multiple drugs or enzyme inhibitors. *Advances in Enzyme Regulation* 1984;22:27-55.

328. Vander Velde R, Yoon N, Marusyk V, Durmaz A, Dhawan A, Miroshnychenko D, Lozano-Peral D, Desai B, Balynska O, Poleszhuk J, Kenian L, Teng M, Abazeed M, Mian O, Tan AC, Haura E, Scott J, Marusyk A. Resistance to targeted therapies as a multifactorial, gradual adaptation to inhibitor specific selective pressures. *Nature Communications* 2020;11(1):2393.

329. Szakacs G, Hall MD, Gottesman MM, Boumendjel A, Kachadourian R, Day BJ, Baubichon-Cortay H, Di Pietro A. Targeting the Achilles heel of multidrug-resistant cancer by exploiting the fitness cost of resistance. *Chemical Reviews* 2014;114(11):5753-5774.

330. Munck C, Gumpert HK, Wallin AI, Wang HH, Sommer MO. Prediction of resistance development against drug combinations by collateral responses to component drugs. *Science Translational Medicine* 2014;6(262):262ra156.

331. Foo J, Michor F. Evolution of acquired resistance to anti-cancer therapy. *Journal of Theoretical Biology* 2014;355:10-20.

332. Imamovic L, Sommer MO. Use of collateral sensitivity networks to design drug cycling protocols that avoid resistance development. *Science Translational Medicine* 2013;5(204):204ra132.

333. Szybalski W, Bryson V. Genetic studies on microbial cross resistance to toxic agents. I. Cross resistance of escherichia coli to fifteen antibiotics. *Journal of Bacteriology* 1952;64(4):489-499.

334. Pluchino KM, Hall MD, Goldsborough AS, Callaghan R, Gottesman MM. Collateral sensitivity as a strategy against cancer multidrug resistance. *Drug Resistance Updates* 2012;15(1-2):98-105.

335. O'Neil NJ, Bailey ML, Hieter P. Synthetic lethality and cancer. *Nature Reviews: Genetics* 2017;18(10):613-623.

336. Vasan N, Baselga J, Hyman DM. A view on drug resistance in cancer. *Nature* 2019;575(7782):299-309.

337. Jariyal H, Weinberg F, Achreja A, Nagarath D, Srivastava A. Synthetic lethality: A step forward for personalized medicine in cancer. *Drug Discovery Today* 2020;25(2):305-320.

338. Bosanquet AG, Bell PB. Novel ex vivo analysis of nonclassical, pleiotropic drug resistance and collateral sensitivity induced by therapy provides a rationale for treatment strategies in chronic lymphocytic leukemia. *Blood* 1996;87(5):1962-1971.

339. Hall MD, Handley MD, Gottesman MM. Is resistance useless? Multidrug resistance and collateral sensitivity. *Trends in Pharmacological Sciences* 2009;30(10):546-556.

340. Shen DW, Akiyama S, Schoenlein P, Pastan I, Gottesman MM. Characterisation of high-level cisplatin-resistant cell lines established from a human hepatoma cell line and human KB adenocarcinoma cells: Cross-resistance and protein changes. *British Journal of Cancer* 1995;71(4):676-683.

341. Bech-Hansen NT, Till JE, Ling V. Pleiotropic phenotype of colchicine-resistant CHO cells: Cross-resistance and collateral sensitivity. *Journal of Cellular Physiology* 1976;88(1):23-31.

342. Loewe S. The problem of synergism and antagonism of combined drugs. *Arzneimittel-Forschung* 1953;3(6):285-290.

343. Loewe S. Antagonism and antagonists. *Pharmacological Reviews* 1957;9:237–242.

344. Loewe S, Muischnek H. Effect of combinations: Mathematical basis of the problem. *Naunyn-Schmiedebergs Archiv für Experimentelle Pathologie und Pharmakologie* 1926;114:313 - 326.

345. Berenbaum MC. A method for testing for synergy with any number of agents. *The Journal of Infectious Diseases* 1978;137(2):122-130.

346. Chou T-C, Talalay P. Analysis of combined drug effects: A new look at a very old problem. *Trends in Pharmacological Sciences* 1983;4:450-454.

347. Foucquier J, Guedj M. Analysis of drug combinations: Current methodological landscape. *Pharmacology Research & Perspectives* 2015;3(3):e00149.

348. Ianevski A, Giri AK, Aittokallio T. Synergyfinder 2.0: Visual analytics of multi-drug combination synergies. *Nucleic Acids Research* 2020;48(W1):W488-W493.

349. Bulusu KC, Guha R, Mason DJ, Lewis RP, Muratov E, Kalantar Motamedi Y, Cokol M, Bender A. Modelling of compound combination effects and applications to efficacy and toxicity: State-of-the-art, challenges and perspectives. *Drug Discovery Today* 2016;21(2):225-238.

350. Meyer CT, Wooten DJ, Lopez CF, Quaranta V. Charting the fragmented landscape of drug synergy. *Trends in Pharmacological Sciences* 2020;41(4):266-280.

351. Beca F, Polyak K. Intratumor heterogeneity in breast cancer. *Advances in Experimental Medicine and Biology* 2016;882:169-189.

352. Fisusi FA, Akala EO. Drug combinations in breast cancer therapy. *Pharmaceutical Nanotechnology* 2019;7(1):3-23.

353. Buchholz TA, Mittendorf EA, Hunt KK. Surgical considerations after neoadjuvant chemotherapy: Breast conservation therapy. *Journal of the National Cancer Institute Monographs* 2015;2015(51):11-14.

354. Cortazar P, Zhang L, Untch M, Mehta K, Costantino JP, Wolmark N, Bonnefoi H, Cameron D, Gianni L, Valagussa P, Swain SM, Prowell T, Loibl S, Wickerham DL, Bogaerts J, Baselga J, Perou C, Blumenthal G, Blohmer J, Mamounas EP, Bergh J, Semiglazov V, Justice R, Eidtmann H, Paik S, Piccart M, Sridhara R, Fasching PA, Slaets L, Tang S, Gerber B, Geyer CE, Jr., Pazdur R, Ditsch N, Rastogi P, Eiermann W, von Minckwitz G. Pathological complete response and long-term clinical benefit in breast cancer: The ctneobc pooled analysis. *The Lancet* 2014;384(9938):164-172.

355. Rose M, Svensson H, Handler J, Hoyer U, Ringberg A, Manjer J. Patient-reported outcome after oncoplastic breast surgery compared with conventional breast-conserving surgery in breast cancer. *Breast Cancer Research and Treatment* 2020;180(1):247-256.

356. Rastogi P, Anderson SJ, Bear HD, Geyer CE, Kahlenberg MS, Robidoux A, Margolese RG, Hoehn JL, Vogel VG, Dakhil SR, Tamkus D, King KM, Pajon ER, Wright MJ, Robert J, Paik S, Mamounas EP, Wolmark N. Preoperative chemotherapy: Updates of national surgical adjuvant breast and bowel project protocols B-18 and B-27. *Journal of Clinical Oncology* 2008;26(5):778-785.

357. Cardoso F, Kyriakides S, Ohno S, Penault-Llorca F, Poortmans P, Rubio IT, Zackrisson S, Senkus E. Early breast cancer: ESMO Clinical Practice Guidelines for diagnosis, treatment and follow-up. *Annals of Oncology* 2019;30(8):1194-1220.

358. Early Breast Cancer Trialists' Collaborative Group (EBCTCG). Comparisons between different polychemotherapy regimens for early breast cancer: Meta-analyses of long-term outcome among 100 000 women in 123 randomised trials. *The Lancet* 2012;379(9814):432-444.

359. Fares J, Kanojia D, Rashidi A, Ulasov I, Lesniak MS. Landscape of combination therapy trials in breast cancer brain metastasis. *International Journal of Cancer* 2020.

360. Kawachi A, Yamashita S, Okochi-Takada E, Hirakawa A, Tsuda H, Shimomura A, Kojima Y, Yonemori K, Fujiwara Y, Kinoshita T, Ushijima T, Tamura K. BRCA1 promoter methylation in breast cancer patients is associated with response to olaparib/eribulin combination therapy. *Breast Cancer Research and Treatment* 2020;181(2):323-329.

361. Gadag S, Sinha S, Nayak Y, Garg S, Nayak UY. Combination therapy and nanoparticulate systems: Smart approaches for the effective treatment of breast cancer. *Pharmaceutics* 2020;12(6).

362. Shimomura A, Yonemori K, Yoshida M, Yoshida T, Yasojima H, Masuda N, Aogi K, Takahashi M, Naito Y, Shimizu S, Nakamura R, Hamada A, Michimae H, Hashimoto J, Yamamoto H, Kawachi A, Shimizu C, Fujiwara Y, Tamura K. Gene alterations in triple-negative breast cancer patients in a Phase I/II study of eribulin and olaparib combination therapy. *Translational Oncology* 2019;12(10):1386-1394.

363. Zhumakayeva A, Rakhimov K, Sirota V, Arystan L, Madiyarov A, Adekenov S. Long-term results of combination therapy for locally advanced breast cancer. *Georgian Medical News* 2018(282):30-35.

364. Malorni L, Curigliano G, Minisini AM, Cinieri S, Tondini CA, D'Hollander K, Arpino G, Bernardo A, Martignetti A, Criscitiello C, Puglisi F, Pestrin M, Sanna G, Moretti E, Risi E, Biagioni C, McCartney A, Boni L, Buyse M, Migliaccio I, Biganzoli L, Di Leo A. Palbociclib as single agent or in combination with the endocrine therapy received before disease progression for estrogen receptor-positive, HER2-negative metastatic breast cancer: TREND trial. *Annals of Oncology* 2018;29(8):1748-1754.

365. Freedman RA, Tolaney SM. Efficacy and safety in older patient subsets in studies of endocrine monotherapy versus combination therapy in patients with HR+/HER2-advanced breast cancer: A review. *Breast Cancer Research and Treatment* 2018;167(3):607-614.

366. Hu ZI, Ho AY, McArthur HL. Combined radiation therapy and immune checkpoint blockade therapy for breast cancer. *International Journal of Radiation Oncology, Biology, & Physics* 2017;99(1):153-164.

367. Xu D, Chen X, Li X, Mao Z, Tang W, Zhang W, Ding L, Tang J. Addition of capecitabine in breast cancer first-line chemotherapy improves survival of breast cancer patients. *Journal of Cancer* 2019;10(2):418-429.

368. West J, You L, Zhang J, Gatenby RA, Brown JS, Newton PK, Anderson ARA. Towards multidrug adaptive therapy. *Cancer Research* 2020;80(7):1578-1589.

369. Lee TD, Lee OW, Brimacombe KR, Chen L, Guha R, Lusvarghi S, Tebase BG, Klumpp-Thomas C, Robey RW, Ambudkar SV, Shen M, Gottesman MM, Hall MD. A high-throughput screen of a library of therapeutics identifies cytotoxic substrates of P-glycoprotein. *Molecular Pharmacology* 2019;96(5):629-640.

370. Iorio F, Garcia-Alonso L, Brammeld JS, Martincorena I, Wille DR, McDermott U, Saez-Rodriguez J. Pathway-based dissection of the genomic heterogeneity of cancer hallmarks' acquisition with SLAPenrich. *Scientific Reports* 2018;8(1):6713.

371. Mullard A. Stemming the tide of drug resistance in cancer. *Nature Reviews Drug Discovery* 2020;19(4):221-223.

372. Pan H, Gray R, Braybrooke J, Davies C, Taylor C, McGale P, Peto R, Pritchard KI, Bergh J, Dowsett M, Hayes DF. 20-year risks of breast-cancer recurrence after stopping endocrine therapy at 5 years. *New England Journal of Medicine* 2017;377(19):1836-1846.

373. Masuda N, Lee SJ, Ohtani S, Im YH, Lee ES, Yokota I, Kuroi K, Im SA, Park BW, Kim SB, Yanagita Y, Ohno S, Takao S, Aogi K, Iwata H, Jeong J, Kim A, Park KH, Sasano H, Ohashi Y, Toi M. Adjuvant capecitabine for breast cancer after preoperative chemotherapy. *New England Journal of Medicine* 2017;376(22):2147-2159.

374. Cardoso F, Senkus E, Costa A, Papadopoulos E, Aapro M, Andre F, Harbeck N, Aguilar Lopez B, Barrios CH, Bergh J, Biganzoli L, Boers-Doets CB, Cardoso MJ, Carey LA, Cortes J, Curigliano G, Dieras V, El Saghir NS, Eniu A, Fallowfield L, Francis PA, Gelmon K, Johnston SRD, Kaufman B, Koppikar S, Krop IE, Mayer M, Nakigudde G, Offersen BV, Ohno S, Pagani O, Paluch-Shimon S, Penault-Llorca F, Prat A, Rugo HS, Sledge GW, Spence D, Thomssen C, Vorobiof DA, Xu B, Norton L, Winer EP. 4th ESO-ESMO International Consensus Guidelines for advanced breast cancer (ABC). *Annals of Oncology* 2018;29(8):1634-1657.

375. Winters S, Martin C, Murphy D, Shokar NK. Breast cancer epidemiology, prevention, and screening. *Progress in Molecular Biology and Translational Science* 2017;151:1-32.

376. Hossain MS, Ferdous S, Karim-Kos HE. Breast cancer in south asia: A Bangladeshi perspective. *Cancer Epidemiology* 2014;38(5):465-470.

377. Allemani C, Matsuda T, Di Carlo V, Harewood R, Matz M, Nikšić M, Bonaventure A, Valkov M, Johnson CJ, Estève J, Ogunbiyi OJ, Azevedo e Silva G, Chen W-Q, Eser S, Engholm G, Stiller CA, Monnereau A, Woods RR, Visser O, Lim GH, Aitken J, Weir HK, Coleman MP, Bouzbid S, Hamdi-Chérif M, Zaidi Z, Meguenni K, Regagba D, Bayo S, Cheick Bougadari T, Manraj SS, Bendahhou K, Fabowale A, Bradshaw D, Somdyala NIM, Kumcher I, Moreno F, Calabrano GH, Espinola SB, Carballo Quintero B, Fita R, Diumenjo MC, Laspada WD, Ibañez SG, Lima CA, De Souza PCF, Del Pino K, Laporte C, Curado MP, de Oliveira JC, Veneziano CLA, Veneziano DB, Latorre MRDO, Tanaka LF, Rebelo MS, Santos MO, Galaz JC, Aparicio Aravena M, Sanhueza Monsalve J, Herrmann DA, Vargas S, Herrera VM, Uribe CJ, Bravo LE, Garcia LS, Arias-Ortiz NE, Morantes D, Jurado DM, Yépez Chamorro MC, Delgado S, Ramirez M, Galán Alvarez YH, Torres P, Martínez-Reyes F, Jaramillo L, Quinto R, Castillo J, Mendoza M, Cueva P, Yépez JG, Bhakkan B, Deloumeaux J, Joachim C, Macni J, Carrillo R, Shalkow Klincovstein J, Rivera Gomez R, Poquioma E, Tortolero-Luna G, Zavala D, Alonso R, Barrios E, Eckstrand A, Nikiforuk C, Noonan G, Turner D, Kumar E, Zhang B, McCrate FR, Ryan S, MacIntyre M, Saint-Jacques N, Nishri DE, McClure CA, Vriends KA, Kozie S, Stuart-Panko H, Freeman T, George JT, Brockhouse JT, O'Brien DK, Holt A, Almon L, Kwong S, Morris C, Rycroft R, Mueller L, Phillips CE, Brown H, Cromartie B, Schwartz AG, Vigneau F, Levin GM, Wohler B, Bayakly R, Ward KC, Gomez SL, McKinley M, Cress R, Green MD, Miyagi K, Ruppert LP, Lynch CF, Huang B, Tucker TC, Deapen D, Liu L, Hsieh MC, Wu XC, Schwenn M, Gershman ST, Knowlton RC, Alverson G, Copeland GE, Bushhouse S, Rogers DB, Jackson-Thompson J, Lemons D, Zimmerman HJ, Hood M, Roberts-Johnson J, Rees JR, Riddle B, Pawlish KS, Stroup A, Key C, Wiggins C, Kahn AR, Schymura MJ, Radhakrishnan S, Rao C, Giljahn LK, Slocumb RM, Espinoza RE, Khan F, Aird KG, Beran T, Rubertone JJ, Slack SJ, Garcia L, Rousseau DL, Janes TA, Schwartz SM, Bolick SW, Hurley DM, Whiteside MA, Miller-Gianturco P, Williams MA, Herget K, Sweeney C, Johnson AT, Keitheri Cheteri MB, Migliore Santiago P, Blankenship SE, Farley S, Borchers R, Malicki R, Espinoza JR, Grandpre J, Wilson R, Edwards BK, Mariotto A, Lei Y, Wang N, Chen JS, Zhou Y, He YT, Song GH, Gu XP, Mei D, Mu HJ, Ge HM, Wu TH, Li YY, Zhao DL, Jin F, Zhang JH, Zhu FD, Junhua Q, Yang YL, Jiang CX, Biao W, Wang J, Li QL, Yi H, Zhou X, Dong J, Li W, Fu FX, Liu SZ, Chen JG, Zhu J, Li YH, Lu YQ, Fan M, Huang SQ, Guo GP, Zhaolai H, Wei K, Zeng H, Demetriou

AV, Mang WK, Ngan KC, Kataki AC, Krishnatreya M, Jayalekshmi PA, Sebastian P, Nandakumar A, Malekzadeh R, Roshandel G, Keinan-Boker L, Silverman BG, Ito H, Nakagawa H, Sato M, Tobori F, Nakata I, Teramoto N, Hattori M, Kaizaki Y, Moki F, Sugiyama H, Utada M, Nishimura M, Yoshida K, Kurosawa K, Nemoto Y, Narimatsu H, Sakaguchi M, Kanemura S, Naito M, Narisawa R, Miyashiro I, Nakata K, Sato S, Yoshii M, Oki I, Fukushima N, Shibata A, Iwasa K, Ono C, Nimri O, Jung KW, Won YJ, Alawadhi E, Elbasmi A, Ab Manan A, Adam F, Sanjaajmats E, Tudev U, Ochir C, Al Khater AM, El Mistiri MM, Teo YY, Chiang CJ, Lee WC, Buasom R, Sangrajrang S, Kamsa-ard S, Wiangnon S, Daoprasert K, Pongnikorn D, Leklob A, Sangkitipaiboon S, Geater SL, Sriplung H, Ceylan O, Kög I, Dirican O, Köse T, Gurbuz T, Karaşahin FE, Turhan D, Aktaş U, Halat Y, Yakut CI, Altinisik M, Cavusoglu Y, Türkköylü A, Üçüncü N, Hackl M, Zborovskaya AA, Aleinikova OV, Henau K, Van Eycken L, Valerianova Z, Yordanova MR, Šekerija M, Dušek L, Zvolský M, Storm H, Innos K, Mägi M, Malila N, Seppä K, Jégu J, Velten M, Cornet E, Troussard X, Bouvier AM, Guizard AV, Bouvier V, Launoy G, Arveux P, Maynadié M, Mounier M, Woronoff AS, Daoulas M, Robaszkiewicz M, Clavel J, Goujon S, Lacour B, Baldi I, Pouchieu C, Amadeo B, Coureau G, Orazio S, Preux PM, Rharbaoui F, Marrer E, Trétarre B, Colonna M, Delafosse P, Ligier K, Plouvier S, Cowppli-Bony A, Molinié F, Bara S, Ganry O, Lapôtre-Ledoux B, Grosclaude P, Bossard N, Uhry Z, Bray F, Piñeros M, Stabenow R, Wilsdorf-Köhler H, Eberle A, Luttmann S, Löhden I, Nennecke AL, Kieschke J, Sirri E, Emrich K, Zeissig SR, Holleczek B, Eisemann N, Katalinic A, Asquez RA, Kumar V, Petridou E, Ólafsdóttir EJ, Tryggvadóttir L, Clough-Gorr K, Walsh PM, Sundseth H, Mazzoleni G, Vittadello F, Coviello E, Cuccaro F, Galasso R, Sampietro G, Giacomin A, Magoni M, Ardizzone A, D'Argenzio A, Castaing M, Grosso G, Lavecchia AM, Sutera Sardo A, Gola G, Gatti L, Ricci P, Ferretti S, Serraino D, Zucchetto A, Celesia MV, Filiberti RA, Pannozzo F, Melcarne A, Quarta F, Russo AG, Carrozzi G, Cirilli C, Cavalieri d'Oro L, Rognoni M, Fusco M, Vitale MF, Usala M, Cusimano R, Mazzucco W, Michiara M, Sgargi P, Boschetti L, Borciani E, Seghini P, Maule MM, Merletti F, Tumino R, Mancuso P, Vicentini M, Cassetti T, Sassatelli R, Falcini F, Giorgetti S, Caiazzo AL, Cavallo R, Cesaraccio R, Pirino DR, Contrino ML, Tisano F, Fanetti AC, Maspero S, Carone S, Mincuzzi A, Candela G, Scuderi T, Gentilini MA, Piffer S, Rosso S, Barchielli A, Caldarella A, Bianconi F, Stracci F, Contiero P, Tagliabue G, Rugge M, Zorzi M, Beggiato S, Brustolin A, Berrino F, Gatta G, Sant M, Buzzoni C, Mangone L, Capocaccia R, De Angelis R, Zanetti R, Maurina A, Pildava S, Lipunova N, Vincerževskienė I, Agius D, Calleja N, Siesling S, Larønningen S, Møller B, Dyzmann-Sroka A, Trojanowski M, Góźdź S, Mężyk R, Mierzwa T, Molong L, Rachtan J, Szewczyk S, Błaszczyk J, Kępska K, Kościańska B, Tarocińska K, Zwierko M, Drosik K, Maksimowicz KM, Purwin-Porowska E, Reca E, Wójcik-Tomaszewska J, Tukiendorf A, Grądalska-Lampart M, Radziszewska AU, Gos A, Talerczyk M, Wyborska M, Didkowska JA, Wojciechowska U, Bielska-Lasota M, Forjaz de Lacerda G, Rego RA, Bastos J, Silva MA, Antunes L, Laranja Pontes J, Mayer-da-Silva A, Miranda A, Blaga LM, Coza D, Gusenkova L, Lazarevich O, Prudnikova O, Vjushkov DM, Egorova AG, Orlov AE, Kudyakov LA, Pikalova LV, Adamcik J, Safaei Diba C, Primic-Žakelj M, Zadnik V, Larrañaga N, Lopez de Munain A, Herrera AA, Redondas R, Marcos-Gragera R, Vilardell Gil ML, Molina E, Sánchez Perez MJ, Franch Sureda P, Ramos Montserrat M, Chirlaque MD, Navarro C, Ardanaz EE, Guevara MM, Fernández-Delgado R, Peris-Bonet R, Carulla M, Galceran J, Alberich C, Vicente-Raneda M, Khan S, Pettersson D, Dickman P, Avelina I, Staehelin K, Camey B, Bouchardy C, Schaffar R, Frick H, Herrmann C, Bulliard JL, Maspoli-Conconi M, Kuehni CE, Redmond SM, Bordoni A, Ortelli L, Chiolero A, Konzelmann I, Matthes KL, Rohrmann S, Broggio J, Rashbass J, Fitzpatrick D, Gavin A, Clark DI, Deas AJ, Huws DW, White C, Montel L, Rachet B, Turculet AD, Stephens R, Chalker E, Phung H, Walton R, You H, Guthridge S, Johnson F, Gordon P, D'Onise K, Priest K, Stokes BC, Venn A, Farrugia H, Thursfield V, Dowling J, Currow D, Hendrix J, Lewis C. Global surveillance of trends in cancer survival 2000–14 (CONCORD-3): Analysis of individual records for 37 513 025 patients diagnosed with one of 18 cancers from 322 population-based registries in 71 countries. *The Lancet* 2018;391(10125):1023-1075.

378. Cortes J, Perez-Garcia JM, Llombart-Cussac A, Curigliano G, El Saghir NS, Cardoso F, Barrios CH, Wagle S, Roman J, Harbeck N, Eniu A, Kaufman PA, Tabernero J, Garcia-Estevez L, Schmid P, Arribas J. Enhancing global access to cancer medicines. *CA: A Cancer Journal for Clinicians* 2020.

379. Buonomo OC, Caredda E, Portarena I, Vanni G, Orlandi A, Bagni C, Petrella G, Palombi L, Orsaria P. New insights into the metastatic behavior after breast cancer surgery, according to well-established clinicopathological variables and molecular subtypes. *PloS One* 2017;12(9):e0184680.

380. Ahmad A. Pathways to breast cancer recurrence. *International Scholarly Research Notices* 2013;2013:290568.

381. Linn SC, Honkoop AH, Hoekman K, van der Valk P, Pinedo HM, Giaccone G. p53 and P-glycoprotein are often co-expressed and are associated with poor prognosis in breast cancer. *British Journal of Cancer* 1996;74(1):63-68.

382. Yamanouchi K, Kuba S, Eguchi S. Hormone receptor, human epidermal growth factor receptor-2, and Ki-67 status in primary breast cancer and corresponding recurrences or synchronous axillary lymph node metastases. *Surg Today* 2019.

383. Prajoko YW, Aryandono T. The effect of p-glycoprotein (P-gp), nuclear factor-kappa b (NF-kappab), and aldehyde dehydrogenase-1 (ALDH-1) expression on metastases, recurrence and survival in advanced breast cancer patients. *Asian Pacific Journal of Cancer Prevention* 2019;20(5):1511-1518.

384. Jeon SH, Shin KH, Kim JH, Kim K, Kim IA, Lee KH, Kim TY, Im SA. Effects of trastuzumab on locoregional recurrence in human epidermal growth factor receptor 2-overexpressing breast cancer patients treated with chemotherapy and radiotherapy. *Breast Cancer Research and Treatment* 2018;172(3):619-626.

385. Chen X, Fan Y, Xu B. Distinct characteristics and metastatic behaviors of late recurrence in patients with hormone receptor-positive/human epidermal growth factor receptor 2-negative breast cancer: A single institute experience of more than 10 years. *Clinical Breast Cancer* 2018;18(6):e1353-e1360.

386. Milata JL, Otte JL, Carpenter JS. Oral endocrine therapy nonadherence, adverse effects, decisional support, and decisional needs in women with breast cancer. *Cancer Nursing* 2018;41(1):E9-E18.

387. Mao JJ, Chung A, Benton A, Hill S, Ungar L, Leonard CE, Hennessy S, Holmes JH. Online discussion of drug side effects and discontinuation among breast cancer survivors. *Pharmacoepidemiology and Drug Safety* 2013;22(3):256-262.

388. Martel S, Bruzzone M, Ceppi M, Maurer C, Ponde NF, Ferreira AR, Viglietti G, Del Mastro L, Prady C, de Azambuja E, Lambertini M. Risk of adverse events with the addition of targeted agents to endocrine therapy in patients with hormone receptor-positive metastatic breast cancer: A systematic review and meta-analysis. *Cancer Treatment Reviews* 2018;62:123-132.

389. Brockway JP, Shapiro CL. Improving adherence to endocrine therapy in women with HR-positive breast cancer. *Oncology (Williston Park)* 2018;32(5):235-237, 249.

390. Wazir U, Mokbel L, Wazir A, Mokbel K. Optimizing adjuvant endocrine therapy for early ER+ breast cancer: An update for surgeons. *American Journal of Surgery* 2019;217(1):152-155.

391. van Hellemond IEG, Geurts SME, Tjan-Heijnen VCG. Current status of extended adjuvant endocrine therapy in early stage breast cancer. *Current Treatment Options in Oncology* 2018;19(5):26.

392. Liu X. Chapter 2 - ABC family transporters. In: Liu X, GuoyuPan, eds. *Advances in Experimental Medicine and Biology*. 2019/10/02 ed. Singapore: Springer; 2019;1141:13-100.

393. Chen Z, Shi T, Zhang L, Zhu P, Deng M, Huang C, Hu T, Jiang L, Li J. Mammalian drug efflux transporters of the ATP binding cassette (ABC) family in multidrug resistance: A review of the past decade. *Cancer Letters* 2016;370(1):153-164.

394. Zhou SF. Structure, function and regulation of P-glycoprotein and its clinical relevance in drug disposition. *Xenobiotica* 2008;38(7-8):802-832.

395. Silva R, Vilas-Boas V, Carmo H, Dinis-Oliveira RJ, Carvalho F, de Lourdes Bastos M, Remiao F. Modulation of P-glycoprotein efflux pump: Induction and activation as a therapeutic strategy. *Pharmacology & Therapeutics* 2015;149:1-123.

396. Robey RW, Pluchino KM, Hall MD, Fojo AT, Bates SE, Gottesman MM. Revisiting the role of ABC transporters in multidrug-resistant cancer. *Nature Reviews Cancer* 2018;18(7):452-464.

397. Fletcher JI, Williams RT, Henderson MJ, Norris MD, Haber M. ABC transporters as mediators of drug resistance and contributors to cancer cell biology. *Drug Resistance Updates* 2016;26:1-9.

398. Slot AJ, Molinski SV, Cole SP. Mammalian multidrug-resistance proteins (MRPs). *Essays in Biochemistry* 2011;50(1):179-207.

399. Keppler D. Multidrug resistance proteins (MRPs, ABCCs): Importance for pathophysiology and drug therapy. In: Fromm MF, Kim RB, eds. *Drug transporters*. Berlin, Heidelberg: Springer Berlin Heidelberg; 2011:299-323.

400. Schinkel AH, Jonker JW. Mammalian drug efflux transporters of the ATP binding cassette (ABC) family: An overview. *Advanced Drug Deliver Reviews* 2003;55(1):3-29.

401. Genovese I, Ilari A, Assaraf YG, Fazi F, Colotti G. Not only P-glycoprotein: Amplification of the ABCB1-containing chromosome region 7q21 confers multidrug resistance upon cancer cells by coordinated overexpression of an assortment of resistance-related proteins. *Drug Resistance* 2017;32:23-46.

402. Albrecht C, Viturro E. The abca subfamily—gene and protein structures, functions and associated hereditary diseases. *Pflügers Archiv - European Journal of Physiology* 2007;453(5):581-589.

403. Childs S, Yeh RL, Hui D, Ling V. Taxol resistance mediated by transfection of the liver-specific sister gene of P-glycoprotein. *Cancer Research* 1998;58(18):4160-4167.

404. Taylor NMI, Manolaridis I, Jackson SM, Kowal J, Stahlberg H, Locher KP. Structure of the human multidrug transporter ABCG2. *Nature* 2017;546(7659):504-509.

405. Esser L, Zhou F, Pluchino KM, Shiloach J, Ma J, Tang WK, Gutierrez C, Zhang A, Shukla S, Madigan JP, Zhou T, Kwong PD, Ambudkar SV, Gottesman MM, Xia D. Structures of the multidrug transporter P-glycoprotein reveal asymmetric ATP binding and the mechanism of polyspecificity. *Journal of Biological Chemistry* 2017;292(2):446-461.

406. Johnson ZL, Chen J. ATP binding enables substrate release from multidrug resistance protein 1. *Cell* 2018;172(1-2):81-89 e10.

407. Callen DF, Baker E, Simmers RN, Seshadri R, Roninson IB. Localization of the human multiple drug resistance gene, MDR1, to 7q21.1. *Human Genetics* 1987;77(2):142-144.

408. Chin JE, Soffir R, Noonan KE, Choi K, Roninson IB. Structure and expression of the human MDR (P-glycoprotein) gene family. *Molecular and Cellular Biology* 1989;9(9):3808-3820.

409. Chen C-j, Chin JE, Ueda K, Clark DP, Pastan I, Gottesman MM, Roninson IB. Internal duplication and homology with bacterial transport proteins in the mdr1 (P-glycoprotein) gene from multidrug-resistant human cells. *Cell* 1986;47(3):381-389.

410. Thiebaut F, Tsuruo T, Hamada H, Gottesman MM, Pastan I, Willingham MC. Cellular localization of the multidrug-resistance gene product P-glycoprotein in normal human tissues. *Proceedings of the National Academy of Sciences* 1987;84(21):7735-7738.

411. Fojo AT, Ueda K, Slamon DJ, Poplack DG, Gottesman MM, Pastan I. Expression of a multidrug-resistance gene in human tumors and tissues. *Proceedings of the National Academy of Sciences* 1987;84(1):265-269.

412. Kathawala RJ, Gupta P, Ashby CR, Chen Z-S. The modulation of ABC transporter-mediated multidrug resistance in cancer: A review of the past decade. *Drug Resistance Updates* 2015;18:1-17.

413. Amawi H, Sim HM, Tiwari AK, Ambudkar SV, Shukla S. ABC transporter-mediated multidrug-resistant cancer. *Advances in Experimental Medicine and Biology* 2019;1141:549-580.

414. Wu S, Fu L. Tyrosine kinase inhibitors enhanced the efficacy of conventional chemotherapeutic agent in multidrug resistant cancer cells. *Molecular Cancer* 2018;17(1):25.

415. Wang J, Seebacher N, Shi H, Kan Q, Duan Z. Novel strategies to prevent the development of multidrug resistance (MDR) in cancer. *Oncotarget* 2017;8(48):84559-84571.

416. Trock BJ, Leonessa F, Clarke R. Multidrug resistance in breast cancer: A meta-analysis of MDR1/gp170 expression and its possible functional significance. *Journal of the National Cancer Institute* 1997;89(13):917-931.

417. Mehrotra M, Anand A, Singh KR, Kumar S, Husain N, Sonkar AA. P-glycoprotein expression in Indian breast cancer patients with reference to molecular subtypes and response to anthracycline-based chemotherapya prospective clinical study from a developing country. *Indian Journal of Surgical Oncology* 2018;9(4):524-529.

418. Badowska-Kozakiewicz AM, Sobol M, Patera J. Expression of multidrug resistance protein P-glycoprotein in correlation with markers of hypoxia (HIF-1alpha, EPO, EPO-r) in invasive breast cancer with metastasis to lymph nodes. *Arch Med Sci* 2017;13(6):1303-1314.

419. Faneyte IF, Kristel PM, van de Vijver MJ. Determining MDR1/P-glycoprotein expression in breast cancer. *International Journal of Cancer* 2001;93(1):114-122.

420. Wishart GC, Plumb JA, Going JJ, McNicol AM, McArdle CS, Tsuruo T, Kaye SB. P-glycoprotein expression in primary breast cancer detected by immunocytochemistry with two monoclonal antibodies. *British Journal of Cancer* 1990;62(5):758-761.

421. Hennessy BT, Gonzalez-Angulo A-M, Stemke-Hale K, Gilcrease MZ, Krishnamurthy S, Lee J-S, Fridlyand J, Sahin A, Agarwal R, Joy C, Liu W, Stivers D, Baggerly K, Carey M, Lluch A, Monteagudo C, He X, Weigman V, Fan C, Palazzo J, Hortobagyi GN, Nolden LK, Wang NJ, Valero V, Gray JW, Perou CM, Mills GB. Characterization of a naturally occurring breast cancer subset enriched in epithelial-to-mesenchymal transition and stem cell characteristics. *Cancer Research* 2009;69(10):4116-4124.

422. Henneman L, van Miltenburg MH, Michalak EM, Braumuller TM, Jaspers JE, Drenth AP, de Korte-Grimmerink R, Gogola E, Szuhai K, Schlicker A, Bin Ali R, Pritchard C, Huijbers IJ, Berns A, Rottenberg S, Jonkers J. Selective resistance to the PARP inhibitor olaparib in a mouse model for BRCA1-deficient metaplastic breast cancer. *Proceedings of the National Academy of Sciences* 2015;112(27):8409-8414.

423. Burger H, Foekens JA, Look MP, Meijer-van Gelder ME, Klijn JG, Wiemer EA, Stoter G, Nooter K. RNA expression of breast cancer resistance protein, lung resistance-related protein, multidrug resistance-associated proteins 1 and 2, and multidrug resistance gene 1 in breast cancer: Correlation with chemotherapeutic response. *Clinical Cancer Research* 2003;9(2):827-836.

424. Tulsyan S, Mittal RD, Mittal B. The effect of ABCB1 polymorphisms on the outcome of breast cancer treatment. *Pharmacogenomics and Personalized Medicine* 2016;9:47-58.

425. Chaturvedi P, Tulsyan S, Agarwal G, Lal P, Agarwal S, Mittal RD, Mittal B. Influence of ABCB1 genetic variants in breast cancer treatment outcomes. *Cancer Epidemiol* 2013;37(5):754-761.

426. Amiri-Kordestani L, Basseville A, Kurdziel K, Fojo AT, Bates SE. Targeting MDR in breast and lung cancer: Discriminating its potential importance from the failure of drug resistance reversal studies. *Drug Resistance Updates* 2012;15(1-2):50-61.

427. Doyle LA, Yang W, Abruzzo LV, Krogmann T, Gao Y, Rishi AK, Ross DD. A multidrug resistance transporter from human MCF-7 breast cancer cells. *Proceedings of the National Academy of Sciences* 1998;95(26):15665-15670.

428. Mao Q, Unadkat JD. Role of the breast cancer resistance protein (ABCG2) in drug transport. *Journal of the American Association of Pharmaceutical Scientists* 2005;7(1):E118-133.

429. McDevitt CA, Collins RF, Conway M, Modok S, Storm J, Kerr ID, Ford RC, Callaghan R. Purification and 3D structural analysis of oligomeric human multidrug transporter ABCG2. *Structure* 2006;14(11):1623-1632.

430. Mo W, Zhang JT. Human ABCG2: Structure, function, and its role in multidrug resistance. *International Journal of Biochemistry and Molecular Biology* 2012;3(1):1-27.

431. Dohse M, Scharenberg C, Shukla S, Robey RW, Volkmann T, Deeken JF, Brendel C, Ambudkar SV, Neubauer A, Bates SE. Comparison of ATP-binding cassette transporter interactions with the tyrosine kinase inhibitors imatinib, nilotinib, and dasatinib. *Drug Metabolism and Disposition* 2010;38(8):1371-1380.

432. Hegedüs C, Ozvegy-Laczka C, Apati A, Magocsi M, Nemet K, Orfi L, Keri G, Katona M, Takats Z, Varadi A, Szakacs G, Sarkadi B. Interaction of nilotinib, dasatinib and

bosutinib with ABCB1 and ABCG2: Implications for altered anti-cancer effects and pharmacological properties. *British Journal of Pharmacology* 2009;158(4):1153-1164.

433. Hegedüs C, Truta-Feles K, Antalffy G, Várady G, Német K, Özvegy-Laczka C, Kéri G, Őrfi L, Szakács G, Settleman J, Váradi A, Sarkadi B. Interaction of the EGFR inhibitors gefitinib, vandetanib, pelitinib and neratinib with the ABCG2 multidrug transporter: Implications for the emergence and reversal of cancer drug resistance. *Biochemical Pharmacology* 2012;84(3):260-267.

434. Tiwari AK, Sodani K, Wang SR, Kuang YH, Ashby CR, Jr., Chen X, Chen ZS. Nilotinib (amn107, tasigna) reverses multidrug resistance by inhibiting the activity of the ABCB1/Pgp and ABCG2/BCRP/MXR transporters. *Biochemical Pharmacology* 2009;78(2):153-161.

435. Tiwari AK, Sodani K, Dai C-l, Abuznait AH, Singh S, Xiao Z-J, Patel A, Talele TT, Fu L, Kaddoumi A, Gallo JM, Chen Z-S. Nilotinib potentiates anticancer drug sensitivity in murine ABCB1-, ABCG2-, and ABCC10-multidrug resistance xenograft models. *Cancer Letters* 2013;328(2):307-317.

436. Sodani K, Patel A, Anreddy N, Singh S, Yang DH, Kathawala RJ, Kumar P, Talele TT, Chen ZS. Telatinib reverses chemotherapeutic multidrug resistance mediated by ABCG2 efflux transporter in vitro and in vivo. *Biochemical Pharmacology* 2014;89(1):52-61.

437. Chearwae W, Shukla S, Limtrakul P, Ambudkar SV. Modulation of the function of the multidrug resistance-linked ATP-binding cassette transporter ABCG2 by the cancer chemopreventive agent curcumin. *Molecular Cancer Therapeutics* 2006;5(8):1995-2006.

438. Pan Y-Z, Morris ME, Yu A-M. Microrna-328 negatively regulates the expression of breast cancer resistance protein (BCRP/ABCG2) in human cancer cells. *Molecular Pharmacology* 2009;75(6):1374-1379.

439. Jiao X, Zhao L, Ma M, Bai X, He M, Yan Y, Wang Y, Chen Q, Zhao X, Zhou M, Cui Z, Zheng Z, Wang E, Wei M. Mir-181a enhances drug sensitivity in mitoxantone-resistant breast cancer cells by targeting breast cancer resistance protein (BCRP/ABCG2). *Breast Cancer Research and Treatment* 2013;139(3):717-730.

440. Ma M-T, He M, Wang Y, Jiao X-Y, Zhao L, Bai X-F, Yu Z-J, Wu H-Z, Sun M-L, Song Z-G, Wei M-J. Mir-487a resensitizes mitoxantrone (MX)-resistant breast cancer cells (MCF-7/MX) to MX by targeting breast cancer resistance protein (BCRP/ABCG2). *Cancer Letters* 2013;339(1):107-115.

441. Meyer zu Schwabedissen HE, Kroemer HK. In vitro and in vivo evidence for the importance of breast cancer resistance protein transporters BCRP/MXR/ABCP/ABCG2). In: Fromm MF, Kim RB, eds. *Drug transporters: Handbook of Experimental Pharmacology*. Heidelberg: Springer-Verlag; 2011;201:325-370.

442. Natarajan K, Xie Y, Baer MR, Ross DD. Role of breast cancer resistance protein (BCRP/ABCG2) in cancer drug resistance. *Biochemical Pharmacology* 2012;83(8):1084-1103.

443. Vulsteke C, Pfeil AM, Maggen C, Schwenkglenks M, Pettengell R, Szucs TD, Lambrechts D, Dieudonne AS, Hatse S, Neven P, Paridaens R, Wildiers H. Clinical and genetic risk factors for epirubicin-induced cardiac toxicity in early breast cancer patients. *Breast Cancer Research and Treatment* 2015;152(1):67-76.

444. Semsei AF, Erdelyi DJ, Ungvari I, Csagoly E, Hegyi MZ, Kiszel PS, Lautner-Csorba O, Szabolcs J, Masat P, Fekete G, Falus A, Szalai C, Kovacs GT. ABCC1 polymorphisms in anthracycline-induced cardiotoxicity in childhood acute lymphoblastic leukaemia. *Cell Biology International* 2012;36(1):79-86.

445. Cole SP. Targeting multidrug resistance protein 1 (MRP1, ABCC1): Past, present, and future. *Annual Review of Pharmacology and Toxicology* 2014;54:95-117.

446. Deeley RG, Westlake C, Cole SP. Transmembrane transport of endo- and xenobiotics by mammalian ATP-binding cassette multidrug resistance proteins. *Physiological Reviews* 2006;86(3):849-899.

447. Liang Z, Wu H, Xia J, Li Y, Zhang Y, Huang K, Wagar N, Yoon Y, Cho HT, Scala S, Shim H. Involvement of mir-326 in chemotherapy resistance of breast cancer through modulating expression of multidrug resistance-associated protein 1. *Biochemical Pharmacology* 2010;79(6):817-824.

448. Guo L, Liu Y, Bai Y, Sun Y, Xiao F, Guo Y. Gene expression profiling of drug-resistant small cell lung cancer cells by combining microRNA and cDNA expression analysis. *European Journal of Cancer* 2010;46(9):1692-1702.

449. Guo J, Gong G, Zhang B. Mir-539 acts as a tumor suppressor by targeting epidermal growth factor receptor in breast cancer. *Scientific Reports* 2018;8(1):2073.

450. Fabbro D, Cowan-Jacob SW, Moebitz H. Ten things you should know about protein kinases: IUPHAR Review 14. *British Journal of Pharmacology* 2015;172(11):2675-2700.

451. Lahiry P, Torkamani A, Schork NJ, Hegele RA. Kinase mutations in human disease: Interpreting genotype-phenotype relationships. *Nature Reviews: Genetics* 2010;11(1):60-74.

452. Du Z, Lovly CM. Mechanisms of receptor tyrosine kinase activation in cancer. *Molecular Cancer* 2018;17(1):58.

453. Jiang W, Ji M. Receptor tyrosine kinases in PI3K signaling: The therapeutic targets in cancer. *Seminars in Cancer Biology* 2019;59:3-22.

454. Anreddy N, Gupta P, Kathawala RJ, Patel A, Wurpel JN, Chen ZS. Tyrosine kinase inhibitors as reversal agents for ABC transporter mediated drug resistance. *Molecules* 2014;19(9):13848-13877.

455. Siveen KS, Prabhu KS, Achkar IW, Kuttikrishnan S, Shyam S, Khan AQ, Merhi M, Dermime S, Uddin S. Role of non receptor tyrosine kinases in hematological malignances and its targeting by natural products. *Molecular Cancer* 2018;17(1):31.

456. Yan Z, Shanmugasundaram K, Ma D, Luo J, Luo S, Rao H. The N-terminal domain of the non-receptor tyrosine kinase ABL confers protein instability and suppresses tumorigenesis. *Journal of Biological Chemistry* 2020;295(27):9069-9075.

457. Kwon M, Hong JY, Kim ST, Kim KM, Lee J. Association of serine/threonine kinase 11 mutations and response to programmed cell death 1 inhibitors in metastatic gastric cancer. *Pathology - Research and Practice* 2020;216(6):152947.

458. Li C, Wang A, Chen Y, Liu Y, Zhang H, Zhou J. Microrna2995p inhibits cell metastasis in breast cancer by directly targeting serine/threonine kinase 39. *Oncology Reports* 2020;43(4):1221-1233.

459. Maloney C, Kallis MP, Edelman M, Tzanavaris C, Lesser M, Soffer SZ, Symons M, Steinberg BM. Gefitinib inhibits invasion and metastasis of osteosarcoma via inhibition of macrophage receptor interacting serine-threonine kinase 2. *Molecular Cancer Therapeutics* 2020;19(6):1340-1350.

460. Hubbard SR, Miller WT. Receptor tyrosine kinases: Mechanisms of activation and signaling. *Current Opinion in Cell Biology* 2007;19(2):117-123.

461. Butti R, Das S, Gunasekaran VP, Yadav AS, Kumar D, Kundu GC. Receptor tyrosine kinases (RTKs) in breast cancer: Signaling, therapeutic implications and challenges. *Molecular Cancer* 2018;17(1):34.

462. Lemmon MA, Schlessinger J. Cell signaling by receptor tyrosine kinases. *Cell* 2010;141(7):1117-1134.

463. Vogelstein B, Papadopoulos N, Velculescu VE, Zhou S, Diaz LA, Jr., Kinzler KW. Cancer genome landscapes. *Science* 2013;339(6127):1546-1558.

464. Fruman DA, Chiu H, Hopkins BD, Bagrodia S, Cantley LC, Abraham RT. The PI3K pathway in human disease. *Cell* 2017;170(4):605-635.

465. Lyashenko E, Niepel M, Dixit PD, Lim SK, Sorger PK, Vitkup D. Receptor-based mechanism of relative sensing and cell memory in mammalian signaling networks. *Elife* 2020;9.

466. Engelman JA. Targeting PI3K signalling in cancer: Opportunities, challenges and limitations. *Nature Reviews Cancer* 2009;9(8):550-562.

467. Pons-Tostivint E, Thibault B, Guillermet-Guibert J. Targeting PI3K signaling in combination cancer therapy. *Trends in Cancer* 2017;3(6):454-469.

468. Roskoski R, Jr. Small molecule inhibitors targeting the EGFR/ErbB family of protein-tyrosine kinases in human cancers. *Pharmacological Research* 2019;139:395-411.

469. Roskoski Jr R. ErbB/her protein-tyrosine kinases: Structures and small molecule inhibitors. *Pharmacological Research* 2014;87:42-59.

470. Jacobi N, Seeboeck R, Hofmann E, Eger A. ErbB family signalling: A paradigm for oncogene addiction and personalized oncology. *Cancers (Basel)* 2017;9(4).

471. Appert-Collin A, Hubert P, Cremel G, Bennasroune A. Role of ErbB receptors in cancer cell migration and invasion. *Front Pharmacol* 2015;6:283.

472. Wee P, Wang Z. Epidermal growth factor receptor cell proliferation signaling pathways. *Cancers (Basel)* 2017;9(5):52.

473. Lee J, Lee EJ, Moon SH, Kim S, Hyun SH, Cho YS, Choi JY, Kim BT, Lee KH. Strong association of epidermal growth factor receptor status with breast cancer FDG uptake. *European Journal of Nuclear Medicine and Molecular Imaging* 2017;44(9):1438-1447.

474. Lee HJ, Seo AN, Kim EJ, Jang MH, Kim YJ, Kim JH, Kim SW, Ryu HS, Park IA, Im SA, Gong G, Jung KH, Kim HJ, Park SY. Prognostic and predictive values of EGFR overexpression and EGFR copy number alteration in HER2-positive breast cancer. *British Journal of Cancer* 2015;112(1):103-111.

475. Park HS, Jang MH, Kim EJ, Kim HJ, Lee HJ, Kim YJ, Kim JH, Kang E, Kim SW, Kim IA, Park SY. High EGFR gene copy number predicts poor outcome in triple-negative breast cancer. *Modern Pathology* 2014;27(9):1212-1222.

476. Larionov AA. Current therapies for human epidermal growth factor receptor 2-positive metastatic breast cancer patients. *Frontiers in Oncology* 2018;8:89.

477. Westover D, Zugazagoitia J, Cho BC, Lovly CM, Paz-Ares L. Mechanisms of acquired resistance to first- and second-generation EGFR tyrosine kinase inhibitors. *Annals of Oncology* 2018;29(suppl_1):i10-i19.

478. Ma F, Li Q, Chen S, Zhu W, Fan Y, Wang J, Luo Y, Xing P, Lan B, Li M, Yi Z, Cai R, Yuan P, Zhang P, Li Q, Xu B. Phase I study and biomarker analysis of pyrotinib, a novel irreversible pan-ErbB receptor tyrosine kinase inhibitor, in patients with human epidermal growth factor receptor 2-positive metastatic breast cancer. *Journal of Clinical Oncology* 2017;35(27):3105-3112.

479. Ben-Baruch NE, Bose R, Kavuri SM, Ma CX, Ellis MJ. HER2-mutated breast cancer responds to treatment with single-agent neratinib, a second-generation HER2/EGFR tyrosine kinase inhibitor. *Journal of the National Comprehensive Cancer Network* 2015;13(9):1061-1064.

480. Toi M, Saeki T, Iwata H, Inoue K, Tokuda Y, Sato Y, Ito Y, Aogi K, Takatsuka Y, Arioka H. A multicenter Phase II study of TSU-68, an oral multiple tyrosine kinase inhibitor, in combination with docetaxel in metastatic breast cancer patients with anthracycline resistance. *Breast Cancer* 2014;21(1):20-27.

481. Perez EA, Barrios C, Eiermann W, Toi M, Im YH, Conte P, Martin M, Pienkowski T, Pivot XB, Burris HA, 3rd, Petersen JA, De Haas S, Hoersch S, Patre M, Ellis PA. Trastuzumab emtansine with or without pertuzumab versus trastuzumab with taxane for human epidermal growth factor receptor 2-positive advanced breast cancer: Final results from MARIANNE. *Cancer* 2019;125(22):3974-3984.

482. Nahleh Z, Botrus G, Dwivedi A, Jennings M, Nagy S, Tfayli A. Bevacizumab in the neoadjuvant treatment of human epidermal growth factor receptor 2-negative breast cancer: A meta-analysis of randomized controlled trials. 2019;10(3):357-365.

483. Beretta GL, Cassinelli G, Pennati M, Zuco V, Gatti L. Overcoming ABC transporter-mediated multidrug resistance: The dual role of tyrosine kinase inhibitors as multitargeting agents. *European Journal of Medical Chemistry* 2017;142:271-289.

484. Pottier C, Fresnais M, Gilon M, Jérusalem G, Longuespée R, Sounni NE. Tyrosine kinase inhibitors in cancer: Breakthrough and challenges of targeted therapy. *Cancers (Basel)* 2020;12(3).

485. Yamaoka T, Kusumoto S, Ando K, Ohba M, Ohmori T. Receptor tyrosine kinase-targeted cancer therapy. *International Journal of Molecular Sciences* 2018;19(11).

486. Roskoski R, Jr. Properties of FDA-approved small molecule protein kinase inhibitors. *Pharmacol Res* 2019;144:19-50.

487. Jiao Q, Bi L, Ren Y, Song S, Wang Q, Wang YS. Advances in studies of tyrosine kinase inhibitors and their acquired resistance. *Molecular Cancer* 2018;17(1):36.

488. Costa RLB, Gradishar WJ. Triple-negative breast cancer: Current practice and future directions. *Journal of Oncology Practice* 2017;13(5):301-303.

489. Oda K, Matsuoka Y, Funahashi A, Kitano H. A comprehensive pathway map of epidermal growth factor receptor signaling. *Molecular Systems Biology* 2005;1(1):2005.0010.

490. Maennling AE, Tur MK, Niebert M, Klockenbring T, Zeppernick F, Gattenlohner S, Meinhold-Heerlein I, Hussain AF. Molecular targeting therapy against EGFR family in breast cancer: Progress and future potentials. *Cancers (Basel)* 2019;11(12).

491. Gradishar WJ. Emerging approaches for treating HER2-positive metastatic breast cancer beyond trastuzumab. *Annals of Oncology* 2013;24(10):2492-2500.

492. Tsang RY, Finn RS. Beyond trastuzumab: Novel therapeutic strategies in HER2-positive metastatic breast cancer. *British Journal of Cancer* 2012;106:6.

493. Wu P, Nielsen TE, Clausen MH. FDA-approved small-molecule kinase inhibitors. *Trends in Pharmacological Sciences* 2015;36(7):422-439.

494. Ciardiello F, Tortora G. EGFR antagonists in cancer treatment. *New England Journal of Medicine* 2008;358(11):1160-1174.

495. Tomasello C, Baldessari C, Napolitano M, Orsi G, Grizzi G, Bertolini F, Barbieri F, Cascinu S. Resistance to EGFR inhibitors in non-small cell lung cancer: Clinical management and future perspectives. *Critical Reviews in Oncology/Hematology* 2018;123:149-161.

496. Bhullar KS, Lagarón NO, McGowan EM, Parmar I, Jha A, Hubbard BP, Rupasinghe HPV. Kinase-targeted cancer therapies: Progress, challenges and future directions. *Molecular Cancer Research* 2018;17(1):48.

497. Parsa Y, Mirmalek SA, Kani FE, Aidun A, Salimi-Tabatabaee SA, Yadollah-Damavandi S, Jangholi E, Parsa T, Shahverdi E. A review of the clinical implications of breast cancer biology. *Electron Physician* 2016;8(5):2416-2424.

498. Pondé N, Brandão M, El-Hachem G, Werbrouck E, Piccart M. Treatment of advanced HER2-positive breast cancer: 2018 and beyond. *Cancer Treatment Reviews* 2018;67:10-20.

499. Loibl S, Gianni L. HER2-positive breast cancer. *The Lancet* 2017;389(10087):2415-2429.

500. Diéras V, Miles D, Verma S, Pegram M, Welslau M, Baselga J, Krop IE, Blackwell K, Hoersch S, Xu J, Green M, Gianni L. Trastuzumab emtansine versus capecitabine plus lapatinib in patients with previously treated HER2-positive advanced breast cancer (EMILIA): A descriptive analysis of final overall survival results from a randomised, open-label, phase 3 trial. *Lancet Oncology* 2017;18(6):732-742.

501. Hanker AB, Brewer MR, Sheehan JH, Koch JP, Sliwoski GR, Nagy R, Lanman R, Berger MF, Hyman DM, Solit DB, He J, Miller V, Cutler RE, Lalani AS, Cross D, Lovly CM, Meiler J, Arteaga CL. An acquired *HER2^{T798I}* gatekeeper mutation induces resistance to neratinib in a patient with HER2 mutant–driven breast cancer. *Cancer Discovery* 2017;7(6):575-585.

502. Lee-Hoeflich ST, Crocker L, Yao E, Pham T, Munroe X, Hoeflich KP, Sliwkowski MX, Stern HM. A central role for her3 in HER2-amplified breast cancer: Implications for targeted therapy. *Cancer Research* 2008;68(14):5878-5887.

503. Jaiswal Bijay S, Kljavin Noelyn M, Stawiski Eric W, Chan E, Parikh C, Durinck S, Chaudhuri S, Pujara K, Guillory J, Edgar Kyle A, Janakiraman V, Scholz R-P, Bowman Krista K, Lorenzo M, Li H, Wu J, Yuan W, Peters Brock A, Kan Z, Stinson J, Mak M, Modrusan Z, Eigenbrot C, Firestein R, Stern Howard M, Rajalingam K, Schaefer G, Merchant Mark A, Sliwkowski Mark X, de Sauvage Frederic J, Seshagiri S. Oncogenic ERBB3 mutations in human cancers. *Cancer Cell* 2013;23(5):603-617.

504. Meric-Bernstam F, Johnson AM, Dumbrava EEI, Raghav K, Balaji K, Bhatt M, Murthy RK, Rodon J, Piha-Paul SA. Advances in HER2-targeted therapy: Novel agents and opportunities beyond breast and gastric cancer. *Clinical Cancer Research* 2019;25(7):2033-2041.

505. Montor WR, Salas A, Melo FHM. Receptor tyrosine kinases and downstream pathways as druggable targets for cancer treatment: The current arsenal of inhibitors. *Molecular Cancer* 2018;17(1):55.

506. Mo H-N, Liu P. Targeting MET in cancer therapy. *Chronic Diseases and Translational Medicine* 2017;3(3):148-153.

507. Ghosh S, Marrocco I, Yarden Y. Chapter One - Roles for receptor tyrosine kinases in tumor progression and implications for cancer treatment. In: Kumar R, Fisher PB, eds. *Advances in Cancer Research*: Academic Press; 2020;147:1-57.

508. Kadkol H, Jain V, Patil* A. Multi drug resistance in cancer therapy-an overview. *Journal of Critical Reviews* 2019:1-6.

509. Brozik A, Hegedus C, Erdei Z, Hegedus T, Ozvegy-Laczka C, Szakacs G, Sarkadi B. Tyrosine kinase inhibitors as modulators of ATP binding cassette multidrug transporters: Substrates, chemosensitizers or inducers of acquired multidrug resistance? *Expert Opinion on Drug Metabolism & Toxicology* 2011;7(5):623-642.

510. Deng J, Shao J, Markowitz JS, An G. ABC transporters in multi-drug resistance and ADME-Tox of small molecule tyrosine kinase inhibitors. *Pharmaceutical Research* 2014;31(9):2237-2255.

511. D'Cunha R, Bae S, Murry DJ, An G. TKI combination therapy: Strategy to enhance dasatinib uptake by inhibiting Pgp- and BCRP-mediated efflux. *Biopharmaceutics & Drug Disposition* 2016;37(7):397-408.

512. Shao J, Markowitz JS, Bei D, An G. Enzyme- and transporter-mediated drug interactions with small molecule tyrosine kinase inhibitors. *Journal of Pharmaceutical Sciences* 2014;103(12):3810-3833.

513. Eadie LN, Hughes TP, White DL. Interaction of the efflux transporters ABCB1 and ABCG2 with imatinib, nilotinib, and dasatinib. *Clinical Pharmacology and Therapeutics* 2014;95(3):294-306.

514. He M, Wei MJ. Reversing multidrug resistance by tyrosine kinase inhibitors. *Chinese Journal of Cancer* 2012;31(3):126-133.

515. Wang XK, Fu LW. Interaction of tyrosine kinase inhibitors with the MDR- related ABC transporter proteins. *Current Drug Metabolism* 2010;11(7):618-628.

516. Ozvegy-Laczka C, Cserepes J, Elkind NB, Sarkadi B. Tyrosine kinase inhibitor resistance in cancer: Role of ABC multidrug transporters. *Drug Resistance Updates* 2005;8(1-2):15-26.

517. Eechoute K, Sparreboom A, Burger H, Franke RM, Schiavon G, Verweij J, Loos WJ, Wiemer EAC, Mathijssen RHJ. Drug transporters and imatinib treatment: Implications for clinical practice. *Clinical Cancer Research* 2011;17(3):406-415.

518. Shibayama Y, Nakano K, Maeda H, Taguchi M, Ikeda R, Sugawara M, Iseki K, Takeda Y, Yamada K. Multidrug resistance protein 2 implicates anticancer drug-resistance to sorafenib. *Biological and Pharmaceutical Bulletin* 2011;34(3):433-435.

519. Krchniakova M, Skoda J, Neradil J, Chlapek P, Veselska R. Repurposing tyrosine kinase inhibitors to overcome multidrug resistance in cancer: A focus on transporters and lysosomal sequestration. *International Journal of Molecular Sciences* 2020;21(9).

520. Janne PA, Gray N, Settleman J. Factors underlying sensitivity of cancers to small-molecule kinase inhibitors. *Nature Reviews Drug Discovery* 2009;8(9):709-723.

521. Khozin S, Blumenthal GM, Zhang L, Tang S, Brower M, Fox E, Helms W, Leong R, Song P, Pan Y, Liu Q, Zhao P, Zhao H, Lu D, Tang Z, Al Hakim A, Boyd K, Keegan P, Justice R, Pazdur R. FDA approval: Ceritinib for the treatment of metastatic anaplastic lymphoma kinase-positive non-small cell lung cancer. *Clinical Cancer Research* 2015;21(11):2436-2439.

522. Zhang Q, Liu Y, Gao F, Ding Q, Cho C, Hur W, Jin Y, Uno T, Joazeiro CA, Gray N. Discovery of EGFR selective 4,6-disubstituted pyrimidines from a combinatorial kinase-directed heterocycle library. *Journal of the American Chemical Society* 2006;128(7):2182-2183.

523. Anastassiadis T, Deacon SW, Devarajan K, Ma H, Peterson JR. Comprehensive assay of kinase catalytic activity reveals features of kinase inhibitor selectivity. *Nature Biotechnology* 2011;29(11):1039-1045.

524. Gewirtz D. A critical evaluation of the mechanisms of action proposed for the antitumor effects of the anthracycline antibiotics adriamycin and daunorubicin. *Biochemical Pharmacology* 1999;57(7):727-741.

525. Arcamone F, Cassinelli G, Fantini G, Grein A, Orezzi P, Pol C, Spalla C. Adriamycin, 14-hydroxydaunomycin, a new antitumor antibiotic from *S. peucetius* var. *Caesius*. *Biotechnology and Bioengineering* 2000;67(6):704-713.

526. Bonadonna G, Monfardini S, De Lena M, Fossati-Bellani F. Clinical evaluation of adriamycin, a new antitumor antibiotic. *British Medical Journal* 1969;3(5669):503-506.

527. Scott RB. Cancer chemotherapy - the first twenty-five years. *British Medical Journal* 1970;4(5730):259-265.

528. Carter SK. Adriamycin—a review. *JNCI: Journal of the National Cancer Institute* 1975;55(6):1265-1274.

529. Lüpertz R, Wätjen W, Kahl R, Chovolou Y. Dose- and time-dependent effects of doxorubicin on cytotoxicity, cell cycle and apoptotic cell death in human colon cancer cells. *Toxicology* 2010;271(3):115-121.

530. Rivankar S. An overview of doxorubicin formulations in cancer therapy. *Journal of Cancer Research and Therapeutics* 2014;10(4):853-858.

531. Pugazhendhi A, Edison T, Velmurugan BK, Jacob JA, Karuppusamy I. Toxicity of doxorubicin (Dox) to different experimental organ systems. *Life Sciences* 2018;200:26-30.

532. Cappetta D, Rossi F, Piegari E, Quaini F, Berrino L, Urbanek K, De Angelis A. Doxorubicin targets multiple players: A new view of an old problem. *Pharmacological Research* 2018;127:4-14.

533. Mealey KL, Barhoumi R, Burghardt RC, Safe S, Kochevar DT. Doxycycline induces expression of P-glycoprotein in MCF-7 breast carcinoma cells. *Antimicrobial Agents & Chemotherapy* 2002;46(3):755-761.

534. Wang L, Zhang L, Liu F, Sun Y. Molecular energetics of doxorubicin pumping by human P-glycoprotein. *Journal of Chemical Information and Modeling* 2019;59(9):3889-3898.

535. Li S, Zhao Q, Wang B, Yuan S, Wang X, Li K. Quercetin reversed MDR in breast cancer cells through down-regulating P-gp expression and eliminating cancer stem cells mediated by YB-1 nuclear translocation. *Phytotherapy Research* 2018;32(8):1530-1536.

536. Li S, Yuan S, Zhao Q, Wang B, Wang X, Li K. Quercetin enhances chemotherapeutic effect of doxorubicin against human breast cancer cells while reducing toxic side effects of it. *Biomedicine and Pharmacotherapy* 2018;100:441-447.

537. Shafiei-Irannejad V, Samadi N, Yousefi B, Salehi R, Velaei K, Zarghami N. Metformin enhances doxorubicin sensitivity via inhibition of doxorubicin efflux in P-gp-overexpressing MCF-7 cells. *Chemical Biology & Drug Design* 2018;91(1):269-276.

538. Li Y, Wang M, Zhi P, You J, Gao J-Q. Metformin synergistically suppress tumor growth with doxorubicin and reverse drug resistance by inhibiting the expression and function of P-glycoprotein in MCF7/ADR cells and xenograft models. *Oncotarget* 2017;9(2):2158-2174.

539. Loehrer PJ, Einhorn LH. Drugs five years later. Cisplatin. *Annals of Internal Medicine* 1984;100(5):704-713.

540. Wang D, Lippard SJ. Cellular processing of platinum anticancer drugs. *Nature Reviews Drug Discovery* 2005;4(4):307-320.

541. de Graeff A, Slebos RJ, Rodenhuis S. Resistance to cisplatin and analogues: Mechanisms and potential clinical implications. *Cancer Chemotherapy and Pharmacology* 1988;22(4):325-332.

542. Yao X, Panichpisal K, Kurtzman N, Nugent K. Cisplatin nephrotoxicity: A review. *American Journal of the Medical Sciences* 2007;334(2):115-124.

543. Adams M, Kerby IJ, Rocker I, Evans A, Johansen K, Franks CR. A comparison of the toxicity and efficacy of cisplatin and carboplatin in advanced ovarian cancer. The swons gynaecological cancer group. *Acta Oncologica* 1989;28(1):57-60.

544. Weiss RB, Christian MC. New cisplatin analogues in development. *Drugs* 1993;46(3):360-377.

545. Galluzzi L, Senovilla L, Vitale I, Michels J, Martins I, Kepp O, Castedo M, Kroemer G. Molecular mechanisms of cisplatin resistance. *Oncogene* 2011;31:1869.

546. Galluzzi L, Vitale I, Michels J, Brenner C, Szabadkai G, Harel-Bellan A, Castedo M, Kroemer G. Systems biology of cisplatin resistance: Past, present and future. *Cell Death & Disease* 2014;5:e1257.

547. Amable L. Cisplatin resistance and opportunities for precision medicine. *Pharmacological Research* 2016;106:27-36.

548. Sun CY, Zhang QY, Zheng GJ, Feng B. Phytochemicals: Current strategy to sensitize cancer cells to cisplatin. *Biomedicine and Pharmacotherapy* 2019;110:518-527.

549. Jiang YQ, Xu XP, Guo QM, Xu XC, Liu QY, An SH, Xu JL, Su F, Tai JB. Reversal of cisplatin resistance in non-small cell lung cancer stem cells by *Taxus chinensis* var. *Genetics and Molecular Research* 2016;15(3).

550. Zhou P, Zhang R, Wang Y, Xu D, Zhang L, Qin J, Su G, Feng Y, Chen H, You S, Rui W, Liu H, Chen S, Chen H, Wang Y. Cepharanthine hydrochloride reverses the mdr1 (P-glycoprotein)-mediated esophageal squamous cell carcinoma cell cisplatin resistance through JNK and p53 signals. *Oncotarget* 2017;8(67):111144-111160.

551. Wolf DM, Lenburg ME, Yau C, Boudreau A, van 't Veer LJ. Gene co-expression modules as clinically relevant hallmarks of breast cancer diversity. *PloS One* 2014;9(2):e88309.

552. Robinson K, Tiriveedhi V. Perplexing role of P-glycoprotein in tumor microenvironment. *Frontiers in Oncology* 2020;10:265.

553. Greene RF, Chatterji DC, Hiranaka PK, Gallelli JF. Stability of cisplatin in aqueous solution. *American Journal of Health-System Pharmacy* 1979;36(1):38-43.

554. Mosmann T. Rapid colorimetric assay for cellular growth and survival: Application to proliferation and cytotoxicity assays. *Journal of Immunological Methods* 1983;65(1-2):55-63.

555. Liminga G, Nygren P, Larsson R. Microfluorometric evaluation of calcein acetoxymethyl ester as a probe for P-glycoprotein-mediated resistance: Effects of cyclosporin a and its nonimmunosuppressive analogue SDZ PSC 833. *Experimental Cell Research* 1994;212(2):291-296.

556. Holló Z, Homolya L, Davis CW, Sarkadi B. Calcein accumulation as a fluorometric functional assay of the multidrug transporter. *Biochimica et Biophysica Acta - Biomembranes* 1994;1191(2):384-388.

557. Tiberghien F, Loor F. Ranking of P-glycoprotein substrates and inhibitors by a calcein-am fluorometry screening assay. *Anticancer Drugs* 1996;7(5):568-578.

558. Polli JW, Wring SA, Humphreys JE, Huang L, Morgan JB, Webster LO, Serabjit-Singh CS. Rational use of in vitro P-glycoprotein assays in drug discovery. *Journal of Pharmacology and Experimental Therapeutics* 2001;299(2):620-628.

559. Goutelle S, Maurin M, Rougier F, Barbaut X, Bourguignon L, Ducher M, Maire P. The Hill equation: A review of its capabilities in pharmacological modelling. *Fundamental and Clinical Pharmacology* 2008;22(6):633-648.

560. Gadagkar SR, Call GB. Computational tools for fitting the Hill equation to dose-response curves. *Journal of Pharmacological and Toxicological Methods* 2015;71:68-76.

561. Wooten DJ, Meyer CT, Quaranta V, Lopez C. A consensus framework unifies multi-drug synergy metrics. *bioRxiv* 2019:683433.

562. Stephenson RP. A modification of receptor theory. *British Journal of Pharmacology and Chemotherapy* 1956;11(4):379-393.

563. Holford N, Sheiner L. Understanding the dose-effect relationship. *Clinical Pharmacokinetics* 1981;6.

564. Kenakin T. Pharmacologic analysis of drug–receptor interaction. New York: Raven Press; 1987.

565. Kenakin KT. Pharmacologic analysis of drug receptor interaction. *Therapeutic Drug Monitoring* 1988;10(3):365-366.

566. Stephenson RP. A modification of receptor theory. 1956. *British Journal of Pharmacology* 1997;120(4 Suppl):106-120; discussion 103-105.

567. Colquhoun D. Pharmacologic analysis of drug–receptor interaction (3rd edn). *Trends in Pharmacological Sciences* 1998;19(12):515-516.

568. Tallarida RJ. Drug synergism and dose-effect data analysis. Boca Raton: Chapman & Hall/CRC Press; 2000.

569. Kenakin T. Pharmacology in drug discovery: Understanding drug response. New York: Academic Press; 2012.

570. Fieller EC. The biological standardization of insulin. *Supplement to the Journal of the Royal Statistical Society* 1940;7(1):1-64.

571. Fieller EC. A fundamental formula in the statistics of biological assay, and some applications. *Quarterly Journal of Pharmacy and Pharmacology* 1944;17:117-123.

572. Fieller EC. Some problems in interval estimation. *Journal of the Royal Statistical Society: Series B (Methodological)* 1954;16(2):175-185.

573. Bliss CI. A simplified calculation of the potency of penicillin and other drugs assayed biologically with a graded response. *Journal of the American Statistical Association* 1944;39(228):479-487.

574. Bliss CI. Confidence limits for measuring the precision of bioassays. *Biometrics* 1956;12(4):491-526.

575. Tallarida RJ, Murray RB. Manual of pharmacologic calculations with computer programs. 2nd ed. London: Springer-Verlag; 1987.

576. Sherman M, Maity A, Wang SJ. Inferences for the ratio: Fieller's interval, log ratio, and large sample based confidence intervals. *Asta-Advances in Statistical Analysis* 2011;95(3):313-323.

577. von Luxburg U, Franz VH. A geometric approach to confidence sets for ratios: Fieller's theorem, generalizations and bootstrap. *Statistica Sinica* 2009;19(3):1095-1117.

578. Beyene J, Moineddin R. Methods for confidence interval estimation of a ratio parameter with application to location quotients. *BMC Medical Research Methodology* 2005;5:32-32.

579. Franz UvLaVH. A geometric approach to confidence sets for ratios: Fieller's theorem, generalizations, and bootstrap. *Statistica Sinica* 2009;19:1095-1117.

580. Franz VH. Ratios: A short guide to confidence limits and proper use. *arXiv preprint arXiv:07102024* 2007.

581. Chou T-C. Theoretical basis, experimental design, and computerized simulation of synergism and antagonism in drug combination studies. *Pharmacological Reviews* 2006;58(3):621-681.

582. Amzallag A, Ramaswamy S, Benes CH. Statistical assessment and visualization of synergies for large-scale sparse drug combination datasets. *BMC Bioinformatics* 2019;20(1):83.

583. Ezechiáš M, Cajthaml T. New insight into isobolographic analysis for combinations of a full and partial agonist: Curved isoboles. *Toxicology* 2018;402-403:9-16.

584. Di Veroli GY, Fornari C, Wang D, Mollard S, Bramhall JL, Richards FM, Jodrell DI. Combenefit: An interactive platform for the analysis and visualization of drug combinations. *Bioinformatics* 2016;32(18):2866-2868.

585. Tallarida RJ. An overview of drug combination analysis with isobolograms. *Journal of Pharmacology and Experimental Therapeutics* 2006;319(1):1-7.

586. Bae SY, Guan N, Yan R, Warner K, Taylor SD, Meyer AS. Measurement and models accounting for cell death capture hidden variation in compound response. *Cell Death & Disease* 2020;11(4):255.

587. Berenbaum MC. What is synergy? *Pharmacological Reviews* 1989;41(2):93-141.

588. He L, Kulesskiy E, Saarela J, Turunen L, Wennerberg K, Aittokallio T, Tang J. Methods for high-throughput drug combination screening and synergy scoring. In: von Stechow L, ed. *Cancer Systems Biology*. New York, NY.: Humana Press, Springer; 2018;1711:351-398.

589. Brooks SC, Locke ER, Soule HD. Estrogen receptor in a human cell line (MCF-7) from breast carcinoma. *Journal of Biological Chemistry* 1973;248(17):6251-6253.

590. Lee AV, Oesterreich S, Davidson NE. MCF-7 cells - changing the course of breast cancer research and care for 45 years. *Journal of the National Cancer Institute* 2015;107(7).

591. Comsa S, Cimpean AM, Raica M. The story of MCF-7 breast cancer cell line: 40 years of experience in research. *Anticancer Research* 2015;35(6):3147-3154.

592. Chiang YS, Huang YF, Midha MK, Chen TH, Shiau HC, Chiu KP. Single cell transcriptome analysis of MCF-7 reveals consistently and inconsistently expressed gene groups each associated with distinct cellular localization and functions. *PloS One* 2018;13(6):e0199471.

593. Cailleau R, Young R, Olive M, Reeves WJ, Jr. Breast tumor cell lines from pleural effusions. *Journal of the National Cancer Institute* 1974;53(3):661-674.

594. Konecny G, Untch M, Slamon D, Beryt M, Kahlert S, Felber M, Langer E, Lude S, Hepp H, Pegram M. Drug interactions and cytotoxic effects of paclitaxel in combination with carboplatin, epirubicin, gemcitabine or vinorelbine in breast cancer cell lines and tumor samples. *Breast Cancer Research and Treatment* 2001;67(3):223-233.

595. Barton VN, D'Amato NC, Gordon MA, Lind HT, Spoelstra NS, Babbs BL, Heinz RE, Elias A, Jedlicka P, Jacobsen BM, Richer JK. Multiple molecular subtypes of triple-negative breast cancer critically rely on androgen receptor and respond to enzalutamide *in vivo*. *Molecular Cancer Therapeutics* 2015;14(3):769-778.

596. Hasan M, Browne E, Guarinoni L, Darveau T, Hilton K, Witt-Enderby PA. Novel melatonin, estrogen, and progesterone hormone therapy demonstrates anti-cancer actions in MCF-7 and MDA-MB-231 breast cancer cells. *Breast Cancer (Auckl)* 2020;14:1178223420924634.

597. Welsh J. Chapter 40 - animal models for studying prevention and treatment of breast cancer. In: Conn PM, ed. *Animal models for the study of human disease*. Boston: Academic Press; 2013:997-1018.

598. Aggarwal S, Verma SS, Aggarwal S, Gupta SC. Drug repurposing for breast cancer therapy: Old weapon for new battle. *Seminars in Cancer Biology* 2019.

599. Schneeweiss A, Lux MP, Janni W, Hartkopf AD, Nabieva N, Taran FA, Overkamp F, Kolberg HC, Hadji P, Tesch H, Wockel A, Ettl J, Luftner D, Wallwiener M, Muller V, Beckmann MW, Belleville E, Wallwiener D, Brucker SY, Schutz F, Fasching PA, Fehm TN. Update breast cancer 2018 (part 2) - advanced breast cancer, quality of life and prevention. *Geburtshilfe Frauenheilkd* 2018;78(3):246-259.

600. Goldvaser H, Barnes TA, Seruga B, Cescon DW, Ocana A, Ribnikar D, Amir E. Toxicity of extended adjuvant therapy with aromatase inhibitors in early breast cancer: A systematic review and meta-analysis. *Journal of the National Cancer Institute* 2018;110(1).

601. Xie Z, Wu K, Wang Y, Pan Y, Chen B, Cheng D, Pan S, Guo T, Du X, Fang L, Wang X, Ye F. Discovery of 4,6-pyrimidinediamine derivatives as novel dual EGFR/FGFR inhibitors aimed EGFR/FGFR1-positive NSCLC. *European Journal of Medicinal Chemistry* 2020;187:111943.

602. Panda M, Biswal BK. Cell signaling and cancer: A mechanistic insight into drug resistance. *Molecular Biology Reports* 2019;46(5):5645-5659.

603. Pegram MD, Konecny GE, O'Callaghan C, Beryt M, Pietras R, Slamon DJ. Rational combinations of trastuzumab with chemotherapeutic drugs used in the treatment of breast cancer. *Journal of the National Cancer Institute* 2004;96(10):739-749.

604. Boone JJ, Bhosle J, Tilby MJ, Hartley JA, Hochhauser D. Involvement of the HER2 pathway in repair of DNA damage produced by chemotherapeutic agents. *Molecular Cancer Therapeutics* 2009;8(11):3015-3023.

605. Seidman A, Hudis C, Pierri MK, Shak S, Paton V, Ashby M, Murphy M, Stewart SJ, Keefe D. Cardiac dysfunction in the trastuzumab clinical trials experience. *Journal of Clinical Oncology* 2002;20(5):1215-1221.

606. Cornen S, Vivier E. Chemotherapy and tumor immunity. *Science* 2018;362(6421):1355-1356.

607. Ponde NF, Zardavas D, Piccart M. Progress in adjuvant systemic therapy for breast cancer. *Nature Reviews Clinical Oncology* 2019;16(1):27-44.

608. Khosravi-Shahi P, Cabezon-Gutierrez L, Custodio-Cabello S. Metastatic triple negative breast cancer: Optimizing treatment options, new and emerging targeted therapies. *Asia Pacific Journal of Clinical Oncology* 2018;14(1):32-39.

609. Wu YS, Quan Y, Zhang DX, Liu DW, Zhang XZ. Synergistic inhibition of breast cancer cell growth by an epigenome-targeting drug and a tyrosine kinase inhibitor. *Biological and Pharmaceutical Bulletin* 2017;40(10):1747-1753.

610. Marinello J, Delcuratolo M, Capranico G. Anthracyclines as topoisomerase II poisons: From early studies to new perspectives. *International Journal of Molecular Sciences* 2018;19(11).

611. Lee S-M, O'Halloran TV, Nguyen ST. Polymer-caged nanobins for synergistic cisplatin-doxorubicin combination chemotherapy. *Journal of the American Chemical Society* 2010;132(48):17130-17138.

612. Li M, Tang Z, Lv S, Song W, Hong H, Jing X, Zhang Y, Chen X. Cisplatin crosslinked pH-sensitive nanoparticles for efficient delivery of doxorubicin. *Biomaterials* 2014;35(12):3851-3864.

613. Wu H, Jin H, Wang C, Zhang Z, Ruan H, Sun L, Yang C, Li Y, Qin W, Wang C. Synergistic cisplatin/doxorubicin combination chemotherapy for multidrug-resistant cancer via polymeric nanogels targeting delivery. *ACS Applied Materials & Interfaces* 2017;9(11):9426-9436.

614. Manohar S, Leung N. Cisplatin nephrotoxicity: A review of the literature. *Journal of Nephrology* 2018;31(1):15-25.

615. Oun R, Moussa YE, Wheate NJ. The side effects of platinum-based chemotherapy drugs: A review for chemists. *Dalton Transactions* 2018;47(19):6645-6653.

616. Casares N, Pequignot MO, Tesniere A, Ghiringhelli F, Roux S, Chaput N, Schmitt E, Hamai A, Hervas-Stubbs S, Obeid M, Coutant F, Métivier D, Pichard E, Aucouturier P, Pierron G, Garrido C, Zitvogel L, Kroemer G. Caspase-dependent immunogenicity of doxorubicin-induced tumor cell death. *Journal of Experimental Medicine* 2005;202(12):1691-1701.

617. Zeng C, Fan D, Xu Y, Li X, Yuan J, Yang Q, Zhou X, Lu J, Zhang C, Han J, Gu J, Gao Y, Sun L, Wang S. Curcumol enhances the sensitivity of doxorubicin in triple-negative breast cancer via regulating the mir-181b-2-3p-ABCC3 axis. *Biochemical Pharmacology* 2020;174:113795.

618. Fan Y, Ma K, Jing J, Wang C, Hu Y, Shi Y, Li E, Geng Q. Recombinant dual-target MDM2/MDMX inhibitor reverses doxorubicin resistance through activation of the TAB1/TAK1/p38 MAPK pathway in wild-type p53 multidrug-resistant breast cancer cells. *Journal of Cancer* 2020;11(1):25-40.

619. Chen JS, Konopleva M, Andreeff M, Multani AS, Pathak S, Mehta K. Drug-resistant breast carcinoma (MCF-7) cells are paradoxically sensitive to apoptosis. *Journal of Cellular Physiology* 2004;200(2):223-234.

620. Abudabbus A, Badmus JA, Shalaweh S, Bauer R, Hiss D. Effects of fucoidan and chemotherapeutic agent combinations on malignant and non-malignant breast cell lines. *Current Pharmaceutical Biotechnology* 2017;18(9):748-757.

621. Tyagi AK, Agarwal C, Chan DC, Agarwal R. Synergistic anti-cancer effects of silibinin with conventional cytotoxic agents doxorubicin, cisplatin and carboplatin against human breast carcinoma MCF-7 and MDA-MB468 cells. *Oncology Reports* 2004;11(2):493-499.

622. Witters LM, Witkoski A, Planas-Silva MD, Berger M, Viallet J, Lipton A. Synergistic inhibition of breast cancer cell lines with a dual inhibitor of EGFR-HER-2/neu and a Bcl-2 inhibitor. *Oncology Reports* 2007;17(2):465-469.

623. Nikolaou M, Pavlopoulou A, Georgakilas AG, Kyrodimos E. The challenge of drug resistance in cancer treatment: A current overview. *Clinical and Experimental Metastasis* 2018;35(4):309-318.

624. Fan YF, Zhang W, Zeng L, Lei ZN, Cai CY, Gupta P, Yang DH, Cui Q, Qin ZD, Chen ZS, Trombetta LD. Dacomitinib antagonizes multidrug resistance (MDR) in cancer cells by inhibiting the efflux activity of ABCB1 and ABCG2 transporters. *Cancer Letters* 2018;421:186-198.

625. Katayama K, Yoshioka S, Tsukahara S, Mitsuhashi J, Sugimoto Y. Inhibition of the mitogen-activated protein kinase pathway results in the down-regulation of P-glycoprotein. *Molecular Cancer Therapeutics* 2007;6(7):2092-2102.

626. Chun SY, Kwon YS, Nam KS, Kim S. Lapatinib enhances the cytotoxic effects of doxorubicin in MCF-7 tumorspheres by inhibiting the drug efflux function of ABC transporters. *Biomedicine & Pharmacotherapy* 2015;72:37-43.

627. Nunez C, Capelo JL, Igrejas G, Alfonso A, Botana LM, Lodeiro C. An overview of the effective combination therapies for the treatment of breast cancer. *Biomaterials* 2016;97:34-50.

628. Nanayakkara AK, Follit CA, Chen G, Williams NS, Vogel PD, Wise JG. Targeted inhibitors of P-glycoprotein increase chemotherapeutic-induced mortality of multidrug resistant tumor cells. *Scientific Reports* 2018;8(1):967.

629. Li P, Zhong D, Gong P-y. Synergistic effect of paclitaxel and verapamil to overcome multi-drug resistance in breast cancer cells. *Biochemical and Biophysical Research Communications* 2019;516(1):183-188.

630. Flores C, Fouquet G, Moura IC, Maciel TT, Hermine O. Lessons to learn from low-dose Cyclosporin-A: A new approach for unexpected clinical applications. *Frontiers in Immunology* 2019;10:588.

631. Abdallah HM, Al-Abd AM, El-Dine RS, El-Halawany AM. P-glycoprotein inhibitors of natural origin as potential tumor chemo-sensitizers: A review. *Journal of Advanced Research* 2015;6(1):45-62.

632. Chen J, Kinoshita T, Sukbuntherng J, Chang BY, Elias L. Ibrutinib inhibits ERBB receptor tyrosine kinases and HER2-amplified breast cancer cell growth. *Molecular Cancer Therapeutics* 2016;15(12):2835-2844.

633. Gelmon KA. Lapatinib for breast cancer: A review of the current literature. *Expert Opinion on Drug Safety* 2011;10(1):109-121.

634. Madden R, Kosari S, Peterson GM, Bagheri N, Thomas J. Lapatinib plus capecitabine in patients with HER2-positive metastatic breast cancer: A systematic review. *International Journal of Clinical Pharmacology and Therapeutics* 2018;56(2):72-80.

635. Voigtlaender M, Schneider-Merck T, Trepel M. Lapatinib. In: Martens UM, ed. *Small Molecules in Oncology*. Cham: Springer International Publishing; 2018:19-44.

636. Guo X-f, Li S-s, Zhu X-f, Dou Q-h, Liu D. Lapatinib in combination with paclitaxel plays synergistic antitumor effects on esophageal squamous cancer. *Cancer Chemotherapy and Pharmacology* 2018;82(3):383-394.

637. Bao B, Mitrea C, Wijesinghe P, Marchetti L, Girsch E, Farr RL, Boerner JL, Mohammad R, Dyson G, Terlecky SR, Bollig-Fischer A. Treating triple negative breast cancer cells with erlotinib plus a select antioxidant overcomes drug resistance by targeting cancer cell heterogeneity. *Scientific Reports* 2017;7:44125.

638. Huang L, Shen C, Chen Y, Yan H, Cheng Z, Zhu Q. Simotinib as a modulator of P-glycoprotein: Substrate, inhibitor, or inducer? *Anticancer Drugs* 2016;27(4):300-311.

639. D'Amato V, Raimondo L, Formisano L, Giuliano M, De Placido S, Rosa R, Bianco R. Mechanisms of lapatinib resistance in HER2-driven breast cancer. *Cancer Treatment Reviews* 2015;41(10):877-883.

640. Liu L-L, Zhao H, Ma T-F, Ge F, Chen C-S, Zhang Y-P. Identification of valid reference genes for the normalization of RT-qPCR expression studies in human breast cancer cell lines treated with and without transient transfection. *PloS One* 2015;10(1):e0117058.

641. Sakil HAM, Stantic M, Wolfsberger J, Brage SE, Hansson J, Wilhelm MT. Δnp73 regulates the expression of the multidrug-resistance genes ABCB1 and ABCB5 in breast cancer and melanoma cells - a short report. *Cellular Oncology* 2017;40(6):631-638.

642. Calcagno AM, Salcido CD, Gillet JP, Wu CP, Fostel JM, Mumau MD, Gottesman MM, Varticovski L, Ambudkar SV. Prolonged drug selection of breast cancer cells and enrichment of cancer stem cell characteristics. *Journal of the National Cancer Institute* 2010;102(21):1637-1652.

643. Jin W, Chen B-b, Li J-y, Zhu H, Huang M, Gu S-m, Wang Q-q, Chen J-y, Yu S, Wu J, Shao Z-m. TIEG1 inhibits breast cancer invasion and metastasis by inhibition of epidermal growth factor receptor (EGFR) transcription and the EGFR signaling pathway. *Molecular and Cellular Biology* 2012;32(1):50-63.

644. Lee J-Y, Kim JM, Jeong DS, Kim MH. Transcriptional activation of EGFR by HOXB5 and its role in breast cancer cell invasion. *Biochemical and Biophysical Research Communications* 2018;503(4):2924-2930.

645. Jacob F, Guertler R, Naim S, Nixdorf S, Fedier A, Hacker NF, Heinzelmann-Schwarz V. Careful selection of reference genes is required for reliable performance of RT-qPCR in human normal and cancer cell lines. *PloS One* 2013;8(3):e59180.

646. Chen KG, Sale S, Tan T, Ermoian RP, Sikic BI. CCAAT/enhancer-binding protein β (nuclear factor for interleukin 6) transactivates the human *MDR1* gene by interaction with an inverted CCAAT box in human cancer cells. *Molecular Pharmacology* 2004;65(4):906-916.

647. Babaer D, Amara S, Ivy M, Zhao Y, Lammers PE, Titze JM, Tiriveedhi V. High salt induces P-glycoprotein mediated treatment resistance in breast cancer cells through store operated calcium influx. *Oncotarget* 2018;9(38):25193-25205.

648. Wang G, Aa J, Ge C. The underlying mechanism contributing to P-gp over-expression and drug resistance in the MCF-7 breast cancer cells induced by adriamycin. *Journal of Clinical Oncology* 2017;35(15_suppl):e12028-e12028.

649. Dyson J, Foll FL, Magal P, Noussair A, Pasquier J. Direct and indirect P-glycoprotein transfers in MCF-7 breast cancer cells. *Journal of Theoretical Biology* 2019;461:239-253.

650. Pasquier J, Galas L, Boulange-Lecomte C, Rioult D, Bultelle F, Magal P, Webb G, Le Foll F. Different modalities of intercellular membrane exchanges mediate cell-to-cell P-glycoprotein transfers in MCF-7 breast cancer cells. *Journal of Biological Chemistry* 2012;287(10):7374-7387.

651. Tryggvadottir H, Huzell L, Gustbée E, Simonsson M, Markkula A, Jirström K, Rose C, Ingvar C, Borgquist S, Jernström H. Interactions between ABCB1 genotype and preoperative statin use impact clinical outcomes among breast cancer patients. *Frontiers in Oncology* 2018;8(428).

652. Shen H, Lee FY, Gan J. Ixabepilone, a novel microtubule-targeting agent for breast cancer, is a substrate for p-glycoprotein (P-gp/MDR1/ABCB1) but not breast cancer resistance protein (BCRP/ABCG2). *Journal of Pharmacology and Experimental Therapeutics* 2011;337(2):423-432.

653. Joko-Fru WY, Jedy-Agba E, Korir A, Ogunbiyi O, Dzamalala CP, Chokunonga E, Wabinga H, Manraj S, Finesse A, Somdyala N, Liu B, McGale P, Jemal A, Bray F, Parkin DM. The evolving epidemic of breast cancer in sub-saharan Africa: Results from the African cancer registry network. *Int J Cancer* 2020;n/a(n/a).

654. Yu K, Rohr J, Liu Y, Li M, Xu J, Wang K, Chai J, Zhao D, Liu Y, Ma J, Fan L, Wang Z, Guo S. Progress in triple negative breast carcinoma pathophysiology: Potential therapeutic targets. *Pathology - Research and Practice* 2020;216(4):152874.

655. Soule HD, Vazguez J, Long A, Albert S, Brennan M. A human cell line from a pleural effusion derived from a breast carcinoma. *Journal of the National Cancer Institute* 1973;51(5):1409-1416.

656. Rich MA, Furmanski P, McGrath CM, McCormick J, Russo J, Soule H. The etiology of breast cancer. *Current Topics in Molecular Endocrinology* 1976;4:15-27.

657. Levenson AS, Jordan VC. MCF-7: The first hormone-responsive breast cancer cell line. *Cancer Research* 1997;57(15):3071-3078.

658. Gallaher JA, Enriquez-Navas PM, Luddy KA, Gatenby RA, Anderson ARA. Spatial heterogeneity and evolutionary dynamics modulate time to recurrence in continuous and adaptive cancer therapies. *Cancer Research* 2018;78(8):2127-2139.

659. Bacevic K, Noble R, Soffar A, Wael Ammar O, Boszonyik B, Prieto S, Vincent C, Hochberg ME, Krasinska L, Fisher D. Spatial competition constrains resistance to targeted cancer therapy. *Nature Communications* 2017;8(1):1995.

660. Hansen E, Woods RJ, Read AF. How to use a chemotherapeutic agent when resistance to it threatens the patient. *PLoS Biology* 2017;15(2):e2001110.

661. Ramya Krishna V, Aswani Dutt V, Dhananjay P, Ashim KM. Mechanisms of drug resistance in cancer chemotherapy: Coordinated role and regulation of efflux transporters and metabolizing enzymes. *Current Pharmaceutical Design* 2013;19(40):7126-7140.

662. Chmielecki J, Foo J, Oxnard GR, Hutchinson K, Ohashi K, Somwar R, Wang L, Amato KR, Arcila M, Sos ML, Socci ND, Viale A, de Stanchina E, Ginsberg MS, Thomas RK, Kris MG, Inoue A, Ladanyi M, Miller VA, Michor F, Pao W. Optimization of dosing for EGFR-mutant non-small cell lung cancer with evolutionary cancer modeling. *Science Translational Medicine* 2011;3(90):90ra59.

663. Yu HA, Sima C, Feldman D, Liu LL, Vaitheesvaran B, Cross J, Rudin CM, Kris MG, Pao W, Michor F, Riely GJ. Phase 1 study of twice weekly pulse dose and daily low-dose erlotinib as initial treatment for patients with EGFR-mutant lung cancers. *Annals of Oncology* 2017;28(2):278-284.

664. Zhang J, Cunningham JJ, Brown JS, Gatenby RA. Integrating evolutionary dynamics into treatment of metastatic castrate-resistant prostate cancer. *Nature Communications* 2017;8(1):1816.

665. Enriquez-Navas PM, Wojtkowiak JW, Gatenby RA. Application of evolutionary principles to cancer therapy. *Cancer Research* 2015;75(22):4675-4680.

666. Schafer JM, Lehmann BD, Gonzalez-Ericsson PI, Marshall CB, Beeler JS, Redman LN, Jin H, Sanchez V, Stubbs MC, Scherle P, Johnson KN, Sheng Q, Roland JT, Bauer JA, Shyr Y, Chakravarthy B, Mobley BC, Hiebert SW, Balko JM, Sanders ME, Liu PCC, Pietenpol JA. Targeting MYCN-expressing triple-negative breast cancer with BET and MEK inhibitors. *Science Translational Medicine* 2020;12(534):eaaw8275.

667. Xu S-W, Law BYK, Qu SLQ, Hamdoun S, Chen J, Zhang W, Guo J-R, Wu A-G, Mok SWF, Zhang DW, Xia C, Sugimoto Y, Efferth T, Liu L, Wong VKW. Serca and P-glycoprotein inhibition and ATP depletion are necessary for celastrol-induced autophagic cell death and collateral sensitivity in multidrug-resistant tumor cells. *Pharmacological Research* 2020;153:104660.

668. Kim KS, Jiang C, Kim JY, Park JH, Kim HR, Lee SH, Kim HS, Yoon S. Low-dose crizotinib, a tyrosine kinase inhibitor, highly and specifically sensitizes P-glycoprotein-overexpressing chemoresistant cancer cells through induction of late apoptosis in vivo and in vitro. *Frontiers in Oncology* 2020;10:696.

669. Zhou Y, Chung PY, Ma JY, Lam AK, Law S, Chan KW, Chan AS, Li X, Lam KH, Chui CH, Tang JC. Development of a novel quinoline derivative as a p-glycoprotein inhibitor to reverse multidrug resistance in cancer cells. *Biology (Basel)* 2019;8(4).

670. Nanayakkara AK, Vogel PD, Wise JG. Prolonged inhibition of P-glycoprotein after exposure to chemotherapeutics increases cell mortality in multidrug resistant cultured cancer cells. *PloS One* 2019;14(6):e0217940.

671. Williams CB, Soloff AC, Ethier SP, Yeh ES. Perspectives on epidermal growth factor receptor regulation in triple-negative breast cancer: Ligand-mediated mechanisms of receptor regulation and potential for clinical targeting. *Advances in Cancer Research* 2015;127:253-281.

672. Danzinger S, Tan YY, Rudas M, Kastner M-T, Weingartshofer S, Muhr D, Singer CF. Differential claudin 3 and EGFR expression predicts BRCA1 mutation in triple-negative breast cancer. *Cancer Investigation* 2018;36(7):378-388.

673. Simond AM, Muller WJ. Chapter five - in vivo modeling of the EGFR family in breast cancer progression and therapeutic approaches. In: Kumar R, Fisher PB, eds. *Advances in Cancer Research*: Academic Press; 2020;147:189-228.

674. Chow LWC, Lie EF, Toi M. Chapter ten - advances in EGFR/HER2-directed clinical research on breast cancer. In: Kumar R, Fisher PB, eds. *Advances in Cancer Research*: Academic Press; 2020;147:375-428.

675. Hegedus C, Ozvegy-Laczka C, Szakács G, Sarkadi B. Interaction of ABC multidrug transporters with anticancer protein kinase inhibitors: Substrates and/or inhibitors? *Current Cancer Drug Targets* 2009;9(3):252-272.

676. Crawford RR, Potukuchi PK, Schuetz EG, Schuetz JD. Beyond competitive inhibition: Regulation of ABC transporters by kinases and protein-protein interactions as potential mechanisms of drug-drug interactions. *Drug Metabolism and Disposition* 2018;46(5):567-580.

677. Comandante-Lou N, Khaliq M, Venkat D, Manikkam M, Fallahi-Sichani M. Phenotype-based probabilistic analysis of heterogeneous responses to cancer drugs and their combination efficacy. *PLoS Computational Biology* 2020;16(2):e1007688.

678. de Nonneville A, Finetti P, Adelaide J, Lambaudie É, Viens P, Gonçalves A, Birnbaum D, Mamessier E, Bertucci F. A tyrosine kinase expression signature predicts the post-operative clinical outcome in triple negative breast cancers. *Cancers (Basel)* 2019;11(8).

679. Crunkhorn S. Combination therapy combats aggressive breast cancer. *Nature Reviews Drug Discovery* 2020;19(5):310.

680. Sudalagunta P, Silva MC, Canevarolo RR, Alugubelli RR, DeAvila G, Tungesvik A, Perez L, Gatenby R, Gillies R, Baz R, Meads MB, Shain KH, Silva AS. A pharmacodynamic model of clinical synergy in multiple myeloma. *EBioMedicine* 2020;54:102716.

681. Seo H, Tkachuk D, Ho C, Mammoliti A, Rezaie A, Madani Tonekaboni SA, Haibe-Kains B. SYNERGxDB: An integrative pharmacogenomic portal to identify synergistic drug

combinations for precision oncology. *Nucleic Acids Research* 2020;48(W1):W494-w501.

682. Potdar S, Ianevski A, Mpindi JP, Bychkov D, Fiere C, Ianevski P, Yadav B, Wennerberg K, Aittokallio T, Kallioniemi O, Saarela J, Östling P. Breeze: An integrated quality control and data analysis application for high-throughput drug screening. *Bioinformatics* 2020;36(11):3602-3604.

683. Bolt HM, Hengstler JG. The rapid development of computational toxicology. *Arch Toxicol* 2020;94(5):1371-1372.

684. Scotti L, Ishiki HM, Duarte MC, Oliveira TB, Scotti MT. Computational approaches in multitarget drug discovery. *Methods in Molecular Biology* 2018;1800:327-345.

685. Molins EAG, Jusko WJ. Assessment of three-drug combination pharmacodynamic interactions in pancreatic cancer cells. *Journal of the American Association of Pharmaceutical Scientists* 2018;20(5):80.

686. Hasselgren C, Myatt GJ. Computational toxicology and drug discovery. *Methods in Molecular Biology* 2018;1800:233-244.

687. Wicha SG, Chen C, Clewe O, Simonsson USH. A general pharmacodynamic interaction model identifies perpetrators and victims in drug interactions. *Nature Communications* 2017;8(1):2129.

688. Toyoda Y, Takada T, Suzuki H. Inhibitors of human ABCG2: From technical background to recent updates with clinical implications. *Frontiers in Pharmacology* 2019;10:208.